2015

Proceedings of the 2015 Coal Operators' Conference

Naj Aziz
University of Wollongong, naj@uow.edu.au

Bob Kininmonth
Illawarra Outburst Committee

PROCEEDINGS OF THE 2015 COAL OPERATORS' CONFERENCE

UNIVERSITY OF WOLLONGONG, NSW

11 - 13 FEBRUARY 2015

PRINCIPAL EDITORS

NAJ AZIZ AND BOB KININMONTH

ORGANISERS

UNIVERSITY OF WOLLONGONG - MINING ENGINEERING
AUSTRALASIAN INSTITUTE OF MINING AND METALLURGY- ILLAWARRA BRANCH
MINE MANAGERS ASSOCIATION OF AUSTRALIA

All papers in these proceedings are peer reviewed

Published on line: http://ro.uow.edu.au/coal
Or via: http://research.uow.edu.au/coal

SPONSORS AND EXHIBITORS

Faculty of Enginering and Information Sciences

FOREWORD

On behalf of the conference advisory and editorial boards I welcome you to the 15th Coal Operators Conference (Coal2015). Since its beginning in 1998 it has seen authors presenting papers on a wide variety of topics. The availability of past papers on line at http://ro.uow.edu.au/coal, currently has provided the industry with all the latest on new and current innovations, cutting edge research, developing technologies in different aspects of coal mining operations. These are relevant to safe, economic and efficient mining operations, and contribute to the professional development of mine employees. At present there are 545 papers on line, which are papers published in 14 proceedings. These papers have attracted around 80 000 downloads since going online in 2008. The figure below shows the number of papers and the attendances for each conference.

An additional 41 papers will be added on line from this conference. These papers are mostly from Australia but include papers from China, Czech Republic, India, Iran, Japan, and USA.

For a number of years, the International Longwall News (ILN), now known as International Coal News (ICN) website has been providing publicity coverage for the conference. This support is deeply appreciated and thanks to Lou Caruana for maintaining support for our conference. I look forward to the continuation of this support.

Number of participants and papers in each year of conference
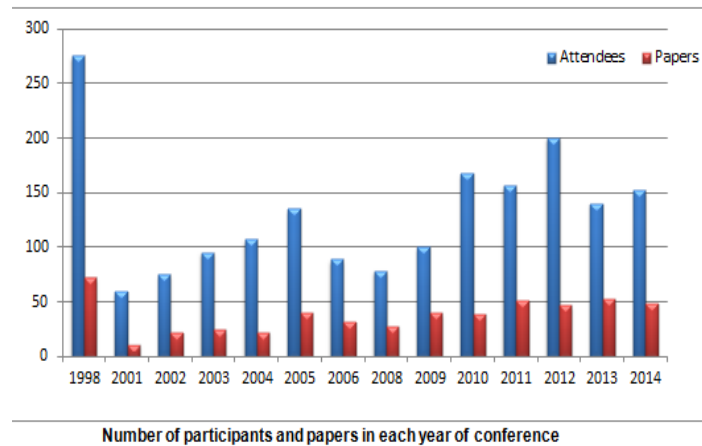
Special thanks to the editorial panel members and the paper reviewers; Dr Ali Mirza for typesetting the conference proceedings; Peter Vrahas of Eventico for his conference general management and efficient administration of the conference website; The University of Wollongong printery staff Gerard Toomey for designing the conference proceedings cover page, Garry Piggott and Maria O' Hearn for printing the conference proceedings, and Uni-Centre for catering. Finally, sincere thanks to authors, and participants, who form the backbone of the conference success.

All papers are peer reviewed to maintain the conference's high standing and recognition.

Professor Naj Aziz
Conference chairman and convenor

TABLE OF CONTENTS

COAL MINE HEALTH AND SAFETY REGULATORY AND ENFORCEMENT APPROACH, NEW SOUTH WALES, AUSTRALIA

Rob Regan

INTRODUCTION

The approach of the New South Wales (NSW) Mine Safety Operations Branch (the Inspectorate) is based on achieving safe work outcomes by controlling the physical work environment in mines through:

- competent people
- fit for purpose plant and equipment, and
- safe systems of work

The Inspectorate's aim is to ensure that the mining industry operates atbest practice in engineering safety and health standards. It is the expectation that industry operators will take responsibility for leading safety efforts by implementing and continuously improving safe systems of work. It is expected that mine workers will take on responsibility for contributing to improvements in safety and health and for complying with the safe systems of work.

This is achived using:

- a comprehensive regulatory framework that requires consultation and collaboration between mine operators, employees, employee unions and the regulator
- strong proactive powers for inspectors
- specific regulations that address the technical engineering requirements to control the electrical, mechanical and mining engineering necessary for safe mining
- codes of practice that recommend the best known ways and greater detail to control the hazards and risks of mining
- mining design guidelines for controlling critical risks
- Australian and international Standards for detailed engineering and procedures necessary for controlling these risks
- legislated requirements for the competency of managers and supervisors of electrical, mechanical and mining engineering and management of mines
- legislated requirements for employers to ensure their employees are competent to undertake the tasks required by the employer
- legislated requirements for the competency of electrical, mechanical and mining inspectors
- continuous training of inspectors to ensure the technical and practical knowledge and experience for a strong capability to advise mine operators in management of risks, and
- a problem solving approach by the Inspectorate to risks arising at mines

HISTORY

Coal was first discovered in Australia in NSW in 1791 and the early exploitation of resources was achieved with convict labour.

The abolition of the convict system resulted in a reduction of convicts in the industry so that by 1847 there were only a few in NSW mines.

Director Mine Safety Operations, Chief Inspector NSW Department of Trade & Investment, Regional Infrastructure & Resources, E-mail: safetyalert@minerals.nsw.gov.au, Tel: 0249 316458

Miners were employed from Great Britain to fill the need for non-¬convict labour. These miners had used industrial action to improve conditions in Britain. They carried on action in NSW. This led in 1854 to the passing in NSW of the first Act for the regulation of coal mines.

British mining acts and associated regulations and the progressive amendments which were made became models for the legislative control of mining in Australia and New Zealand.

The amendment, repeal and replacement of coal mining Acts has occurred progressively. The stimulus for change has arisen in a number of ways including development of mining technology, a better understanding of the inherent risks of mining, industrial action for improved working conditions and implementation of recommendations of inquiries into mining disasters.

From the introduction of the first Act for the "Registration and Inspection of Coal Mines in the Colony of NSW", in November 1854, successive legislation was introduced to prescribe controls required to improve safety in mines (Regan and kininmonth, 2009).

The critical activities requiring improved technology and management were;

- Mine ventilation by fans instead of furnace fires.
- Regular inspections for detection of methane.
- Watering of dry and dusty places, stone dusting including explosion suppression with stone dust and water barriers.
- Use of explosives including prohibition of gunpowder and the introduction of permitted explosives for gassy and dusty mines.
- Use of electricity in coal mines.
- Competency certification of managers, mining supervisors, electricians and winding engine drivers.
- Appointment of a certified manager to every mine employing more than twenty employees.
- The issue of a summary of the Act to all employees.
- Appointment of Coal Mine Inspectors in 1875 followed by an Electrical Inspectors in 1908.
- Appointment of a Chief Inspector in 1897.

Since the 1912 Coal Mines Regulation Act, improvements have upgraded these same basic mining engineering safety requirements and added;

- Systematic timbering rules,
- Use of cutting and welding apparatus.
- Water reticulation to the mining place,
- Installation and use of belt conveyors in mines.
- Fire precautions and fire fighting organisation,
- Gas monitoring, and
- Preparation of rules and schemes for prescribed activities specific to an individual coal mine

In 1999 the Coal Mining (General, Underground and Open Cut) Regulations (NSW government,1999) established the concepts of duty of care and risk management   into coal mining legislation.
The revised Occupational Health and Safety Act 2000 (NSW Gov, 2000) was passed.   This replaced the 1983 Act and reinforced the duty of care and risk management responsibilities for coal mining employers. This was updated to the NSW Work Health and Safety Act and Regulation(NSW Gov, 2011). The Coal Mine Health and Safety Act 2002 further strengthened the requirements for duty of care and risk management.

NSW has recently updated the coal, metalliferous and quarrying safety legislation to a nationally consistent act and regulation, the Work Health and Safety (Mines) Act 2013 and Regulation 2014. It makes provisions for all mining in NSW and maintains the health and safety standards of the previous legislation. This legislation commenced on 1 February 2015.

NSW MINE SAFETY OPERATIONS

Mine Safety Operations has nine regional offices and a Technology Centre. The main office is at Maitland in the Hunter Valley. The Mine Safety Technology Centre is at Thornton, east of Maitland. Mine Safety Operations is responsible for supporting and encouraging health and safety compliance to meet community expectations for some 2000 mining operations, 6,000 mineral claims and 700 exploration licences in NSW.

There is a huge diversity of mining techniques, people, procedures, locations and working conditions.

The bulk of the mineral claims are for opal mining which have different needs from the mining operations.

The mining operations range from heavy mineral sands, through a range of open cut clay, gold, copper and other mineral mines, extensive coal mines in the Hunter and Illawarra, to large underground gold and base metal mines in central and far western NSW.

Mine Safety Operations is independently funded by a levy imposed on the owners of mining operations in all sectors in NSW. The levy is controlled by the Mine Safety (Cost Recovery) Levy Act of December 2005. The levy is to be set to be no greater than 1% of the value of wages and salaries paid by employers to their employees including contracting companies and their employees. The monies are collected via the workers compensation insurance systems that cover the mining, onshore petroleum and exploration sectors in NSW. The monies must be used only for the administration and enforcement of mine safety in NSW. The levy has been set between 0.85% and 0.95% of wages and salaries resulting from budgets ranging from $23 to $27million per annum.

There are 108 positions including 55 full-time field officers, eight senior inspectors, one chief inspector, 10 specialist technical inspectors, 19 technical service officers and 15 administrative officers.

The NSW Coal Mining industry has some 35 underground coal mines and 34 open cut coal mines. There are nine coalmining inspectors and 5 mine safety officers dedicated to coal mines. In addition seven mechanical and seven electrical inspectors and mine safety officers have responsibility for all types of mines

CONTROLLING THE WORK ENVIRONMENT

Relationship of NSW WHS Acts and Regulations, Codes and Standards and guidelines

In NSW the WHS Act 2011 and Regulation provide the minimum health and safety requirements that all employers must meet. The WHS (Mines) Act and Regulation require specific provisions as stated in the objectives. These are additional to the WHS Act. Failure to comply with the provisions of the Acts and Regulations is subject to enforcement action including advice, improvement notices, prohibition notices or prosecution.

Due to the technical detail required to ensure safety in certain high risk work places including mines and particularly underground coal mines, Codes of Practice have been developed to establish electrical, mechanical and mining engineering requirements.

The Codes of Practice provide information about the best known ways to achieve satisfactory safety standards for the particular hazard that they deal with.

A Code of Practice is not mandatory, however a mine operator that does not follow the code must show that it is applying an equal or better practice to control the risk associated with the hazard. If an inspector forms the reasonable opinion that the mine operator is not following a practice that is up to the standard of the code, the inspector is able to require the mine operator to follow the code or be in breach of the notice that is served on the mine operator.

Objectives of NSW Health and Safety Legislation

Should there be a short lead in saying how or what means the mines safety operations group was formed . See last page of this paper in Page 21.

The Mine Safety Operations unit of the Trade and Investment, Regional Infrastructure and Resources has the opportunity and responsibility to maintain the mining industry's corporate technical and practical knowledge. This is what the Inspectorate will continue to work on this to assist the unions and mine operators to protect workers.

Mine Safety Operations undertakes the regulatory function for health and safety Acts for mining, explosives and onshore petroleum activities, and works to ensure that the industry satisfies community and government expectations for safety, health, mine subsidence and resource extraction. These Acts are the Work Health and Safety Act 2011 (WHSA), the Work Health and Safety (Mines) Act 2013, the Explosives Act 2003 and the Petroleum (Onshore) Act 1991 (POA).

There are six objectives of the key health and safety legislation in NSW that Mine Safety Operations has been established for and provided with powers and functions to enforce achievement of:

- a balanced and nationally consistent framework to secure the health and safety of workers and workplaces
- securing the objectives of the Work Health and Safety Act at mines, including securing and promoting the health and safety of people at work at mines or related places
- to protect workers at mines and other persons against harm to their health and safety through the elimination or minimisation of risks arising from work or from specific types of substances or plant
- to ensure that effective provisions for emergencies are developed and maintained at mines
- to establish a scheme for ensuring that persons exercising certain functions at mines are competent to do so
- to establish the Mine Safety Advisory Council
- to provide for worker safety and health representatives in coal mines
- to facilitate interstate regulatory co-operation
- to establish Boards of Inquiry
- to provide for enforcement powers that are in addition to those in the Work Health and Safety Act 2011.
- Mine Safety Operations is provided with powers and functions to secure these objectives and
- provide for fair and effective workplace representation, consultation, co-operation and issue resolution in relation to work health and safety
- encourage unions and employer organisations to take a constructive role to promote improvements in work health and safety practices, and assisting persons conducting businesses or undertakings and workers to achieve a healthier and safer working environment
- promote the provision of advice, information, education and training in relation to work health and safety
- secure compliance with the Acts through effective and appropriate compliance and enforcement measures
- ensure appropriate scrutiny and review of actions taken by persons exercising powers and performing functions under the Acts
- provide a framework for continuous improvement and progressively higher standards of work health and safety, and
- maintain and strengthen the national harmonisation of laws relating to work health and safety and to facilitate a consistent national approach to work health and safety in NSW.

To further ensure the achievement of the objectives of the legislation, Mine Safety Operations, duty holders, officers, workers and other persons must have regard to the principle that workers and other persons should be given the highest level of protection against harm to their health, safety and welfare from hazards and risks arising from work or from specified types of substances or plant as is reasonably practicable.

As the regulator's delegates Mine Safety Operations also has through its inspectors the following legislated functions:

- to advise and make recommendations to the Minister and report on the operation and effectiveness of the Work Health and Safety Act   (the Act)
- to monitor and enforce compliance with the Act
- to provide advice and information on work health and safety to duty holders under the Act and to the community
- to collect, analyse and publish statistics relating to work health and safety
- to foster a co-operative, consultative relationship between duty holders and the persons to whom they owe duties and their representatives in relation to work health and safety matters
- to promote and support education and training on matters relating to work health and safety
- to engage in, promote and coordinate the sharing of information
- to achieve the objective of the Act, including the sharing of information with a corresponding regulator
- to conduct and defend proceedings under the Act before a court or tribunal
- any other function conferred on the regulator by the Act.

Inspectors have the following functions and powers under the Acts:

- to provide information and advice about compliance with this Act
- to assist in the resolution of:
- work health and safety issues at workplaces
- issues related to access to a workplace by an assistant to a health and safety representative
- issues related to the exercise or purported exercise of a right of entry
- to review disputed provisional improvement notices
- to require compliance with the Acts through the issuing of notices
- to investigate contraventions of the Acts and assist in the prosecution of offences, and
- to attend coronial inquests in relation to work-related deaths and examine witnesses.

SAFE SYSTEMS OF WORK

The Acts and Regulations place requirements on mine operators to establish implement and apply health and safety management plans to control all the prescribed major hazards that arise at their mine. They must also prepare such plans for any particular major hazard that is peculiar to their mine.   No mining can take place until such plans are implemented.   Once mining commences it is the inspector's function to apply his powers to drive implementation and application of these plans as well as compliance with the legislation in general.

Management plans and systems

There are a number of control and management plans comprising the safety management system requirements to develop safe work methods, and how to deal with high risk activities: .

Safety management system

This is the primary plan that the mine operator must prepare and implement; its contents are prescribed in the WHS (Mines) Regulation 2014.

If no functional safety management system or any part relevant to mining operations is established, such mining operations are not to take place.

The approach specifically calls up each of the NSW WHS Act key requirements of Consultation, Hazard Identification, Risk Assessment, Risk Management, Information Provision, Instruction and Training, Supervision, Monitoring, Reviewing and Revising.

The outline and policy are required to be submitted to the Inspector of Mines and to the Industry Check Inspector who can object where the system is deficient. The inspector can then issue a prohibition and/or improvement notice to ensure a satisfactory standard is achieved.

The following are major components of the Safety Management System.

- Health and Safety Policy
- Management Structure for operation
- Management Register for operation
- Contractor Management Plans
- Principal Hazard Management Plans
- Principal Control Plans, including a Health Control Plan
- Specific Control Measures
- Emergency Management Plans, and

Procedure and arrangement details for these plans and measures

Contractor management plans:

These address both mine operators and contractors to the mine operator.

- Contractors must either prepare a plan and obtain the mine operator's written agreement that the plan is consistent with the SMS for the mine, or
- Contractors must review the relevant parts of the mine SMS and give the operator written notice that the contractor's arrangements for managing health and safety are consitant with the SMS.
- Contractors are defined as those conducting a business or undertaking at a mine, i.e. general mining and construction but not those engaged in a delivery, office equipment service, office cleaning or catering business or those specified in a regulator published Gazette order.
- It is the duty of both the mine operator and contractor to ensure that contractors comply with the Contractor Management Plan and the requirements of the Acts and Regulations

Principal mining hazard management plans

The nine Principal Mining Hazards (PMH) to be considered are prescribed in Schedule 1 of the Regulation. They are:

- Ground or strata failure
- Inundation or inrush of any substance
- Mine shafts and winding systems
- Roads and other vehicles operating areas
- Air quality or dust or other airborne contaminants
- Fire or explosion
- Gas Outbursts
- Spontaneous combustion
- Subsidence

PMHare also identified by a mine operator's own identification and risk assessment.

A separate plan must be prepared for each separate principal hazard and each must be considered individually and cumulatively with other hazards at a mine.

The plans must

- provide for the management of all aspects of risk control in relation to the PMH
- be set out and expressed in a way that is readily understandable by persons who use it
- describe the nature of the PMH, how it relates to other hazards, analysis used to identify it, record of most recent risk assessment, investigation and analysis methods to determine control measures, all control measures, arrangements to provide information, training and instruction
- refer to design principles, engineering and technical standards, and

- set out reasons for adopting or rejecting each control measure considered.

Principal control plans

Schedule 2 of the regulation prescribes matters to be addressed by each of the four plans.

- Health
  o controlling exposures and impairments and monitoring health hazards and health of workers
- Mechanical engineering
  o consider the life cycle of plant and structures, reliability of mechanical safeguards, work practices and competency of workers, possible injury to workers working on plant or structures, ignition sources, mechanical energy sources, plant fires and toxic or harmful substances
- Electrical engineering,
  o consider the life cycle of plant and structures, reliability of electrical safeguards, work practices and competency of workers, possible injury to persons caused by direct or indirect contact with electricity or working on electrical plant or installations, ignition sources and fires, and
- Explosives
  o Consider unintended detonation, characteristics for intended use and places of use, charging and firing activities, theft, misuse, deteriorated or damaged explosives, handling misfires, manufacturing, storing, transporting and delivering and accounting of explosives and ejection of flyrock.

Emergency Management Plan (Emergency Response Control Plan)

The mine operator must prepare an up to date emergency management plan including the following matters having regard to the nature, complexity and location of the mining operations and the risks associated with those operations:

- emergency control structure
- key personnel, internal and external
- consult with primary emergency services and workers
- resources and equipment
- rescue training
- procedures including evacuation and accounting for all persons at the mine, control points for utilities, in event of ventilation failure for more than 30 minutes, fire fighting, emergency sealing from a safe place and for safely inserting inertisation equipment
- training of workers in relation to the plan
- testing of plan
- regularly review the plan
- copy available at the mine
- provide copy to consulted emergency service organisation

Ensuring effective provisions for emergencies is one of nine objectives of the WHS (Mines) Act. This means that the Emergency Management Plan is of critical importance.

High risk activities

The High Risk Activities are prescribed by schedule 3 of the Regulation and include:

- All mines
  o Electrical work on energized equipment
- Underground mines
  o Development of a new mine entry
  o Connected voltage becoming greater than 12,000 volts

- Underground coal mines
  - Working in an inrush control zone
  - Roadway or drift without intersection for 250 metres
  - Shotfiring
  - Sealing part of a mine, other than   in an emergency
  - Conduct of hot work in a hazardous zone
  - Driving underground roadway that is wider than 5.5 metres
  - Widening underground roadway to more than 5.5 metres
  - Use of high voltage plant and cables in a hazardous zone
  - Formation of non-conforming pillars
  - Secondary extraction or pillar extraction, splitting or reduction
  - Shallow depth of cover mining
  - Mining in outburst control zones
  - First applications of explosion inhibitors
  - Use of explosives designed for use in coal mines
  - Use of explosive not designed for use in coal mines
  - First use of a vehicle with a fire-protected diesel engine
  - First use of an explosion barrier other than a water barrier or bagged stone dust
- Coal mines other than underground coal mines
  - Highwall mining, entry of persons
- All coal mines
  - Emplacement areas
  - Highwall mining
  - Barrier mining

A mine operator is not permitted to commence any of theses activities without preparation of suitable plans and notification to the inspector and industry check inspector and observing a waiting period, while the plans are examined.

The principal hazard management plans and high risk activity notifications are required for the

- Prevention of unplanned falls of ground or strata,
- Prevention of inrushes of mud, water, gas,
- Prevention of gas and dust explosions,
- Prevention of electric shock and burns,
- Prevention of fires,
- Prevention of uncontrolled explosives blasts,
- Prevention of injury and death from unintended operation of equipment,
- Prevention of high pressure hydraulic fluid injection
- Provision of electrical safeguards with a correct safety integrity level (reliability vs failure on demand or failure per hour), and
- Prevention of health risks from airborne pollutants such as diesel particulate matter, diesel exhaust gases and coal and silica dust

MANAGEMENT SYSTEMS

The management system approach is systematic, rigorous and auditable involving:

- System safety engineering
- Hierarchy of risk controls
- Hazard reduction precedence
- Provision of information used to provide:
  - Fit for purpose equipment
  - High focus on hazardous area equipment
  - Competent people

  o Proper procedures

System safety is a compilation of engineering analyses and management practices that:

- Uses consultative processes
- Identifies hazards in the system
- Determines underlying causes of hazards
- Develops engineering and management controls to eliminate the hazards or mitigate their consequences
- Verifies the controls are adequate and in place
- Monitors the system
- Puts appropriate supervision in place
- Provides information, instruction and training to employees, and
- Reviews and revises the system.

COMPETENTENCY LEVELS

Mining management, supervisors and workers

Mine operators must ensure that each person is competent to undertake the duties, tasks and functions required of them by the mine operator and the mine safety legislation.

The legislation requires competence standards to be set and met by persons undertaking various roles at a mine.

The mine operator must ensure only competent people are employed to perform specified functions such as the mining, electrical and mechanical engineering managers, underground mine supervisors, supervisors of mining crews, electrical, mechanical and ventilation engineers, electrical and mechanical tradespersons, quarry managers and shotfirers (blasting explosives users).

Likewise any contractors must ensure they employ only competent people to undertake these functions. To oversee the setting and assessment of competency standards a Mining Competence Board is constituted with an independent chairperson, two employer representatives, two employee representatives, between two and four persons who have expertise in the development and assessment of competence of people performing functions at mines, and two officers of the Department appointed by the Minister.

The Mining Competence Board sets examinations through examination panels convened by inspectors of the Department, electrical, mechanical and mining, and assesses the competency of persons through written examinations in mining practices and mine safety legislation and an oral examination by two or three examiners, being one inspector and one or two competent persons from the mining industry.

Before a person is permitted to sit for the examinations they must have at least three years experience in or about a mine. If a person has a tertiary qualification in mining engineering at university degree or technical and further education advanced diploma level they are not required to be examined in mining practices but must sit a legislation examination and oral examination.

Certificates of competency are granted if the person passes the written examinations with at least 65% overall and at least 60% in any one examination paper and are recognised as competent in the oral examination. The oral examination assesses competence in all aspects of the (legislation specified) function for which they wish to obtain a certificate. Candidates often pass the written examinations but are not recognised as competent after the oral assessment. Candidates are permitted three attempts at the oral examination once the written examinations are passed before they must resit the written examinations. There are strict requirements governing the granting of certificates of competency with penalties for false and misleading statements regarding experience and qualifications, use of other person's certificates and forged certificates.

Workers must be assessed after training in the functions or activities they are to undertake as part of their work at a mine, e.g. continuous miner operator, longwall shearer operator, longwall chock operator, shuttlecar driver, roofbolter operator, fire officer, roadway dust sampler, etc

INSPECTORS OF MINES

A person may be appointed as an inspector only if the regulator is satisfied that the person has:

- appropriate knowledge and skills, and adequate experience in mining operations to effectively exercise the functions of an inspector, and
- the qualifications prescribed by the regulations or qualifications that the regulator determines to be equivalent of those qualifications, i.e.
  - the qualifications required to be nominated to exercise the statutory function of mining, mechanical or electrical engineering manager or quarry manager at the mine to which the person's inspections will relate

Powers and functions of inspectors

Inspectors have several powers under the WHS Act 2011and the WHS (Mines) Act 2013.

- Advice

The inspector has a duty to bring concerns regarding health, safety or welfare to the attention of mine operators when an inspector obtains any information or becomes aware of any practice at a mine that may, in their opinion, be relevant to the continued safe operation of a mine or the health, safety or welfare at work of the people who work at a mine. The inspector must, as soon as possible, advise the most senior person in the management structure of the mine who is at the mine.

- Proactive improvement or prohibition notices

This enables an inspector to act on information received or observed about any matter or activity that is not yet taking place but is in the inspector's opinion not being planned to be undertaken with the necessary standard of safety or health. If the inspector is of the opinion that a mine or any part of a mine or any matter, thing or practice at a mine or connected with the control or management of a mine is, or is liable shortly to become, dangerous to the safety or health of any persons employed at the mine the inspector may serve on the operator of the coalmine a notice:

- stating that the inspector is of that opinion, and
- giving particulars of the inspector's reasons for being of that opinion.
- The inspector may, by way of that notice:
- impose upon the operator such prohibitions and restrictions, and require the operator to carry out such works or do such things:
  - as appear to the inspector to be necessary for the purpose of safeguarding the safety or health of the persons employed at the operation, and as are set out in the notice, or
- direct that operator to cause the   mine or any part of the   mine:
  - to be evacuated immediately, or
  - to be closed, either indefinitely or for such period as is specified by the inspector, or
  - give such directions as appear to be necessary, or
  - both impose prohibitions and restrictions and give directions.

The inspector may require any notice to be complied with immediately or within a period specified in the notice. Any notice served remains in force until it is varied or revoked by the inspector unless it sooner expires.

- Reactive improvement notices

If an inspector is of the opinion that any person:

a. is contravening any provision of the Act or the regulations, or
b. has contravened such a provision in circumstances that make it likely that the contravention will continue or be repeated, the inspector may issue to the person a notice requiring the person to remedy the contravention or the matters occasioning it within the period specified in the notice.

An inspector may specify a period that is less than 7 days after the issue of the improvement notice if satisfied that it is reasonably practicable for the person to comply with the requirements imposed by the notice by the end of that period.

- Reactive prohibition notices

If an inspector is of the opinion that at any place of work there is occurring or about to occur any activity which involves or will involve an immediate risk to the health or safety of any person, the inspector may issue to the person who has or may be reasonably presumed to have control over the activity a notice prohibiting the carrying on of the activity until the matters which give or will give rise to the risk are remedied.

- Power of entry

Inspectors have powers to enter any premises they have reason to believe is a mining place of work or associated with a mine.

The inspector may enter the premises without notice and then notify the mine operator unless that would defeat the purpose of the inspection. Entry may be at any time the mine is worked. If necessary, reasonable force may be used for the purpose of gaining entry to a mine if the regulator gives written authority to the inspector. Inspector may apply for a search warrant if the inspector has reasonable grounds for believing that a provision of Act or the regulations has been or is being or is about to be contravened in or about any premises.

Powers on entry

When an inspector goes to a mine he has the power to do any of the following:
- make searches, inspections, examinations and tests (and take photographs and make video and audio recordings),
- take samples of substances or things which in the inspector's opinion may be a risk to health, require any person in or about those premises to answer questions or otherwise furnish information, require the mine operator to provide the inspector with such assistance and facilities as is or are reasonably necessary to enable the inspector to exercise the inspector's functions,
- require the production of and inspect any documents in or about those premises, take copies of or extracts from any such documents, dismantle any plant or other thing on the premises for the purpose of examination, take any plant, substance or other thing (or any sample of any substance) from the premises. Having taken a thing an inspector may:
  - o move the thing from the place where it was taken, or
  - o leave the thing at the place but take reasonable action to restrict access to it, or
  - o if the thing is plant—dismantle it.

Access may be restricted by:

- sealing a thing and marking it to show access to it is restricted,
- sealing the entrance to a room where the thing is situated and
- marking it to show access to it is restricted.
- keep any plant, substance, sample or other thing taken that:
  - o may reasonably be required as evidence in proceedings for an offence , or
  - o might, if not so kept, be used to continue or repeat the offence.

An inspector may, by notice in writing served on a person, require the person to do any one or more of the following things:

- to give an inspector, in writing signed by the person (or, in the case of a body corporate, by a competent officer of the body corporate) and within the time and in the manner specified in the notice, any such information of which the person has knowledge,
- to produce to an inspector, in accordance with the notice, any such documents,

- to appear before an inspector at a time and place specified in the notice and give either orally or in writing any such evidence and produce any such documents.

An inspector may inspect a document produced in response to his notice and may make copies of, or take extracts from, the document. An inspector may take possession and retain possession for as long as is necessary for the purposes of the Act, of a document produced in response to his notice if the person otherwise entitled to possession of the document is supplied, as soon as practicable, with a copy certified by an inspector to be a true copy. An inspector may require a person whom the inspector reasonably suspects has committed an offence against this Act or the regulations to state the person's full name and residential address. The inspector may request the person to provide reasonable proof of the person's identity.

An inspector may take a police officer to accompany and take all reasonable steps to assist an inspector in the exercise of the inspector's functions in executing a search warrant, or if the inspector reasonably believes that he may be obstructed in the exercise of those functions.

Inspector to consult with employee's local check inspector

An inspector who is proposing to undertake an inspection of a place of work with respect to a matter that may affect the health, safety or welfare of employees at the place of work: must, to the extent that it is practicable, consult a representative of the employees or an industrial organisation of employees whose members are employed at the place of work, and must, if requested to do so by the representative, take the representative on any such inspection.

Duty to notify the regulator of certain incidents:

1. A mine operator of a mine must ensure that the regulator, and at a coal mine an industry safety and health representative, is notified immediately after becoming aware that a notifiable incident arising out of the conduct of any business or undertaking at the mine has occurred.
2. A person conducting a business or undertaking at a mine must ensure that the regulator is notified immediately after becoming aware that a notifiable incident arising out of the conduct of the business or undertaking at the mine has occurred.
3. Notice under this section must be given in accordance with this section and by the fastest possible means.
4. The notice must be given:
5. by telephone, or
6. in writing.

Example. The written notice can be given by facsimile, email or other electronic means.

- Notifiable incidents
  o the death of a person
  o a serious injury or illness of a person prescribed by the regulations, i.e.
  a. an injury or illness requiring the person to have immediate treatment as an in-patient in a hospital,
  b. an injury or illness requiring the person to have immediate treatment for any of the following:
  o the amputation of any part of his or her body,
  o a serious head injury,
  o a serious eye injury,
  o a serious burn,
  o the separation of his or her skin from an underlying tissue (such as
  o degloving or scalping),
  o a spinal injury,
  o the loss of a bodily function,
  o serious lacerations,
  c. an injury or illness requiring the person to have medical treatment within 48
  d. hours of exposure to a substance,

e.   a fracture to a person's bone other than a bone in the person's hand (including a finger) or foot (including a toe),

f.   a condition prescribed as a serious illness for the purposes of section 36 of the WHS Act, or

o   a dangerous incident prescribed by the regulations, i.e.

a.   an incident in relation to a workplace that exposes a worker or any other person to a serious risk to a person's health or safety emanating from an immediate or imminent exposure to:

i)   an uncontrolled escape, spillage or leakage of a substance, or

ii)   an uncontrolled implosion, explosion or fire, or

iii)   an uncontrolled escape of gas or steam, or

iv)   an uncontrolled escape of a pressurised substance, or

v)   the fall or release from a height of any plant, substance or thing, or

vi)   the collapse, overturning, failure or malfunction of, or damage to, any plant that is required to be authorised within the meaning of Part 4 of the WHS Act, or

vii)   the collapse or partial collapse of a structure, or

viii)   the collapse or failure of an excavation or of any shoring supporting an excavation, or

ix)   the inrush of water, mud or gas in workings in an underground excavation or tunnel, or

x)   the unintended interruption of the main system of ventilation in an underground excavation or tunnel, or

xi)   the loss of control of heavy earthmoving machinery (including any failure of braking or steering), or

xii)   the unintended activation, movement, or failure to stop of vehicles or machinery, or

xiii)   a collision involving a vehicle or mobile plant, or

xiv)   damage to, or failure of, any part of a powered winding system or a shaft or shaft equipment, or

xv)   damage to any plant or structure, or

xvi)   a failure of ground, or of slope stability control measures, or

xvii)   rock falls, instability of cliffs, steep slopes or natural dams, occurrence of sinkholes, development of surface cracking or deformations or release of gas at the surface, due to subsidence, or

xviii)   a vehicle or plant making contact with an energised source having a voltage greater than 1,200 volts (other than testing equipment applied to energised equipment in accordance with the WHS Regulations),

a.   a fire in the underground parts of a mine, including where the fire is in the form of an oxidation that releases heat and light,

b.   an electric shock to a person (other than a shock from an extra low voltage source),

c.   any initial indication that any underground part of a coal mine is subject to windblast, outbursts or spontaneous combustion,

d.   the unintended overturning of any vehicle or of plant weighing more than 1,000 kilograms,

e.   ejection of rock from blasting that falls outside the blast exclusion zone (being the area from which persons are excluded during the blasting).

The mine operator must take all reasonable steps to ensure that the regulator, via the inspector of the mine, is notified after becoming aware of an incident, other than a notifiable incident, if the incident results in illness or injury that requires medical treatment suturing wounds, treating fractures, bruises and second and third degree burns. Similarly the industry safety and health representative is notified in case of an incident at a coal mine.

The time frame is 7 days after becoming aware of the incident or 48 hours after becoming aware that the incident resulted in an illness or injury.

- High potential incidents
  o   incidents that would have been dangerous incidents had a person reasonably been in the vicinity at the time, and
  o   detection of methane in the general body or air at 2.5% or greater

o   an unplanned fall of a roof or sides that impedes passage, extends beyond the bolted zone or disrupts production or ventilation

o   a failure of ground support where persons could potentially have been present

o   the burial of machinery such that it cannot be recovered under its own tractive effort

o   a progressive pillar failure or creep

o   a sudden pillar collapse

o   an electric arc occurring in the hazardous zone in an underground coal mine that is directly observed or that leaves visible evidence on an electric cable

o   the failure of the explosion-protection characteristics of explosion-protected plant while that plant is in-service in an underground coal mine

o   a misfire or unplanned explosion of an explosive or explosive precursor (but not in the case of a misfire at a mine other than a coal mine if the misfired explosive can be fired without any significant risk to a person

o   an unplanned event that causes the emergency evacuation of more than once person from the mine or part of the mine

o   an unplanned event that causes less than 2 exits from an underground mine to be available for use

o   any indication from monitoring data of thee development of subsidence which may result in any incident referred to in clause 179 (a) (xvi) or (xvii), i.e. a failure of ground, or slope stability control measures or rock falls, instability of cliffs, steep slopes or natural dams, occurrence of sinkholes, development of surface cracking or deformations or release of gas at the surface, due to subsidence

o   an injury to a person (supported by a medical certificate) that result in or is likely to result in the person being unfit, for a continuous period of at least 7 days, to perform the person's usual activities at the person's place of work

o   the illness of a person (supported by a medical certificate) that is related to a work process and that results in or is likely to result in the person being unfit, for a continuous period of at least 7 days, to perform the person's usual activities at the person's place of work.

Investigation notices

An inspector investigating any matter whether notified to him or not may issue an investigation notice to the mine operator if it is necessary to issue the notice in order to facilitate the exercise of the inspector's powers.

An investigation notice extends the time for non-disturbance of a site for a period, not exceeding 7 days, as specified in the notice. The notice may be renewed more than once by an inspector by issuing a further investigation notice.

The inspector may, after consulting with an industry check inspector (employees WHS representative), notify the operator of a mine that the scene of the incident may be released less than 24 hours after the notification of the relevant incident.

Despite the strong powers of the inspector and the role to fairly but firmly enforce compliance with satisfactory standards of health and safety, I expect inspectors to have a relationship with industry stakeholders such that the inspector is the first person mine operators, industry check inspectors, union officials and workers will call when planning an activity or when they have a problem.

The Mine Safety Operations approach is to extend the capabilities of mine operators by:

- Sanctioning or stopping the "vulnerable" mines
- Directing the "rule followers" to be better organised
- Encouraging the "robust" to achieve credible systems through involvement and information
- Partnering the "enlightened" to demonstrate the value of leadership with committed employees
- Championing the "resilient" to achieve mines truly prepared for any contingency

- Assisting the mining industry to eliminate unsafe work practices and achieve a safe working environment,
- Enabling industry and stakeholders to demonstrate commitment to the principles of duty of care and due diligence and adopt a systems approach to managing risks, and
- Implementing positive and clear safety interventions with continuous improvement for better safety and health management

Mine Safety Operations has the responsibility is to administer the legislation firmly, fairly and consistently, for example by

- appropriate licensing and certification; but with greater emphasis on assessment, education, advice, persuasion and enforcement of acceptable health and safety standards in the legislation and other sources
- checking the applicability of industry standards
- coordinating the improvement of standards
- where necessary retaining a leading role in standard setting
- monitoring industry compliance and taking appropriate enforcement action where it does not comply

The enforcement process is a relationship between assessment, investigation and application of directive powers and functions in the legislation.

Assessment or investigation can lead, with or without enforcement, to improved standards and to greater conformity with standards through standard improvement, education and information transfer, which are processes of encouragement.

Prosecution is one form of sanction in the overall process of enforcement. It is used to demonstrate that serious incidents are not acceptable and will be dealt with by use of the strongest measures available in the legislation. It is reserved for the most serious non-compliance outcomes as it is an often lengthy and adversarial process that requires enormous resources, skill and dedication both of the organisation and individual inspectors and investigators.

The Department Mine Safety Operations unit maintains this ongoing enforcement approach because our serious injury and fatality rates are not zero for long enough periods.

Enforcement of the legislation is the strategy for obtaining or maintaining conformity of operations with acceptable standards. Enforcement responses range from giving advice and expressing concern orally through to giving directions in writing as detailed above. For serious incidents or repeated non-compliance prosecution, and suspension or cancellation of 'right to mine' may result. Responses at the earlier end of the spectrum have the advantages of immediacy. The latter responses invariably take greater time and resources to give effect to.

The appropriate response will depend on the particular circumstances, the relevant provisions and the appropriate exercise of legislative discretions. The broad range of sanctions available allows the Inspectorate to tailor responses to particular circumstances including the breach, the actual or possible consequences of the breach and the relative immediacy of any danger.

Responses may be directed to the mining company, company directors, the mining engineering manager, particular mine workers, contractors, suppliers or combinations of these people.

CONCLUSION

The enforcement principles adopted by the Department are to:

- protect the safety and health of the mining workforce and those who may be affected by mining in a firm, fair and reasonable way consistent with community attitudes
- co-ordinate development,   review and promulgation of acceptable standards
- examine that compliance with acceptable standards for the management of health and safety is accepted and the primary responsibility lies with mine operators

- ensure that sanctions, applied from the wide range of available responses, are applied consistently, fairly, commensurate with the seriousness of a situation and should escalate where previous responses have not been complied with
- ensure that non-compliances should be met with timely and effective responses but n the first instance, subject to the seriousness of a situation, a cooperative response is preferred

This is done by:

- by maintaining a database and records of non-compliances and of Department action
- checking to ascertain remedial actions taken by industry and maintaining records of the remedial action
- supporting the enforcement policy through assessment and investigation programs
- identifying and solving specific problems in the industry, and
- developing and maintaining the competency of inspectors and adopting operating procedures to effectively administer the strategy

Improvement

The Department will know the strategy is successful while safety performance measures show continuing trends of improvement.

These are

- a continuous reduction in serious incident rates
- more and longer periods fatality free
- an increased ability to counsel industry, rather than apply penalties
- more time spent on assessment and verification, major hazard identification, risk assessment planning, risk management, emergency preparedness planning, targeted safety campaigns, practical workshops, guidelines and investigation of problems rather than reaction to serious incidents and breaches of legislation.
- implementing solutions to specific problems.
- a reduction in the number and type of certifications, notifications and exemptions required by legislation.
- continued management, recruitment and training consolidation of inspectors to enable delivery of the programs.

REFERENCES

Regan, R W and Kininmonth, R J. 2009, The development of safety legislation in Australasian Coal Mining Practices, Monograph 12, 12, 3rd edition, *The AusIMM.*
NSW government 1999.
NSW government 2000.
NSW government 2011.

MINING LEGISLATION -THE QUEENSLAND PERSPECTIVE

Andrew Clough

ABSTRACT: Following a series of coal mine disasters in the 80s and early 90s in Australia, a trend to move away from prescriptive to risk based legislative frameworks for mine safety gathered significant momentum. In one Australian jurisdiction, the state of Queensland, two mine safety Acts built on the risk based approach were introduced in 1999 - one for coal mines and one for metalliferous mines - which have led to arguably the best safety performance in a mining jurisdiction in the world. The approach relies on a single integrated safety management system for each mine, anticipation of hazards, control of risk and prevention of incidents. The legislation has high standards of duty and awareness requirements for everyone involved in the industry, and it demands extensive knowledge at the mine site about managing risk and the need for workforce involvement on mine sites. Formal risk management competencies are required by legislation for many of those holding management and other statutory positions in mines. This paper will cover how the risk based legal framework operates and the role and approach of the mines inspectorate in regulating mine safety under this type of framework.

HISTORICAL BACKGROUND

On the 7th August 1994 an explosion occurred at the Moura No 2 underground coal mine in central Queensland. Rescue attempts of the 11 trapped miners were abandoned after a second more violent explosion 18 hours later. The mine was sealed from the surface and the bodies of the 11 miners were never recovered. This was the third disaster that had occurred in the Moura district over the previous 20 years resulting in a total loss of 36 lives.

The Wardens inquiry into the Moura No 2 explosion was held in 1995 and a number of significant recommendations were made including a recommendation to revise the existing Coal Mining Act and regulations.

The Queensland Government committed to investigating each of the Wardens recommendations and a number of task groups were formed consisting of representatives from Government organisations, mine management, union bodies and the general workforce. The results of the task groups and subcommittee investigations have had impacts into the areas of legislative changes, operational changes and research activities.

A MOVE TOWARDS RISK BASED LEGISLATION

The Wardens inquiry saw no inherent objection to introducing self-regulation at mines. The Warden however commented that self-regulation must, however, be established within a framework of legislation that prescribes minimum requirements in respect to safety. It seems that high probability, low consequence matters might be suitably addressed by self-regulation but that low probability, high consequence matters should remain subject to prescriptive legislation.

The Coal Mining safety and Health Act (CMSHA) Qld Government 1999 and the Mining Quarrying Safety and Health Act (Qld Govt, 1999) were passed in 1999. The approach adopted in both Acts was one of self-regulation and advocacy of greater consultation between workers and employers. This was termed Robens style legislation in that the new legislation was structured around the findings of the UK 1972 Robens Report on Safety and Health at Work   (Sefety and Health at Work 1972a)CMSHA1999 and the Mining and Quarrying Safety and Health Act (Gld Govt, 1999) provide the framework for the legislative management of Safety. Both these Acts outline the goals or objectives of the legislation and provide the broad principals. The Acts are underpinned by specific Regulations, Codes of Practice, Recognised Standards and Guidance notes. Safety and Health Management Systems developed by the employer in consultation with the work force form the next tier of the scheme.

The Acts provide for placing safety and health obligations on those persons whose decisions affect the safety and health of others. The manner in which those obligations are discharged is through taking a systematic risk based approach to managing the hazards in the workplace. This necessitates consulting

Chief Inspector of Coal Mines, Department of Natural Resources and Mines, Queensland, E-mail:
Andrew.Clough@dnrm.qld.gov.au

with the workforce on safety and health matters and also providing ways to monitor the effectiveness of the systems.

This paper present further detail on the legal framework and policies that support the safe operation of the mines in Queensland. Specific reference will be made to the CMSHA) and the underpinning regulations and policies although the material presented here is applicable to both Acts.

THE OBJECTIVES OF THE ACT AND HOW IT INTENDS TO ACHIEVE THESE

The objectives of this Act are:

   (a) to protect the safety and health of persons at coal mines and persons who may be affected by coal mining operations;
   (b) to require that the risk of injury or illness to any person resulting from coal mining operations be at an acceptable level; and
   (c) to provide a way of monitoring the effectiveness and administration of provisions relating to safety and health under this Act and other mining legislation.

To ensure that risk is at an acceptable level, the legislation requires that management and operating systems must be put in place for each coal mine. The systems must incorporate risk management elements and practices appropriate for each coal mine to:

   - Identify, analyse, and assess risk;
   - Avoid or remove unacceptable risk;
   - Monitor levels of risk and the adverse consequences of retained residual risk;
   - Investigate and analyse the causes of serious accidents and high potential incidents with a view to preventing their recurrence;
   - Review the effectiveness of risk control measures, and take appropriate corrective and preventive action; and
   - Mitigate the potential adverse effects arising from residual risk.

This approach is in line with the Australian and New Zealand Standard *AS/NZS 4360:1999 Risk Management*.

CONSULTATION AND COOPERATION

The Act seeks to achieve cooperation between coal operators, mine management and coal workers to achieve the objects of the Act.

Cooperation is an important strategy in achieving the objects of the Act and is achieved at an industry level by:

   (i)   the establishment of the coal mining safety and health advisory committee
   (ii) the appointment of industry safety and health representatives

Cooperation is achieved at a coal mine level by:

   (i)   the election of site safety and health representatives; and
   (ii) the process of involving coal mine workers in the management of risk.

SAFETY AND HEALTH MANAGEMENT SYSTEMS

The CMSHA prescribes the requirements for the development of a safety and health management System. The CMSHR (Qld Govt, 2001) prescribe many of the components that must be included in the safety and health management system. The CMSHA has the force of legislation in that there is a requirement to comply with the procedures contained within.

It is the responsibility of the most senior officer employed by the operator who has responsibility for the mine Site Senior Executive (SSE) to develop the safety and health management system.

The safety and health management system must be:

- Be a documented and auditable system for implementing the organisations OHS policy
- Define the management structure necessary for safety and health
- Outline the processes and resources needed to manage the mine so that risk is at an *acceptable level*
- Deliver the strategy and plan to ensure that the mine is run safely
- Include principal hazard management plans and standard operating procedures;
- Contain a plan to regularly review and continually improve so that risk to persons at the coal mine is or *an acceptable level*; and
- Whenthere is a significant change to the coal mining operations of the coal mine—contain a plan to immediately review the safety and health management system so that risk to persons is at an acceptable level.

The prescribed structure of the safety and health management plan must be consistent with the Australian and New Zealand Standard AS/NZS 4804:2001 Occupational health and safety management systems.

Principal hazard management plans are developed to manage hazards that could result in multiple fatalities. The regulations prescribe the minimum principal hazard management plans that must be developed for underground coal mines.

These are;

- emergency response;
- gas management;
- methane drainage;
- mine ventilation;
- spontaneous combustion;
- strata control; and
- inrush management

Each principal hazard management plan outlines the preventive controls required to lower the possibility of an incident occurring, the monitoring controls to ensure the preventive controls are effective, first response procedures to mitigate the effects of an incident if the preventive controls should fail and emergency procedures to recover from an incident.

SELF-ESCAPE AND MINES RESCUE

Self-escape in the event of an emergency is a first response component of principal hazard management plans and is also prescribed under regulation.

An underground mine's safety and health management system must provide for the self-escape of persons from the mine, or a part of the mine, to a place of safety.

The system must be developed through a risk assessment that includes a consideration of at least the following matters;

- the location of devices for assisting self-escape;
- the number of devices, including self-rescuers, to be distributed throughout the mine;
- selecting and marking the location for reserve self-rescuers;
- the number and location of changeover stations and refuges;
- selecting and marking escape routes;
- communication equipment and ways of using the equipment;
- training persons in self-escape; and
- fitness of coal mine workers to enable self-escape.

It is a legislative requirement that an underground mine also has emergency response strategies for mines rescue services.

Mines rescue strategies must include a mines rescue agreement with the Queensland Mines Rescue Service. It must also include a system of providing mutual assistance to adjacent mines and be capable of being implemented whenever a person is underground.

The final legislative requirement is that underground coal mines must be capable of being safely sealed in the event of an emergency and provide for means to inertise the underground atmosphere in the event of an underground fire or explosion.

The Queensland Mines Rescue Service provides a jet engine that can introduce exhaust gasses into the mine to inertise the atmosphere.

COMPETENT MANAGEMENT AND TRAINING

There are a number of measures in the Queensland legislation to ensure competent management.

A Board of Examiners is established under the Act to examine and issue statutory certificates to certain statutory position holders. A written examination in Mining Safety Law is required followed by an oral examination to determine required technical knowledge to safely perform the function.

There is also a requirement that all supervisors have training in risk management.

Training schemes must be established for the workforce. Each person who performs work at a coal mine must be trained and assessed against a national competency standard.

DISCHARGE OF OBLIGATIONS

The Act provides for placing safety and health obligations on those persons whose decisions affect the safety and health of others. All coal mine workers or other persons at coal mines or persons who may affect safety and health at coal mines or as a result of coal mining operations, have safety and health obligations.

The following class of persons also have obligations under the legislation:

- a holder of the mineral tenure;
- a coal mine operator;
- a site senior executive;
- a contractor;
- a designer, manufacturer, importer or supplier of plant for use at a coal mine;
- an erector or installer of plant at a coal mine;
- a manufacturer, importer or supplier of substances for use at a coal mine; and
- a person who supplies a service at a coal mine.

There are three ways in which a person may discharge their safety and health management obligations;

1. If a regulation prescribes a way of achieving an acceptable level of risk, a person may discharge the person's safety and health obligation in relation to the risk only by following the prescribed way.
2. If a recognised standard states a way or ways of achieving an acceptable level of risk, a person discharges the person's safety and health obligation in relation to the risk only by:
    (a)   adopting and following a stated way; or
    (b)   adopting and following another way that achieves a level of risk that is equal to or better than the acceptable level.

3. If there is no regulation or recognised standard prescribing or stating a way to discharge the person's safety and health obligation in relation to a risk, the person may choose an appropriate way to discharge the person's safety and health obligation in relation to the risk.

However, the person discharges the person's safety and health obligation in relation to the risk only if the person takes reasonable precautions, and exercises proper diligence, to ensure the obligation is discharged

A recognised standard is made by the Minister and states ways to achieve an acceptable level of risk to persons arising out of coal mining operations.

The requirement for a person to take reasonable precautions and exercise proper diligence is fundamental to the concept of self-regulation using risk management principles.

INDUSTRY SAFETY AND HEALTH REPRESENTATIVES AND SITE SAFETY AND HEALTH REPRESENTATIVES

There are a number ways in which worker representation on safety and health matters is facilitated through the legislation. At an industry level, the union representing the majority of coal mine workers may elect, after ballot of their members, up to three persons to be Industry Safety and Health Representatives.

An Industry Safety and Health Representative has the following functions;

- to inspect coal mines to assess whether the level of risk to the safety and health of coal mine workers is at an acceptable level;
- to review procedures in place at coal mines to control the risk to safety and health of coal mine workers so that it is at an acceptable level;
- to detect unsafe practices and conditions at coal mines and to take action to ensure the risk to the safety and health of coal mine workers is at an acceptable level;
- to participate in investigations into serious accidents and high potential incidents and other matters related to safety or health at coal mines;
- to investigate complaints from coal mine workers regarding safety or health at coal mines; and
- to help in relation to initiatives to improve safety or health at coal mines.

The Industry safety and Health representative has considerable powers under the Act including the ability to suspend operations if he believes that there is an unacceptable level of risk.

At a site level coal mine workers at a coal mine may elect up to two of their number to be Site Safety and Health Representatives for the mine for the term decided by the coal mine workers.

The Site Safety and Health Representative for a coal mine has the following functions—

- to inspect the coal mine to assess whether the level of risk to coal mine workers is at an acceptable level;
- to review procedures in place at the coal mine to control the risk to coal mine workers so that it is at an acceptable level;
- to detect unsafe practices and conditions at the coal mine and to take action to ensure the risk to coal mine workers is at an acceptable level; and
- to investigate complaints from coal mine workers at the mine regarding safety or health.

THE ROLE OF THE REGULATOR

The Chief Executive appoints officers to be Mines Inspectors. Inspector's functions include;

- Inspecting, auditing and monitoring coal mines
- Investigating accidents
- Provide help, advice and assistance
- Ensure corrective actionis taken

- Investigate complaints and
- Issue directives and recommend prosecutions as necessary

Inspectors are highly experienced industry professionals with tertiary qualifications. They are also holders of statutory qualifications and are highly trained by the department.

The inspectors have considerable powers under the legislation to ensure that corrective actions are taken at mines to achieve an acceptable level of risk.

Where it is necessary for a compliance action to be taken against persons who have safety and health obligations under this Act, the department has developed a compliance policy to give guidance on the appropriate action.

The compliance policy recommends five possible levels of action from simply providing advice up to a prosecution under this legislation.

THE COAL MINING SAFETY AND HEALTH ADVISORY COMMITTEE

One of the objectives of the Act is to provide a way of monitoring the effectiveness and administration of provisions relating to safety and health under the Act and other mining legislation.

The Coal Mining Safety and Health Advisory Committee primary function is to give advice and to make recommendations to the Minister about promoting and protecting the safety and health of persons at coal mines. To achieve this, the committee must periodically review the effectiveness of the Act, regulations and recognised standards.

The committee is a tripartite arrangement appointed by the Minister and has representatives from Government, coal mine operators and industrial organisations representing coal mine workers.

As soon as practicable, but within 4 months, after the end of each financial year, a report must be prepared and given to the Minister outlining the committees operations for the year.

CONCLUSIONS

This paper has outlined how the risk based legislative framework is applied in Queensland to manage the risks at coal mines. The paper provides an overview and for the sake of brevity, has omitted some aspects of the legislative framework.

This Robens style legislation adopted after the Moura No. 2 disaster has led to a dramatic improvement in mine safety in the state. It has now been twenty years in Queensland since there has been a major underground disaster.

There still remain challenges however in ensuring that the current provisions are not diluted in the pursuit of cost savings in difficult economic times. It is also imperative that the lessons learnt from the past disasters that shaped this legislation are not forgotten by subsequent generations.

The Queensland legislative framework has been effective in assisting coal mine workers to return home safe and healthy every day.

REFERENCES

Report of the Committee 1970 -72, Chairman, Lord Robens, Cmnd. 5034 H.M.S.O, 1972a. *Safety and Health at Work* (Volume 1: London).
Wardens, I*, 1994. *Report on an Accident at Moura No.2 Underground Mine*, Sunday 7, AUGUST 1994.
Risk Management, Australian and New Zealand Standard, AS/NZS 4360:1999.
Occupational Health and Safety Management Systems, Australian and New Zealand Standard, AS/NZS 4804:2001.
Coal Mining Safety and Health, Act 1999. Queensland Government.
Coal Mining Safety and Health Regulations, 2001. Queensland Government.
Mining and Quarrying Safety and Health, Act 1999. Queensland Government.
Mining and Quarrying Safety and Health Regulations, 2001. Queensland Government.

MINING ENGINEERING: WHAT THEY DIDN'T TEACH YOU AT UNI!

Joe Clayton

INTRODUCTION

I understand this is a technical conference but I'm not a technical person. I was thrilled when Naj asked me to present a paper at my old alumni but I explained that it won't be full of technical detail.

I have been in mining now for 38 years. I started as a "Fed" underground and am now a CEO of a mining services business, the SubZero Group. I have been made redundant five times. I have lived in Wollongong, Singleton and Muswellbrook in the Hunter Valley, Collie in South West WA, Gunnedah in North West NSW, Lihir Island in PNG, Melbourne, Perth, Adelaide, the Central Coast of NSW and Sydney. My kids went to eight different schools. I have managed mining operations in all the mainland states of Australia, New Ireland Province PNG, South Kalimantan, East Kalimantan and North Sulawesi in Indonesia. I have directly reported to Chinese, Japanese, American, Malaysian, Indonesian, English and Australian bosses. The Chinese boss did not speak a word of English. Mining is not for the fainthearted.

THE EARLY DAYS

I was fortunate enough to do my degree all part time while working fulltime in an underground coal mine in Wollongong. I lived at North Beach and could ride my pushbike to work at Kemira Colliery, half way up Mt Kiera Road, and to Uni. Where else in the world can someone do that? Then I was silly enough to move away to Collie in WA when I finished Uni!!

I worked in Kemira as a "Fed" for 4 years and worked on every shift in every panel in an AIS Collieries cadetship. A fantastic grounding in dealing with shiftwork and people. It is so important that mining engineers understand the impact of their decisions on the workforce and the only real way to achieve that understanding is to spend time working on shift and operating equipment. It should be compulsory. Kemira still had a pit pony in 1976 and one of my first jobs was to build a stable underground while working in "Cocky's" outbye crew. A significant part of the old Coal Mines Regulation Act 1912 was devoted to management of horses underground. When the stable was completed a Mines Inspector came underground and carried out air speed and volume tests for the stable and decreed it did not meet the regulations and had to be removed. So we took the stable out and installed a crib room for the workers in the exact same spot. The same Mines Inspector came underground and passed it! Not good enough for a horse but suitable for men. I knew at that point I was in an interesting industry.

In those days man management was a skill passed down from the Undermanagers to the trainees and Deputies. I remember my Undermanager In Charge, Ron Peace, saying to me one day "We have set up a little test for you and will discuss how you handle it afterwards. Not telling you any more detail but you will know when it happens." As it turned out they set up a demarcation issue underground with the crew I was working with and the Union Delegate, who shall remain nameless, got pretty irate about what happened. I sorted out a mutually agreed solution which got the union delegate even angrier. At shift end he challenged me in the bath house to sort it out in the carpark. I kept a cool head and convinced him he was older than me and may not be up to it but also that we would both be throwing away our jobs over such a relatively minor incident. I was known at the time as being pretty volatile on the rugby field and wasn't used to taking a backward step. But this was work and was different. Ronny was very pleased with the outcome. The issue being, I could have thrown away my job and Ron was prepared to let me do that in the course of allowing me a great life lesson. Where does that happen in industry now? Are you prepared to allow your staff to grow in that way?

When I was 22 and a new father we had a fall in the main travelling road to the panel in which I was working. To recover the fall people would scramble up on the top of the fall and roof bolt the newly exposed roof then remove the fall material. We did all the tests for 'Baggy" roof and it appeared all was safe but, while passing equipment up to two operators on top of the fall, the lip gave way and buried me leaving, luckily, only my head exposed. Also luckily we were in a seam that had a coal roof. If it was rock

Interim CEO and Excutive director, SubZero group limited, E-mail: jclayton@subzeroservices.com.au. Tel: +61 437763477

I don't think I would have survived the initial impact. All the tools were buried so the crew scratched me out by hand and had Entonox ready for pain relief. To everyone's astonishment I got up and walked away. The Deputy sent me back to the crib room to have a cup of coffee to which I protested loudly that I was fine and should keep working. He insisted. I made a coffee and when I went to drink my hand started trembling so much I couldn't keep the coffee in the cup. Shock had set in and the Deputy knew it would happen.

This episode made me seriously reconsider a career in mining. Over a week I did a lot of soul searching about where I wanted to go in life. I realized mining was really all about people, being able to operate in teams to overcome extreme, at times dangerous, work challenges. It is personally extremely rewarding. It builds life long bonds. It is the closest I have come to the camaraderie of a winning rugby team! Hence I am still in the game.

I stayed in for the people issues and the different experiences I would not have had in a conventional office job. This is an eclectic collection of those experiences.

ETHNICITY

I am often asked the difference between Japanese and Chinese management.

Japanese senior management admit they like bottom up management so they don't have to make, or take responsibility, for any critical decisions. As an example, I needed a new fleet of 300 tonne excavators. I carried out a review of all excavators on the market in that class, short listed three brands, completed a detailed suitability review of each for capital and operating costs, selected one brand and negotiated terms. I did a paper to my boss explaining the process and the reason for the selection. The report recommendation stated an order would be placed in two weeks' time and if he was not happy with the recommendation he should inform me before the order was placed. I did not hear from him and placed the order and the payments were approved.

Whereas the Chinese do things by "consensus". The Chinese version of consensus is the boss is always right and do what you think he wants.

I was running an exploration program for a Chinese company and had to select a project management group to run the program. An Owner's Selection Team of eight people were appointed, five of whom were non-English speaking Chinese who had no idea what an exploration program entailed. We mutually agreed a set of weighted criteria for the selection. Of course, as with everything Chinese, the cost was the heaviest weighted criteria so basically the best price would win anyway. After five proponents were short listed and presented to the selection panel (with everything translated) two proponents were shortlisted. The final hurdle was a request for each proponent to take 20% out of their costs to win the work. One of the proponents said they could not work in the circumstances and pulled out of the race. All respect. Five people on the panel were astounded and three people completely understood. The company that won the contract was basically endorsed by Beijing Head Office and the local Chinese staff did everything in their power to appoint that company even though that company had never previously managed an exploration program. The result was an inordinately overpriced and problematic exploration program. The Project Management Company was cheap but, due to their lack of acumen in the field, they allowed cost and time over runs in all areas of the project.

Another good example of ethnicity is the difference between Australian and Indonesian equipment operators.

In Australia where you have a less experienced dozer operator the best way to lift his productivity is to put him alongside an experienced operator. The less experienced operator will do everything he can to lift his performance to the level of the experienced operator. A natural competitive Australian instinct.

Do the same thing in Indonesia and the experienced operator will slow down to match the less experienced operator because he doesn't want the other person to "lose face". It is based around the Muslim/Indonesian culture of respecting everyone and not standing out from the pack.

I was working for an Australian Contractor in Indonesia. The company put in place a new MD who wanted to rebrand the company and called the program "We Make a Difference". At my weekly senior staff meeting I talked about the program and suggested we could get some caps made up with the slogan in Indonesian and select an employee of the week to be awarded a cap. I was reasonably new in

Indonesia at the time and didn't yet speak Bahasa so I asked them to translate "I Make a Difference". A raging argument ensued. Eventually I asked the supervisor with the best English what was going on. He explained that in Indonesian culture people didn't want to stand out and they called people who did a very derogatory term that roughly translated in English to "You are different". He said I was proposing to select the best operator for the week and make him were a hat that proclaimed "I am a Dickhead". Everyone at the table dissolved in laughter and the campaign was dropped on the minesite.

The campaign continued at the corporate level with every staff member receiving a multimedia DVD with an upmarket roll out of the new slogan and campaign in both English and Bahasa Indonesian. At that time half the workforce of the company, 2,000 people, were Indonesian. Surely the translator for the DVD would have alerted the production team to the problem? Such a waste of resources and energy.

I am lead to believe I broke a long held taboo and employed the first female operator in PNG. After a few months in the role she started losing a lot of time so I asked the human resource manager to sort it out. He asked me to attend the counselling session as I might not believe him when he explained the reason for her losing time. The operator told us straight faced that a witch doctor had been paid to put a hex on her by some jealous male operators. The hex made her very tired and she couldn't even accept food from her mother in case it had been hexed. When quizzed on what she was doing about it she had hired her own witch doctor to remove the hex but no-one could know as someone may hire another witch doctor to re-apply the hex. She committed that she would be hex free in a further 10 days. Sure enough she was in fact back in full swing in ten days.

The human resource manager was a national trained at university. He told me that all PNG nationals believed in witch doctors which made them real! Self-fulfilling prophets!

CAMBERWELL COAL

My first role as Mine Manager was at Camberwell Coal in the Hunter Valley in 1990. Camberwell was the first mine constructed since the early eighties rush of coal mine construction. It was the first mine in the Hunter to have only one union, no seniority, pay by the number of skills not by the size of the equipment and eight and a half hour shifts. It was a break through operation with no seniority or demarcation. We trained operators and tradesmen in Targeted Selection and included them on employment selection panels, a first for the industry. We completed a full week induction for all employees and filled them full of management theory. In my previous roles I had found that workers didn't understand management "speak". To counteract this we taught the operators and tradesmen management theory and carried out role plays so they would understand what it was like to be a boss and to understand the pressures on their supervisors. We put the operators first by inverting the traditional organisation chart. The senior managers were at the bottom called the "Foundation Team". The supervisors were in the middle and called the "Support Team". Operators and tradesmen were on top and called the "Winning Team". The new approach was based on sound human resource principles of the two factory theory of Frederick Herzberg, Theory Z of Abraham Maslow, the ABC of Management by Elliott Jaques and Socio-Technical Systems of Fred Emery. Have any of you heard of these?

Camberwell had an "Open Store" without storemen. Anyone could enter the store and everyone was trained to book out stores stock to maintain inventory levels. Prior to the mine opening a pallet of port was in the store for two weeks and not one bottle was stolen.

We called our system "The Camberwell Way". In the first year of operation we were the lowest cost operator in the Hunter and won the Sentinels of Safety Award. My time at Camberwell is one of the highlights of my career. I still bump into people I worked with at Camberwell and invariably it is like catching up with family. No matter how long it has been we are immediately in tune. That is the magic of treating people like adults, setting the right work culture and entrusting people to do the right thing.

LIHIR GOLD MINE

Lihir Gold Mine would be the most unique open cut mining operation in the world. The mine is in a dormant caldera. Not extinct just dormant! This produces ground temperatures of 150^0C, noxious gas outbursts, boiling groundwater and old exploration drill holes producing geysers spewing Sulphuric Acid 50 metres into the air. On top of this 1998 produced over six metres of rain. This was the start of the mine so we were mining the soft leached oxides so there was no rock for road building. The island had plenty of suspended coral material which we used to build the roads. Coronus material is thixotropic so it

sets like concrete if let alone after being compacted into a road surface. But when driven on straight away it will never set.

We had an indigenous workforce of four hundred and fifty with about twenty expatriate staff/management. Fifty percent of the workforce were local Lihirians who had never operated mining equipment and many had never driven a car. We taught them to operate one hundred and fifty tonne trucks.

The stop work

In my first month we had to retrench some troublesome souls and after setting it up with meticulous planning it all turned to trouble. I had a stop work meeting and about 300 Nationals in the meeting area at the mine looking for trouble. After 4 hours of talking, night shift drifted off to bed so I knew we were starting to get on top. An hour later day shift drifted off to work. We were left with a core of people who were being retrenched. I had a pay office there doling out the payout cash and people gradually started to take the money and leave. I was left with the last, and most emotional, 3 Nationals. Eventually they succumbed and took the money but had to be transported to the airfield 20 minutes away where an airplane was on standby to fly them back to Moresby. All Nationals have bush knives which are two foot long machetes with which they can inflict a lot of damage. They were leaving the island so they had all their possessions including their bush knives! I felt I couldn't delegate the risk to anyone else so I drove them to the airport myself. Immediately they were in the car I asked them all about their families and got them talking about their kids and their villages and told them all about my family and where I grew up. I kept them talking for the full twenty minutes all of which I could feel the sensation of a bush knife coming through the back of my seat and skewering me. One of the longest twenty minutes in my life! But at the airport they embraced me like an old buddy, said goodbye, got on the plane and I never saw them again.

The strike

About six months into the role we had a project defining three week strike over an Expat being belittling of the same hexed female National operator in the story above. The workforce took over the mining camp as their stronghold and built a road block between the town and the mine and manned it and threatened to defend it with Molotov cocktails. Helicopters were hired to fly people over the roadblocks to work so the staff could keep the ROM crusher in work. Ten mercenaries were hired through the local police sergeant and I had them on a one minute alert on my two way. They were only a deterrent and never to be used. They cruised around in a blacked out police troop carrier so people knew they were in town.

Three weeks into the strike a meeting was called at the local Landowners' Group compound. The compound was U-shaped with tiered seating on one side the back of which opened onto a grass lawn that ran about 20 m back to a backdrop of dense jungle. The other two sides contained offices which included a barred window pay office. All my expats were looking extremely twitchy and nervous so I went to the meeting on my own. On arrival no-one was in sight but over 15 minutes about 250 people melted out of the jungle and filled up the seating with not a word spoken. It was absolutely awesome to witness. The meeting commenced and I was supported by about six senior National staff who were standing with me. During the proceedings a young sizable National got very agitated and started down the stairs next to seating while threatening me. My adrenalin started pumping and I was asking myself "If I hit him I will get wiped out and if I don't hit him he will clobber me". But he lost his footing and started to stagger into me, arms akimbo, so I just chested him off and he fell backwards onto the floor at which stage two of the senior Nationals got stuck into him, then half a dozen of the other nationals got stuck into them. The place just erupted. My senior Nationals surrounded me and managed to get us into the barred window pay office and locked the door and we had a window seat for the mayhem that was playing out in front of us. The Police Sergeant was screaming down the two way "Clayton do you need the guns?" and I was screaming back "No I am safe don't let them out of the troopy!" Eventually I made it to safe ground. My Expat staff couldn't believe I didn't have a scratch on me. They were standing about five hundred metres back up a hill looking into the meeting and saw the whole drama unfold and thought I was gone for sure.

That meeting actually ended the strike. We met again two days later at the same place and signed a mutual agreement to end the strike. It was like a football grand final. Everyone cheered and clapped and every worker stood in line and shook my hand. Over the next 12 months we increased the truck fleet productivity by 38%. Once sorted the workforce became extremely loyal and worked with me to improve the mining.

INDONESIA

Papua New Guinea is a soft landing for a first time Expat. Australia ruled PNG until 1975 and the locals remember that as a very prosperous time as they like and respect Australians. PNG has the same court systems, school systems, government institutions and banks as Australia. Indonesia has none of that and they dislike upstart Expats telling them what to do.

Java Man roamed Indonesia over a million years ago. Early Indonesians cultivated rice at 800BC and traded with India and China at 300BC. The Majapahit Dynasty ruled Java and were the first to beat Kubla Khan's army in the Thirteenth Century. Indonesians began trading with Europeans in 1512. They have a long proud history and do not take kindly to brash Australian engineers lauding it over their people. They are an industrious and complicated people who deserve respect and consideration.

Illegal miners

The first mine I managed had an illegal miner problem. Within five kilometres of strike length ahead of the opencut mining operations there were 32 illegal 20 t and 30 t excavators stealing our subcrop coal. A security post at the main intersection with the highway and the mine access road counted the number of 8 t road truckloads of illegal coal hailed each day. Some days they hauled more coal than the mine. An illegal barge loading port was upstream of the mine's port. The illegals only used one tug to tow the coal barges (to our two) so routinely became stuck on the ever moving river delta at the mouth of the tidal river. We had to hire a third barge to tow the illegal barges off the river delta so we could get our coal through!

The line of demarcation between our mining operations and the illegal operations manned by our mercenaries, named Brimob, who were paramilitary hired through the regional General. The line consisted of ATCO huts, lighting plants and armed security 24/7. This was during the East Timor crisis and the mercenaries used to joke that the government hired them to shoot at Aussies in the jungles of Timor while Aussies hired them for protection in the jungles of Kalimantan! No problem. They worked for whoever paid and rotated between roles!

Every three months we would bring police from Jakarta to impound the illegal excavators in a police station three hours away by road. It would take the illegals two or three days to bribe the impounding police at the station and regain their equipment. In that time we would move the lighting plants, ATCO huts and guns a kilometre up strike and reclaim part of our mine before the illegal excavators moved back to site.

This was a contract operation and the illegal activity actually completely changed the mine plans on which the contract was costed. Because the illegals were dozing back overburden from on top of the subcrop coal then took the coal we had to move the same dirt but mined less coal. This accelerated the mining rate along the strike length to maintain the coal schedule which created a thinner operating pit and a longer waste haul. The main haulroad to the port was a regional logging road shared by us and the illegals. The local town residents would not let the illegals haul during the day to keep the dust down because the illegal port was on the other side of town. So at 8pm each night we would have 40 illegal haul trucks entering the haul road all at once and stopping us getting on the road for half an hour or more. We also had to maintain the haulroad. Haulroad maintenance is based on the number of axle loads. Higher axle loads, higher maintenance. To make our trucks run efficiently with good haulroads, the illegals were also running more efficiently and we were paying for it!

It is the one and only time I submitted a variation claim on a contract for illegal mining.

Swamp mining

At another operation in Indonesia we mined coal less than 20 metres of mud in a swamp, below sea level on a small island with 3.5 metres of annual rainfall. Below the mud was 10 metres of rock which we treated like gold. Without this we could not operate. Large cells were built out of the rock in mined out areas of the pit adjacent to the operating face to create a two truck haul to the nearest edge of the cell to dump loads of mud. Long hauls to the far side of the cell were not necessary because the mud simply ran there and saved us haul trucks. It turned out to be a very low cost operation but quite complex waste haulage scheduling. The rehabilitation plan entailed allowing the rehabbed waste area to be inundated by the ocean. Areas were built up above the water level for birds to roost. A unique part of this operation

was building a coal haul road with a water buffalo underpass! Also a ten foot python was caught behind the workshop.

COMMUNITY RELATIONS

This has taken many guises. In Indonesia the locals struggled to accept Expats drinking alcohol in the camps. To compensate I implemented a fifty cents darg per beer. When enough money was collected we would by equipment for the local orphanages. Every regional town in Indonesia has at least one orphanage. We made sure it was a media event so the locals knew we were helping. It allowed us to build relationships with the wonderful, selfless people who managed these institutions.

In North Sulawesi I convinced the local Bupati (Mayor) to donate rice paddies to the two local orphanages and we hired people to teach the kids how to grow their own rice and to grow pepper on the walls of paddies as a cash crop. It underpinned the independence of the orphanage from relying on donations as well it gave the kids life skills and self-respect.

Recently in Australia I was involved with a similar exercise but on a much bigger scale. In Gunnedah I had a Community Donation budget of $1,000,000 per year for five years. We advertised for Community Fund Committee volunteers. Over sixty people applied and we chose ten people from a cross section of the whole community. I stepped back from the process leaving our Stakeholder Manager to facilitate the group. A Charter was developed by the Committee and advertisements were placed for community groups to apply for funding. In the first year over one hundred applications were received. The committee members then ranked these applications individually then came together and agreed a consensus ranking of the projects. The first fifteen projects managed to gain funding.

This was the community telling the mining company where the community funding was best needed. It wasn't wasted on football jumpers or pressure from council for projects. The community groups put together budgets, funding applications that sold their dream to achieve success and then managed their projects. They went from lamington drives and dreams to self-empowered reality. Strong resilient communities can be built on the back of the transitory mining industry.

CONCLUSION

The mining industry can throw up some extraordinary and unique challenges. My challenges pale into insignificance with the great mining engineering and social feats achieved throughout the world. But they were my challenges. When some of the old buggers who have worked in these situations get that far away look in their eyes I hope I have given you a glimpse behind their thoughts.

There are people here yet to have their epiphanies and make the world a better place through their considered application of mining engineering. When that has played out for you, I hope you too get the opportunity to come back here and ramble on to the next generation.
Thank you for this wonderful opportunity.

Estimation of Uniaxial Compressive Strength of Coal Measures of Pranhita-Godavari Valley, India Using Sonic Logs

Makesh Shanmukha Rao[1], Gudlavalleti Uday Bhaskar[2] and Shivakumar Karekal[3]

ABSTRACT: The Singareni Collieries Company Limited (SCCL) carries out exploration and exploitation of coal deposits of Early Permian Barakar Formation in the 350km long NNW-SSE trending Pranhita Godavari Valley located in the state of Telangana, India. Empirical studies undertaken by SCCL established an exponential relationship between Vp obtained from sonic logs and UCS determined on core samples of sandstones of from all parts of Godavari Valley. Polynomial and exponential relationships are also established between Vp and Tensile Strength (TS) and Vp and Young's Modulus (E) respectively. The empirical relationships can give a major opportunity to understand the implications of regional and local geological and geotechnical conditions on planning and managing various types of mines.

INTRODUCTION

The uniaxial unconfined compressive strength (UCS) is an important mechanical property of the rock mass having several implications in planning and designing both underground and opencast coal mines. UCS is usually determined on core samples obtained from exploratory boreholes and tested either in the field or preferably in the laboratory. McNally (1987 and 1990) has the unique distinction of establishing empirical relationships between compressional wave velocity (Vp) obtained from sonic logs and UCS determined on core samples collected from various coal mines in Australia. These studies paved the way towards generating a continuous strength profile of the interburden strata between coal seams using Vp-UCS relationships. Turvey and Hanna (1998) highlighted the importance of UCS predicted from Vp logs to evaluate the immediate roof and floor conditions of longwall mines to determine roof bolting requirements. These studies help improve productivity in difficult geomining conditions and evaluating blasting requirements and rippability in open cast mines. Studies by Payne and Ward (2002), Payne (2008) carried out at Crinum mine; Australia delineated roof strata into geomechanical units along the main gate sections which helped define mining conditions and roof support requirements. Hatherly *et al.*, (2001, 2004), Gordon (2002), Hoelle (2004) and Stam *et al.,* (2012) extended the studies to various coalfields of Australia. Hatherly (2013) reviewed the Vp-UCS empirical studies made by several workers in Australia and USA and concluded that site specific empirical estimates of Vp-UCS are established all over Australia and extensively used in all types of coal mining. Butel *et al.,* (2014) have further improved Vp-UCS correlations at Hunter Valley, Australia. Pell *et al.,* (2014) have extended the Vp-UCS empirical studies to the coalfields of New South Wales and Queensland, Australia. Vp derived UCS contour maps can be created for use in a number of important mine planning and design applications. The Vp obtained from sonic logs are therefore a very important and even a key component of roof control in underground coal mines of Australia. The experiences and benefits gained by the Australian coal mining industry clearly document a great need to extend sonic logging to other coal basins of the world to make mining safer and more productive.

FIELD STUDIES

A similar uptake of geophysical logging was made by Singareni Collieries Company Limited (SCCL) a state owned public sector carrying out detail exploration and extraction of coals of Early Permian Barakar Formation of Godavari Valley located in the state of Telangana, India (Figure 1).

SCCL introduced tri-receiver Full Waveform Sonic (FWS) logging in 2007 to obtain the complete geotechnical spectrum of the interburden strata of coals and complement the testing of core samples

[1] *Superintending Geophysicist, Exploration Division, The Singareni Collieries Co Ltd, Kothagudem, India 507 101, E-mail: ms_rao_gp@yahoo.com*
[2] *Deputy General Manager (Geophysics), E-mail: uday_bhaskar_g@yahoo.com*
[3] *Energy Flagship, CSIRO, E-mail: Shivakumar.Karekal@csiro.au*

and laboratory studies. SCCL has so far carried out sonic logging in about 600 closely spaced boreholes of various exploration blocks of Godavari Valley. UCS and TS determined on core samples of 10 boreholes and YM determined on core samples of four boreholes were empirically related to Vp obtained from sonic logs.
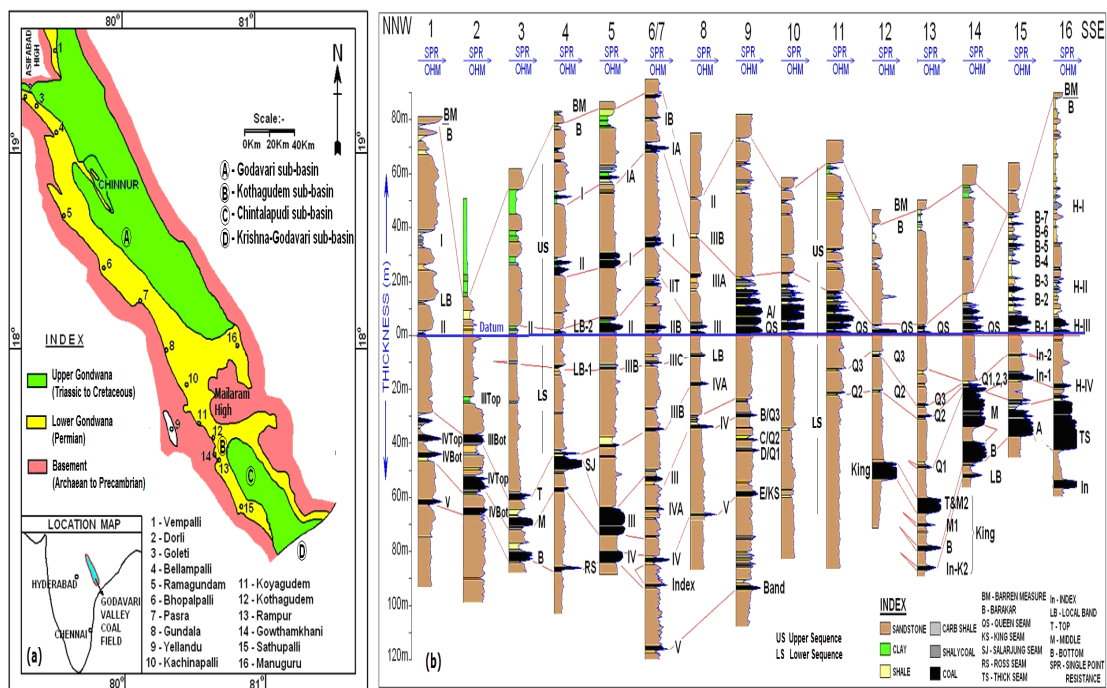
Figure 1: (a) Outline of Pranhita-Godavari Valley, (b) Nomenclature and Correlation of Coals. Queen Seam (QS) is the datum of section (locations in Figure 1, modified after Uday Bhaskar *et al.*, 2002 and 2011)

The empirical equations thus developed were further successfully tested using the subsequently generated UCS and TS values of core samples of about forty boreholes from different coal exploratory blocks of Godavari Valley. Empirical relationships established between Vp from sonic logs and UCS, TS and YM provided bed-wise geotechnical characteristics of interburden strata. The procedures followed to derive the empirical equations to estimate geotechnical properties from Vp are discussed in the following pages.

SCCL uses a tri-receiver full waveform sonic probe made by M/s Robertson Geologging, UK to generate the elastic wave velocities. This probe consists of a piezoelectric transmitter operating at 23 kHz and firing at approximately 2ms intervals. Data is received at 4µs interval by the three receivers located 20 cm apart along the body of the logging tool. The distance between the first receiver and the transmitter is 60 cm. The probe records the full sonic wave-train at all receivers simultaneously.   The source/receiver pair distance is sufficiently large to ensure that first arrivals are waves refracted along the borehole walls, rather than direct rays. A water or mud-filled (and uncased) hole is required to ensure adequate acoustic coupling. Two centralizers are used to ensure the vertical movement of the probe. Propagation of sonic waves through coal measures and determination of UCS are extensively reviewed by Oyler *et al.,* (2008), Stam *et al.,* (2012) and Butel *et al.,* (2014)

WellCAD software is used to interpret the sonic data. Data from three receivers are processed to pick up the arrival times of compressional (DTP), shear (DTS) and Stoneley (DTSTN) waves through velocity/semblance analysis which are shown as dark and thick black stripes in Figure 2.

Arrival times are converted into the respective Vp, Vs and Vstn wave velocities, which are in turn compared with acoustic mean amplitude (AMA), single point resistance (SPR), neutron (NEUT), density (DENS), natural gamma (NGAM), short normal resistivity (SNR), self potential (SP)), caliper (CALP) logs. Such an approach improves the reliability of depth estimates and geological interpretation of geophysical logs. The compressional wave velocities (Vp) obtained from the tri-receiver full waveform sonic probe (FWS) is used to empirically estimate UCS and TS of sandstones. Figure 2 also shows the comparison between geotechnical properties estimated from Vp logs and those determined on core

samples at laboratories. UCS_VP, TS_VP and YM_VP are the uniaxial compressive strength, tensile strength and Young's Moduls estimated from Vp logs respectively. UCS_SCC, TS_SCC are UCS and TS determined on core samples at SCCL laboratory respectively. UCS_CMRI and YM_CMRI are UCS and YM determined on core samples at the Central Institute of Mining and Fuel Research of India, Dhanbad, India.
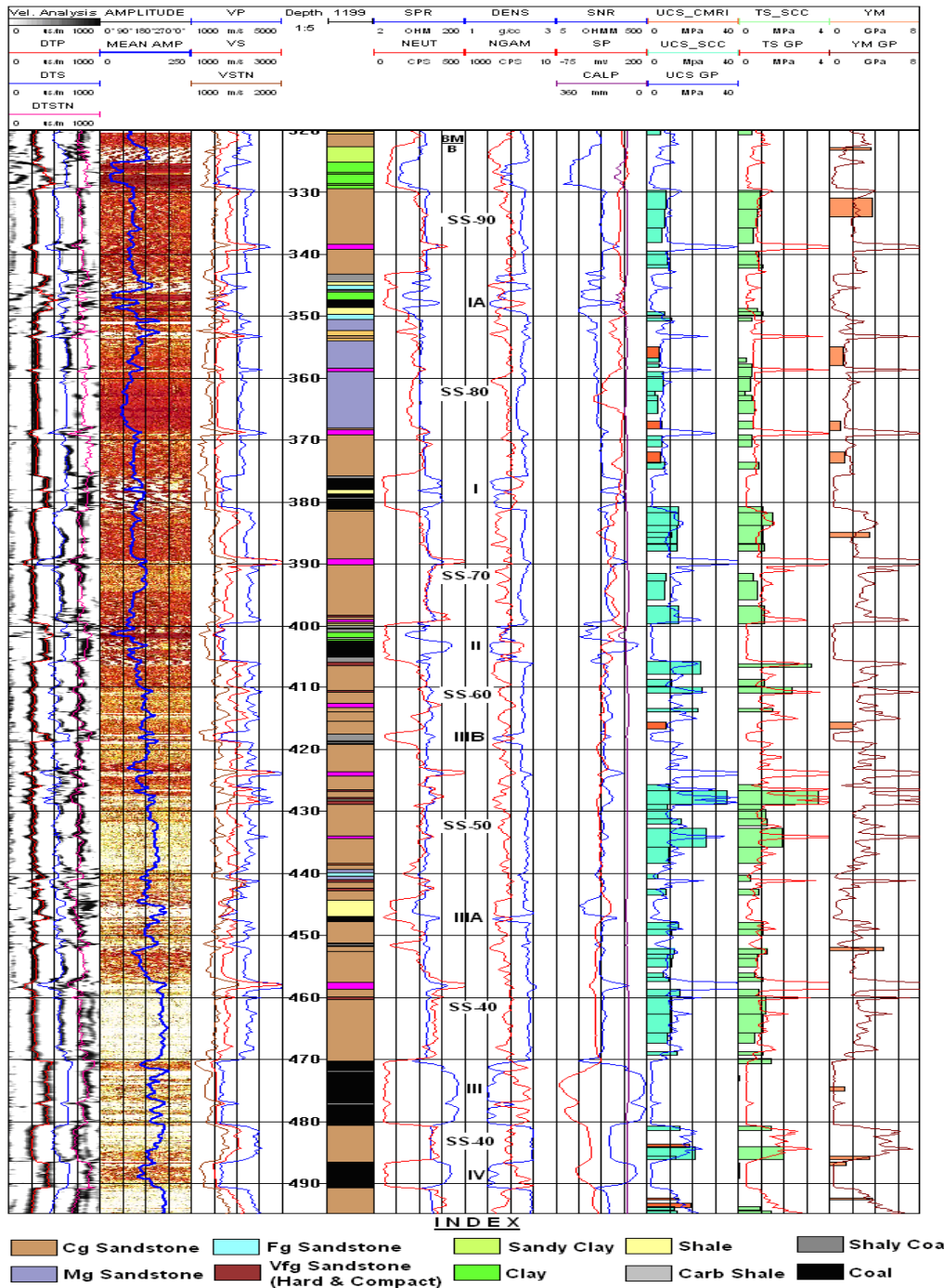
Figure 2: Interpretation of Lithologies and Geotechnical properties of Barakar Formation using Geophysical Logs, Borehole RG-1199, Adriyala Longwall Block, Ramagundam area

The empirical studies relating Vp of sonic logs and laboratory determined geotechnical properties were initiated using the data of Adriyala longwall block, Ramagundam (Figure 3). The coal-bearing Barakar Formation of Adriyala longwall block shown in Figure 2 is about 170m thick and contains seven correlatable coals. The Seam-II resolves the Barakar into lower and upper sequences. The lower sequence is mostly made up of well sorted, compact fine to coarse grained quartzose sandstones with cement. The Vp of sandstones of lower sequence is around 3750 m/s to 4000 m/s. The grey to greyish

white sandstones of upper sequence is mostly very coarse to pebbly, porous and friable whose Vp varies from 3000m/s to 3500 m/s. SS-80 and SS-30 constituting the overburden of Seam-IA and Seam-IV respectively have minimum and maximum Vp of 3000m/s and 4000 m/s respectively. The interburden strata of coals also contain 1m to 2 m thick very fine grained sandstones which are very hard, compact and silicified whose Vp varies from 4500 m/s to 6500 m/s. The determination of UCS of these sandstones is difficult because they are usually fractured and not intact.

McNally (1990) and Oyler *et al.,* (2008) concluded that the correlation of Vp of sonic logs and UCS determined on core samples depends on how well the depths and thicknesses obtained from core and geophysical logs tally with each other. They framed broad guidelines and procedures to improve the correlation between Vp and core data which are followed in the present study. Sonic data is initially correlated with geophysical logs followed by core data (Figure 2). The determination of UCS and TS on core samples was carried out by SCCL at its own laboratories. UCS and YM are also determined at Central Institute of Mines and Fuel Research of India (CIMFRI). Vp values were selected from homogenous zones of thickness greater than twice the sonic tool receiver spacing. The core samples falling close to the Vp values were selected for laboratory testing. The average of three test values of UCS, TS and YM were considered.

GEOLOGICAL SETTING

The Pranhita-Godavari Valley is a major north-northwest-south-southeast trending belt on the Precambrian platform extending over 470km in strike length from Eluru on the east coast of Andhra Pradesh in the southeast of India through the State of Telangana   in the central parts   to Boregaon of Maharashtra in the northwest (Figure 1). It is the largest single Gondwana basin belt of 'Crevice' type of platform rift zone containing 4,000 m to 5,000 m fluviatile sediments of Early Permian to Early Cretaceous (Ramana Murty and Parthasarathy, 1988). The major southeast part of the valley lying in the States of Telangana and Andhra Pradesh, India is called the Pranhita-Godavari Valley and the northwest part falling in the State of Maharashtra is called the Wardha Valley. The Godavari Valley having a strike length of 350km covers an area of about 17,000sq. km whose stratigraphic succession is provided by King (1881), Raja Rao (1982), Raiverman *et al.,* (1985), Ramana Murty and Madhusudan Rao (1996) and Lakshminarayana (1996). Based on geological and geophysical data the valley is divided into four sub-basins from north to south as Godavari, Kothagudem, Chintalpudi located in Telangana and Krishna-Godavari located in Andhra Pradesh (Raja Rao, 1982; Ramana Murty and Parthsarathy, 1988) (Fig. 1a). 'Mailaram High' disposed transverse (northeast-southwest) and located in the southcentral parts of the valley is a major tectonised zone of basement rocks of Middle/Upper Proterozoic Pakhal and older gneissose group and was uplifted during the Early Jurassic (Lakshminarayana, 1996). Asifabad High' is another such tectonised zone located in the northcentral parts of the valley.

In this valley, the potential coal deposits occur essentially in the Early Permian Barakar Formation and partly in the Late Permian Lower Kamthi/Raniganj Formation. These are separated by 100 m to 500 m thick non coal-bearing strata of the Barren Measure Formation mostly made up of medium to coarse grained sandstone and shales/clay. The Barakar is resting conformably over the Talchir Formation along the western margin of the valley and at a few places on the eastern margin.   Structural disturbances resulted in the occurrence of Barakar in different pockets or coalbelts/coalfields. The Barakar of 250-300 m thickness is divisible into the Lower and Upper Members. The 70 m to 120 m thick Lower Member (Basal Barakar) is devoid of coal seams and consists of medium to coarse grained sandstones with lenses of conglomerates and a few shale bands. The Upper Member (coal bearing) has a maximum thickness of 200m and exhibits a cyclic repetition of sandstone, shale and coal seams (Ramana Murty and Madhusudan Rao, 1996). Workable coal seams of two metres to 30 m thickness vary in number from two to eight and on an average three to four seams occur in the sub-basins.

Rao *et al.,* (1989, 1992 & 1996) applied single point resistance and gamma logs to identify and correlate coal seams of Godavari Valley and detect geological faults within the sedimentary strata. Rao *et al.,* (1996), Uday Bhaskar (2006) and Uday Bhaskar *et al.,* (2002 & 2011) resolved the Upper Barakar into Lower and Upper sequences and established regional extent and correlation of coals from one sub-basin to the other of the valley (Figure 1b). The lower set of coals coalesce at selective portions of the valley to form major composite seams locally known as combined Ross-Salarjung-IIIA, combined IV-III-IIIA and Thick Seam and King Seam at Belampalli, Ramagundam, Manuguru and and Kothagudem respectively. The top set of coals is locally by different names including Seam-II, LB, I, IA. These coals exist as independent entities in northern parts of Godavari sub-basin and coalesce at the southern parts of Godavari where the seam is referred to as Queen Seam (QS) and extends further south into Kothagudem and Chintalpudi sub-basins (Uday Bhaskar *et al.,* 2011).

UNIAXIAL COMPRESSIVE STRENGTH (UCS)

Uniaxial Compressive strength (UCS) of an intact rock sample is the amount of compressive force per unit area in a single direction required to induce failure (Figure 3). It is obtained by dividing the compressive load at failure by the cross sectional area of the sample. UCS measurements were carried out as per IS norms IS: 9143-1979 by Central Institute of Mining and Fuel Research of India (CMFRI) and also by SCCL. According to the norms the length to diameter ratio of the intact cylindrical rock sample was maintained two and compressed parallel to the longitudinal axis. The UCS of the specimen in dry condition was calculated by dividing the maximum load by original cross-sectional area. Young's Modulus of the sample was also measured simultaneously during UCS tests.

UCS (MPa) = P/A

where, P is Compressive Load at Failure (kN) and A is cross sectional area (mm) of the rock sample.
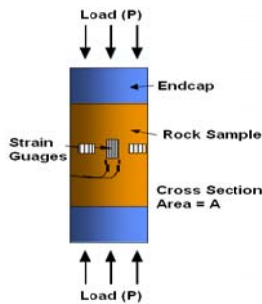
Figure 3: Schematic diagram showing test setup for measuring UCS

Empirical studies initiated with 58 data samples from four boreholes drilled at the Adriyala mine produced an exponential strength relationship which is shown in Figure 4a.

$$UCS\_ADR = 0.0429e^{0.0016Vp} \qquad R^2 = 0.82 \qquad\qquad (1)$$

where UCS is in MPa and Vp in m/s.

Equation (1) was developed during the year 2007.
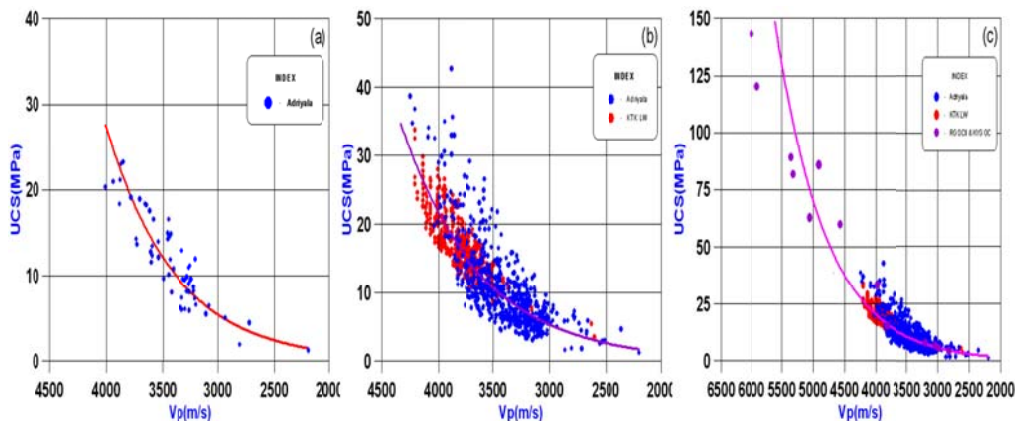
Figure 4: Exponential Curve showing the relation between log determined Vp and laboratory determined UCS values of (a) Adriyala mine of Ramagundam (b) Adriyala of Ramagundam and Kakatiyakhani longwall block of Bhopalpalli (c) Adriyala, Kakatiyakhani and high strength sandstones of Opencast-II of Ramagundam and Koyagudem blocks

Equation (1) when applied to the Adriyala boreholes produced UCS values similar to laboratory determined UCS values for Vp of 3000 m/s to 4000 m/s however log derived UCS values are very greater than the laboratory determined UCS values for Vp of 4000 m/s to 6000 m/s (see circles in Figure 5). It was therefore concluded that the empirical relationship could be improved by considering the Vp-UCS data of wider range of test data from various mining blocks.
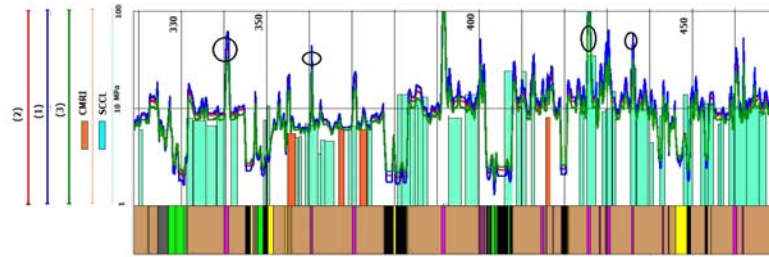
Figure 5: Comparison of Laboratory determined UCS and UCS obtained by different equations (1), (2) and (3), Borehole RG-1199 (Index in Figure 2)

Studies continued by considering 1005 data points of Kakatiyakhani and Adriyala longwall blocks of Bhopalpalli and Ramagundam areas mines respectively (Figure 4b). This combined data set produced the exponential relationship:

$$UCS\_ADRKTK = 0.0798e^{0.0014Vp} \qquad R^2 = 0.72 \qquad (2)$$

where UCS is in MPa and Vp in m/s.

Equation (2) was developed in the year 2010 (Figure 3b).

Equation (1)   and (2) when tested produced UCS values similar to laboratory determined UCS values for Vp of 3000 m/s to 4000 m/s (Figure 5). Equation (2) is close to the laboratory determined UCS values for Vp of 4000 m/s to 6000 m/s but the UCS was still greater than laboratory determined UCS values overall. Studies were continued by generating some more data of Vp of 4000 m/s to 6000 m/s from the Opencast-II of Ramagundam and Koyagudem mining blocks to produce the following exponential relationship:

$$UCS\_ALL = 0.1401e^{0.0012Vp} \qquad R^2 = 0.73 \qquad (3)$$

where UCS is in MPa and Vp in m/s.

Equation (3) as shown in Figure 3c was developed during 2012.

Equation (3) incorporating Vp up to 6000 m/s fits quite well with the laboratory data and performs better than (1) and (2) at Vp range of 4000 m/s to 6000m/s. Results thus reflect that the wide range of data increases the accuracy of cross correlation studies. Equation (3) is good enough to predict the UCS values of various exploratory blocks of SCCL.
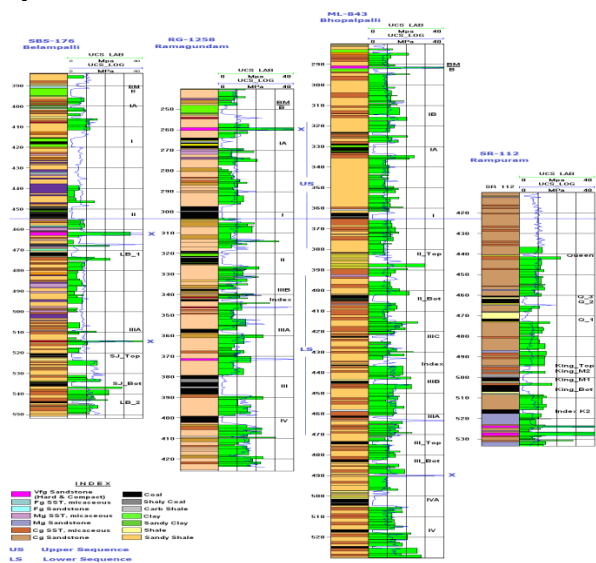
Figure 6: Comparison of Vp derived and Laboratory determined UCS values of various blocks

Figure 6 displays the UCS profile derived using equation (3) and laboratory determined UCS values of various exploratory blocks. It is concluded that the data from geophysics and laboratory tally very well with each other.

Figure 6 indicates a broad consistency in the UCS values of sandstones from one block to another of the various Godavari sub-basins. The UCS of sandstones of the upper sequence (US) are around 10 MPa and those of the lower sequence (LS) are 10 MPa to 30 MPa. 'X' in Figure 6 are very fine grained sandstones silicified whose UCS ranges from 40 MPa to 100 MPa. The Figure can not depict their true values because the upper limit is scaled to 40 MPa.

The fractures in sandstones would have a tendency of holding more water due to which Vp decreases. Accordingly, the Vp derived UCS values will be less than the UCS determined on dry samples as observed in the case of borehole SR 112 of Rampur block shown in Figure 6. In this case the laboratory determined UCS is around 10 MPa to 15 MPa against the Vp derived UCS of around 6MPa around the depths of 470 m to 490 m of SR112. UCS determined on dry core samples would be greater than the UCS of sandstones saturated at insitu conditions. Figure 7 shows the core samples of fractured sandstones at depths of 487m. The impact of fracturing on UCS values is also well depicted in the UCS map shown in Figure 8.
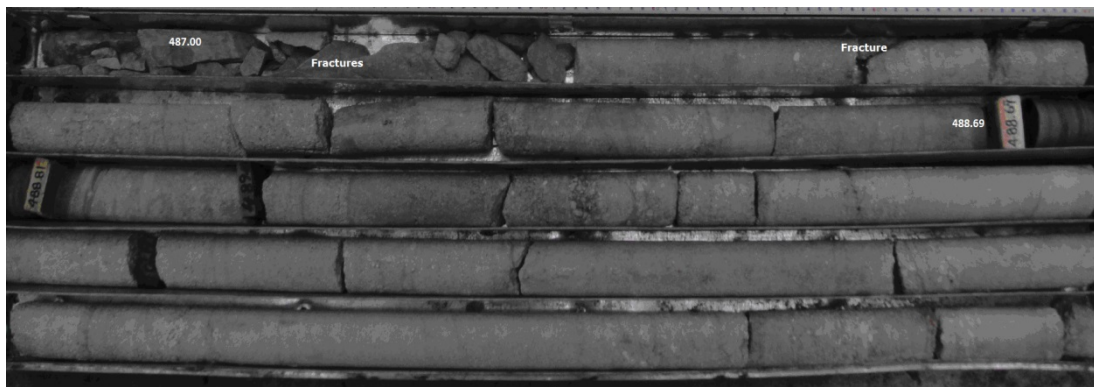
Figure 7: Sandstones fractured around 487m depth, Borehole SR 112, Rampur Block
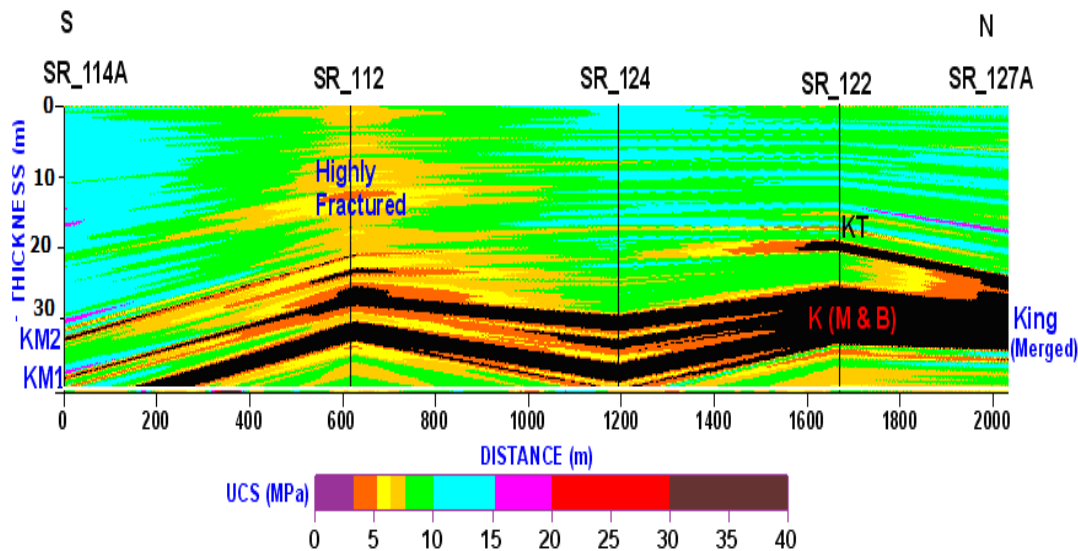
Figure 8: UCS map of overburden strata of King Seam, Rampuram Block. '0' is the datum

Figure 8 displays the UCS map of overburden strata of the King Seam of Rampuram block including the impact of fracturing on UCS values. Overburden strata of King Seam have an UCS of 10 MPa to 15 MPa which is reduced to 5 MPa to 7.5 MPa at SR-112, and it is concluded that this is due to the saturation of fractured sandstones with water (Figure 7). Vp logs document such sensitive structural features influencing the strength of rocks whereas the UCS determined on dry core samples might not record the

impact of insitu conditions. Differences between the laboratory determined and Vp derived UCS can therefore be visualised as differences in laboratory and insitu conditions.

Figures 9 and 10 enable classification of the Permian sequences based on the UCS values. The Middle Permian Barren Measure having a thickness of 200 m to 250 m is resolved into Upper and Lower sequences dominated by UCS values of 3 MPa to 5 MPa and 5 MPa to 10 MPa respectively. Early Permian coal-bearing Barakar Formation of 200 m thickness is also resolved into Upper and Lower sequences dominated by UCS values of 5 MPa to 15 MPa and 15 MPa to 20 MPa respectively. Sandstones of Barren Measure are poorly sorted, less compact and less cemented and friable than the sandstones of the Barakar. Sandstones of the Barren Measure are also more kaolinised and are prone to weathering into clay bearing rocks which seem to influence UCS values. Competency of Permian sequences increases in the descending order. Figure 8 also indicates regional consistency and near parallelism of the various beds making up the Permian sequences. UCS maps can be very useful to plan and manage the opencast mines.
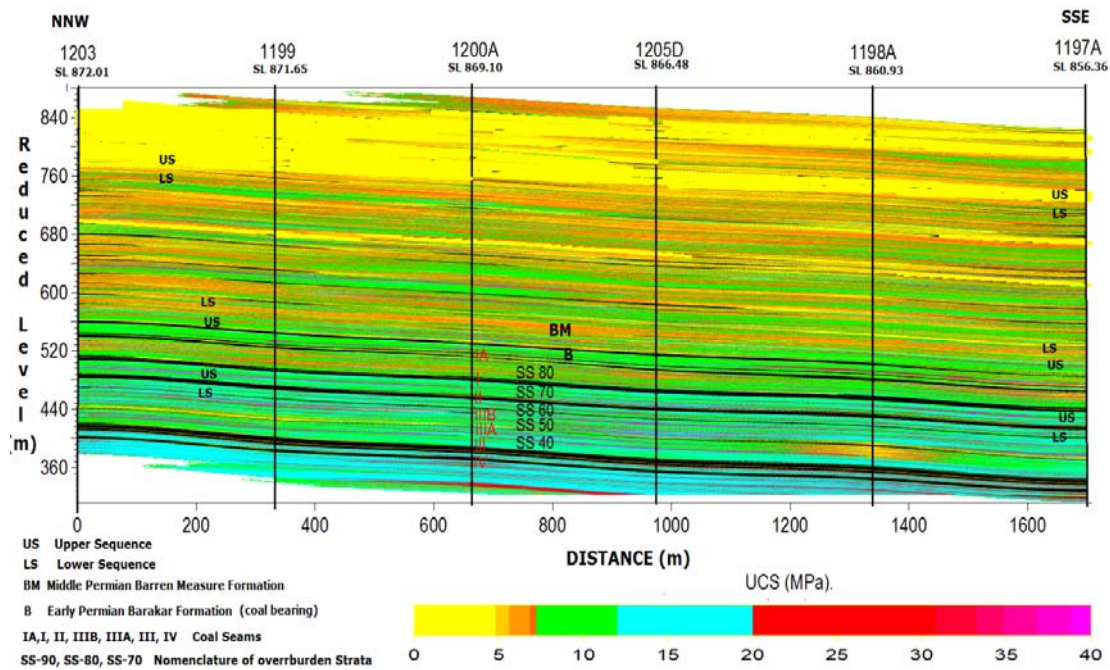
Figure 9: Vp derived UCS Map of Permian Sequences of Adriyala Longwall block, Ramagundam
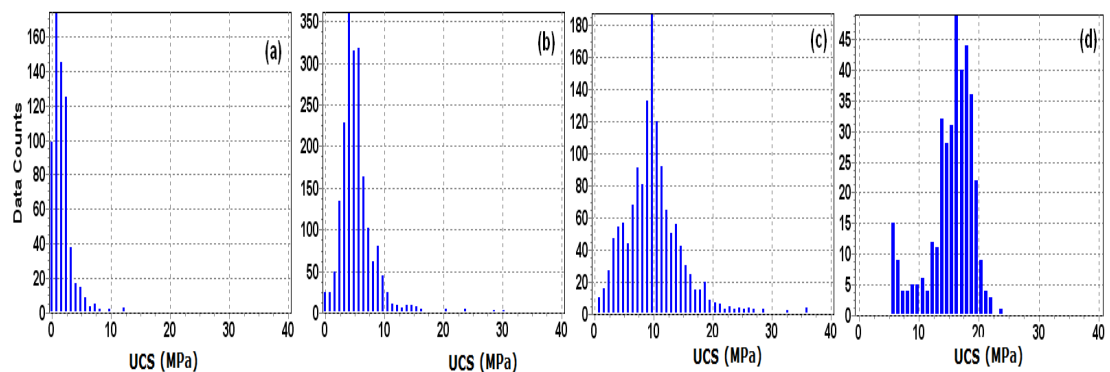
Figure 10: Classification of Permian Sequences on the basis of UCS values, Adriyala Longwall block, Ramagundam. (a) and (b) Upper and Lower sequences of Barren Measure. (c) and (d) Upper and Lower sequences of Barakar Formation

TENSILE STRENGTH (TS)

Tensile Strength is the maximum resistance offered by the rock to tensile loading. Due to practical difficulties tensile strength was determined by the indirect Brazilian method, wherein the cylindrical rock

sample was placed horizontally between the bearing flat platens of a testing machine and subjected to failure by compressional loading as shown (Figure 11). TS measurements were carried out as per IS norms IS: 10082-1981 by CMFRI and also by SCCL. According to the norms the length to diameter ratio of the intact cylindrical rock sample was maintained 0.5. Tensile Strength was calculated by the following formula.

TS (MPa) = 0.636 x P/Dt

Where, P is load at failure (kN), D is diameter (mm) of the rock sample and t is thickness (mm) of the rock sample.
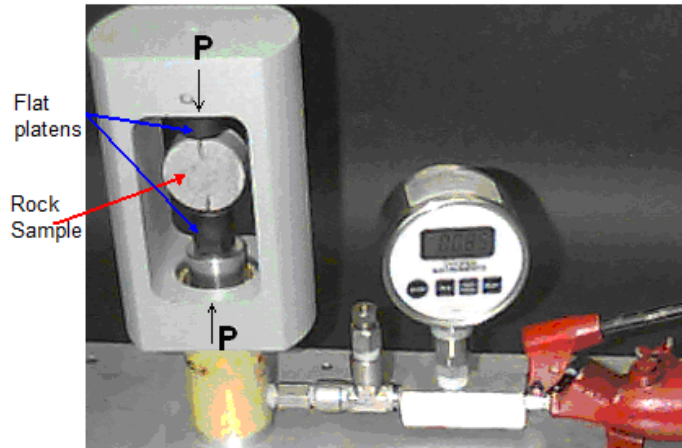
Figure 11: Testing setup for measuring Tensile Strength

Figure 12(a) shows the polynomial relation between Vp from sonic logs and laboratory determined Tensile Strength. The Figure 12(b) shows the linear relationship between laboratory determined TS and UCS. The respective equations are as follows. 762 data points are considered in the study.

$$TS = 9.1109E\text{-}007Vp^2 - 0.0047Vp + 6.2757 \qquad\qquad R^2 = 0.76 \qquad\qquad (4)$$

$$UCS = 9.5729 * TS \qquad\qquad R^2 = 0.95 \qquad\qquad (5)$$

where TS and UCS are in MPa and Vp is in m/s.

Equations (4) and (5) give similar values of Tensile Strength.
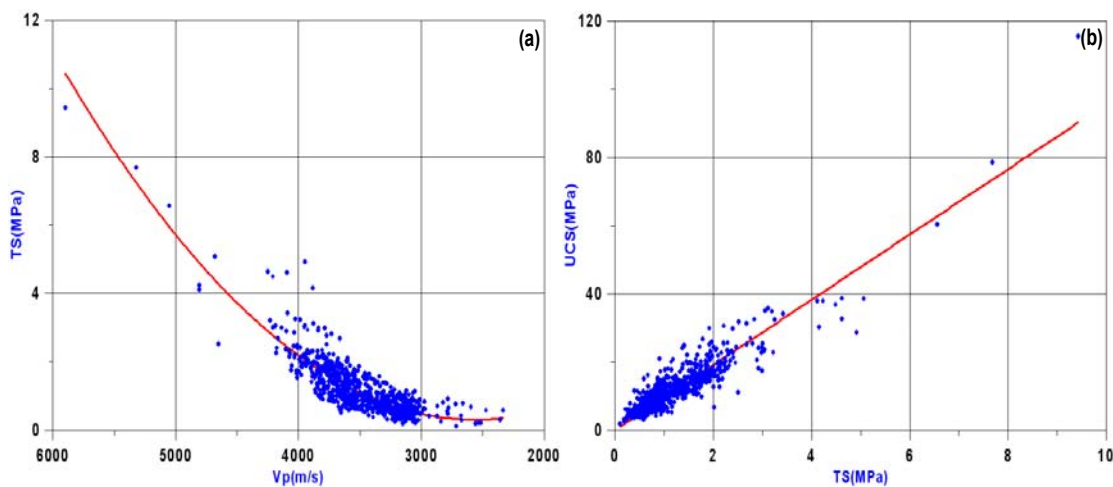
Figure 12: (a) Sonic P-wave Velocity (Vp) versus Laboratory determined TS of Sandstones. (b) Laboratory determined UCS versus Laboratory determined TS of sandstones

Figure 2 shows that the laboratory determined and Vp derived values of Tensile Strength tally very well with each other.

YOUNG'S MODULUS (E)

Young's modulus is the measure of change in strain parallel and normal to the direction of the applied stress. Measurement was conducted by applying load on the specimen continuously at a constant stress rate to a certain extent and then unloading in the same stress rate. The applied load and the resultant axial and circumferential strains or deformations were recorded through electronic load cell, LVDT's (Linear Variable Differential Transformer) and Data Logger connected with the computer during the investigation. Young's modulus was measured as detailed in Figure 13. This modulus was measured simultaneously with the UCS tests as per IS norms IS: 9221-1979 by Central Institute of Mining and Fuel Research of India.
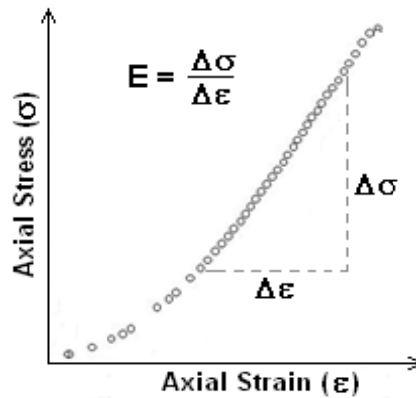
Figure 13: Determination of Young's Modulus (E) from stress and strain graph

Figure 14(a) shows the exponential relation between Vp from sonic logs and laboratory determined Young's Modulus under loading conditions. Figure 14(b) shows the linear relationship between laboratory determined Young's Modulus (E) and laboratory determined UCS values. 135 data points from Adriyala and Kakatiyakhani Longwall Block (Bhopalpalli) are considered. The respective equations are as follows:

$$E = 0.0069e^{0.0017Vp} \qquad R^2 = 0.73 \qquad\qquad (6)$$

$$E = 0.2442 * UCS + 0.0205 \qquad R^2 = 0.79 \qquad\qquad (7)$$

Where Young's Modulus (E) is in GPa, UCS is in MPa and Vp in m/s.

Equations (6) and (7) give similar values of Young's Modulus.
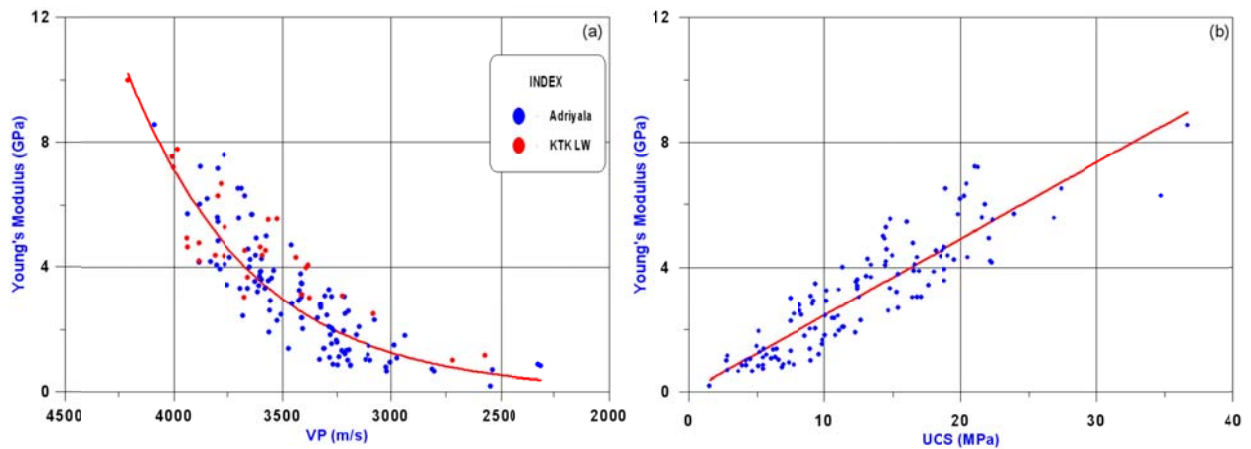
Figure 14: (a) P-wave velocity (Vp) versus Laboratory determined Young's Modulus (GPa). (b) Laboratory determined Young's Modulus (GPa) versus Laboratory determined UCS (MPa)

Figure 2 shows that the laboratory determined and Vp derived values of Young's Modulus tally very well with each other.

CONCLUSIONS

Uniaxial unconfined compressive strength (UCS) can now be empirically estimated from sonic geophysical logs and can be used in planning and designing both underground and opencast coal mines. It is found that the laboratory determination of UCS and TS being a regular affair offers a continuous scope to monitor and improve the relationships. A continuous down-hole profile of UCS is obtained from the Vp logs providing a visualisation of strata strength. Data from multiples boreholes can be modelled to provide a full UCS picture of the behaviour of the strata along strike and dip. Geological and geotechnical layering and the areas which have particular geotechnical significance are identified. These models provide better strata characterisation than that based on point-wise geotechnical testing of core samples. The generation of these models give a major opportunity for geological and geotechnical characterisation on local to regional scales to understand the implications of regional and local geological conditions on mine planning. Vp and UCS maps of interburden strata of coals bringing out the spatial distribution of weak and fissile horizons and the thick strong beds that can cause periodic weighting.

ACKNOWLEDGMENTS

REFERENCES

Butel, N, Hossack, A and Kizil, M. S. 2014, Prediction of in situ rock strength using sonic velocity, *14th Coal Operators' Conference, University of Wollongong*, The Australasian Institute of Mining and Metallurgy & Mine Managers Association of Australia, pp 89-102.

Gordon, N. 2002, The Development of Hazard Plans at Kestrel Mine, *in Aziz, N (ed), Coal 2002: Coal Operators' Conference*, University of Wollongong & the Australasian Institute of Mining and Metallurgy, pp 159-168.

Hatherly, P, Medhurst, T, Zhou, B and Guo, H. 2001, Geotechnical evaluation for mining – assessing rock mass conditions using geophysical logging, Final report, *ACARP Project C8022b*.

Hatherly, P, Sliwa, R, Turner, R and Medhurst, T. 2004, Quantitative geophysical log interpretation for rock mass characterization. End of Grant Report, *ACARP Project C11037*.

Hatherly, P. 2013, Overview on the application of geophysics in coal mining, *International Journal of Coal Geology*, http://dx.doi.org/10.1016/j.coal.2013.02.006.

Hoelle, J. 2004, Exploration for Results: Moura Coal Mine*, in Aziz, N (Ed), Coal 2004: Coal Operators' Conference*, University of Wollongong & the Australasian Institute of Mining and Metallurgy, pp 85-89.

IS-9143. 1979, Method for the determination of unconfined compressive strength of rock materials [CED 48: Rock Mechanics], *Bureau of Indian Standars*.

IS-9221. 1979, Method for the determination of modulus of elasticity and Poisson's ratio of rock materials in uniaxial compression [CED 48: Rock Mechanics], *Bureau of Indian Standards*.

IS-10082. 1981, Method of test for the determination of tensile strength by indirect tests on rock specimens [CED 48: Rock Mechanics], *Bureau of Indian Standards*.

King, W. 1881, The geology of the Pranhita-Godavari Valley, *Memoirs of Geological. Survey of India*, 18 (20), pp 150-311.

Lakshminarayana, G. 1996, Stratigraphy and structural framework of the Gondwana sediments in the Pranhita-Godavari Valley, Andhra Pradesh, *in P. K. S. Guha, S. Sengupta, and K. Ayyasami, R. N. Ghosh, eds.*, Gondwana Nine, Oxford & IBH Publishing Co. Pvt. Ltd., New Delhi, v. 1, pp 311-330, (Proceedings of the 9th International Gondwana Symposium, Hyderabad, 1994.).

McNally, G.H. 1987, Estimation of coal measures rock strength using sonic and neutron logs, *Geoexploration*, 24(4-5):381–395.

McNally, G.H. 1990, The prediction of geotechnical rock properties from sonic and neutron logs, *Exploration. Geophysics*, 21: 65–71.

Oyler, D C, Mark, C, Molinda, G. 2008, Correlation of sonic travel time to the uniaxial compressive strength of U.S. coal measure rocks, *Proceedings of the 27th International Ground Control in Mining Conference*, Morgantown, WV, pp 338–346.

Payne, D A and Ward, B. 2002, Strata Management in Weak Roof Conditions at Crinum Mine, *in Aziz, N (ed), Coal 2002: Coal Operators' Conference*, University of Wollongong & the Australasian Institute of Mining and Metallurgy, pp 126-134.

Payne, D A. 2008, Crinum Mine, 15 Longwalls 40 Million Tonnes 45 Roof Falls-What did we learn? *In Aziz, N (Ed), Coal 2008: Coal Operators' Conference*, University of Wollongong & the Australasian Institute of Mining and Metallurgy, pp 22-43.

Pell, S, Seedsman, R and Straub, K. 2014, Geotechnical data from geophysical logs: stress, strength and joint patters in NSW and QLD coalfields, *14th Coal Operators' Conference, University of Wollongong*, The Australasian Institute of Mining and Metallurgy & Mine Managers Association of Australia, pp 25-33.

Raiverman, V, Rao, M R and Pal, D. 1985, Stratigraphy and structure of the Pranhita-Godavari Graben, *Petroleum . Asia Journal*, 5(2):175-189.

Raja Rao, C S.1982, Coalfields of India-coal resources of Tamilnadu, Andhra Pradesh, *Orissa and Maharastra, Geological. Survey of India*, Bulletin Series A, 45(2), pp 9-40.

Ramana Murty, B V and Parthasarathy, E V R. 1988, On the evolution of the Godavari Gondwana graben based on LANDSAT imagery interpretation, *Journal of Geological Society of India*, 32(5): 417-425.

Ramana Murty, B V and Rao, C M. 1996, A new lithostratigraphy classification of Permian (Lower Gondwana) succession of Pranhita-Godavari basin with special reference to Ramagundam Coalbelt, Andhra Pradesh, India, *in P. K. S. Guha, S. Sengupta, K. Ayyasami, and R. N. Ghosh, eds., Gondwana Nine, Oxford & IBH Publishing Co. Pvt. Ltd, New Delhi*, v. 1, pp 67-78, (Proceedings of 9th International Gondwana Symposium, Hyderabad, India, 1994).

Rao, K V, Venkatappaiah, A, Basava Chary, M and Prasad, G V S. 1989, Practical application of geophysical well logging in a coal mine, production support drilling and economic case studies from Godavari Valley Coalfield, *India, in R. K. Verma, ed., Advances in Coal Geophysics, AEG, Hyderabad, India*, pp 105-118.

Rao, K V, Srinivasa Rao, A and Prasad, G V S. 1992, Identification and correlation of coal seams in Godavari Valley: an approach with geophysical logs, *Proceedings of National Workshop on Coal Exploration, SCCL, Kothagudem, India*, pp 631-634.

Rao, K V, Uday Bhaskar, G, Prasad, K A V L. and Durga Prasad, G D V. 1996, Solutions to the stratigraphic paradoxes of Chintalpudi sub-basin from electrologs, *Extended Abstracts of Proceedings of the 2nd International Seminar & Exhibition, Geophysics beyond 2000, Association of Exploration Geophysicsists, Hyderabad*, pp 263-266.

Stam, S, Guy, G and Gordon, N. 2012, Back analysis of roof classification and roof support systems at Kestrel North, *12th Coal Operators' Conference, University of Wollongong & the Australasian Institute of Mining and Metallurgy*, pp 42-51.

Turvey, C and Hanna, P, Coal Geology - where to from here? 1998, *in Aziz, N (Ed), Coal 1998: Coal Operators' Conference, University of Wollongong & the Australasian Institute of Mining and Metallurgy*, pp 126-132.

Uday Bhaskar, G. 2006, Electro lithofacies analysis for depositional history and stratigraphy of Manuguru Coafield using geophysical logs, *Journal of Indian Geophysical Union*, V 10(3): 241-254.

Uday Bhaskar, G, Srinivasa Rao, A and Shanmukha Rao, M. 2002, Coal seams correlation and Permian Stratigraphy of Kothagudem and Godavari sub-basins of Pranhita-Godavari Valley-An example from geophysical logs, *Journal of Indian Association of Sedimentologists*, 21(1 and 2):15-29.

Uday Bhaskar, G, Srinivasa Rao, A G V S Prasad, K A V L Prasad and Shanmukha Rao, M. 2011, Sondilla Seam and its implications on Permian stratigraphy of Pranhita Godavari Valley, Review based on geophysical logs, *proceedings of Proterozoic and Phanerozoic Evolutionary trends and Coal Exploration and Exploitation, Geological Survey of India and Singareni Collieries Company Limited, Kothagudem, India*, Abstracts volume, pp 29-30.

ANALYTICAL PROCEDURE TO ESTIMATE THE HORIZONTAL ANISOTROPY OF HYDRAULIC CONDUCTIVITY IN COAL SEAMS

Mahdi Zoorabadi[1&2], Winton Gale[3] and Serkan Saydam[4]

ABSTRACT: The horizontal hydraulic conductivity anisotropy of coal seams is a controlling parameter for designing gas drainage boreholes. The ratio between the maximum and minimum horizontal hydraulic conductivity (RkH-kh) and the orientation of maximum horizontal conductivity defines this anisotropy in horizontal plane. This paper presents a new analytical procedure based on the field stress data and geometrical properties of coal cleats to calculate these two parameters. The application of this procedure for a real case in Eastern of Australia resulted in an average ratio of 20.9 for RkH-kh and orientation of NE for maximum horizontal conductivity. The comparison between these results with the measured values validated the accuracy of proposed procedure to estimate the anisotropy of horizontal hydraulic conductivity of coal seams.

INTRODUCTION

Hydraulic conductivity of coal seams is a key parameter for successful designing of gas drainage operations. For gas drainage, the pore pressure (reservoir pressure) is lowered which causes desorption of gas molecules from coal matrix. Then the free gas flows toward drainage borehole through coal fractures (cleats) and its diffusion within coal matrix. Contribution of diffusion to the fluid flow in coal seam is negligible compared to flow throughout cleat network (Robertson and Christiansen, 2008). Therefore, coal seam is simulated as fractured reservoir with respect to fluid flow. Similar to all fractured rocks, hydraulic conductivity of coal seam is an anisotropic character and flow rate of gas and water mixture (two phase flow) would be higher in the direction with higher hydraulic conductivity.

For practical applications, anisotropy in hydraulic conductivity can be explained by two ratios; 1) ratio between maximum and minimum horizontal conductivity and 2) ratio between maximum horizontal conductivity and vertical conductivity (R_{kH-kV}). R_{kH-kh} controls the orientation of drainage boreholes. Massarotto *et al.,* (2003) found that the reported RkH-kh of coal varies from 1.8 to 17. They performed triaxial permeability tests on Permian coals from Bowen Basin, Queensland, and Sunan Basin, China. Based on these experiments, they reported a range of 1.35 to 19 for RkH-kh. Furthermore, they found that the RkH-kV varies from 0.11 to 4 for Permian coal.

In this paper, an analytical procedure was introduced to estimate RkH-kh based on cleat geometry and in-situ stress. The new procedure was applied to a real case which is located in Eastern Australia. A comparison was made between estimated value and results obtained from field interference tests.

METHODOLOGY

In practical applications, water flow within rock joints (rough surfaces) is simulated as laminar flow through two parallel plates, (cubic law) (Snow, 1969). Based on this assumption, hydraulic conductivity of individual joints is obtained as:

$$k_j = \frac{g a_j^2}{12\vartheta} \tag{1}$$

where, *g* is the gravitational acceleration, ϑ is the kinematic viscosity and a_j is the joint hydraulic aperture. This formulation can be extended to a joint set with spacing of *S* as:

$$k_j = \frac{g a_j^2}{12 S \vartheta} \tag{2}$$

1 *Senior Geotechnical Engineer, SCT Operations, Wollongong. Email: MZoorabadi@sct.gs, Tel: 0432552816*
2 *Adjunct Lecturer, School of Mining Engineering, UNSW,*
3 *Managing Director, SCT Operations, Wollongong, Australia. Email: wgale@sct.gs, Tel: 42222777*
4 *Associate Professor, School of Mining Engineering, UNSW. Email: S.Saydam@unsw.edu.au, Tel : (02) 93854525*

Snow (1969) introduced the first comprehensive analytical method for hydraulic conductivity of jointed rocks:

$$k_{ij} = \frac{g}{12\vartheta} \sum_{k=1}^{n} \frac{a_k^3}{s_k} \left(\delta_{ij} - n_{ik} n_{jk} \right) \tag{3}$$

where, k_{ij} is hydraulic conductivity tensor, n is number of joint sets, a_k and s_k are hydraulic aperture and spacing of k_{th} joint set, δ_{ij} is the Kronecker Delta and nik and n_{jk} are direction cosines of the unit vector normal of each joint set in the x, y and z direction. Rock joints are considered as infinite plane; therefore, they extend all over the considered volume of rock mass (objective volume) and intersect its boundary. Orthogonal geometry (Figure 1) is common to simulate the network for cleats within coal (Robertson and Christiansen 2008). Then Snow's formulation can be further applied to the cleat network to estimate its hydraulic conductivity tensor.
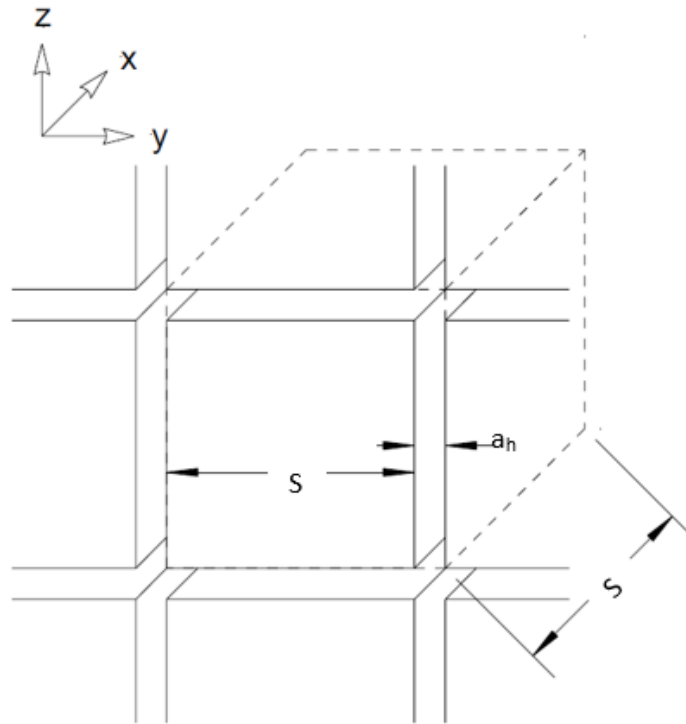
Figure 1: Schematic orthogonal geometry for coal cleats (Modified after Robertson and Christiansen, 2008), ah is hydraulic aperture and S is spacing

The orientation and spacing of cleats can be measured by using defect logs, acoustic scanner and field mapping. As can be seen from Equation (3), hydraulic aperture of cleats is the main controlling parameter (hydraulic aperture gets power of 3). Nevertheless, there is no direct method to estimate the hydraulic aperture of rock discontinuities. Zoorabadi *et al.,* (2014) proposed empirical formulations to estimate the hydraulic aperture of rock discontinuities at different depth (Figure 2).

In this method, approximate acting stress on each discontinuity set is determined firstly by considering the orientation of that discontinuity set and field stress orientation (Figure 3). Then equivalent depth (Zeq) for each discontinuity set can be estimated as follows:

$$z_{eq} = \sigma_i / \gamma \tag{4}$$

where σ_i is the applied stress on the discontinuity set of i and γ is the unit weight of rock mass. Following the calculation of the equivalent depth for each discontinuity sets, the hydraulic aperture is calculated using following equation (Zoorabadi *et al.,* 2014).

$$a_h = 250 \left(1 - \frac{z_{eq}}{40 + 0.98\, z_{eq}} \right) \tag{5}$$

where a_h is hydraulic aperture of rock discontinuity considering applied stress.
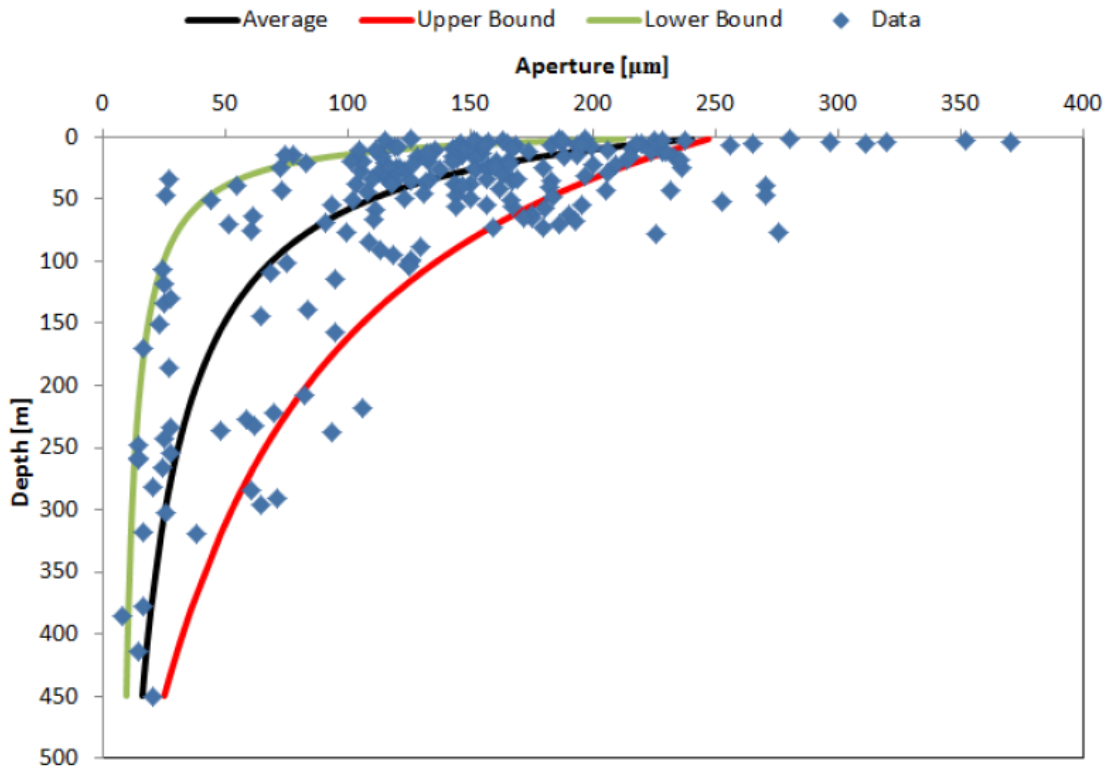
Figure 2: Variation hydraulic aperture of rock fractures by depth (Zoorabadi *et al.,* 2014)
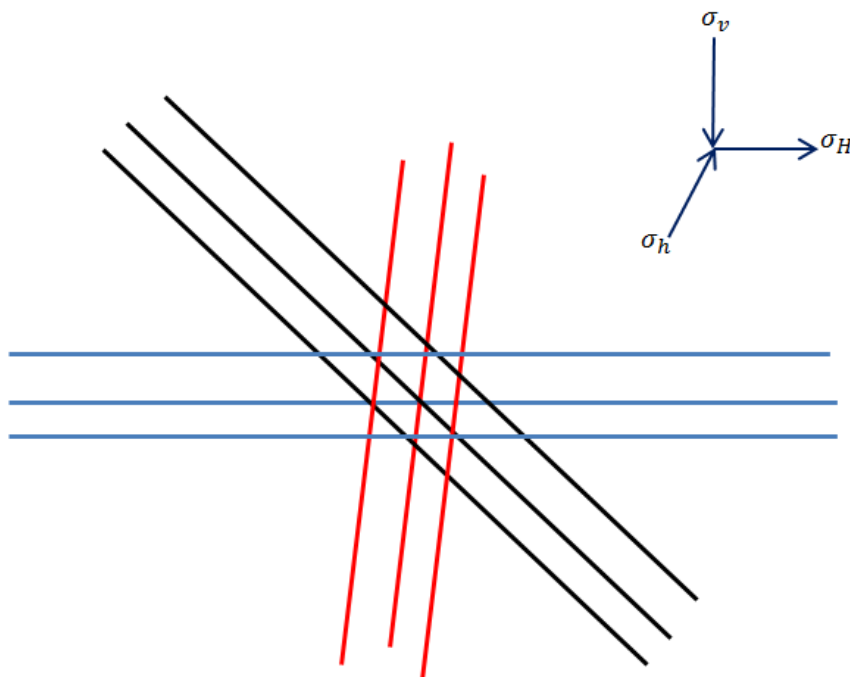
Figure 3: Approximate acting stress on each discontinuity set as a function of field stress orientation and orientation that discontinuity set

CASE STUDY

The above mentioned procedure was applied to a real case. This case was a mining project which was located in Eastern Australia. Detected cleats in different boreholes were statistically analysed to determine the orientation and spacing of cleats. Figure (4) shows contours diagrams of detected cleats in different scanned boreholes. Furthermore an average spacing of 0.53 m was estimated for cleats.
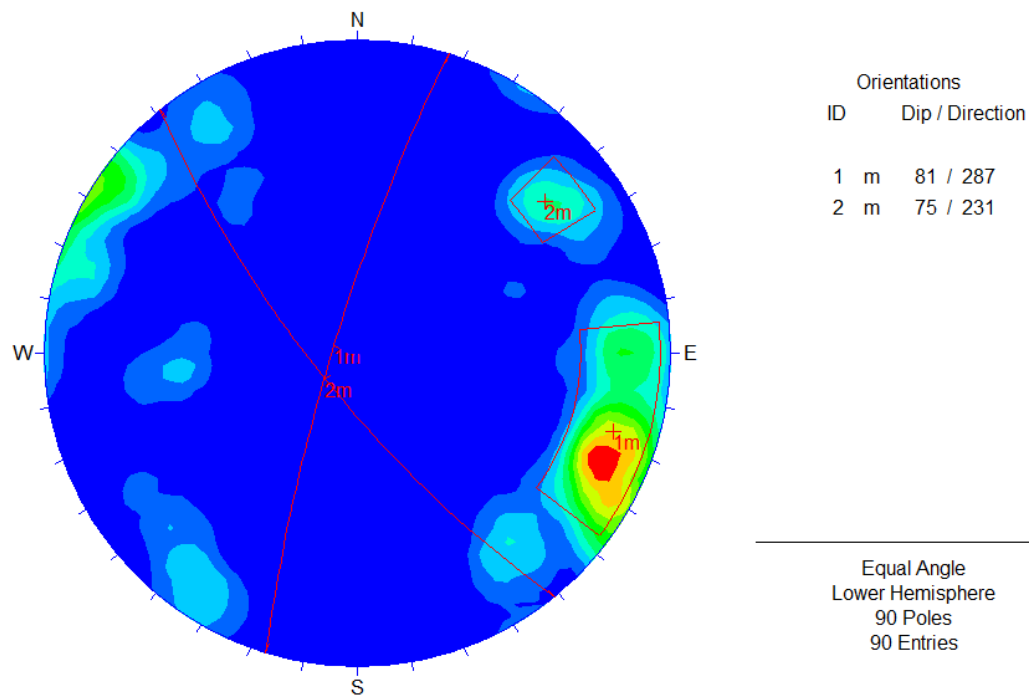
Figure 4: Contour diagram of all cleats detected by acoustic scanner

In this study, the average depth of coal seam was 225 m. Field stress measurement and borehole breakouts analysis demonstrated that the direction of maximum horizontal stress was NE. Based on the field measurements the tectonic factor for this site varied between 0.7 and 1. The data which was published by Nemcik *et al.,* (2005) gave approximately the same range for the tectonic factor at depth around 200 m. By considering the elastic modulus of 3 GPa for coal and by using the concept of tectonic stress concept (Nemcik *et al.,* 2005), the ratio between maximum horizontal stress and vertical stress for this site would be between 0.8-1.

Before starting of interference tests, the step-rate-test was performed to determine the maximum allowable flow rate. Moreover the inflection point on water pressure – flow rate curve of step-rate-test provided an estimate for the minimum stress within coal seam (Figure 5). Using this method, the ratio between minimum horizontal stress and vertical stress for this project was determined from 0.26 to 0.36. Combination of filed stress orientation and magnitude with orientation of cleats, resulted in equivalent depth of and hydraulic aperture for cleat sets as in Table 1 (using Equations 4 and 5).

Table 1: Geometrical properties of discontinuity sets for depth 150 m (100-200 m)

Cleat Set	Dip/Dir	Dip	Spacing [m]	Equivalent Depth [m]	Hydraulic Aperture [μm]
C1	287	81	0.53	58 - 81	80-100
C2	231	75	0.53	180-225	34-42

The hydraulic conductivity tensor of coal seam was calculated by applying Equation (3) to the geometrical properties for cleat sets. In Table 2, the calculated results including the range of RkH-kh and the orientation of the maximum horizontal conductivity are listed.

In this study, hydraulic interference test was carried out in a coal seam to evaluate the horizontal hydraulic conductivity of the seam. The interference test included an injection well, which was fully screened in seam thickness and three observation boreholes in around the injection well. Water injects with a constant flow rate and the corresponding head changes were measured in the observation wells (Figure 6). The recorded head change versus time provided data to calculate the principal hydraulic conductivities in horizontal plane (Papadepulos 1965).
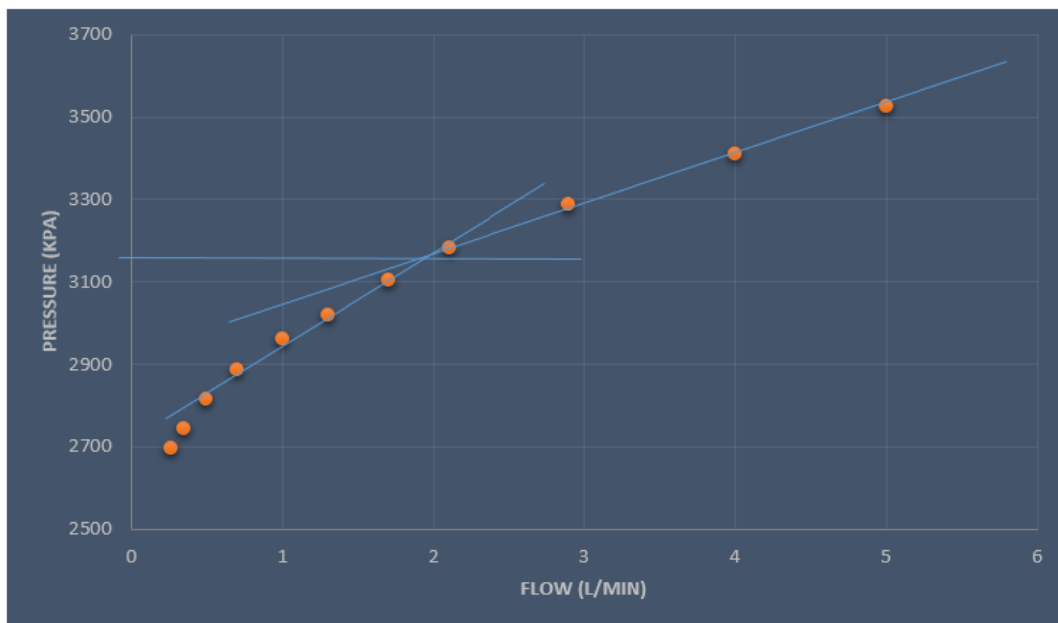
Figure 5: An example for estimating of minimum stress by step-rat-test

Table 2: Calculated RkH-kh and it orientation

	For Minimum Hydraulic Aperture	*For Maximum Hydraulic Aperture*
$R_{kH\text{-}kh}$	20.5	21.2
Orientation	NE	NE

Different combinations of recoded head change curves in this project were considered to calculate the anisotropic horizontal hydraulic conductivity. The average measured RkH-kh was 20.2 at NE orientation. Comparison between the measured and calculated anisotropy ratios demonstrates that proposed analytical procedure has the capability to be used for practical estimations. This procedure has potential to be used to calculate the hydraulic conductivity changes which happen by water withdrawal as well. As it commonly known, the water withdrawal increases the effective stress which results in reducing of cleat aperture. On the other hand, coal shrinkage due to gas release increases that hydraulic aperture of cleats (Robertson and Christiansen 2008). The combination of proposed procedure with the Sorptive-Elastic models such as Palmer and Mansoori (1998), Shi and Durucan (2003), Robertson and Christiansen (2006) provides the capability to calculate the variation anisotropic horizontal hydraulic conductivity by water withdrawal.
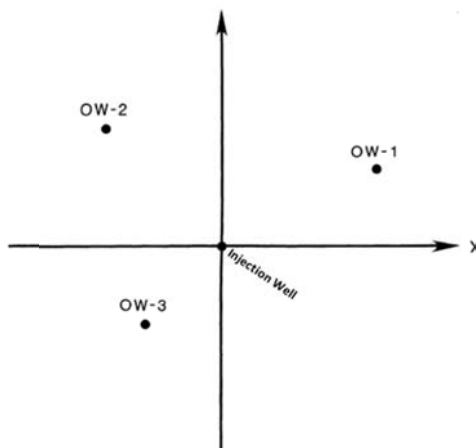
Figure 6: Schematic view of interference test (ow, observation well)

CONCLUSIONS

A new analytical procedure is proposed in this paper to calculate the ratio between the maximum and minimum horizontal conductivity of coal seam by combination field stress data with the geometrical properties of coal cleats. The proposed procedure was applied to a real case in Eastern Australia. The calculated ratio between the maximum and minimum horizontal conductivity and the orientation of maximum horizontal conductivity were compared with the measured values from interference test. The comparison showed that the proposed analytical procedure has a reasonable accuracy to predict the anisotropic conductivity of coal seams.

REFERENCES

Massarotto, P, Golding, S D and Rudolph, V. 2003, Anisotropic permeability characterisation of Permian coals. *Proceedings of the International CBM Symposium*. University of Alabama, USA.

Nemcik, J, Gale, W and Mills, K. 2005. Statistical analysis of underground stress measurements in Australian coal mines, *Bowen Basin Symposium*, Yeppoon, Qld, Australia.

Palmer, I and Mansoori, J. 1998, How Permeability Depends on Stress and Pore Pressure in Coal beds: A New Model, *SPEREE 1* (6):539-544. SPE-52607-PA doi: 10.2118/52607-PA.

Papadopulos, I S. 1965, Notsteady flow to a well in an infinite anisotropic aquifer, *Duabrovnik Symposium on the Hydrology of Fractured Rocks*, Intern. Assoc. Sci. Hydrol, pp 21-31.

Robertson, E P and Christiansen, R L. 2008. A permeability model for coal and other fractured, Sorptive-elastic media, *SPE Journal*, 13 (03).

Shi, J Q and Durucan, S. 2003, Changes in Permeability of Coal beds During Primary Recovery--Part 1: Model Formulation and Analysis, *Paper 0341 presented at the International Coalbed Methane Symposium*, Tuscaloosa, Alabama, USA.

Snow, D T. 1969. Anisotropic permeability of fractured media, *water resources research*, 5: 1273-1289.

Zoorabadi, M, Saydam, S, Timms, W and Hebblewhite, B. 2014. New empirical equations to estimate the hydraulic aperture of rock discontinuities at different depths, *Ausrock 2014: Third Australian ground control in mining conference*, Sydney, Australia.

Stress Measurement in Coal Seam Ahead of Longwall Face – Case Study

Radovan Kukutsch, Petr Konicek, Petr Waclawik, Jiri Ptacek, Lubomir Stas, Martin Vavro and Alice Hastikova

ABSTRACT: Stress measurement and stress monitoring is an important task in mining geomechanics, because knowledge of the stress-strain state in a rock mass is the determining factor for the proper planning of roadway support and for the correct design of underground mining. This strategy is useful for ensuring mining safety, because increasing depth causes several issues, especially in areas with rockburst hazard, when roadways are loaded by the pressure ahead of an advanced longwall or by the stresses induced by destress blasting in overlying rock. Besides, mining is influenced by stress induced by previous excavations, mining edges in the overburden or abandoned workings in the same seam. The paper presents experiments with Compact Conical-endedBorehole Monitoring (CCBM) probes, which were used for stress monitoring in the area of a high-capacity coal face at Karvina Mine at the Lazy site (Czech Republic). This longwall panel is influenced by all the factors mentioned above. Monitoring of stress changes was carried out by using conical probes (CCBM) glued into a special cement body, which was installed directly into the coal seam. The basic description of the probe installed in the coal, the method of installation and the measurement results are the subject of this contribution. Another aim of the paper is to compare the measured values with the theoretical assumptions and mathematical model results.

INTRODUCTION

Knowledge, that is as accurate as possible, of the stress-strain state in the rock mass is the determining factor for the proper planning of roadway support and for the correct design of underground mining. That is why monitoring of the changes in stress induced by longwall mining was included within this experiment.

The problems of rock stress and its determination have been under investigation at the Institute of Geonics for a long time. For the determination of all the components of the stress state, a Compact Conical-ended Borehole Overcoring (CCBO) system was used, which was first used by K. Sugawara and Y. Obara from Kumamoto University (Sugawara and Obara 1999; Obara and Sugawara 2003). The conical shape of the CCBO probe provides a sufficient number of strain measurements in independent directions in one probe position in the borehole, so that all the values of the stress tensor can be determined. Two variants of the CCBO probe were developed and used at the Institute of Geonics. The latter, called a Compact Conical ended Borehole mMonitoring (CCBM) method device, was used for long-term monitoring of stress tensor changes (Stas *et al.,* 2005, 2011). Several measurements of stress tensor changes by the CCBM were performed (Soucek *et al*., 2013, Konicek *et al*., 2014). However, all the probes were installed in compact rocks, into the overburden of the coal seam. The flat conical shape of the borehole bottom is necessary for these types of probes in order to obtain relevant monitored data. In order to monitor the stress changes in the coal seam, a CCBM conical probe was glued into a special cement body. The body containing the CCBM probe was installed into a borehole in a selected longwall panel in the Karvina Sub-basin (see Figure 1) in the Upper Silesian Coal Basin (USCB). The system of the embedded cement body with the conical probe was implemented due to the impossibility of directly installing the conical probe into the coal due to the properties of coal (a brittle material that fails easily).

MINING AND GEOMECHANICAL CONDITIONS

The longwall t explored was the second panel in seam No. 4, which has a thickness of 3 to 8 m; the average seam thickness is 6.2 m. The seam lies about 800 m below the surface. The bed dip ranges from +10° to –17° (differing in the eastern and western limbs of the anticline). The longwall face length was 191 m. The explored area is documented in Figure 2. The hard coal seam is covered by solid and competent sandstone and sandy siltstone layers in this area.

Institute of Geonics AS CR, v.v.i. & Institute of Clean Technologies, E-mail: kukutsch@ugn.cas.cz, Tel: +420 596979 242

Figure 1: Location of the Karvina Sub-basin in the Upper Silesian Coal Basin (USCB)

In addition, seams No. 1, 2, and 3 have been irregularly mined out in the overburden. This causes irregular stress distribution in the rock mass and consequently a high risk of rockburst in the course of longwall mining. Seam No. 4 lies in the lower part of the Sedlove Member of the Namurian age. The main tectonic structures are obvious from Figure 2. A very flat anticline (maximum dip up to 20°) divides the geological block into two different parts, and three faults A, B and C. The influence of the mine edges of seams No. 2 and 3 in the overburden is evident from Figure 2 as well. For stress distribution in the area of the explored longwall, it is necessary to consider the mining in seams No. 2 and No. 3 in the next colliery B (east and north east of the explored area – see Figure 2). The first panel in seam. No. 4 was already mined out south of the explored long wall. Additional stress caused by this goaf caused a stress concentration in the south part of the explored panel. It was necessary toconsider the additional stresses caused by residual pillars in seams No. 2 and No. 3 too. These were left in the overburden at a distance of about 50 m and 80 m respectively. The location of experimental stress measurement in seam No. 4 (see CCBM 21 in Figure 2) was in the area of the border of the shaft protective pillar, where the additional stress concentration produced by the edges of seams No. 2 and 3 was considered.
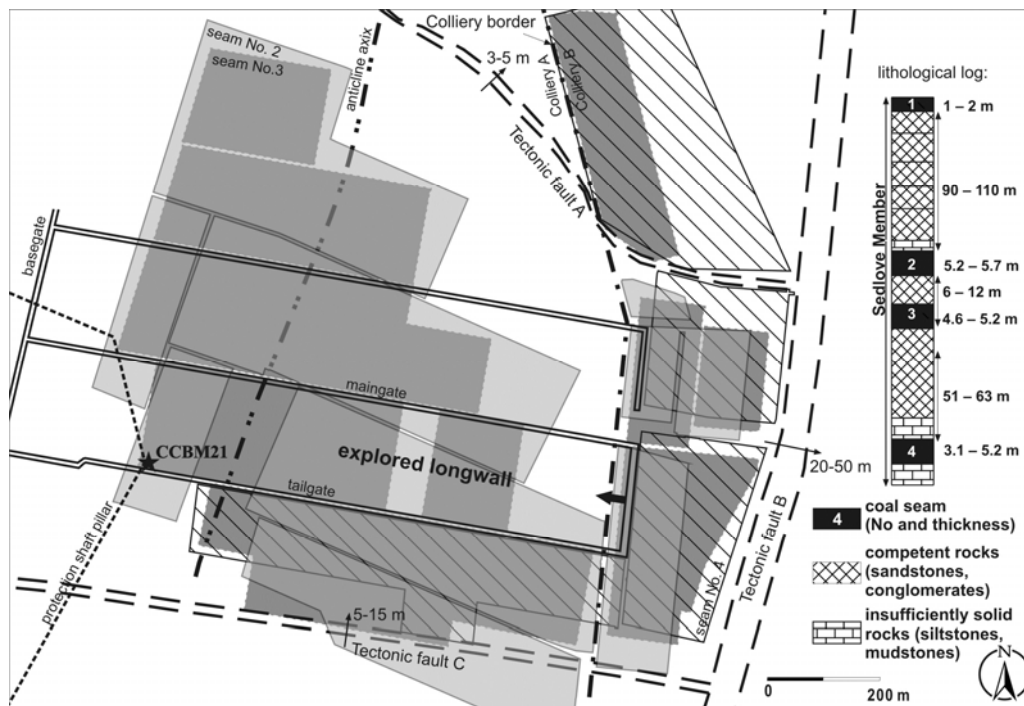

Figure 2: Geological and mining condition of explored area

DESTRESS BLASTING

Destress blasting in the area of the longwall termination was adopted (see Figure 3). The main goal of the destress blasting was to weaken the strength/massiveness of the overlying competent rock strata before the underground mining began in the area of additional stress from previous mining in the overburden seams (seams No. 2 and 3 in Figure 2). First, the horizon of the competent overlying strata was identified through the procured core samples. Then, different sets of predefined, long boreholes were drilled from the gate-roads, targeting these competent strata and the existing mining activity in and around the panel.

A schematic diagram of the adopted design for the long borehole drilling for the destress rock blasting in the termination part of the panel is shown in Figure 3. Boreholes for the first main goal of destress blasting were drilled upwards at angles between 15° and 35° from both of the longwall gate-roads (boreholes perpendicular to gates and inclined boreholes towards the north from the maingate, all in Figure 3). The borehole lengths varied from 50 m (boreholes north from the maingate) to 100 m (boreholes perpendicular to gates). In view of the calculated amount of explosive required for the destress rock blasting, the diameter of these boreholes was 93 mm and the spacing of the boreholes was 10 m (boreholes perpendicular to gates). With suitable length and angle combinations for these boreholes, the bottoms (ends) of all of the boreholes were situated at a similar horizon inside the roof, nearly 25 m above coal seam No. 4.

All of these upward-drilled boreholes were charged pneumatically by the gelatine-type explosive Perunit 28E (heat of explosion 4100 kJ.kg^{-1}), and sand was used for the stemming. The length and amount of explosive in each borehole varied according to the surrounding geo-mining conditions. According to the condition of explored panel No. 140 704, the lengths of the charge in the different holes varied from 32 m to 80 m, and the length of the sand stemming varied from 18 m to 46 m. An individual group of loaded boreholes, typically ranging from 4 to 5 boreholes, was fired in advance according to the predefined firing order. All of the charged boreholes in a certain group were fired simultaneously, without any delay. The weight of the explosive charged in different holes varied according to the adopted length of the borehole. The amount of the explosive charged in a hole of the panel varied from 250 kg to 700 kg. The total amount of explosive (for the 4 to 5 boreholes in a group) blasted at a time in the panel varied from 1275 kg to 3050 kg.

According to the site conditions, boreholes Nos. 41–46, 61–64, and 161–164 (Figure 3) were adopted to dilute the influence of the edges between the mined and the un-mined parts of the seams in the overburden. Blasting in boreholes Nos. 71–75 and 171–175 were used to isolate the mining in the longwall panel and the protection shaft pillar. These borehole blastings were designed to develop continuous fractures in the rock mass, which is likely to be responsible for the generation and the accumulation of stress concentrations due to the mining. The competent overlying rock strata, which are continuously fractured due to these blastings, were also observed to be caving friendly. The decision to blast different individual groups of boreholes at different stages was made according to the surrounding workings and the strata, the development of seismic activity during mining and the advancement of the longwall face. As per the geo-mechanical properties of the overlying rock strata and existing legislation, the positions of the fired boreholes were kept in the range of 30 m to 100 m ahead of the longwall face (stages 21–23) and at a distance more than 100 m ahead of the longwall face (stages 19 and 20). The amount of explosive to be charged in each borehole is derived from the dimensions of the selected boreholes for firing. Finally, the selection of boreholes depends on the existing mining conditions, natural conditions and agreement of the registered seismic activity with the legislation.

The efficiency of the adopted destress blasting at the different mining stages is evaluated in terms of seismic effect (SE), which is calculated through the available seismic monitoring data and the weight of the explosive charged (Konicek 2013). These technical evaluation methods provided satisfactory results for the destress blasting design process. Results as well as destress blasting parameters are shown in Table 1. In spite of the fact that the main goal of the destress blasting was different (see text above), the seismic effect, which represents the effect of stress release in the rock mass, was very high (see Table 1). For the first three stages of destress blasting (stages No. 19, 20 and 21 in Table 1), the stress release effect of destress blasting was evaluated as Excellent (SE= 24.8, 44.6 and 14.9), while in the last stages it was extremely good and very good. This corresponds to previous knowledge of destress blasting in similar conditions (e.g. Konicek *et al.,* 2013).
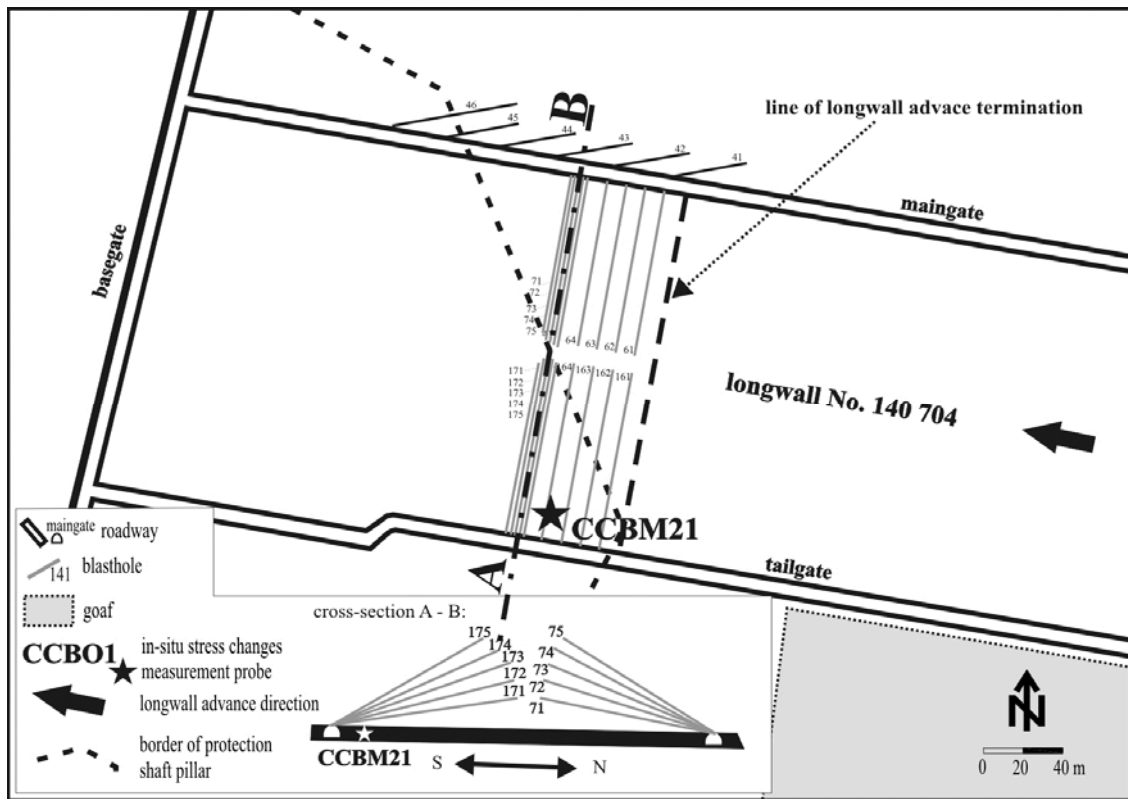
Figure 3: Destress blasting design in area of longwall termination

Table 1: Destress rock blasting parameters conducted in explored longwall

Stage	Numbers of boreholes	Explosive charge [kg]	Released seismic energy [J]	Seismic effect By Konicek 2013 [J.kg^{-1}]	Seismic effect evaluation
19	71, 72, 73, 74, 75	2 900	1.5E+05	24.8	Excellent
20	171, 172, 173, 174, 175	2 975	2.8E+05	44.6	Excellent
21	61, 62, 41, 161, 162	3 050	9.8E+04	14.9	Excellent
22	63, 64, 42, 163, 164	3 050	5.8E+04	8.7	Extremely good
23	43, 44, 45, 46	1 275	1.3E+04	5.0	Very good

EXPERIMENT DESCRIPTION

The objective of the experiment was to determine the stress-strain changes in the coal seam. As noted, the location of the experiment was chosen in an area where an additional stress concentration was contributed by the edges of seams in the overburden near the protective shaft pillar. Because the probe was not installed in the overlying rocks, where installation is relatively easy, it was necessary before installation in the coal seam to solve several problems.

These consisted of two main technical aspects:

- coal is a brittle material and close contact between the conical probe and coal is problematic,
- suitable consistency of grouting mixture.

The approach to these issues and the solution of these problems is the subject of the followingsections.

Parameters of filling material for fixing probe in the borehole in the coal seam

The basic input requirements for the composition and properties of the cementitious filling (grouting) mixture applied to a borehole in the coal seam, which had to be taken into account when designing the recipe, were:

1. The mixture in the fresh state has to exhibit a very high degree of plasticity so that it is able to spontaneously (by gravity) fill the space of a borehole with a very low inclination (10-15°);
2. Aggregates with grain sizes as small as possible must be used as filler in the mixture, with regard to the maximum homogeneity of the hardened mixture and the minimum porosity;
3. During the process of the setting and hardening of the mixture, shrinkage must not occur, so that the maximum possible contact between the cement filler and surrounding coal can be maintained during subsequent stress measurement.

The grouting compounds in fresh state were prepared and tested in the laboratory, showing properties comparable with the cast self-compacting and self-levelling materials that are commonly applied in the construction industry (e.g. as floor screeds). These are characterised by a high degree of spill (260-280 mm according to EN 13454-2: 2008), a relatively high flow rate (approximately 100 mm.s^{-1}) even in a low tilt test in PVC pipe (15°), and a low content of air pores (max. 2%).

During setting and hardening, the mixture exhibited moderate expansion of its volume. After 28 days of hydration of the mixture, the total value of the length change was approximately +0.3 mm.m^{-1}. The resulting mechanical and deformation properties of the hardened mixture are characterised by unconfined compressive strength in the range of 35-40 MPa, tensile bending from 5.0 to 6.0 MPa, indirect tensile strength from 3.0 to 4.0 MPa, static tensile modulus of 12-15 GPa and Poisson number from 0.15 to 0.22.

Installtion

The installation procedure in a coal seam is different from the installation in the overlying rocks. Since the probe would not stick to the coal and close contact between the probe and rock would not be possible, it was decided to put theprobe into a concrete body and then install this "container" in the borehole. The problem of inserting the probe into the concrete was solved by sticking the probe into a concrete body 75 mm in diameter (Figure 4). After solidification, this body was inserted into the casting vessel and secured with concrete, which increased the body dimensions of the probe to 280x100 mm. In order to approach a condition similar to that of the inserted probe in the body when it was sealed in the borehole, a free space was created behind the probe. Subsequently, centralisers with the same diameter as the borehole were mounted in front of and behind the probe in order to centre the body in the borehole. The orientation of the probe in the borehole was solved by using a pointer on the centraliser. Due to the dimensions of the probe, it was necessary to adjust the borehole diameter to the final proportions of the concrete container including the centralisers.

The experimental data shows how the coal will behave at the cave front.   Under low confining stress, cleating has a dominant role and results in a weakening effect on the coal (this effect is similar to rib spall). Further into the coal mass, confining stresses are higher and shearing is more predominant. The caving model needs to be able to mimic the expansionary effect of coal at low confining stress, whilst adequately reflecting the effect of scale on strength.
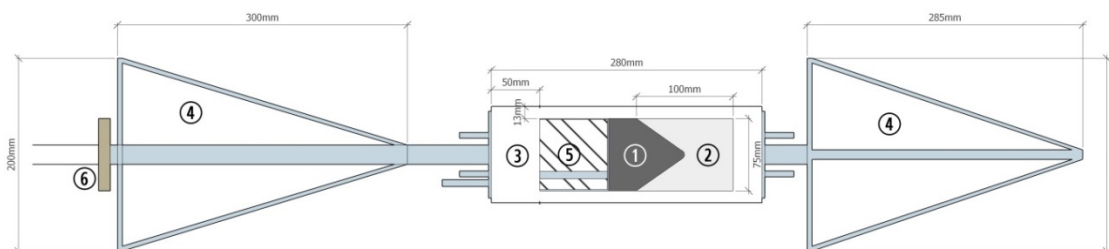
Figure 4: Cement body probe scheme: (1) CCBM probe (2) Inner cement body (3) Outer cement body (4) Centralizers (5) Free space (6) Pointer

Installation of the CCBM probe in front of the longwall No. 140 704 was done on the tailgate at the 128 m station. A borehole 10 m in length and 200 mm in diameter was drilled. The borehole was made perpendicular to the gate side at an inclination of 10° so that the end of the borehole was located in the coal (Figure 5).
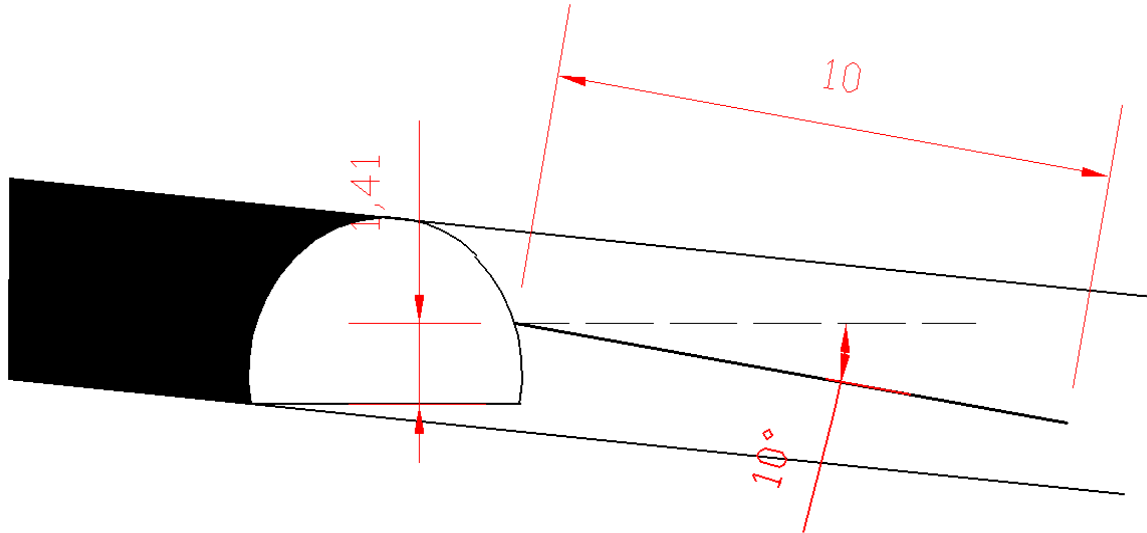
Figure 5: Cross-cut at tailgate 40 703

After drilling and cleaning the borehole, a video inspection of the borehole was performed. After a positive result (the borehole was accessible over its entire length), installation proceeded. This consisted of inserting the concrete container with the CCBM probe into the borehole using the installation rods and grouting the cement mixture. The dry, bagged mixture was mixed with the predetermined quantity of water and other additives. To transport the mixture to the end of the borehole, a PVC pipe was used to ensure that the mixture reached the bottom of the borehole and not elsewhere. The last step was to verify communication of the probe with a data logger.

24 hours after installation, the borehole was inspected using a video camera to verify successful solidification of the mixture. Subsequently, readings from the probe were taken and regular daily monitoring started. Mine employees took values from the probe and recorded the real daily advance and stationing of the coalface at the tailgate. The last step was to fill the mouth of the borehole with fitting foam.

STRESS CHANGES MONITORING AND MODELLING

The stress field induced ahead of a longwall face is affected by many factors, especially by:

- speed of advance of longwall,
- influence of previous mining activities (pillars and mining edges in the overburden),
- additional stress from the goaf of the previous longwall panel,
- occurrence of rigid strata between thick coal seams, and
- destress blasting and other rockburst prevention measures.

For the appropriate and correct interpretation, it is desirable to analyse all factors and to search for mutual relations. As it turns out, each of these factors play an important role in the development and change of the stress field. It should be pointed out that the longwall advance was irregular (from 0.5 m to 4.2 m per day) in the monitored period. Geological and geomechanical conditions were the main causes of it. Local coal seam erosion as well as tectonic faults caused fractures in the overburden and consequently rockfall in the longwall space. It took numerous drilling and blasting works to strengthen the longwall face.

Experiments of principal stress monitoring during longwall advance were modelled using the finite element method via Midas GTS 3D software. The linear elastic material model was used to obtain trends of principal stress changes during longwall face advance. The lengths of longwall advances in the model were chosen as 50 m. The final 50 m advance interval was separated into 5 m long sequences. Together, 17 stages were defined in the construction wizard – the primary stage and 16 advance stages defined by two phases. The first phase of each advance stage was "excavation of the working unit" and the following phase was "caving" of the working unit, including roof units. Finally, goaf areas were connected from the left side and front of the longwall panel and on the right side the original rock massif remained. Total volume of the model was 0.05 km^3.

The total stress field represented by its tensor (σ) was considered as the superposition of the basic stress tensor measured at the time of the probe installation (σ_0 – start of monitoring) and supplementary stress changes monitored in the course of longwall advance (S) (Figure 6).

$$\sigma = \sigma_0 + S$$
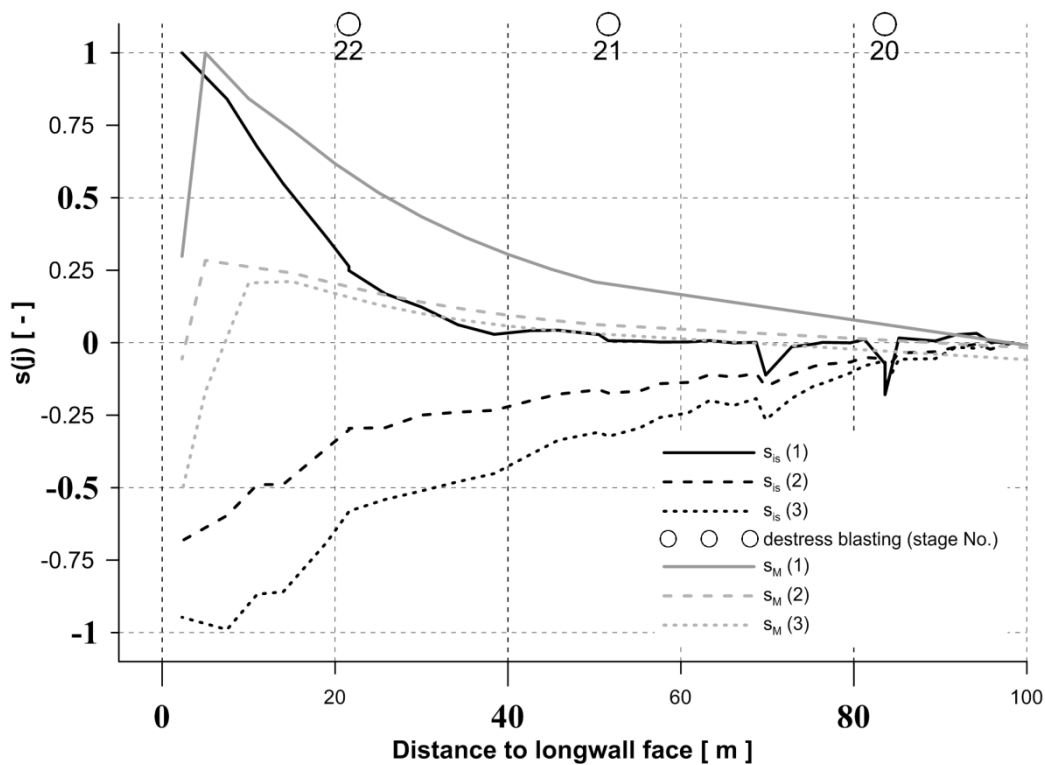
Figure 6: Relative principle components s(j) of tensor {S} ahead of longwall face

Supplementary stress change monitoring as well as mathematical modelling were done at a distance of 200 m before the CCBM probe. But only a 100 m section was selected for presentation (Figure 6). To better distinguish the shape of the graphs, the *in situ* monitored tensor (S_{is}) and modelled tensor (S_M) were normalised by their maximal achieved value using the following relations:

$$s_{is}(j) = S_{is}(j)/S_{is}(1)_{max} \text{ – for } in\ situ \text{ monitoring}$$
$$s_M(j) = S_M(j)/S_M(1)_{max} \text{ – for model}$$

where (j) is adequate three normalised principal components.

The trend in this case is more important than the stress change magnitude (strong, different elastic modulus of coal and elastic modulus of concrete material of cylinder). In Figure 6 the trend of the normalised principal component monitored by CCBM $s_{is}(1)$ illustrates that values monitored by the probe in the concrete body are in compliance with normalised principal components calculated by the mathematical model $s_M(1)$. Different trends are evident from comparison of both of the other components: $s_{is}(2,3)$ and $s_M(2,3)$. This could be caused by simplification of the mathematical model against real conditions.

CONCLUSION

The article describes an experiment of measuring the stress changes induced by longwall face advance in a coal mine and presents results of the induced stress changes determined by the CCBM method. The CCBM probe itself was situated in the coal seam and was embedded in a concrete body. The results of the experiment show that it is possible to measure induced stress change by this method as the trends of the 3D model are in agreement with the results of the ones *in situ*. The next step of this research will be to determine the stress surrounding the concrete body (in the coal seam) and to determine the relationship between stress within the concrete body and outside of the concrete body in the coal seam. Mathematical model calibration according to the measured data must follow as well. Other variants of the placement of the probe in the concrete body will also be the topic of future work.

ACKNOWLEDGEMENTS

REFERENCES

Obara, Y and Sugawara, K. 2003, Updating the use of the CCBO cell in Japan: overcoring case studies, *International Journal of Rock Mechanics and Mining Sciences*, Vol.40, pp 1189-1203.

Sugawara, K and Obara, Y. 1999, Draft ISRM suggested method for in-situ stress measurement using the compact conical – ended borehole overcoring (CCBO) technique, *International Journal of Rock Mechanics and Mining Sciences*, Vol.36, pp 307-322.

Stas, L, Knejzlik, J and Rambousky, Z. 2005, Conical strain gauge probes for stress measurement, *In proceedigs Eurock 2005 - Impact of Human Activity on the Geological Environment*, Leiden: A.A.Balkema Publishers, pp 587-592.

Stas, L, Soucek, K, Knejzlik, L, Waclawik, P and Palla, L. 2011, Measurement of Stress Changes Using a Compact Conical- Ended Borehole Monitoring, *Geotechnical Testing Journal*, 34(6), pp 685-693.

Soucek, K, Konicek, P, Stas, L, Ptacek, J and Waclawik, P. 2013, Experimental Approach to Measure Stress and Stress Changes in Rock ahead of Longwall Mining Faces in Czech Coal Mines, *In Proceedings of the 2013 Coal Operators´ Conference*, Wollongong, Australia, 14-15 February, pp 115-123.

Konicek, P, Ptacek, J, Stas, L, Kukutsch, R, Waclawik, P and Mazaira, A. 2014, Impact of destress blasting on stress field development ahead of a hardcoal longwall face, *In Proceedings of the International Symposium of the International Society for Rock Mechanics*, EUROCK 2014, Vigo, Spain, 27-29 May, A. A. Balkema, pp 585-590.

Konicek P, Soucek K, Stas L and Singh R. 2013, Long-hole destress blasting for rockburst control during deep underground coal mining, *International Journal of Rock Mechanics and Mining Sciences*, Volume 61, pp 141–153.

Longwall Salvage Roof Fall Recovery Experience

Richard Campbell

ABSTRACT: Longwall (LW) salvage and relocation operations are a high-pressure period for all mine personnel, where any delays in the scheduled works are unacceptable, have a significant financial penalty and can increase mine worker's exposure to hazardous conditions. Successful longwall salvages rely on geotechnically controlled conditions, which allow for rapid shield recovery, often in dynamic environments. Recent longwall salvage at Mine A in Queensland experienced long operational delays, abnormal strata conditions, weighting events and shield convergence, culminating in a significant fall of ground outbye of the e-frame. This paper presents a case study of the geotechnical and operational conditions leading up to the fall of ground. In addition, some of the challenges faced and specific details of the fall recovery methods, successfully employed, are discussed, which allowed the safe and efficient resumption of salvage operations.

INTRODUCTION

Over many years, as the result of significant research and operational studies, numerous geotechnical roof support design methodologies have been developed for coal mine strata control. Each method, whether it's based on empirical, analytical and/or numerical methods, relies on understanding the geotechnical environment, applicability of the model and induced changes as a result of mining. As an industry progress in this field has been rapid and success is evident, with increasing design certainty and decreasing risk, hence it is possible to mine increasingly challenging deposits, safely and economically.

Longwall salvage situations however, remain an area where the risks are consistently present in terms of actual geotechnical understanding. These inherent risks affect the ability to design with absolute confidence and reduce the geotechnical control of the strata during salvage operations. Much of the geotechnical risk is actually due to logistical issues, such as time, equipment selection and ventilation. Past experience at the mine in question, or adjacent mines, remains the benchmark for "design". Longwall moves, being complex and unavoidable, are the least studied geotechnical challenges remaining in the industry. Perhaps the most concise summary and state of the art guideline for conventional recovery continues to be ACARP report C13022 by Hill (2006).

BACKGROUND, GEOTECHNICAL SETTING AND PREVIOUS EXPERIENCE

Mine A   operates a set of 2 m wide shields in a 146 shield face, which are designed for mining a thick seam with a cutting height range of 3.0 to 5.2 m. Planned cut height for LW salvage is 3.8 m.

The geotechnical inputs for the LW salvage design called for 1280 t capacity shields, 320 bar (80 t/m^2) set pressure, 380 bar high set pressure and 420 bar (100 t/m^2 yield pressure) and a tip to face of 650 mm while cutting a 1.0 m web. During this relocation all LW shields were scheduled to come out to the surface for major maintenance, including replacement of all leg cylinders and re-hosing.

Geotechnical setting

Depth of cover across Mine A ranges from 80 m, close to the pit bottom, to in excess of 400 m in the down dip northern extents of the lease. The experience base of LW salvages is within the 100 to 180 m range, with the fall of ground occurring at a depth of 165 m. The LW operates by extracting the lower 4.6 m of the seam, maintaining a 0.6 m - 1.0 m banded coal roof beam. The strata about the target seam is characterised by a moderate strength immediate siltstone/shale roof overlain by moderately bedded, stronger siltstone and sandstone units. Figure 1 shows the general stratigraphic column expected in the area of interest and the typical strata strength for the seam section.

Analysis of the numerous boreholes across the lease indicates an average Coal Mine Roof Rating (CMRR) of 32 within the coal roof and 52 for the overlying stone roof. Figure 2 depicts the range of CMRR values in the data set for the coal roof and stone roof environments. Based on a study conducted

Director & Principal Geotechnical Engineer. Blackrock Mining Solutions Pty Ltd, E-mail: r.campbell@blackrockmining.net,
Tel: +61 4396-93266

by Mark and Molinda (2003), the coal roof can be classified as "Moderate to Weak" and the stone roof is classified as "Strong".
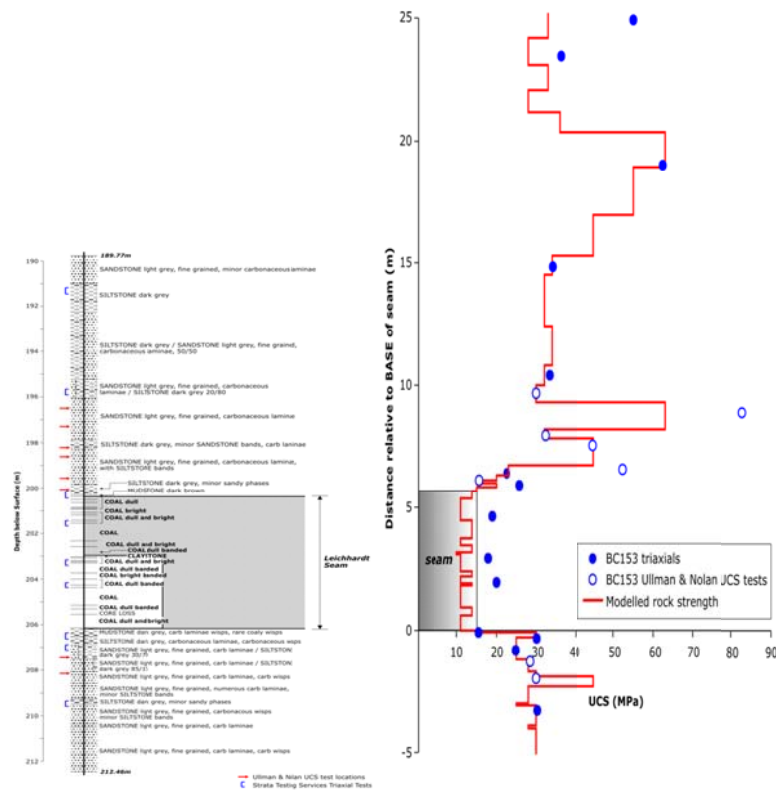
Figure 1: Typical stratigraphic column and strata strength profile
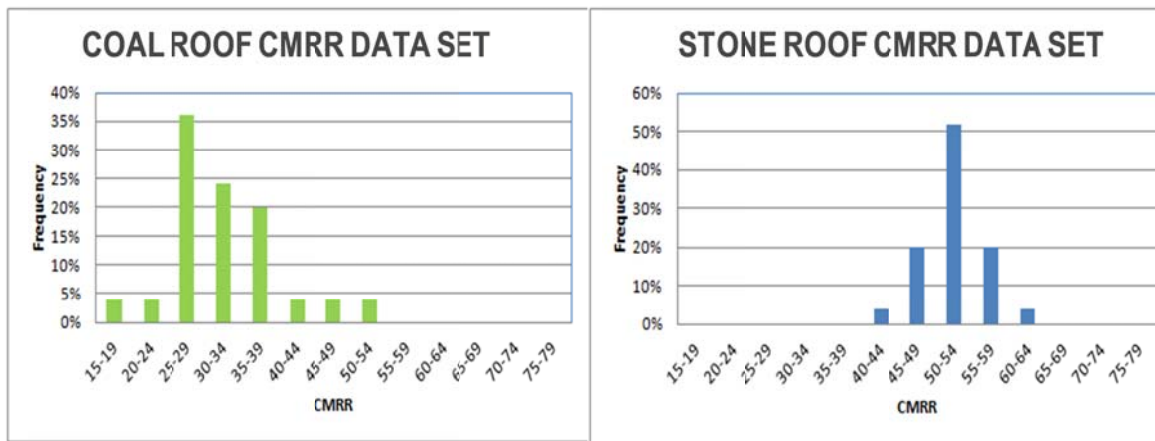
Figure 2: Summary of the CMRR data set

The target seam is heavily faulted with most LW blocks having full seam displacement structures, multiple fault zones and full seam displacement fault features being common place.

The roof strata are prone to periodic weighting cycles, typically at a 10 to 15 shear frequency. The common result of these frequent periodic weighting events, which are expressed as periods of rapid loading, and multiple yield events on shields in the affected zone, is an increased face spall and a roof gutter which runs parallel to the face – 600 mm wide and 500 mm high. Typically these events do not cause significant production issues. Figure 3 illustrates the typical time weighted average pressure TWAP & weighting events, loading rates and yield events leading up to the LW bolt up and salvage.
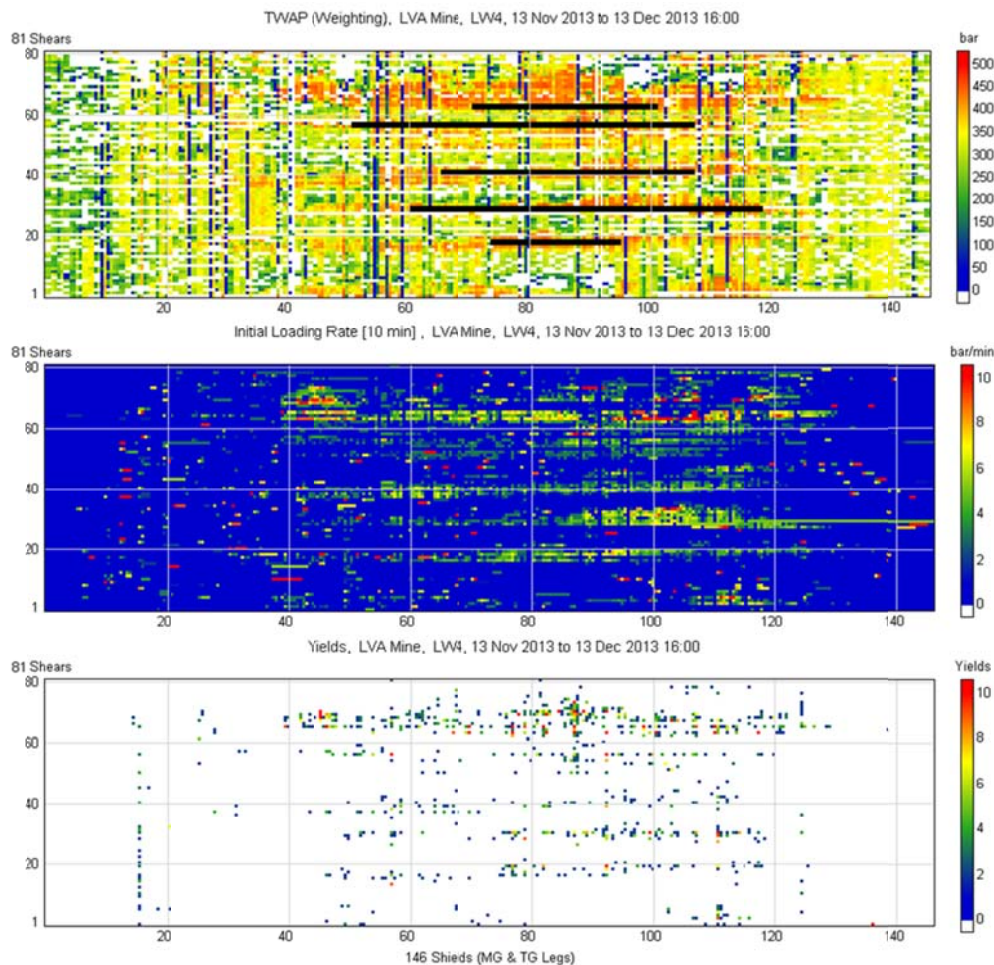
Figure 3: LVA data showing TWAP and weighting events, loading rates and yield events leading upto the LW bolt up and salvage

Previous experience

In the preceding six years the Mine A had undertaken five relatively successful and uneventful longwall relocations. Support plans and recovery strategies had been refined based on site experience, where a "leap-frog" shield recovery sequence was considered optimal, and the mine used a three shield E-frame. The tip to face for the forward shields was designed at 3 m, and 4 m for the back shields. The support strategy used bolts, 8 m cables and recovery mesh, with link'n'locks installed in place of each second shield, once removed, in normal conditions. A Trigger Action Response Plan (TARP) was in place for varying conditions during bolt up and shield recovery, including tell-tales and convergence monitoring. If conditions deteriorated, the salvage would convert to a sequential pulling sequence, with standing support in place of each shield recovered and rock-props used along the face side.

SEQUENCE OF EVENTS PRIOR TO THE FALL OF GROUND

The LW bolt up and salvage was scheduled to begin leading up to the Christmas period and be completed early in the New Year. Bolt up was completed using rapid face bolters. Shield recovery was from TG to MG with two chute roads in place for access and ventilation.

A time line for the LW salvage is detailed below:

- December 2nd - Mesh on
- December 12th - Bolt-up completed
- December 18th - TG shields removed
- December 23rd - Tear down completed
- December 23rd - Salvage of run of face shields started

- Shields 146 to 133 recovered
- December 24th to December 27th- operations stopped for Christmas break
- 27th December to 1st January - Salvage of shields 132 to 87 occurred as planned.
  o Convergence levels of 0-15 mm/24hrs recorded for shields, with the highest levels around mid-face. 200-300 mm total convergence recorded across the face
  o The goaf/roof behind the E-frame was noted as mostly standing from the E-frame to TG (approx.124 m). This is not considered typical behaviour. Some sag noted on the face side.
  o Tell tales (not adjacent to shields being pulled) showing minimal or no movement
  o Other visual indicators showed no indication of abnormal deterioration
- 1st January - During the salvage of shield 86 significant convergence of shields 75 to 50 was noted (adjacent to the MG chute road), resulting in clearance issues for the dozer.
  o Shields 86 to 80 recovered
  o Convergence rates of 40 to 70 mm per 12 hrs recorded.
  o Total convergence of 700 mm in mid face region
  o Tell tales (not adjacent to shields being pulled) showing minimal or no movement
  o Other visual indicators showed no indication of abnormal deterioration
  o Some areas required the floor to be shot out to get clearance
- 2nd to 3rd January - Significant weighting event on shields 50 to 75.
  o Shields 79 to 77 recovered
  o Shields in yield between 50 to 75, convergence of 200-300 mm occurring in 24 hrs
  o Total convergence at mid face now 1000 to 1200 mm
  o Tell tales (not adjacent to shields being pulled) showed minimal movement
  o Goaf behind e-frame still standing, estimated to have sagged down to 1.5- 2 m off the floor.
- 4th January – At 3.30am, during the salvage of shield 76, a fall of ground occurred from shield 55 to the E-frame (40 m).
  o Shield 76 under the fall
  o Shields iron bound from 75 to 64
  o Goaf remained open from E-frame to TG – slowly getting closer to the floor from its initial height of 1.5-2 m at the time of the fall

The fall was limited from the tips of the forward shields to the face line (approx. 3 m – 4 m wide). The face line had crushed out significantly leading up to the fall.   The height of the fall was estimated to be at least 8m (full length of cables visible and laser range finder used). Access and inspection of the fall was possible by traveling along the back of the remaining shields to the E-frame. Figures 4, 5 and 6 illustrate the extent of the fall.

Figure 4: Fall of ground from shield 55 looking towards the E-frame

Figure 5: Shield 76 under the fall – in the middle of the face road

Figure 6: View from the E-frame looking towards the MG

RECOVERY PLAN

Immediate actions taken

As with all falls of ground, the immediate concern is the safety of the surrounding environment. A detailed inspection was undertaken to define the areas of concern outbye of the fall and a stabilisation plan was implemented on the MG side of the fall, including the E-frame and adjacent shields. The main aim of this immediate stabilisation was to limit any further deterioration, provide a safe working place for the crews and allow a detailed recovery plan to be implemented. The inspection identified rapid deterioration of the roof and face from the fall outbye to around shield 27. Figure 7 illustrates the re-support installed outbye of the fall.

Immediate response included:

1. Standing rock-props along the face side from shield 25 to the lip of the fall to limit any shearing vertically along the block.

2. Install cable trusses from shield 25 inbye to the fall, with the cables angled well out over the face and the shield canopies.
3. Installation of 4m cables and dowels into the face side rib and also within the MG chute road, in order to strengthen the coal block.
4. Install monitoring devices down the length of the roadway and develop an inspection regime
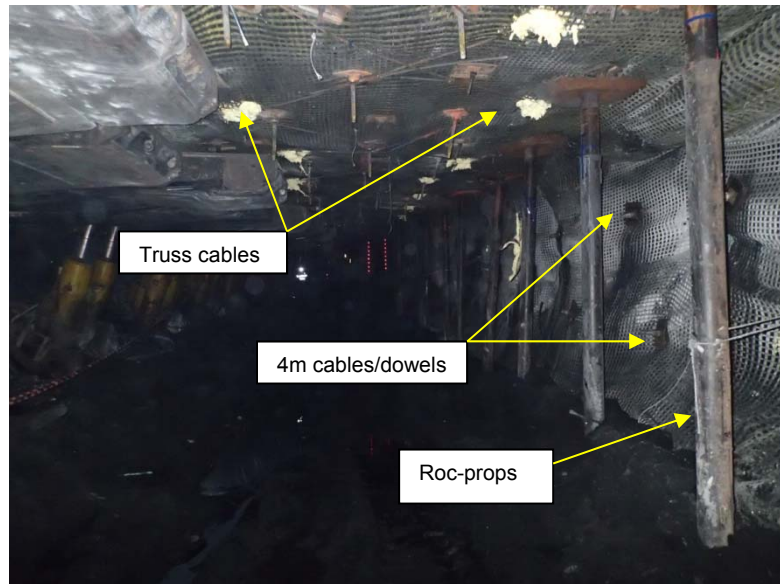
Figure 7: immediate response re-support outbye of the fall

Fall recovery plan

Immediately following the notification of the fall, the mine management formed an Incident Management Team (IMT) to ensure the correct risk based systems were followed and correct resourcing priorities were given to the fall.

The immediate task post-stabilisation was to gain an understanding of what the likely cause or causes of the fall were and define the mechanisms involved. This task was given priority, so as to give all stakeholders an understanding of the risks involved in the recovery of the remaining shields. The intended outcomes being:

- Gain an understanding of the cause of the fall in order to gain confidence in the recovery plan; and
- Determine whether a similar fall of ground was possible once salvage operations resumed.

A simple representation of the fall mechanism is depicted in the illustration below (Figure 8), where the mechanism described is very similar to that identified by Hill, D (2006) ACARP C13022.

Once the basic understanding of why the fall occurred was developed, a staged recovery plan was formulated with the underlying principal being;

- Provide a safe working environment, now and during salvage operations.
- The ability to resume LW salvage operations to recover all equipment.
- The final design had to be fit for purpose and allow normal salvage operations to recommence.
- No additional risks or impediments were to be introduced through remedial actions taken.

At this point in the operation many different strategies and ideas for how to go about the remediation works had been tabled; from the crews underground and adjacent mine sites, through to the head office staff - each strategy having its own merits and limitations. The IMT as a group worked to decide the actual stages to be taken based on the risk each task introduced. Each stage of the strategy was well-defined, quantifiable and included stop and go review points at the completion of each task so as to ensure the applicable design outcomes were achieved.

Each stage was subjected to a formal risk assessment and the workforce was kept up-to-date with regular briefings, including any changes to the plan going forward and revised completion dates. This regular forum gave each and every person the opportunity to raise any concerns.

Stage 1: Tensile cracking and abutment loading	Stage 2: Cantilever of roof and convergence of shields
Stage 3: On going convergence and crushing of the rib	Stage 4: Delamination on weakness plane in roof
Stage 5: Fall of ground	
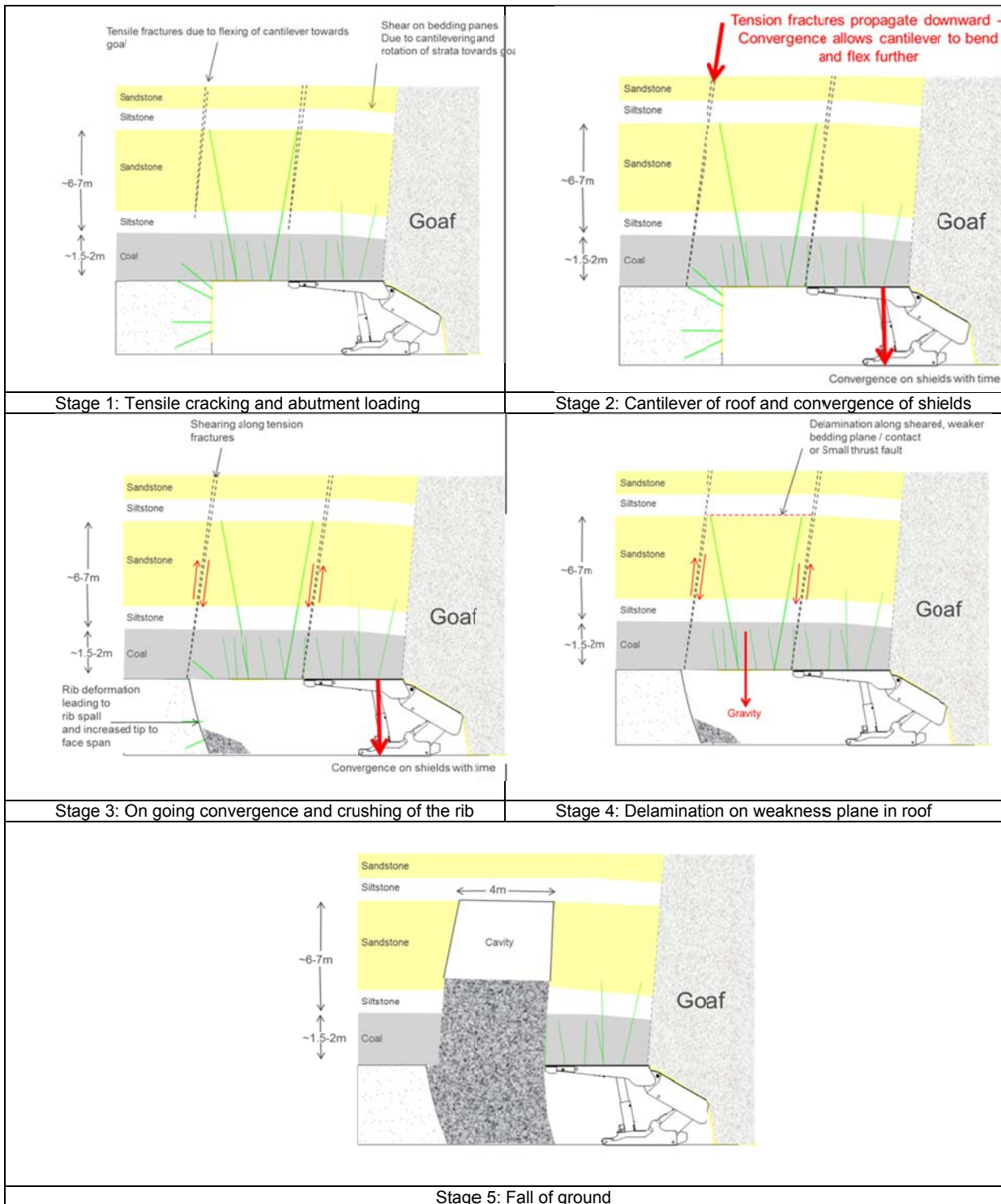
Figure 8: Failure mechanism and failure stages

The recovery plan was divided into five separate stages:

1)   Place a "cocoon" of foam around Shield 78, as it would be encased in the planned back fill operations., This material had to be weak enough to allow Shield 78 to be pulled free when the time came.

2) Shutter off the fall area in preparation for backfilling with a weak grout mix. Drill proving holes and install stand pipes to ensure the grout fills the cavity above the fall (Figure 9).
3) Pump a weak cement fill material from the ground up, in stages to fill the void and consolidate the fall material.
4) Re-mine and re-support the tip to face zone from the MG side of the fall to the E-frame, using a road header – ensuring the excavated profile is fit for purpose for the resumption of shield salvage.
5) Resume salvage operations.

Figure 9: Shuttering off the fall material in preparation for consolidation of the muck pile and backfilling of the void in the roof

During the consolidation and back filling of the void above the fall a set of quality assurance tests were developed, aimed to ensure that the void above and adjacent to the face was effectively filled, the grout had cured as planned and to determine the condition of the rock mass above the canopies and over the coal face. A detailed programme of UG drilling and core sampling was undertaken to provide this information. As the results became available, they were reviewed and where necessary action was taken. Samples of the grout batches were also taken during pumping and sent to laboratories for strength and density testing.

The drilling confirmed that the muck pile was sufficiently consolidated and that the voids within the shutter and above the roof-line were filled. In addition, results showed that the rock mass above both the canopies and over the block was competent.

In conjunction with the pumping operations, and in preparation for the roadheader mobilisation into the panel, a series of discussions were held regarding the best method to re-support the roof and face as the roadheader re-mined the tip-to-face area. Two basic strategies were decided on as being worthy of investigating.

These being:

- Re-mine through consolidated fall material and stand steel sets, or
- Re-mine through consolidated fall material and install roof bolts and truss cables.

Both ideas were subjected to a design study and were tested in terms of; effective support capacity, safety during installation and subsequent shield recovery, and practicality during shield salvage. The workforce was involved in developing work methods for both options, which included risk assessments being undertaken for each.

The outcome was to re-mine and re-support the fall material using roof bolts and truss cables - this being the technically preferable option which had the least risk in terms of potential injury during installation as well as providing a higher actual support capacity. In addition, the installation of bolts and cables provided the best end result when salvage operations resumed. Steel sets would inherently be exposed to significant damage during the recovery of shields, where their structural integrity could come into

question. Once damaged or knocked out of alignment the support capacity is reduced and potentially they can collapse or become entangled with the shields. Potentially introducing a significant hazard to the operation.

A design and applicable support plan was developed for the installation of this support, which included, a monitoring system to provide adequate warning of any movement or further deterioration in conditions. Furthermore, a quality assurance program was initiated whereby a series of short encapsulation pull tests were undertaken in both the consolidated fall material as well as the in situ rock mass either side of the consolidated fall material, in order to quantify the actual support capacity that would be generated.

Re- mining and re-support

Once the method was finalised and the excavation geometry and support plans were issued, the roadheader began mining through the shutter. Re-mining took place from the 20th January and had completed mining onto the E-frame on 16th February, including the recovery of Shield 76 from within the consolidated muck pile. Figures 11 to 14 illustrate the re-mining process.
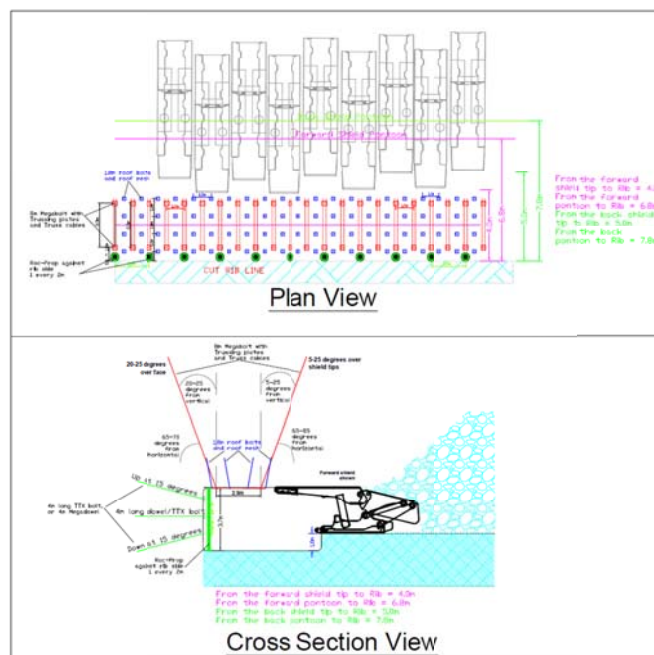
Figure 10: Support plan for re-mining through consolidated muck pile

Figure 11: Roadheader re-mining through the consolidated muck pile under the backfilled void

Figure 12: Consolidated muck pile and grout filled voids

Figure 13: Recovery of shield 76 from within the consolidated muck pile

RECOMMENCING LONGWALL SALVAGE OPERATIONS

Longwall salvage recommenced on the 18th February and was completed past the outbye edge of the fall on 22nd February. During this time there were no strata related delays, with minimal movement on tell tales installed through the consolidated fall material and no convergence recorded on non-ironbound shields. The goaf caved readily behind the E-frame as per normal conditions. All iron bound shields required the floor beneath the pontoons and bases to be shot fired, in order to provide some space to allow them to be pulled free. By the 28th February the last shields were taken off the face and the E-frame was disassembled.

LESSONS AND EXPERIENCE GAINED

Post recovery of the final remaining shields and prior to the resumption of LW operations in the adjacent block, several investigations and ICAM/Root Cause analyses were undertaken. The aim of these was to fully understand the root causes and future mitigation methods available, to avoid a repeat of the situation.

Areas assessed included:

1) The longwall move schedule and resourcing
2) Salvage equipment selection and availability
3) Geotechnical environment

4) Adequacy of the support plans, TARP's, monitoring and responses
5) Longwall system health
6) Delays in the salvage operations

Each aspect above was critically reviewed and evaluated, with the relevant outcomes documented in preparation for the next longwall salvage in order to avoid a reoccurrence.

CONCLUSIONS

Longwall salvages remain a time of elevated risk at every operation, where high pressure situations for all mine personnel are the norm.   Conflicting resource demands and delays in the scheduled works has a significant financial penalty and can increase mine workers exposure to hazardous conditions.

Successful longwall salvages rely on geotechnically controlled conditions which allow for rapid shield recovery in often dynamic environments. There is currently a lack of engineering tools available to adequately assess the conditions, or address changes as they occur, and a general reliance on experience from within the mine or adjacent operations is often the primary design tool utilised.

This paper presents a case study of methods used to recover a significant fall of ground on a longwall salvage face. The case study provides an example of where a staged, risk based method was successfully developed and implemented. The importance of a collaborative approach, including a thorough quality assurance program, is thought to be fundamental to the success of any salvage operation and to ensure the resumption of normal operations is achieved.

ACKNOWLEDGEMENTS

REFERENCES

Hill, D. 2006, Improving the Efficiency of Longwall Face Recoveries by Managing the Geotechnical Threats, *ACARP Final Project Report*, Project No: C13022.

Mark, C and Molinda, G M. 2003, The Coal Mine Roof Rating in Mining Engineering Practice, *Proceedings of the 2003 Coal Operator's Conference*, Wollongong, NSW, pp 50-62.

INVESTIGATION INTO A NEW APPROACH FOR ROADWAY ROOF SUPPORT DESIGN THAT INCLUDES CONVERGENCE DATA

Terry Medhurst

ABSTRACT: The results of a recent investigation into roadway roof support design using the Geophysics Strata Rating (GSR) are presented. A key aim of the investigation was to identify an ability to relate changes in roof conditions and support performance to our primary roof stability indicator, roof convergence. By developing these links, an ability to differentiate between operating factors such as support type and installation practice; and traditional geotechnical factors can be established. This paper outlines progress on the development of a convergence based roof support design method that is complementary to the current TARPS based strata management process. Some examples are provided.

INTRODUCTION

Mining at increasing depths of cover, in weaker and more variable strata conditions and with greater emphasis on optimisation of mining practice is driving the need for improvements in roof support design. Whilst existing methods have served the industry well, an ability to identify specific factors affecting roof support performance is required. Through recent ACARP projects we have developed the Geophysical Strata Rating (GSR) to be an objective measure of rock quality. GSR results can be modelled in 2D and 3D along with other parameters derived from geophysical logs such as the clay content. By developing such models at various mines it has become evident that this information may improve the link between roof behaviour and strata characteristics. Roof displacement monitoring provides the main source of information in most strata control management systems. GSR is also fundamentally related to the stiffness of the rock mass and thus can be directly linked to displacement based estimates of failure processes.

The investigation was directed towards developing an analytical framework to quantify/establish stress related impacts and/or strain/displacement correlations with support data. An analytical method was proposed as it can be more easily adopted as a site based tool. The proposed model is based on beam-column principles and incorporates bending, horizontal loading and shear. Using this model, estimates of roof convergence for various heights of softening (or surcharge loading) above a roadway can be obtained for a given support pressure. The model relies upon inputs from the Geophysics Strata Rating (GSR), roof bolt pull-out stiffness/load, H:V stress ratio and UCS. An ACARP funded study (Project C22008) was undertaken to assess the viability of the concept at a few sites to determine if a more comprehensive design methodology can be developed. The full results of the study are provided in the project report (Medhurst, 2014).

ANALYSIS METHODOLOGY

Strata characterisation

The Geophysics Strata Rating (GSR) is based on physical measurements that are related to the composition, density and elastic properties of the strata. This means that parameters such as strata modulus can be estimated from the GSR borehole analysis. The details of the GSR will not be repeated here but can be found in previous project studies (Hatherly *et al.*, 2008; Medhurst *et al.,* 2009). Table 1 shows an indicative range of rock quality as it relates to GSR.

GSR provides a continuous measure through the borehole column over the full height of the strata. This allows a measure of the change and distribution of rock mass quality over the supported interval. Such features are amenable to assessing changes in bending stiffness and section properties for beam analysis. Beam analysis requires section properties such as the 2nd moment of area (I), the position of the neutral axis of the beam (y) and a measure of strata modulus (Estrata). Previously, these have been chosen simply as a function of bolt length without regard to the strata. Various methods are available to

PDR Engineers Pty Ltd,E-mail: tmedhurst@pdrengineers.com.au*,Tel: (07) 4051 5599*

estimate in-situ modulus from rock mass quality estimates such as GSI, Q and RMR. Through previous work on development of GSR comparison with Q and other classification systems have been undertaken. Using these results, the current Bowen Basin data and in-house experience extraction a basic estimate of strata modulus has been developed where:

Table 1: GSR applied to Australian coal measures

GSR Range		Description
0	15	Very poor
15	30	Poor
30	45	Fair
45	60	Good
60	80	Very good
80	100	Extremely good

$$E_{strata} = 1.75e^{3 \cdot GSR/100} \quad \text{(GPa)} \tag{1}$$

The position of the neutral axis over a given beam thickness can be estimated using the parallel axis theorem. Using this approach the beam is treated as being comprised of many layers of different stiffness, which is determined from the GSR analysis. The true bending behaviour of the beam is then accomplished by transforming the dimensions of the beam parallel according to the ratio of the elastic modulus of the materials. This is the standard approach for the design of composite beams in structural engineering.

Beam formulation

For the purposes of this study a model was developed based on beam-column principles that incorporates both bending and axial loading (Timoshenko and Gere, 1963). The analytical procedure is based upon classification of four different types of roof conditions as shown in Table 2. The beam models require estimates of strata modulus and beam section properties which are obtained from analysis of GSR logs over the relevant bolting interval.

The beam models also include the influence of horizontal loading on deflection. The beam deflection due to bending is estimated using the standard method and the influence of the horizontal load (P) is treated as a multiplier (u) on both the deflection and maximum bending moment. The formulation for Type 1 (fixed end beam) conditions is shown in Figure 1.

The multiplying effect produced from the horizontal load is a function of beam thickness via the 2nd moment of area (I). Areas of high deformation/low confining stress occur at the boundary of the excavation, and are concentrated in the immediate roof. In this case there is a critical strata/beam thickness in which this deformation occurs that is not related to that defined by the bolt length, but more about the strata properties in the immediate roof. Previous studies conducted to estimate the stability of unsupported roadways in highwall mining found that for each set of roof conditions, there is a critical beam thickness at which failure occurs. This minimum thickness can be defined by a mechanism of snap-through at the mid-span (CSIRO, 1996) as shown in Figure 2.

If the span (roadway width) is known and an estimate of modulus is available from GSR then the critical thickness (t) for snap-though can be obtained. This critical thickness can then be used to estimate the multiplier (u) in the beam models. In other words, roof convergence caused by horizontal stresses is estimated based on a critical thickness for snap-thru of the beam rather than just conventional bending analysis.

In the case where stresses might be very high or the roof is very weak, then plastic beam analysis might apply, i.e. Type 3 analysis in Table 2. This is generally applied to beams of ductile material that do not ordinarily fracture under static loading but fail through excessive deflection. In this case the plastic

section modulus, Zp, is used rather than the elastic section modulus, Z = I/y. For this condition, the plastic section modulus is used (Roark and Young, 1975).

Table 2: Summary of beam analysis methodology

Case	Beam Type
1. Fixed end beam Moderate to strong roof conditions Minimal stress influences No jointing effects	
2. Propped cantilever Moderate to strong roof conditions Potential stress influences (guttering) and/or influenced by sub-vertical jointing effects	
3. Plastic fixed end beam Weak roof conditions characterised by potential yielding and inelastic roof behaviour	
4. Plastic propped cantilever Weak roof conditions characterised by excessive yielding, guttering and bedding plane shear	

Deflections

when load is in centre of beam

$$\delta = (y)_{x=l/2} = \frac{ql^4}{384EI} \cdot \frac{12(2\sec u - 2 - u^2)}{5u^4} \quad \text{where}$$

$$u = \frac{kl}{2} = \frac{l}{2}\sqrt{\frac{P}{EI}}$$

$$u = \frac{\pi}{2}\sqrt{\frac{P}{P_{Cr}}}$$

Maximum Bending Moment

$$M_{max} = \frac{ql^2}{8} + \frac{ql^4}{384EI} \cdot \frac{12(2\sec u - 2 - u^2)}{5u^4} P \quad \text{where} \quad I = \frac{t^3}{12}$$
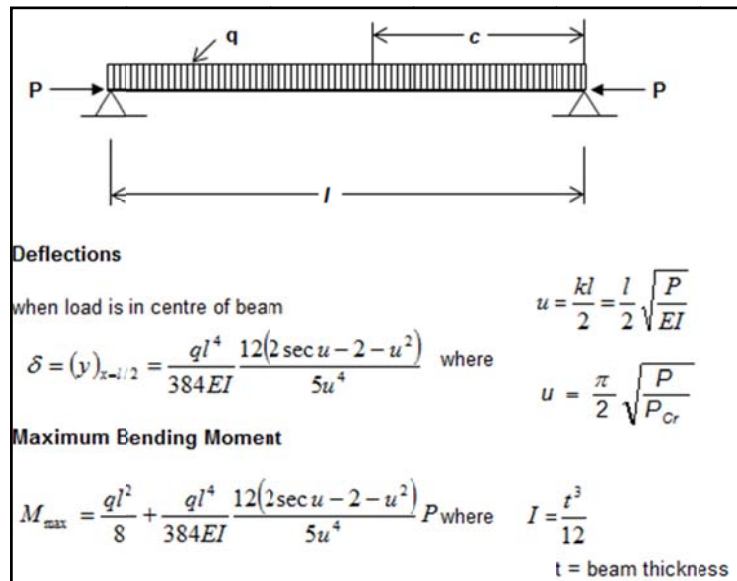
t = beam thickness

Figure 1: Beam formulation for Type 1 conditions

$$S = 2s = 2 \cdot \left[\frac{4}{3\sqrt{3}}\right]^{1/4} \cdot t \cdot \left(\frac{E}{p}\right)^{1/4}$$

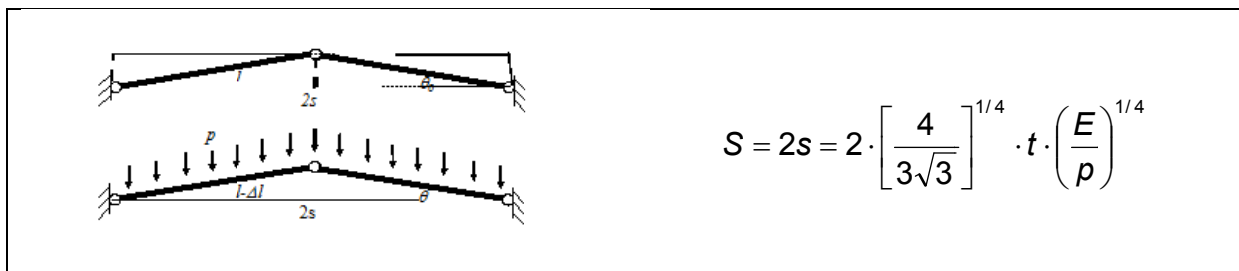**Figure 2: Definition of critical thickness for beam snap-thru**

By following through this analysis, it can be seen that roof deflections can be estimated from an estimate of vertical surcharge load (p), horizontal stress/load (P), GSR, and roadway width. The vertical load (p) is simply estimated by choosing the height (or range) of softening above the roadway and the horizontal load (P) by the normal in-situ stress regime and concentration factors about roadways.

In contrast to previous beam models used for support design, the aim here is to provide an analytical model that does not require estimates of cohesion, friction angle, tensile strength or other properties that are commonly difficult to measure or estimate. It can also be used to estimate load-convergence relationships across a range of roof conditions as a function of differing end constraints and includes a term to allow for increased deformation in the immediate roof due to localised failure. However in order to estimate roof convergence, the effect of the roof support must also be considered. Roof support has the effect of increasing roof stiffness, which is also usually not present in beam based analysis. Hence an ability to estimate the combined stiffness of the roof strata and roof support is required.

Support characteristics

In the case of a coal mine roadway, the above mentioned beam formulation can be used to estimate roof convergence as a function of height of softening (or surcharge loading) for a given support pressure. One then needs to estimate the change in stiffness of the roof beam as a function of the installed roof support. Brady and Brown (2004) provide detailed analytical solutions for rock-support interaction analysis and show that the support stiffness can be treated as two springs connected in series one being the stiffness of the roof bolt and the other the stiffness characteristics of the bolt/anchor system under pull-out load or so-called grip factor as follows:

Support stiffness

$$\frac{1}{k_b} = \frac{W}{N_b}\left(\frac{4L}{\pi d_b^2 E_b} + Q\right) \qquad (2)$$

Where   W = roadway width
   N_b = number of bolts or cables
   L = length of bolt or cable
   D_b = diameter of bolt or cable
   E_b = bolt or cable modulus
   Q = load deformation constant or grip factor of bolt or cable in mm/kN

The combined stiffness of the roof beam can then be treated as the strata stiffness and the support stiffness acting in parallel, which is the summation of the two. This provides the estimate of roof stiffness used for analysis.

Mark *et al.,* (2002), provides estimate of grip factors for fully resin grouted bolts in both Australian and U.S. coal mines. However Q values can also be obtained by short encapsulation pull-out tests or other related data. Thomas (2012) provides an outline of a series of lab-based tests on cable anchorages commonly used in Australia.

A final consideration is estimation of roof beam stiffness where roof failure has developed. In this case an estimate of strata stiffness in its residual state is used rather than intact strata stiffness. Previous experimental work on coal is used as a guide (Medhurst and Brown, 1998). In general terms a 50% reduction in stiffness is typically encountered in coal and strata of similar strength. This reduction was used for estimating roof beam stiffness in failure zones within the analytical model.

Pull-out load is an important parameter for any roof support element and there are a range of methods to estimate this. The yield capacity of the bolt or cable itself is one measure, or another that includes some measure of the rock strength itself is also common, depending upon the length of anchorage. Littlejohn (1993) provides one measure, which requires an estimate of the cohesive strength of the resin/rock interface. Farmer (1975) provides a similar but simpler expression based on the unconfined compressive strength (UCS) as follows:

P = 0.1·UCS·π·R·L (3)

Where   *P* = pull-out load
    R = borehole radius

L = bond length

The UCS can be obtained from relevant test data or estimated from sonic velocity derived values as is often used at most operations. Depending upon the support installation, the lesser of the bolt yield capacity or pull-out load is used.

Bolt placement

Several experimental studies in the 80's into the effectiveness of bolt placement showed that roof deflections reduce as the number of bolts increases, but it's effect becomes less significant after about 6 bolts/m. However, this effect is most effective when extra bolts are installed close to the roadway abutments (Spann and Napier, 1983; Stimpson, 1983).
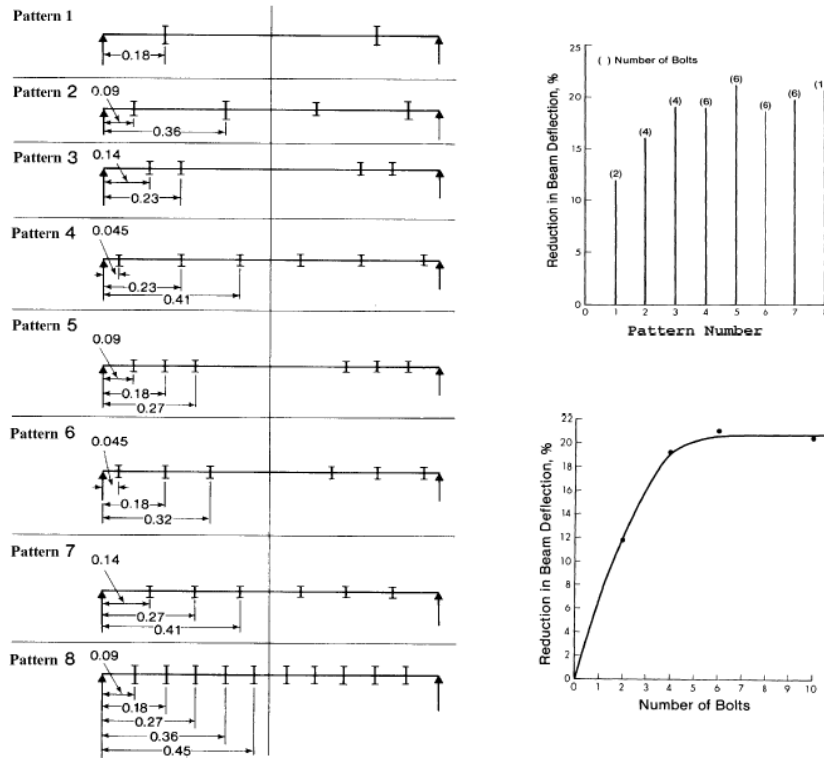
Figure 3: Effect of bolt placement on roof behaviour (Stimpson, 1983)

This effect is well known in structural engineering in which beams and suspended slabs are often thickened at the supports or in this case corners as an efficient way to increase stiffness and reduce shear stresses. These are known as drop panels and specific formulae have been developed to estimate deflections of these "stepped" beams (Yamamoto, 1985), as shown in Figure 4.

$$\Delta_{\mathcal{C}} = \frac{WL^4}{EI_2}\left[\frac{1}{384} - \frac{c^3(4-3c)}{24}\right] + \frac{WL^4}{EI_1}\left[\frac{c^3(4-3c)}{24}\right]$$
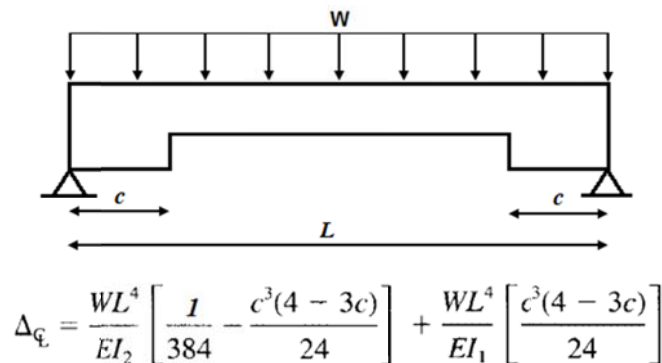
Figure 4: Deflection of fixed end stepped beam

If the distance (c) is taken as the position of the extra intermediate bolt, for example in a 6:2 pattern, then an estimate of deflection can be made using the stepped beam formula. This can result in up to a 20% reduction in roof deflection.

STABILITY ASSESSMENT

Ground response

Brown *et al.,* (1983) provided the first real analytical framework in which to calculate tunnel support pressure and roof convergence relationships, or ground response curves (Figure 5). It should be noted that ground response curves (GRC) are a generic tool in which to plot the results of stability analyses. They are not a design method as such, but are the simplest way in which to assess support pressure in conjunction with roof convergence.
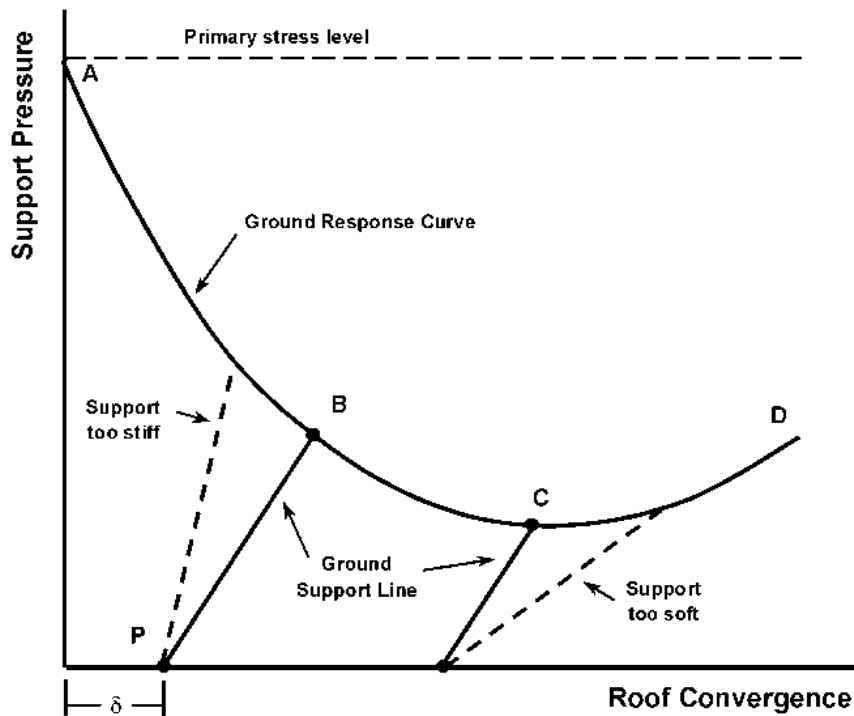
Figure 5: Ground response curve

The aim of the approach is to optimise support requirements, i.e. to determine the best load/convergence balance for a given set of conditions. Seedsman (2014) recently noted that the classic discussion of the GRC concept involves the early installation of stiff support. This in fact is not the intention of the GRC approach, but it is true that this concept has been used in the past to argue for stiffer support as a means to reduce roof convergence. Whilst such debate may have occurred it is important to reiterate that a GRC is simply the plotting of estimates of load and convergence from any particular analysis model.

A key aspect of GRC analysis is it can only represent the results from the model in which they were generated. In the case of elastic analysis under one set of boundary conditions, a single GRC can be generated bounded by the virgin load on the vertical axis and on the horizontal axis by a convergence limit bounded by the elastic state. In the progressive failure case, it can be envisaged that once one elastic state has been achieved and failure begins to occur, then a second set of conditions/properties/geometry may apply with a different curve; and a third and so on.

In order to overcome the limitation of elastic analysis in a practical manner, one approach might be to use an appropriate analytical model and then apply it at different stages in the loading and supported condition and plot it on a cumulative basis. Again, this is a simplified approach, but potentially avoids the requirement to undertake plasticity analysis whilst capturing increasing levels of deformation that cannot be estimated by a single elastic analysis. The general concept is shown in Figure 6.
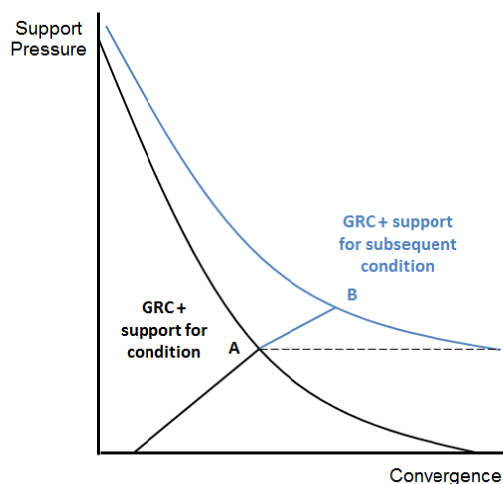
Figure 6: General concept of cumulative GRC analysis

Longwall installation road in weak roof

In this example, the roadway was driven in conditions where the immediate roof was weak, with a UCS ≈ 10 to 15 MPa and GSR ≈ 22 to 29. Support generally comprised 8 AX bolts/m and secondary support of 2 x 7 m Megabolts/m on the first pass and another 1 x 7 m Megabolt every 2m on the second pass. Roof conditions and monitored roof convergence is shown in Figure 7.

A key aspect of this approach is that by introducing a convergence measure then serviceability limits can be used as the primary design criteria. For example, secondary support may have been designed with a strength limit (Factor of Safety, FoS = 1.5), but roof convergence levels may be in excess of say 100 mm leading to the requirement for further support. The issue here is the uncertainty between the relationship between roof load, the size of the failure zone in the roof and convergence.

The approach here attempts to address this issue in which a new measure is introduced based on the support pressure generated that includes the effect of cumulative roof convergence. In this case an alternative term will be used called the Serviceability Factor (SF) = ratio of nominal support capacity to the estimated support pressure for a given roof convergence. This is intended to be more representative of the load generated in the roof, and to develop the relationship between observed conditions and the ability to assess the risk of instability.

Figure 8 shows the analysis using the supplied data. The extensometer data indicated that roof convergence was about 20 mm on first pass development. The corresponding analysis shows a height of softening (HoS) of 2 m at this convergence level as denoted by the intersection of the 2 m Primary GRC and the AX bolt support line (the intersections of the curves are marked by the dotted red lines). The outcome here suggests that the HoS may be around the 2 m level and some load sharing between bolts and megabolts would occur that develops about 17 t/m^2 capacity.
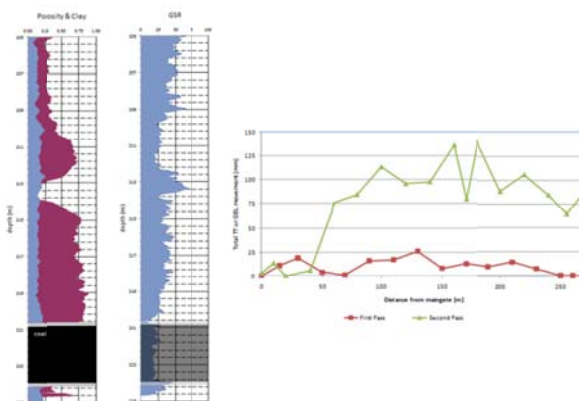
Figure 7: GSR and convergence for weak roof
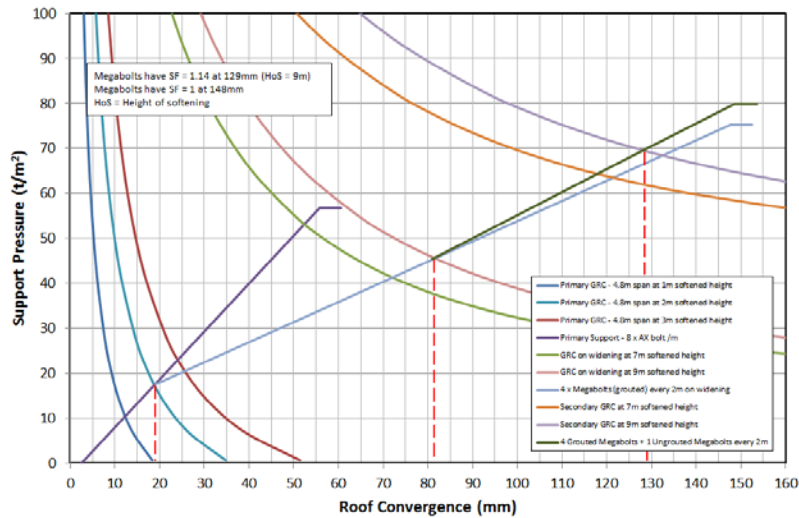
Figure 8: Stability analysis for weak roof

Upon widening roof convergence levels initially increase to about 80mm. The analysis suggests that this corresponds to a height of softening of about 9m upon widening with the initial four megabolt per 2 m pattern installed, i.e. prior to the additional tendon being installed. This is consistent with underground observations. Support demand at this point is around the 45t/m^2 level, however the HoS is above the length of the megabolts. At this point the potential for bedding plane shear needs to be checked. For the 7 m long tendons, the neutral axis of the beam was calculated to be 4.1 m above the roof using the GSR data. Based on a shear flow analysis for beams this yields a Factor of Safety (FoS) = 0.8 for the 4 megabolt per 2 m pattern. On this basis it can be presumed that the roadway would continue to deform.

The ground response characteristics for the 5 megabolt pattern (additional ungrouted tendon installed) are also shown in Figure 7. The analysis predicts that the roof would stabilise at the 129 mm level with a SF = 1.14 based on the 0.82 MN capacity of the megabolts. The megabolts were also estimated to reach serviceable capacity, SF = 1, at about 148mm of roof movement.

There are several factors that need to be considered to follow the analysis. Firstly, how to determine the height of softening upon primary development? In an operating environment, this can simply be based on telltale data or other monitoring information. This then provides the basis for prediction of the next stage of excavation. In the case of a virgin site, it could be based on previous monitoring data, comparison with roof conditions via GSR, or other geotechnical data.

Type 3 was initially selected for primary development since GSR ≤ 30, i.e. poor roof (Table 2). The reason to choose Type 4 for widening is based on the extent of damage that developed in the roadway, indicated by either large values of monitored roof convergence and observed damage or the calculation check on shear flow high in to the roof strata. Alternatively, the ratio of GSR/σh, i.e. ratio of GSR to horizontal stress can be used as a trigger for assessing whether roof softening is likely to be above the primary bolt horizon. In this and other examples, GSR/σh < 3 has been found to provide a useful threshold.

The second issue becomes checking the adequacy of the secondary support. Again, monitoring is the first option. The alternative, however, is to check the potential for bedding plane or horizontal shear in the roof as demonstrated. The beam analysis here provides some indication of the zone of maximum shear and provides an estimate of the load generated. This can be checked against installed/designed capacity. The criterion being that the roof would stabilise when the FoS ≥ 1 for horizontal shear and the Serviceability Factor SF ≥ 1. It is noteworthy that shearing of megabolts did occur in the roadway. Discussion with staff indicated that significant movements were recorded above the 4.5m GEL and some above the 7m GEL extensometers.

Intersection in strong, jointed roof

In this example, the roadway was driven in conditions where the immediate roof was strong with a series of intersecting joints, with a UCS ≈ 47 MPa and GSR ≈ 62. Roof support consisted of 6 x 1.8 m bolts/m

plus 2 x 4 m superstrands every 2m. Bowen cables (6m) were installed at intersections. Roof conditions and monitored roof convergence is shown in Figure 9.

Figure 10 shows the analysis using the supplied data based on a Type 2 model (Table 2). The analysis includes the initial analysis based on the roadway width and the use of the diagonal span for the intersection. The extensometer results showed initial roof convergence up to 20mm at the 1.5 m anchor horizon. The corresponding impact on the superstrands is also present in the analysis. The loss of end constraint on the roof beam suggests that the HoS = 4 m could be reached in the roadways at about the 44 mm roof convergence level and the superstrands would reach serviceable capacity at about the 48 mm mark. This suggests that roof convergence in the roadways was probably around the 40mm to 50 mm level given that roof convergence later increased in the intersection, i.e. HoS was greater than 4m and might have increased up to 6 m.
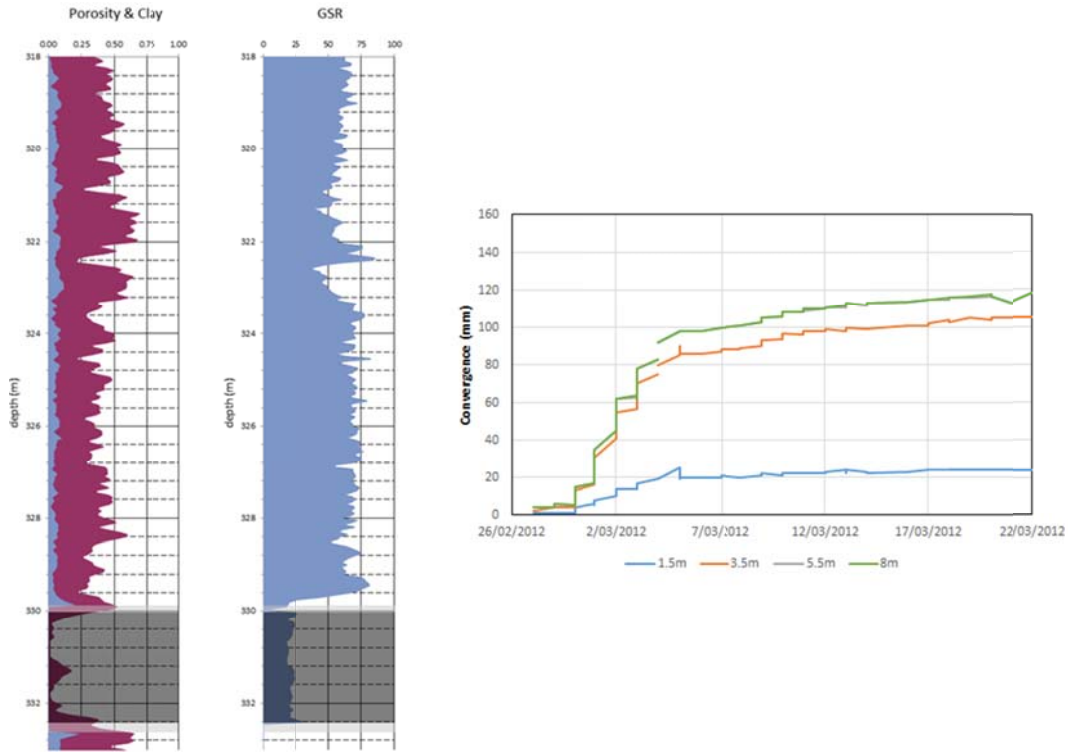

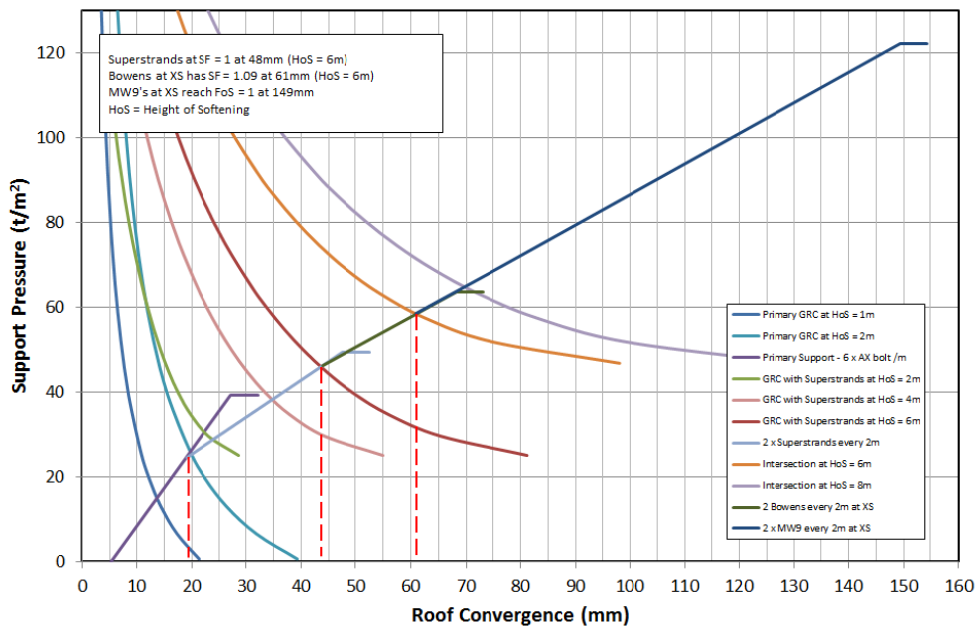**Figure 9: GSR and convergence for strong, jointed roof**

Figure 10: Stability analysis for strong, jointed roof

At the intersection roof convergence initially increases at a higher rate to about 80mm high into the strata before reducing to a lower rate from 80mm to 110 mm. The analysis suggests that the HoS =   6 m was reached at the intersections at about 60mm and the Bowen cables reached serviceable capacity at about 70 mm corresponding to a softening height of about 7 m. At this point it is understood that 11 m MW9 cables were installed at around 80mm displacement to stabilise the area.

The analysis shows that the installed support was unable to control the roof movement when it reached 70mm. At this point it is estimated that the softening height was above the cable length, i.e. > 6 m. Roof convergence increased relatively quickly to about 80mm then extended up to about 120 mm over a steady rate. This is reflected in the analysis as it appears that when the Bowen cable capacity was overcome at about the 70 mm mark, the MW9 cables were mobilised to maintain stability.

CONCLUSIONS

Through analysis of various examples, relationships were identified between roof conditions, depth, bolt placement, bolt length, support density and timing of installation. It allows an estimate of roof convergence and provides an ability to calculate load sharing between the support elements and within the roof itself. In particular the project has been able to quantify the relative roles of primary and secondary support and thus provide an opportunity to optimise the support cycle.

The approach provides the ability to investigate support behaviour in relation to different types of roof conditions and support strategies. This flexibility, whilst powerful for investigating different behaviour mechanisms, also requires further work in its application. Detailed stability analysis in combination with convergence monitoring has many obvious benefits. In some instances, the height of softening, choice of roof interval and associated trigger point may be easy to define. In other cases it will not, such as that governed by complex stress/structure affected zones or unidentified blocky roof behaviour.

The initial work has provided some indicators at to what may guide various inputs. For example, the GSR/σv ratio and particularly the GSR/σh ratio appear to be a useful first pass indicator of potential conditions when no other information might be available. In combination with GSR models, additional tools could be developed in combination with stress maps to allow better prediction and hazard planning assessments. Further research is proposed to extend this approach to a more general framework and design methodology applicable to all underground mines. In the interim, it appears useful for site specific applications provided monitoring data is available.

ACKNOWLEDGEMENTS

REFERENCES

Brady, B H G and Brown, E T. 2004, Rock Mechanics for Underground Mining, *Kluwer Academic Publishers*.

Brown, E T, Bray, J W Ladanyi, B and Hoek, E. 1983, Ground response curves for rock tunnels, *Journal of Geotechnical Engineering*, ASCE, Vol 109, pp 15-39.

CSIRO Exploration and Mining. 1996, Span Stability Assessment for Highwall Mining - Analytical and Numerical Studies, *Report 316F prepared for ACARP*, October 1996.

Farmer, I W. 1975, Stress Distribution along a resin grouted rock anchor, *Int. J. Rock Mech. Min. Sci*, Vol 12, pp 347-351.

Hatherly, P, Medhurst, T and MacGregor, S. 2008, Geophysical strata rating, *End of Grant Report, ACARP Project C15019*.

Littlejohn, S. 1993, Overview of rock anchorages, *Comprehensive Rock Engineering*, Vol 4, pp 413-450. Pergamon.

Mark, C, Compton, C, Oyler, D and Dolinar, D. 2002, Anchorage pull testing for fully grouted roof Bbolts, *Proc. 21st Int. Conf. on Ground Control in Mining*, Morgantown, WV, pp 105-113.

Medhurst, T. 2014, Investigation into roadway roof support design using the geophysics strata rating, *ACARP Report C22008*, December 2014.

Medhurst, T P and Brown, E T. 1998, A study of the mechanical behaviour of coal for pillar design, *Int. J. Rock Mech. Min. Sci*, Vol 35, pp1087-1105.

Medhurst, T, Hatherly, P, Zhou, B and Ye, G. 2009. Application of the geophysical strata rating in production settings, *ACARP end of grant report C17009*.

Roark, R J and Young, W C. 1975, Formulas for Stress and Strain, *5th ed., McGraw Hill*, 624pp.

Seedsman, R. 2014, Implementing a suspension design for coal mine roadway support, *Proc. 2014 Coal Operators' Conf, AusIMM*, pp 70-81.

Thomas, R. 2012, The load transfer properties of post–groutable cable bolts used in the Australian Coal Industry, *Proc. 31st Int. Conf. on Ground Control in Mining*, Morgantown, WV, pp 1-10.

Timoshenko, S and Gere, J. 1963, Theory of Elastic Stability, *2nd Ed., McGraw Hill*.

IMPORTANCE OF MONITORING TECHNOLOGIES AND *IN SITU* TESTING, WITH RELATION TO NUMERICAL ANALYSIS FOR GROUND CONTROL DESIGN

Charles Sweeney

ABSTRACT: As Underground (UG) coal mining companies look to reduce costs, whilst attempting to mine through increasingly difficult ground conditions, UG strata monitoring and testing data is becoming more and more important to acquire. The current monitoring technologies have their uses, but with mines getting deeper and entering new areas these laborious technologies are becoming too labour intensive and potentially subjecting personnel to potentially hazardous situations. With certain difficulties surrounding the implementation of electronic remote monitoring systems in UG coal mines, acquiring this data has seen little headway in terms of being able to expand the range of monitoring equipment being used in UG coal mines. There are a number of products on the market today which are effective in remotely monitoring strata deformation, however these can be very specialised and not entirely established or user friendly. Where an experience base of strata deformation is not available for a particular mine site, UG strata sampling and relevant *in situ* testing is able to compensate in the validation of numerical models. The data obtained from this testing can be used to build calibrated numerical models for site-specific ground control issues - to be used in predicting the behaviour of UG strata deformation. The rapid increase in computer power and affordability has seen enormous growth in the development of sophisticated computer codes. This paper discusses a number of limitations surrounding the collection of UG monitoring data and its use in mine design. The relevance of *in situ* data collection is also discussed in relation to the emergence of numerical modelling, as a tool to predict ground behaviour in UG coal mines.

INTRODUCTION

There are many different requirements for monitoring the environment in an Underground (UG) coal mine; from groundwater and gas drainage, to strata movement and seismicity. There currently exists little in the form of cost effective, reliable and user friendly remote monitoring technologies for strata control and its associated hazards. The majority of extensometer and tell tale instrumentation available today require mine site personnel to read the instrumentation directly, with the potential of putting themselves in harm's way. Limitations exist in the practical application of electrical remote monitoring equipment in UG coal mines, especially in explosion risk zones (ERZ0) where these devices are required to have intrinsically safe and explosion proof certification which can be difficult to acquire. With regard to strata monitoring instrumentation, limitations exist not only in terms of the equipment being used but also the ability to capture the changing geological conditions over short distances through extrapolation. With a lack of access and staffing/resources due to recent cut backs and initiatives to run low-cost mines, time intensive reading of UG instrumentation and conducting the appropriate analysis has led to an increasing need for remote monitoring and real time reporting. There are products on the market today which are capable of remote monitoring, however these are mostly in the developmental stage and can be expensive and impracticable. At this point in time, the limitations of using historical monitoring data for use in complex mine design scenarios is taken up through *in situ* testing of support elements in the UG environment as well as laboratory testing of UG samples - to be used to develop applicable predictive numerical models for site-specific UG environments. As mines enter new domains or green/brown field sites, an insufficient experience base exists. The development of predictive models is an alternative to this lack of monitoring data, until it can be readily obtained. The development of a field-based monitoring program is still essential in order to build up an inventory of relevant data and to warn personnel of pending movement during mining activities, as well as to validate numerical models.   In terms of support design, most mines will use a

combination of historical monitoring data (if available), together with calibrated numerical models, in order to design their pillar systems and strata support requirements.

This paper will detail the various monitoring techniques available for strata deformation and design, and discuss the rise in using *in situ* and laboratory test results to build calibrated numerical models for use in complex ground control design scenarios within UG coal mines.

AVAILABLE MONITORING TECHNIQUES

The development of monitoring technologies and techniques, to provide early warnings of hazardous strata conditions, has been underway for many years. The purpose of monitoring the underground environment during mining is to characterise and define the relevant failure mechanisms that are occurring around particular UG excavations. This is in order to provide an understanding of the design requirements and effectiveness of roadway support systems on the stability of the roadway, as well as to warn personnel of pending strata deformation. The following section details the available monitoring devices in UG coal mines today and highlights some emerging technologies in the field of remote monitoring of strata movement.

Extensometers

In-house mechanical extensometer devices have been used in parts of the USA for decades (Lannacchione *et al.*, 2005). Extensometers generally comprise of a series of anchors located at set intervals along a borehole, in either the roof or rib (SCT, 2000). Results are interpreted to determine the displacement/strain between anchors with time and face advance/retreat (SCT, 2000). Two types of extensometers are:

1. The sonic probe extensometer - for detailed monitoring and design purposes, and
2. Roadway deformation indicators for routine monitoring – for verification/checking purposes.

These instruments are used to measure deformation around a roadway – roof, floor and rib-sides. For design purposes the height of strata softening into the roof and depth of failure of the roadway sides is critical, but this information only comes with much experience and is available post-mining.

A play on the typical extensometer is the tell-tale (mechanical extensometer), which was first introduced in France in the 1970's (Lannacchione *et al.*, 2005) and is used to warn miners of strata movement. Tell-tales are considered a deflection monitor and are common place in any ground control management plan in most UG Australian coal mines. The definition of a tell-tale is typically a strata extensometer which incorporates a visual indication of strata movement into an excavation and is intended to provide a visible warning of excessive ground deformation (Bigby, *et al.*, 2010). Altounyan, *et al.*, (1997) found that uncontrolled falls of ground in British coal mines were reduced from 267 to six between 1990 and 1995, partially due to the use of tell-tales (Lannacchione, *et al.*, 2005). These instruments are currently used to gain widespread coverage of roof deformation throughout the mine, and are very common in Australian UG coal mines due to the low cost and low level of skill required for installation and monitoring. A limitation of these devices however, is that they are only capable of assessing the behaviour of a localised section of the immediate roof – generally within and above the bolted horizon. The geology and geotechnical conditions within any coal mine can change rapidly within a very short distance and therefore coverage around geological structures, for example, tends to necessitate an increase in instrument density. High roofs and stone/coal dust/fines however, can obstruct the view of the visual indicator making it difficult to monitor.   In addition, if movement is triggered, the routine reading of these tell-tales, in an area where the roof is readily deforming, can be hazardous to coal mine workers if the appropriate Trigger Action Response Plan (TARP) based actions are not implemented.

An intrinsically safe, remote reading tell-tale monitoring system has been developed which allows a number of tell-tales to be read remotely, along a linear line. This reduces the difficulty in monitoring these devices and allows for up-to-date data analysis and real time alarming of trigger levels, however depending on the density, it still only assesses the localised behaviour in the immediate roof around the tell-tale location.   High densities can be costly and impractical, as the system is still in the development stage and only allows a certain number of instruments onto the one 'daisy-chain' link of instruments. A huge benefit of any remote reading system is the ability to monitor the area in question, 24 hours a day/7 days a week, with alarms set to alert on movement triggers. The alarms need to be practical however, and relate to the appropriate mining practice. To date, remote reading systems have been implemented in Tailgates (TG's), installation faces left standing for a long period of time as well as in mine critical

infrastructure areas such as belt chambers, however the system was typically designed for the monitoring of the TG during LW retreat and is under development to be used in other parts of the mine as a long term monitoring system.

The GEL-extensometer, which is a 5 anchor tell-tale, has a potentiometer built into the casing to enable the instrument to be read from a distance with a readout box. These instruments are intrinsically safe, however they only have a small excitation of 0.96V. This amount of excitation severely limits its use as a remote monitoring extensometer – where with increasing distance the reduction in voltage and impedance will get too great to register. A further limitation for the potential of the GEL-extensometer to become a remote monitoring device in UG coal mines is the lack of an intrinsically safe data logger and stand-alone transmitting system able to be used in ERZ0 zones of an UG coal mine.

Several intrinsically safe wireless devices, for transmitting sigals, are currently available, however these are typically very expensive and not practical in relation to the variable and extensive network of monitoring instruments to be monitored in the elaborate network of UG coal mines. By utilising wireless devices in the UG environment, data acquisition and analysis time can be minimised significantly. The ability to set alarms of total movement on certain triggers is fundamental to any remote monitoring system. With the extent of UG mines continuing to escalate as mines go deeper and broader, having to read extensometers manually in every part of the mine becomes laborious and the data interpretation can be very time consuming.

The Roof Monitoring Safety System (RMSS) was established by the National Institute for Occupational Safety and Health (NIOSH) in 1999, as a means to remotely read mechanical extensometers. The RMSS is used to monitor the sag, or vertical movement of the roof. The instrument is still required to be read from UG however, reading the resistivity off a multimeter at a distance from the monitoring site, as opposed to monitoring it from the surface.

Emerging remote reading technologies

An emerging monitoring/prediction technique is that of monitoring for microseismicity, which has shown that there is some correlation between measurable rock noise and ground movement. The first evaluation of this technology was in the 1940's by Obert and Duvall, as a means of tracking general stability conditions (Ellenberger and Bajpayee 2007). The technique has recently been used, with varying levels of success, to predict roof falls.   Roof falls are generally preceded by a period of elevated microseismic activity, but not all periods of elevated activity result in a roof fall (Ellenberger, 2007).

Performance of UG microseismic monitoring systems depends on a number of inter-related issues, namely; maintaining ever increasing cable runs, preventing component damage from mining activities and avoiding signal degradation due to interference from mining equipment (Bajpayee *et al*., 2008). A potential solution for this is to use a surface-based monitoring system, where sensors are placed in boreholes above and adjacent to UG mine workings (Bajpayee *et al*., 2008). Mine-wide microseismic monitoring technology has the capability to collect and analyse a share of the total energy released as localised strata fractures prior to, during, and after rock falls (Ellenberger and Bajpayee, 2007). Despite an advantage of continuous detection and relatively low instrument-to-coverage ratio (geophones cover areas in the range of hundreds of square meters), the use of microseismic monitoring has been limited due to a lack of published data as well as high initial purchase costs (Ellenberger and Bajpayee, 2007). Both NIOSH and CSIRO in the United States are currently undergoing evaluation of this technique as a predictive tool.

A recent research thesis, by Logan, 2008, showed the diverse nature of tiltmeters to measure roof movement in the UG mining environment. Logan went on to explain how wireless tiltmeters, with inbuilt accelerometers, can be used on any surface with a measureable angle. This enables the tiltmeter to record angles of roof alignment change over extended periods of time, where change in readings can infer instabilities in the rock mass. By placing these tiltmeters on the roof mesh, a large area can essentially be monitored.

Acceptance of each monitoring technique is varying within the mining industry as a whole, primarily based on cost and ease of installation/monitoring, as well as intended life-of-mine. As discussed above, most monitoring technologies, especially remote reading monitoring systems, are presently in the development stage and are somewhat being held back by limited interest.

NUMERICAL MODELLING AS A PREDICTIVE TOOL

An accurate understanding of the complex behaviour of rock mass, and jointed rock mass in particular, has always been a difficult task for geotechnical engineers to ascertain. To provide a safe mining operation under complex and difficult conditions, reliable planning and design is of the utmost importance.   In order to compensate for the lack of detailed information able to be gained from current strata monitoring techniques, in relation to the prediction and warning of pending strata failure, numerical modelling has emerged as a popular tool to predict strata movement and to assist in proper strata control design and setting of TARP levels in most Australian mines Principal Hazard Management Plans (PHMP) for ground control.

Importance of reliable and accurate input data

Numerical modelling techniques provide for complex geometries and material behaviour, with the models that are generated being heavily dependent on accurate input data. Main sources for this input data are site investigations, and laboratory and field tests (Kumar *et a.l*, 2010).

The testing methods that are used to acquire the input data required, and which are useful in building relevant and accurate numerical models, are as follows:

Stress measurements

Knowledge of *in situ* stress is fundamental to coal mine ground control. Over the last 20 years, it has become clear that horizontal stress is a critical factor affecting roof stability in UG coal mines (Mark *et al.*, 2010). A number of theories have been proposed to explain the presence of horizontal stress, with a major break-through occurring in the 1970's which established the theory of plate tectonics and a dynamic earth crust (Mark *et al.*, 2010). The stress orientation in Australia is considered unique by World Stress Map (WSM) standards, as the stress orientation varies considerably between regions (Figure 1) (Mark *et al.*, 2010). The major stress orientation in the Bowen Basin coalfields in central Queensland is horizontal and orientated at NNE, with the vertical stress being the minor or intermediate principal stress (Mark *et al.*, 2010). In order to get accurate stress magnitude and orientation data, the overcoring method, utilising Strata Control Technologies ANZI 3-dimensional stress cell or the CSIRO cell, is typically used in Australian mines (Figure 2). Stress magnitudes and orientations will vary from site-to-site across Australia, where a general indication of the *in situ* stress field can assist in rock bolting design in virgin ground.   Mining induced stress on the other hand, will vary in direction and magnitude depending on the position with respect to previous mine workings (SCT, 2000). Hence increased specific testing of the mining induced stress, when designing roadways around existing goafs etc, will be a key factor for effective rock bolting design. The measuring of stress change around a retreating longwall can also be advantageous, in the effective design of maingate and tailgate support and for chain pillar design for longwall extraction purposes.
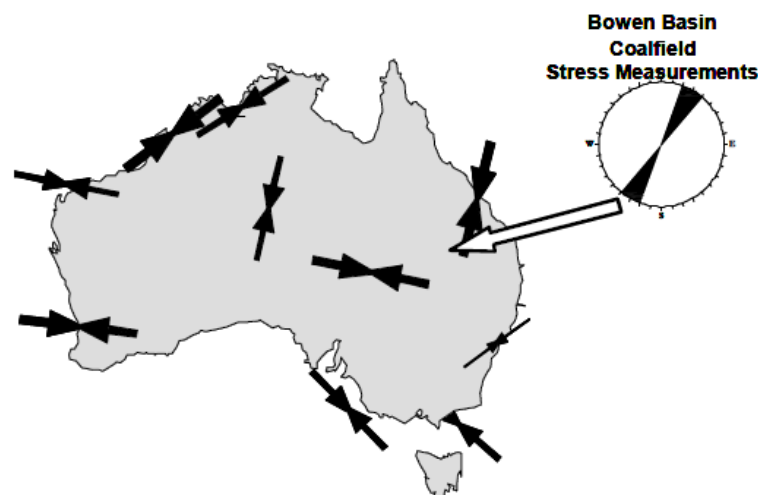
Figure 1: World Stress Map of Australia, compared with stress orientations determined from Bowen Basin coalfield stress measurements (Map after Hillis *et al.*, 1999; Stress measurements after Nemcik *et al.*, 2005)
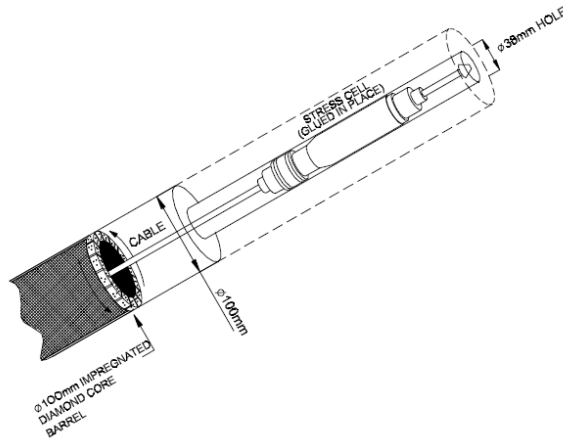
Figure 2: Overcore method for CSIRO HI 3-dimensional stress cell (SCT, 2000)

Key properties of coal and rock

Accurate coal and rock input data is paramount in building representative numerical models. There are multiple methods for predicting the *in situ* strength of coal/rock throughout UG coal mines. Sonic velocity is one of these methods, which is cheap, fast and easy to produce (Butel *et al.*, 2014). *In situ* testing of coal and rock samples collected from the UG mining environment is essential in correlating UCS with geophysical characteristics, to allow extrapolation of rock strength data about the proposed mining areas and also to assist in calibrating the applicable numerical models.

Rocks have a number of properties that determine their behaviour in the UG mining environment. An example of the variation of rock properties for different coal measure strata can be seen in Figure 3. In order to gain detailed knowledge of the key rock properties from any proposed mining area, a detailed testing program is required. The following key rock properties should be determined for proper design and modelling purposes (SCT, 2000):

- Unconfined compressive strength (UCS)
- Confined compressive strength properties of intact and failed rock (triaxial strength)
- Bedding plane properties
- Rock modulus properties
- Moisture content
- Tensile strength (if appropriate)
- Moisture sensitivity and mineralogical analysis of clay-rich strata (if present)
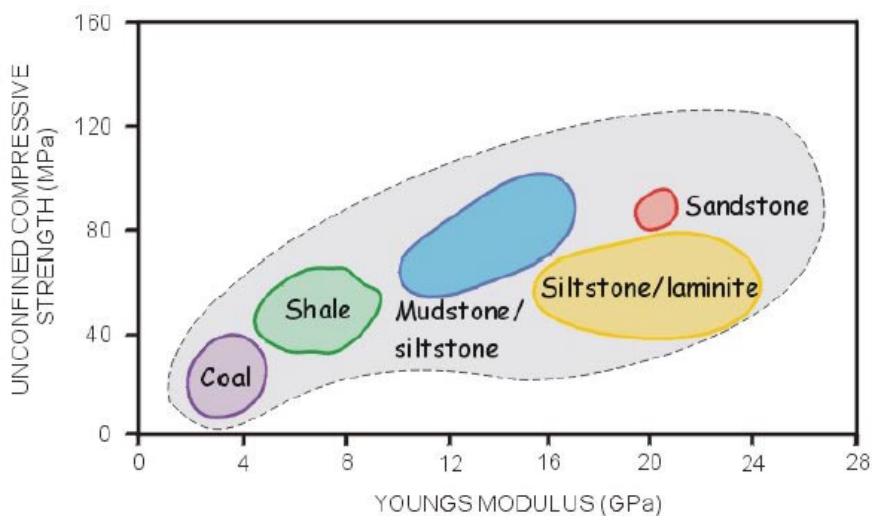
Figure 3: Examples of variation of rock properties for different coal measure strata (SCT, 2000)

Core sampling is the typical method of collecting samples appropriate for laboratory testing. The location and number of sampling sites would normally be determined following an evaluation of the existing data and a consideration of the likely variation in geological conditions within the proposed mining area (SCT, 2000). An example of the method of coring can be seen in Figure 4, whereby core is taken from both the floor and roof horizons. The boreholes are drilled with specific orientations to sample rock strength and bedding planes.
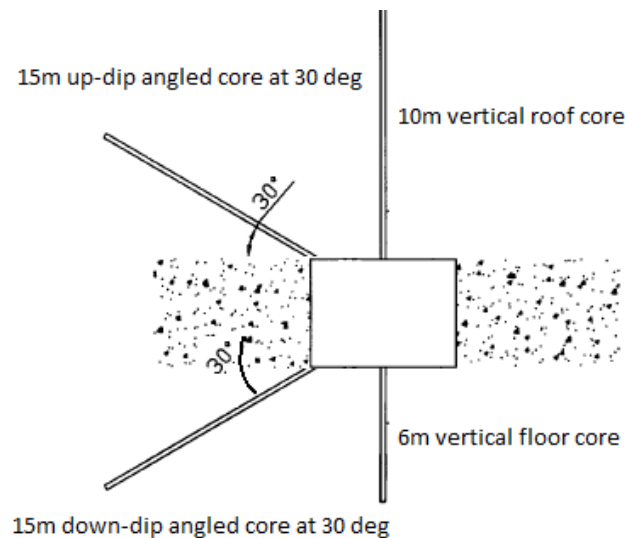
Figure 4: Typical coring requirements for rock property determination about the immediate roadway zone (SCT, 2000)

When testing samples in the laboratory, a number of things need to be taken into account to accurately represent the natural environment. Sample size and moisture content are two examples of this. Moisture content can significantly affect the rock properties of a wide range of rock types (SCT, 2000), therefore in order to obtain representative results the natural moisture content should be maintained prior to testing (SCT, 2000). Sample size is also known to have an effect on many rock experiments, where smaller sample sizes of a particular rock can exhibit much higher strengths than that of the *in situ* rock. The effect of sample size on specimens of coal can be seen in Figure 5, where the tested strength is required to be corrected i.e. reduced, compared with that of the *in situ* strength (SCT, 2000).
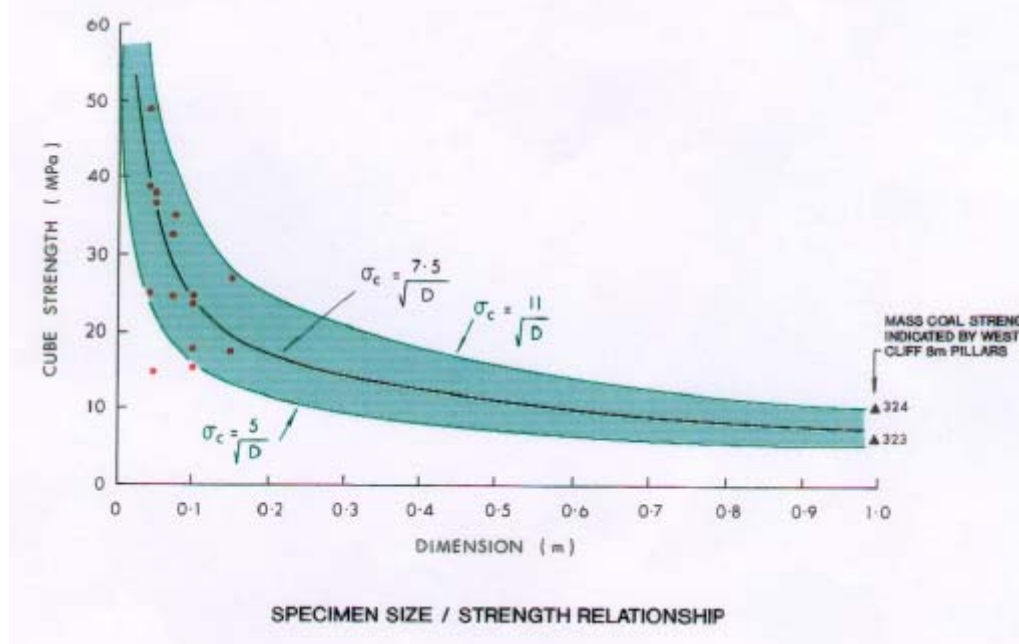
Figure 5: Sample size versus strength relationship for coal (SCT, 2000)

Any investigation program should also provide a detailed understanding of the immediate roof and floor lithology's, as this is an important component of rock bolting design and will give you an understanding of how the strata is likely to behave around any UG excavation in a coal seam.

Rock reinforcement performance characteristics

An assessment of load transfer and system stiffness is an integral component of effective reinforcement design. To assess the bolting system characteristics, a typical test is the Short Encapsulation Pull Test (SEPT).

The SEPT is an internationally recognised method of measuring the resin anchorage or bond properties of fully bonded roof bolts. The bond strength of a resin bonded roof bolt is a fundamental parameter determining its effectiveness. The stronger the bond, and the length of anchorage applied to the bolt, determines the resistance zone over which the full bolt strength is available to resist roof movement. With the modern high-strength, high-stiffness, polyester resins that are in use today, it has been found through numerous tests that a bond length of 300mm is appropriate for determining the resin bond for a standard roof bolt. In terms of system stiffness, in weak roof materials the resin-rock interface controls the failure mechanism whereas in stronger rock material the bond failure may occur on the resin-bolt interface. In order to measure the bond strength, it is necessary to shear the bond on the bolt-resin or resin-rock interface.

A schematic of the typical SEPT test can be seen in Figure 6 below. The data obtained from the SEPT test provides vital information on the shear stress capacity of the system. In correlation with laboratory test results, this provides a rational approach for the selection of consumables to suit specific reinforcement requirements.
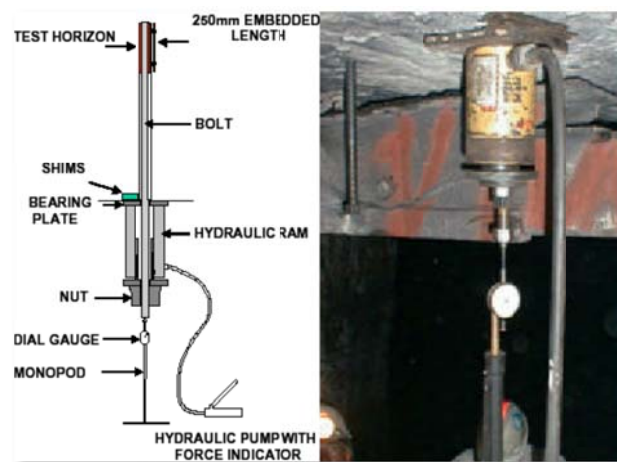
Figure 6: Schematic of typical SEPT set up

Applications of Numerical Modelling Technologies

One of the major problems that engineers are faced with in the geotechnical design of underground coal mines is the change in the displacement field around the coal seam and surrounding rock after extraction (Oraee *et al.*, 2013). Effective mine design has long been recognised as an essential element in establishing safe and productive mining operations (Karabin and Evanto, 1999). Numerous empirical and analytical methods have been developed over the years to analyse pillar stability and support design, with the work of Holland and Gaddy (1964), Obert and Duvall (1967), and Bieniawski (1984), to name a few (Karabin and Evanto, 1999). With the introduction of longwall mining, new methodologies were developed to address design considerations for that technology i.e. ALTS, ARMPS, (Larson and Whyatt, 2009).   Each of these technologies can provide a reasonable estimate of pillar strength and stability in certain conditions and simple mining geometries, and have unique underlying assumptions (Karabin and Evanto, 1999). In practice though, the geology of the mine can change dramatically and situations may arise that justify a complex mixture of pillar configurations with varying entry and crosscut widths, spacings, and orientations (Karabin and Evanto, 1999). To validate any model, the input properties should be calibrated to site-specific conditions and observations (Larsonand whyatt, 2009).

Numerical modelling is a tool to obtain detailed predictions of stresses and deformations around UG excavations (Suchowerska *et al.*, 2014). Typically, two categories of numerical modelling approaches exist – these are Continuum and Discontinuum.

Continuum

- Finite Difference Method (FDM) e.g.FLAC
- Finite Element Method (FEM) e.g. Phase2
- Boundary Element Method (BEM) e.g. LaMODEL, MAP 3D

Discontinuum
- Discrete Element Method (DEM) e.g. UDEC, 3DEC

A high level of detail is generally required for any particular scenario which warrants the use of a numerical model, but with rapid growth in computer power and affordability since the 1970's this has led to significant developments in numerical modelling computer codes. Sophisticated material behaviour, such as yielding of the rock mass strata, strain softening and non-associated plastic flow rules are now able to be modelled with a certain degree of accuracy. As mentioned previously however, confidence in numerical modelling as a predictive tool, especially relating to stress, is dependent on accurate field data.

The appropriateness of a numerical modelling methodology depends on the approach adopted and the ability to estimate the relevant key rock parameters. Site-specific information must be used to calibrate and assess the appropriateness of each methodology – for instance LaMODEL does not consider tectonic stress and therefore it might be a poor choice if high horizontal stresses are present (Larsonand whyatt , 2009). Field observations confirm that high horizontal stresses can cause instability to mine roadways. This being a 3-dimensional problem, a full 3-dimensional analysis is needed to capture the details of these damaging effects. Table 1 indicates the applicable pillar design methodologies for certain areas of the mine. Once an understanding of the likely strata failure mechanism is gained, with associated hazards, this will inevitably enable the engineer to design an effective strata support system to suit.

Table 1: Pillar design methodologies (Gale and Hebblewhite, 2005)

Pillar Type	Design issue	Applicable Methodologies
Subsidence protection	Load-bearing stability	experiential
		numerical
		empirical-mechanistic
		hybrid
Barrier pillars	Load-bearing stability	experiential
		numerical
		empirical-mechanistic
		hybrid
	Abutment stress protection	experiential
		numerical
		empirical-statistical
	Partition pillars	experiential
		numerical
Main development	Load-bearing stability	experiential
		empirical-mechanistic
		numerical
		hybrid
Chain pillars	Load-bearing stability	experiential
		numerical
		empirical-mechanistic
		hybrid
	Abutment stress protection	experiential
		numerical
		empirical-statistical
Bord & pillar (production)	Load-bearing stability	experiential
		numerical
		empirical-mechanistic
		hybrid
Fenders	Load-bearing stability	experiential
		numerical
		empirical-mechanistic
		hybrid
	Abutment stress protection	experiential
		numerical
Yield pillars	Load-bearing stability/yield	experiential
		numerical
		empirical-mechanistic
		hybrid
Highwall web pillars	Load-bearing stability	experiential
		numerical
		empirical-mechanistic
		hybrid

In choosing a methodology appropriate to the issue, the geotechnical engineer should work within the limitation of this methodology and understand the significance of the applied parameters. No one methodology should be used in isolation and therefore the numerical model that is generated should be calibrated against an appropriate empirical or analytical method and site-specific conditions.

CONCLUSIONS

With a lack of recent developments in the field of UG monitoring technology, particularly as mines venture into "unchartered territory" and mining through complex geological environments, the use of calibrated numerical models is becoming increasingly important. Numerical models need to be built with reliable and accurate input data, which is only achievable from sampling and testing in the UG environment and laboratory. Field monitoring during development also plays an enormous role in validating these models, as monitoring of the UG environment helps build a site-specific experience base. This field monitoring data is typically used for empirical and analytical design for simple mine geometries. With the increase in powerful 3-dimensional (3D) codes available today, which allow for complex 3D problems to be solved, multiple failure modes can be modelled around discrete block behaviour. Validation and correlation of these models to actual mining environments is critical to their effectiveness as a predictive tool. Numerical modelling is a vital tool in the prediction of ground behaviour in UG coal mines and to obtain a detailed extrapolation of stresses and deformations for complex mining geometries.

REFERENCES

Altounyan, P F R, Bigby, D N, Hurt, K G and Peake, H V. 1997, Instrumentation and procedures for routine monitoring of reinforced mine roadways to prevent falls of ground. In Proceedings, *27th Intern. Conf. of Safety in Mines Research Inst,1997, New Delhi, India,* pp 759-766.

Bajpayee, T S, Lannacchione, A T and Schilling, S R. 2008, Detecting strata fracturing and roof failures from a borehole based microseismic system, *27th International Conference on Ground Control in Mining*.

Bigby, D, MacAndrew, K and Hurt, K. 2010, Innovations in Mine roadway stability monitoring using dual height and remote reading electronic tell tales, *UG Coal Operator's Conference, The AusIMM Illawara Branch, University of Wollongong,* pp 146–160.

Butel, N, Hossack, A and Kizil, M. 2014, Prediction of *in situ* rock strength using sonic velocity, *UG Coal Operator's Conference, The AusIMM Illawara Branch, University of Wollongong,* pp 89-102.

Ellenberger, J L and Bajpayee, T S. 2007, An evaluation of microseismic activity associated with major roof falls in a limestone mine: A case study*, 2007 SME Annual Meeting and Exhibit, Denver, Colorado, preprint 07-103*, pp 1-5.

Gale, W J and Hebblewhite, B K. 2005, Systems approach to pillar design; Module 1 – pillar design procedures, *Final report, Volume 1 (of 3) – ACARP Project C9108, 68p.*

Hillis, R R, Enever, J R and Reynolds, S D. 1999, In situ stress field of eastern Australia, *Australian Journal of Erath Sciences,* Vol. 46, pp 813-825.

Karabin, G J and Evanto M A.1999, Experience with the boundary-element method of numerical modelling to resolve complex ground control problems, *Proceedings, 2nd International Workshop on Coal Pillar Mechanics and Design, NIOSH IC*, Vol. 9448.

Kumar, B R, Deb, D, Prasad, V N S and Siva Sanker, U. 2010, Numerical modelling – an effective tool for strata control in coal mines, *National Seminar on Underground Coal Mining*.

Lannacchione, A, Bajpayee, T and Edwards, J. 2005, Forecasting roof falls with monitoring technologies, *Proceedings, 24th International Conference on Ground Control in Mining, West Virginia University*, Morgantown, WV, Aug. 2-4, 2005, pp. 44-51.

Larson, M K and Whyatt, J K. 2009, Deep coal longwall panel design for strong strata: The influence of software choice on results, *Pages 75–87 of: Proceedings of the International Workshop of Numerical Modelling for Underground Mine Excavation Design*, Vol. IC 9512. Pittsburgh, PA: National Institute for Occupational Safety and Health.

Logan, K S. 2008, Analysis of wireless tiltmeters for ground stability monitoring, MSc thesis, Virginia Polytechnic Institute and State University.

Mark C.1991, Horizontal stress and its effects on longwall ground control, *Mining Engineering*, pp 1356-1360.

Mark, C and Gadde, M. 2010, Global trends in coal mine horizontal stress measurements, *10th UG Coal Operator's Conference, University of Wollongong & the Australian Institute of Mining and Metallurgy,* pp 21-39.

Nemcik, J, Gale, W and Mills, K. 2005, Statistical analysis of underground stress measurements in Australian Coal Mines, *in Proceedings of the Bowen Basin Symposium,* pp 117-122.

Oraee, B, Zandi, S and Oraee, K. 2013. A comparison of numerical methods and analytical methods in determination of tunnel walls displacement–A case study, *32nd International Conference on Ground Control in Mining http://icgcm.conferenceacademy.com/.*

SCT Operations Ltd, 2000. Coal Mine Rock Properties – Training Manual.

Suchowerska, A M, Carter, J P, Merifield, R S. 2014, Horizontal stress under supercritical longwall panels, *International Journal of Rock Mechanics & Mining Sciences*, Vol 70, pp 240-251.

Successful Construction of a Complex 3D Excavation Using 2D and 3D Modelling

Yvette Heritage[1], Adrian Moodie[2] and James Anderson[3]

ABSTRACT: Austar Coal Mine (Austar) successfully constructed an underground coal storage bin at a deep mine in challenging conditions. SCT Operations (SCT) was involved in various geotechnical assessments related to the bin excavation including vertical separation of the bin drift and underlying seam roadways, bin top area roof design and support and seam roof support at the bin base. Traditional methods used for determining support recommendations can be difficult to apply to complex three dimensional excavations. SCT used a combination of two dimensional and three dimensional numerical modelling using FLAC 2D and FLAC 3D to understand the key drivers and modes of failure about the bin excavation.The staged process of construction and an interactive approach between Austar and SCT enabled review and validation of the modelling process to occur throughout the construction. A key lesson from this program of work is that there is value in an interactive approach whereby site monitoring and review of model properties during construction provides early validation of the model. This ensures that natural geological variability, which can have significant impacts on rock failure and deformation, can be incorporated into the model as an ongoing process.

INTRODUCTION

Austar Coal Mine (Austar) is located approximately 10 km southwest of Cessnock in the Newcastle coal fields, New South Wales, Australia, as shown in Figure 1. Austar is owned by Yancoal and mines premium coking coal from the Greta Seam of the Greta Coal Measures at current overburden depths of approximately 500-550 m.

Figure 1: Location of Austar Coal Mine.

In 2012-2013, Austar installed a 1500 t underground coal storage bin for their expansion into Stage 3 of their mine plan consisting of Longwalls A7-A19. The underground coal storage bin was constructed by Mancala using a technique of raise boring then benching down in 1.5 m levels to form an elliptical 24 m high bin with axes 10 m and 14 m. A conveyor drift was firstly driven from seam level to the top of the

[1] *Senior Engineering Geologist, SCT Operations, NSW, Australia. E-mail: yheritage@sct.gs, Tel: +61 0429881 771*
[2] *Technical Services Manager, Austar Coal Mine (Yancoal), E-mail: adrian.moodie@yancoal.com.au, Tel: +61 02 4993 7293*
[3] *Senior Mining Engineer, Austar Coal Mine (Yancoal), E-mail: janderson@austarcoalmine.com.au, Tel: +61 02 4993 7362*

underground bin to gain access for construction. The base of the bin is at approximately 460 m overburden depth.

SCT Operations (SCT) was involved in design and support recommendations for various geotechnical scenarios relating to the bin installation. Specific assessments conducted by SCT include:

- Drift and Greta Seam roadway vertical separation
- Bin top roof support and design, and,
- Greta Seam roof support at the bin base.

This paper consists of a high level summary of the geotechnical approach used for the design and support recommendations highlighting key controls, model outcomes and model validation from underground monitoring.

BACKGROUND

The underground coal storage bin design consists of the bin, bin top area, bin base area and drift. The bin design is presented in Figure 2. The sequence of bin excavation consisted of the drift, followed by the widening and floor excavation of the bin top area, then the benching down of the bin, followed by the seam level widening of bin base area.
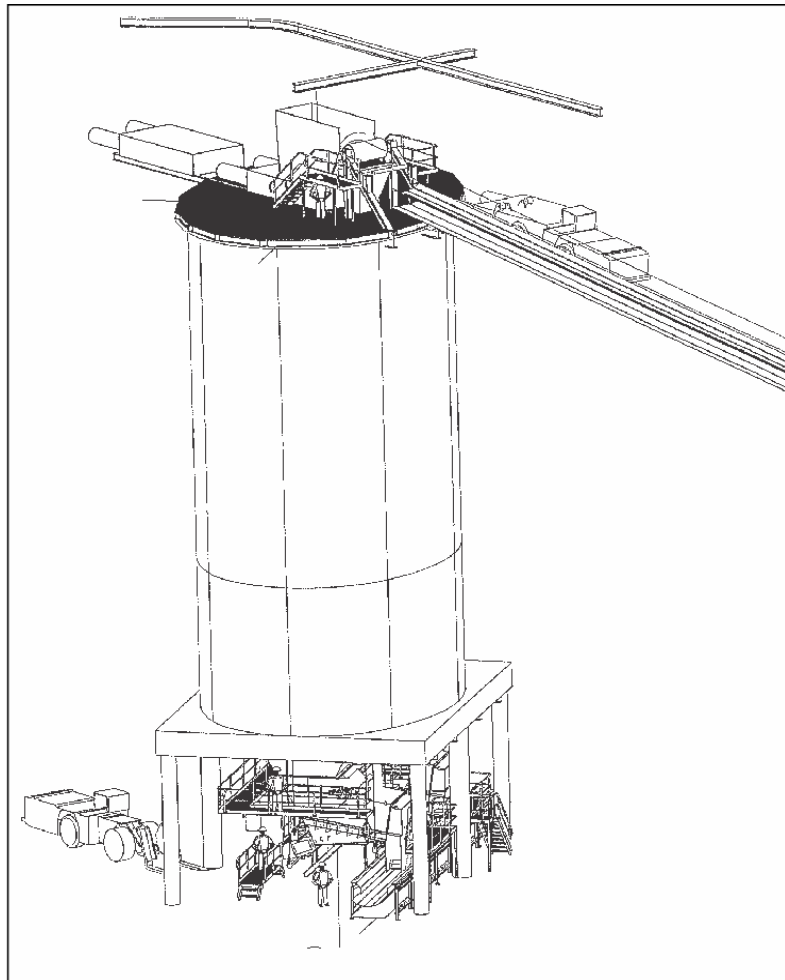
Figure 2: 3D diagram of underground coal storage bin arrangement. *(Courtesy of Arkhill Engineers.)*

The bin is an elliptical design with its long axis oriented in line with the maximum horizontal stress. The bin top area is an irregular shape of approximately 14 m by 20 m, with the drift entering approximately from the south. The bin top area design is presented in Figure 3a. The bin base area is an irregular area with an approximate roof span of 14 m by 8 m adjacent to the bin. The bin base area design is presented in Figure 3b. The location of the bin and its orientation to stress is presented in Figure 3c.

a) Bin top area   b) Bin base area   c) Bin location
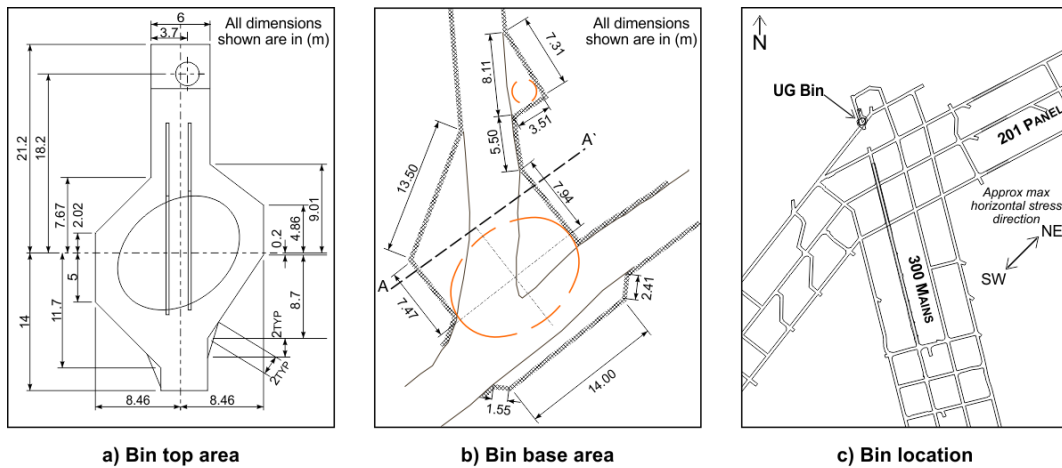
Figure 3: Bin location with bin top and bin base area dimensions.

SCTs investigations were staged with the sequence of bin construction where drift separation was conducted first, followed by bin top and then bin base investigations. The sequence of assessments allowed validation and refinement of the model inputs during the investigations.

METHODOLOGY

A combination of two dimensional and three dimensional numerical modelling, using FLAC 2D and FLAC 3D, was used to assess the key drivers for deformation about the bin and associated excavations. Project time constraints dictated a combination of two dimensional and three dimensional models.

Unless stated otherwise, the two dimensional modelling using FLAC 2D uses SCT's "in house" rock failure code based on Mohr-Coulomb criteria relevant to confining conditions in the ground. The code in FLAC 2D uses a coupled mechanical and fluid flow system to simulate rock failure and pressure effects A detailed description of SCT's rock failure routines used in FLAC can be found in a number of references, in particular Gale *et al.,* (2004) and Gale and Tarrant (1997).

The modelled strata is based on geotechnical properties from a combination of Austar's rock test data, geophysical relationships and prior experience. The model UCS based on geophysics and rock test data from Austar, for both the drift separation models and the updated bin models, is presented in Figure 4. The UCS is determined from borehole sonic velocity and laboratory UCS relationships empirically described by various researchers such as McNally (1987) and Hatherly *et al.,* (2008).

The three dimensional modelling used the constitutive model of the bilinear strain-hardening/softening ubiquitous joint model in FLAC 3D. Rock properties were again based on Austar's rock test data, geophysical relationships and prior experience. The three dimensional models were generally used to assess the stress distribution around the bin and to assess bolt loads. The three dimensional models were not used to assess detailed rock failure due to the larger element sizes required to run the models in a shorter time frame.

Numerical modelling using FLAC 2D was conducted by SCT to assess the deformation between the Greta Seam roadway and the drift to determine a minimum vertical separation to prevent roadway instability. The key design guideline is to keep the seam roof deformation and the drift floor deformation separate. A conservative separation is also advised due to unknown joints and structure.

SCT's original modelling recommended a minimum separation of a 20 m rock head between the seam roadway roof and the drift floor. This recommendation took into account an upper bound of estimated tectonic stress where the model results showed a barrier between deformation of the two excavations.

For the purpose of validation, models were run at roadway separations coincident with the actual excavated separations for A, B and C Headings of 12.5 m, 16.5 m and 21.5 m. These models included simulation of both roadway and intersection scenarios where the mine site monitoring and observations were found to be consistent with the model results.
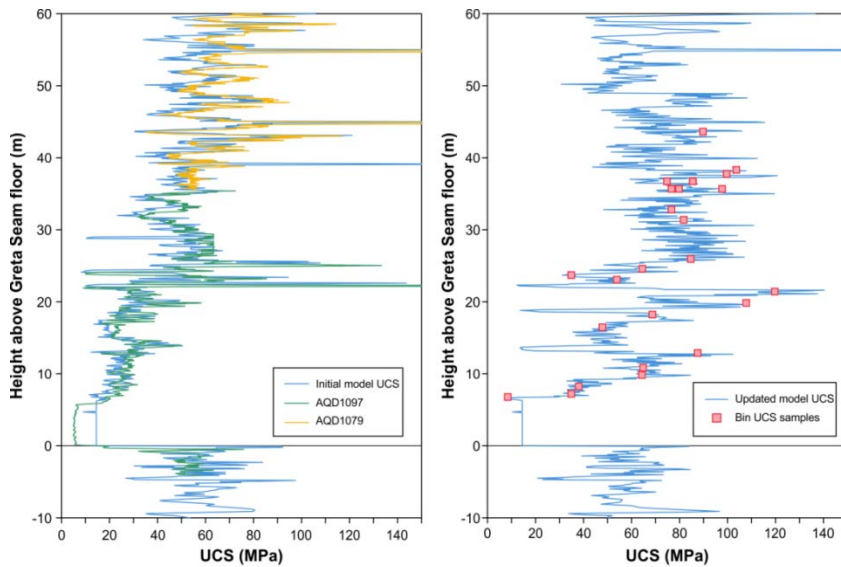
Figure 4: Modelled UCS for a) drift separation model, and b) bin models.

DRIFT AND ROADWAY VERTICAL SEPARATION ASSESSMENT

Pogo sticks in 1 cut-through between C and B headings monitored roadway convergence and showed convergence up to 120-140 mm. The model results for roadway convergence from 12.5-16.5 m separation were approximately 105-120 mm which is in the same order of magnitude as the pogo stick monitoring.

The primary modes of failure determined in the FLAC 2D models are shear failure and bedding shear failure. The roadway roof failure and drift floor failure are observed to connect for a 12.5 m separation while no connection is observed for the deformation of the 16.5 m and 21.5 m separation model. The mode of failure for the 12.5 m and 16.5 m models are presented in Figure 5. Models were also run with a widened roadway representing an intersection at seam level. In this scenario there is a connection between the intersection roof deformation and the drift floor deformation at 16.5 m separation, however a barrier exists for the 21.5 m separation.
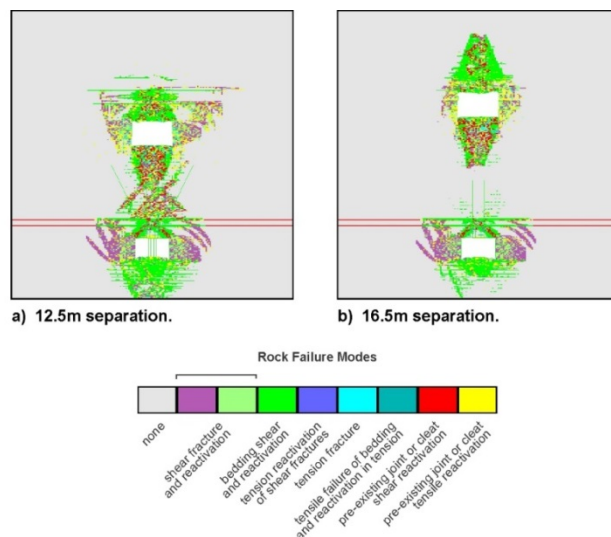
Figure 5: Mode of deformation for roadway interaction models at
12.5m and 16.5m and 21.5m separation.

The model results for vertical displacement between the roadway and drift are presented in Figure 6a. Negative displacements are downwards related to the roof of the coal seam intersection, while positive displacements are due to floor heave and failure in the floor of the drift. Figure 6b shows the vertical displacement relative to the seam roadway roof in order to compare the GEL extensometer and Tell Tale data. The monitoring data is consistent with the model data. The Tell Tales and GELs located between

C and B heading are between the B and C heading extensometer profiles within the models. The Tell Tale between A and B heading is between the 16.5 m and 21.5 m model extensometer outputs. The monitoring data for the seam roadway intersections is also consistent with the model extensometer results.

Key outcomes from the drift separation assessments are as follows:

- Numerical modelling provided a means for determining an appropriate vertical separation between the seam level roadways and drift
- Monitoring and observations validated the model outputs

BIN TOP ROOF SUPPORT ASSESSMENT

The bin top area is a roof expanse of approximately 20 m by 14 m with the long axis oriented with the major horizontal stress direction. SCT conducted numerical modelling of the 14 m and 20 m roof expanses using FLAC 2D to assess the deformation in the roof and determine appropriate support recommendations. The bin top area is a three dimensional problem, however due to time constraints the approach was limited to two dimensional representation whilst taking into account the limitations of the two dimensional model.
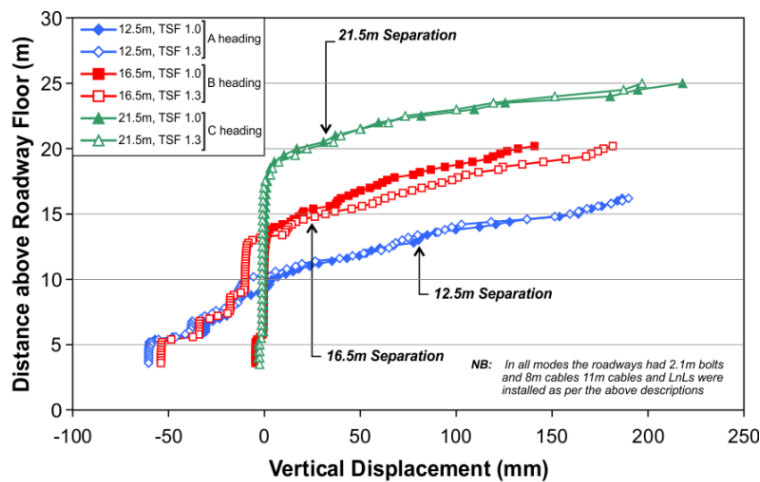
a) Vertical displacement for roadway roof through to drift floor for 12.5m, 16.5m and 21.5m separation.
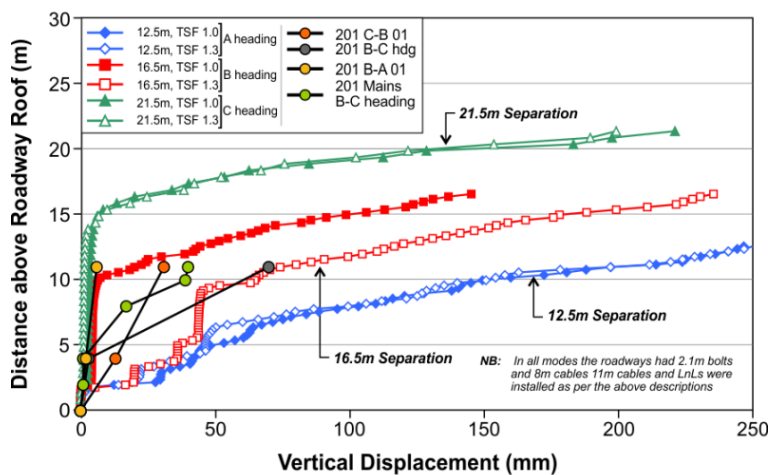
b) Roof displacement relative to the roadway floor for model and Tell Tale/GEL comparison.

Figure 6: Modelled and observed vertical displacement for roadway and drift separation.

The two dimensional models show the height of softening for the bin top roof at approximately 7-10 m for the 14-20 m roof expanse. Height of softening to this extent is problematic due to cables of similar

lengths not being able to pin back into intact strata. Figure 7a shows the mode of deformation for a 20 m wide bin top excavation with modelled primary and secondary support required to limit the roof deformation.

The height of softening is due to the reduction in vertical stress in the roof reducing confinement. The reduction in confining stress reduces the strength of the immediate roof and exposes the strata to the horizontal stress concentrations above the excavation. An arched roof model shows that the height of softening does not increase with the increase in roof height. The arched roof design removes the unconfined strata without redistributing stress. The mode of deformation for the arched roof of the 20 m roof expanse model is presented in Figure 7b where the secondary support is observed to extend into competent ground.
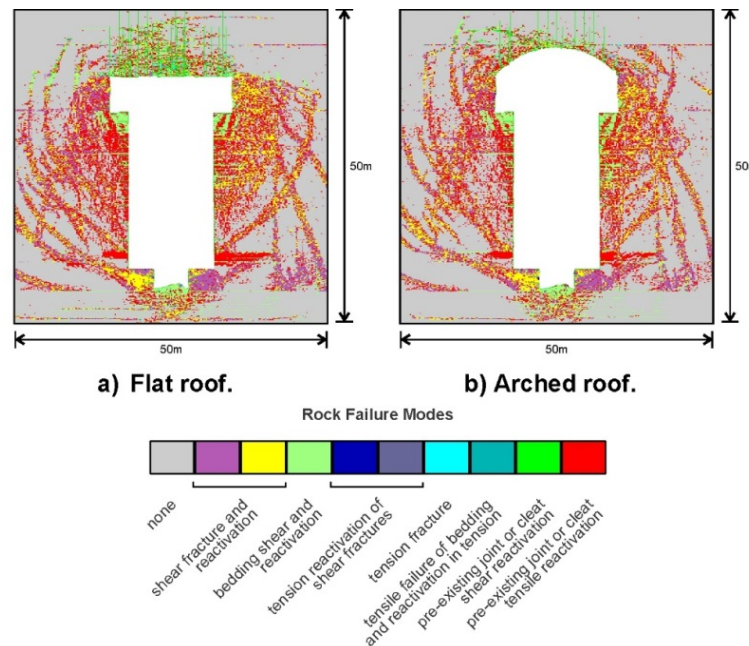
Figure 7: Mode of deformation for a 20m wide bin top section for a 14m wide bin.

Elastic models were run in FLAC 2D and FLAC 3D to compare the horizontal stress concentration in a flat roof, shown in Figure 8. Elastic models do not simulate stress transfer due to rock failure, however they provide an indication of the initial stress concentrations about the excavation. The stress concentrations in the two dimensional model are approximately 1.4 times the stress concentrations in the three dimensional model. The reduction in horizontal stress concentration in the roof indicates that the deformation may not be as much as observed in the two dimensional models and that the two dimensional models are a worst case scenario. The excavation is also expected to be controlled by its minimum width (such as an infinite roadway is). The deformation in the 14 m model is therefore expected to be more indicative of the three dimensional deformation than the 20 m model.
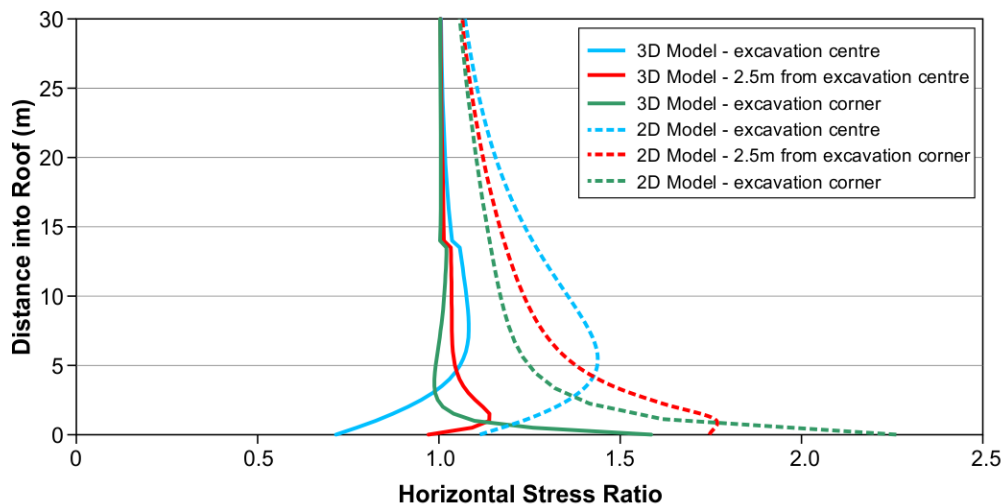
Figure 8: Horizontal stress profile for the roof of the bin top excavation.

The two dimensional model overestimates the stress concentration in the roof and the 14 m expanse model is likely to be the controlling expanse on the height of softening. Therefore a support pattern was recommended that involved a lower level of primary support (8 m cables at 2 m by 2 m grid), followed by a secondary support pattern (11 m infill cables creating 1 m x 1 m support pattern) if and after significant deformation occurs. This allows the strata to deform before adding in secondary support, thus adding confinement to the deformed strata using pre-tension cables, whilst also allowing a lower level of support to be used in the likely case that less deformation is observed than in the models.

Validation of the bin top modelling shows the arched roof is a stable shape with a maximum of 10 mm roof displacement measured, see photograph in Figure 9 of arched roof. The bin top deformation shows greater displacement in the modelling than observed which prompted a review of the rock model properties which included a new borehole drilled at the bin site. Rock properties were changed to fit the local rock test data with a higher Modulus to UCS ratio and less tectonic stress for higher strength lensing units. A 1x1 m constitutive Mohr Failure Model, to check the differences in rock properties, shows significantly less failure about the bin and bin top with the updated rock properties. There appears to be a different set of properties in the Branxton Formation that reduces rock failure in the bin top.

Figure 9: Panoramic photo of bin top area.

Key outcomes form the bin top modelling are as follows:

- The arched roof design provides a more stable roof shape than the flat roof
- The smaller roof span of 14 m diameter is likely to be the controlling diameter
- Two dimensional models are likely to overestimate deformation due to:
  o Overestimating the stress concentration in the roof, due to the two dimensional model not redistributing the stress in three dimensions, and,
  o Underestimating the rock strength due to not correctly modelling the confining stress in the third dimension
- The roof support recommendations allowed a lower level of support to be used with a response plan for additional support

SEAM ROOF SUPPORT ASSESSMENT AT BASE OF BIN

The bin base area consists of a roadway intersection widened to accommodate bin infrastructure. This creates a roof expanse of approximately 14 m by 8 m adjacent to the bin. The stress and deformation is a complex three dimensional problem where the widened intersection is unconfined in one plane and hosts bin deformation in the seam roof before widening of the seam intersection. The model approach used a combination of FLAC 2D and FLAC 3D to assess the key controls of roof deformation.

The impact of the bin excavation on the seam roof stability was assessed in three dimensions using a bilinear strain-hardening/softening ubiquitous joint model in FLAC 3D. The reduction in stress about the bin shows that the bin deformation extends across the span of the seam roof. The major and minor horizontal stresses show stress redistribution around the whole excavation leaving minimal stress transfer and confinement in the seam roof. Figure 10 shows a slice of the stress distribution at 1 m from the edge of the bin while at 5m from the bin a similar stress distribution where the stress transfer is near zero is observed.

a) Major horizontal (on plane).   b) Minor horizontal (out of plane).
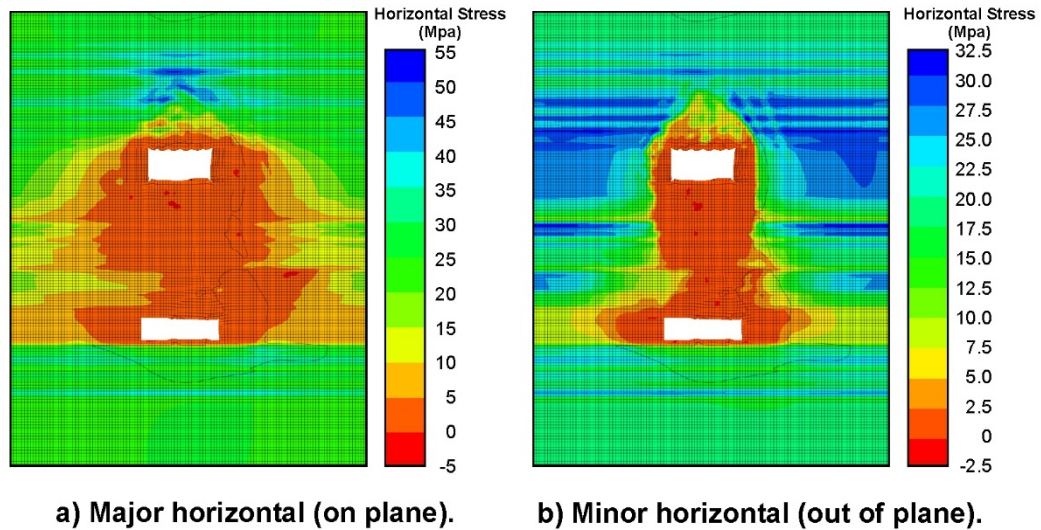
Figure 10: Stress redistribution about bin on vertical plane A-A' (See Fig 3b).

Two dimensional modelling was aimed to assess the seam roof deformation for expected residual rock properties due to rock failure from the excavation of the bin. The main limitation of the two dimensional modelling is that it assumes an infinite roadway, where as in reality the roof span is confined on one side and open on the other where it meets the bin. Residual rock properties and stresses input into the seam roof prior to the widening of the bin bottom roadways reduce the appearance of shear failure in the roof however due to the residual rock properties and the lack of confinement, large displacements were observed in the roof strata of the model.

A two dimensional plan view Mohr failure model was run in the horizontal plane to observe the stress vectors about the bin excavation. Figure 11 shows the major stress vectors running tangentially around the bin excavation with the minor stress running perpendicular to the bin surface. The vertical stress is also larger than the minor horizontal stress and fractures would therefore form in the vertical plane about the bin.
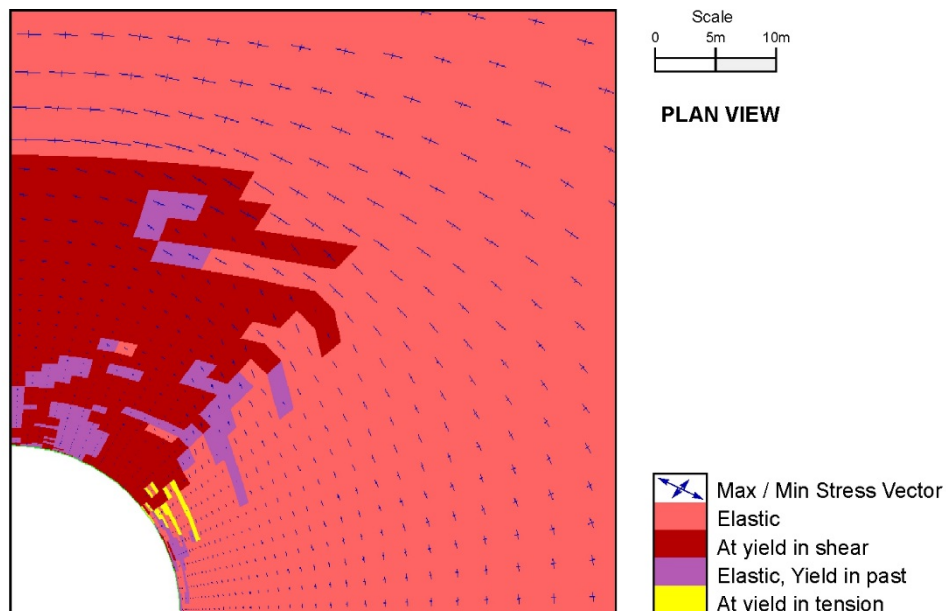
Figure 11:   Mohr Failure model with stress vectors around bin excavation.

Parallel horizontal 8 m cables extending from the bin wall at 3 m spacing per 1.5 m bench were recommended to provide seam roof confinement. Fifteen degree from vertical 10 m cables angled away from the bin were recommended at a 2 m by 2 m grid. The three dimensional bilinear strain-hardening/softening ubiquitous joint model shows that secondary support in the recommended

pattern does not yield, thus creating the required confinement on the vertical fractures formed about the bin.

Key outcomes from the seam roof support assessment at the base of the bin are as follows:

- There is very little confinement in the immediate roof and so there is a need to generate confinement with pre-tensioned secondary support
- Horizontal and angled vertical cables are required to confine the vertical fractures forming around the bin
- The models show that although primary support yields, secondary cables do not yield and therefore create the required confinement in the seam roof strata

CONCLUSIONS

A combination of two dimensional and three dimensional numerical modelling enabled assessment of a complex excavated volume to be assessed. Each model was designed to assess specific controls on deformation about the bin excavation, ensuring that the key controls of deformation were assessed.

The underground coal storage bin at Austar was successfully excavated and constructed without significant deformation. The deformation at the assessed locations adjacent to the bin was controlled by the support recommendations determined in this program of work.

This program of work highlights that numerical models are a valuable tool if used to their strengths and limitations.

A key lesson from this program of work is that there is value in an interactive approach whereby site monitoring and review of model properties during construction provides early validation of the model. This ensures that natural geological variability, which can have significant impacts on rock failure and deformation, can be incorporated into the model as an ongoing process.

ACKNOWLEDGMENTS

REFERENCES

Gale, W J and Tarrant, G C. 1997, Let The Rocks Tell Us, *Proceedings, Symposium on Safety in Mines*, The Role of Geology Nov. 24-25, pp 153-160.

Gale, W J, Mark, C, Oyler, D C and Chen, J. 2004, Computer simulation of ground control behaviour and rock bolt interaction at Emerald Mine, *in Proceedings, 23rd International Conference on Ground Control in Mining*, Morgantown, WV, Aug. 3-5, pp 27-34.

Hatherly, P, Medhurst, T and MacGregor, S. 2008, Geophysical Strata Rating, *ACARP Project C15019*, July 2008.

McNally, G H. 1987, Estimation of coal measures rock strength using sonic and neutron logs, *Geoexploration*, Vol. 24, Issues 4-5, Nov 1987, pp 381-395.

Risk-Benefit Analysis in Coal Mine Roof Support Design Using Stochastic Modelling Technique

Hongkui Gong[1], Ismet Canbulat[2], Mehmet S Kizil[1], Anna Mills[3] and Jason Emery[3]

ABSTRACT: Various roof support design methodologies have been used in Australian coal mines, which include analytical, numerical and empirical models. These models are mainly based on the deterministic approach in which a single factor of safety is calculated for the roof support design. The main limitation of this design methodology is that it fails to account for the inherent variations existing in rock mass properties and other roof reinforcement elements. To overcome this issue, an improved design methodology based on stochastic approaches has been developed in which both the design inputs parameters and the outcomes (i.e., factor of safety) are expressed as probability distribution functions. This paper focuses on the application of stochastic modelling technique to evaluate the underground roof support strategies currently used in an underground coal mine located in the Bowen Basin. The starting point of the analysis is the existing analytical roof support models that identified the relevant design inputs in consideration. Based on the best fit probability distributions of input parameters determined by goodness of fit tests, a risk based design is conducted to quantitatively evaluate the risk of roof fall fatality under specific roof support system by using the probability of failure from Monte Carlo simulation and the associated underground personnel exposure.

INTRODUCTION

Roof strata control is one of the most critical components of underground coal mining. Without proper reinforcement, the roof strata may be destabilised resulting in catastrophic consequences to the health and safety of employees and significant financial loss due to the production downtime. It is widely accepted that in an underground environment rock mass properties and support elements can vary significantly within a short distance; roof stability is strongly dependent on these varying properties. Traditional roof support design for underground coal mine are primarily based on deterministic approaches in which the inputs parameters are presented as single values. Although such approaches provide a straightforward design process and the design outcome can be easily evaluated against the long established design criteria (i.e. factor of safety), they are unable to account for uncertainties governing the roof support performance in a quantifiable manner. In order to address this issue, the application of the stochastic modelling technique has been proposed. Stochastic modelling simply allows for the randomness of the input parameters in the roof support design.

In a stochastic design approach, the input parameters are expressed as probability distribution functions rather than single values. The design outputs (i.e. factor of safety) are also statistically distributed, based on which the probability of failure (POF) for a given roof support design can then be calculated. As such, the associated risk from the varied design inputs can be quantified, which in turn assists geotechnical engineers and mine management with the risk-based decision-making.

An improved stochastic approach will directly contribute to better risk assessment and management in underground roof support (Brown, 2012). This design methodology potentially accounts for all sources of inherent geotechnical uncertainties and field investigation errors and can enable geotechnical engineers to produce a risk-based roof support design for underground roadways. The decision-making process with respect to many of the risk-based problems such as potential fatality analysis and evaluation of roof support design against the relevant safety standards can be improved by representing risk quantitatively in terms of the probability of failure and the associated underground workforce exposure.

[1] *School of Mechanical and Mining Engineering, The University of Queensland, St Lucia Qld 4072, E-mail: m.kizil@uq.edu.au Tel: +61 07 3365 4499*

[2] *School of Mining Engineering, The University of New South Wales, Sydney, NSW, 2052, Tel: +61 02 9385 0721*

[3] *Anglo American Coal, 201 Charlotte Street, Brisbane Qld 4000; Tel (H) +61 07 3834 1333*

UNDERGROUND ROOF SUPPORT DESIGN

Roof behaviour in underground coal mines

For the purpose of designing and implementing effective strata control strategies in underground coal mines, the overall design methodology is to obtain an improved understanding of the roof behaviour of laminated, weak coal mine strata. The stability of roadways in underground coal mines is vulnerable to two major causes: the mining induced stress redistribution around the underground excavation and the geologic discontinuities in the immediate roof, such as beddings planes, faults and joints (Horne, Ferm and Currucio, 1978). Both of these causes will result in a zone of roof softening that influences the roof behaviour and controls the transverse loading pattern on the immediate roof. In a case study on South Africa collieries, a roof monitoring program using sonic extensometer suggested that a parabolic surcharge is loaded on the immediate roof by the formation of softened weak strata under the effect of sagging due to the lack of the nature support from beneath the strata (Canbulat and Van der Merwe, 2009), as shown in Figure 1.
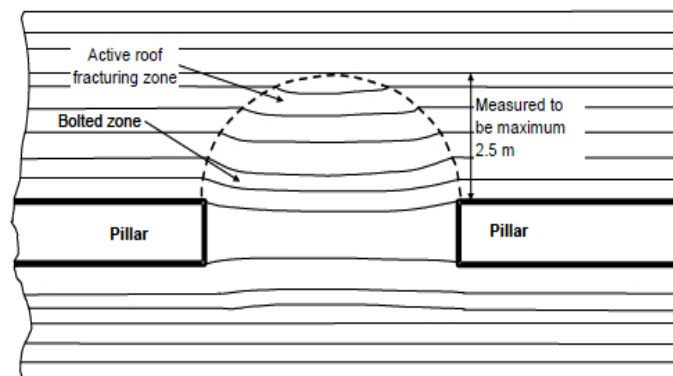
Figure 1: Roof behaviour model with zone of softening (Canbulat and Van der Merwe, 2009)

Roof support design approaches

The general idea behind the underground roof support is to reduce the magnitude of horizontal and vertical movements of the laminated strata by clamping them together and closing the separation of any pre-existing fractures that might have contributed by roof sagging after excavation (Hoek, Kaiser and Bawden, 1995). As there is no universally accepted design methodology in roof support system, many mines adopt an integrated methodology that combines the numerical, analytical and empirical methods. Three analytical failure modes, including shear, roof bolt tension and bond sliding are considered, with the design outputs back analysed by empirical modelling and geotechnical classification techniques (Canbulat, 2011). In these analytical models the aim is to ensure that the shear failure is prevented in the first place by installing sufficient number of roof bolts (i.e. reinforcement); however, if the shear failure occurs the roof should be stabilised in suspension mode, mainly using cables (i.e. post roof failure). These failure mechanisms can be classified under two well-known design models, namely, suspension and beam building, as shown in Figure 2.
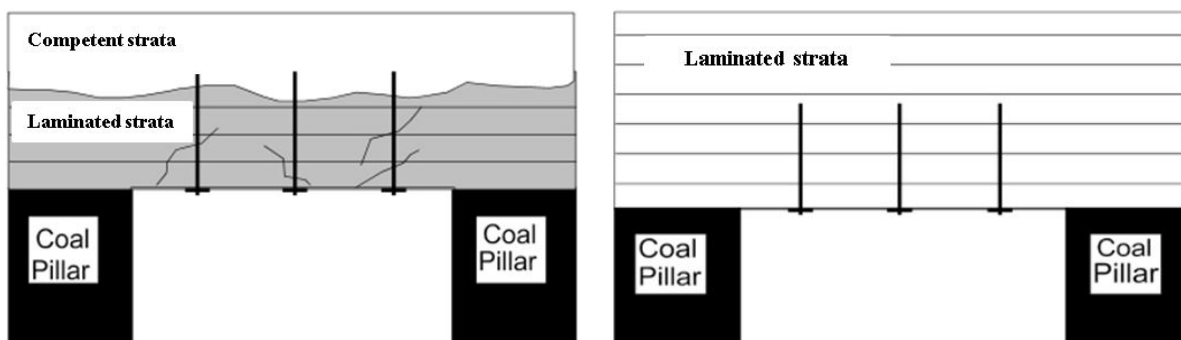
Figure 2: Analytical roof support models (After Mark, Molinda and Dolinar, 2001)
(Left: Suspension; Right: Beam building)

Suspension support mechanism is applicable to those situations where the immediate roof is comprised of weak strata or failed immediate (i.e. bolted) strata with stronger bedding or unfailed strata existing higher in the roof. The dead weight of the lower weak rock strata is suspended by using roof bolts or cables clamping these weak strata together and anchoring in the upper stronger strata. Two design criteria must be met the following conditions:

- The roof bolt or cable strength has to be greater than the weight of the loose or failed roof layers;
- The anchorage capacity of the support system is greater than the weight of the loose roof layers suspended; and

In shear failure mode it is assumed that the support mechanism is influenced by the interbedding shear stress induced under transverse loading and the shear resistance provided by the bolting system, including frictional resistance from bolt pre-tensioning and intrinsic shear strength of the bolts.

The details of these failure modes and the factors of safety against shear and suspension failures are given by Canbulat and van der Merwe (2009). It is of note that in this current study it is assumed that the load distribution across the beam is parabolic in all failure modes in order to achieve a consistent approach in calculation of loading on the roof support.

REVIEW OF STOCHASTIC MODELLING TECHNIQUES

Stochastic roof support design methodology

The underground roof support design is influenced by many elements, such as rock mass properties, mining geometries and bolting specifications. It is widely recognised that the rock mass properties can vary significantly within a short distance in a coal mine, leading to the roof stability to be considered as a random system where the occurrence of failure is a random event depending on the outcome of random variables involved (Chen, Jia and Ke, 1997). When compared with the traditional deterministic approach where single values are assigned to each design input, stochastic modelling technique has the advantage in dealing with the inherent uncertainties in the underground roof support design. The design inputs in the support system with the random values are represented as probability distributions, with the resulting factor of safety also expressed by a density function. Therefore, the associated risk of each support design can be quantified by calculating the area beneath the density function of FoS within a specified interval (i.e. less than unity). The following steps summarise the stochastic approach used in this paper in evaluating the roof support design:

- Select appropriate analytical models that produces a deterministic solution to the roof stability;
- Decide which input parameters are to be modeled probabilistically and the representation of their variability in terms of probability distributions;
- Repeatedly run the design output using the deterministic model by Monte Carlo simulation
- Obtain the probability density function of the design output (i.e. factor of safety) for each roof support design; and
- Evaluate the risks for each roof support design by considering the probability of failure, as illustrated in Figure 3.

Figure 3: Risk representations by the probability distribution of factor of safety

Monte Carlo simulation

In order to obtain the density function of the design output, Monte Carlo Simulation is used to conduct a repeated deterministic calculation for a large number of times where single values of each input

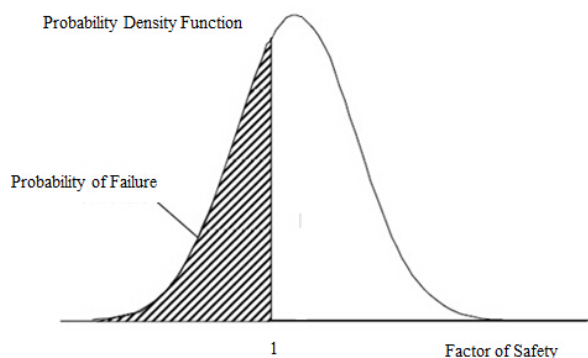parameters are sampled randomly from their dataset and each loop can produce a single value of design output (Rubinstein, 1981). The accuracy of the Monte Carlo simulation is related to the number of trials run, which is dependent on a variety of factors. Equation 1 shows the quantitative relationship between the number of simulation trials required and the desired confidence level in solution to the design output as well as the number of input variables included, based on the studies in civil engineering (Harr, 1987).

$$\mathbf{M}_{mc} = [\frac{d^2}{4(1-\varepsilon)^2}]^m \tag{1}$$

Where:

M_{mc} = number of Monte Carlo simulation trials
d = standard normal z value corresponding to the confidence level
ε = the required confidence level (0 to 100%)
m = number of inputs variables

The number of Monte Carlo trials increases exponentially with the level of confidence and the number of variables. The factor of safety in bolt tensile failure contains three random variables (Canbulat and van der Merwe, 2009), the number of Monte Carlo simulation required is 309,445 under a desired confidence level of 90%. However, in the case of shear failure model seven random variables are involved, the number of Monte Caro trials increases significantly to 6.8×10^{12}. Furthermore, with an increased confidence level to 95%, 1.2×10^{18} runs are required. Such large number simulations is extremely time consuming and therefore is not technically feasible for personal computers. The number of Monte Carlo simulation trials can be reduced by using Latin Hypercube Sampling (LHS). With this sampling technique, the entire space for each parameter is partitioned into an arbitrary number of dimensions and only one value will be selected within each dimension. The benefit of this sampling method is that it allows the value to be selected across the entire variable space and can be used to generate a representative distribution curve of a function of multiple variables with less sampling iteration (McKay, Beckman and Conover, 1979).

Goodness of fit tests

In the stochastic model, the randomness of the input parameters is accounted for by using appropriate probability distributions. Goodness of fit test is a broad class of statistical test that determines the best fit distribution model for each of the input parameters. It measures the compatibility of a random sample with a theoretical probability distribution function. The idea behind the goodness of fit tests is to calculate the value of a test statistic that measures the 'distance' between the actual data and the candidate probability distribution, and compare that distance to some threshold value. It is obvious that the probability distribution with the lowest test statistic value is considered as most compatible to the actual data sample. There are three common types of goodness of fit tests, Kolmogorov-Smirnov, Chi-square and Anderson-Darling tests. They differ in how the test statistics and critical values are calculated (Easyfit, 2014).

Chi-Squared test is used to determine if a sample comes from a population with a specific distribution. The main disadvantage of Chi-square test is that the sample data has to be binned and there is no optimal choice for the number of bins. Different formulas can be used to calculate this number based on the sample size (Harris and kanji, 1983).

Kolmogorov-Smirnov (K-S) test is used to decide if a sample comes from a hypothesised (fully defined) continuous distribution. The main limitation of K-S test is that it gives more weight near the centre of the distribution than at the tails (Berry and Lindgren, 1996).

The Anderson-Darling (A-D) test is a general test to compare the fit of an observed cumulative distribution function to a defined cumulative distribution function. A-D test can be used to overcome the limitations of the other two tests mentioned above as it is applicable to both of the binned and unbinned data and also provide a more sensitive result at the tail region (Sinclair, Spurr and Admad, 1990).

Fundamentals of probability theory

For the joint probability between two events, two conditions need to be considered based on the dependency between them (Berry and Lindgren, 1996). If two events A and B are independent where the occurrence of any one does not affect the probability of the other, the joint probability of both of A and B to occur is given by multiplying the probability of events A and B, as shown in Equation 2.

$$P(A \cap B) = P(A) \times P(B) \tag{2}$$

If the probability of occurrence of event A is dependent on that of event B, the joint probability is then determined by:

$$P(A \cap B) = P(A) \times P(B \mid A) \tag{3}$$

Where P*(B|A)* is defined as the probability of A to occur when B takes place.

Based on the assumed failure modes (and sequences), the overall probability of failure can be calculated using the above relationships. For the purpose of this study the overall probability of roof failure is calculated as follows:

Let *A* be the event that the roof fails in shear, and *B* be the event that the roof fails in suspension mode. The event *B* can only occur if shear failure has already occurred. Also, let *B*1 be the event that the roof fails due to cable failure and *B*2 be the event the roof fails due to weak bonding. If either *B*1 or *B*2 occur than *B* occurs. Based on these assumptions, the overall probability of failure, $\Pr(i)$ of any given support system can be calculated as follows (Stoklosa, 2014):

$$\Pr(i) = \Pr(A) \, [\Pr(B_1) + \Pr(B_2) - \Pr(B_1 \cap B2)] \tag{4}$$

CASE STUDY

Input parameters in stochastic modelling

To evaluate the current roof support design at Mine A using stochastic modelling technique, a set of design inputs are selected based on the analytical support mechanism discussed above. These parameters include:

- Roadway width;
- Intersection span;
- Height of roof softening;
- Thickness of immediate weak strata;
- Unit weight of immediate weak strata;
- Roof bolt and cable pretension;
- Roof bolt ultimate tensile strength;
- Bond strength obtained from underground short encapsulated pull tests (SEPT);
- Coefficient of friction of laminated roof strata;
- Roof bolt, cable spacing;
- Roof bolt, cable length.

All of the above input parameters are to be expressed in probability distribution with a large field data set collected, except for roof bolt, cable spacing and length that will be modelled as single value applicable to the whole mine. In addition, some other variables are also collected in assessing the variation in underground geotechnical environment and characterising different geotechnical domains that may be subject to varied roof support strategies. Those parameters are as follows:

- Major horizontal principal stress;
- k-ratio (horizontal stress to vertical stress ratio);
- Young's modulus of overlaying roof at bolting horizon; and
- UCS of roof strata at bolting horizon.

Uncertainties in roof support design

A comprehensive understanding of the immediate roof is a critical component in the roof support design. Geological boreholes are used at Mine A in conjunction with geophysical logging to perform a detailed geological and geotechnical characterisation up to 10 m into the roof strata, which corresponds to the longest cable bolts available at the mine site and represents the highest bolting horizon. Geotechnical domains are then defined using these data, with the purpose of differentiating the roof support designs across zones with different geotechnical environment. The following geotechnical properties are discussed:

- Lithology, including thickness of laminated roof;
- Roof strata competency at primary bolting horizon (UCS, CMRR);
- Roof deformation; and
- Height of roof softening.

Immediate roof lithology

The case mine extracts the German Creek Seam within the Bowen Basin coalfield. The cover depth of current panels varies from 300 to 350 m. The lithology of immediate roof is characterised into five distinct roof zones based on the geophysical investigation, as shown in Figure 4.
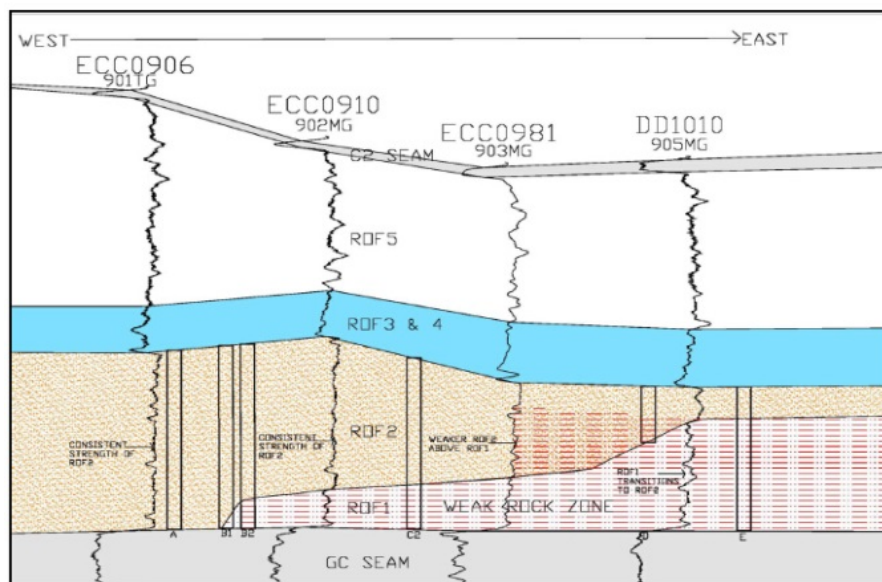
Figure 4: Sonic signatures in four boreholes (provided by the mine)

It can be seen that the weak, laminated roof, as represented by ROF1, has the potential to delaminate and soften under high horizontal stress and these roof zones are both critical to roadway performance and geotechnical design. Therefore, the thickness of the immediate weak rock strata can be used to define the geotechnical domains. To obtain a mine-wide profile of ROF1, geological data from 588 boreholes across the mine site is used and the contour map for the thickness of laminated roof is produced by using Surfer, as shown in Figure 5.

The lithological contour map in Figure 5 shows that the current panels that are in operation can be classified into two geotechnical domains based on the thickness of the laminated immediate roof. In the western panels from 901 to 904, the laminated roof varies from 0 to 1.2 m while in the eastern panels from 905 to 908 the thickness is consistently larger varying from 1.5 to 2.7 m. Therefore, different bolting strategies may be considered in these two geotechnical domains.

The competency of the roof was assessed using the Coal Mine Roof Rating (CMRR) technique. Molinda and Mark (1994) suggest the following broad categorisation of roof competency:

- CMRR<45, weak roof;
- 45<CMRR<65, moderate roof; and
- CMRR>65, strong roof.

Based on an analysis of 588 boreholes at the mine's current workings, the roof strata at primary bolting horizon of 1.8 m has an overall CMRR of approximately 45, indicating that the roof competency can be generally classified as 'moderate'.

Roof deformation

Roof deformation at a total of 162 intersection and roadway measurement sites from 900s panels are shown in Figure 6. It can be seen that the magnitudes of roof deformation at intersections are consistently higher than those observed at roadways with the average being 6 and 18 mm at roadway and intersection respectively. With the proposed roadway and intersection span of 5.5 and 9 m

respectively, the results indicated that for approximately 80% (as mined) per cent increase in the diagonal span at intersections relative to the roadway spans, on average, the magnitude of the displacement in the roof increased by approximately three times.
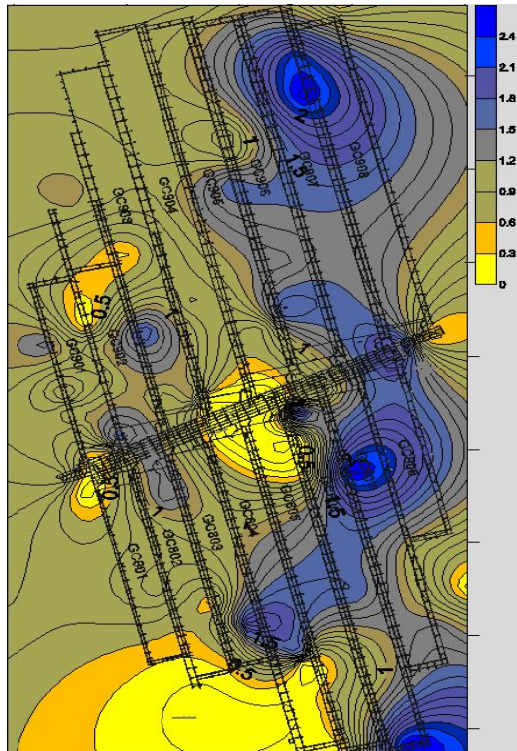
Figure 5: Contour map of thickness of ROF1 unit

Height of softening

As part of the roof monitoring program, 4-anchor tell-tales were used to monitor roof deformations once the primary supports are installed. For the purpose of this study, the height of roof softening is defined as the highest roof horizon where the deformation is larger than 2 mm. The data of height of softening obtained from 284 tell-tales at the mine site and the simulated continuous data using Monte Carlo trials is presented in Figure 7. The maximum measured height of softening is limited to 8 m into the roof, and there is no evidence of substantial roof instabilities beyond this height in the absence of the reported roof failure. The average HoS is approximately 2.7 m that is larger than the primary roof bolt length of 1.8 m currently used on site.
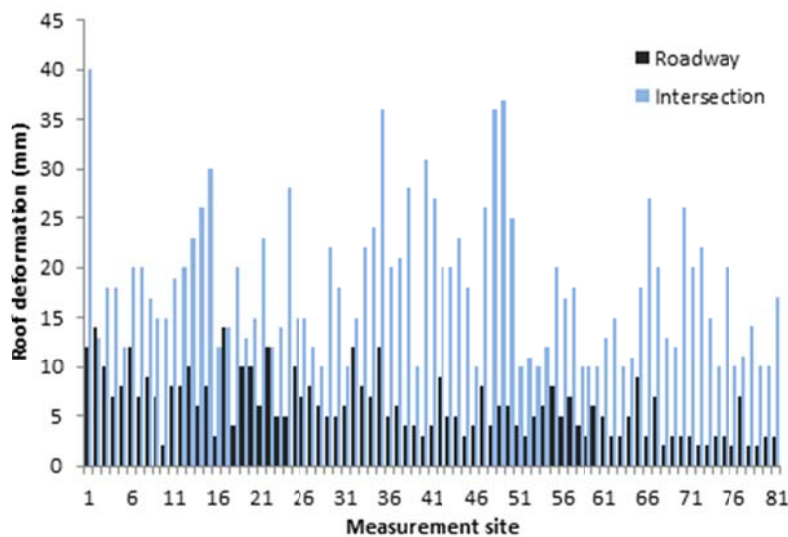
Figure 6: Measured roof deformation at roadway and intersections
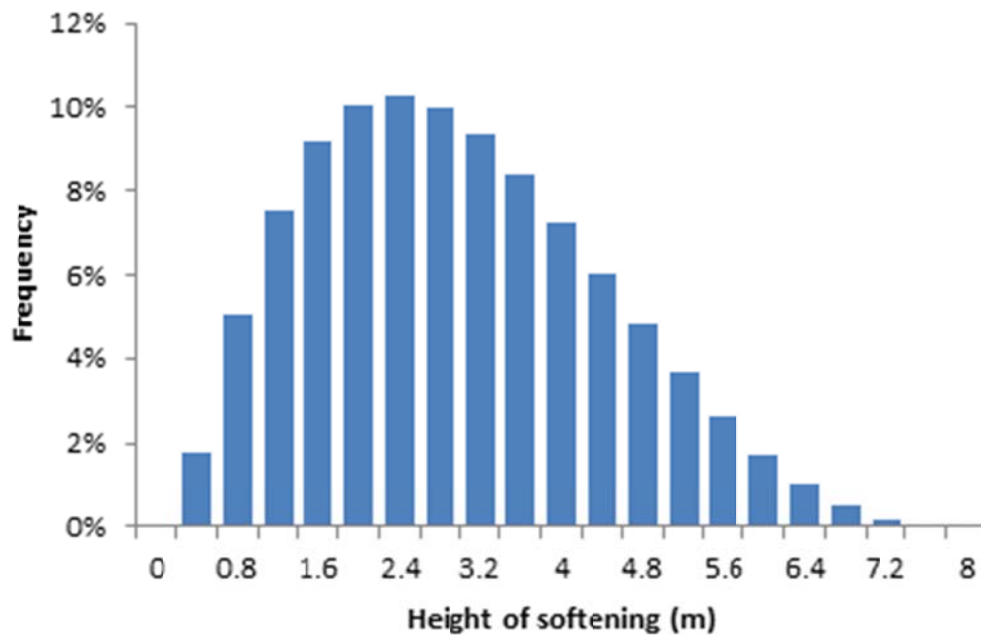
Figure 7: Measured height of roof softening

The roof deformation results show that the intersections are subjected to roof deformations almost three times of the roadways, which strongly suggest the necessity to divide the entire underground roof into two study areas: namely, roadways and intersections. The average HoS at roadway and intersection are 2.5 and 3.2 m respectively (excluding the cases with zero height of softening), as shown in Figure 8. It is evident from this figure that similar to the roof deformation measurements, the magnitude of HoS at intersections is larger on average than that in roadways, which is attributable by a larger roof span and also may indicate relatively higher risk of roof instability if insufficient roof support is installed in intersections.
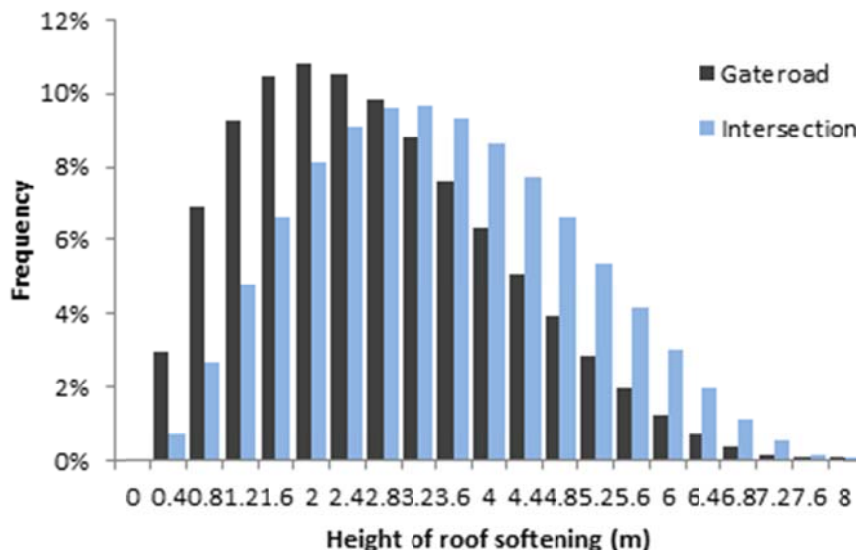
Figure 8: Subset of height of softening

Roof bolt and resin bond strength

The ultimate tensile strength tests are conducted for the primary roof bolts that are used in the current panels. Over 320 roof bolts with a nominal length of 1.8m have been tested. The results showed that the bolt ultimate tensile strength varied from 304 to 348 kN with an average value of 324 kN.

A series of underground short encapsulation pull tests were also carried out at the mine in various locations with relatively high strength of roof strata using 200 mm and 300 mm encapsulation of spin to

stall and spin and hold resins using 1.8 m roof bolts currently being used by the mine. Roof bolt pull-out resistance demonstrates a high degree of variation, ranging between 0.25 and 1.18 kN/mm (maximum load achieved in kN/encapsulation length in mm). The most likely cause of poor anchorage measured in these tests is varying rock competency. Some of the extremely low bond strength results are considered to be anomalies caused by resin losses and/or incorrect testing practices such as resin under or overspinning.

Bolt pretension

The pretension on the roof bolts can be estimated by the conversion from the torque measured during the bolt installation using a torque-wrench. Unfortunately, the relationship between tension and torque for fastened bolt is difficult to predict and in the real world variation as high as 30% can occur (Bickford and Nassar, 1998). Nevertheless, the installation audit reports indicated that the magnitude of pretensioning on the roof bolts varied from 33 to 75 kN.

PROBABILITY DISTRIBUTION OF INPUT PARAMETERS

Before the statistical determination of the best fit distribution fitting, it is necessary to conduct a preliminary study on the nature of data collected. Such process can screen out those candidate distributions that are explicitly not fit to the data set. This can help to narrow the choice to a limited number of distributions and save computational time, especially for those inputs with a large number of data points. The following factors of data set are considered:

- Data domain (continuous/discrete);
- Bound of data (fixed/open); and
- Negativity.

In general, specifying a fixed bound can enable the resulting distributions fitted to better reflect the randomness of the underlying data points. However, the number of candidate distributions decreases significantly if fixed bound is used otherwise. A preliminary analysis shows that for most of the design inputs the tail region of the proposed best fit distribution that is beyond the actual measured data range has a limited impact on the design output (i.e. on factor of safety and probability of roof failure). However, that is not the case for height of roof softening as the design outputs is very sensitive to the tail region in the proposed distribution. Without truncating the tail values the probability of roof failure will be significantly high, which is considered to be unrealistic. Therefore, for the purpose of this project, open bound is used for all of the design inputs, except for the height of roof softening, to introduce a larger candidate pool in the distribution fitting. The results of Anderson-Darling goodness of fit test are included in Table 1.

Table 1: Best fit distributions used in Monte Carlo simulation using Easyfit©

Parameters	Samples	Min	Max	Ave	Distribution	Scale	Shape	Location
Bolt strength (kN)	319	306	347	324	Lognormal	5.78 (µ)	0.03 (σ)	0
Bolt pretension (kN)	100	33.0	75	57.0	Weibull	61.3	6.25	0
Coefficient of friction	27	0.52	1.14	0.86	Weibull	0.92	5.33	0
Roof density (t/m^3)	115	2.34	2.70	2.54	Pearson5	44.5	96.9	0
Young's modulus (MPa)	90	2.2	28.9	9.25	Lognormal	1.80 (µ)	0.71 (σ)	1.47
Laminate thickness (m)	119	0.04	2.5	0.86	Erlang	0.43	2	0
HoS – Roadway (m)	112	0	8.0	1.93	Pert	0 (min)	8 (max)	1.80 (mode)
HoS – Intersection (m)	172	0	8.0	3.42	Pert	0 (min)	8 (max)	2.85 (mode)
Major stress (MPa)	61	5.93	22.8	12.0	Gamma	1.16	10.4	0
Roadway width (m)	1136	4.72	7.87	5.48	Pearson5	1502	275	0
Intersection span (m)	257	7.35	11.9	9.93	Weibull	10.28	14.6	0
Bond strength (kN/mm)	17	0.25	1.18	0.83	Gamma	0.04	27.7	0

It should be noted that the some of the results (e.g., interbedding coefficient of friction, bond strength) presented in Table 1 are based on a limited number of data points and/or the limits of the software

utilised to conduct the Monte Carlo simulations. Therefore, the best fit probability distributions of these design inputs obtained from GoF tests are only marginally better than the others.

RISK-BENEFIT ANALYSIS OF ROOF SUPPORT DESIGN

Required number of Monte Carlo simulation

A sensitivity analysis is conducted to investigate the optimum runs of Monte Carlo trials with the main objective to determine the minimum number of Monte Carlo trials from which further increasing the trials will not significantly improve the computational performance. In order to achieve this, the probability of roof failure under shear failure mechanism is calculated 10 times with various numbers of trials and the variation in the results are compared. The results are presented in Figure 9. The computed PoF from the Monte Carlo simulations becomes insensitive to the number of trials after 100,000 trials, implying potentially an optimum trial runs for the analytical models used in this study.
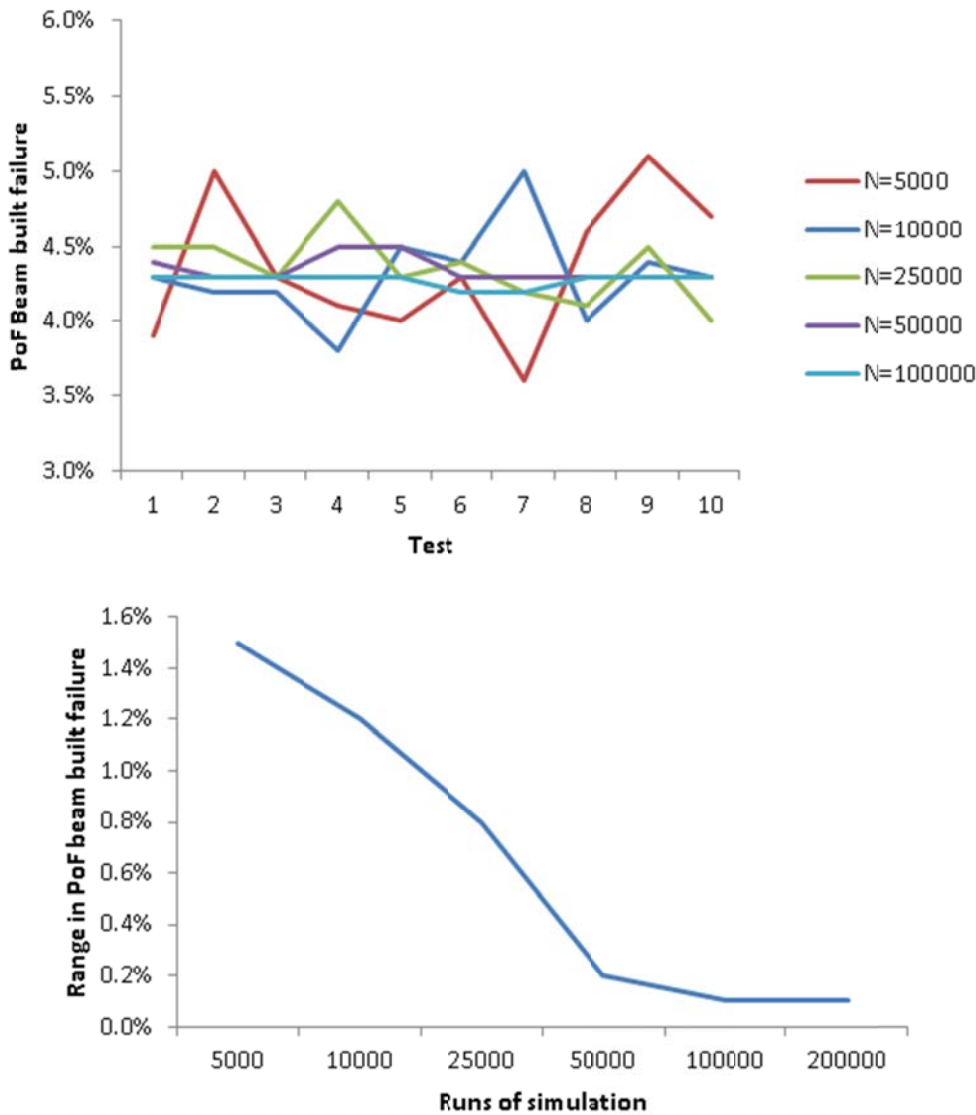
Figure 9: Sensitivity analyses on optimum Monte Carlo trials

Probability of failure and roof support design

A risk-benefit analysis of roof support design involves the evaluation of the overall probability of roof failure that incorporates three types of failure modes, including shear failure, bolt tensile and bond sliding failure in suspension mechanism. Individual probability of failure of these failure modes is determined by calculating the area under the density curve of safety factor <1 from a total of 100,000 Monte Carlo simulation trials. The mine's current bolting density is used in the analysis. 4 or 6 roof bolts

are installed in a row with row spacing of 1 m. The cables are in a bolting pattern of 2 bolts in a row with 2 m row interval.

Roadway roof support design without cable bolts

Table 2 summarises the probabilities of stabilities for 6 roof bolt patterns with 1 m row spacing. It is evident that increased roof bolt length will reduce the probability of failure in all three failure modes. In general, the risk of roof failure under suspension supporting mechanism can be reduced by using longer roof bolts. However, even with the longest 2.4 m roof bolt, the resulting PoF can still be as high as 53%. The possible reason is that the analytical model of suspension mechanism is only considered effective when the height of roof softening does not exceed the bolt length. For any roof strata with height of softening beyond bolting horizon, a safety factor of zero is assumed. Therefore, cable bolts are required to reinforce the roof zone with a relatively high elevation of softening in suspension mechanism.

Table 2: Probability of failure in a roadway with currently used roof bolt densities

		Roof bolt length (m)	
Bolting pattern	*PoF*	*1.8*	*2.1*
6 bolts in a row with 1 m row spacing	Shear loading	0.045%	0.002%
	Bolt suspension failure*	67.6%	59.5%
	Bond suspension sliding*	68.4%	60.4%
	Overall	0.040%	0.002%

* calculated only for the heights of softening that are less than the roof bolt length

Roadway roof support design with cable bolts

As indicated above, although the overall probability of roof failure can be significantly reduced by using longer roof bolts, the suspension failure modes still remain the main sources of roof instability. In order to mitigate such risks, cable bolts are recommended. Bolting patterns that consist of 1.8 m roof bolts with six bolts in a row at 1.0 m row spacing and cable bolts in varied lengths of 4, 6 and 8 m with two cables in a row at 2.0 m row spacing are evaluated in suspension and shear failure mechanisms. The resulting PoF for each bolting plan is presented in Table 3.

It is evident in this table that that the risks of roof failures in all failure modes are substantially reduced when cable bolts are introduced. In addition, the PoF of bolt tensile and bond sliding failure can be decreased by increasing the length of cable bolts from 4 m to 6 m. Further increase in the cable length will not benefit the roof stability substantially. Figures 10 and 11 present the distributions of factor of safety for the roof support design with a combination of 1.8 m roof bolt and 6 m cable bolt, based on which PoF is calculated.

Table 3: Probability of failure in a roadway with currently used 1.8m long roof bolt and cable densities

		Cable bolt length (m)			
Bolting pattern	*PoF*	*Roof bolts only*	*4*	*6*	*8*
Six 1.8 m roof bolts, 1 m row spacing with two cable bolts, 2 m row spacing	Shear loading	0.045%	~0	~0	~0
	Bolt suspension tensile*	67.6%	18%	1.8%	1.3%
	Bond suspension sliding*	68.4%	23%	3.4%	0.029%
	Overall	0.040%	~0	~0	~0

* calculated only for the heights of softening that are less than the cable lengths

Intersection roof support design

Roof strata at intersections is expected to have a higher risk of failure due to inherently larger spans, higher levels of deformations and height of softening, as shown in Figures 6 and 8. The roof span is defined as the average diagonal width of the intersection and the required support density is calculated for this length. A preliminary study showed that the minimum PoF at intersection that can be achieved by using 2.4 m roof bolts solely is approximately 2%, which is significantly higher than the PoF in roadways. Therefore, cable bolts are required to reinforce the roof strata at intersections. Table 4 summarises the probability of failure of the current intersection support with cables. Similar to the cases in roadway support, introducing additional cables can significantly improve the roof stability by reducing the bolt

tensile and sliding failures. The probability of failure in shear failure mode can also be reduced by installing cables. However, as the cables increase the shear capacity only in the bolted horizon, an increased in cable length will not result in reduced PoF in shear failure mode.

Table 4: Probability of failure in an intersection with currently used cables

Bolting pattern	PoF	Cable bolt length (m)			
		0	*4*	*6*	*8*
Twelve 1.8 m rock bolts, 1 m row spacing with two cables, 1 m row spacing**	Shear loading	10.6%	2.5%	2.4%	2.4%
	Bolt suspension tensile*	81.2%	32.7%	4.5%	1.5%
	Bond suspension sliding*	81.8%	39.2%	8.2%	0.1%
	Overall	10.25%	1.50%	0.30%	0.04%

* calculated only for the heights of softening that are less than the cable lengths

**twelve 1.8 m rock bolts as counted across the intersection diagonal width

Exposure and quantitative risk

In the above section, a stochastic approach was demonstrated to calculate the probability of failure with various roof support design. However, a probability of failure alone is not useful unless it is used to calculate the quantitative risk by combining the consequence in the consideration (i.e. Risk = PoF × Consequence). In this section an example is given, with the aim of calculating the annual probability of having a fatal accident across an underground working section. A similar concept for South African gold mines was also published by Stacey and Gumede (2007) and utilised in this paper.
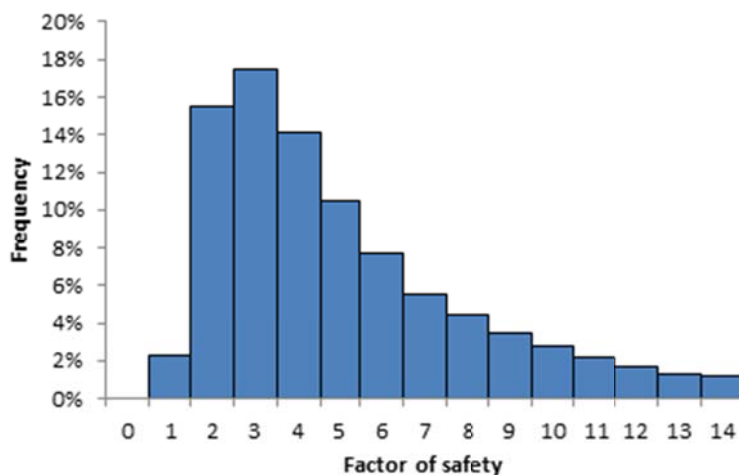
Figure 10: Distribution of factor of safety in shear failure mechanism (1.8 m roof bolt/6 m cable)
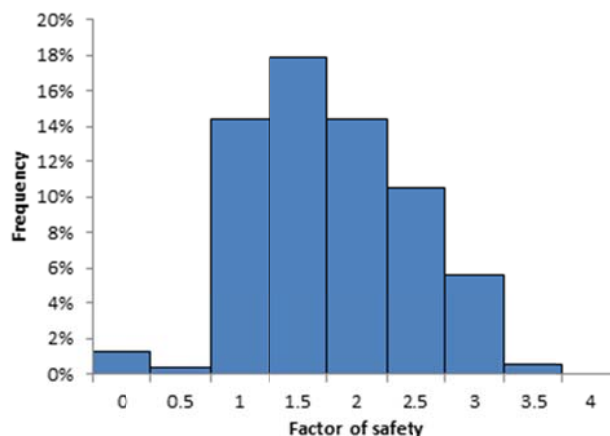
Figure 11: Distribution of factor of safety in suspension failure mechanism (1.8 m roof bolt/6 m cable)

For a double heading gateroad with 100 m long chain pillar and 5.5 m roadway width, the total area of exposure is 1,100 m^2.   The roof support used in this section is assumed to be 6×1.8 m long roof bolts installed at 1 m spacing interval. Assuming the following:

- There are 6 miners in this panel area for a period of 12 hours during the day and night shifts;
- Each miner expects to occupy an area of 1 m^2;
- The work within this panel area is scheduled for 30 days a month and 12 months a year;
- The probability of roof failure with the assumed roof support is 0.036%; and
- The roof fall will result in a fatality.

The total annual exposure hours can be calculated as follows:
Total hours per year = 365 days×24 hours = 8,760 hours
Total shift exposure = 12 months×30 days×24 hours = 8,640 hours
Panel area = 100 m×5.5 m×2 = 1,100 m^2
Area occupied by miners on day/night shifts = 6 miners×1 m^2
Probability of annual occurrence of roof fall fatality = (2×8,640/8,760×6/1,100)×0.04% = 3.8×10^{-6}

The results calculated above indicate that, with a six roof bolt pattern, the risk of a fall of ground fatality is approximately 4 in 1,000,000 employees or 1 in 250,000 employees in all ground conditions, i.e., without a TARP based pro-active strategy. Since the mine uses a comprehensive TARP system, it is considered that the actual probability of failure should be lower than this number as additional roof bolts are installed by triggering the TARP in the case of deteriorating ground conditions. Nevertheless, the acceptability of this roof support design can be evaluated against the relevant design criteria. The acceptable fatality rates have been proposed by various publications. Wong (2005) states that risks which have a fatal injury rate of 10^{-5} or more are unacceptable. Terbrugge *et al.* (2006) and Steffen and Terbrugge (2004) suggested the use of internationally accepted design criteria that proposed an annual probability of fatality of 1 in 10^{-4}.

CONCLUSIONS

The data collected as part of this study confirms that the rock mass properties and support-rock interface exhibit high degrees of variations. These variations should ideally be quantified using probability distributions in a roof support design. Using the Anderson-Darling goodness of fit test, best probability distributions for various input parameters have been identified. The results indicated that specifying a fixed bound can enable the resulting distributions fitted to better reflect the randomness of the underlying data points. However, the number of candidate distributions decreases significantly if fixed bound is used otherwise. A preliminary analysis also indicated that for most of the design inputs the tail region of the proposed best fit distribution that is beyond the actual measured data range has a limited impact on the design output (i.e. on factor of safety and probability of failure). However, the results revealed that the design outputs is highly sensitive to the tail region in the proposed distribution in the case of height of softening. Without truncating the tail values the probability of roof failure will be significantly high, which is considered to be unrealistic. Therefore for the purpose of this project, open bound is used for all of the design inputs, except for the height of roof softening, to introduce a larger number of possible distributions.

An attempt has also been made to demonstrate the significance of quantifying the risks associated with roof failures. Three failure mechanisms, namely shear failure, bolt tensile failure and bond failure, have been used in this study. The results revealed that in general, the highest probability of failure is associated with bolt tensile failure and bond sliding from dead-weight loading if rock bolts are used solely in roof reinforcement, implying the necessity of longer roof bolts and/or cables. Analysis results indicated that both of the risks associated with bolt tensile and bond sliding failures can be significantly reduced by additional cables with increased bolt length, resulting in an improvement in the overall roof stability.

Various roof support designs with a combination of roof bolts and cables were investigated for roadway and intersections, based on which an example was demonstrated to assess the quantitative risk of roof fall fatality for an underground working section by considering both of the probability of roof failure and underground workforce exposure.

ACKNOWLEDGEMENTS

REFERENCE

Berry, D A and Lindgren, B W. 1996, *Statistics: Theory and Methods*, pp 46-52 (Duxbury Press: Belmont, US).

Bickford, J and Nassar, S. 1998, *Handbook of Bolts and Bolted Joints*, 428 p (Marcel Dekker, Inc: New York).

Brown, E T. 2012, Risk assessment and management in underground rock engineering, *Journal of Rock Mechanics and Geotechnical Engineering*, 4(3):193-204.

Butel, N, Hossack, A and Kizil, M. 2014, Prediction of in situ rock strength using sonic velocity, in *Proceedings of 2014 Coal Operators' Conference*, University of Wollongong, pp 89-102 (The Australasian Institute of Mining and Metallurgy & Mine Managers Association of Australia).

Canbulat, I and Van Der Merwe, J N. 2009, Design of optimum roof support systems in South African collieries using a probabilistic design approach, *Journal of the South African Institute of Mining and Metallurgy*, 108:71-88.

Canbulat, I. 2011, Improved roadway roof support design for Anglo American Metallurgical Coal's underground operations, *Transactions of the Institutions of Mining and Metallurgy, Section A: Mining Technology*, 120(1):1-13.

Canbulat, I, Mills, A, Stevens, C and Emery, J. 2013, Underground Geotechnical Engineering Design, Monitoring, Mapping and Hazard Plan Guidelines, Anglo American Metallurgical Coal.

Canbulat, I, 2014. Personal communication, 20 September.

Chen, G, Jia Z H and Ke, J C. 1997, Probabilistic analysis of underground excavation stability, *International Journal of Rock Mechanics and Mining Sciences,* 34(3):51-66.

Harr, M E. 1987, *Reliability-based design in Civil Engineering*, pp 102-112 (McGraw-Hill Inc: New York).

Harris, R R and kanji, G K. 1983, On the Use of Minimum Chi-Square Estimation, *Journal of the Royal Statistical Society*, 32(4):379-394.

Hoek, E, Kaiser, P K and Bawden, W F. 1995, *Support of underground excavations in hard rock,* pp 163-173 (Balkema: Rotterdam).

Horne, J C, Ferm, J C and Currucio, F T. 1978, *Depositional models in coal exploration and mine planning*, pp 544 - 575 (Deptartment of Geology, University of   South Carolina: Columbia).

Mark, C, Compton, C S, Oyler, D C and R, D D. 2002, Anchorage pull testing for fully grouted roof bolts, in *Proceedings of 21st International Conference on Ground Control in Mining*, Morgantown, West Virginia, 6-8 August, pp 105-113 (West Virginia University).

Mark, C and Molinda, G M. 2005, The coal mine roof rating (CMRR) - a decade of experience, *International Journal of Coal Geology*, 64:85-103.

Mark, C, Molinda, G M, Dolinar, D R. 2001, Analysis of roof bolt systems (ARBS), in *Proceedings of 20th International Conference on Ground Control in Mining*, Morgantown, West Virginia, pp 218–225 (West Virginia University)

MathWave Technologies. 2014, EastFit - Distribution Fitting Software [Online]. Available from: < http://www.mathwave.com > [Accessed: 29 October 2014].

McKay, M D, Beckman, R J and Conover, W J. 1979, A comparison of three methods for selecting values of input variables in the analysis of output from a computer code., *Technometrics*, 21(2):239-245.

Rubinstein, R, 1981. *Simulation and the Monte Carlo Method*, pp 11-12 (John Wiley & Sons: New Jersey).

Sinclair, C D, Spurr, B D and Admad, M I. 1990, Modified anderson darling test, *Communications in Statistics - Theory and Methods*, 19(10):3677-3686.

Stacey, T R and Gumede, N. 2007, Evaluation of risk of rock fall accidents in gold mine stopes based on measured joint dataprobabilistic design approach, *Journal of the Southern African Institute of Mining and Metallurgy*, 107:345-350.

Steffen, O K H and Terbrugge, P J. 2004, Designing open pit slopes with risk, in *Colloquium The Management of Risk in the Minerals Industry*, 10 pp, (South African Institute of Mining and Metallurgy)

Stoklosa, J, 2014. Personal Communication.

Terbrugge, P J, Wesseloo J, Venter, J and Steffen, O K H. 2006, A risk consequence approach to open pit slope design, *South African Institute of Mining and Metallurgy*, 106(7):503-511.

Van der Merwe, J N and Madden, B J. 2002, Rock engineering for coal mining, *Safety in Mines Research Advisory Committee (SIMRAC),* SAIMM Special Publications Series 7.

Wagner, H. 1985, Design of roof bolting patterns, Chamber of Mines workshop on roof bolting in collieries, Republic of South Africa, Johannesburg.

Wong, W. 2005, *How did that happen? Engineering Safety and Reliability*, (Professional Engineering Publishing Limited: London).

PREINSTALLED CABLE BOLTS IN LONGWALL INSTALLATION ROADS

Ross Seedsman

*ABSTRAC*T**:** Long tendon support is typically installed in the first pass of an installation roadway meaning that it is pre-installed as the full roadway width is developed. The recognition of additional compressive failure in a rock mass as the roadway is widened results in a set of challenges for the design of the pre-installed long tendons support. Cable bolts cannot prevent the onset or progression of failure and hence must be able to survive the associated deformations. After failure there are stress reductions in the immediate roof that may cause the cables to debond. In certain geological conditions pre-installed, pre-tensioned, fully grouted cables may be too stiff and could fail due to their inability to accommodate deformations of the excavation. A case study is presented and analysed using some readily available analytical tools that capture what are considered as the key aspect of the behaviour model.

INTRODUCTION

Sedimentary rocks are often referred to as soft rocks to contrast them with igneous and metamorphic rocks. As well as being geotechnically soft (low modulus) they have lower strengths and this means that at comparable depths with respect to hard rock mines (where the dominant roof collapse mode is gravity fall of joint bounded wedges), soft rocks can undergo compressive failure. As identified in the logical framework (Seedsman, 2012), there can be several situations in longwall coal mines where compressive failure is possible – at the development face in low strength/high stress environments, at the maingate corner and in "super stress notches".

Hutchinson and Diederichs (1996) provide a detailed coverage of all aspects of cable bolting. In the section on mechanistic design, they present discussions on how cables may interact with the rock mass during mining. They comment (page 254): "*cablebolts are unlikely to arrest the onset of rock failure under high stress, and may do little to alter the progression of such failure into the rockmass…. In highly plastic (deformable) rockmasses under high stress, it is also unlikely that cables will be effective in arresting the progression of failure.   In addition, in these environments, the induced displacements may be too great for the system to handle and cable strand rupture may be inevitable in pre-installed systems.".*

The ground reaction curve concept is well established in mining rock mechanics (Brady and Brown, 1985). The concept is to allow the roof to move to some degree so as to minimise the required support density but not sufficient movement to allow a large failure zone to develop. It allows (requires?) roof deformation to redirect stresses away from the roadway. The concept requires consideration of both the strength and strain capacity of the ground support, with the concern that strong, stiff, but brittle support members may break before their load bearing capacity can be mobilised in the roof. Over the last decade, there has been a trend in the Australian underground coal industry to install fully grouted pre-tensioned cables as close as possible to the face so as to limit roof deflection with the view that this reduces the height of softening. This trend would appear to be at odds with the ground reaction curve concept.

Once compressive failure develops, the ground stresses are redistributed to elsewhere in the rock mass. This means that the stresses within the failure zone itself reduce. Hutchinson and Diederichs (1996) also discuss stress shadowing and relaxation effects (page 255): "*Zones of relaxation pose additional hazard for cablebolting.   … stress decreases across a cable array can seriously impair the bond strength of plain strand cablebolts.   Rockmass stiffness is also dependent on confinement in fractured rockmasses and decreases with relaxation.   ….It is for this reason that plating and the use of modified strand cablebolts are recommended in fractured-destressed rock"*

Longwall installation roadways can be required to be excavated in low strength/high stress environments. In a two-pass installation, say a 5.2 m wide roadway stripped to 9 m wide, long tendons are typically installed in the first pass and are hence pre-installed with respect to the second pass. Additional compressive failure as the second pass is extracted could induce displacements that could

Seedsman Geotechnics Pty Ltd, NSW, Australia, E-mail: sgplross@bigpond.com

cause cable rupture. The use of pretensioned fully grouted-cables could cause premature failure if the magnitudes of the deformations in the roof are too large. Subsequent destressing of the zone of compressive failure could lead to debonding of the cable.

This paper presents a summary of large and unexpected movements in a recent installation roadway and considers what may have happened in the light of these comments. As is common with mine operational problems there is inadequate data on the geological and geotechnical conditions atthe site. It is acknowledged that there may be other explanations to what occurred.

CASE STUDY

A summary of the geology and geophysical logs of a borehole within 150 m of the site is presented in Figure 1. The siltstones have a unit rating of 42 and the medium grained sandstone a unit rating of 59 giving a Coal Mines Roof Rating (CMRR) of 54 without a strong bed adjustment. Based on the sonic-derived strengths, the Roof Strength Index (RSI) of the siltstones is in the order of 4.0 for a depth of 250 m. The mine is known to have a relatively high horizontal to vertical stress ratio (possibly in the order of 1.8 to 2.0) so a stress-relieving roadway was used.
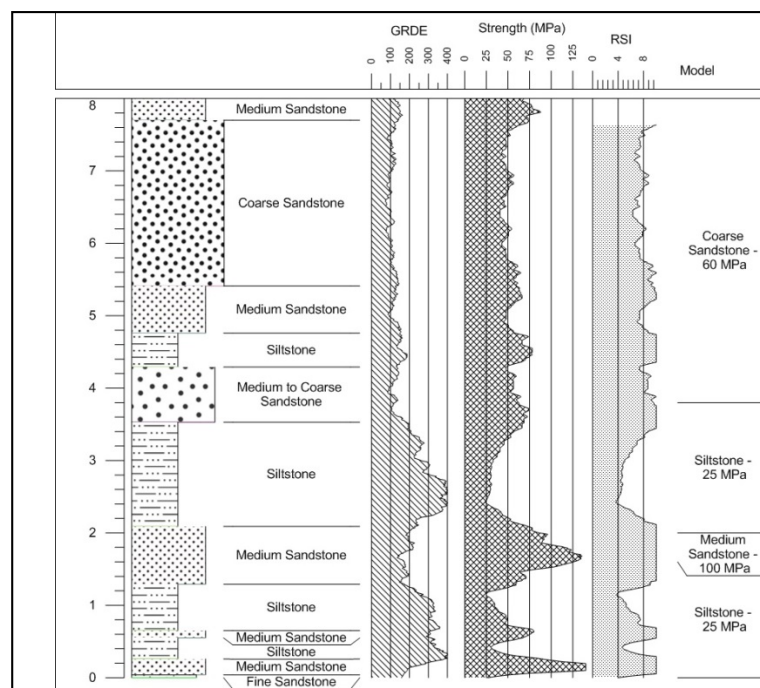
Figure 1: Roof geology and simplified geotechnical model

The installed roof support in the 5.2 m wide first pass roadway was 6 of 2.1m X grade bolts every metre with 3 of 8.0 m long pre-tensioned fully-grouted 630 kN cables subsequently installed every two metres. The second pass to 9.0 m was supported with an additional 5 of 2.1 m X grade bolts every metre and one additional cable every two metres. The primary roof density index (Thomas, 2010) was 0.8 MN/m and the secondary roof density index was 1.12 MN/m. Based on Colwell and Frith (2013), the Primary Roof Support Rating PRSUP was 81.9 for the first pass and 63.3 for the second pass.

The stress relief roadway encountered some roof/rib guttering and some cables were installed. The first pass roadway was offset by about 14 m and excellent roof conditions were encountered. There was negligible movement recorded on the GEL extensometers on the first pass. Some minor guttering was observed on the outbye rib and indicated an apparent change in the stress direction.

During the second pass the roof extensometers consistently showed movement at both the 1.8 m and 2.5 m horizons and at the 5.5 m horizon in some locations. This movement was accompanied with some stress guttering on the outbye rib and some minor distress to the roof line between the first and second cables on the inbye side. There was no evidence of loading on the cable plates and only a few of the bolt plates. Operators and company mining engineers reported loud sharp noises that they related to strand rupture. In a previous installation roadway, broken cables had been recovered from the fall debris.

The GEL extensometers were installed no more than 1.5 m from the to-be-stripped rib and within 1.4 m of a cable installation. After 24 hours the movement at the roof line was in the range of 40 mm to 55 mm, at the 1.8 m horizon the movement was between 14 mm to 28 mm, and these then increased to about 28 mm to 42 mm in the next 24 hours. The creep rates after 48 hours were 10 mm/day and 5 mm/day respectively. The surge measured at the roof line would have been in excess of 100 mm.

The decision to re-support was based primarily on the movements at the 1.8 m and 2.5 m horizons, reference to published guidelines, the interpreted breakage of support based on the noises in the roof given the recovery of broken cables in the collapse of an earlier installation roadway.

NUMERICAL SIMULATION

There is not a complete set of geological or geotechnical data so there are major constraints to the selection of geotechnical parameters for the numerical simulations. Consistent with the approach of Lambe (1973), there may be greater confidence in the interpretation of the outcomes if the sophistication of the analyses matches the available data. In this way Phase2 finite element analyses were used to examine the impact of the geological layering and to "calibrate" a simpler Examine2D model that allows ready sensitivity/parametric assessments. The Examine2D model considered just the siltstone with a revised UCS to account for the sandstone layer. The siltstone was modelled with brittle parameters and transverse isotropy (Seedsman, 2013). The Examine2D model can only be interpreted in terms of the roof conditions and possibly the floor (but not the ribs as the coal was not modelled).

An implication of the failure zones identified in the stress models will be a redirection of the stress field. This was simulated in the simple elastic stress models by forming a new excavation shape for the analysis of the next stress change. The same redirection of stresses allows the application of published voussoir beam methods to the sandstone layer as the layer will not have imposed stresses onto it.

It is acknowledged that the Examine2D model is very much simplified compared to the geotechnical conditions but is somewhat compatible with the available data. It is assessed to reflect an appropriate behaviour model for this installation road.

Stress relieving roadway

The Phase2 model showed compressive failure in the siltstones above and below medium grained sandstone (Figure 2). The calibrated Examine 2D model has a compressive failure zone extending 3.9 m into the roof. Simulating this failure zone as a new excavation, the model then indicates that there would have been substantial relaxation of the horizontal stresses at the location of the first pass roadway – the predicted horizontal stresses at the roof line may have been in the order of 7 MPa to 8 MPa (left side of Figure). It is noted that is consistent with some of the observations. Stress relief at this distance is also consistent with reports in the literature from the Southern Coalfield of New South Wales.
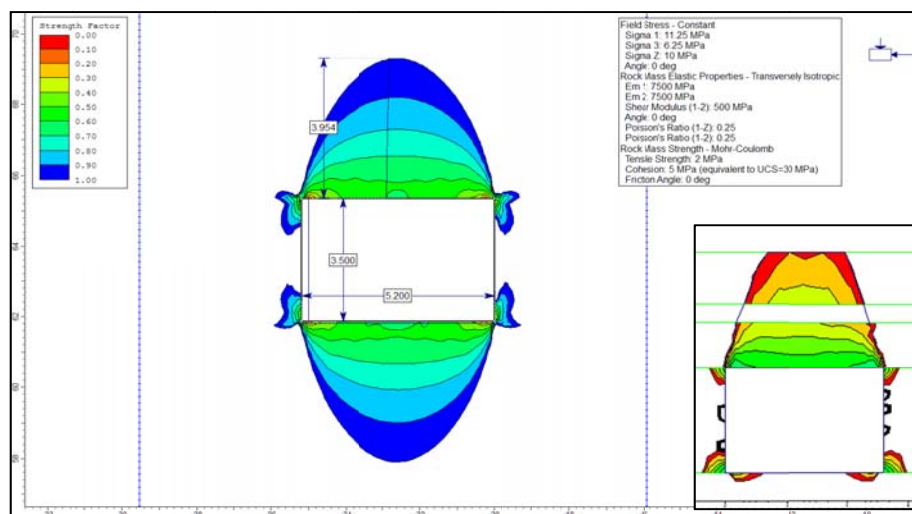
Figure 2: Failure zone (strength factor < 1.0) developed around the stress relieving roadway (inset – Phase2 model)

First pass

By comparing Figure   with Figure , it can be seem that there is a significant reduction in the extent of compressive failure and it is now less than 2 m above the roof line. In reality, this would be seen as failure in the siltstones below the sandstone layer and such material could have been readily suspended from the sandstone layer with the 2.1 m long bolts. The model suggests that there may have been some stress guttering developed on the outbye rib as was observed.
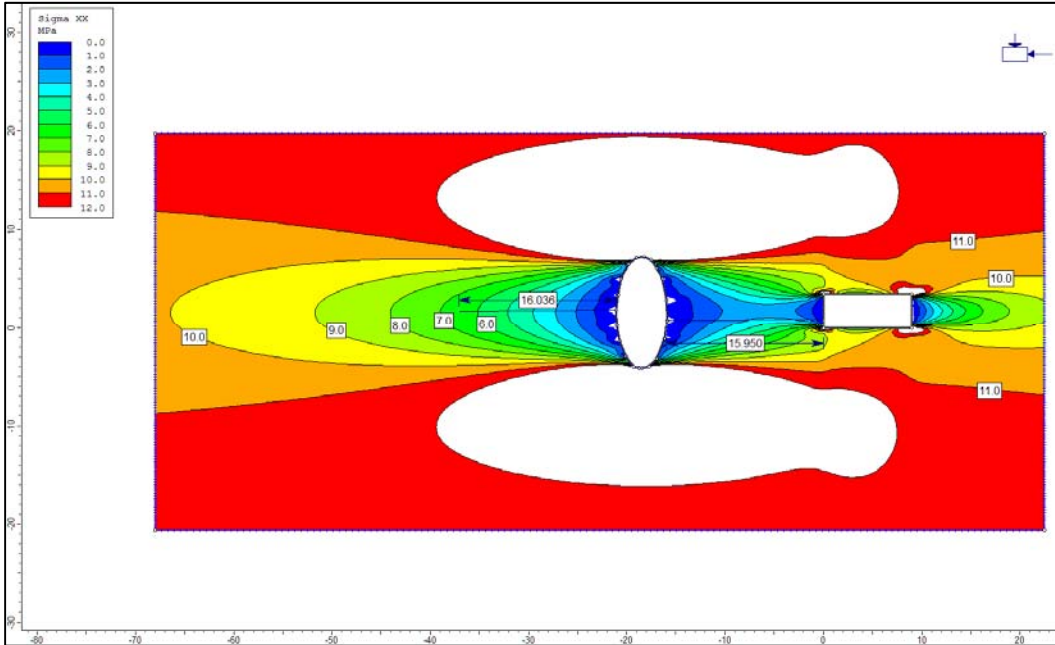
Figure 3: Reduction in horizontal stresses associated with the stress relieving roadway (note simulated excavation)
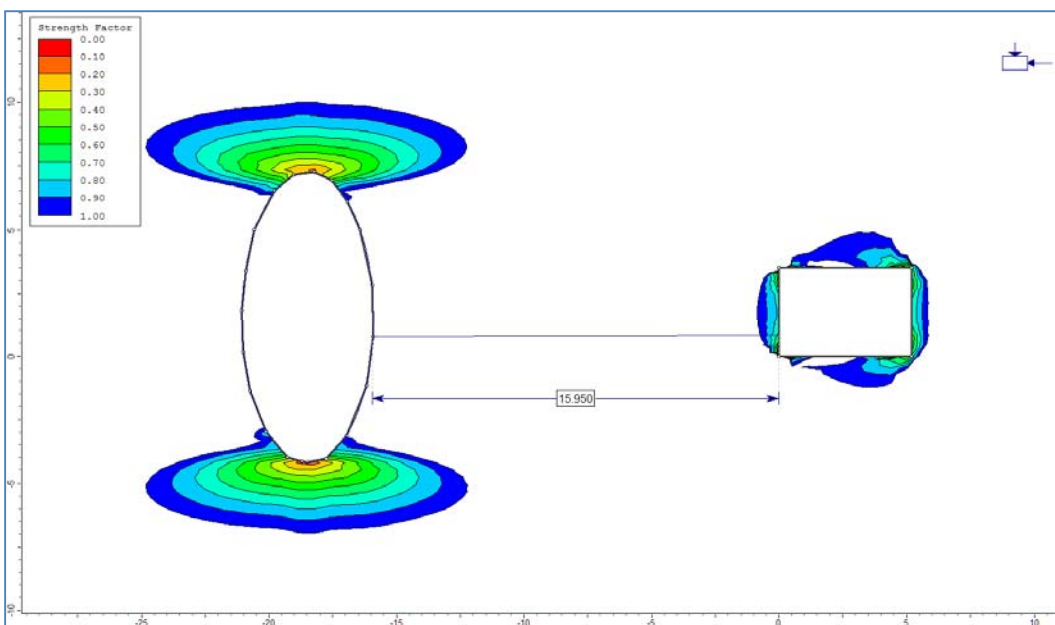
Figure 4: Failure zone developed above the first pass roadway in the shadow of the stress-relieving roadway

Second pass

In Figure , the shape of the first pass roadway has been modified to account for the compressive failure modelled in the first pass (Figure). There is additional compressive failure in the roof, extending 5.8 m above the original roof line (to the base of the coarse sandstone?). It is noteworthy that there is very minor

stress guttering at the outbye roof/rib corner. The associated elastic strains (those before failure) in the roof at this time are only in the order of 1 mm/m to 1.5 mm/m.
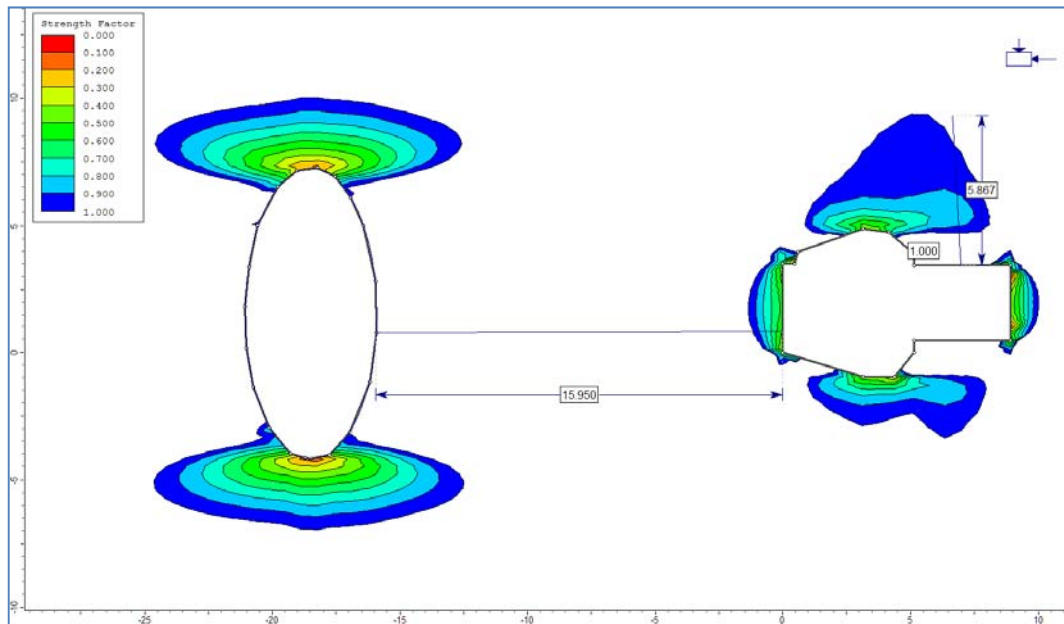
Figure 5: Failure zone developed as the roadway is widened to 9 m

BACK ANALYSIS

The surge certainly exceeded the published databases for acceptable outcomes (Colwell and Frith, 2013). The databases are unpublished and it may be the definition of an acceptable surge is based on very conservative assessment of approach to the required serviceability of installation roadways. It is noted that the decision to resupport was not based on the surge value alone. The decision to resupport the roadway was made primarily on the basis of the roof movements at 1.8 m and 2.5 m as it was acknowledge that there was some delamination in the immediate roof.

Extensometers and borescopes confirmed that the highest movement is located at the base of the coarse sandstone. By reference to Figure , a possible collapse mass assuming a general parabolic shape is 0.67 * 5.8 * 9 * 2.5 t/m = 87 t/m.   The installed capacity of the cables was 128 t/m. If the load was evenly distributed between the cables, each cable would be carrying 43 tonnes, representing a "factor of safety" of 1.5.
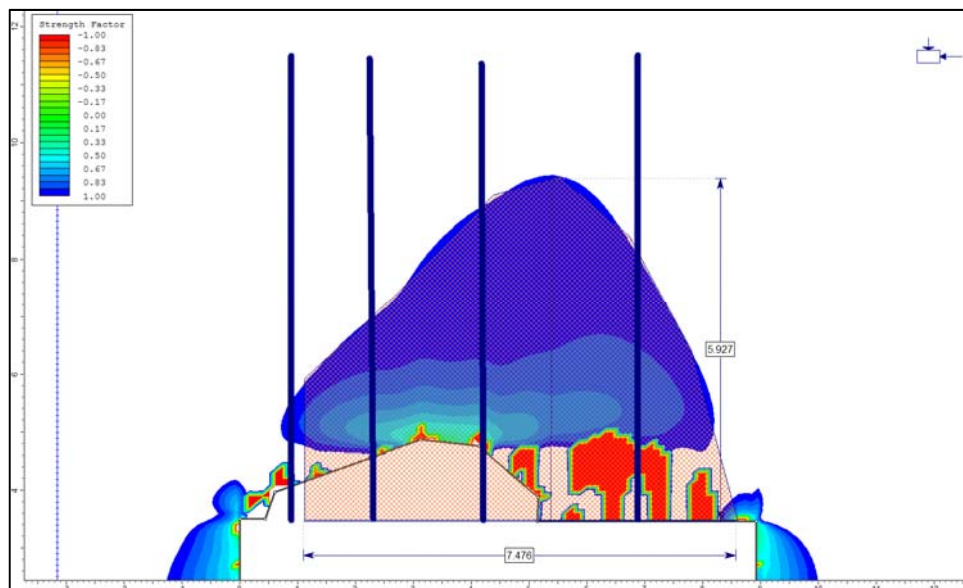
Figure 6: Close up of the modelled failure zone above the 9 m wide roadway

So four questions need to be answered:

1. Why did the immediate roof skin move so much?
2. Why did the 1.8 m and 2.5 m anchors move?
3. Why does the calculated factor of safety based on suspension of a possible detached block not reflect the unsatisfactory outcome?

In the following discussion, it will be assumed that the materials supplied to the mine were to specification and that they were installed by the experience and well trained workforce.

Adequacy of the geological model

Subsequent roof drilling has identified highly variable lithologies along the length of the installation roadway. It is possible that the geological and geotechnical properties of the borehole were not representative of the bulk of the installation roadway.

Adequacy of the behaviour model

The design was based on precedent and practice at the mine and hence a specific behaviour model was not proposed. Precedent/practice is an acceptable design approach if it can be demonstrated that conditions have not changed. The drilling referred to above highlighted the weakness of this assumption.

The a-posteriori application of a simple suspension model certainly needs more consideration. Frith and Colwell (2011) have stated that suspension is fundamentally flawed, while Seedsman (2014) has argued that it continues to have validity once the survivability of stiff cables in a compressive failure regime is considered. The following discussion is based on a suspension support model and the logical framework.

The empirical Analysis and Design of Faceroad Roof Support (ADFRS) model was not used by the mine. The key tenet of ADFRS that "*roof softening can be reduced by limiting roof displacement, this then increasing overall roof stability*" is not accepted. Instead it is considered that roof displacement beyond the elastic regime is a consequence of failure, be it opening of angled structures, shear along joints, and compressive failure of the rock mass or delamination of thin beams. The roof stress model invoked in ADFRS is also not supported by mine instrumentations (Seedsman 2014). Given the extreme divergence of views, it would be inappropriate to discuss the possible application of ADFRS to this case study.

The onset of compressive failure requires the application of brittle behaviour proposed by Martin, Kaiser and McCreath (1999) and implemented in soft rock by the method of Seedsman (2014).

Compressive failure and strand rupture

Most of the compressive failure on the first pass will have developed prior to the installation of the cable bolts. At the time of installation both the vertical and horizontal stresses in immediate roof will have already relaxed. The combination of the bolts and the cables will have resulted in negligible roof movement – at the stage the installed capacity would have been 366 tonnes compared to the weight of say 2 m layer of siltstone which would have been 27.5 tonnes.

Now consider the failure zone above the second pass into which the cables were pre-installed. According to the simple numerical model the elastic deviatoric stress in this zone are in the order of 10 MPa to 20 MPa and this is sufficient to cause failure. Consistent with Hutchinson and Diederichs (1996), the localised deformations within the failed rock may have been sufficient to cause strand rupture.

Destressing and relaxation

During the second pass and after the onset of compressive failure in the roof there would have been a substantial relaxation of the stresses; at a simple level the elastic deviatoric stresses would have reduced to zero. At the same time the broken rock mass would now have a much reduced deformation modulus. This is not to say there were zero horizontal stresses in the mine roof; the interaction of the broken rock with other blocks and with the support elements would result in some induced body stresses.

The mechanism here is stress reduction allowing the hole diameter to increase and hence cause a reduction in the shear strength of the rock/grout interface through a reduction in mechanical interlock.

If the gap exceeds the asperity height at the interface there can be no stress transfer. There are two interfaces where this can happen – the steel to grout and the grout to rock (Figure). Continued shear resistance requires a rough interface so the surfaces interlock: hence the adoption of bulbing for the steel/grout interface. At the grout to rock interface the problem is greater in lower modulus (= soft/sedimentary) rocks because the deformation per unit stress change is greater and hence a potentially larger gap. If a deformation modulus of 400 MPa is assumed for broken and sheared mudstone, a 45 mm borehole would have expanded by 1 mm which is well in excess of the likely roughness of the borehole wall especially the low strength and clayey composition of the rocks.

Inspection of Figure 6 indicates that such relaxation could have developed over a minimum length of 2.4 m.   If a yield strain of 1% and an ultimate stain of 3.5 % are assumed, such a free length could allow 24 mm to 84 mm of deformation. For a 4 m free length the deformations would be 40 mm to 140 mm.
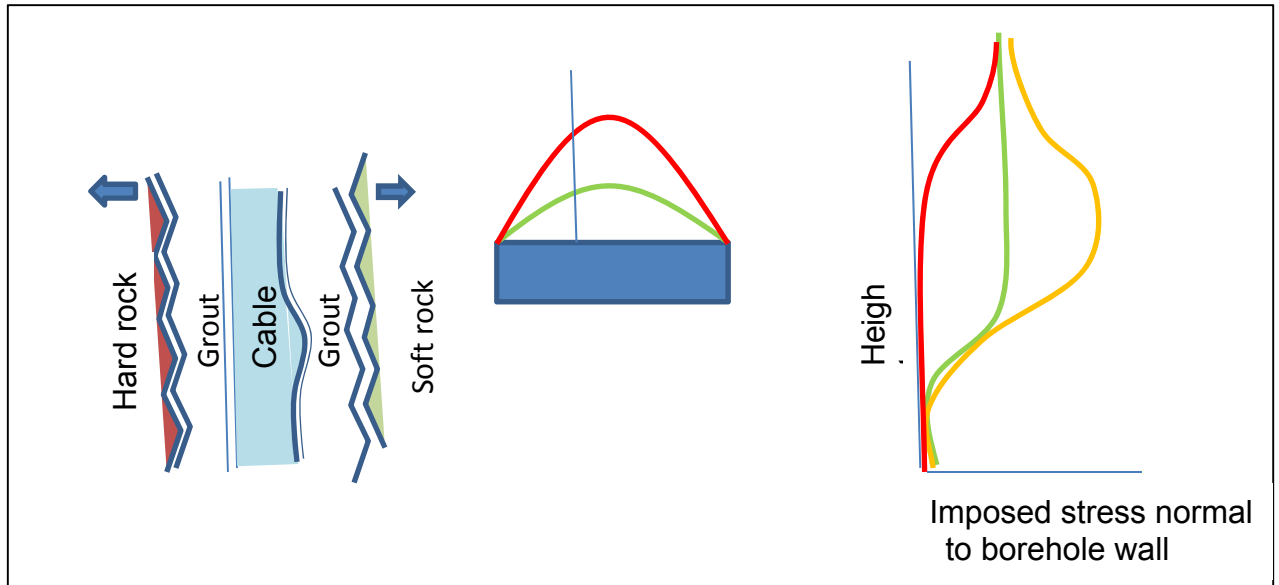
Figure 7: Stress relaxation and its impact on anchorages

It is not known if such debonding developed. Whilst such debonding would be anticipated to transfer loads to the plates (which was not observed) it is important to note that relaxation of stresses does not occur at the roof line during the second pass. This area underwent compressive failure prior to the installation of the cables and hence was already relaxed. There may have been a suitable length of grouted anchorage at the roof line such that loads were not transferred to the plates.

Installation of pre-tensioned fully grouted cables too stiff

Referring once again to Hutchinson and Diederichs (page 274): "*the cablebolts installed normal to the laminations covering the span area should be designed as stiff reinforcement within the zone of rock equivalent in thickness to a self supporting beam as calculated in this analysis…..Beyond this limit, an optimum cable array should have a more ductile response to allow the beam to deflect a small amount to generate the required compression for stability.   Beyond this should be a suitable anchorage length.*"

Currently in the Australian underground coal industry much is made of the supposed advantages of the stiffness inherent in fully-grouted and pre-tensioned cables. Seedsman (2014) has argued that this may be due to the habit of plotting the maximum height of movement (height of softening) as the Y axis against displacement at the roof line as the X axis. This plot leads to an interpretation that the height of softening can be controlled by limiting roof displacement, which is the key tenet of ADFRS.   If the data is plotted the other way around, it can be equally valid to assert that roof displacement is the consequence of the dilation associated with rock failure in the roof.

Laboratory tests on cables grouted into steel tubes result in the cables breaking at about 8 mm of opening of a joint in a double embedment pull test using steel tubes (Clifford *et al.,* 2001). It is not known if this test is at all representative of loading conditions in the field. Immediately prior to the onset of compressive failure, it could be argued that the elevated stresses result in compression of the boreholes in the same way that relaxation leads to dilation and this compression could lead to very stiff

anchorages. At the simplest level, the inference would be that the fully grouted cables may have ruptured as a result of the measured bedding dilations which are inferred to be well in excess of 8 mm.

GROUND CHARACTERISTIC AND SUPPORT REACTION

The ground characteristic of a gravity-driven collapse is a horizontal line, and hence the ground reaction concept has limited application to suspension designs in the compressive or tensile failure steps of the logical framework (Seedsman, 2012). The concept can be applied if there is some capacity of the rock mass to arch across an excavation and hence transfer stresses. One of the difficulties in applying the ground reaction concept in practice is the difficulty in determining the ground characteristic – numerical methods are required. In the two-pass installation roadway context, numerical analyses are further complicated by the stage formation of the roadway requiring complex three-dimensional considerations. When considering the bolts, the method can only consider a support pressure, expressed as equivalent stress applied to the roof: a support load density as kN/m^2. Consequently, the following back analysis has required numerous simplifications.

In the first pass driveage, the roof will respond by relaxing elastically into the roadway. These movements are substantially complete by the time the bolts and tendons are installed. In the following analysis, the elastic movements associated with the second pass will also be ignored as they are likely to be very small.

At the same time as the elastic movements develop, compressive failure will develop in the lower strength materials*. In situ* stresses are transferred away and it will be assumed that the immediate roof performance will be determined by the spanning capacity of the high strength sandstone layer. This layer will need to carry the failed material above as well as that associated with the bolted roof below. This layer may be adequately thick to span the 9 m wide roadway; if not the roof will fully detach and possibly collapse to a height determined by the failure of the low strength mudstone. In this section, these two mechanisms will be considered separately and then combined into a simplified ground characteristic.

Figure   presents the results of a voussoir beam analysis giving the relationship between thickness, deflection and stability for 5.2 m and 9 m spans. For a 5.2 m span and assuming a 0.4 m thick layer, the indicated stability is high and the deflection is in the order of 4 mm. Bearing in mind much of this will develop before an extensometer is installed this result is consistent with the measurements underground. For a 9 m span, the same 0.4 m thick layer would be self-supporting and deflect 30 mm while 0.3 m and 0.2 m thick units would not be self-supporting. The analysis indicates that a stable beam would need to be at least 0.34 m thick.
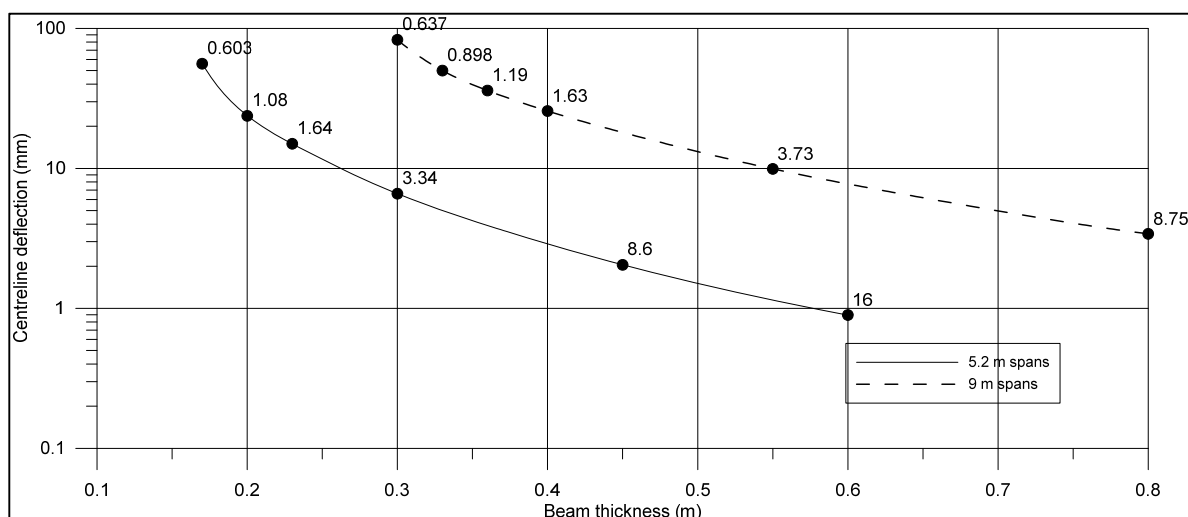
Figure 8: Deflection and stability of voussoir beams in medium grained sandstones (100 MPa, E= 25 GPa, 5 m failure height)

A possible ground characteristic can be obtained by altering the density of the material in the voussoir beam. In this way Figure   presents the ground characteristic for 9 m spans of the medium grained sandstone as a function of the thickness of the layer. The 0.4 m thick unit is self-supporting (the double

yellow line intersects the horizontal axis) and would not require any additional cables. The 0.3 m and 0.2 m units are not self-supporting.
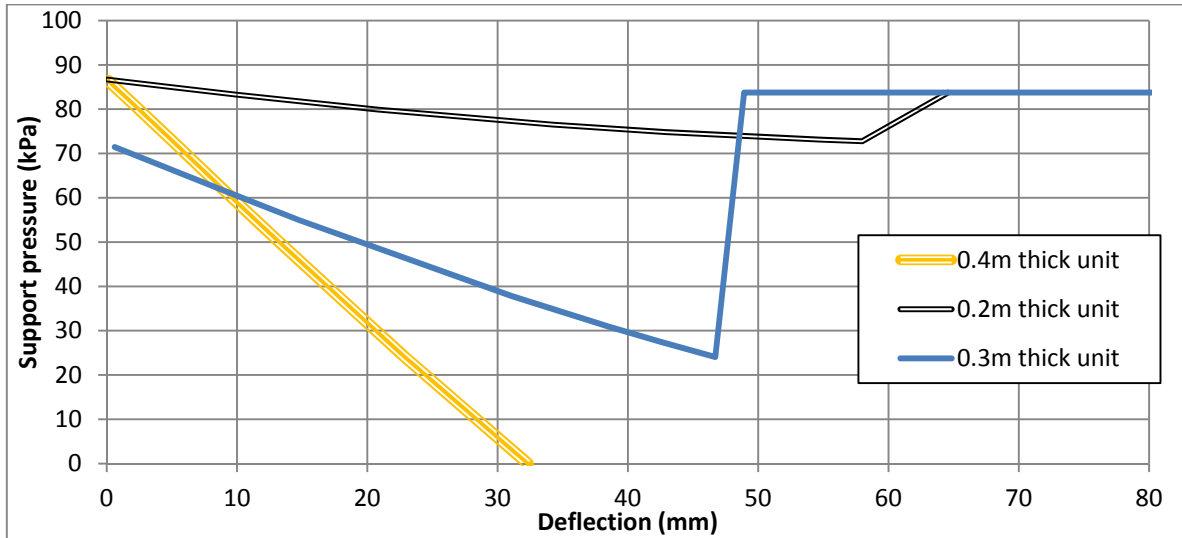
Figure 9: Composite ground characteristic of voussoir beam and collapse of the compressive failure mass

For the 0.3 m and 0.2 m sandstone layers the voussoir beams fail eventually (at 46 mm and 58 mm deflection respectively). When this happens the ground characteristic is determined by the weight of the detached block. For a 5 m high parabolic block over a 9 m span this is equivalent to a horizontal ground characteristic of 84 kN/m^2 as shown in Figure .

When considering pre-installed cables it is necessary to consider their efficiency in dealing with the moments associated with their location with respect to the centre of the 9 m wide roadway: it is possible that they are not equally loaded. Prior to the installation of the cable in the second pass the effective locus of the support reaction is located well inside the line of action for the weight (Figure 10). This results in a 30 % reduction in the efficiency of the installation. When the cable is installed in the second pass the efficiency improves to 93 % assuming the first pass cables have not ruptured.
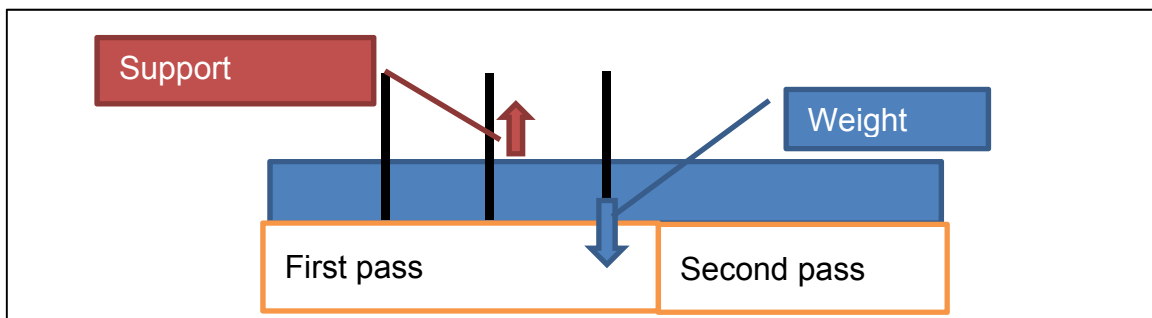
Figure 10: Moment loading of the pre-installed cables

The cables have been modelled assuming a tensile load of 540 kN at 1 % strain and 610 kN at 3.5 % strain. To simulate the laboratory test, a debonded length of a fully grouted cable is assumed to be 0.23 m. The point anchored cable has a debonded length of 3 m. It has been assumed that the roof deflects 30 mm before the final cable is installed in the second pass. The analysis has not considered the impact of pre-tensioning.

The ground characteristic and the support reactions are shown in Figure . The figure suggests that neither cable patterns would be required if the sandstone layer was 400 mm thick. Since the fully-grouted line does not intersect the 200 mm thick ground characteristic, failure of the support design is indicated prior to the installation of the cable in the second pass. The fully-grouted pattern would be considered marginal for a 300 mm thick unit. It is noteworthy that the point-anchored cable line indicates

that its full capacity is mobilised at in excess of 80 mm of movement; importantly the roof would be stabilised at 33 mm of deflection.
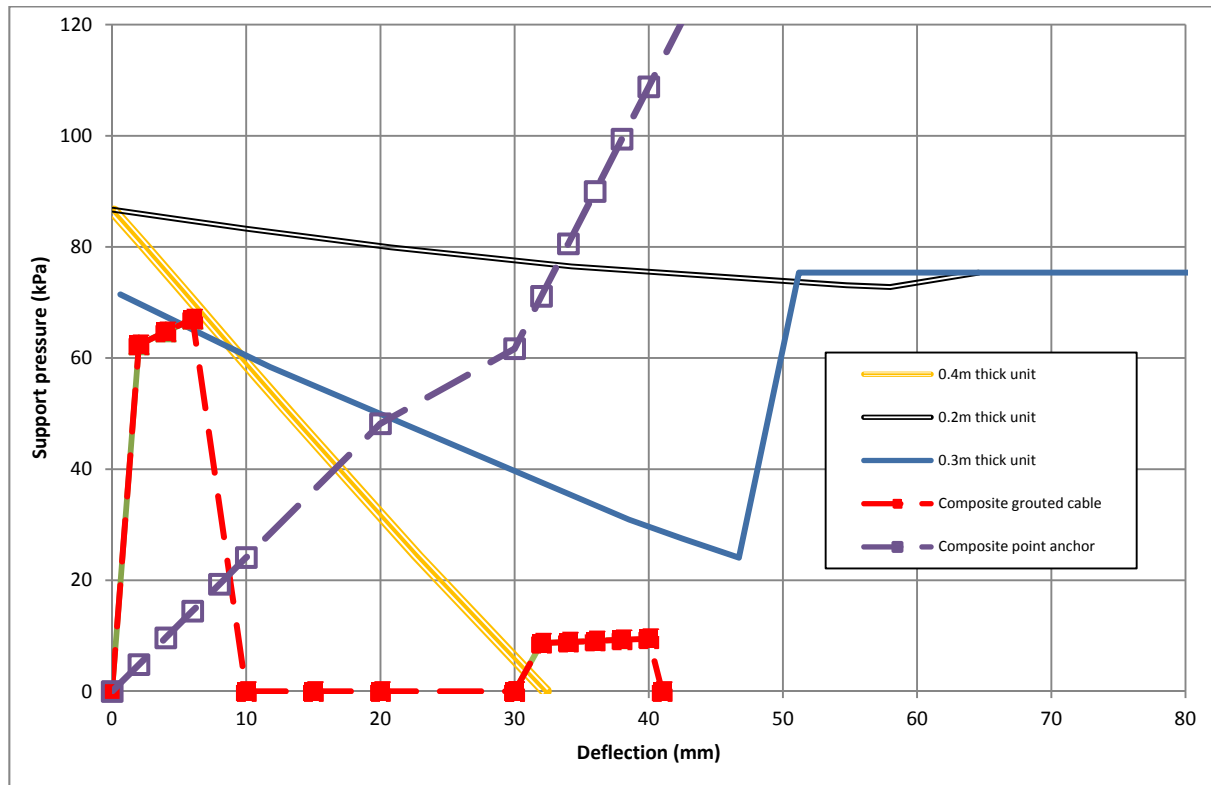
Figure 11: Full ground/reaction curves for the case study installation road

DISCUSSION

It is not possible to know what happened within the rock mass above the installation road as the mine decided to install additional support to prevent collapse. Putting emphasis on the observations of high frequency noises, it is considered likely that there was strand rupture at some location in the roof. The mine had recovered broken cables from previous installation roadways. It is noted that there are frequent reports of broken fully grouted cables in the Australian underground coal sector (Frith and Colwell, 2011). The state of knowledge of what happens with pre-installed cable bolts in a rock mass undergoing compressive stress failure condition is inadequate and the decision to re-support was justifiable based on the available information.

Based on an assessment of the geotechnical conditions and the presumed stress field, it is highly likely the low strength siltstones within the first 5 m of the roof underwent compressive failure. A possible consequence of such compressive failure was the breakage of the preinstalled fully grouted cables during the overstressing of the rock mass. If this compressive failure mechanism did not develop, it is possible they were too stiff and broke as they tried to prevent the roof deformation associated with the development of a voussoir beam.

A "softer" cable installation method would certainly address the hazard of deformations associated with the deflection of a voussoir beam, and would possibly address the survivability of the cables in a compressive failure environment by providing greater deformation capacity (Figure 12). As discussed by Hutchinson and Diederichs (page 104), such an installation can be achieved with paint, grease, or preferably plastic tubing; reference is made to deboning of bulbed cables. The anchorage is located outside the zone of compressive failure, and the collar is grouted to minimise loading on the plate and the barrel and wedge. In critical situations even if the cable survives the onset of compressive failure, relaxation and debonding probably develops at the rock/grout interface so there is now real concern if debonding at the steel to grout interface is engineered into the tendons before installation.
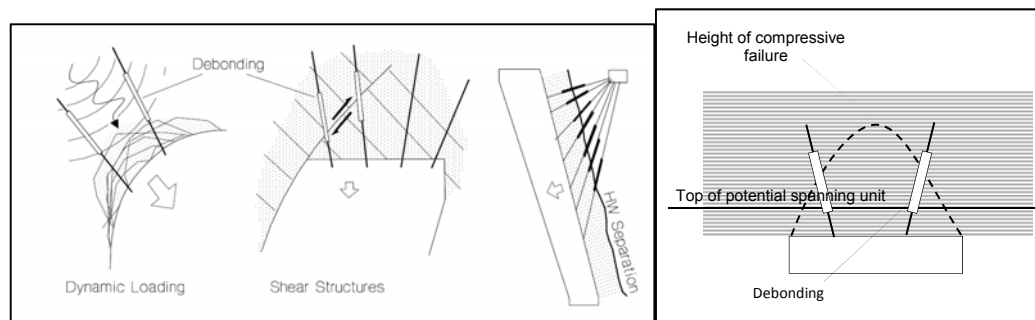
Figure 12: Desirable debonding situations (left – metal mines (Hutchinson and Diederichs), right – coal mines)

Recommendations for future installation roadways at the site of the case study included:

1. Site characterisation before driveage of the first pass including roof core at tailgate of previous face line, geological and geotechnical log, rock strength testing. It is acknowledged that fracture logging may not be indicative of the pre-mining condition of the rock mass if the rock strength is relatively low.
2. Prediction of likely ground behaviour using simple stress elastic and voussoir beam models.
3. Support design based on dead-weight suspension and site precedent practice.
4. Use of full grouted but de-bonded cables to provide unquestioned deformation capacity.
5. Revision of critical roof deflection levels based on acceptable strain over de-bonded length of the cable.
6. Core drilling down the length of the first pass of the installation to confirm the geotechnical model used in the design.
7. Detailed extensometry and bore scopes to confirm predictions made during design.

REFERENCES

Brady, B H G and Brown, E T. 1985, Rock mechanics for underground mining, London, UK: George Allen & Unwin.

Clifford, B, Kent, L, Altounyan, P and Bigby, D. 2001, Developments in the long tendon systems used in coal mining reinforcement, *In Proceedings, 20th International Conference on Ground Control in Mining*, Morgantown WV August 7-9, 235-241. http://icgcm.conferenceacademy.com/papers/detail.aspx?subdomain=icgcm&iid=735.

Colwell, M G and Frith, R. 2013, ACARP C19008. Analysis and design of faceroad roof support (ADFRS) – a roof support design methodology for longwall installation roadways, *Colwell Geotechnical Services*.

Frith, R and Colwell, M G. 2011, Why Dead Load Suspension Design For Roadway Roof Support Is Fundamentally Flawed Within A Pro-Active Strata Management System, *Proceedings 30th International Conference on Ground Control in Mining*, http://icgcm.conferenceacademy.com/papers /detail.aspx?subdomain=icgcm&iid=890.

Hutchinson and Diederichs. 1996, Cable bolting in underground mines, *BiTech Publishers*, British Colombia.

Lambe, T W. 1973, Predictions in soil engineering, *Geotechnique*, 23 (2) 149-202.

Martin, C D, Kaiser, P K and McCreath, D R. 1999, Hoek-Brown parameters for predicting the depth of brittle failure around tunnels, *Canadian Geotechnical Journal*, 36(1), 136-151.

Seedsman, R W. 2012, The development and application of a logical framework for specifying roof and rib support/reinforcement in Australian underground coal mines, *7th International Symposium on Rock bolting and Rock Mechanics in Mining*, Aachen 30-31 May.

Seedsman, R W. 2013, Practical strength criterion for coal mine roof support design in laminated soft rocks, *Mining Technology*, 122(4), 243-249.

Seedsman, R W. 2014, Suspension Designs Required in the Logical Framework, *33rd International Conference on Ground Control in Mining*. 97-104, http://icgcm.conferenceacademy.com/papers/detail.aspx?subdomain=ICGCM&iid=2105.

Thomas, R. 2010, The design and management of wide roadways in Australian coal mines, *29th ICGCM* Morgantown, 191-197, http://icgcm.conferenceacademy.com/papers/detail.aspx?subdomain=icgcm&iid=325.

IMPROVED ROOFBOLTING METHODOLOGIES: REDUCING HYDRAULIC FRACTURE OF STRATA

David William Evans

ABSTRACT: Induced hydraulic fracture of strata during roof bolt installation is a potentially prevalent, but masked phenomenon within the underground coal industry. Previously reported resin testing programs (McTyre *et al.,* 2014) examined the relationship between resin mixing effectiveness and varying bore hole diameter. The methodology employed within this earlier test program facilitated a further critical area of research – the measurement of back pressures generated within the bore hole during standard rock bolt installation practices. Experimental data has indicated that fluid resin can be pressurised to levels where it exceeds the compressive strength of the strata, inducing hydraulic fracture within the immediate area of the bolting horizon. The routine cycle of roof bolting serves to propagate this effect, progressively fracturing and delaminating the roof during mine advancement. This masked phenomenon can lead to a perception of difficult ground conditions - mining efficiencies and costs are therefore affected, with increased need for additional support subsequently required to re-stabilise the inadvertently damaged roof.

Further analysis of the parameters associated with resin bolt installation has now been conducted, assisting in the development of an empirical relationship between bore hole pressure, bore hole diameter and bolt insertion times. This relationship has been analysed for 15:1 ratio resins and 2:1 ratio resins, within 28 mm and 30 mm boreholes. Further to this, load transfer performance has been comparatively assessed for both 28 mm and 30 mm boreholes, suggesting that for 2:1 resins, acceptable resin mixing and load transfer can be obtained within a 30 mm bore hole. The combination of 2:1 resins, utilised within a 30 mm bore hole, may well provide the optimal solution to reduce the risk of hydraulic fracture in weaker strata during resin bolt installation.

INTRODUCTION

A number of industry papers have previously investigated areas of concern associated with the performance of cartridge style resins in roof bolting, predominantly focussing on the effects of plastic film gloving, inadequate resin mixing and the pressurisation of resin within the bore hole. These three effects have a critical influence on the load transfer of the steel bolt element, through the cured resin and into the surrounding strata.

Gloving occurs due to the plastic film of the resin cartridge partially encasing or wrapping around the steel roof bolt element – a known phenomenon over many years (Pettibone, 1987). The plastic film creates regions of discontinuity between the bolt, cured resin and borehole, reducing effective load transfer into the strata. Experiments conducted into the effects of bolt ends fully encased by plastic film (Pastars and MacGregor, 2005) revealed that load transfer can be reduced by 85 to 90% in worst-case occurrences. It is also known that the aggregate filler size used within the resin can assist in shredding and breaking up the plastic film – this effect was observed in a previous study on resin mixing effectiveness (McTyer *et al.,* 2014).

Beyond the immediate impact of gloving discontinuities, is the issue of poor resin component mixing – where sections of resin remain unmixed and uncured after bolt installation is complete. The film casing of a resin cartridge has two internal compartments, each respectively holding the 'mastic' and 'catalyst' components. Note that the referred ratios for resin cartridges are simply the volumetric ratio of mastic to catalyst. When the mastic and catalyst are mixed in the correct ratio, the resin will cure and harden. However, it has been reported that for some resin cartridge designs, the catalyst compartment is dimensionally too small to be fully ruptured by the rotation of the bolt in the borehole (Campbell and Mould, 2003). Laboratory trials within a 28.5 mm borehole indicated that under initial insertion of the bolt, the resin cartridge expands and the catalyst compartment is pushed against the wall of the borehole. In this instance, the geometrical configuration can permit the ribbed bolt profile to pass through without fully rupturing and dispersing the catalyst through the resin mix, causing significant areas of uncured resin. While the cartridge and bolt are not fully defined within the 2003 paper, given the date of publication and

the New Zealand origins of the experimentation, it can be assumed that the bolts were an M24 left hand anchor bar and that the resin cartridges were a 24 mm diameter 15:1 mastic to catalyst ratio.

Pressurisation of fluid resin within boreholes has also been an area of investigation. Earlier research focussed on the relationship between resin pressurisation and gloving, with theorisation that the plastic film cartridge may radially expand under the initial thrust of the bolt, then rupture and slip over the bolt end – hence the derivation of the term 'gloving'. Resin pressurisation was also associated with the loss of resin volumes into strata voids, reducing resin encapsulation of the bolt and weakening of the corresponding load transfer. (Giraldo *et al.,* 2006) proposes a mathematical model for the burst pressure associated with rupture of resin cartridges. However, as seen from the derived pressure verses displacement curves, while the point of cartridge rupture provides an initial pressure increase, it is certainly not associated with the peak pressures that are measured on full bolt insertion. Pressures observed by Giraldo, for different bolting systems, ranged from 3,500 psi (*24.13 MPa*) up to 7,000 psi (*48.26 MPa*). It was also observed that bolting systems with greater annulus around the bolt, as well as slower installation speeds, produced lower insertion pressures. While pressures of this magnitude have been measured, the exact modes that lead to the generation of such elevated pressures have not been fully explored.

THE DEVELOPMENT OF AN EMPIRICAL MODEL

The determination of internal borehole pressures due to resin flow presents a highly complex fluid mechanics model, involving numerous parameters. These parameters can be compiled under three main groupings, being the *fluid characteristics* of the resin, the *dimensional geometry* of the resin, borehole and bolt, as well as the *rate of insertion* of the bolt. These parameters are outlined below:

- Fluid characteristics of the resin
  - Dynamic Viscosity (N.sec.m^{-2})
  - Density (kg.m^{-3})
- Dimensional geometry – resin, borehole and bolt
  - Resin cartridge diameter (m)
  - Resin cartridge length (m)
  - Bore hole diameter (m)
  - Bolt core diameter (m)
  - Bolt rib profile (various dimensions) – height, width, flank angles, radial profile, pitch spacing (m, degrees)
  - Relative surface roughness of the borehole (dimensionless)
- Rate of insertion of bolt
  - Bolt insertion velocity (m.s-1)
  - Bolt rotational speed (rad.s-1)

Two points are worthwhile noting in regards to these parameters. The first is that for a mining resin, viscosity is only a notional concept. The resin is actually a suspension of solids in liquids – it is not a uniform, homogenous fluid. Further to this, resin cartridges are of course a two component system – a chemical reaction transforms the properties of the resin during bolt installation. Therefore, a true measurement of viscosity is actually indeterminate. Similarly, the measurement of true density values is also difficult.

The second key point relates to bolt insertion velocity. It is the velocity of the bolt through the resin that generates the flow of the liquid and the corresponding back pressures in the bore hole. The insertion force (N) of the bolt will of course influence the bolt velocity – a greater thrust force will insert the bolt faster – however it is the velocity of the rockbolt that determines the velocity of the resin flow and associated borehole pressures. This is schematically shown below in Figure 1.
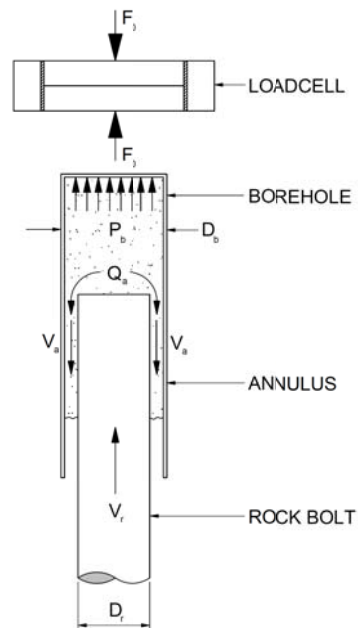
Figure 1: Representation of resin flow within borehole due to advancement of rock bolt

In Figure 1 the following values have been used:
V_r = Insertion velocity of rockbolt (m.s^{-1})
P_b = Borehole internal fluid pressure (Pa)
Q_a = Flow rate of fluid in annulus (m^3.s^{-1})
V_a = Fluid velocity in annulus (m.s^{-1})
D_b = Borehole diameter (m)
D_r = Rockbolt core diameter (m)
F_o = Output force (N)

Further complicating the analysis of borehole pressures is the fact that the resin flow is highly turbulent – due to speed, rotation and geometry. For applications of internal incompressible viscous flow, it is known that "In turbulent flow the pressure drop cannot be evaluated analytically, but this can be achieved by experimental results and dimensional analysis to correlate the experimental data" (Fox and McDonald, 1985).

For bolt insertion through resin, in order to develop a working empirical model that makes sense of experimental data, the added complexity of minor or indeterminate parameters must be initially set aside. Only parameters that are determinate and have a major influence on back pressure have been selected for use. For the purposes of this initial mathematical model, the bolt rib dimensions, relative roughness and rotational speed are not included as explicitly defined parameters – even though their influences will be captured within the experimental data sets. Also, note that the experiments and associated data are exclusively grouped by resin type. This is due to the fact that resin viscosity and density cannot be truly measured and therefore cannot be explicitly defined within the empirical model. The influences of plastic remnants from the film cartridge are also not specifically accounted for – however, these would only serve to further restrict flow and increase annulus pressure.

The fundamental premise of the empirical model is that the back pressure of the liquid resin in the borehole (Pa) is predominantly a function of the velocity of the liquid resin (m.s^{-1}) through the annulus created between the bolt and the borehole. From a fluid mechanics perspective, this is a logical relationship – as the bolt progressively advances, the static volume of the liquid resin must rapidly accelerate and flow through the comparatively small cross sectional area of the annulus – hence the velocity of the resin through the annulus becomes high. Further to this, note that pressure losses for sudden constrictions in fluid flow are based on the square of the fluid velocity divided by two (Fox and McDonald, 1985, 367).

So, the basic empirical model becomes:

$$P_b = f \left(V_a^2 / 2 \right) \tag{1}$$

Where: P_b = Borehole internal pressure (kg.m^{-1}.s^{-2})
              V_a = Fluid velocity in annulus (m.s^{-1})
              f = functional correlation between pressure and resin fluid velocity

Excluding minor and indeterminate parameters, the thesis is that this empirical relationship holds true at the point of peak pressure and annulus velocity – when measured at full bolt insertion. At the peak of insertion and specific to individual resin types, a ratio can then be assumed between peak pressure and velocity - and the equation becomes:

$$P_b = R_{pv} (V_a^2 / 2)$$ (2)

Where: R_{pv} = pressure-velocity ratio, *at peak pressure* (kg.m^{-3})

EXPERIMENTAL METHODOLOGY

The experimental method utilised for this report was documented in an earlier publication (McTyre *et al.,* 2014). This involved internally sleeving the borehole utilising a PVC pipe of specific diameter, contained within and structurally supported by an external, heavy walled steel pipe to prevent swelling of the inner PVC pipe. The PVC pipe was capped at the top end to prevent resin loss and constrained at each end to prevent internal slipping and rotation. The internal PVC pipe could be readily removed after each installation test was completed, permitting quick changeover and multiple tests to be conducted. The PVC pipe could also be easily cut open and peeled away, to fully view and inspect the entire resin annulus. Various pipe combinations could be utilised to simulate both a 28 mm and a 30 mm borehole. This sleeving method was further supported with calibrated instrumentation on the drill rig, including a toroidal load cell, linear displacement transducer and tachometer. For every bolt installation, a data logger was utilised to capture force (kN), displacement (mm) and rotational speed (rpm) against time (sec) to a resolution of 0.1 sec per data event. Figure 2 outlines the experimental arrangement.

Experimental results – pressure / flow relationships

Utilising this experimental method, a series of bolt installations were conducted and average data sets were compiled. Two resin types were investigated - a 2:1 resin and a 15:1 resin. Two bore holes were also investigated, 28 mm and 30 mm. A single bolt type was used across all installations, being standard left hand anchor bar with a nominal core diameter of 21.7 mm. The bolt steel grade was HSAC840, commonly available on the Australian market. The following installation graphs shown in Figures 3 to 6 provide the experimental data derived from this test program – each graph represents the average data set from multiple tests for each experimental combination.
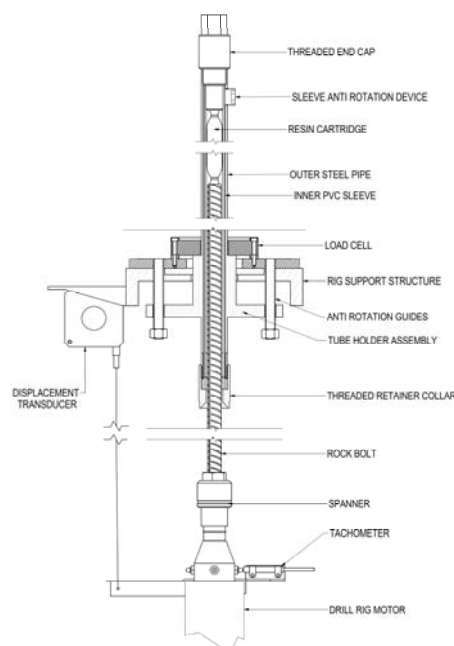
Figure 2: The 'Borehole Sleeving' experimental method, including instrumentation features
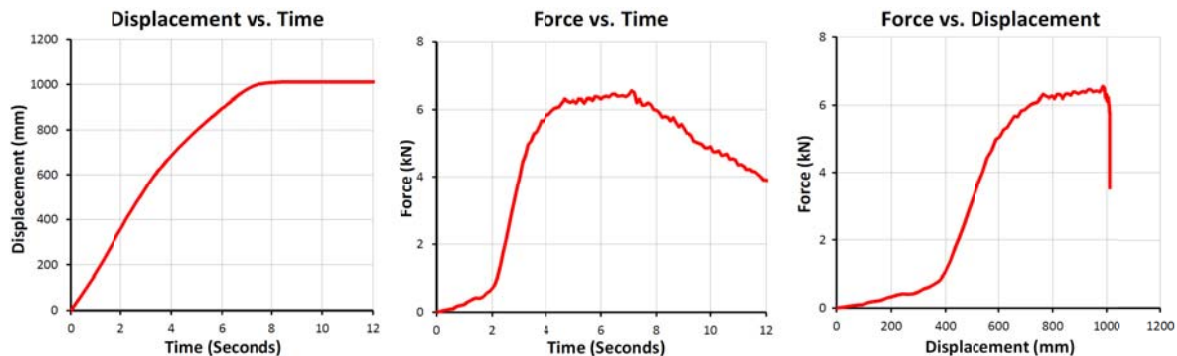
Figure 3: Installation graphs for 15:1 resins, 1000 mm long, into a 28 mm borehole. Data shown is the average curve for 20 tests
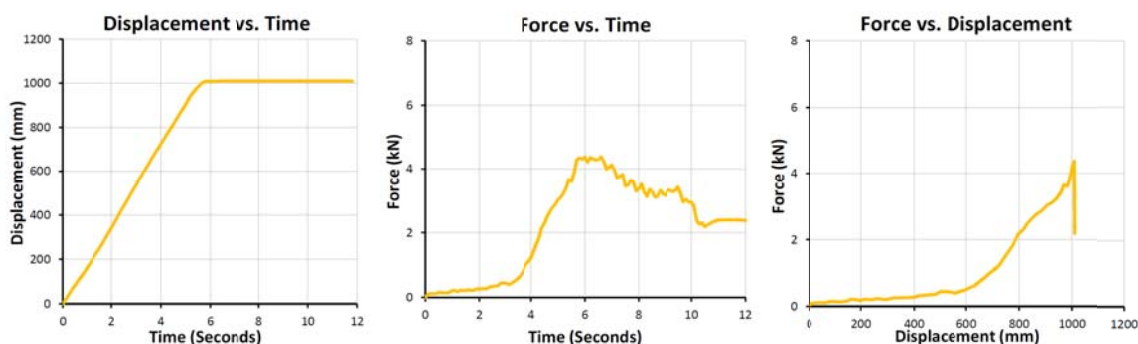
Figure 4: Installation graphs for 15:1 resins, 1000 mm long, into a 30 mm borehole. Data shown is the average curve for five tests
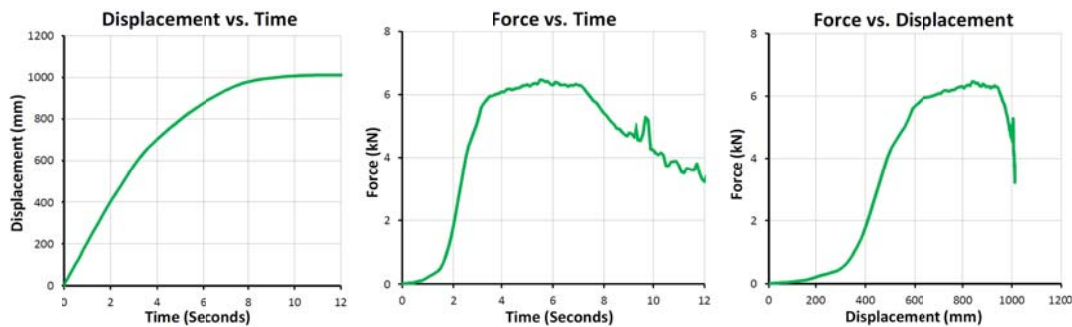
Figure 5: Installation graphs for 2:1 resins, 1000 mm long, into a 28 mm borehole. Data shown is the average curve for 20 tests.
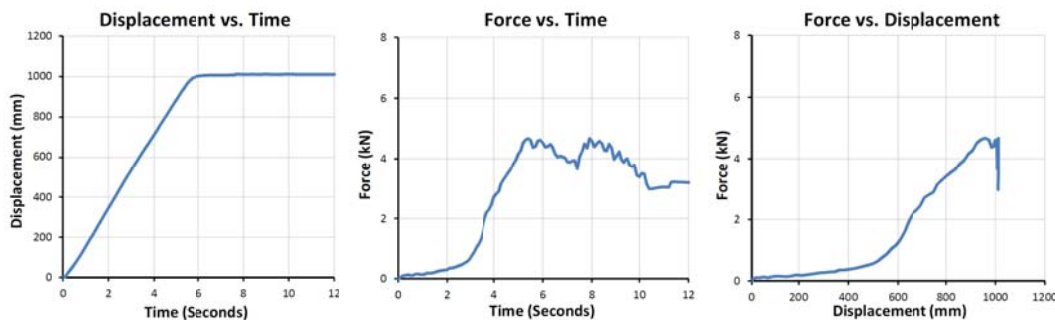
Figure 6: Installation graphs for 2:1 resins, 1000 mm long, into a 30 mm borehole. Data shown is the average curve for ten tests.

For each experiment, the average insertion time was determined - this was used to calculate the flow rate of resin through the annulus. The total resin volume is of course known, simply by measurement of the cartridge dimensions. Upon full insertion of the bolt into the resin, the flow rate into the annulus, Q_a, is then the total resin volume divided by the full insertion time. The peak velocity of resin in the annulus, upon full bolt insertion, is therefore the flow rate divided by the annulus area. This is expressed in the following equations:

$$Qa = vc / tf \qquad \text{and} \qquad Va = Qa /Aa \qquad\qquad (3)$$

Where: Q_a = volumetric flow rate of resin into annulus ($m^3.s^{-1}$)
               v_c = volume of Resin Cartridge (m^3)
               t_f = time for full insertion through the resin cartridge (s)
               V_a = velocity of resin within the annulus ($m.s^{-1}$)
               A_a = annulus area (m^2)

Referring to Figure 1, the internal pressure of the bore hole is determined by the measured output force, divided by the area of the borehole, calculated simply as:

$$Pb = Fo / Ab \qquad\qquad\qquad\qquad\qquad\qquad (4)$$

Where: P_b = Borehole Internal Pressure ($kg.m^{-1}.s^{-2}$)
               F_o = Output Force (N)
               A_b = borehole area (m^2)

Utilising the experimental methodology as described and the mathematical relationships defined above, data sets were compiled for each experimental combination, provided in Table 1 - this permitted calculation of the Peak Pressure-Velocity Ratio, R_{pv}.

Table 1: Calculation of Peak Pressure-Velocity Ratio (R_{pv}), based on the various experimental data sets

| *Resin Type*	**15:1 Resin, 1000 mm Long**		**2:1 Resin, 1000 mm Long**	
Borehole Diameter (mm)	28	30	28	30
Bolt Type / Core Diameter (mm)	AT / 21.7	AT / 21.7	AT / 21.7	AT / 21.7
Cartridge Diameter (mm)	23.7	23.7	23.4	23.4
Cartridge Volume (mm^3)	441,208	441,208	430,108	430,108
Annulus Area (mm^2)	245.95	337.07	245.95	337.07
Bolt Full Insertion Time (s)	7.5	5.7	9	5.7
Effective Resin Flow Rate ($mm^3.s^{-1}$)	58,828	77,405	47,790	75,458
Annulus Flow Velocity ($mm.s^{-1}$)	239	230	194	224
Peak Load (N)	6,600	4,300	6,500	4,700
Peak Pressure (Pa)	10.717×10^6	6.082×10^6	10.555×10^6	6.648×10^6
Peak Pressure-Velocity Ratio ($kg.m^{-3}$)	3.747×10^8	2.307×10^8	5.591×10^8	2.653×10^8

Derivation of peak pressure installation curves

Given that the Peak Pressure-Velocity Ratio is determined for each experimental data set, this relationship can now be used to mathematically determine the Peak Pressure for varying flow velocities within the annulus. The annulus flow velocity correlates to bolt insertion velocity and bolt insertion time, pushing through 1000 mm of resin. Note that these empirical relationships are only assumed for each individual resin type and length – the R_{pv} value is assumed to be different for different resin types and fluid characteristics. The following charts of predicted peak pressure in Figures 7 and 8 have been determined by individual resin type and borehole size. Also, the R_{pv} value for the 27 mm borehole is a linear extrapolation, based on the R_{pv} values determined from the 28 mm and 30 mm data sets.

The peak pressure charts clearly indicate the nature of the relationship between bolt insertion velocity, borehole size and peak pressure. An important observation is that the pressures derived within this empirical model are of a similar magnitude to the borehole pressures measured by Giraldo, *et al*., (2006). The empirical model also shows that increasing the borehole size and reducing the insertion velocity substantially reduces the peak pressure. Further to this, it can also be noted that the 2:1 pressure curves are slightly more elevated compared to the equivalent 15:1 curves – this outcome in the empirical relationship notionally captures the fact that the 2:1 resins are slightly 'thicker' or more 'viscous' compared to the 15:1 resins.

Further experimentation – load transfer for 30 mm boreholes

The inherent concern is that, with increasing borehole annulus size, the load transfer performance to the strata is assumed to reduce. In order to assess this potential difficulty, load transfer tests were conducted within a pre-cast concrete block, using a series of drilled holes 300 mm deep, both 28 mm and 30 mm in diameter. The boreholes were blown clear of debris with compressed air after drilling, internally inspected with a bore camera and dimensionally measured prior to bolt installation. Each resin and bolt combination were installed using recommended manufacturers spin times to ensure correct mixing and then left for a 24 hr period before pull testing commenced. Each installed bolt was of the same profile type (AT grade) and approximately 600 mm in length, in order to pass continuously through the hollow bore cylinder jack body. This avoided the use of couplers, eliminating displacement errors during initial loading and take-up of the system. The hollow bore jack and pressure gauge had current 3rd party calibration for force against hydraulic pressure. Displacements were measured using a dial gauge indicator mounted on a heavy steel block. 20 tests were conducted in total – 10 tests for 15:1 resin in a 28 borehole and 10 tests for 2:1 resin in a 30 mm borehole. Figures 9a and 9b show the setup for the pull test experimentation.
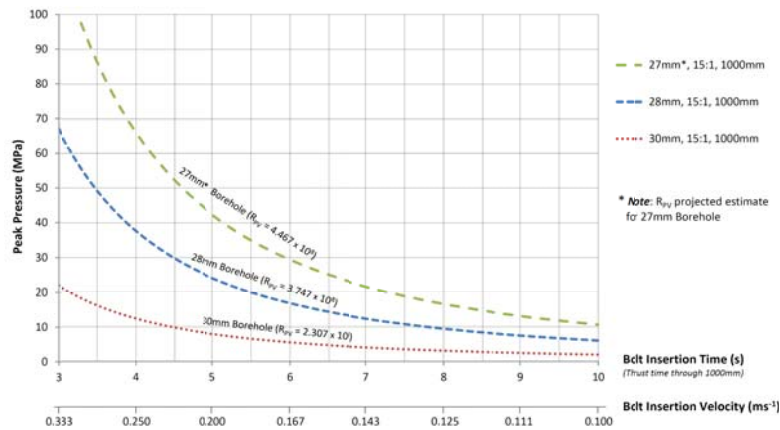
Figure 7: Predicted peak pressures for 15:1 ratio x 1000 mm long resin cartridges, against bolt insertion velocity – for 27 mm, 28 mm and 30 mm boreholes
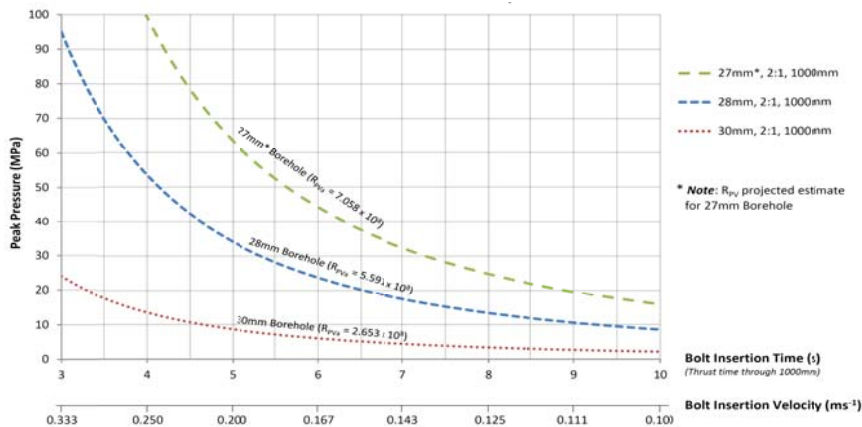
Figure 8: Predicted peak pressures for 2:1 ratio x 1000 mm long resin cartridges, against bolt insertion velocity – for 27 mm, 28 mm and 30 mm boreholes

Figures 9a and 9b: Pull test experimental setup – 300 mm embedment, 28 mm and 30 mm hole diameters
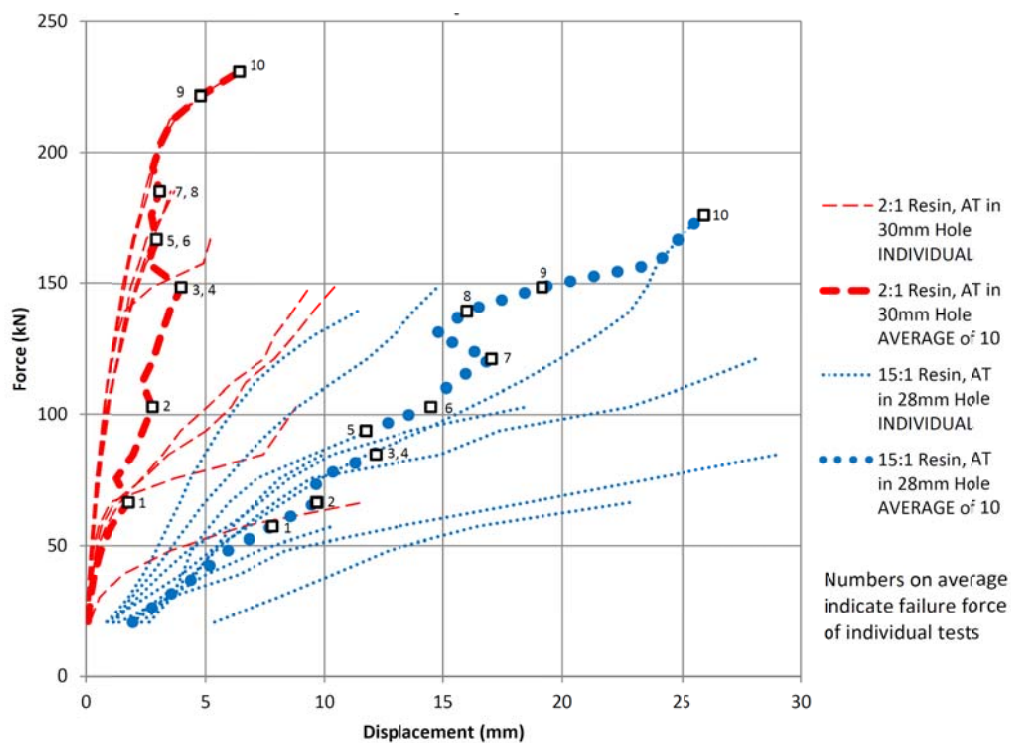
Figure 10: Pull test results for 300 mm embedment tests – 15:1 resins in 28 mm boreholes, 2:1 resins in 30 mm boreholes

The results from the pull tests are given below in Figure 10. The major curves indicate the progressive average of the ten tests, while the minor data curves show each individual test result. Note that the numbers indicated on the averaged curves show the peak load position of each individual test result. Based on the averaged curves, the 2:1 resins within 30 mm boreholes show a stiffer result compared to the 15:1 resins within 28 mm boreholes. The peak load transfer results are also higher for the 2:1 resins.

CONCLUSION

Plastic gloving and poor resin mixing are known concerns with 15:1 ratio resin cartridges – particularly in boreholes greater than 28 mm in diameter. However, for boreholes smaller than 28 mm, resin pressurisation during bolt installation can be elevated to levels that induce hydraulic fracture and delamination of weaker strata. At elevated insertion pressures, resin volumes are also lost into strata voids and bolt encapsulation is subsequently affected. The derivation of an empirical relationship

between borehole size, bolt insertion velocity and peak borehole pressure is useful in determining the risk of hydraulic fracture of strata and resin loss during bolt installation - this risk is seen to substantially reduce with the utilisation of boreholes 30 mm in diameter. Further to this, 2:1 resins are observed to mix well within a 30 mm borehole, providing load transfer results that appear to exceed that of 15:1 resins within a 28 mm borehole. Taking all factors into account, the combination of 2:1 resins, utilised within a 30 mm bore hole, may well provide the optimal resin bolting solution - reducing the risk of hydraulic fracture and resin loss in weaker strata, while maintaining adequate load transfer performance

REFERENCES

Campbell, R and Mould, R. 2003, Investigation into the Extent and Mechanisms of Gloving and Un-mixed Resin in Fully Encapsulated Roof Bolts, In *Proceedings of the 22nd International Conference on Ground Control in Mining,* Morgantown, WV, pp 256-262.

Fox, R W and McDonald, A T. 1985, *Introduction to Fluid Mechanics*, John Wiley and Sons, New York.

Giraldo, L, Cotton, S and Farrand, J. 2006, Characterisation of Internal Insertion Pressure During Installation of Fully Grouted Bolts, In *Proceedings of the 25th International Conference on Ground Control in Mining,* Morgantown, WV, pp 395-399.

McTyer, K, Evans, D, Reed, G and Frith, R. 2014, The borehole sleeving test method of resin anchored roof bolt installations, In p*roceedings of the 2014 Coal Operators Conference*, University of Wollongong, NSW, pp 118-127.

Pastars, D and Mac Gregor, S. 2005, Determination of load transfer aharacteristics of gloved resin bolts from laboratory and *in situ* field testing, In *proceedings of the 24th International Conference on Ground Control in Mining,* Morgantown, WV, pp 329-337.

Pettibone, H. 1987, Avoiding anchorage problems with resin-grouted roof bolts*, Report of Investigations (United States Bureau of Mines) 9129*.

THE IINFLUENCE OF CONCRETE SAMPLE TESTING DIMENSIONS ON ASSESSING CABLE BOLT LOAD CARRYING CAPACITY

Ibad Ur-Rahman, Paul Hagan and Jianhang Chen

ABSTRACT: This paper presents the results of a study into the influence of size of the test sample on the maximum load carrying capacity of 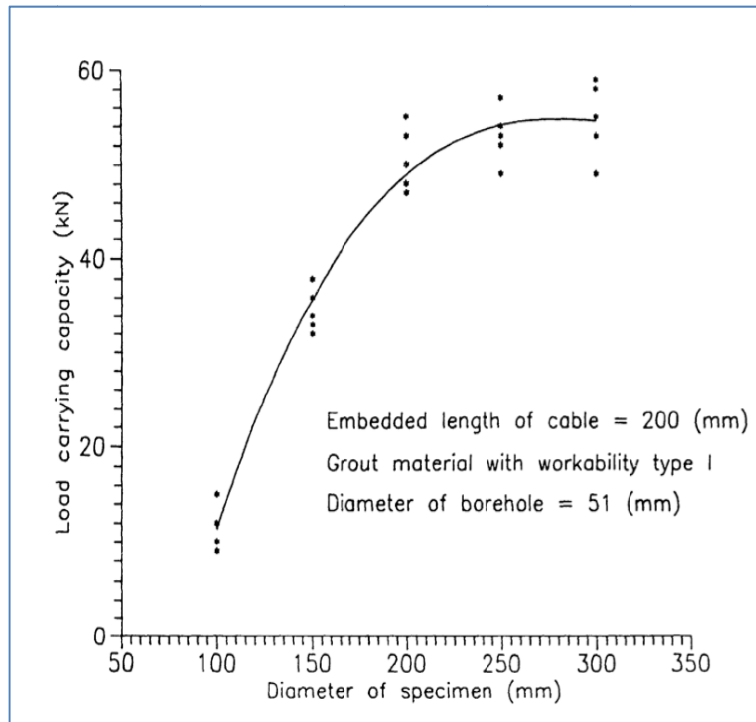cable bolts. As part of the design for the standardisation of the laboratory pullout test, it was previously found that the size of the sample in which the cable bolt is embedded can influence the behaviour of the cable bolt in terms of the peak load carrying capacity. This testing was done with a low capacity plain strand cable bolt with the sample in an unconfined state. Confinement of the sample during testing better simulates the *in situ* condition of the interaction between the cable bolt and surrounding rock mass. A test program was undertaken to assess whether there was any significant difference in the load carrying capacity with varying diameter of test samples and at different levels of confinement. A series of pull-out tests were conducted on cable bolts embedded into samples varying between 150 mm and 500 mm in diameter that were placed within a steel cylinder to provide confinement to the test samples. It was found maximum load varied with the test sample diameter up to some threshold diameter but that confinement pressure also had a significant effect on the load carrying capacity of a cable bolt.

INTRODUCTION

The application of cable bolt systems has advanced rapidly in recent years due to better understanding of the load transfer carrying capacity mechanisms and the advances made in cable bolt system technology. Cable bolts are used as part of temporary and permanent support systems in both civil tunnelling and mining operations throughout the world. In mining they are used for slope stability applications in surface mining and a variety of ground support purposes in underground operations such as stoping, roadway development and shaft sinking. Cable bolts are used to prevent the movement between discontinuity planes by transferring load across the discontinuity when relative strata layer movement takes place with separation.

The most common type of failure mechanism identified in the field is failure at the cable-grout interface (Hyett, Moosavi and Bawden, 1996; Singh *et al.*, 2001). This type of failure is common due to insufficient frictional resistance between the cable strand ridges and the grout material usually due to poor ground conditions and/or poor quality control at installation which leads to weak shear bond strength at the interface. This will often result in premature failure of the system before the steel capacity is mobilised. Due to the vast majority of failures being identified at the cable-grout interface, it can be concluded that a standardised testing methodology should focus on failures at the cable-grout interface (Rajaie, 1990; Hutchinson and Diederichs, 1996)

As reported by Hagan, Chen and Saydam (2014), a range of testing methods has been developed over the years including the double embedment and more recently the Laboratory Short Encapsulation Pull Test (LSEPT). The latter overcomes many of the deficiencies in the earlier tests. An issue with the LSEPT method highlighted by Thomas (2012) is the use of a small diameter test sample of approximately 142 mm placed within a pressurised Hoek cell arrangement and its inability to withstand the torsional loads generated during a pull-test. Rajaie (1990) reported a study on the anchorage strength of cable bolt and the effect of the diameter of the test sample. Nearly 300 pull-tests were conducted using test samples in an unconfined state in order to define the characteristic and behaviour of the cable bolt element using conventional grout and grout-aggregate. The cable bolt used was a plain strand cable with a diameter of approximately 15 mm in test samples having a constant embedment length and borehole diameter. Tests were conducted in test rock samples having diameters ranging between 100 mm and 300 mm. As the results in Figure 1 show, the load carrying capacity of the cable bolt varied with sample diameters up to 200 mm beyond which there was no change. This phenomenon was due to the stress generated with the test sample as a result of the load transfer between the cable bolt, grout and rock. Rajaie recommended that pull out tests be standardised to test samples having a diameter of 250 mm.

School of Mining Engineering, UNSW Australia, Sydney, NSW 2052, Australia, E-mail:p.hagan@unsw.edu.au

Figure 1: Variation in load carrying capacity with sample diameter (Rajaie, 1990)

Since that time, there have been a number of significant developments in the design of cable bolts including the availability of modified bulbed cable bolts having much greater load bearing capacity then the plain strand cable bolts as used by Rajaie. These higher capacity cable bolts are likely to generate much higher stresses in the surrounding rock mass when tested to full capacity. Subsequent work reported by Holden and Hagan (2014) repeated the work by Rajaie using a high capacity cable bolt. They report the pull-out load continued to increase beyond the 200 mm diameter limit as shown in Figure 2.
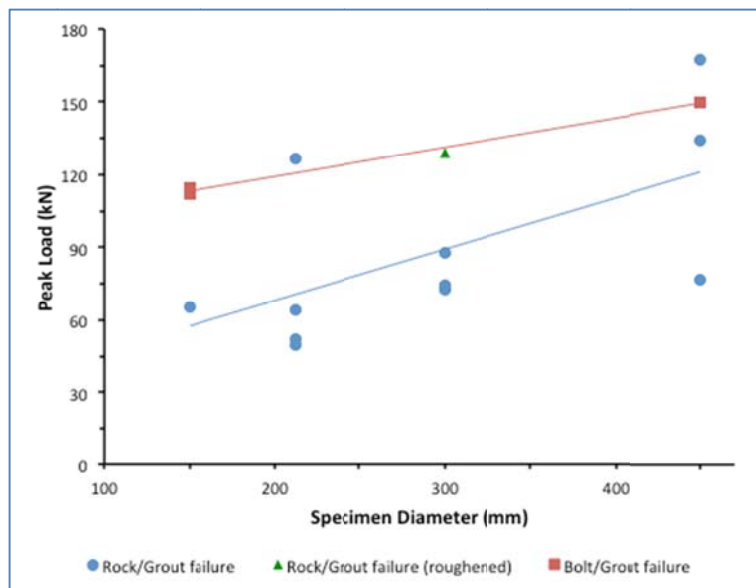
Figure 2: Variation in peak load with composite medium diameter (Holden and Hagan, 2014)

The approach used for cable bolt embedment and test sample confinement has also changed. In tests such as the double embedment tests, the cable bolt is grouted in a small bore steel tube. Confinement within the tube creates a constant stiffness-testing environment that inhibits any dilation effect otherwise induced by the cable bolt when under load due to load transfer. As Thomas (2012) noted, this arrangement does not allow assessment of the rock to grout interface. In the LSEPT test method, the cable bolt is grouted within a sample of rock that itself is confined within a biaxial cell pressurized to

10 MPa. The use of a biaxial cell creates a constant stress environment that "is not necessarily a true and consistent reflection of the underground environment in that (1) very little is known in regard to the *in situ* magnitude of borehole closure in underground coal mines and (2) it is almost certainly a dynamic variable that will vary both along the length of the cable and during the 'life' of the cable" (Thomas, 2012). To overcome this issue, the LSEPT was modified in the test program of Thomas with the sample instead grouted in a thick-walled steel cylinder.

METHODOLOGY

In line with the developments in testing methodology, the work of Holden and Hagan (2014) was repeated, but in this case instead of the test sample being unconfined, the samples were confined within a steel cylinder for each sample diameter. To ensure a more consistent mode of failure, the borehole in which the cable bolt was grouted was rifled to provide better and more consistent bonding between the grout and test sample.

Sample preparation

For testing, the test samples were made from a cement-based material cast in moulds ranging in diameter from 150 mm to 500 mm with an overall length of 320 mm and borehole diameter of 42 mm. An indented Sumo strand cable bolt, manufactured by Jennmar Australia, was selected as it is a high load transfer capacity cable bolt commonly used in the underground coal mining industry. Figure 3 shows the bulb design Sumo strand cable bolt as used in the tests.

Figure 3: Sumo strand cable bolt

The Sumo stand cable bolt was chosen as it represents the worst-case scenario in terms of the high loads generated and hence high stresses induced within the test sample as a result of load transfer. Hence the findings would be equally applicable to lower capacity cable bolts. Preparation involved the following:

1. Preparing moulds (including a rifling mould) and pouring of mortar to create test samples;
2. Initial curing for 24 hr at which time the rifling mould and the casting mould were removed and the test sample allowed to cure for the remainder of the 28 day period under fully saturated conditions; and
3. Grouting a cable bolt into the test sample using a polyester resin.

The test samples were cast in moulds made from thick walled cardboard cylinders with a height of 320 mm and diameters ranging between 150 mm and 350 mm. The cardboard moulds were glued to the base of a wooden board as shown in Figure 4a using industrial silicone to ensure the moulds retained its round shape and prevented any leakage during the cement pouring stage.
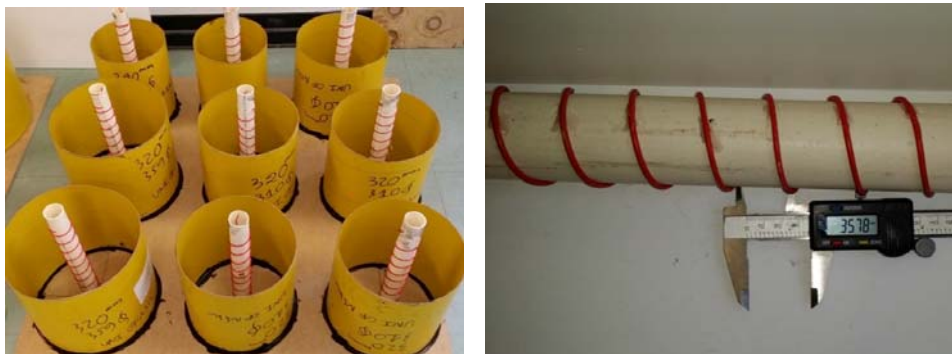
Figure 4: a) Prepared moulds prior to pouring of cement (left) and b) PVC tube used to create borehole with rifling effect (right)

The manufactured rifled boreholes were prepared from a hollow PVC tube around which were wrapped 3 mm electrical wire at a pitch of 36 mm as shown in Figure 4b. The purpose of the wire was to create the rifling effect in the borehole wall that would better promote interlock with the infill resin simulating the load transfer mechanism between resin and rock.

The cement based product used to prepare the sample had an ultimate compressive strength of 32 MPa. Once the silicone dried and set, cement was poured into the moulds as shown in Figure 5. A mechanical vibrator was used to remove air bubbles in the cement during the mixing stage.

Figure 5: Post the pouring of cement into the casting moulds

Within 24 hours of pouring the mortar, both the middle PVC tube and the outer cardboard mould were removed leaving a test sample with the rifled borehole as shown in Figure 6**:** .

Figure 6: Test sample (left) with rifling borehole (right)

After removing the outer cardboard casting mould and the rifling PVC tube, the samples were left to cure fully submerged for 28 days in either a large holding tub or plastic bags as shown in Figure 7.

Figure 7: Test samples fully submerged in water for curing

After curing of the rock cylinder samples, a cable bolt was grouted into each rock cylinder using a slow set resin with a setting time of 20 to 25 min. The resin and oil based catalyst were mixed for 13 min. An electric mixer was employed to combine the two components to ensure a thorough and even distribution of catalyst throughout the resin, which is imperative in achieving the ultimate strength of the cured resin. The mixed resin was poured into the boreholes to a height 50 mm below the collar of the borehole. This allowed room for displacement of the resin after the cable bolt was installed into the borehole. Excess resin was removed from around the rim of the borehole. The resin was left to cure for a day before it was used for testing. An example of the cured resin with cable bolt and rock is shown in Figure 8.

Figure 8: Cable bolt embedded in test sample using a slow set resin

Test arrangement

The setup arrangement for the tests is illustrated in Figure 9. The cable bolt was grouted in the test sample shown in the lower section of Figure 9 and load applied to the cable bolt using hollow hydraulic cylinder acting against a steel plate located on the top surface of the test sample. The level of applied load was measured using a pressure transducer and load cell and, the displacement was measured using a Linear Variable Differential Transformer (LVDT).
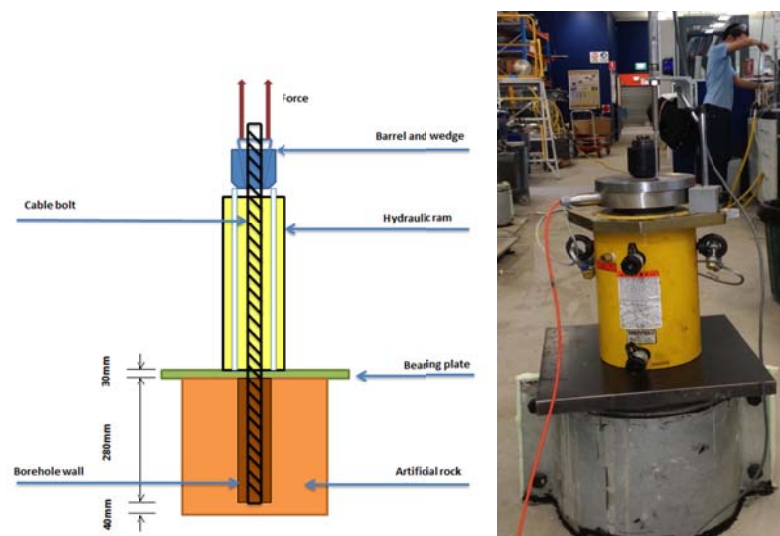
Figure 9: a) Test arrangement (not to scale) (left) and b) fully assembled test arrangement (right)

Prior to each test, the test sample was placed within a split steel cylinder as shown in Figure 10 and the narrow gap or annulus between the sample and cylinder backfilled with cement. A 15 mm gap was left

between the faceplates that were bolted together to join the two halves of the steel cylinder. This gap was filled with foam to prevent spillage of cement during backfilling. To ensure a consistent level of contact between the test sample, cement and steel cylinder that might otherwise alter the maximum pullout load, pre-confinement was applied to the steel cylinder and test sample by tensioning the bolts with a micrometre torque wrench.

Figure 10: a) Test sample placed in assembled steel cylinder (left) and b) gap filled with foam and bolts on side of cylinder that were tensioned before a test (right)

Test variables

Tests were undertaken to determine the size effect of the test sample on pull-out load under:

- unconfined conditions;
- confined conditions with zero torque;
- confined conditions with 40 N m; and
- confined conditions with 80 N m.

RESULTS AND ANALYSIS

Unconfined conditions

The peak load carrying capacities of each size of test sample in the unconfined state is plotted in Figure 11. Three test replications were undertaken at each level of sample diameter.
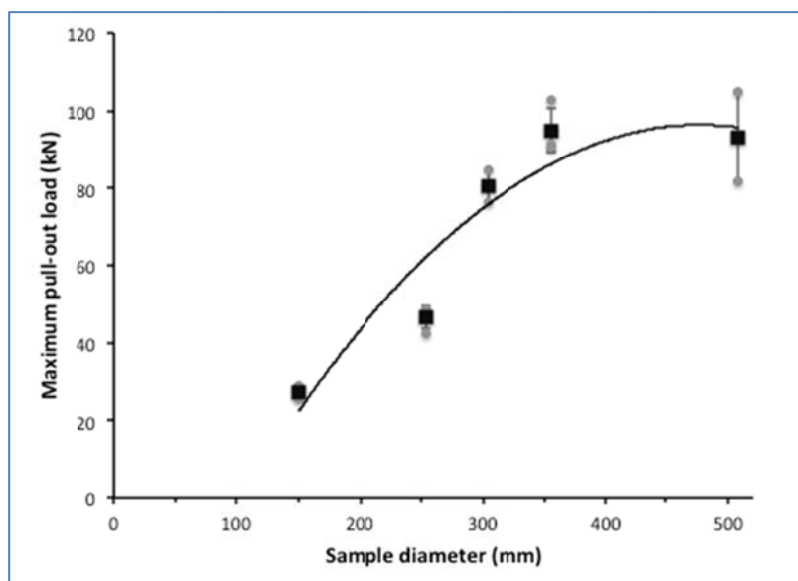
Figure 11: Variation in maximum pullout load with test sample diameter in the unconfined state

There was a near three-fold variation in maximum pull-out load from approximately 30 kN with the smallest size of sample up to over 100 kN achieved in the largest of test samples. This reaffirms the earlier findings by Rajaie (1990) and Holden and Hagan (2014) of the sensitivity of changes in pull-out being dependent on sample size in any laboratory determination of cable bolt performance.

The maximum pull-out load increased with size of the test sample until some threshold value was reached beyond which there was no further increase in load. This is in line with the observation made that in the unconfined condition, the smaller size samples tended to dilate creating two or often three fracture planes as shown in Figure 12. The larger test samples generally remained intact after testing. The general trend is similar to that reported by Rajaie (1990) except the threshold value of sample diameter was in this case in the order of 400 mm, much larger than the diameter of 250 mm as recommended by Rajaie.

Figure 12: Typical failure mode of test samples with two or three fractures

Confined with zero torque

In this series, the test samples were all placed in a steel cylinder that was intended to provide confinement to the sample similar to that experienced by a rock mass surrounding a cable bolt *in situ*. The maximum pull-out load in this confined condition of the test samples is plotted in Figure 13. In this case no torque was applied to the bolts joining the two halves of the steel cylinder.
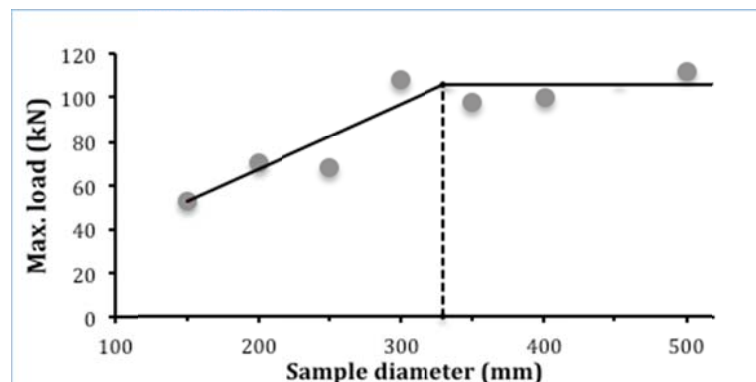
Figure 13: Variation in maximum load with test sample diameter with sample contained in steel cylinder

Similar to the unconfined tests, the maximum pull-out load was sensitive to changes in sample diameter. The main effect of confinement was that it reduced the threshold size above which there was little change in load. In this case the threshold diameter was found to be in the order of 330 mm, down from the 400 mm observed in the unconfined tests.

Confinement with a bolt torque of 40 Nm

In this series, the samples were again placed in a steel cylinder, but in this case the joining bolts were tightened with a torque wrench to a torque level of 40 Nm are shown in Figure 14. A similar result was achieved with a reduction in the threshold diameter with confinement in the steel cylinder.
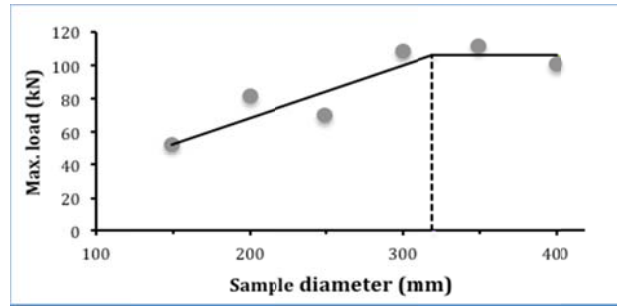
Figure 14: Variation in maximum load with test sample diameter at a bolt torque of 40 Nm

Confinement with a bolt torque of 80 Nm

The variation in load with sample diameter in the case of tightening the joining bolts to a torque level of 80 Nm is shown in Figure 15. A doubling in the level of bolt torque of the bolt did not appear to have any significant effect in reducing the threshold diameter.
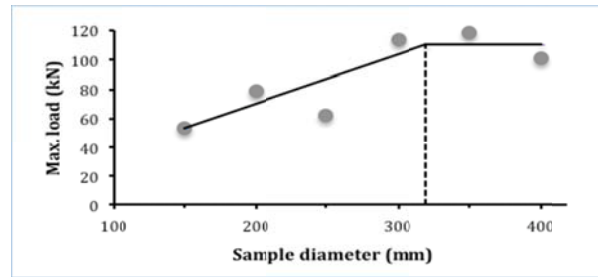
Figure 15: Variation in maximum load with test sample diameter at a bolt torque of 80 Nm

Further analysis

The results from the unconfined test combined with the three different scenarios of confinement are plotted in Figure 16. The graph shows a definite upward shift in the maximum pull-out load attained with the confined test samples especially for test samples with diameters less than 300 mm. The difference, however, reduces as the diameter approaches 400 mm. Interestingly, the pull-out load is insensitive to the level of confinement, at least over the range of confinements investigated in this test program in terms of both the maximum pull-out load of approximately 100 kN and threshold sample diameter of 300-330 mm as there is very little apparent difference.

Overall it can be concluded that consistent pull-out test results can be obtained with a test sample that is in the confined condition with a diameter of at least 300mm. Moreover while the maximum pullout load varies little with the amount of confinement, a tangible amount of confinement provided by tightening the joining bolts to the same low level of torque of 40 Nm will provide a standardized testing environment and hence is more likely to provide more consistent results.
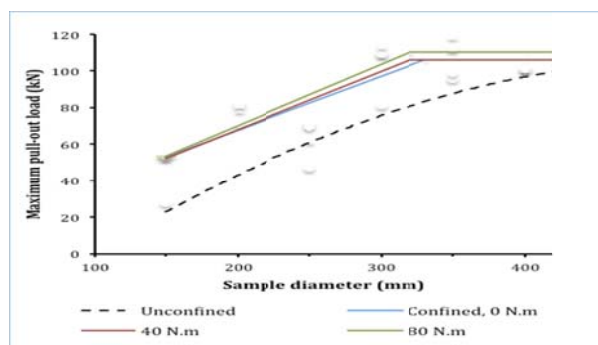
Figure 16: Comparison of the effect of varying levels of confinement on the maximum pull-out load for different sample diameters.

CONCLUSIONS

The results obtained from performance testing a high capacity modified bulb Sumo cable bolt embedded in test samples in an unconfined state found a similar trend to that reported by Rajaie (1990) in that there is an increase in the maximum pull-out load with diameter of the test sample up to some limiting or threshold diameter. Beyond this threshold diameter there is little change in the load of the cable bolt. Rajaie stated the threshold to be around 200 mm in tests that used a low capacity plain strand cable bolt, whereas with the high capacity cable bolt used in this project the threshold is nearly double at 400 mm. Confinement of the test sample by placing it in a rigid steel cylinder was found to reduce this threshold diameter to around 300 mm. Interestingly, over the range of confinement levels studied, the performance of the cable bolt was essentially insensitive to the actual level of confinement. In order to provide a standardised testing environment for the range of cable bolts now available it is recommended that the test sample in which the cable bolt is embedded is placed within a split steel cylinder of at least 300 mm diameter and the bolts that join the two halves of the cylinder be tightened to a torque of 40 Nm to ensure a consistent level of confinement.

ACKNOWLEDGEMENTS

REFERENCES

Hagan C P, Chen J and Saydam S. 2014, The load transfer mechanism of fully grouted cable bolts under laboratory tests, *in Coal2014: Proceedings 14th Coal Operators' Conference*, Wollongong, Australia, pp 137-146 (University of Wollongong: Wollongong), http://ro.uow.edu.au/coal/507/.

Holden M and Hagan P. 2014, The size effect of rock samples used in anchorage performance testing of cable bolts, in *Coal2014: Proceedings 14th Coal Operators' Conference*, Wollongong, Australia, (University of Wollongong: Wollongong), http://ro.uow.edu.au/coal/506/.

Hutchinson D J and Diederichs M S. 1996, *Cablebolting in Underground Mines* (BiTech Publishers: Richmond, Canada).

Hyett A J, Moosavi M and Bawden, W F. 1996, Load distribution along fully grouted bolts with emphasis on cable bolt reinforcement, *International Journal for Numerical and Analytical Methods in Geomechanics,* 20(7):517-544.

Rajaie H. 1990, Experimental and numerical investigations of cable bolt support systems, PhD thesis (published), Montreal, Canada, McGill University.

Singh R, Mandal P K, Singh A K and Singh T N. 2001, Cable-bolting-based semi- mechanised depillaring of a thick coal seam, *International Journal of Rock Mechanics and Mining Sciences*, 38(2):245-257.

Thomas R. 2012, The load transfer properties of post-groutable cable bolts used in the Australian coal industry, in *Proceedings 31st International Conference on Ground Control in Mining*, Morgantown, USA, http://icgcm.conferenceacademy.com/papers/detail.aspx?subdomain=ICGCM&iid=1011.

BEHAVIOUR OF CABLE BOLTS IN SHEAR; EXPERIMENTAL STUDY AND MATHEMATICAL MODELLING

Naj Aziz[1], Peter Craig[2], Ali Mirza[1], Haleh Rasekh[1], Jan Nemcik[1] and Xuwei Li[1]

ABSTRACT: The application of cable bolts for ground support is on the increase in underground coal mines worldwide. Currently, two methods of evaluating the performance of the cable bolt are favoured; the short encapsulation pull test and shear test. The former method can be used both in the laboratory and the field, while the latter can be undertaken mainly in the laboratory. There are two methods of shear strength testing, single and double shear tests. This paper examines the double shear testing of several cable bolts currently marketed in Australia under various pre-tension stresses. Both plain and indented wire cable bolts were tested. It was found that, the shear strength of the cable bolt was a function of the wire geometry and initial pre-tension. Indented wire cable bolts were lower in shear strength than the plain wire cable bolts. A mathematical model was proposed to evaluate the shear strength of cable bolts using Fourier series and Mohr-Coulomb failure criterion. The model coefficients were determined based on the experimental results. The findings from the mathematical modelling tallied well with the experimental results.

INTRODUCTION

Cable bolts have been used for ground support in mines worldwide since the 1960s. Cable bolts have been mostly used as a secondary support in addition to conventional rebar type primary support. Longer cable bolts act to reinforce strata above the primary bolted beam, and also to suspend the primary bolted beam to the higher competent stratification layers. Shorter cable bolts have also been used as flexible primary roof support, known as FLEXIBOLT, replacing the ordinary rigid rebar (Fuller and O'Grady, 1993).

Traditionally the mechanical integrity of cable bolts and rebar is evaluated for tensile strength and axial load transfer assessed by the pull testing method. Various publications have reported on the subject, covering studies undertaken both in the laboratory and field; Hyett *et al.,* (1992), Hyett *et al.,* (1996), Clifford *et al.,* (2001); and Thomas (2012). Pull tests are generally carried out to evaluate the axial reinforcement behaviour of cable bolts as the necessary requirement for cable bolt application to strata support in underground coal mines. Cable bolts are typically installed vertically above a coal mine opening, perpendicular to the sedimentary rock bedding planes. Rock movement resulting from *in situ* and mining intensified horizontal stresses often occurs along these horizontal bedding planes, resulting in shearing loads across the cable bolts.

Recently in Australia's coal mining industry, there has been increasing interest on the evaluation of the cable bolt shear behaviour. Generally, there are two main methods of testing cable bolts in shear, single and double shear methods. Goris and Martin (1996) reported on single shear tests conducted in pairs of 0.025 m³ concrete blocks having joint surfaces ranging from smooth to rough. The failure of cable bolt strands in the field may not occur in shear alone, but could be a combination of tensile and shear due to the movement of bedded strata formations in various directions.

The understanding of cable bolt behaviour in shear is still in its infancy as there are various practical issues to be examined and many theories and mechanisms involved are yet to be fully explored, which could provide better understanding of any particular cable bolt's behaviour in shear. The double shear testing study reported by Aziz *et al.,* (2004) used a three piece concrete block double shear apparatus to simulate shear behaviour of rock bolts in rock at the University of Wollongong. Aziz, 2010, Craig and Aziz *et al.,* (2010*a* and *b*) used a similar but larger apparatus and examined the failure behaviour of 28 mm hollow strand "TG" cable bolts taken to complete failure. Their findings demonstrated the symmetric characteristics of the double shear equipment with the cable bolt being sheared to failure on each side of

---

[1] *School of Civil, Mining and Environmental Engineering, University of Wollongong, NSW, Australia. E-mail: naj@uow.edu.au, Tel: +61 242213449*

[2] *Jennmar Australia, 40-44 Anzac Ave, Smeaton Grange, NSW, Australia, 2567*

the sheared joints. Analysis of the failure mode and loads achieved indicated that the cable strand undergo bending and crush the concrete surrounding the borehole at the shear plane. This kind of behaviour of the cable will not occur when the cable bolt is grouted in steel pipes instead of rock, as the case of the single shear method as recommended by the British Standard BS 7861-part 2 (British Standards 2009). The equipment used in BS 7861 is a guillotine style tool, where the cable bolt is sheared fully in the steel frame (see Figure 1). Crushing of the rock will enable a cable bolt to bend and subsequently load in both shear and tension; hence, the British Standard methodology using steel pipe is inappropriate and may be misleading.
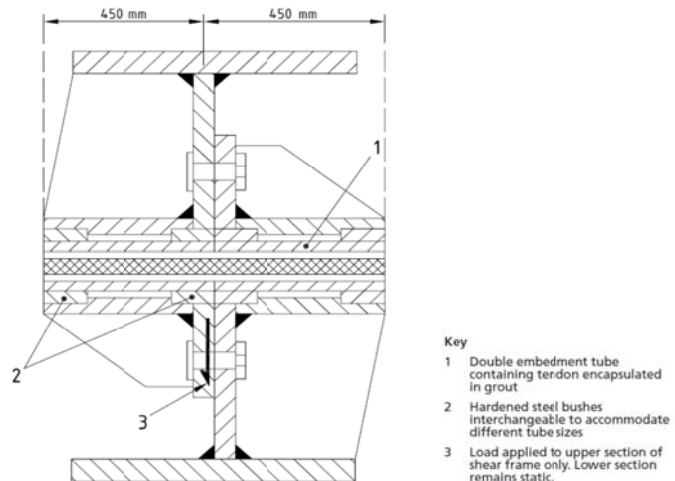
Figure 1: Sectional diagram of double embedment shear frame with the united being tested (BS 7661-2: 2009)

With Australia having the largest variation of high capacity, pre-tensioned and post-grouted cable bolts in the world, there exist a minimum of literature on shear testing of these products using a recognised shear testing methodology. While pull testing of cable bolts can be practiced both in the field and in the laboratory, testing of cable bolts in shear is normally carried out in the laboratory. The difficulty of monitoring shearing process in holes drilled in the ground formation in remote location renders testing in the field an inconvenient approach.

Further, Aziz *et al.,* (2014) carried out a comparative study on 22 mm diameter plain and indented wire cable bolts, as the cable bolt surface indentation remains an issue of concern, particularly in shear. The study indicated that shear properties of indented wire cables were inferior to plain wire cables of the same type. The indentation appeared to cause a reduction in the cable strand cross section, leading to the loss of strength (see Figure 2), including the failure in shear initiated at the indent. The three types of cable tested to date included hollow plain wire, PC plain wire and PC indented wire. Thomas (2012) reported on laboratory axial pull tests of all the Australian cable bolts on the market including the design variables of bulbs, nutcages (birdcages), hollow, PC, multi-strand, indented and plain wires. It was requested of manufacturers to provide shear performance of cable bolts with these multiple variables, and Jennmar proceeded to test their cable bolts at the University of Wollongong. The University has since expanded upon the laboratory tests to include mathematical modelling of the cable bolt behaviour in shear.

EXPERIMENTAL STUDY

A total of six different cables were subjected to double shear testing in 40 MPa concrete. Figure 3 shows the schematic view of various cables as assembled in concrete blocks. Each double shear testing process requires three concrete blocks with two outer 300 mm side cubes and a central rectangular block 450 mm long. The casting of the concrete blocks can be carried out either in a specially prepared plywood mould or directly in the confining steel frame of the double shear apparatus. A plastic conduit 20 mm in diameter, set through the centre of the mould lengthways, will create a centralised hole for cable installation in the concrete blocks. Once the concrete blocks are allowed to set, and the plastic conduit is taken out, the hole in each block hole is reamed to the desired diameter. The concrete blocks are left immersed in a concrete curing solution to cure for a minimum period of 28 days.
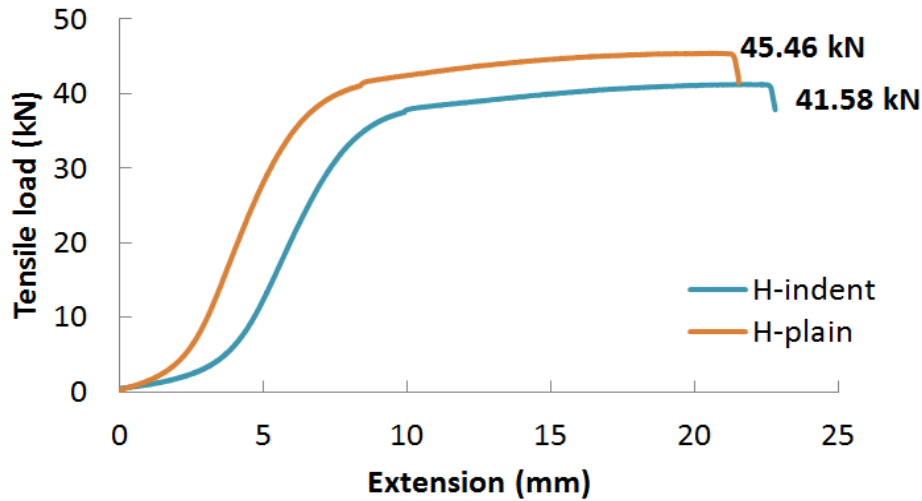
Figure 2: Tensile load / elongation profiles of both plain and indented 5.5 mm wire from cable bolts
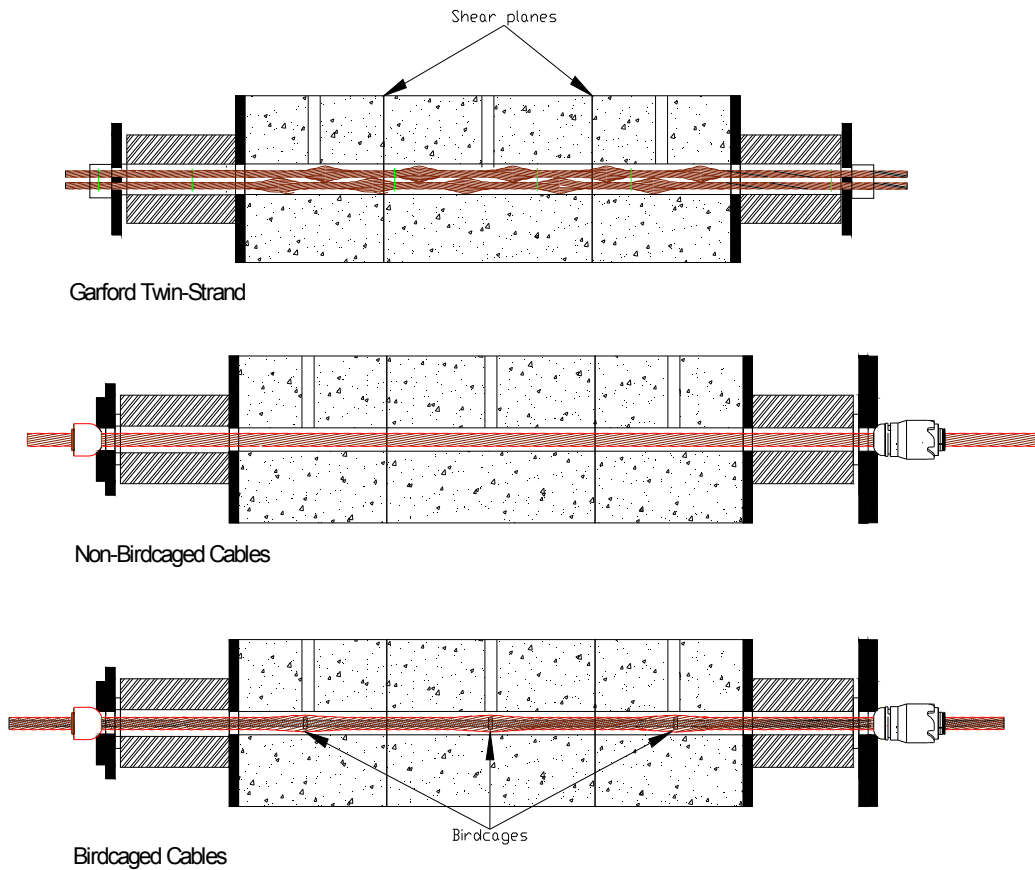
Figure 3: Cross section of double shear blocks and cables

The cured blocks are then mounted in the double shear confining steel frames and the cable bolt specimen placed into the borehole. Two 60 t load cells were inserted onto each end of the cable followed by the typical cable bolt end fitting. The load cells were connected to the data logger during tensioning. Once the cable is pretensioned, the grout is injected to the annulus between the cable and borehole through the intersecting small holes on top of the block. Cables with hollow central tubes were also filled with grout, and the grout or polyester resin left to cure for at least 7 days. The top of the concrete blocks are covered by the bolted steel plates and the whole assembly is then mounted on the carried base platform. The whole double shear assembly and the base frame is then mounted on to the 500 t compression testing machine for shearing process as shown in Figure 4.
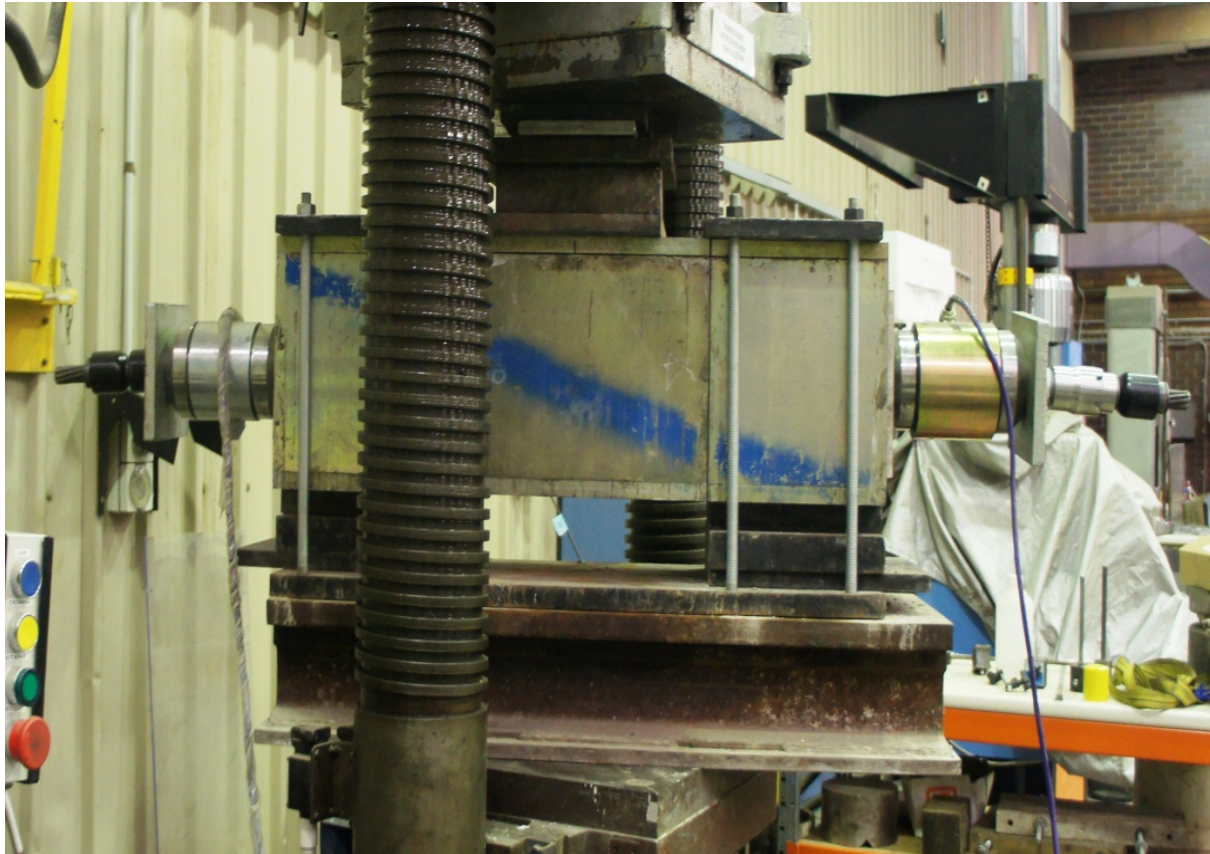
Figure 4: Arrangement of shearing apparatus on compression machine

The properties of the eight different cable bolts are described in Table 1. The study focussed on the main cables in the market as supplied by Jennmar, with indented wire hollow cable included for additional research. Cables were subjected to three different values of initial axial load ranging from 0 to 25 t. Three types of bonding agent were used in this particular study; Jennmar bottom-up grout (BU100), Jennmar top-down grout (TD80) and J-Lok standard oil based resin. The values of shear and axial loads versus shear displacement were monitored and recorded. The shear and axial stresses were calculated using following equations:

$$\sigma_n = \frac{N}{CA} \tag{1}$$

$$\tau = \frac{0.9 \times S}{2 \times CA} \tag{2}$$

where, σ_n is the normal stress, N is the normal load, CA is cable area, τ is the shear stress and S is the shear load.

It is noted that 10% of the shear load was ascribed to the rubbing of concrete surfaces and therefore 90% of the measured shear load incorporated as shown in Equation (2) in calculating the value of shear stress. The rubbing of concrete surface was evaluated by painting the concrete surfaces in checkered pattern before shearing. The damaged pattern on concrete surfaces was then carefully examined after dismantling the double shear apparatus. Figure 5 shows a typical checkered sheared face, which clearly shows approximately the percentage part of the surface damage during the shear process. Due to the significant stiffness of the cable, it is therefore rational to postulate that the shear load almost concentrates on the cable cross sectional area rather than on the concrete surfaces.

The process of double shear testing consists of loading the central block vertically in the 500 t compression testing machine (Figure 4). The 450 mm long middle section of the double shear apparatus is then vertically shear loaded at the rate of 1 mm/min for the maximum100 mm vertical displacement.

The rate of loading and displacement are monitored and simultaneously displayed visually on a PC monitor.

Table 2: list of tested cables and the test environment

| Test No. | Cable Bolt Properties | | | | | Drill bit (mm) | Bonding agent | Pre-tension load (t) | Peak shear load (kN) [½ double shear] |
	Product name	Cable Ø (mm)	Wire geometry	Cable cross-section	Cable geometry				
1	Twin-strand	15.2	Plain	2 x 7 wire, PC strand	25mm Bulbs	55	BU100 Grout	0	501
2	Indented TG	28	Indented	9 wires, hollow centre	Non-birdcaged	42	TD80 Grout	25	604
3	SUMO	28	Plain	9 wires, hollow centre	35mm birdcage	42	TD80 Grout	10	659
4	SUMO	28	Plain	9 wires, hollow centre	35mm birdcage	42	TD80 Grout	25	711
5	Indented SUMO	28	Indented	9 wires, hollow centre	35mm birdcage	42	TD80 Grout	10	488
6	Indented SUMO	28	Indented	9 wires, hollow centre	35mm birdcage	42	TD80 Grout	25	414
7	Superstrand	21.8	Plain	19 wire, PC strand	Non-birdcaged	28	Oil based resin	25	628
8	Indented Superstrand	21.8	Indented	19 wire, PC strand	Non-birdcaged	28	Oil based resin	25	558

Figure 5: A typical concrete block surface after shearing

MATHEMATICAL MODELING

The mathematical model was developed by assuming the linear Mohr-Coulomb relationship between the shear and normal stresses as (in below equation, surface roughness has been omitted):

$$\tau - \sigma_n \tan(\varphi) - c = 0 \tag{3}$$

where, φ is the friction angle and c is the cohesion.

The Fourier series concept as described below is applied to replicate the variation of normal stress against shear displacement. Fourier series is a mathematical technique incorporated to solve a large variety of engineering problems mainly adopting the principle of superposition:

$$\sigma_n = \frac{a_0}{2} + \sum_{n=1}^{\infty} \left[a_n \cos(\frac{2n\pi u}{T}) + b_n \sin(\frac{2n\pi u}{T}) \right] \tag{4a}$$

$$a_n = \frac{2}{T} \int_0^T \sigma_n \cos(\frac{2n\pi u}{T}) du \tag{4b}$$

$$b_n = \frac{2}{T} \int_0^T \sigma_n \cos(\frac{2n\pi u}{T}) du \tag{4c}$$

where, a_n and b_n are Fourier coefficients, n is the number of Fourier coefficient, u is the shear displacement and T is the shearing length.

Introducing Equations (4a, b, and c) in equation (3) by considering a_0 to a_3, the shear strength is obtained as:

$$\tau = (\frac{a_0}{2} + \sum_{n=1}^{3} \left[a_n \cos(\frac{2n\pi u}{T}) \right]) \tan(\varphi) + c \tag{5}$$

The shear displacement at peak shear strength is determined by taking derivation of the above relationship respect to the shear displacement and equating to zero as:

$$\frac{d\left\langle \frac{a_0}{2} + \sum_{n=1}^{3} \left[a_n \cos(\frac{2n\pi u}{T}) \right]) \tan(\varphi) + c \right\rangle}{du} = 0 \tag{6}$$

Thus, the peak shear displacement at peak shear strength (u_p) is obtained as:

$$u_p = \frac{T}{2\pi} \cos^{-1} \left[\frac{-4a_2 + \sqrt{16a_2 - 48a_1 a_3 + 432a_3^2}}{24a_3} \right] \tag{7}$$

Introducing equation (7) in equation (5), the peak shear strength (τ_p) is proposed as:

$$\tau_p = (\frac{a_0}{2} + \sum_{n=1}^{3} \left[a_n \cos(\frac{2n\pi \frac{T}{2\pi} \cos^{-1} \left[\frac{-4a_2 + \sqrt{16a_2 - 48a_1 a_3 + 432a_3^2}}{24a_3} \right]}{T}) \right]) \tan(\varphi) + c \tag{8}$$

The model coefficients including Fourier coefficients (a_n), cohesion (C) and angle of friction (φ) were determined according to the measured data for various conditions of cable type and pre-tension as listed in Table 2. Generally, the values of Fourier coefficients showed a decreasing trend with the increasing the number of Fourier coefficients.

RESULTS AND ANALYSIS

Figures 6 to13 show the shear stress and axial stress profiles against shear displacement for the tests conducted in this study. The initial changes in some of the shear stress graphs after the elastic state may be related to the barrel/wedge settlement as the cable ends begins to take axial load due to cable bending at the shear planes. Various shear drops beyond the peak value are attributed to individual cable strand failures. The larger shear drop corresponds to the higher diameter strand failure while the smaller ones are due to the small strand failures. It is of interest to note that the number of visible sudden drops in stress upon shear displacement is equal or slightly less than the number of failed strand, which might be due to two strands snapping near the same time. The strand failure in the cable at the shear plane was also observed as load drop at the load cells measuring axial load near the end fittings. Figure 14 shows snapped strands of the tested cables. It is obvious that the failures of strands in the cable is a mix of tensile and shear, depending on the location of the strand in the cable cross-section, the direction of the shearing and cable construction. For multiple mixed wire diameter cables of the superstrand cable, it was observed that smaller diameter strands of the inner layer appears to fail in tension with con and cup pattern (Aziz *et al.,*2014 a, b).

Table 2: Model coefficients for different types

Test number	a_0	a_1	a_2	a_3	C (GPa)	φ (°)
1	0.63	-0.42	0.11	-0.012	0.32	44.72
2	2.51	-0.266	-0.06	0.07	0.03	51.59
3	1.56	-0.47	0.06	-0.01	0.22	53.47
4	2.06	0.01	-0.29	0.21	0.26	56.83
5	1.36	-0.11	-0.26	0.16	0.18	55.23
6	2.09	0.45	-0.19	-0.02	0.37	44.71
7	2.15	-0.05	-0.25	0.23	0.36	47.21
8	2.63	-0.24	-0.13	0.09	0.21	47.21

Table 3 summarises the peak shear strength of the different cable bolt and testing configurations. It is obvious from the results that the plain wire birdcaged cables had higher shear strength when compared to the indented wire birdcaged cables. The shear performance of non-birdcaged superstrand and hollow TG cable was lower when wires were indented, but the shear strength was still close to the UTS (Uniaxial Tensile Strength) of the cable bolts.

The lower shear behavior of the indented wire of the same cable type was likely attributed to the fact that the indented wires have a small cross section and the indent geometry forms a stress raiser to initiate failure. The indented wire cable bolts display lower deflection (stiffer) than the plain wire equivalent type. No cable rotation was observed in either the plain or indented strand cable bolts during the double shearing tests. As can be seen from Figure 15, the shear strength of cable bolted concrete block subjected to shearing can be represented reasonably by the proposed model for different initial pretension stresses, bonding agents and cable bolts.

In order to compare the method of double shearing used in this study with single shear test of British Standard, Superstrand cables both indented and plane ones were also sheared as suggested by British Standards (2009). Figure 16 shows the comparison between the shear load against shear displacement using double shear and single shear test methods. It is inferred that the single shear testing method significantly underestimates the shear strength of Super strand cable bolts. The conspicuous difference between the value of shear load in single shear and double shear tests can be related to the fact that the single shear test is only a metal to metal shearing and does not carry any pretension or axial load during shearing. Thus, all the strands only experience shear failure without having any tension failure as

observed in double shearing and shown in Figure 14. Nevertheless, in the process of double shearing, the initial pretension value is subjected to the cable before shearing and increases upon shearing due to the cable deformation. This profoundly increases the strength at which cables can resist against shearing and simulate properly the field conditions.
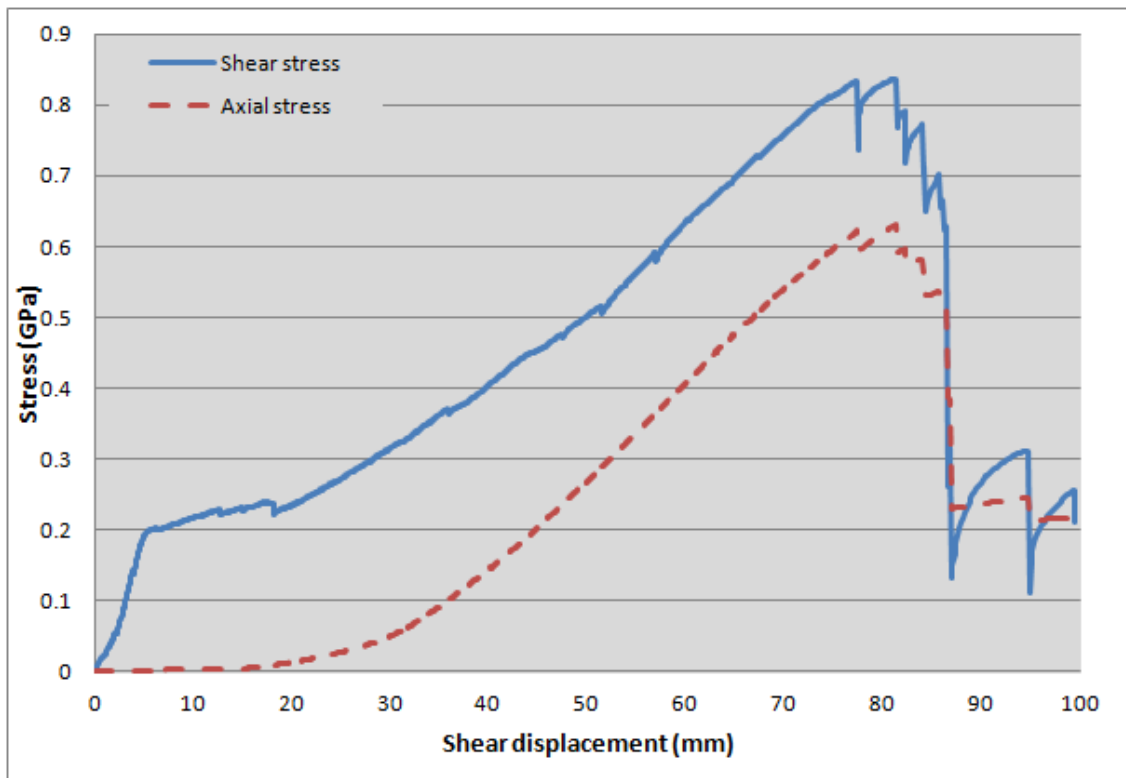
Figure 6: Shear behaviour of cabled concrete [test 1]
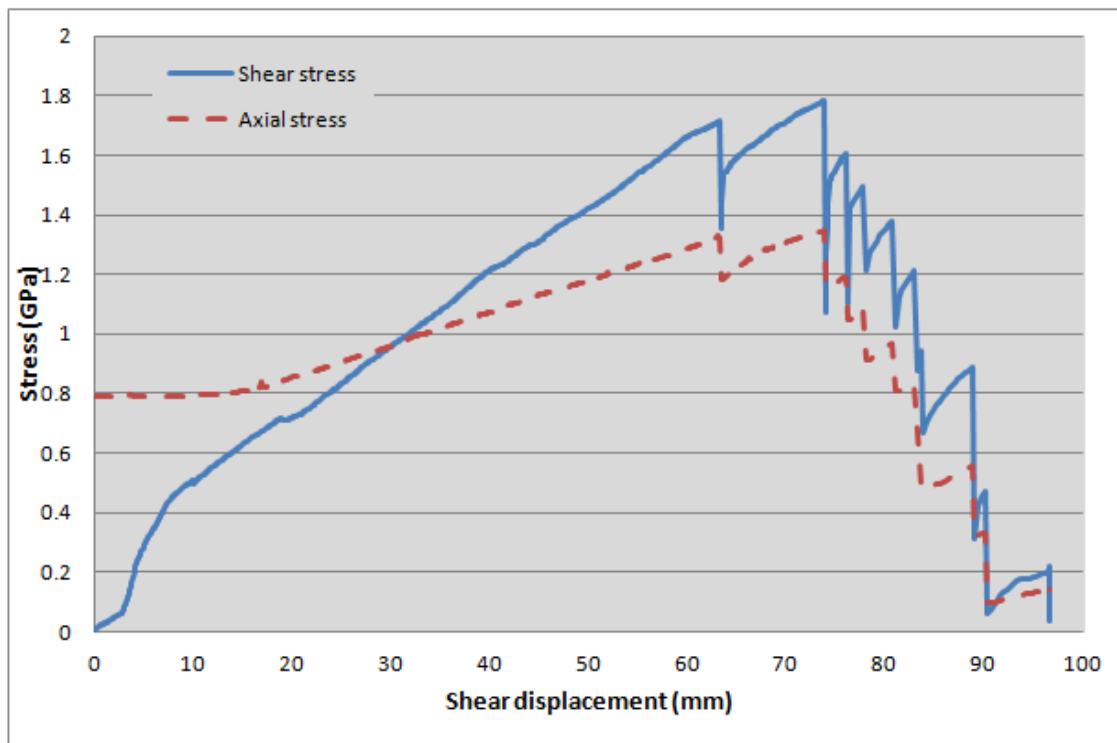
Figure 7: Shear behaviour of cabled concrete [test 2]
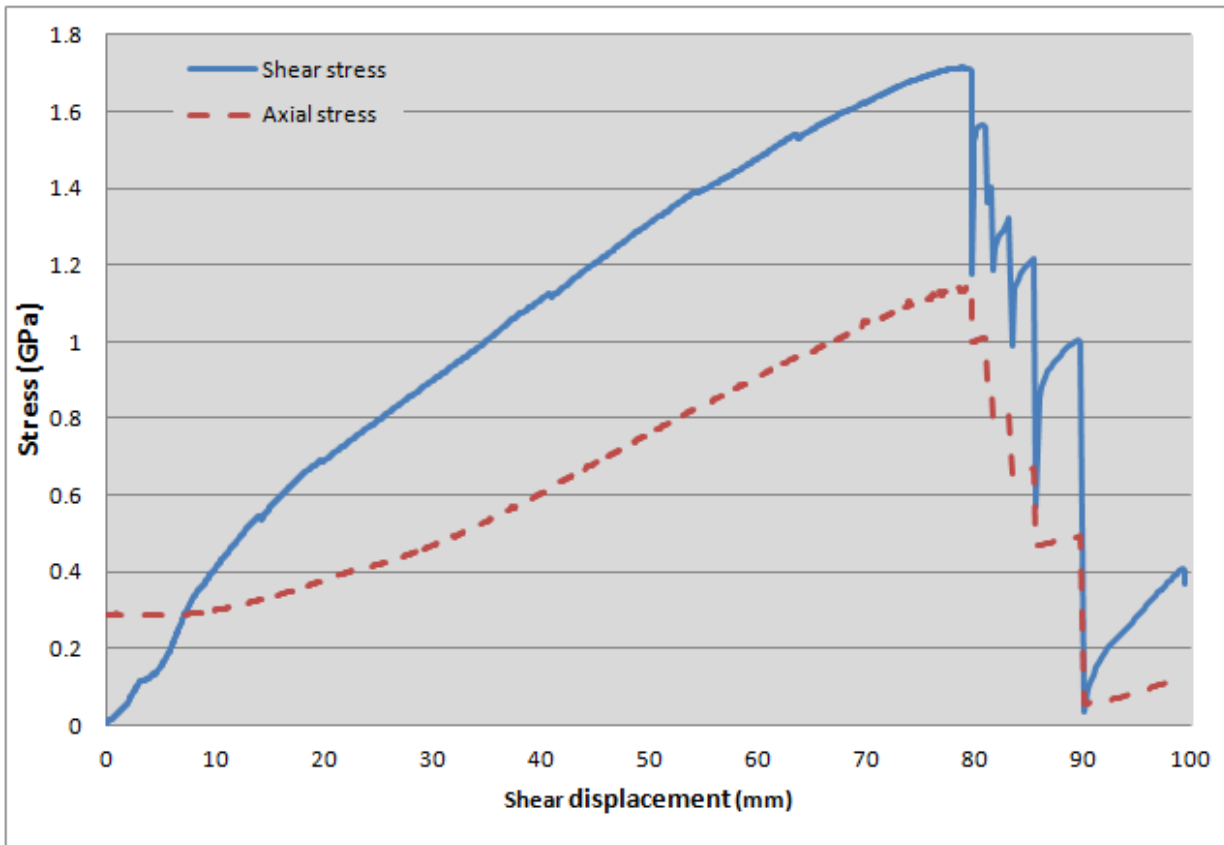
Figure 8: Shear behaviour of cabled concrete [test 3]
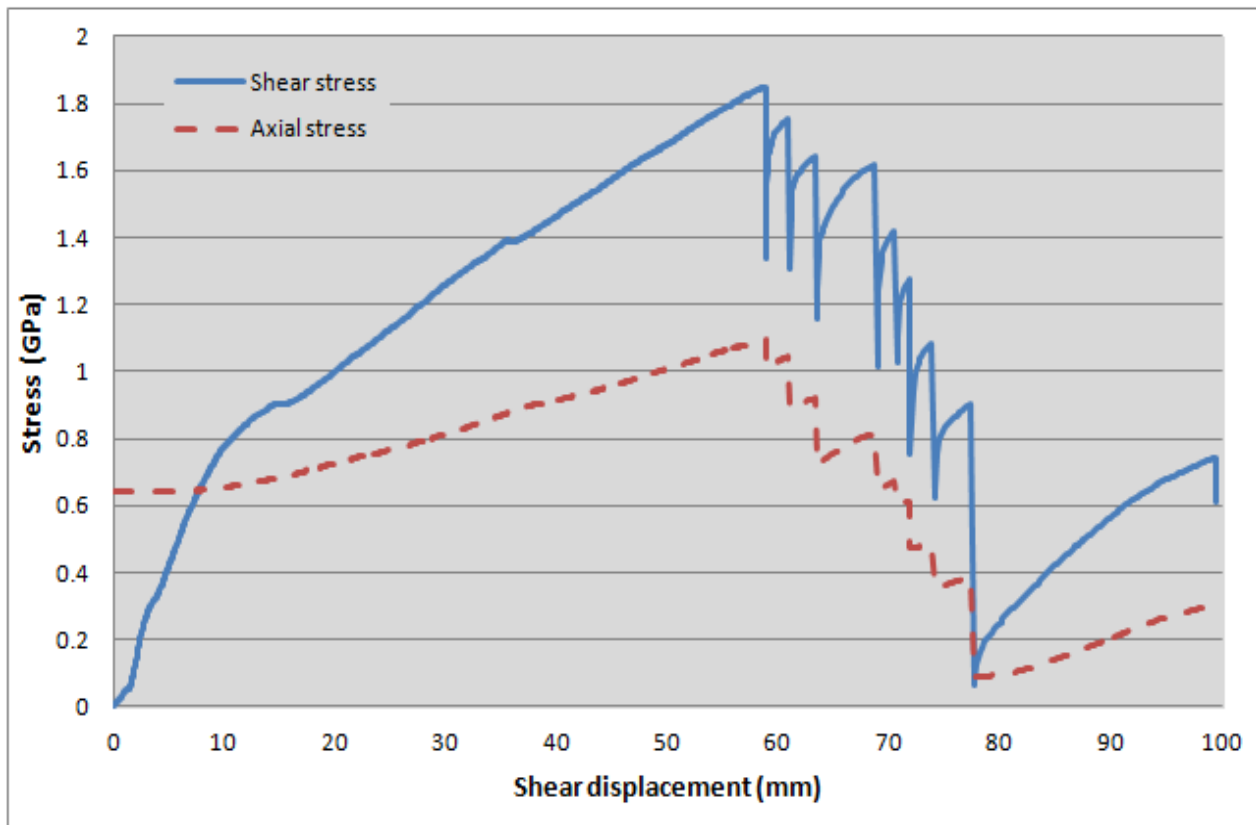
Figure 9: Shear behaviour of cabled concrete [test 4]
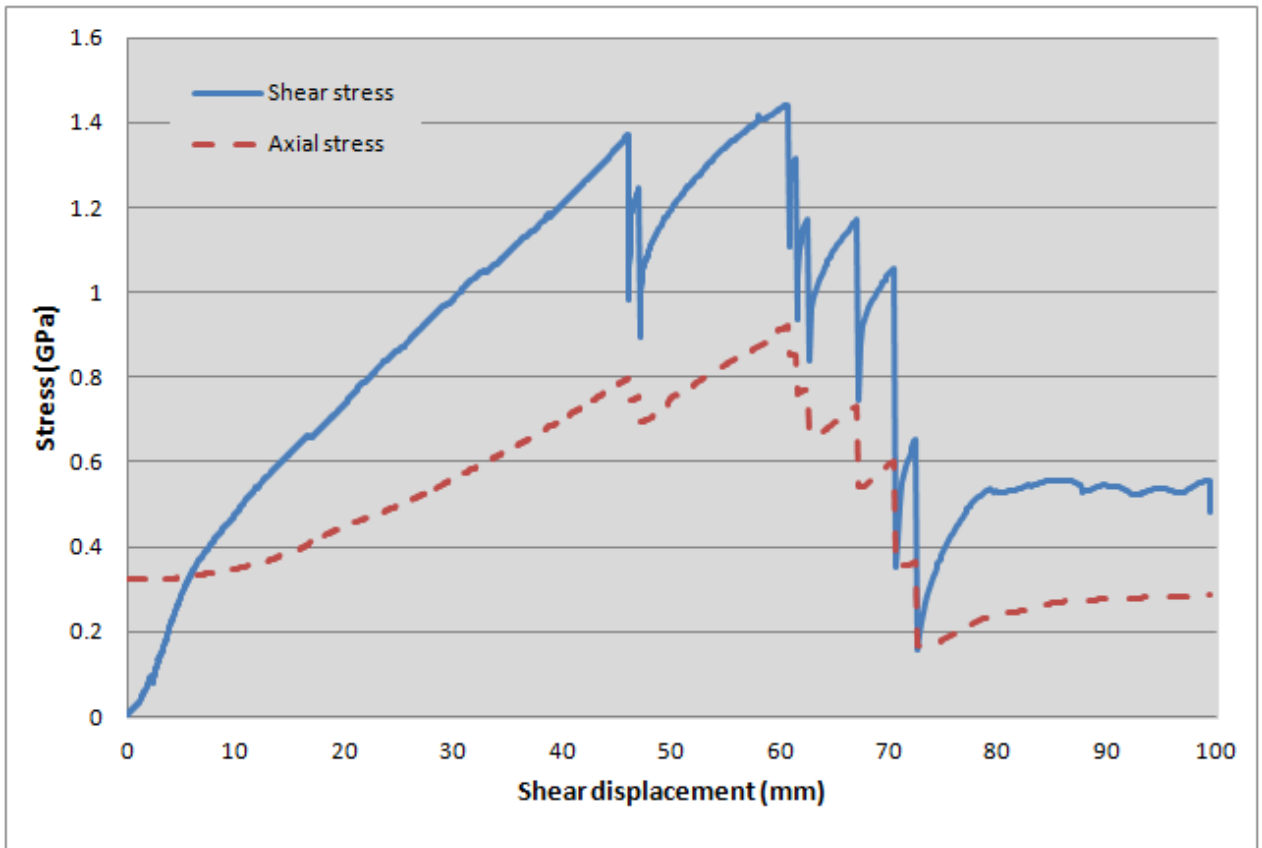
Figure 10: Shear behaviour of cabled concrete [test 5]
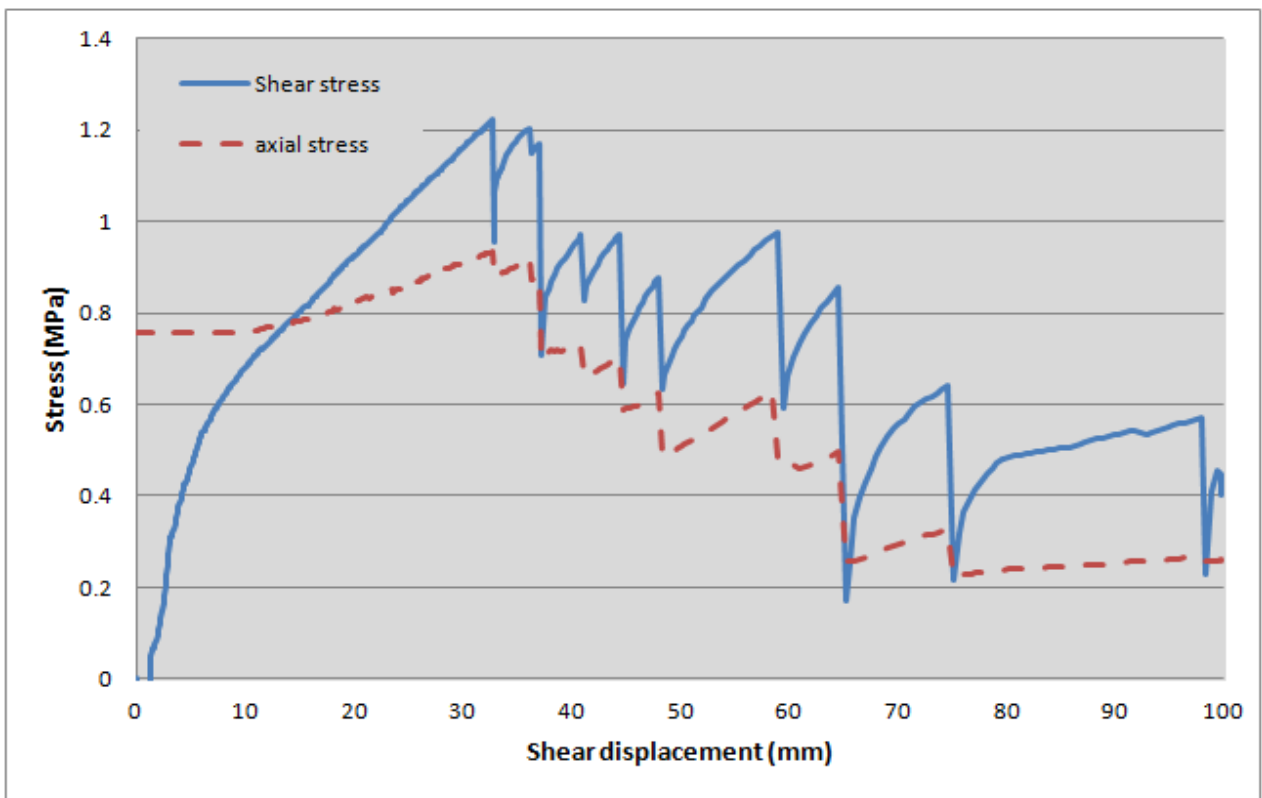
Figure 11: Shear behaviour of cabled concrete [test 6]
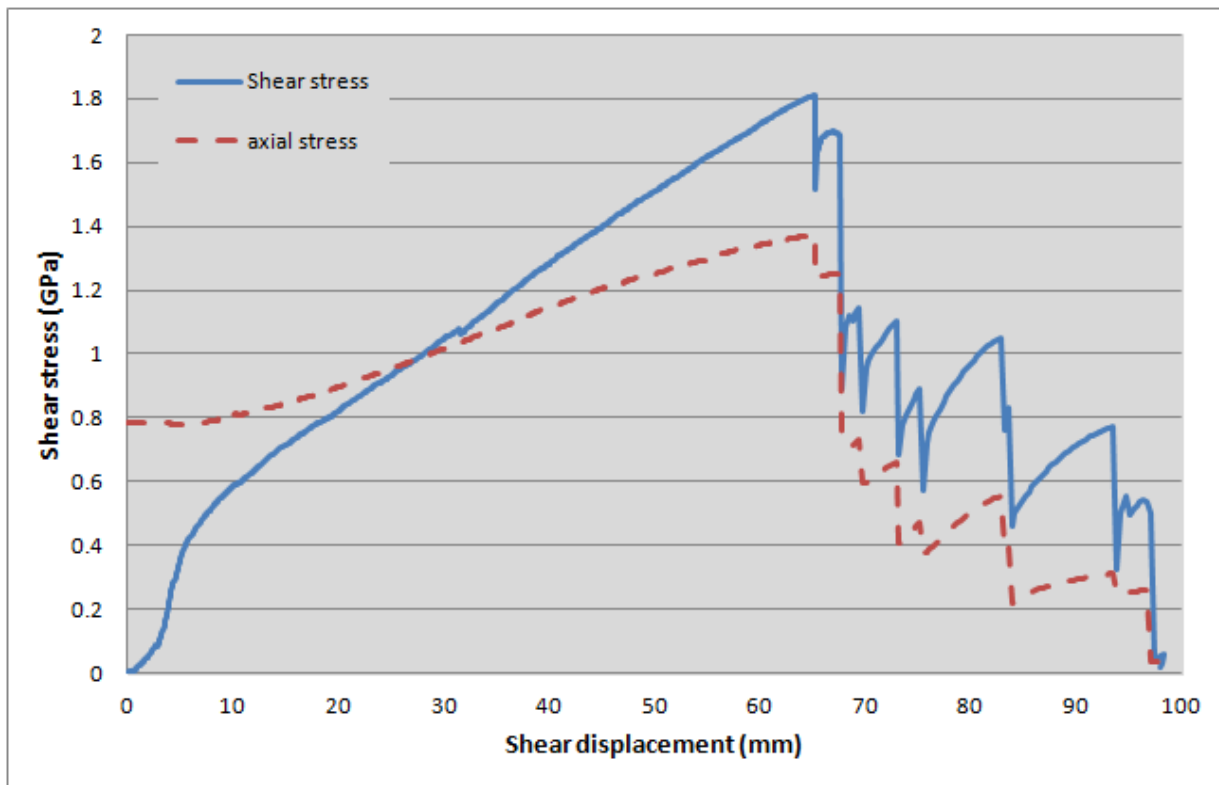
Figure 12: Shear behaviour of cabled concrete [test 7]
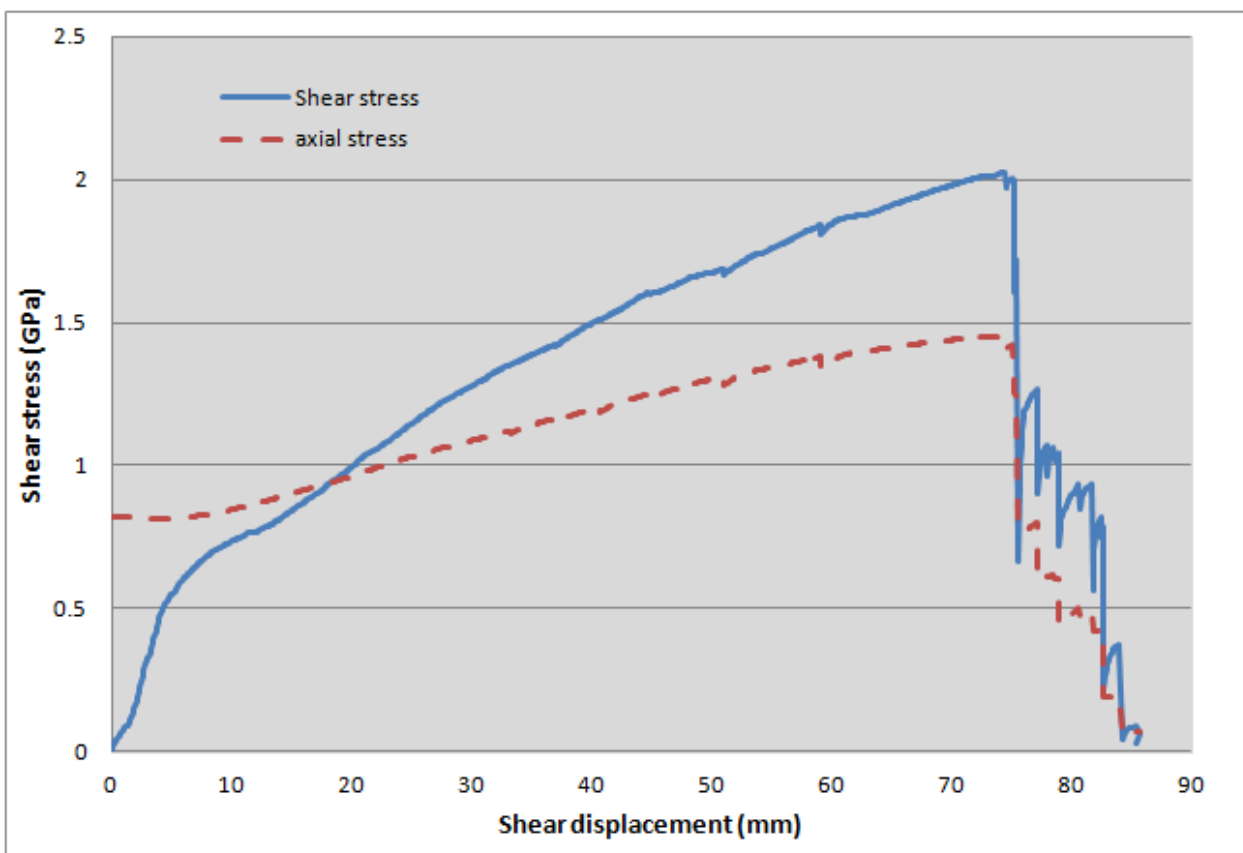
Figure 13: Shear behaviour of cabled concrete [test 8]

Table 3: Peak shear stress for different cabled concrete blocks

Test number	Peak shear stress per surface (*GPa*)
1	0.84
2	1.79
3	1.71
4	1.85
5	1.44
6	1.22
7	1.81
8	2.02

Figure 14: strands snapped of the tested cables
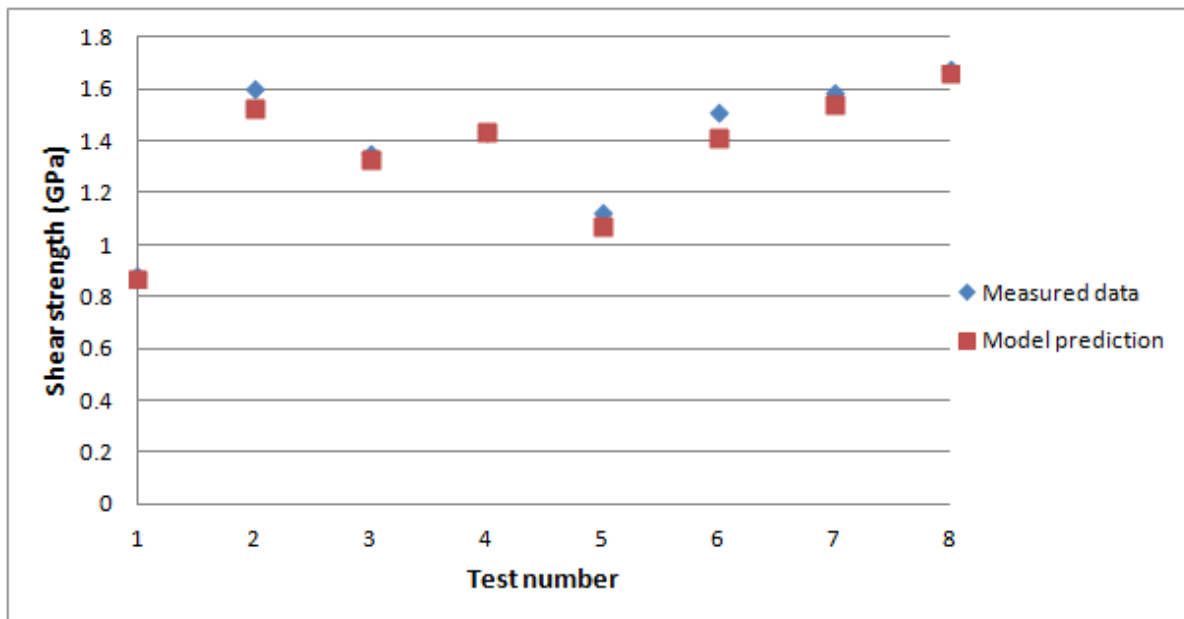
Figure 15: Comparison between the model results and measured data
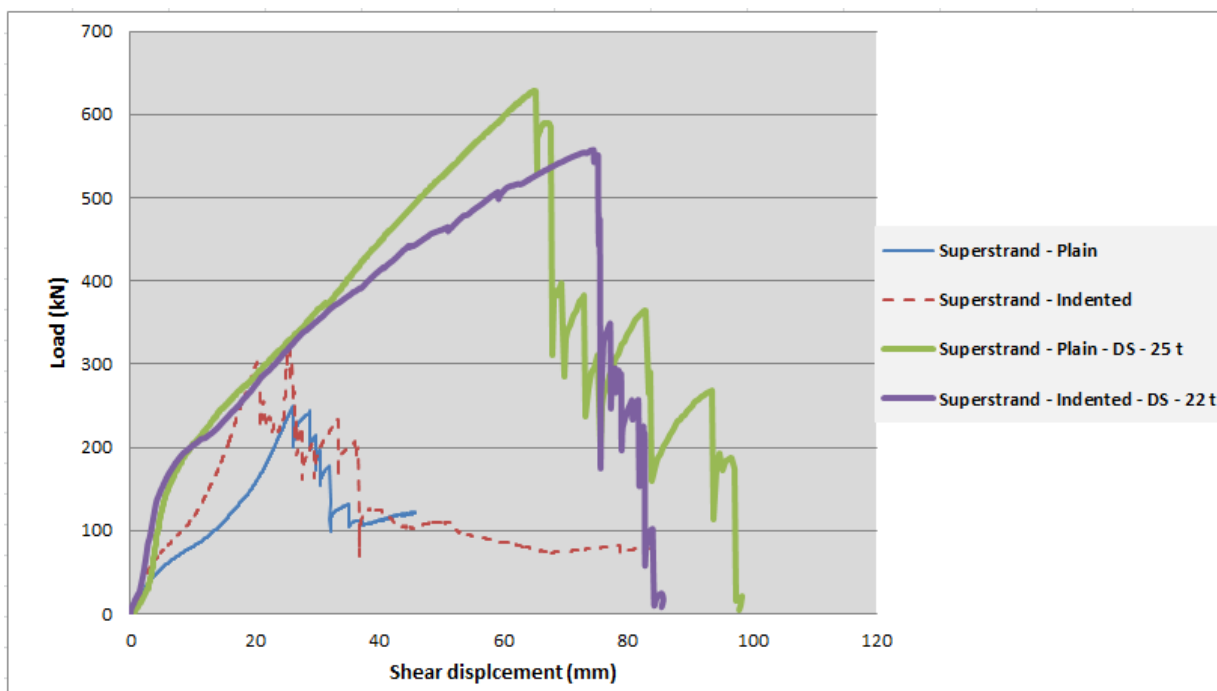
Figure 16: Comparison between the double and single shear methods

CONCLUSIONS AND RECOMMENDATIONS

The following conclusions are drawn from this investigation:

a) Indented wire combined with birdcaging of cable bolts is detrimental to the cable shear performance.
b) Shear strength of non-birdcaged cables bolts are less affected by indentation of the wire.
c) It is likely that the reduced cross-section reduces tensile strength and the geometry forms a stress raiser to initiate failure.
d) A mathematical model was proposed incorporating Mohr-Coulomb failure criterion and Fourier series concept to simulate the shear strength of cabled concrete blocks.
e) The values of Fourier coefficients decreased as the number of Fourier coefficients increased.

Recommendations include:

a) Due attention must be given to the study of the cable shear across closed and interlocking sheared beds as well as across separated beds with no contacts between sheared faces.
b) More experiments are suggested to calibrate the model for practical purposes.
c) The double shear method in simulated rock has proven to provide valuable insight into in-situ performance. The British Standard BS 7861 (part 2)* cannot be applied to the study of shear behaviour of the cable bolt in rock. The equipment used in the BS 7861 (part 2) is a guillotine style tool, where the cable bolt is sheared fully in the steel frame. Shearing of the cable bolt in rock normally undergoes both shear and tension; hence, the British standard methodology is inappropriate and may be misleading.

REFERENCES

Aziz, N. 2014*a*, Double shear testing cable-bolts for Jennmar Australia, a report of study prepared for Jennmar Australia, *School of Civil, Mining and Environmental Engineering, University of Wollongong*, May 27, 9p.

Aziz, N. 2014*b*, Double shear testing of Secura Hollow Groutable Cable-bolt (SHGC) for Orica Australia Pty Ltd, *a report of study, School of Civil, Mining and Environmental Engineering, University of Wollongong*, July, 9p.

Aziz, N, Heemann, K, Nemcik J and Mayer, S. 2014, Shear strength properties of Hilti plain and indented strand cable bolts, *in proceedings Coal Operators Conference (Coal 2014), Wollongong, February 12-14, ISBN 978 1 925100 02 0, pp156-162 (Eds. N Aziz, B Kinninmonth)*, http://ro.uow.edu.au/coal/509/.

Aziz, N, Nemcik, J, Jalalifar, H. 2011, Double shearing of rebar and cable bolts for effective strata reinforcement, *in proceedings 12th ISRM International Congress on Rock Mechanics, Beijing, China, 18-21, October. Pp 1457-1460. Published in Harmonising Rock Engineering and the Environment –Qian and Zhou (Eds)*, 2012 Taylor and Francis Group, London, ISBN, 978-0-415-80444-8.

British Standard BS 7861- Parts 1 and 2. 1996, Strata Reinforcement support system components used in Coal Mines-Part 1, *Specification for rock bolting and Part 2: Specification for Flexible systems for roof reinforcement*.

Clifford, B, Kent, L, Altounyan, P, Bigby, D. 2001, Systems used in Coal Mine Developments in Long Tendon Reinforcement, *20th International Conference on Ground Control in Mining. ICGCM*, http://icgcm.conferenceacademy.com/papers/detail.aspx?subdomain=icgcm&iid=735.

Craig, P and Aziz, N. 2010*a*, Shear testing of 28 mm Hollow Strand "TG" Cable Bolt*, in proceedings 10th Underground Coal operators Conference, Wollongong, February 11/12*, pp171-179 (Ed.N Aziz   and Jan Nemcik. 375 p), http://ro.uow.edu.au/coal/303/.

Craig, P and Aziz, N. 2010*b*, Shear testing of 28 mm hollow strand "TG" cable bolt, *In proceedings 29th International Conference on Ground Control in Mining, ICGCM (pp. 169-174), (Publication ID=35591)*, http://icgcm.conferenceacademy.com/papers/detail.aspx?subdomain=icgcm&iid=273.

Goris, JM, Martin LA.1996, Shear behaviour of cable bolt supports in Horizontal bedded deposit. Laboratory pull tests of resin –grouted cable bolts, *15th International Conference on Ground Control in Mining*, Golden, Colorado, August 13-15, pp 511-521, http://icgcm.conferenceacademy.com/papers/paperlist.aspx?iid=407.

Fuller PG, O'Grady P. 1993, FLEXIBOLT flexible roof bolts: A new concept for strata control, *12th International Conference on Ground Control in Mining*, Morgantown, West Virginia, USA, pp 24-34, http://icgcm.conferenceacademy.com/ebook/view.aspx?PaperID=1235.

Hyett AJ, Bawden WF, and Reichert RD. 1992, The effect of rock mass confinement on the bond strength of fully grouted cable bolts, *Int. J. Rock mechanics and Min. Sci. & Geomech. Abstr*, 29(5), pp 503-524.

Hyett AJ, Mossavi M and Bawden WF. 1996, Load distribution along fully grouted bolts, with emphasis on cable bolt reinforcement, *Int. J. for Numerical and Analytical Methods in Geomechanics*, 20, pp 517-544.

Thomas, R. 2012, The load transfer properties of post-groutable cable bolts used in the Australian coal industry, *31st International Conference on Ground Control in Mining*, Morgantown, 10p, http://icgcm.conferenceacademy.com/papers/detail.aspx?subdomain=icgcm&iid=1011.

STRENGTH CHARACTERISTICS OF SECURA HOLLOW GROUTABLE CABLE BOLTS

Naj Aziz[1], Robert Hawker[2], Ali Mirza[1], Jan Nemcik[1], Xuwei Li[1] and Haleh Rasekh[1]

ABSTRACT: The strength properties of Secura Hollow Groutable Cable-bolts (HGC) were examined for tensile and shear failures. The 30 mm diameter, nine strand, cable bolt consisted of a mixture of five 7.5 mm plain and four 7.0 mm indented strands wrapped around a central 14 mm steel grouting hole to make a round cable with lay length of 500 mm with bulbs at 500mm centres of diameter 35mm. The tensile strength of the cable was tested in accordance with the British Standard (BS7861-part 2:2009) using the double embedment pull test. The shear strength of the cable bolt was tested by both the BS7861 single and UOW double shear methods. The single shear double test used a guillotine shear frame of double embodiment tendon/grout assembly in a steel tube, while the double shear method enabled shear testing of the cable bolt in concrete to simulate rock. It was found that the tensile strength of the cable was in the order of 680 kN, the shear load by single shear test, based on the average of three tests, was around 448 kN. The shear failure load of the cable bolt from double shear testing based on two tests averaged around 786 kN which is significantly higher than achieved from the single shear test. Thus the shear value, obtained from the double shear method was between 13 and 18 % greater than the single shear test method. The use of the guillotine shear frame for the single shear method was considered an unrealistic method of evaluating the shear characteristics of the cable bolts in rock.

INTRODUCTION

Australia uses a variety of cable bolts as a secondary system of support for strata reinforcement. The use of cable bolts initially began in metalliferous mines in mid-1960 and was later introduced to underground coal mines by the early 1970's. Initially, cable bolts were of a conventional 7 single wire strand round cable and soon other cable types of different strand configurations followed. Presently, there are a variety of cable bolts which vary in size, structural formation, and strength to suit different ground stratification and conditions.

In general, installed cable bolts in situ are subjected to complex ground forces, which range from axial loading, to shearing and unwinding leading to the loss of encapsulation. The variation of the various loading force categories is dependent of the changes in ground conditions. Accordingly, methods used to evaluate the cable bolt strength characteristics should embrace various factors that influence the competency of the cable bolt in providing the necessary reactions to the prevailing ground forces. Thus, the forces applied on the cable bolt for strength evaluation tests must simulate the ground forces that the cable element is subjected to in situ.

The strength performance of cables bolts is currently based on both pull and shear tests. Thomas (2012) documented a total of 19 cable bolts, which were subjected for load transfer studies by pull testing. Few of these cables have since being tested in shear in addition to pull testing studies. Testing in shear has been carried out in accordance to British Standard (BS7861-Parts 2: 2009) for strata reinforcement support system components (Figure 1). The British Standard for both Pull and shear tests are normally carried out in embedment tubes with an internal diameter equal to the size of the hole as recommended by the manufacturer for tendon installation and with the steel tube wall thickness of at least 10 mm. The internal surface of the tubes is threaded to a 2 mm pitch and 1 mm deep to maintain bonding of the resin / grout between and steel wall. One notable reported investigation using the British Standard of shear testing was carried out by Rock Mechanics Technology (RMT) on the mechanical performance tests on Megastrand flexible bolts (Clifford, 2002) Cementitious and resin based grouts were used for these tests, depending on the type of tested cable in steel tube.

Craig and Aziz (2010 a and b) and later on by Aziz *et al.,* (2014 a,b) have evaluated the shear strength of cable bolts by double shear testing in concrete to simulate rock formation. Testing of cable bolts in

---

concrete was considered a rational method of simulating cable shear failure *in situ*, particularly where the sheared cable occurs without bed separation and sagging.
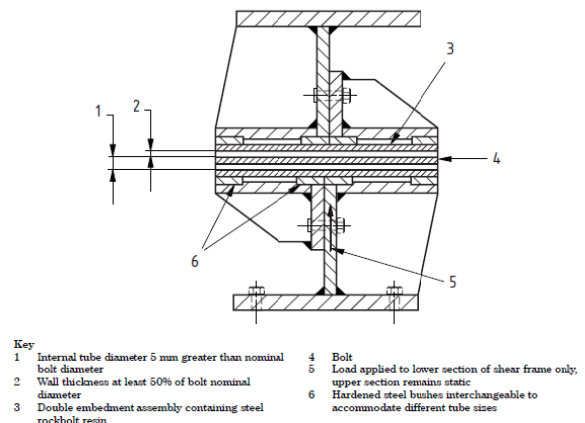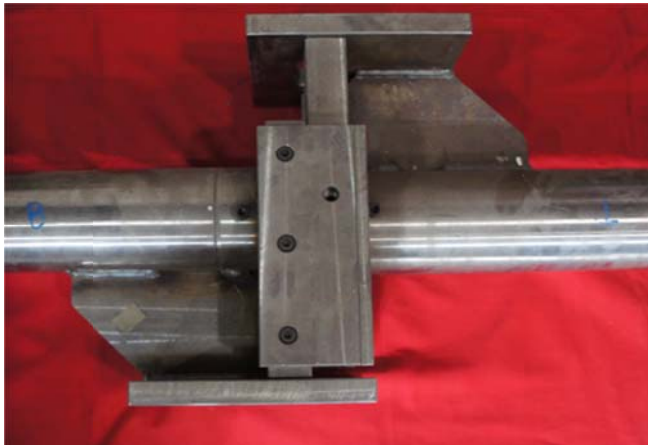
Figure 1: Single shear frame for testing of cable bolt (BS7861- part 2: 2009)

In this paper a newly marketed cable bolt known as Secura HGC-bolt has been studied for load transfer capability and performance. The cable bolt was tested for tensile and shear failures in the laboratory. In particular the performance of the cable for shear failure was carried out using the BS standard of double embedment tube as shown in Figure 1 and by the double shearing method in concrete blocks as reported by Graig and Aziz (2010 a,b). A particular emphasis has been given to the variations in shear strength performance of the cable bolt by both methods of testing.

CABLE BOLT DESCRIPTION

Secura HGC is the latest type of cable bolt that is currently undergoing trials in Australian mines and soon to be marketed by Orica Pty Ltd. Structurally, the cable bolt consists of a mixture of five plain and four indented single wire strands laid around central 14 mm dia. hollow grout tube. The plain wire strand is 7.5 mm in diameter and the indent wire strand is a 7 mm (7.5mm on largest cross section and 6.7mm on smallest cross section). The completely laid mixed strands will, therefore have two plain wire strands side by side as shown in Figure 1. The indented spiral pitch of the strand in the order of 40 mm however, the cable strand lay length, in general, is in the order of 500 mm. The cable bolt is bulbed type with the bulbs set at 500 mm spacing. The tensile strength of the cable is in the order of 69 t. Table 1 shows the specifications of both plain and indented wire strands. Clearly there is a variation in strength loss of around 11.85 % between plain and spiral strands as shown in Figure 2, which corresponds to a cross section area reduction of 12.9 %. The shear characteristics of the Secura HGC cable bolts were evaluated by both single and double shear tests

Table 1: Cable strands specification

Type	Diameter (mm)	Cross section Area (mm2)	Rib width (mm)	Pitch length (mm)	Failure load (kN)	Variation in cross section area (%)	Variation in failure load
Plain	7.5	44.2	1.8-2.2	35-45	75.08	*12.9*	*11.85*
Spiral	7.0	38.5	-	-	67.12	-	-

TENSILE STRENGTH TESTING OF CABLE BOLT

The tensile failure testing of the cable bolt was carried out in accordance to the British Standard (BS7861-Parts 2: 2009) and was carried out by ALS Australia Pty Ltd, NSW (ALS Report, 2014). The grouted hollow cable samples were held between the two jaws of the universal tensile tester a laser

distance reader was used to measure movement of the platens of the testing machine (refer to Figure 4a for test set up). The samples were encapsulated in the embodiment tubes with FB400 Orica Grout.　A tensile load was exerted using a ram travel speed of approximately 5 mm per minute. The displacement was recorded at regular load intervals of 50 kN until the maximum load was achieved. This was repeated with two other grouted hollow cable samples. The average failure load of the cable bolt was 679 KN (68 t) and Figure 4b shows the snapped faces of the cut strands of the cable, which clearly indicate the failed section of the cable in tension. Figure 5 shows the load-displacement profiles of three pull tested SHGC cable bolt sections.

Figure 2: Secura hollow groutable cable bolt
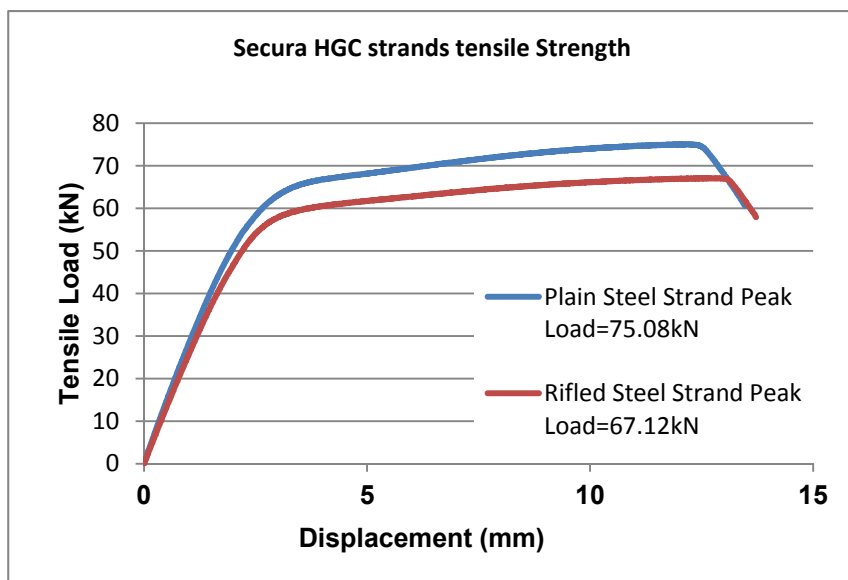
Figure 3: Load displacement graphs of both plain AND INDENT strands of the SHGC
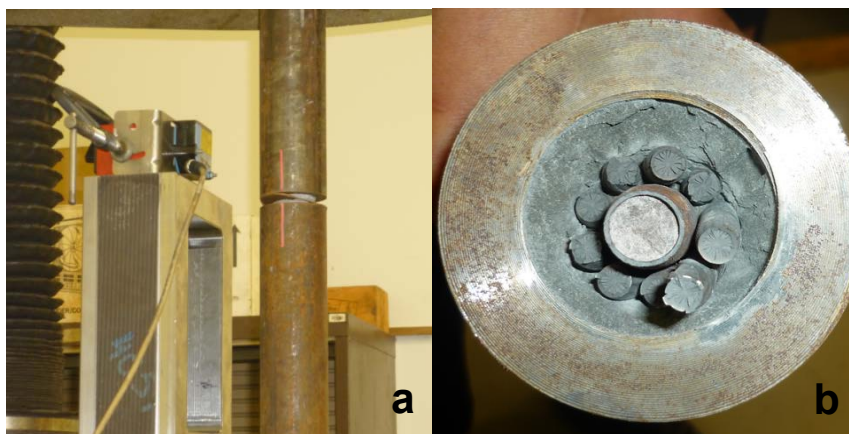
Figure4: (a) Tensile pull test set up and (b) snapped section of the cable bolt
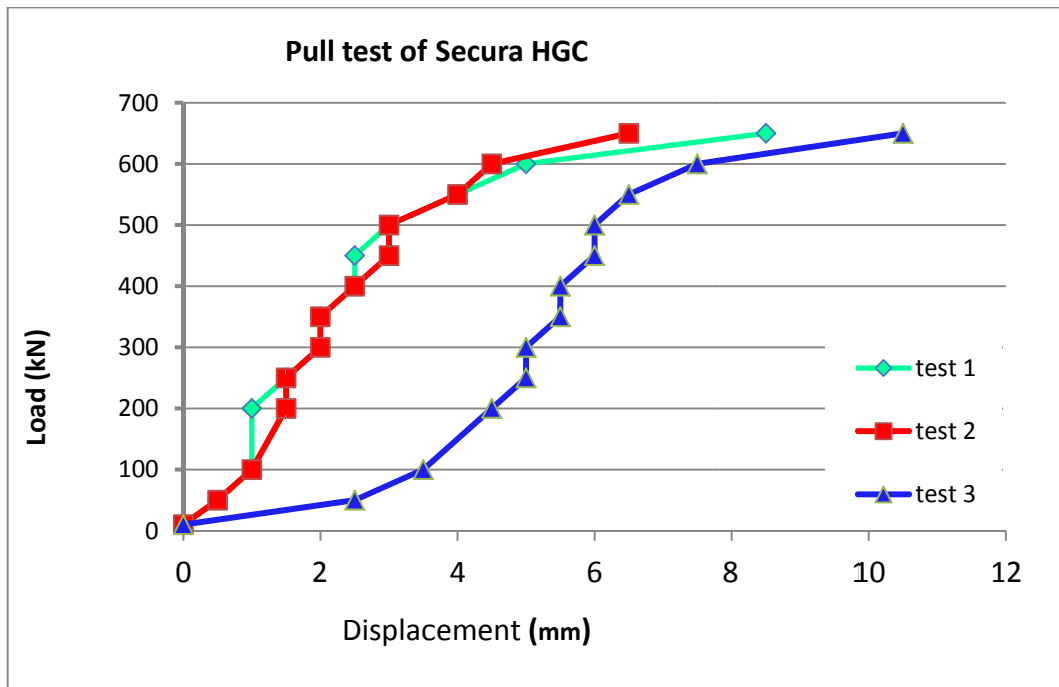
Figure 5: Load displacement profiles of three pull tested Secura HGC cable bolt sections

SHEAR TESTING

Single shear test

Three more samples grouted in the double embedment tubes were tested for shear. The grouted hollow cable samples were positioned into the specifically designed shear testing jig and placed between the two platens of the universal tensile tester a laser distance reader was used to measure movement of the platens of the testing machine (refer to Figure 6a for test set up). A shear load via a compression load on the jig was exerted using a ram travel speed of approximately 2.5 mm per minute. A preload of 10 kN was applied to the sample and the initial displacement was then measured. The displacement was recorded at regular load intervals of 50 kN until the maximum load was achieved. This was repeated with two other grouted hollow cable samples.

Figure 6: Shear test and a view of the sheared sample. Note the interaction between the strands and the steel tube
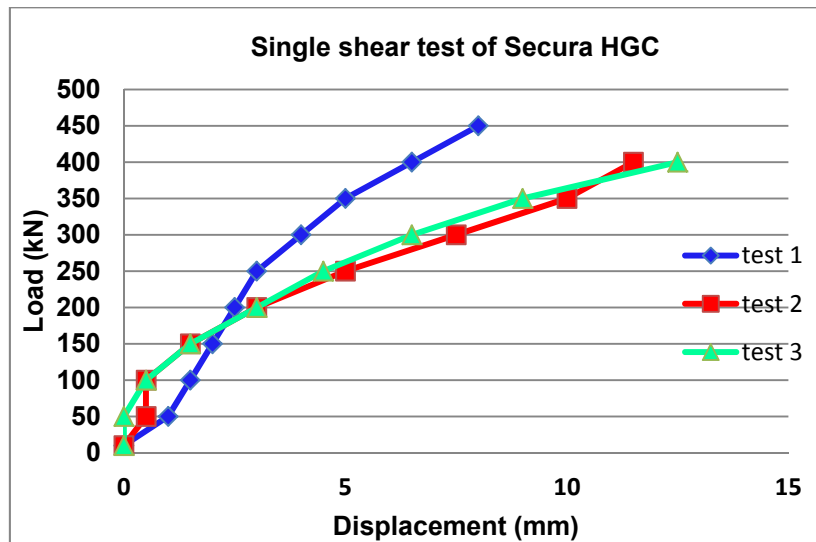
Figure 7: Load-displacement graphs of single shear tests

Double shear testing

Two double shear tests were carried out on SHGC cable bolts. The procedure used for casting concrete blocks was the same as described by Aziz *et al.,* (2014). The UCS value of the concrete was 40 MPa, determined from testing 100 mm diameter cylindrical concrete samples. The first cable bolt was installed in the concrete blocks using FB400 grout and the second was encapsulated with a two component pumpable resin Carbothix (Meikle *et al.,* 2013). The position of birdcages in respect to the shear planes are illustrated in Figure 8. One 60 t load cell was mounted on each protruding side of the assembled concrete blocks and tensioned to the predetermined axial pretension load, using a "Blue Healer" tensioner. Tensioning of the cable was retained by the barrel and wedge retainer. This was followed by the injection of the grout in the central concrete blocks hole for bolt encapsulation. Grouting of the cable in the concrete block was achieved via 20 mm diameter holes drilled on top of each concrete block as shown in Figure 8.
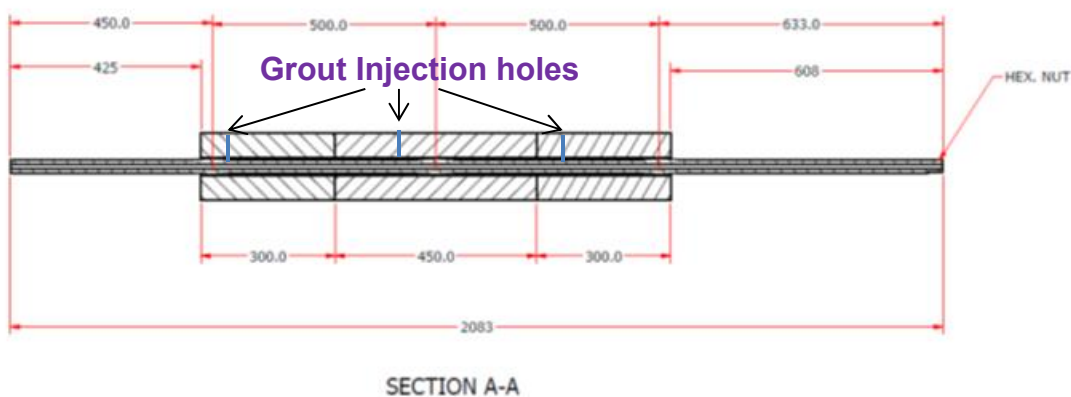
Figure 8: Cross section of double shear blocks and cable

After seven days of grout/resin curing time, the double shear assembly was then placed on the carrier base frame consisting of a parallel pair of rail track sections welded to a 35 mm thick steel plate. The outer side 300 mm3 cube blocks of the double shear apparatus was mounted on 100 mm steel blocks, leaving the central 450 mm long block free to be vertically sheared down a diameter of up to 100 mm as shown in Figure 9.

The process of double shear testing consisted of loading the central block vertically in the 500 t compression testing machine. The 450 mm long middle section of the double shear apparatus was then vertically shear loaded at the rate of 1 mm/min for the maximum 100 mm vertical displacement. The rate of loading and displacement was monitored and simultaneously displayed visually on a PC monitor. Cables and blocks were then dismantled and manually split open after shear testing was complete. An example of post-test broken cable and blocks are shown in Figure 10.
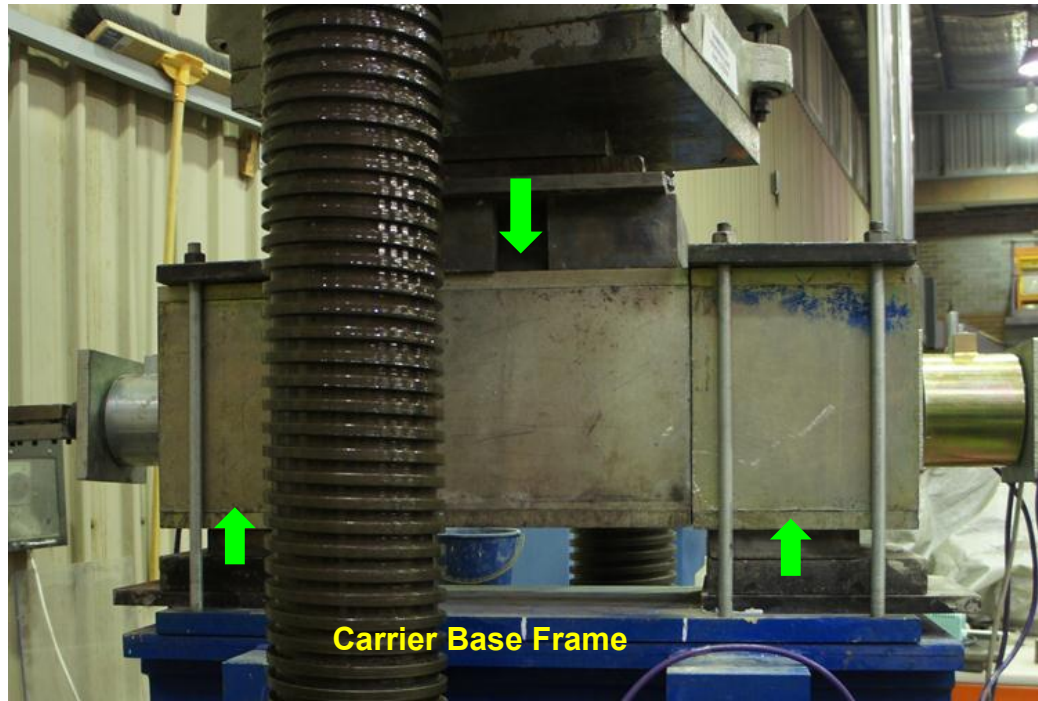
Figure 9: Double shear cable and concrete blocks assembly
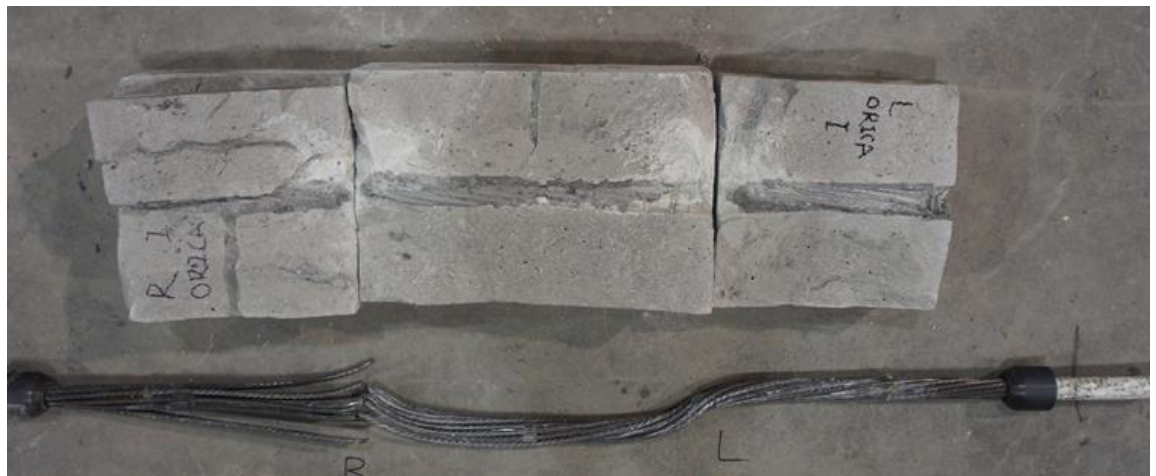
Figure 10: Post-test dismantled cable double shear assembly

RESULTS AND DISCUSSION

Table 2 shows both single and double shear test results of the Secura HGC cables. Figure 11 shows the combined shear and axial pretension load of each tested cables. The average test result of single shear guillotine shear test was carried out independently and in accordance with the British Standard BS 7861-Part 1 [ALS Report No 27244248-1, May 15, 2014]. However, the highest shear load on each joint face obtained from the double shear test was 800 kN with the cable being grouted with FB400 cementitious grout, which is pretensioned to an axial load of 270 kN. The second double face shear test yielded 772 kN. The second test was encapsulated with Carbothix and loaded axially to 97 kN.
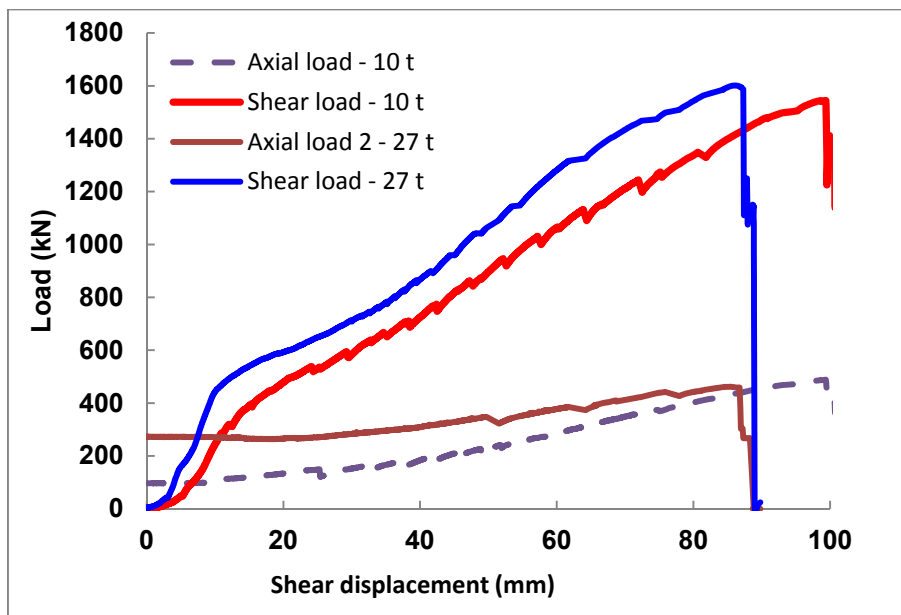
Figure 11: Load-displacement graphs of shear loads together with two shear tests at 10 and 27 t initial axial loads

The relatively lower shear force due to single shear testing can be attributed to; (a) the cable being sheared at zero pretension and (b) the cable being subjected to the guillotine effect, with cable strands being damaged by the steel tube wall. This damage is clearly visible from the post shear view of the cable cut in Figure 6. The shear load per side for each double shear cable bolt was significantly higher than results of testing cables in the single guillotine shear test. These increases were 18 and 13 % respectively. Also, testing by double shearing method may require some portion of the shear force to overcome the shearing forces of the concrete surfaces of joint planes. This level of joint surface shear is dependent on the cable pretension. Currently, two methods are investigated to define the shear component of the concrete faces or eliminate it completely, in a manner similar to the cable being sheared across separated bedding planes with no contacts. No cable rotation or unwinding was observed during shear testing.

The shear failure load of the cable was influenced by the strength loss of the indented strand (about 11%) of the cable as demonstrated by the load displacement profiles shown of Figure 3. The mass loss due to strand indentation clearly has contributed to the strength loss.

Table 2: Single and double shear test results of the Secura HGC cables and single shear test result based on BS7861 test

NB: hole diameter: 42 mm,

Test	Bonding agent (resin or Grout)	Cable UTS (MPa)	Initial pre-tension load in kN	Final ave. peak axial pretension load (kN)	Double joint peak shear load (kN)	Shear load per joint plane (kN)	Single (Guillotine) shear test (BS 7861) (kN)	DS test / BS SS Ratio
1	FB400 grout	680	270	460	1600	800	679	1.18
2	Carbothix	680	97	487	1544	772	679	1.13

CONCLUSION

The overall results of tested cables showed that:

- The level of shear load appears to be influenced by the cable bolt pretension load
- As expected single shear guillotine testing of the cables (based on BS7861 test procedure) yielded lower shear loads.
- The shear failure load of indented strand cable is lower than that of plain strand. This is expected because of the strength loss and mass loss of indented strands.

- No cable rotation was detected in double shear testing in either cable bolt test.

REFERENCES

ALS Industrial Report prepared for Orica Australia Pty Ltd, on the load test of grouted hollow cable samples, No 27144348-1, May 15, 2014, NSW, 5P.

Aziz, N I. 2014, Double shear testing of Secura Hollow Groutable Cable-bolt (HGC) for Orica Australia Pty Ltd, *a report of study, School of Civil, Mining and Environmental Engineering, University of Wollongong*, July, 9p.

Aziz, N, Heemann, K, Nemcik J and Mayer, S. 2014, Shear strength properties of Hilti plain and indented strand cable bolts, *in proceedings Coal Operators Conference (Coal 2014)*, *Wollongong, (Eds. N Aziz, B Kinninmonth)*, Wollongong, February 12-14, ISBN 978 1 925100 02 0, pp156-162.

Aziz, N, Nemcik, J, Jalalifar, H. 2011, Double shearing of rebar and cable bolts for effective strata reinforcement, *in proceedings 12th ISRM International Congress on Rock Mechanics, Beijing, China, 18-21*, October, pp 1457-1460. Published in Harmonising Rock Engineering and the Environment (Eds. Qian and Zhou), 2012 Taylor and Francis Group, London, ISBN, 978-0-415-80444-8.

British Standard BS 7861- Parts 1 and 2, 1996. Strata Reinforcement support system components used in Coal Mines-Part 1. Specification for rock bolting and Part 2: Specification for Flexible systems for roof reinforcement.

Clifford, B. 2002, Mechanical performance tests on Megastrand flexible bolts, *Rock Mechanics Technology Ltd*, February, UK, February, UK, 18 P.

Craig, P and Aziz, N. 2010a, Shear testing of 28 mm Hollow Strand "TG"Cable Bolt, *in proceedings 10th Underground Coal operators Conference*, (Eds.N Aziz and Jan Nemcik. 375 p), Wollongong, February 11/12, pp171-179, http://ro.uow.edu.au/coal/303/.

Craig, P and Aziz, N. 2010b, Shear testing of 28 mm hollow strand "TG" cable bolt. *In proceedings 29th International Conference on Ground Control in Mining, ICGCM* (pp. 169-174). (Publication ID=35591), http://icgcm.conferenceacademy.com/papers/detail.aspx?subdomain=icgcm&iid=273.

Meikle, T, Tadolini, S C, Hawker R and Pollack D. 2013, Improvements in long tendon support with pumpable resin, *in Proceedings 13th Coal Operators' conference, (Eds. N Aziz, B Kinninmonth)*, Wollongong, 14-15 February, pp124-130, http://ro.uow.edu.au/coal/445/.

Thomas, R. 2012, The load transfer properties of post-groutable cable bolts used in the Australian coal industry, *in Proceedings 31st International Conference on Ground Control in Mining*, Morgantown, 10p, http://icgcm.conferenceacademy.com/papers/detail.aspx?subdomain=icgcm&iid=1011.

AN EXPERIMENTAL STUDY ON THE CONTACT SURFACE AREA OF CABLED BOLTED STRATA

Haleh Rasekh, Naj Aziz, Jan Nemcik, Ali Mirza and Xuwei Li

ABSTRACT: The application of cable bolts in underground mines is an increasing trend all over the world; therefore, it is necessary to determine the axial and shear stresses on cable bolts. One important factor is to determine the coefficient of friction of concrete joint surface. This paper examines the contact coefficient of several cabled strata under various pre-tension loads subject to double shearing test. The result shows that the contact surface area can vary between 70-90% of the total surface area. This empirical value helps to figure out shear and axial stresses, where it is impossible to determine the exact amount of contact coefficient.

INTRODUCTION

Cable bolts, as a secondary support system in the mining industry, have been used since the 1960s (Fuller and O'Grady, 1993). The cable bolt provides reinforcement for the bed rock to support it-self. There are different methodologies to determine the behaviour of cable bolts, which are pull out tests and shear tests. Hawkes and Evans (1951), Fuller *et al.,* (1978), Diederichs (1993), Bouteldja (2000), and Yassein (2004) reported the strength of cable bolts for evaluating the tensile failure and load transfer capacity by using the pull test methodology. Nowadays, the performance of cable bolts under shearing is a topic of interest which can be conducted in the laboratory by using either the single shear or double shear tests. Generally, cable bolt failure in the field is a combination of shear and tensile loading. The single shear test as an approach to determine the shear performance of cable bolts has been conducted by a large number of researchers although double shear tests simulate the field condition in a better way. Aziz, *et al.,* (2003) conducted 28 double shear tests on three common types of bolt in Australia with concrete block strengths of 20MPa and 40MPa. The strength of concrete contributed to increase in load transfer capacity of the bolt for the given axial pre-tension load and the value of system stiffness was higher for higher strength concrete (see Figure 1).

(a) Bolt Type 1 in 20 MPa Concrete   (b) Bolt Type 1 in 40 MPa Concrete
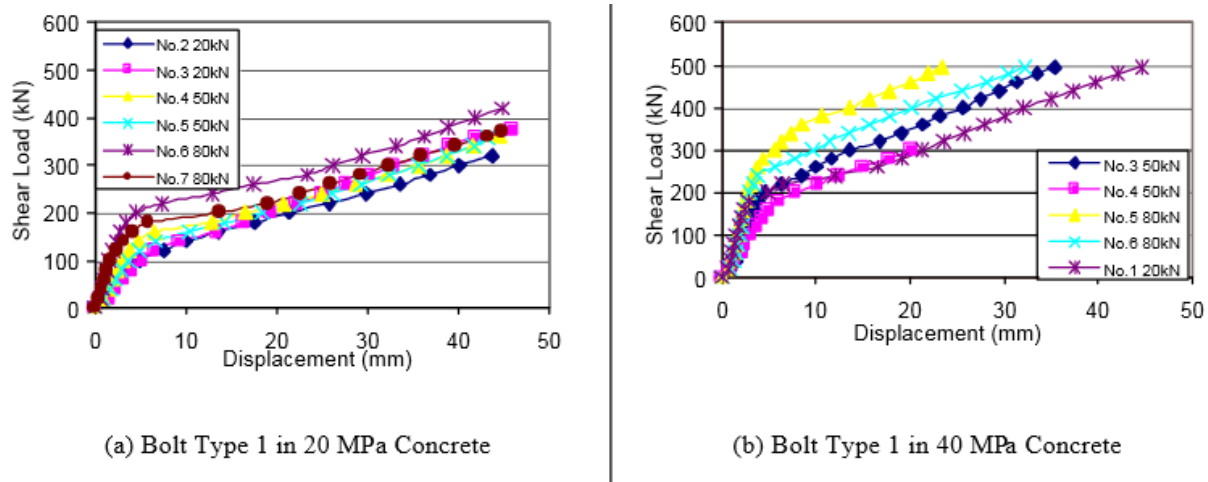
Figure 1: Effect of concrete type in the peak shear load of different rock bolts

Aziz, *et al.,* (2005) investigated the effect of resin thickness in shear for bolt-grout-concrete interaction by double shear testing. Two types of concrete blocks with different strength of 20 MPa and 40 MPa were used for the tests and the study was further reinforced with ANSYS numerical simulation. The results show that the thickness of resin is an important factor in transferring load from bolt to concrete. Increasing the thickness of resin reduces the load transfer capacity, when the bolt was axially loaded (pulling or pushing). The result from the numerical model was in agreement with the experimental

School of Civil, Mining and Environmental Engineering, University of Wollongong, NSW, Australia. E-mail: naj@uow.edu.au,
 Tel: +61 242213449

results. The shear resistance and shear displacement are more influenced by the strength of concrete block when compared to the resin thickness (Figure 2). Grasselli (2005) carried out a series of double shearing tests on two different types of bolt; fully grouted solid bolt and Swellex bolts. The numerical study was carried out using three-dimensional Finite Element (FEM) code. The experimental curve for both bolt types had three similar steps, but the ultimate contribution to the shear resistance for the steel bar was rather higher than for that of the hollow Swellex bolt. The study by Jalalifar (2006) shows the effect of pre-tensioning on the maximum tensile load as shown in Figure 3. Craig and Aziz (2010) conducted two double shear tests on the 28 mm hollow strand "TG" cable bolt. The initial pre-tensioning were 50 kN and 90 kN and the maximum permitted shear displacement were 50 mm and 75 mm respectively. The increase in the initial pre-tension load contributed to increased shear load at reduced shear displacement, which is evident in Figure 1. Aziz *et al.,* (2014 a) carried out double shearing tests on the 19 wire HTT-IXG Hilti plain and indented cable bolts to study their performance. It was found that the maximum shear load and axial load for the plain cable was higher compared to the indented one while the vertical displacement was lower for the plain cable compared to the indented cable. The result of the tensile test of the single strand shows that the strength of indented strand was also 10% less than the plain one. Aziz *et al.,* (2014 b) studied the series of double shear test on the fibre glass cable bolts. The result of this study highlighted the impact of pre-tensioning and grout type on the peak shear load.

This paper is aimed at identifying the amount of the applied force required to overcome the shear generated across the joint faces as a component of the overall force required for double shear testing.

SHEAR FORCE COMPONENETS

In double shear testing of a reinforcement element installed in concrete, the applied shear force is consumed in overcoming the shear resistance of both the reinforcement element and shear joint surface. The shearing load applied is consumed in;

    a)   Shearing and bending of the cable bolt, and
    b)   Overcoming the shearing friction of the two concrete joint faces
    c)   Shearing of the grout annulus which is small and can be considered as part of the concrete joint faces.

Thus, it is imperative that the above three shearing components be quantified so that their or near realistic force values can be determined. This can be achieved by either;

1. Determination of the shear strength of concrete blocks joint surfaces, which can be deducted from the total shear strength to calculate the shear strength of cable bolt, or
2. Eliminate completely the effect of shearing concrete faces by leaving small gaps between concrete blocks to neglect the contact resistance between concrete blocks. By this method, the total shear strength is the strength of cable bolt.

The focus of this paper is on the first method, while the second method represents an alternative approach, which can realistically determine the contribution quantities from that due to concrete and grout.
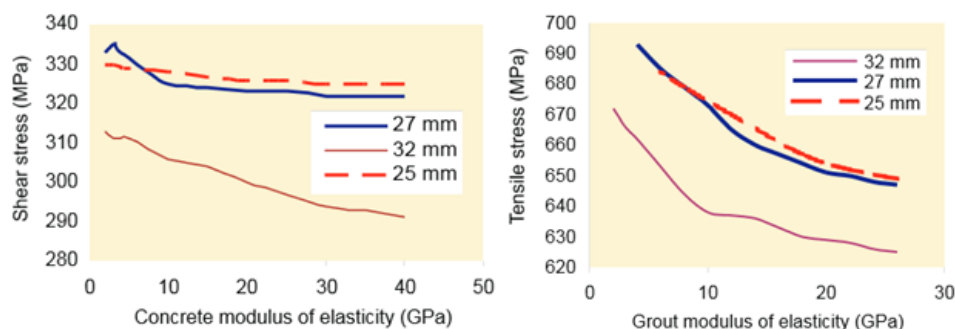
Figure 2: Induced shear and tensile stresses versus grout modulus of elasticity in, left: different resin thickness, right: soft concrete Aziz *et al.,* (2005)
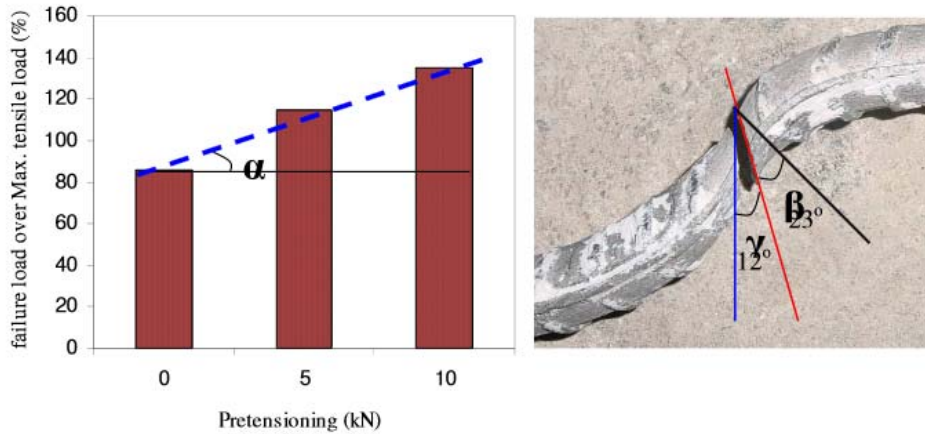
Figure 3: Effect of pre-tensioning on the maximum tensile load (Jalalifar 2006)

Several uncertain factors remain in the double shear test for the first method, such as the contact coefficient of concrete blocks. This factor is an important factor in calculating the shear and axial stresses of the cable bolts using the shear and axial loads according a series of tests were undertaken to evaluate and quantify the coefficient factors under different test conditions.

TEST APPARATUS, SAMPLE PREPARATION, AND EXPERIMENTAL PLAN

The double shear assembly consisted of three concrete blocks with cross sectional area of 300 x 300 mm^2 while the outer concrete blocks length was 300 mm and the middle one was 450 mm (see Figure 4). The concrete blocks had a compressive strength of 40 MPa. They were cast in the steel frame of the double shear apparatus while a 20 mm thick plastic conduit was positioned through the mould for cable bolt installation. The concrete blocks were kept wet for 28 days for curing purposes.

Subsequently, the surfaces of concrete blocks were painted using special painting pattern shown in Figure 5. Each surface was divided to 36 squares that helped to precisely determine the contact surface area after the test. Then, the concrete blocks were mounted in the steel moulds. In order to monitor the axial loads generated on the cable bolt during pre-tensioning and shearing test, two 60 t load cells were incorporated. The cable bolt was retained in tension by installation of two sets of barrels and wedge. After pre-tensioning the cable bolt, chemical resin or cementitious grouts were injected to the holes on top of the concrete blocks depending on the test requirements, and tests were conducted seven days later. The 500 t machine at the rock mechanics laboratory of University of Wollongong was used to perform the double shear tests. Figure 6 shows the installed cabled bolt in double shear test assembly in the 500 t machine. The rate of shear displacement was set by the digital controller. The shear load was applied to the sample using a hydraulic jack located on top of the instrument. The middle concrete block was moved in a vertical direction. The amount of shear and normal load and shear displacement were recorded by the data taker.

Figure 4: Concrete block dimensions
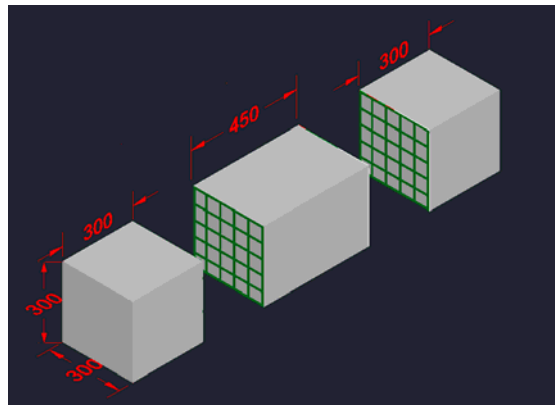
Figure 5: Concrete block painting
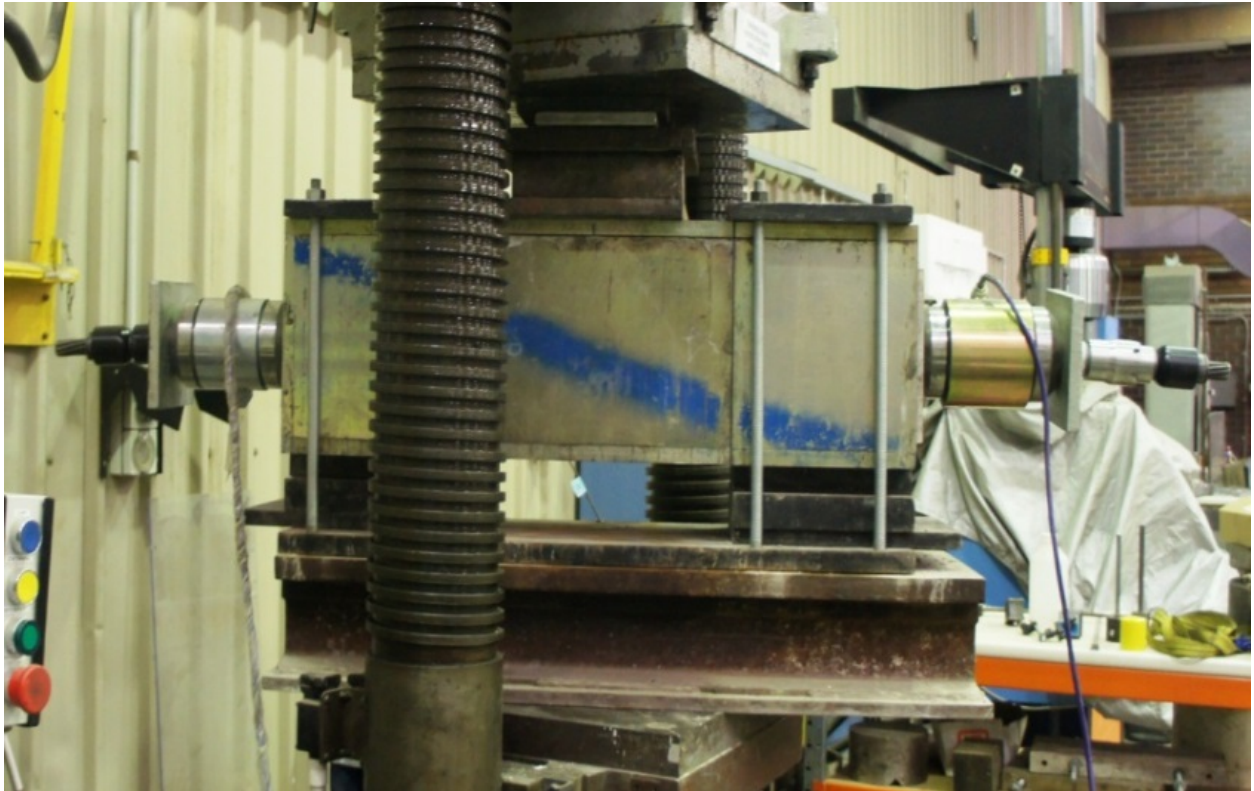
Figure 6: Arrangement of shearing apparatus in compression machine

More than 10 double shear tests were conducted on various samples. The value of initial normal load varied between 0, 100 and 250 kN while the rate of shear displacement was set to 1 mm/min. The first test was conducted without installing cable bolts in the concrete block and the purpose was to investigate the pure shear strength of concrete blocks. Seven different types of cable bolts were tested with different type of grout and pre-tension loads as shown in Figure 7 and Table 1.

TEST RESULTS AND DISCUSSION

The aim of this research was to determine the pure shear strength of cable bolts; therefore, it was essential to calculate the shear strength of the concrete blocks joint surfces at the desired value of the applied axial stress. Figure 8 shows the relationship between the normal and shear stresses for the sliding concrete blocks. By using the Mohr Coulomb equation, the friction angle was drawn as 26.94°. The cable bolt   shear strength, can then be obtained by deducting the shear strength of concrete block joints surfece from the total shear strength obtained from shearing test.

Figure 9 shows the concrete blocks after shearing. As previously mentioned, each surface was divided into 36 squares. The Contact Coefficient (CC) was calculated as:

$$CC = \frac{Number\ of\ damaged\ squares}{Total\ square\ numbers\ (=36)} \times 100 \tag{1}$$

The amount of CC for experimental tests of this study are summarised in Table 2. The average of CC of the cabled concrete, after shearing, was 80% of the total area. This value can be considered between 70% and 90% where it is impossible to determine the contact coefficient of concrete blocks precisely.

Then, the axial stress and shear stress can be calculated using the following equations:

$$\sigma_n = \frac{N}{CA} \tag{2a}$$
$$\tau = \frac{0.9 \times S}{2 \times CA} \tag{2b}$$

where, σ_n is the normal stress, *N* is the normal load, *S* is the shear load and CA is cable area.

The damage on the concrete blocks was mostly concentrated around cable bolts. It was noted that by increasing pre-tensioning, the contact coefficient increases. The reason is that the load applied to the concrete blocks and cable bolt subjected the sheared concrete joint faces tight and increased the contact forces between concrete blocks. This is evident in tests 5 and 7 and also in tests 7 and 8. For instance, CC values for the Indented SUMO-Hollow 28mm cable with pre-tensioning forces of 10 t and 25 t, the CC values were 75% and 81% respectively. The stiffness of cable is more compared to the concrete block, and this is the reason why the cable bolt carries 90% of the total shear load. Table 2 shows the total shear strength and the pure shear strength of cable bolts. The result from this method of testing is approximately and hence required a closer look. Figure 10 shows an alternative approach to eliminate the effect of the Joint surfaces shear values. The new design of the double shear apparatus should prevent shearing joint faces coming in contact with each other, thus the applied shear load will enable accurate determination of the cable bolt shear strength.

21.8mm super strand 19 wire cable

21.8mm super-strand 19 wire cable

TG- Hollow 28mm

SUMO-Hollow 28mm c/w 35mm birdcaged

SUMO- Hollow 28mm c/w 35mm birdcaged

Garford 15.2mm twin strand cable

Secura hollow groutable cable bolt

Figure 7: Cable bolts used for double shearing test purpose

Table 3: Detail of double shear tests carried out on various cables with different pretension loads and grouts

Test No.	Cable Bolt Properties					Drill bit (mm)	Bonding agent	Pre-tension load (t)	Peak shear load (kN) [½ double shear]
	Product name	Cable Ø (mm)	Wire geometry	Cable cross-section	Cable geometry				
1	Indented Superstrand	21.8	Indented	19 wire, PC strand	Non-birdcaged	28	Oil based resin	25	558
2	Superstrand	21.8	Plain	19 wire, PC strand	Non-birdcaged	28	Oil based resin	25	628
3	Indented TG	28	Indented	9 wires, hollow centre	Non-birdcaged	42	TD80 Grout	25	604
4	Indented SUMO	28	Indented	9 wires, hollow centre	35mm birdcage	42	TD80 Grout	25	414
5	Indented SUMO	28	Indented	9 wires, hollow centre	35mm birdcage	42	TD80 Grout	10	488
6	Plain SUMO	28	Plain	9 wires, hollow centre	35mm birdcage	42	TD80 Grout	25	711
7	Plain SUMO	28	Plain	9 wires, hollow centre	35mm birdcage	42	TD80 Grout	10	659
8	Gardford twin-strand	15.2	Plain	2 x 7 wire, PC strand	25mm Bulbs	55	BU100 Grout	0	501
9	Orica Secura HGC cable	30	Plain & indented	5 plain wire +4 indented wire	Non-birdcaged	42	FB400	25	800.5
10	Orica Secura HGC cable	30	Plain & indented	5 plain wire +4 indented wire	Non-birdcaged	42	Carbothix resin	10	772
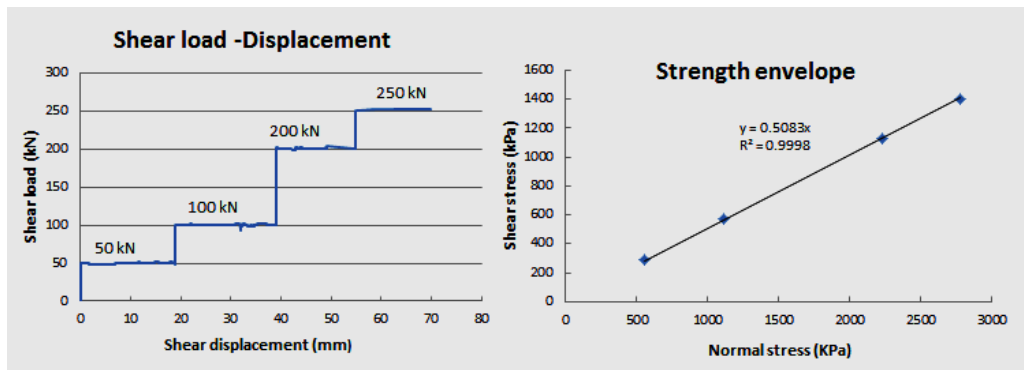
Figure 8: test results of the concrete blocks sliding test

CONCLUSION

- Testing of cable bolts in concrete represent a realistic away of simulating shear failures in rocks in underground.
- There is a significant level of shear force spent in overcoming the sheared concrete joint surfaces friction. The level of forces is rather difficult to quantify accurately by using CC by the painted pattern damage. One approach will be the elimination of the joint surfaces coming in contact with each other during shearing. Also, by increasing the pre-tensioning leads to increase in the contact coefficient.

Table 2: Peak shear strength for different cabled concrete blocks

Test Number	Contact coefficient (%)	Total Shear strength (GPa)	Shear strength of cable (GPa)
1	86.1	2.24	2.02
2	89	2.01	1.81
3	83.3	1.99	1.79
4	61	1.36	1.22
5	81	1.6	1.44
6	75	2.06	1.85
7	83.3	1.9	1.71
8	69.4	0.93	0.84
9	83.3	2.31	2.08
10	88.9	2.23	2.01

Figure 9: Concrete block surfaces after shearing
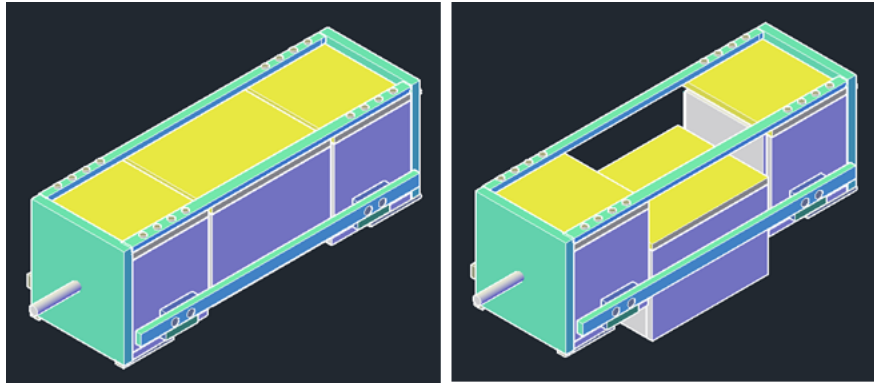
Figure 10: Schematic design of double shearing apparatus with no contacts between concrete blocks

ACKNOWLEDGEMENT

REFRENECES

Aziz N, Heemann K, Nemcik J and Mayer S. 2014 a, Shear strength properties of Hilti plain and indented strand cable bolts, *in proceedings Coal Operators Conference (Coal 2014)*, Wollongong, February 12-14, ISBN 978 1 925100 02 0, pp156-162 (Eds. N Aziz, B Kinninmonth,) [http://ro.uow.edu.au/coal/509/].

Aziz N, Gilbert D, Nemcik J, Mirzaghorbanali A and Burton R. 2014 b, The strength properties of fibre glass and other polymer based dowels for strata reinforcement in coal mines, *in Proceedings, Third Australaisan Ground control in Mining Conference (AusRoc 2014)*, Nov. 5 and 6, Sydney, pp 363-368.

Aziz N, Jalalifar H and Hadi M. 2005, The effect of resin thickness on bolt-grout-concrete interaction, *in shear , Coal Operators' Conference. - Wollongong : University of Wollongong*, pp 3-9.

Aziz N, Pratt D and Williams R. 2003, Double shear testing of bolts, *[Conference] // Coal 2003: Coal Operators' Conference. - Wollongong : University of Wollongong*, pp 154-161.

Bouteldja M. 2000, Design of cable bolt using numerical modelling [Report]. - Montreal : McGill University.

Craig P and Aziz N. 2010, Shear testing of 28 mm Hollow Strand "TG" Cable Bolt, *10th Underground Coal operators Conference, Wollongong, February 11/12, pp171-179, (Ed.N Aziz and Jan Nemcik*, 375 p), [http://ro.uow.edu.au/coal/303/].

Diederichs M S. 1993, A Model For Evaluating Cable Bolt Bond Strength: *An Update [Journal]*, - Balkema : International Society for Rock Mechanics.

Fuller P G, O'Grady P. 1993, FLEXIBOLT flexible roof bolts: A new concept for strata control, *12th International Conference on Ground Control in Mining*, Morgantown, West Virginia, USA.

Fuller P G and Cox R.H T. 1978, Rock reinforcement design based on control of joint displacement - a new concept, *Proc. 3rd Aust. Tunneling Conference*, Sydney : [s.n.], pp 28-35.

Grasselli G. 2005, 3D behaviour of bolted rock joints: experimental and numerical study, *International Journal of Rock Mechanics and Mining Sciences*, pp 13-24.

Hawkes J M and Evans R H. 1951, Bond stresses in reinforced concrete columns and beams, *Structural Engineering*, Vol 29, pp 323-328.

Jalalifar H. 2006, A new approach in determining the load transfer mechanism in fully grouted bolts [PhD thesis] – Wollongong, University of Wollongong Thesis Collection.

Yassein A, Wahab K and Peng S. 2004, 3D FEM simulation for fully grouted bolts, *International conference on ground control in mining*, West Virginia : [s.n.], pp 273-277.

MODELLING OF REBAR AND CABLE BOLT BEHAVIOUR IN TENSION/SHEAR

Xuwei Li, Jan Nemcik, Naj Aziz, Ali Mirza and Haleh Rasekh

ABSTRACT: Cable bolting and rock/rebar bolting are the two main reinforcement techniques used in underground coal mines to maintain the stability of openings. Due to the structural features of cable strands, cables and solid bolts behave differently in reinforcing rock strata. Since the generation of a cable model is different in a numerical program, and especially impossible in a 2D program, some researchers tend to replace cable bolts with rebar bolts in numerical models, which is still pretty suspicious. To compare their performance differences when subjected in tension and/or in shear, numerical models of cable and rebar bolt were built and analysed using Flac3D program. The generated models of cables and rebar bolts were assigned identical geometrical dimensions and basic mechanical properties to ensure comparability. Attention was mainly given to the strength and stiffness of cables and rebar bolts both in tension and in shear. Conclusions are drawn from these models, which can be a reference for other studies in this area.

INTRODUCTION

Bolting is an important main reinforcement technique used in openings to control and reinforce rock strata. To better use the bolting technique, a good understanding of the interaction and loading transfer mechanism of bolts and the surrounding media is necessary. Compared to experimental methods, numerical simulation is a good way to investigate the evolution and propagation of stress and strain in detail inside the shear system. It is also cheaper and easily repeatable. Many studies have been carried out with numerical simulation. Spang and Egger (1990) carried out numerical 3D simulation using the Finite Element Method to quantitatively investigate the various phenomena occurring during shear tests on bolted rock blocks. Stankus and Guo (1996) conducted numerical tests on bolted rock joints with various lengths of bolts and pretensions and drew some interesting conclusions on the effects of the pretension and cable length. Grasselli (2005) studied and compared the shear performances of both full steel dowels and frictional swellex using a commercial three-dimensional finite element code, ZSOIL_3D. Tests were also done by Turmo *et al.,* (2006) using a Finite Element Method to study the structural behavior of segmental concrete structures with bolt reinforcement. Song *et al.,* (2010) conducted numerical tests on Double Shear Model (DSM) using a 3D program to study the deformability and stress state of bolted jointed rock blocks. Obviously, past studies with simulation mainly focused on the interaction of rebar bolt and rock strata but did not include cable bolts, because of the structural complexity of cable bolts. For modelling of cable bolts, the grid zones used will be dozens times that used for rebar bolts. The contact interface of strands is also a tough problem in simulation. So when attention is shifted to cable bolting in simulation, especially considering the effect of cables' surface structure, many problems will emerge. An easy means of this could be to replace the cable bolt with a rock bolt in numerical simulation. But the feasibility of this means has not yet been determined, which requires further research prior to its adoption.

In this paper, the preliminary work carried out to study the performance differences of rebar and cable bolts is reported. Attention was mainly given to the strength and stiffness of cable and rebar bolts both in tension and in shear. For the cable bolts, only its main structural feature, the spiral structure, was considered. No consideration was given to the cables' bird structure or strand indentation.

CONSTITUTIVE MODEL OF BOLT COMPOSITE

Deformability of cable strand

The deformability of cables in tension and in shear plays an essential role in their performance when loaded in shear. Since they are made from steel, their main deformability is determined by the steel material. Steel material normally has four typical stages in its stress strain curve, elastic stage, yield stage, strain hardening stage, and strain softening stage. Several cable strands have been tested in

tension and two stress strain relationship profile were gained and illustrated in Figure 1 and Figure 2. The cable strand results are consistent with the typical relationship except the strain softening stage since cable strands do not have an obvious strain softening stage. In these figures, the yield stage and the strain hardening stage are combined and represented by another strain hardening stage which simplifies the stress strain relationship as a linear relation and is easy to be used in analysis. In addition, both two stages can be considered as linearly elastic with two different moduli.
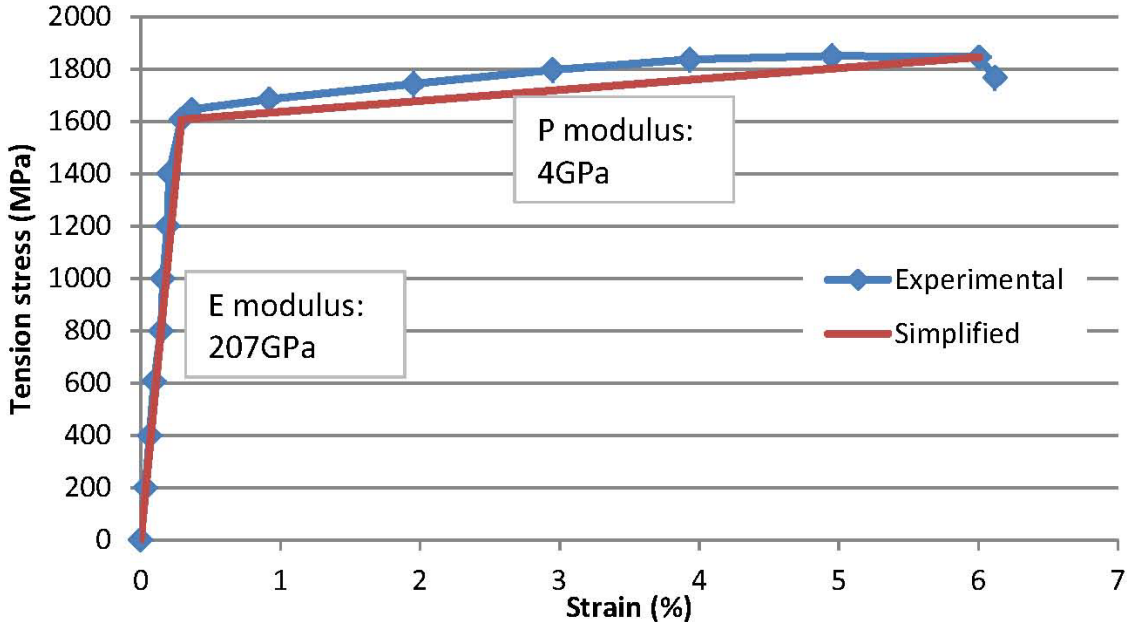
Figure 1: Stress strain relationship of a plain cable strand (source Orica)
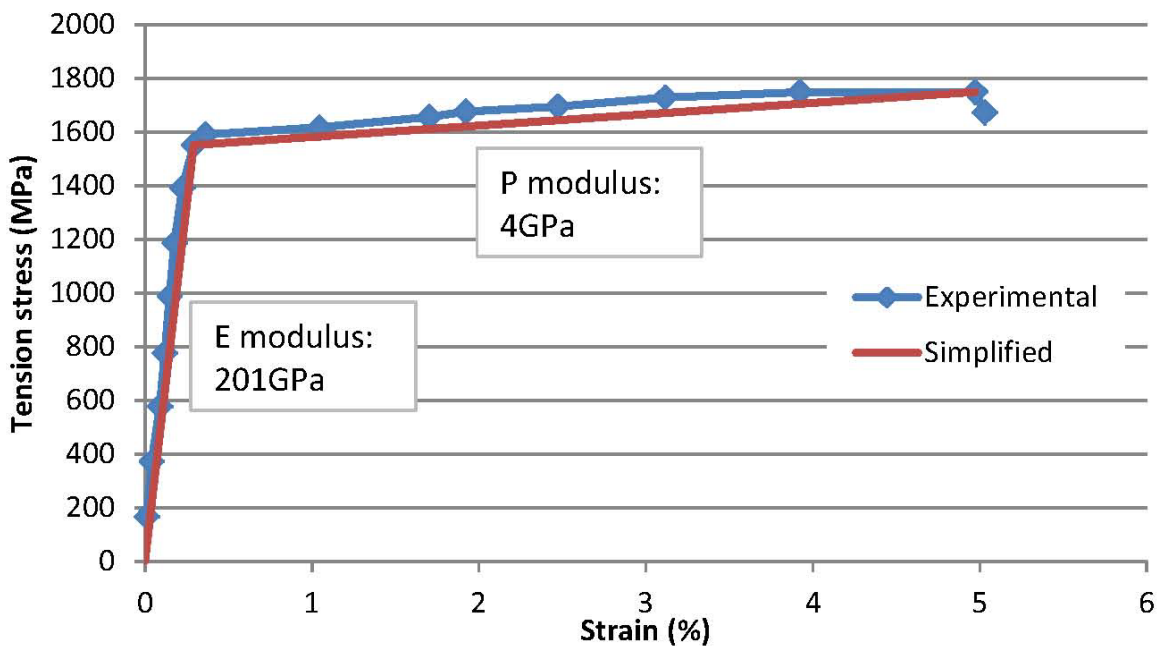
Figure 2: Stress strain relationship of an indented cable strand (source Orica)

Constitutive model of cable composite

Considering the tensile tests conducted on the cable strand, two linearly elastic stages were assumed for both in tension and in compression as its constitutive model, as shown in Figure 3. In numerical simulation elastic model with varied moduli was applied to the cable according to its stress state. The tensile moduli used in simulation were 200GPa and 4GPa for the elastic stage and plastic stage, respectively.
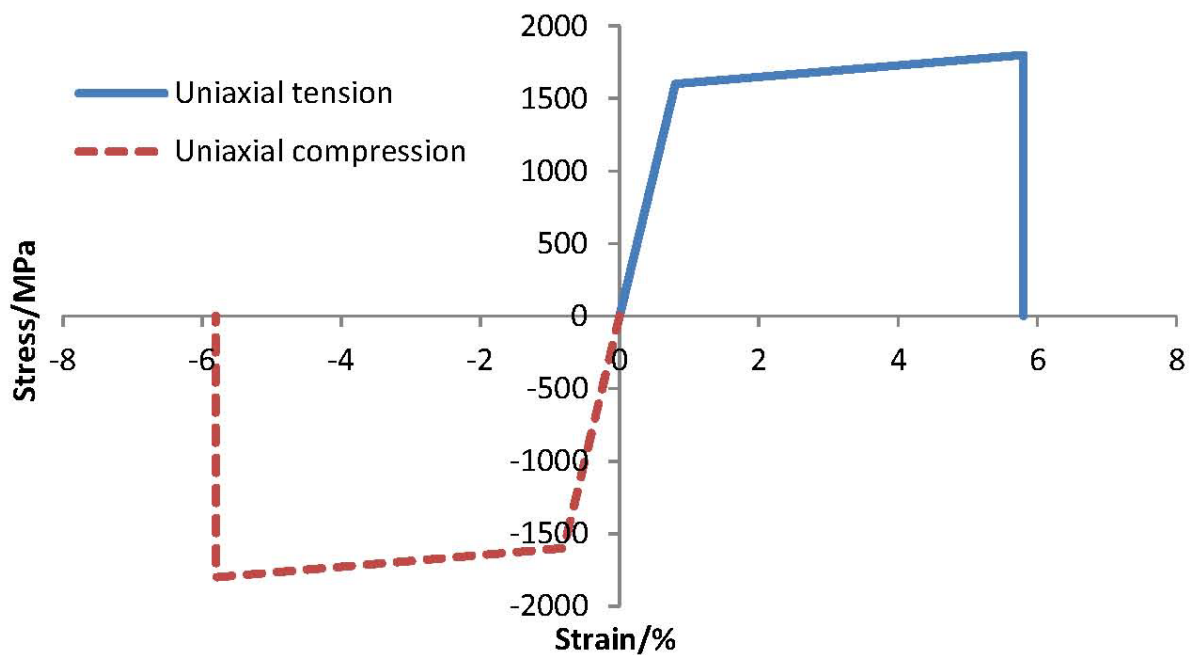
Figure 3: Constitutive model used in Flac3D model for both cable and rebar bolts

Verification of the constitutive model

A single cable strand was generated and assigned the above constitutive model and mechanical properties to verify the effectiveness of this model. The modelled cable strand is 200 mm long by 7 mm in diameter as shown in Figure 4. The steel strand was fixed at one end and tensioned to failure at the other end. The recorded tension load at the fixed end is shown in Figure 5, which is rigidly consistent to the assumed constitutive model in Figure 3, and thus this model can be used in the following study.
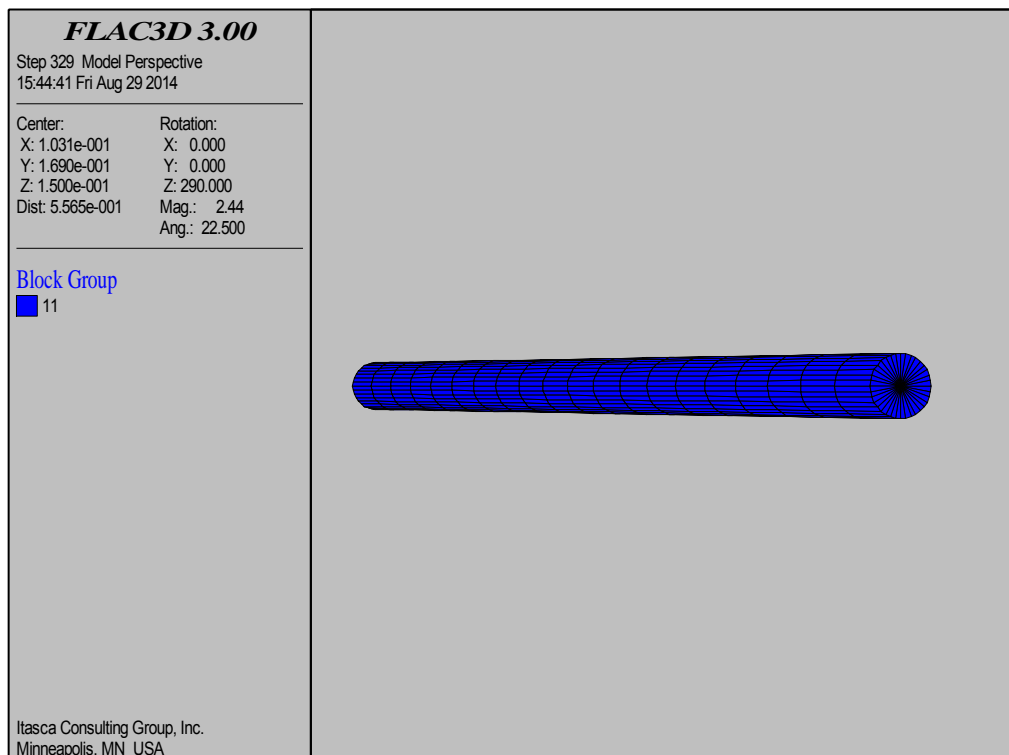
Figure 4: Model of a single cable strand
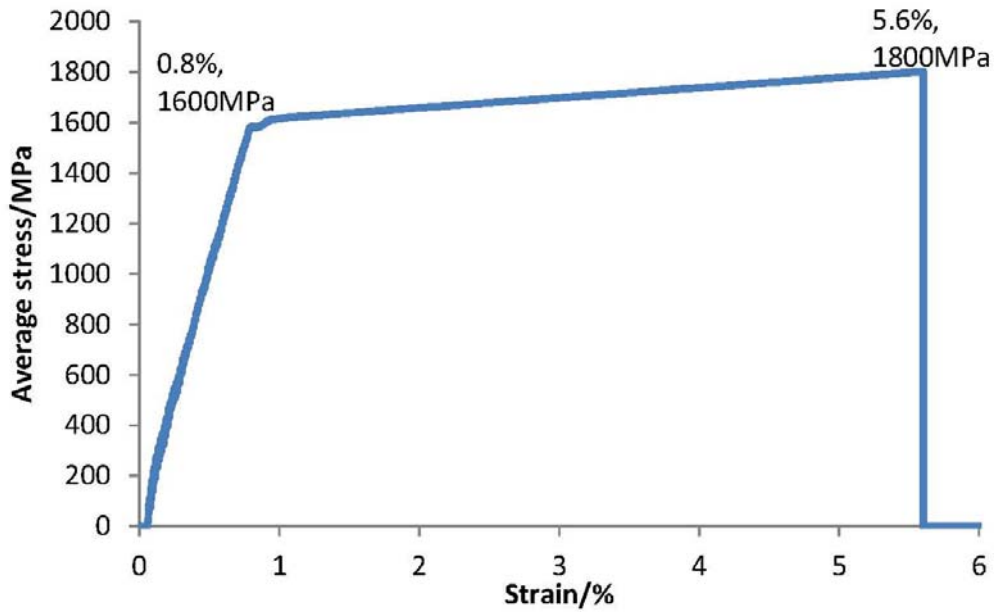
Figure 5: Tension stress vs. strain of a single cable strand

COMPARISON OF CABLE AND REBAR BOLT IN TENSION

The uniaxial tensile tests on a section of cable bolts and rebar bolts were conducted in FLAC3D to compare the reaction of cable and rebar bolt. The cable model was created based on an extensively used hollow cable bolt and its counterpart rebar bolt was generated with the identical dimensions. The dimension details of the cable and rebar bolt are given in Figure 6. Figure 7 shows the generated models of cable and rebar bolt.
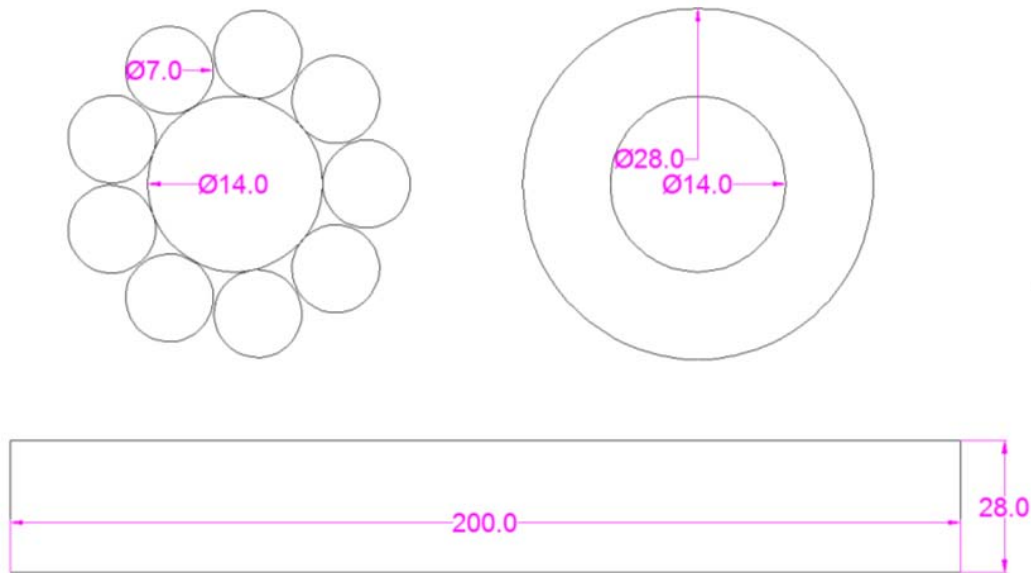
Figure 6: Geometrical dimensions of cable and rebar bolt
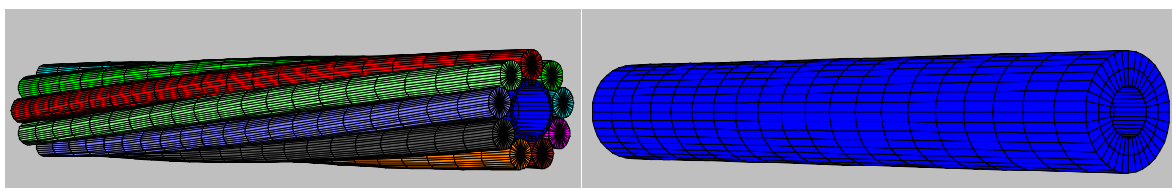
Figure 7: Model of cable and rebar bolt
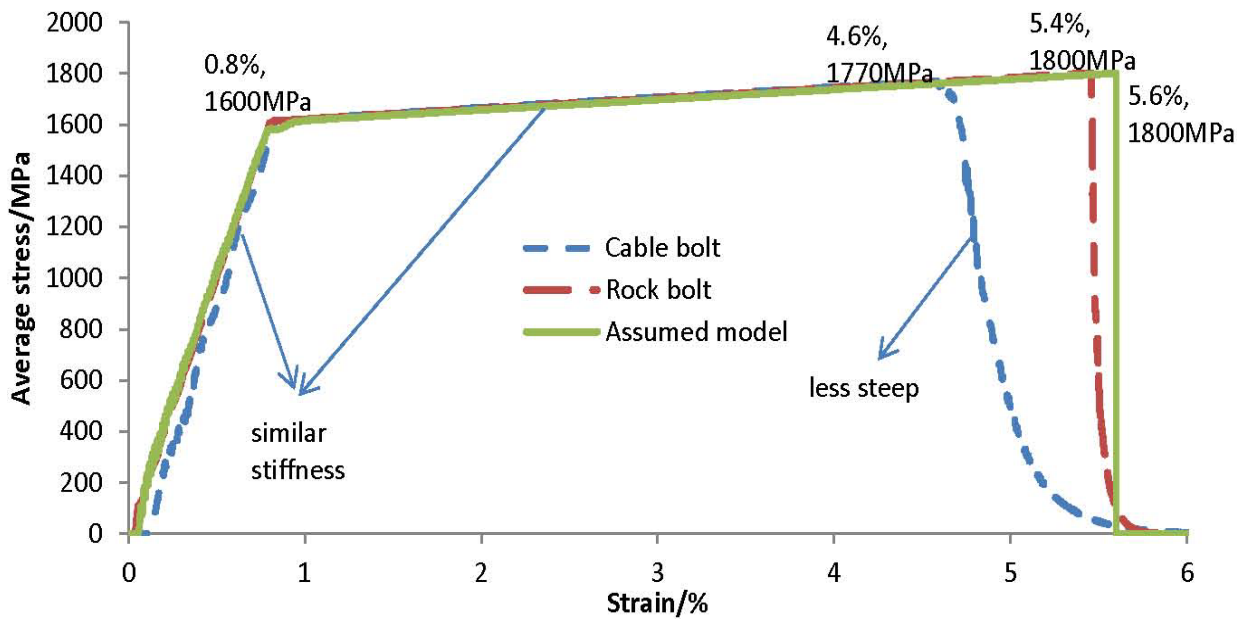
Figure 8: Stress vs. strain relationships of tendons in tension

The cable bolt, rebar bolt and steel strand all behaved with nearly identical stiffness in tension for both elastic and plastic stages. The main difference is located at the failure point. The cable bolt failed at a smaller strain of about 4.6%, the average tension stress peaking at just under 1800 MPa (1770 MPa to be exact), while breaks of the rebar bolt and steel strand occurred at a similar strain which is bigger than that of the cable bolt due to its early failure. The reason of this could be that stress propagation along the cable bolt was less uniform than the rebar bolt and the steel strand, which led to stress concentration in some cable strands and stress decentralization in others and because of this the cable strands ruptured separately rather than simutaniously. The post-peak stages also support this view point since the average stress of cable bolt decreased much slower than the other two.

Comparison of cable and rebar bolt in shear

Numerical double shear tests were carried out on solid cable bolt and rebar bolt to study their performance and to compare with the experimental result. Regarding these two simulations, all used properties and parameters were in reference to the experimental test. What is worth mentioning is the normal stiffness of contact interfaces was assigned a nearly infinite value to prevent interpenetration of the bolt, concrete and grout. Figure 9 shows the assembly of the shear apparatus with cable and rebar bolt, and the shear force variation is given in Figure 10.
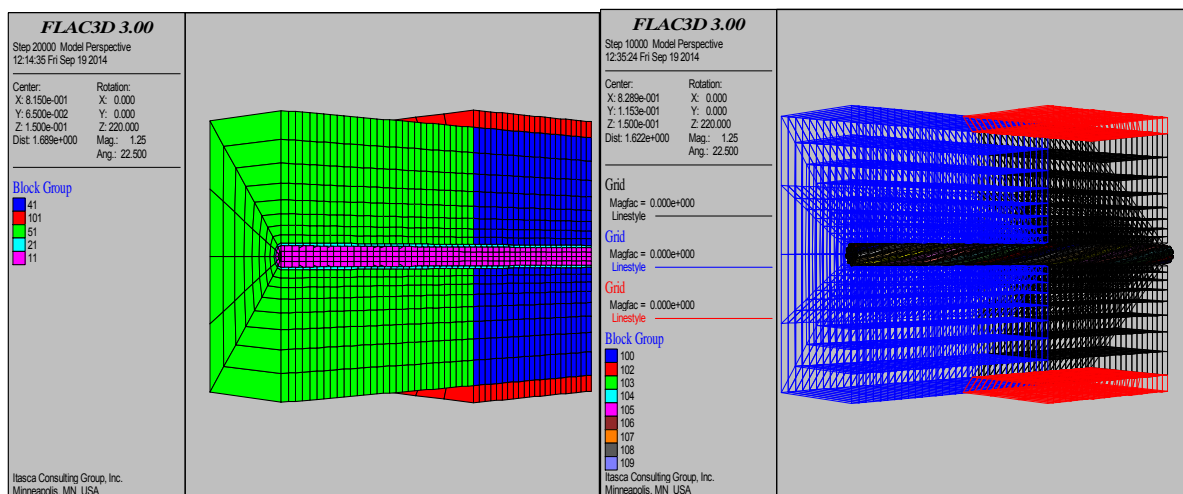
Figure 9: Assembly of shear system
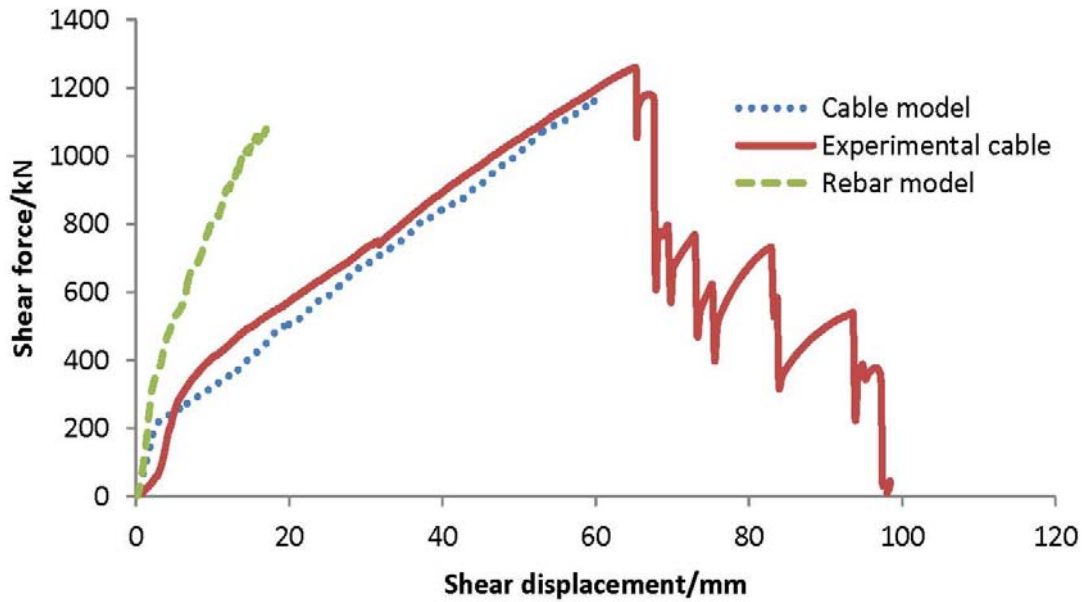
Figure 10: Relationship of shear force vs. shear displacement of solid bolts with 25 t pretension

It is seen that for solid reinforcement elements the rebar and cable bolt behaved in different stiffness for both pre- and post- plastic hinge. The shear stiffness of the entire system with rebar bolt is roughly two times that with cable bolt. Failures of rebar bolt and cable bolt happened at similar strength as the experimental result, at a displacement of less than 20 mm for rebar bolt and about 60 mm for cable bolt. The consistency of the cable model and the experimental test is good in general.

Figure 11 shows the numerical and experimental results of shear systems with hollow cable and rebar bolt. Similar to the solid ones discussed above, the hollow cable bolt had good agreement with the experimental result but was less stiff than the hollow rebar bolt in the shear resistance.
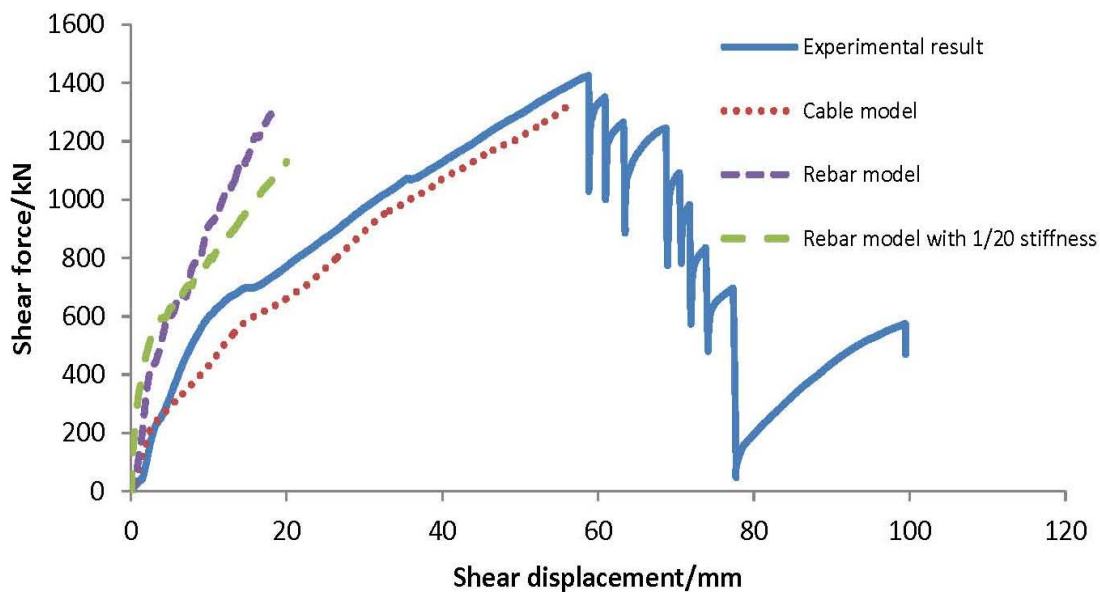
Figure 11: Relationship of shear force vs. shear displacement of grouted hollow bolts with 25 t pretension

So cable and rebar bolt acted differently in reinforcing jointed rock strata, and the former cannot be replaced directly with the latter. The main difference rests on the stiffness, so an assumption can be made that the cable bolt can be matched with the rebar bolt by lowering the stiffness of the latter. Thus, another test was conducted on rebar bolted concrete with one twentieth of the original rebar stiffness, the result of which is also shown in Figure 11. Unfortunately, it seems this method does not help a lot since the shear force – shear displacement curve still deviates from the cable model.

CONCLUSIONS

Numerical tests were conducted on jointed concretes reinforced with cable and rebar bolt, respectively, to study their performance difference. Both tensile and shear tests were done and compared with the experimental test result.

Numerical results show that the rebar bolt with identical geometrical dimensions and mechanical properties displayed similar shear strength to the cable bolt subjected in shear. Thus it is reasonable to use a rebar bolt model for a cable in studying the reinforcement effect. However, the rebar bolt behaved in different stiffness compared to the cable bolt, and the former was twice the latter. So it is reasonable to qualitatively investigate the deformability of the reinforced joint with rebar for cable bolt, but unreasonable to quantitatively do this.

REFERENCE

Grasselli, G. 2005, 3D behaviour of bolted rock joints: experimental and numerical study, *International Journal of Rock Mechanics and Mining Sciences*, 42(1): 13-24.

Orica. 2014, Mechanical property test report, Orica.

Song, H, Duan, Y and Yang, J. 2010, Numerical simulation on bolted rock joint shearing performance. *Mining Science and Technology (China)*, 20(3): 460-465.

Spang, K and Egger, P. 1990. Action of fully-grouted bolts in jointed rock and factors of influence, *Rock Mechanics and Rock Engineering*, 23: 201-229.

Stankus, J. and S. Guo. 1996, Computer automated finite element analysis-a powerful tool for fast mine design and ground control problem diagnosis and solving, *5th Conference on the Use of Computers in the Coal Industry*, West Virginia University, pp 108-115.

Turmo, J, Ramos, G and Aparicio, A. 2006, FEM modelling of unbonded post-tensioned segmental beams with dry joints, *Engineering Structures*, 28(13): 1852-1863.

NEW GENERATION POLYMER TECHNOLOGY AVAILABLE TO BE USED IN PLASTER AND CEMENTITIOUS FIBRE AND NON-FIBRE SPRAY ON AND GROUT SYSTEMS

Allison Golsby

ABSTRACT: Polymer plaster forms part of a group of spray on products that use polymers to supplement or replace cement as a binder in grout systems. The types include but are not limited to polymer plasters, polymer-impregnated concrete, polymer concrete, and polymer-Portland-cement concrete. Polymer plaster and concrete has historically not been widely adopted due to the high costs and difficulty associated with traditional manufacturing techniques. However, recent progress has led to significant reductions in cost, meaning that the use of polymer plaster and concrete is gradually becoming more widespread.This paper will focus on addressing aspects of the use of polymers.

INTRODUCTION

Engineered Cementitious Compounds (ECCs), unlike common fibre reinforced concrete, is a family of micromechanically designed material. As long as a cementitious material is designed/developed based on micromechanics and fracture mechanics theory to feature large tensile ductility, it can be called an ECC. Therefore, ECC is not a fixed material design, but a broad range of products under different stages of research, development, and implementations. The ECC material family is expanding. The development of an individual mix design of ECC requires special efforts by systematically engineering of the material at nano-, micro-, macro- and composite scales.

Some polymers can be added plasters or concretes and used to supplement or replace an original binder. The types include polymer-impregnated concrete, polymer concrete, and polymer-Portland-cement concrete, as well as applications using gypsum and other cementitious products. In these ECCs, thermosetting resins are used as the principal polymer component due to their high thermal stability and resistance to a wide variety of chemicals. ECCs can also be composed of aggregates may include silica, quartz, gypsum, granite, limestone, and other high quality material. The aggregate must be of good quality, free of dust and other debris, and dry. Failure to fulfil these criteria can reduce the bond strength between the polymer binder and the aggregate.

ECC may be used for new construction or repairing old concrete. The adhesive properties of ECCs allow patching of both polymer and conventional cement-based and non-cement based compounds. The low permeability and corrosive resistance of ECCs allows it to be used in civil, road and mining applications, such as sewer structure applications, drainage channels, electrolytic cells for base metal recovery, geomechanics, Ventilation Control Devices (VCDs) and other structures that contain liquids, toxic or corrosive chemicals. It is especially suited to the construction and rehabilitation of manholes due to its ability to withstand toxic and corrosive sewer gases and bacteria commonly found in sewer systems. ECC does not require coating or welding of PVC-protected seams.

ECC has historically not been widely adopted due to the higher costs and difficulty associated with traditional manufacturing techniques. However, recent developments in polymer production and ECC assembly has led to significant reductions in cost, meaning that the use of polymer concrete is gradually becoming more widespread.

RELATIONSHIP TO THE MINING INDUSTRY

Portland cement and gypsum based products are currently the most widely used construction materials in underground mining. The historical characteristics of Portland cement include:

- Low cost,
- high stiffness,
- high compressive strength,
- non-flammability,

CEO, ConsultMine, PO Box 358, Brisbane 4001, E-mail: allison@golsby.org

- ease of fabrication,
- whilst low tensile strength,
- brittleness, and
- long -term durability.

Reinforcing cement with steel provides increased tensile strength and the incorporation of fibres increases its toughness (resistance to crack propagation). Polymers increase ECC tensile and flexural strength and reduces its brittle nature by increasing toughness. In this paper field of ECC will be reviewed.

Geopolymer cements are inorganic hydraulic cements and are based on the polymerization of minerals (Davidovits, Davidovits, and James 1999). The term more specifically refers to alkali-activated alumino-silicate cements, also called zeolitic or polysialate cements. They are used in construction, with high-early strength applications, and waste stabilisation. These cements do not contain organic polymers or plastics.

BRIEF HISTORY

The ancient history of using natural polymers, like asphalt to modify mortars, goes back to the Babylonians, Egyptians and ancient India.

The concrete history timeline according to Auburn 2000 and Brown 1996:

- 9000 BC – Cement floor discovered in Israel in 1985
- 3000 BC-Egyptian Pyramids. The Egyptians were using concrete over 5000 years ago to build pyramids.
- 300 BC - 476 AD-Roman Architecture. The ancient Romans used a material that is remarkably close to modern cement to build many of their architectural marvels, such as the Colosseum, and the Pantheon. The Romans also used animal products in their cement as an early form of admixtures.
- 1824-Portland Cement Invented.
- 1836-Cement Testing. The first test of tensile and compressive strength took place in Germany.
- 1889- The first concrete reinforced bridge was built.. Alvord Lake Bridge is over two hundred years old.
- 1903-The first concrete high rise was built.
- 1908-Thomas Edison designed and built the first concrete homes.
- 1913-The first load of ready mix was delivered.
- 1915-Coloured Concrete. L.M. Scofield, products included colour hardeners, colourwax integral colour, sealers, and chemical stains.
- 1930-Air Entraining Agents. Air entraining agents were used for the first time in cement to resist against damage from freezing and thawing.
- 1938-Concrete Overlay. Latex was added to Portland cement, aggregate, and other materials to make a covering for ship decks.
- 1950's-Decorative Concrete Developed. The Bomanite process was developed, the original cast-in-place, coloured, textured and imprinted architectural concrete paving.
- 1970's-Fiber Reinforcement
- 1980's-Concrete Countertops
- 1990-Concrete Engraving
- 1992-Tallest Concrete Building
- 1999-Polished Concrete

Europeans in the Middle Ages, used ox blood and egg white to increase the durability of lime mortars. The modern history of man-made modifiers starts in the late forties, with the development of butadiene styrene, polychloroprene and acrylic latex in modified mortars and concrete. The main application of latex polymer modified cements at that time was for concrete repair. The use of polymers in the fabrication of bridges and parking garage overlays was developed in the early seventies.

The prime function of the polymer was to reduce concrete permeability and increase resistance to chloride penetration, toughness and adhesion. Dry polymer modifiers, so called redispersable powders, based on Ethyl-Vinyl Acetate (EVA), polyvinyl acetate-vinyl arboxylate, (VA/VeovVa), acrylics, styrene-acrylics and others were introduced in the early eighties. Dry polymer modifiers allow the formulation of one-component systems.

Initially dry polymer modifiers were inferior in many aspects to early polymers.

DESCRIPTION OF POLYMERS

A polymer is a high molecular weight molecule, usually a linear chain of many repeat units. All plastics fall under the category of polymers, but also natural products such as cellulose, proteins, DNA etc. The repeat units are called monomers, and these are polymerised in a wide variety of processes. The polymers we are referring to in this paper are dispersions and their spray-dried, dispersible versions. Dispersible polymers are produced in a process called emulsion polymerisation – the monomers are emulsified and reacted in water, and the end result is a dispersion of small particles (typically 100 nm to several microns in diameter, containing up to 10,000 polymer chains) in water, stabilised by surfactants or colloids such as polyvinyl alcohol.

In this application, the water evaporates, the particles come closer to each other and fuse (film formation) and can bind other ingredients (such as sand or limestone) together in the process. Depending on the nature of the monomers and their other properties, the dispersions can be used in a wide variety of applications, such as water-based paints, adhesives, carpet backing, paper and cardboard coatings, and in construction products. The last application area – construction – is the area from which the use of such polymers in mining, has been derived.
The polymer dispersions are used as admixtures to cement mortars in two-component products.

Initial findings, using this combination, were obtained as far back as the twenties and early thirties. A milestone in the mortar modification was reached with the invention of dispersible polymer powders, by the Munich-based company Wacker Chemie AG. Their first polymer powder was launched in 1957 under the trade name VINNAPAS®.

Polymer powders are spray-dried dispersions. The production of these powders is not simple: dispersions which will form continuous and, in some cases, tacky films at room temperature. They have to be converted into free-flowing and storage stable, water-free powders. Before the spray-drying process is run, a water soluble protective colloid (for example polyvinyl alcohol) is added, which surrounds the dried emulsion particles to keep them separate and to protect them against premature coalescence. Once the applicator (or pump) adds water to the mortar on site, the polymer disperses and the mortar is practically indistinguishable from a mortar modified with dispersion.

Since the seventies, there has been an increasing trend towards the substitution of mortar additives in dispersion form, with polymer powders. This allowed the producers of a construction mortar to add the polymer to the cement or plaster mixes in their pre-blended, bagged form, whereas the liquid dispersion needed to be added on site. This process has the advantage that the amount of polymer could be controlled, and that the logistics of bringing product to a site became a lot easier, especially underground applications.

Since then the use of these dry versions in construction mortars has been growing steadily. The modification of cement based mortars with thermoplastic film forming polymers for a variety of applications is very common today in the Australian construction industry.

Examples for these applications are thin-bed tile adhesive mortars and tile grouts, self-levelling flooring compounds, renders, cement paints, concrete repair mortars, injection grouts, and even concrete itself.

CURRENT USE IN PLASTER AND CEMENT-BASED PRODUCTS

The addition of polymer powders to mineral binders, both cement and gypsum, hydrated lime or high alumina cement, improves a range of properties of hardened and fresh mortar. They include:

- increased open time for adhesives,
- better cohesion for sprayed products,

- better rheology once placed on the target surface (either more flowing, or the opposite to keep the product in place),
- improved adhesion to critical substrates,
- increased flexibility and deformability,
- crack-free curing,
- increased abrasion resistance,
- water-proofing,
- In some cases a higher compressive strength,
- better freeze/thaw resistance where it is relevant.

HOW POLYMER POWDERS WORK

At low polymer dosage, the polymers help bind together the other constituents of the ECC, mostly the fillers, just as the cement does in concrete. The polymers are often found in discernible local domains as well as in enhanced concentrations at the surface of a mortar, or between the mortar and the substrate the mortar was applied to, increasing the adhesion, especially if the substrate is not porous but smooth and dense.

Electron micrographs are used to investigate the structure of a mortar containing polymer powders in their cement matrix. In Figure 1, the dried polymer can be clearly seen. The polymer powder works as a second binder in the cementitious system. The polymer is concentrated in the voids where the water was during the drying process. As the water evaporates or is used to hydrate the cement, the polymer particles form a film – a polymer domain (compare arrows). The tensile adhesive strength of such a resin domain is higher than the tensile adhesive strength of a cementitious mortar. Therefore the domains act like a reinforcing material to enhance the adhesion between the mortar and the dense tiles, as shown in Figure 1.
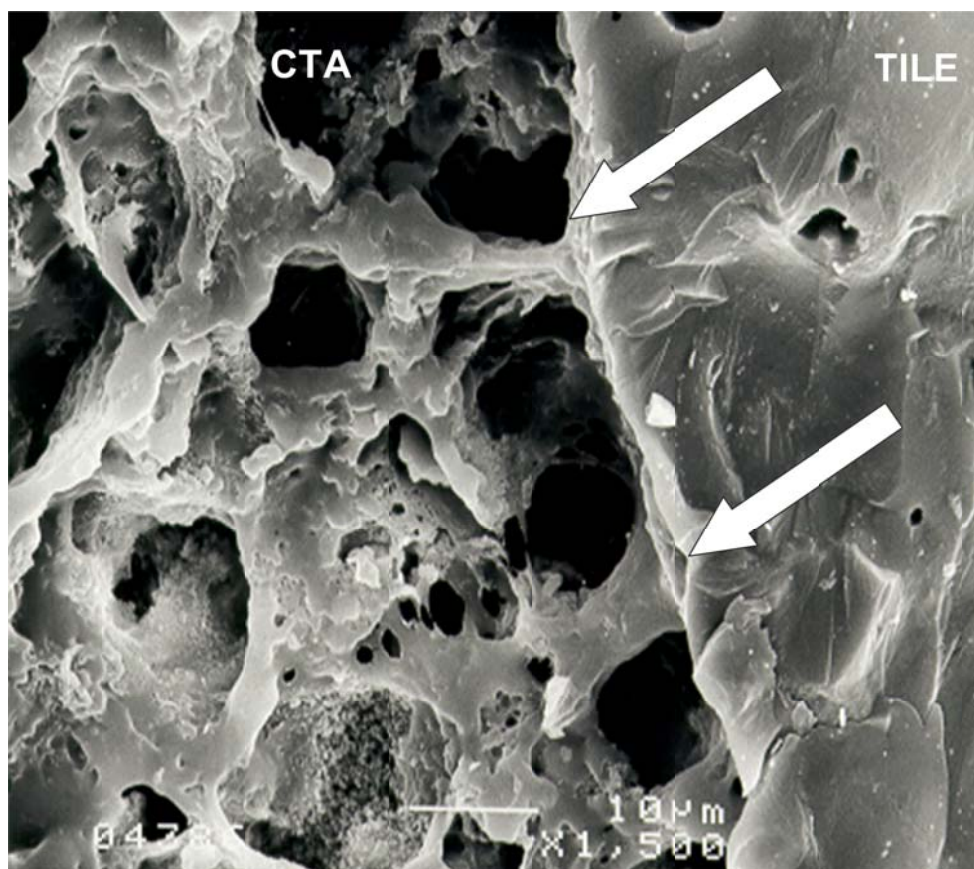
Figure 1: ceramic tile adhesive (CTA), modified with VINNAPAS® polymer powder, on porcelain tile x1500 (Wacker Chemie AG)

At a higher dosage the volume of polymer starts to dominate the cement, and at very high dosages, such as used in water-proofing membranes, the polymers form the matrix, and the cement can be considered as the reinforcement.

Graphic examples of the properties conferred by the polymers can be seen in Figures 2 and 3.

Figure 2 shows the deformation in a three-point bending test of a cementitious mortar where the level of polymer modification was varied between 0% and 15%. The Figure shows the substantial increase in deformation the mortar can sustain before breaking. This mortar is used to make flexible cementitious tile adhesives and mining grouts.

Figure 3 shows examples of cement-polymer mixtures at the same polymer: cement ratio, where the inherent flexibility of the polymer was changed. This illustrates the ability to control the properties of the mortar by controlling the type of polymer used. There are many polymers available.

Figure 4 is a photograph of the dry-spray shotcrete application modified by these types of polymers in a mine. The modification resulted in a marked improvement of the water-proofing properties of the shotcrete, even though the percentage of polymer was not high enough to create continuous film of polymer in the concrete. Instead the polymer domains allowed the shotcrete to cure crack-free to the extent that the shotcrete itself was water-proof.
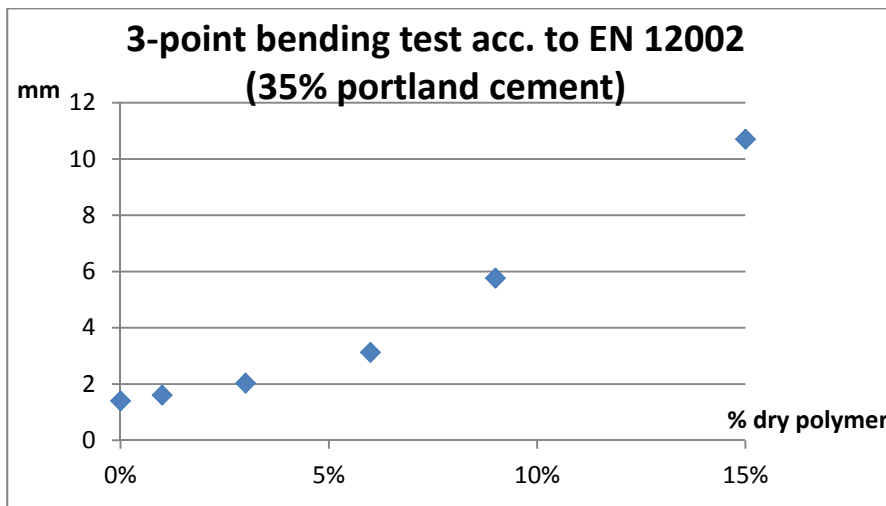
Figure 2: 3 point bending test acc. to EN 12002 (35% Portland cement) (Wacker Chemie AG)
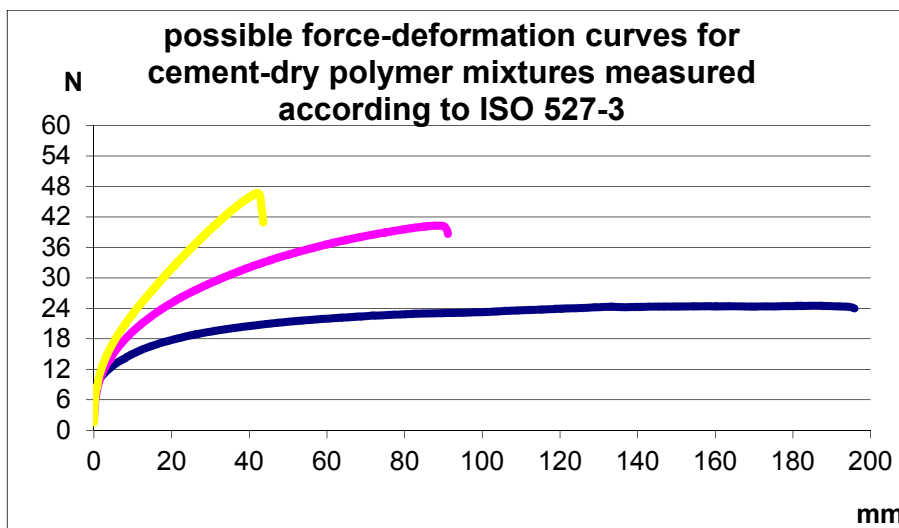
Figure 3: possible force-deformation curves for cement-dry polymer mixtures measured according to ISO 527-3 (Wacker Chemie AG)

Figure 4: ECC application (Wacker Chemie AG)

CASE STUDY

Despite concrete in general not being a widely used product in underground coal compared to hard rock – much less specialised fibre concrete, there have been uses dating back many years.

Fibre in concrete can be divided into two sections:

- Macro fibre – any type of fibre that is generally in excess of 30mm in length. The first Macro fibre was made of steel, which is still used in civil applications however; "plastic macro fibre" is the preferred additive in just about 100% of hardrock shotcreting in Australia. The use of course concrete and macro fibre in underground coal mines has been very limited. The limiting factors include: the size of pumping equipment, logistics to site and the poor adhesion relationship between coal and general concrete).
- Micro fibre – again "plastic" fibre dominates this market with the fibre length ranging from 6mm to about 15mm. This type of fibre is compatible with the dry gunite pumping systems which are the primary source of concrete and plaster spraying in U/G coal. The additional benefit of micro fibre is that it is relatively easy to integrate it into pre bagged dry mix products.

In the 1990's Thin Skin Liners (TSL's) was an experimental product that many manufactures focused on. Micro fibres were an integral part of these TSL's. They all lacked structural integrity. The TSLs were simple surface and crack sealers. The TSL market has diminished greatly with several products morphing into very thin crack sealers, without fibre to improve crack penetration.

More recently high strength ductile cement based products have made their way in to the market using micro fibres – the term Thin Structural Liners has been adopted for these products. These TSL's are highly refined engineered pre bagged products. The TSLs are designed so the cement based matrix works in unison with the characteristics of the micro fibres. This allows for a unique "strain hardening" cracking system to occur. Basically, the matrix is designed to micro crack thus transferring the load to the fibres. As the fibres increase the load bearing ability the matrix continues to micro crack over the entire loaded area thus bringing into play many more fibres. This strain hardening effect permits the matrix to have a high compressive strength (40MPa +) and exhibit high flexural ductility of around 10% plus high tensile strength of 5% plus.

Testing undertaken of the product (PMG 64) used in this case study and the products that are currently on the market are compared in Table 1 below. These tests were conducted at 14 days after application.

From the data in Table 1, PMG 64 has higher flexial strength and crack bridging properties than standard grout.

Table 1: Comparison of case study ECC (PMG 64) to current products (After Moore 2014)

Property	PMG 64	Standard Grout	Phoenelic Resin	PUR
UCS (Mpa)	32	45		
Tensile on Sandstone (MPa)	0.75	0.3	0.74	1.46
Crack Bridging (mm) at 1MPa	1.8	0.4		
Flexial Strength (Mpa)	11	1.2		

An example of the use of such a product was the rib consolidation on the non-walk side of an aging belt road which was starting to spall badly. The entire consolidation was completed from off the stationary belt over a ten day maintenance period. The success of this project has led into the assessment of using such products and techniques as an alternative to secondary support in general as the product costs are similar, the speed of application is much faster with both sides of a 100m pillar roadway being able to be sprayed from a single setup by three men plus a loader in a single shift. Currently, such products are being tested to gauge their effectiveness for pillar confinement and have demonstrated to be tougher in vehicle impact situations which have the potential of extending travel road maintenance periods extensively. The main benefits discovered from this application was that by using the penetration and gluing strengths of these products, that very little needed to be used to give structural strength (around 15 mm over competent coal). The ability to "glue" back into the rib large spalling blocks and put them back to work as support members was a distinct benefit.
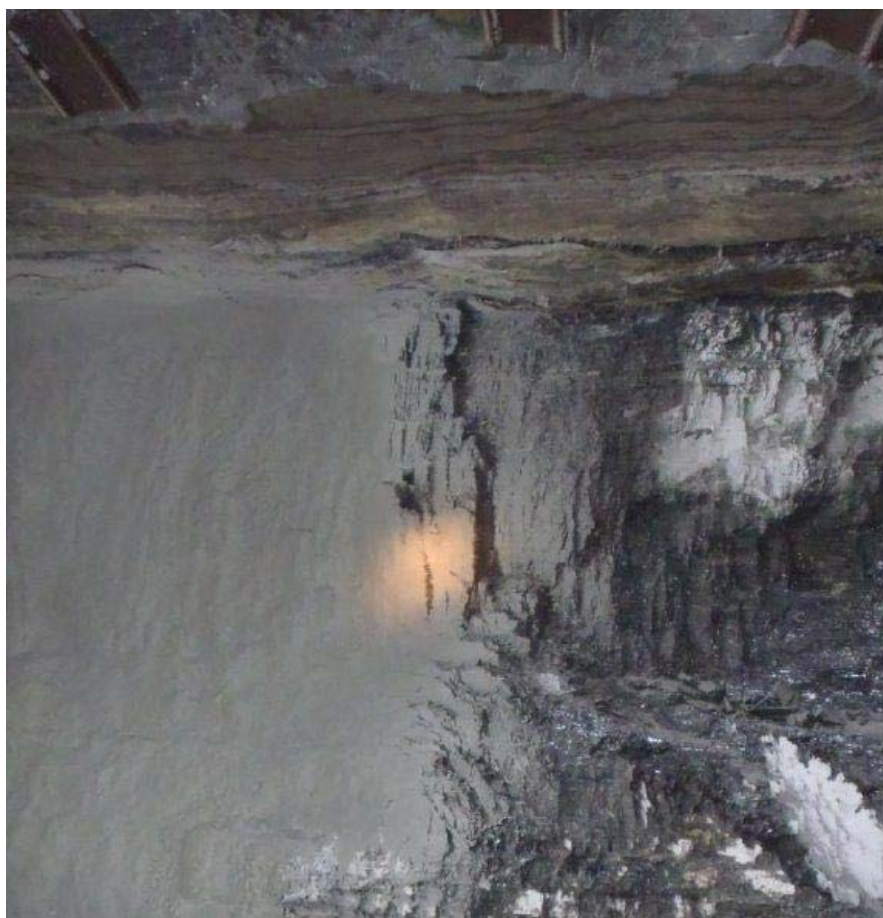
Figure 5: Applied Thin Skin Liner in an underground coal mine (Moore 2014)

Another successful program was the selection of one of these products to replace all the stoppings in a New South Wales underground coal mine. The priorities for this job were – minimal construction time, minimal thickness for the required rating, a high safety factor and the ability to resist convergence. This program is ongoing today with over 100 new stoppings having been built alongside the existing old non rated block stoppings.

One application example of the product was sprayed in this case study at between 2mm to 5mm, covering 1000m2 in 5.5 hours using 350 20kg bags of the product as shown in Figure 5 below. Less of the product is needed to be applied to achieve a similar outcome to standard grout. So, for the same surface area, less product is required and the total product cost is much lower. The site requires no special machinery, skilled staff to apply the product and less challenging OHS issues for a similar result to Phoenelic Resin and PUR (Polyurethane resin). Phoenelic Resin and PUR are commonly used in underground coal mines.

CONCERNS ABOUT POLYMERS

The success of the above program along with the modernising of the dry gunite systems to make them virtually dustless (which is essential for compliance) and the dust reducing additives now available have made the option of using both fibre reinforced cement and plaster based systems more than viable. Figure 6 shows physical comparisons between ECCs and other composite materials.

Properties	FRC	Common HPFRCC	ECC
Design Methodology	N.A.	Use high Vf	Micromechanics based, minimize Vf for cost and processility
Fiber	Any type, Vf usually less than 2%; df for steel ~ 500 micrometre	Mostly steel, Vf usually > 5%; df ~ 150 micrometre	Tailored, polymer fibers, Vf usually less than 2%; df < 50 micrometre
Matrix	Coarse aggregates	Fine aggregates	Controlled for matrix toughness, flaw size; fine sand
Interface	Not controlled	Not controlled	Chemical and frictional bonds controlled for bridging properties
Mechanical Properties	Strain-softening:	Strain-hardening:	Strain-hardening:
Tensile strain	0.1%	<1.5%	>3% (typical); 8% max
Crack width	Unlimited	Typically several hundred micrometres, unlimited beyond 1.5% strain	Typically < 100 micrometres during strain-hardening[1]

Note: FRC=Fiber-Reinforced Cement. HPFRCC=High-Performance Fiber Reinforced Cementitious Composites

Figure 6: Comparison between ECC and other composite materials (wikipedia)

CONCLUSIONS

ECCs historically have not been widely adopted because of higher costs and difficulty associated with traditional manufacturing techniques. However, recent developments have led to significant reductions in cost, meaning that the use of polymer concrete is gradually becoming more widespread.

Advantages of polymer concrete include:

- Rapid curing at ambient temperatures
- High tensile, flexural, and compressive strengths
- Good adhesion to most surfaces
- Good long-term durability with respect to freeze and thaw cycles
- Low permeability to water and aggressive solutions
- Good chemical resistance
- Good resistance against corrosion
- Lighter weight (only somewhat less dense than traditional concrete, depending on the resin content of the mix)
- May be vibrated to fill voids in forms
- Allows use of regular form-release agents (in some applications)
- Dielectric
- Less product required compared to similar applications with standard grouts

Disadvantages of polymer concrete include:

- Product hard to manipulate with conventional tools such as drills and presses due to its strength and density. Getting pre-modified product from the manufacturer is recommended

ACKNOWLEDGEMENT

The author wishes to acknowledge the generosity in time and knowledge of the following technical personnel:

- Dr Harold Schoonbrood
    Director Construction Polymers Australia/New Zealand
    Wacker Chemicals Australia
    affiliated with:
    o   ACS (American Chemical Society)
    o   SCAA (Surface Coatings Association Australia)
- Maxwell Moore
- Technical Manager
    OPC Specialties

REFERENCES

Auburn. 2000, Historical Timeline of Concrete, AU BSC 314, *Auburn University*, http://www.auburn.edu/academic/ architecture/bsc/classes/bsc314/timeline/timeline.htm, June 2000.

Brown, G E. 1996, Analysis and history of cement, Gordon E. Brown Associates, Keswick, Ontario, 1996, 259 p.

Davidovits, J, Davidovits, R and James, C. 1999, editors, Geopolymer '99, The Geopolymer Institute, Wikipedia.org. "Comparison between ECC and other composite materials http://en.wikipedia.org/wiki/Engineered_cementitious_composite . Retrieved 11 November 2014, from http://en.wikipedia.org/wiki/Engineered_cementitious_composite.

Wikipedia.org. "Comparison between ECC and other composite materials'', Retrieved 11 November 2014, from http://en.wikipedia.org/wiki/Engineered_cementitious_composite.

Wacker Chemie AG, electron microscope (ceramic tile adhesive (CTA), modified with VINNAPAS® polymer powder, on porcelain tile x1500 photo.

Wacker Chemie AG, possible force-deformation curves for cement-dry polymer mixtures measured according to ISO 527-3 photo.

Wacker Chemie AG, ECC application photo.

Moore M, Applied Thin Skin Liner in an underground coal mine 2014 photo.

INVESTIGATION ON ADHESION STRENGTH OF THIN SPRAY-ON LINERS IN AN UNDERGROUND COAL MINE

Zecheng Li, Serkan Saydam, Rudrajit Mitra and Duncan Chalmers

ABSTRACT: A Thin Spray-on Liner (TSL) is defined as a chemically based layer or coating (3-5 mm) that is sprayed onto the rock surface to support mining excavations (Saydam and Docrat, 2007). Since the introduction, TSLs have received success in some applications in hard rock mines; however, their use has been slow in coal mining. The adhesion strength between a TSL and a rock surface is an important parameter controlling the design and performance of liner support systems. The i*n situ* adhesion tests have been conducted to study the bonding between a TSL material and the coal substrate in an underground coal mine in NSW. A direct pull-off adhesion tester was adopted to conduct adhesion tests on the ribs of the roadway. In this paper, the *in situ* adhesion test results on coal substrate are analysed and presented.

INTRODUCTION

A Thin Spray-on Liner (TSL) is defined as a thin chemically based coating or layer that is applied onto mining excavations with a thickness of 3 to 5 mm (Saydam and Docrat, 2007). The adhesion strength between a liner and rock is one of the most important parameters in terms of support resisting capacity (Li *et al*., 2014). When liners are used for area support, there is an intimate contact between the liner and rock surface. Where adequate adhesion bonds exists, TSLs can carry or transfer the load created by gravity falls or loose rock onto stable or unfractured rock surface (Archibald, 2001).

The adhesion strength of a TSL can be defined as its ability to adhere to a particular surface (Swan and Henderson, 2001). Over the years, many adhesion test procedures have been proposed by researchers to assess the adhesion strength of TSLs. These adhesion test procedures can be divided into core adhesion test, embedded dolly test and glued dolly test. The glued dolly test method is the most widely used procedure by researchers due to its ease of application and accuracy of results (Mercer, 1992; Espley-Boudreau, 1999; Tannant *et al.,* 1999; Archibald, 2001; Spearing, 2001; Kuijpers *et al.,* 2004; Saydam and Docrat, 2007; Li *et al.,* 2014).

Kuijpers (2004) reported that two types of bond strength have to be considered: tensile and shear, as shown in Figure 1. Tensile bond strength is a measure of the ability of TSL to remain in contact with the rock when a tensile stress is applied normal to the rock-TSL interface. Shear bond strength is concerned with the ability to resist stresses that act parallel to the rock-TSL interface. In practice, there is usually some combination of these stresses acting on the interface (Saydam and Docrat, 2007).

(a) Tension　　　　　　　　　**(b) Shear**
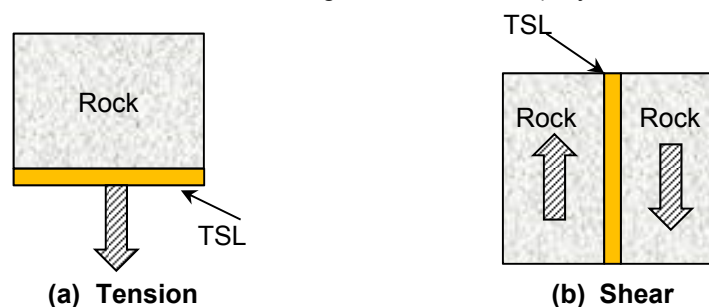
Figure 1: De-bonding mechanisms of TSLs (modified from Kuijpers *et al.,* 2004)

The use of TSL as a gas management tool in underground coal mines is currently being investigated by the School of Mining Engineering, UNSW Australia at an underground coal mine in NSW, Australia. A polymer based TSL was applied to the ribs of the coal mine. As part of the investigation, *in situ* adhesion tests were conducted to study the bonding between TSL and coal substrate. The test method adopted

School of Mining Engineering, UNSW Australia, Sydney, NSW 2052, Australia, E-mail: zecheng.li@student.unsw.edu.au, Tel: 02 9385 6118

was a direct pull adhesion test which was adapted from ASTM D4541 standard. Due to the agreements with the mine and the TSL manufacturer, the mine name and the product name will not be disclosed in this paper.

In this paper, the in-situ adhesion test results on coal substrate are analysed and presented.

TEST PREPARATION AND EXECUTION

Test area description

A polymer based TSL was sprayed onto the ribs of the roadway. Figure 2 shows the adhesion test area before and after the TSL application. Due to the excavation disturbance and the stress concentration, the coal in the top part is more fractured, while the coal in the bottom part is relatively intact. Adhesion strength tests were conducted on both these regions to evaluate the influence of substrate integrity on the adhesion strength results.
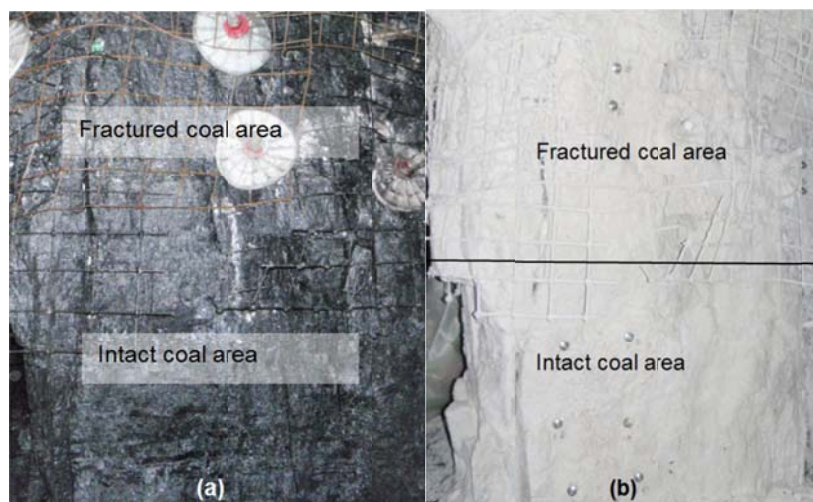
Figure 2: *In situ* adhesion test area (a) before TSL application, (b) after TSL application

Test apparatus and procedure

The PAT GM01-Elcometer testing apparatus was used in this test. The test apparatus works on a distributed force pull off system, which can apply a maximum force of 6.3 kN. The steel test dollies are 28.2 mm in diameter which is the standard size supplied with the equipment. The range of the test pressure is 0-10 MPa for the size of the dollies used.

The test dollies were glued to the surface with araldite epoxy. The test area was over-cored by using a coring bit to make sure the pull force will only be applied on the test dolly area. Then a pull force was applied normal to the coal surface until de-bonding occurred. The liner was allowed to cure for 1 day, 7days, 14 days, 21 days and 42 days before testing. At least 5 tests were conducted for each condition. Figure 3 shows an in-situ test execution on the rib of the roadway.

Figure 3: *In situ* adhesion strength test (a) overcoring, (b) dolly under test

TEST RESULTS AND ANALYSIS

Adhesion strength test results

In total, 58 adhesion strength tests were conducted at the mine on both intact and fractured coal areas. Table 1 provides the average adhesion test results and image processing results with different curing times of 1 day, 7 days, 14 days, 21 days and 42 days.

Table 1: Adhesion strength test results

Test area	Curing time days	Adhesion strength MPa	Standard deviation MPa	Percentage of coal on failure surface %	Standard deviation %
Intact coal area	1	0.23	0.03	47.41	18.26
	7	0.59	0.05	75.63	12.19
	14	0.91	0.23	81.00	7.17
	21	0.91	0.13	84.32	4.18
	42	0.95	0.17	87.61	1.97
Fractured coal area	1	0.12	0.03	43.20	20.03
	7	0.53	0.10	84.33	7.47
	14	0.52	0.21	83.38	8.72
	21	0.57	0.26	85.18	4.03
	42	0.58	0.25	84.86	4.55

Effect of curing time

As curing time increases, the adhesion strength increases and then stops for both intact coal and fractured coal, as shown in Figure 4. For intact coal, the adhesion strength increases from 0.23 MPa to 0.59 MPa from 1 day to 7 days, and then reaches the final value at 14 days. After 14 days, the adhesion strength is almost the same. While for fractured coal, the adhesion strength reaches the final value at 7 days, and there is no significant change to the adhesion strength after 7 days.

For each curing time, the adhesion strength for intact coal is much higher than that on fractured coal, with final adhesion strength of about 0.9 MPa, and 0.55 MPa for intact coal and fractured coal respectively, as shown in Figure 4. The results revealed that the integrity of the substrate has a great influence on the adhesion strength.

It is also interesting to compare the standard deviation of adhesion strength for both intact coal and fractured coal. As shown in Figure 5, the standard deviation for fractured coal is much higher than that for intact coal. For 21 days testing, the standard deviation of adhesion strength result on fractured coal almost doubled compared that on intact coal. It can be concluded that the adhesion strength results on fractured coal varies considerably compared to those on intact coal. This may be due to variability of the friability of the coal at each dolly site.
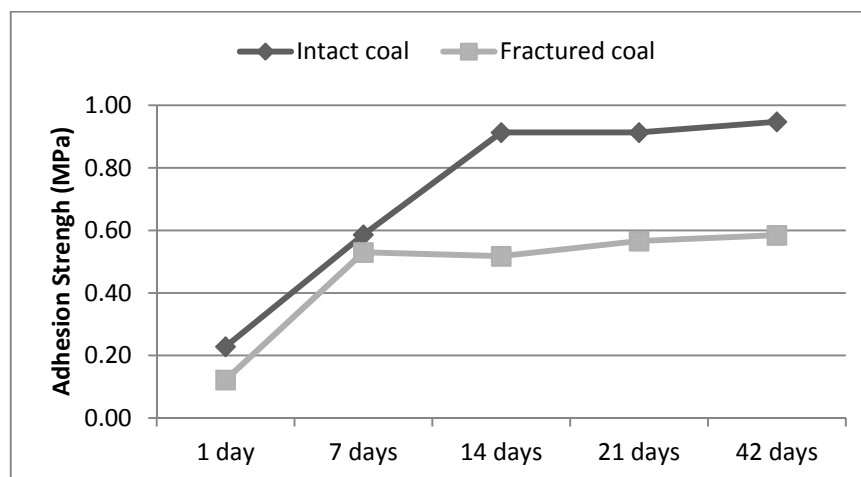
Figure 4: Adhesion strength with different curing time
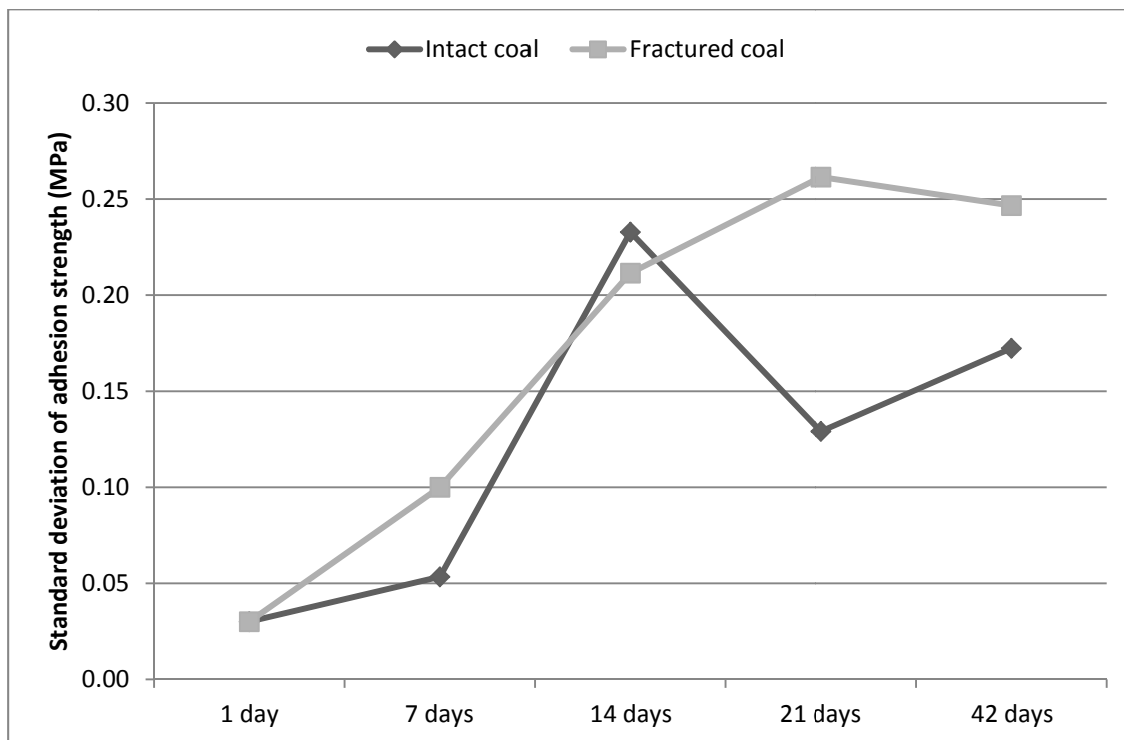
Figure 5: Standard deviation of adhesion strength with different curing time

Failure mode analysis

Failure of the adhesion test can occur in several ways. These include failure between the liner and the host rock (which is coal in this case), internal failure of the host rock, de-bonding of the adhesive material between either the liner or the steel dollies (Saydam and Docrat, 2007; Gilbert *et al.,* 2010). A new methodology was adopted for analysing the failure mode of the adhesion test. This involved using an image processing software to calculate the percentage of coal and liner on the failure surface. This procedure is outlined in Figure 6. Figure 6 (a) is the original photo of the failure mode and the chosen area for analysing is shown in Figure (b). Then the chosen area is converted into an 8-bit image which only contains black and white colour. As shown in Figure 6 (c), the black area represent the coal and the the white area represent the liner. The proporation of coal and liner on the failure surface can be obtained by calculating the percentage of black and white area.

Figure 6: Image software processing

Image processing results reveal that the failure mode for both intact coal and fractured coal is mainly attributed to the internal failure of the coal substrate besides 1 day testing. As shown in Figure 7, for 1 day testing, the failure mode is a combination of internal failure of the coal substrate and the liner, with a percentage of coal on the failure surface about 47.41% and 43.20% for intact coal and fractured coal respectively. This is due to the fact that the TSL material is still very weak after 1 day curing, and the material fails eapsily in tension. While for testing after 7 days of curing, the TSL material has developed a relatively strong tensile strength compared with the adhesion strength between coal substrate and the liner. The percentage of coal on the failure surface almost   exceeds 80%, which indicates an internal failure of the coal substrate, as shown in Figure 7. Typical view of failure surface with different curing time is shown in Figure 8.
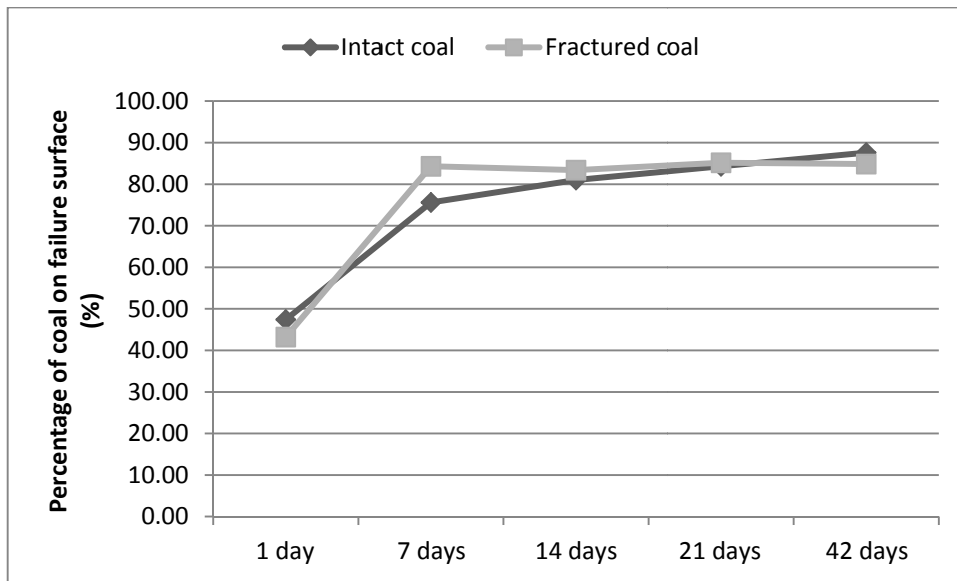
Figure 7: Percentage of coal on failure surface with different curing time

Figure 8: Typical view of failure surface with different curing time

Unlike the standard deviation for adhesion strength results, as the curing time increases, the standard deviation of percentage of coal on the failure surface tends to decrease and then reaches a steady value, as shwon in Figure 9.
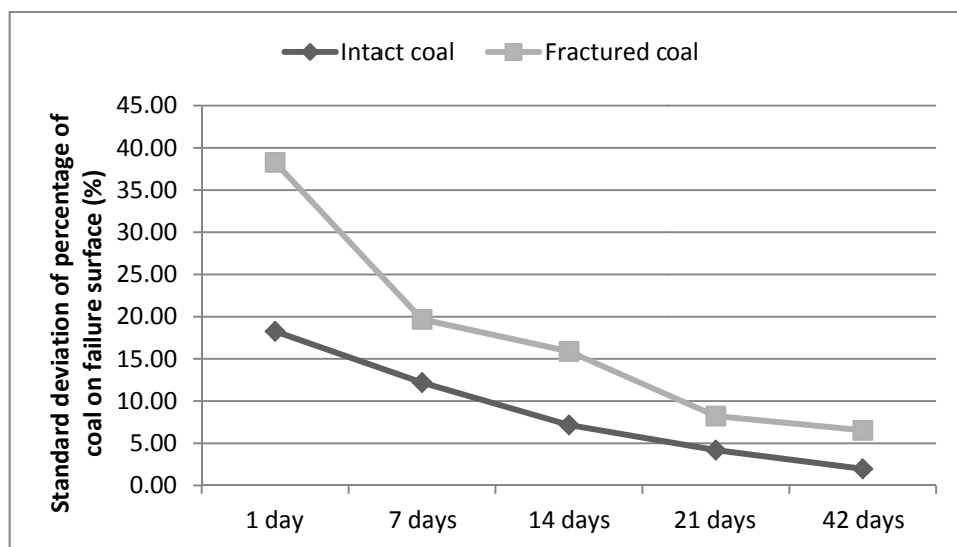
Figure 9: Standard deviation of percentage of coal on failure surface

DISCUSSION

The adhesion test is designed to determine the bond strength existing between a liner material and the substrate. The test results revealed that the TSL material chosen can bond firmly to the coal substrate *in situ*. However, the tests were only conducted with a maximum curing time of 42 days, and TSL's long-term performance should be investigated in the near future.

Previous laboratory research revealed that the coal bedding plane directions have a significant influence on the adhesion strength. Previous laboratory tests also indicated that the adhesion strength parallel to the bedding planes was much higher than that normal to bedding planes (Gilbert *et al.,* 2010; Li *et al.,* 2014). However, for the in-situ applications, the adhesion strength tests were only able to be conducted on the ribs of the roadway, so all the tests conducted were parallel to bedding planes. For adhesion strength normal to bedding planes, laboratory adhesion tests should be conducted as a replacement of the in-situ tests.

The adhesion strength tests are part of the project that investigates the potential use of TSLs as a gas management tool in underground coal mines. The adhesion strength results should also be combined with other test results to evaluate the performance of the TSL chosen.

CONCLUSIONS

In-situ adhesion tests were conducted to investigate the bond strength properties of a polymer based TSL on coal in an underground coal mine in NSW, Australia.

For comparison of the adhesion strength results, tests were conducted on both intact coal and fractured coal areas. With the increase of curing time, the adhesion strength increases for both intact coal and fractured coal, and the adhesion strength on the intact coal area is much higher than that on the fractured coal area.

The adhesion strength results on fractured coal are much more scattered with a higher standard deviation of adhesion strength compared with that on intact coal. The standard deviation tends to increase with the increase of curing time.

The adhesion strength results from this research indicate that the TSL material tested could be implemented for underground coal mining conditions. This is due to the main failure mode of the adhesion strength test observed being   the internal failure of the coal substrate.

RECOMMENDATIONS

This is a pilot research to study the potential applications of TSLs in underground coal mines. However, in order for this technology to become a viable tool for undergrond coal mining, research emphasis should be put on multiple field trials of TSLs under various conditions.

Apart from the use of TSLs as a complementary ground support medium, the application of TSLs could also bring many other benefits, such as gas management and ventilation benefits. A systematically economic model should also be built to evaluate the cost and benefits of TSLs for underground coal mines.

ACKNOWLEDGEMENTS

REFERENCES

Archibald, J F. 2001, Assessing acceptance criteria for and capabilities of liner for mitigating ground falls, *Mining Health and Safety Conference.* Sudbury, Ontario, Canada.
Espley-Boudreau, S J. 1999, Thin spray-on liner support and implementation in the hardrock mining industry*,* Master thesis (unpublished), Laurentian University, Sudbury, Ontario, Canada.

Gilbert, S, Saydam, S and Mitra, R. 2010, Laboratory investigation of the potential use of thin spray-on liners in underground coal mines, *The symposium of extracting the science: a century of mining research.* Littleton, CO, USA.

Kuijpers, J S. 2004, Evaluation of thin spray-on liners support behaviour, *in Surface Support in Mining* (eds: Potvin, Y, Stacey, D and Hadjigeorgiou, J)*,* 103-112 (Australian Centre for Geomechanics: Perth, WA, Australia).

Kuijpers, J S, Sellers, E J, Toper, A Z, Rangasamy, T, Ward, T, Rensburg, A J, Yilmaz, H and Stacey, D. 2004, Required technical specifications and standard testing methodology for thin sprayed linings, *SIMRAC project 200206.* Johannesburg, RSA.

Li, Z, Mitra, R, Saydam, S and Chalmers, D. 2014, Experimental study on support mechanism of thin spray-on liners in underground coal mines, *in Proceedings the 3rd International ISRM Young Scholars' Symposium on Rock Mechanics*, Xi'an, China, 717-721 (CRC Press/Balkema: Leiden, Netherlands).

Mercer, R A. 1992, The investigation thin polyurethane linings as an alternative method of ground control*,* Master thesis (unpublished), Queen's University, Kingston, Ontario, Canada.

Saydam, S and Docrat, Y S. 2007, Evaluating the adhesion strength of different sealants on Kimberlite, *in Proceedings the 11th Congress of International Society of Rock Mechanics*, Lisbon, Portugal, 585-588 (Taylor and Francis: London, UK).

Spearing, A J S. 2001, MBT's approach to thin support membranes in mines. Underground Construction Group MBT International, *Unpublished PowerPoint Presentation*.

Swan, G and Henderson, A. 2001, Water-based spray-on liner implentation at Falconbridge Limited, in *Proceedings the 1st International Seminar on Surface Support Liners: Membrane, Shotcrete and Mesh*, Perth, Australia.

Tannant, D D, Swan, G, Espley, S J and Graham, C. 1999, Laboratory test procedures for validating the use of thin sprayed-on liners for mesh replacement, *Canadian Institute of Mining and Metallurgy Annual Meeting.* Calgary, Canada.

COMPRESSIVE STRENGTH TESTING OF TOUGHSKIN THIN SPRAY-ON LINER

Qiuqiu Qiao, Jan Nemcik, Ian Porter and Ernest Baafi

Abstract: Thin spray-on liners (TSLs) have been attracting more and more attention as an alternative to the steel mesh in underground roadway support. In order to investigate and compare the compressive strength of glass fibre reinforced ToughSkin TSL developed at the University of Wollongong, a compression test was developed using the cube samples of 40 mm in size. The effect of a small amount of glass fibre in the polymer matrix was tested. The test results indicate that the compressive strength and the material stiffness of the cube samples increased with the increase of glass fibre. All of samples exhibited ductile stress strain curve as they had a yield point and a fracture point. The ductile ToughSkin yield characteristics are very important as sudden brittle failure is considered unsafe for mining practices.

INTRODUCTION

Thin spray-on liner (TSL) is a relative new form of rock support in underground coal mines. ToughSkin which is a glass fibre reinforced polymeric material liner has been under development as part of the ACARP project at the University of Wollongong. The polymeric ToughSkin has the properties that satisfy the specified safety requirements for the underground coal mining industry. Experiments indicate that ToughSkin TSL support is able to provide reinforcement to the substrate immediately when rock movement begins which is desirable for rock reinforcement. ToughSkin is currently investigated as being an effective substitution for the steel mesh which is of a passive nature and does not contribute significantly to roadway skin reinforcement.

Many experimental tests such as tensile, shear, tear, bond in tension and shear, buckling and flexural strength have been conducted at the University of Wollongong laboratory, and the tested results were published (Nemcik *et al.,* 2008; 2009a; 2009b; 2009c; 2011a; 2011b; 2012; Nemcik *et al.,* 2013a; 2013b; Qiao *et al.,* 2014a; 2014b; 2014c; 2014d; 2015; Shan *et al.,* 2014;). This paper reports the experimental results on the compressive strength of ToughSkin. There is no standard testing method to determine the compressive strength of TSL materials therefore cubes 40 mm in size reinforced with various amounts of glass fibre were chosen for testing. The aim of this test is to determine the compressive strength of TSL and attempt to establish a standard testing method for the compression test for TSL materials.

SAMPLE PREPARATION

Selection of sample shape and size

It is desirable to perform compression testing of the fibre reinforced ToughSkin material. This has proven difficult as the polymeric material is not viscous enough to evenly distribute the fibre within the large sample. To obtain reliable results, the glass fibre should be evenly distributed within the polymeric material. Due to limited curing time (approximately 10 minutes) it was very difficult to mix large amounts of fibre into the material and almost impossible to prevent air bubbles entering the mixture. It was decided to use the 40 mm steel cube moulds that are commonly used in the industry to test various materials. The cube mould assembly is shown in Figure 1..

The steel mould assembly consisted of 12 small cubical moulds placed on a metal block. The dimensions of the multiple moulds were cubes of 40 mm side. This setup had an extra advantage as multiple samples can be poured at the same time reducing the sample preparation time. The cube has a further advantage that its sides do not need to be machined prior testing as the steel plates make five out of six sides perfectly smooth ready for the compressive test. Being a steel mould, it does not deform or crack during the TSL sample preparation and curing time. In addition, it is easy to grease the mould which makes the process of removing the samples easy.

School of Civil, Mining and Environmental Engineering, University of Wollongong, NSW, Australia. E-mail:jnemcik@uow.edu.au,

Figure 1: Steel mould assembly of 40 mm cubes

Procedure of toughskin sample preparation

a) All contact surfaces of the mould were greased using a thin film of sprayed oil to ensure that samples can be easily removed from the mould.

b) The polymer components were mixed evenly according to the manufacturer's recommendations using a plastic cup and a wood spatula.

c) The glass fibre was mixed evenly into the ToughSkin solution while in the plastic cup.

d) The final polymer mix was poured into the mould ensuring that the glass fibre was evenly distributed.

e) The previous steps were repeated for all samples within the mould assembly.

f) The assembly was placed in the oven at 60°C overnight to cure the polymer.

g) The samples were carefully removed and the sharp surfaces sanded down until smooth and ready for testing (Figure 2).

The chosen mould enabled quick sample preparation for the compression tests however, several problems occurred during the process. The polymer became harder to mix as the glass fibre content increased. It was practically impossible to mix more than 1% of glass fibre into the mould. This amount of fibre is far less than would be normally sprayed in ToughSkin application. The sprayed product would normally consist of more than 30% glass fibre. Other methods must be trialled to achieve much greater fibre percentage for testing and therefore, new methods need to be devised to solve this problem. Typically air bubbles entrapment within the solution occurs when introducing the fibres into the mixture. This problem can be overcome using vibration or a vacuum chamber treatment however, due to the fast curing this approach is also limited.

Three sets of samples with varying glass fibre content were prepared. Three cubes had no glass fibre, three cubes had 0.5% of glass fibre and three samples contained 1% of glass fibre.

Compression test setup

The compression test was carried out using the Instron hydraulic testing rig. The polymer samples were loaded to failure, while load and deformation were recorded. The Instron testing device is shown in Figure 3 below.

Figure 2: Completed samples

Figure 3: Compression strength – test setup

Test results

Testing of the first two samples with 1% glass fibre and no fibre showed that the polymer samples gradually failed with violent outbursts of small debris flying at considerable velocities away from the yielding samples. This made the experiments unsafe so the initial tests were terminated prematurely. To solve the problem, a cloth was wrapped around the subsequent samples and testing resumed.

The average compressive strength for the samples without glass fibre reinforcement was 77.7 MPa, for the samples with 0.5% glass fibre reinforcement was 82.1 MPa, and for the samples with 1% glass fibre reinforcement was 86.9 MPa as shown in Table 1. The test results are shown in Figure 4 depicting the stress strain behaviour of the polymer samples during the uniaxial compression tests.   All test results are summarised in Table 1 below.

The compressive test results indicate two distinct elastic zones. Within the first 6% of strain the material stiffness is approximately 7.8 GPa after which the strain softening occurs reducing the stiffness to

approximately 1.4 GPa. Small increase of the fibre glass content has slightly increased the overall material stiffness.
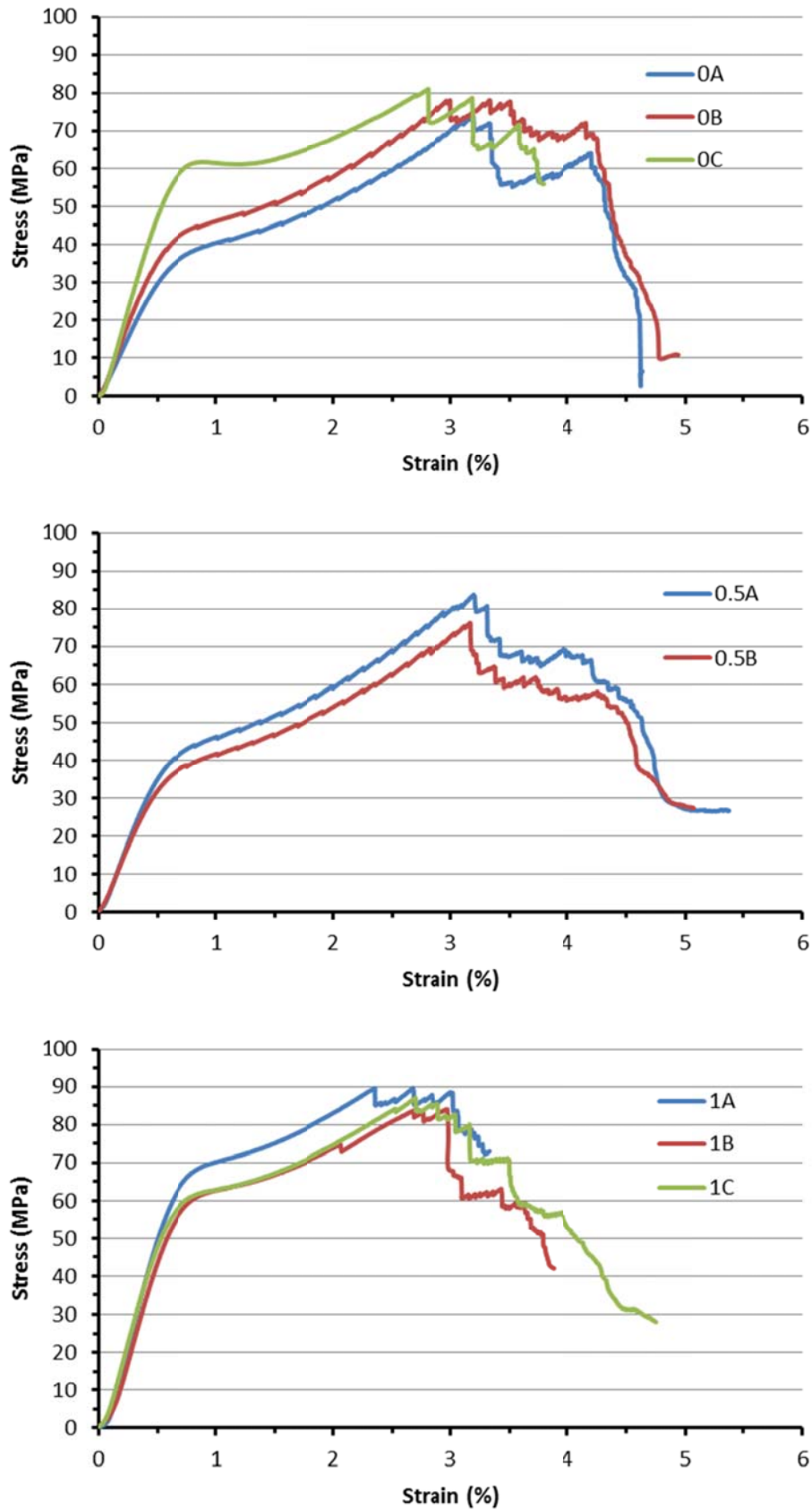
Figure 4: Stress versus strain graphs for all the samples with different glass fibre content

Table 1: Test results - summary of all ToughSkin samples (40 mm cubes)

Glass fibre content	Test Number	Compressive strength	Mean strength
0%	A	73.84	77.67
	B	78.15	
	C	81.04	
0.5%	A	83.79	82.09
	B	76.21	
	C	86.27	
1%	A	89.64	86.91
	B	84.04	
	C	87.07	

DISCUSSIONS

The test results indicate that as expected the averaged compressive strength values were similar as the glass fibre concentration in the reinforced samples was low. Despite the low fibre concentrations the samples with 1% of fibre were on average approximately 11% stronger than the samples with no fibre. This result indicates that the compressive strength of the ToughSkin samples with larger fibre content should dramatically increase the material strength. Further compressive tests of samples with higher glass fibre content are recommended to enable strength determination of the sprayed ToughSkin material. This can be achieved by repetitive spraying of the material components to build up a thick layer of material that can be cut and tested.

The measured strain softening of the material prior to peak load appears to be significant and independent on the glass fibre content. This behaviour can be desirable for material formulations with low glass fibre content as the material provides a significant reinforcement at the initial stage of loading and retains relatively high loads at higher strains. This behaviour is further complimented by high strains during the post failure loading. Higher glass fibre contents within the polymeric material may produce much higher stiffness of the material in compression. Further tests need to be undertaken for formulations with higher fibre to quantify the results.

The stress-strain test data shown in Figure 4 indicate that after the peak strength is exceeded there is a gradual reduction of the load. No abrupt failure of the material was observed until the load reduced significantly. A gradual reduction in post-failure strength reduction is desirable in underground application. It is expected that increase of the glass fibre would further improve the post-failure behaviour with large strains before the total separation of the material occurs. This can be confirmed by testing the sprayed material. Brittle failure characteristics of the ToughSkin would be sudden and unsafe for mining practices.

The violent outbursts of small debris flying at considerable velocities away from the yielding samples need to be studied further to ensure safety. It is envisaged that large amounts of the glass fibre within the loaded material would eliminate such brittle failure mechanism. Further tests are necessary to validate this comment.

The percentage of the glass fibre and the air entrapment within the polymer mixture needs to be researched as they can significantly affect the compressive strength. When spraying the material on the rock surface, the external mixing and the air assist spray stream can produce variable outcomes. The effect of air entrapment together with the fibre content needs to be quantified once the sprayed samples are available.

CONCLUSIONS

The aim of this study was to develop a suitable method to measure the compressive strength of the glass fibre reinforced TSL material and to provide compressive strength comparison of different TSL products. The method using the steel cube mould was selected as it is practicable and able to withstand the heating of large samples caused by the exothermic reaction during the resin setting period. The test results indicate that the compressive strength of all tested 40 mm cube samples ranged from 78 MPa to 87 MPa. The compressive strength of cube samples increased slightly with the small increase of glass fibre content. The measured sample stiffness also slightly increased with the small glass fibre content.

These results indicate that larger glass fibre contents may produce more dramatic increase in stiffness, compressive strength and the post failure strain.

REFERENCES

Nemcik J, Porter I, Baafi E, Spinks G and Lukey C. 2008, Polymeric alternative to steel mesh for underground coal mine roadway support. *In Proceedings of 17th International Symposium on Mine Planning and Equipment Selection*, Beijing, pp 642-647.

Nemcik J, Porter I, Baafi E and Lukey C. 2009a, Geotechnical assessment of polymeric materials as skin reinforcement in underground mines, *In Proceedings of 9th Coal Operators' Conference*, Wollongong, pp 69-76.

Nemcik J, Baafi E, Porter I and Lukey C. 2009b, Computer Modelling of Polymer Liner Reinforcement in Underground Mines, *In Proceedings of the Application of Computers and Operations Research in the Mineral Industry (APCOM) 2009 Conference*, Vancouver, pp 532-547.

Nemcik J, Porter I, Baafi E and Lukey C. 2009c, Geotechnical assessment of skin reinforcement in underground mines, *In Proceedings of 28th International Conference on Ground Control in Mining*, Salt Lake City, pp 1-5.

Nemcik J, Porter I, Baafi E and Joshua T. 2011a, Bearing capacity of a glass reinforced polymer liner, *In Proceedings of 11th Coal operators Conference*. Wollongong, pp 148-153.

Nemcik J, Porter I, Baafi E and Navin J. 2011b, Determination of ultimate strength of tough skin, a glass reinforced polymer liner, *In Proceedings of 11th Coal operators Conference*, Wollongong, pp 154-158.

Nemcik J, Porter I and Baafi E. 2012, Performance of polymer skin spray-on liner in coal mines, *In Proceedings of 12th ISRM International Congress on Rock Mechanics-Harmonising Rock Engineering*, Beijing, pp 1565-1568.

Nemcik J, Porter I and Baafi E. 2013a, Tear tests of glass fibre reinforced polymer skin spray-on liner, *In Proceedings of 13th Coal operators Conference*, Wollongong, pp 170-175.

Nemcik J, Baafi E and Porter I. 2013b, Stabilising rock surfaces with a glass reinforced polymer skin, *Acta Geodynamica et Geomaterialia*,10, No. 2(170): 207-213.

Porter I, Shan Z, Nemcik J and Baafi E. 2014, Full scale tests to compare the strength of polymer liners with high tensile steel mesh, *In Proceedings of 14th Coal Operators' Conference*, Wollongong, pp 193-201.

Qiao Q, Nemcik J, Porter I, Baafi E, Zhang Z and Shan Z. 2014a, Development of testing methods of thin spray-on liner shear-bond strength, *In Alejano R, Perucho A, Olalla C and Jimenez R (Eds.)*, *Proceedings of EUROROCK: Rock Engineering and Rock Mechanics: Structures in and on Rock* ,Masses, pp 125-130. United Kingdom: Taylor & Francis Group.

Qiao Q, Nemcik J and Porter I. 2014b, Shear strength testing of glass fibre reinforced thin spray-on liner, *Géotechnique Letters*, 4: 250-254, http://dx.doi.org/ 10.1680/geolett.14.00057.

Qiao Q, Nemcik J, Porter I and Baafi E. 2014c, Laboratory tests on thin spray-on liner penetrated rock joints in direct shear, *Rock Mechanics and Rock Engineering*, DOI: 10.1007/s00603-014-0669-7.

Qiao Q, Nemcik J, Porter I and Baafi E. 2014d, Laboratory investigation of support mechanism of thin spray-on liner for pillar reinforcement, *Géotechnique Letters*, 4: 317-321, DOI: 10.1680/geolett.14.00076.

Qiao Q, Nemcik J and Porter I. 2015, A new approach for determination of the shear bond strength of thin spray-on liners, *International Journal of Rock Mechanics and Mining Sciences*, 73: 54-61.

Shan Z Porter I, Nemcik J and Baafi E. 2014, Comparing the reinforcement capacity of welded steel mesh and a thin spray-on liner using large scale laboratory tests, *International Journal of Mining Science and Technology*, 24 (3): 373-377.

Pillar Abutment Loading – New Conceps for Coal Mining Industry

David Hill[1], Ry Stone[2], Anastasia Suchowerska[3] and Robert Trueman[4]

ABSTRACT: Chain and barrier pillar design for longwall mining and production pillar design for room-and-pillar retreat mining have tended to rely on simplistic abutment angle concepts for the estimation of pillar stress increases during and subsequent to extraction. Historically, the underpinning database of monitored abutment loading has been small and displayed considerable variation, leading to the application of a number of mine site-specific approximations and often necessarily conservative assumptions. Also, over the last decade, the trend towards wider longwall faces and narrower room-and-pillar sections in deeper areas has challenged established design practices. However, in recent years, considerable effort has been made both in the US and Australia with regard to expanding the abutment loading database and developing an improved understanding of the pillar loading environment. This paper examines some of the progress made and the implications thereof, with a focus on the derivation of formula for abutment angle prediction.

INTRODUCTION

Since the early 1970s, chain and barrier pillar design for longwall mining and production pillar design for room-and pillar retreat mining have relied very largely on the simple abutment angle (φ) concepts developed by King and Whittaker (1971) and Wilson (1973) for the estimation of pillar stress increases during and subsequent to extraction. A typical representation is shown in Figure 1. This model has been incorporated into numerical and empirical methodologies for pillar sizing.

The early researchers suggested abutment angles of between 16.7° and 25° as being appropriate for design purposes, based largely on comparisons to subsidence results. However, it is generally understood that the link between the abutment angle and any observable angle of break or caving angle is tenuous at best. The abutment angle utilised in the design of pillars is usually only a mathematical convenience, simply the number that best fits with measured pillar stresses and / or observed ground behaviour. It is only loosely associated with the actual physical overburden behaviour. As such, the abutment angle concept implicitly reflects the sum of the outcomes of a complex set of overburden behaviours.

The variance between abutment load and observable ground / caving behaviour is understandable given that in practice:

i)   The span to depth ratio of many longwall panels is such that the panel is sub-critical with respect to caving and therefore the calculated abutment load is limited by the half-span of the panel.

ii)   Caving characteristics vary with lithology, with weaker, less stiff rock types generally failing at angles closer to the vertical than stronger materials.

Historically, the underpinning database of monitored abutment loading has been very small and displayed considerable variation, leading to the application of a number of mine site-specific approximations and often necessarily conservative assumptions. Although early studies in both Australia and the USA suggested an abutment angle of 21° as being typically appropriate and reasonably conservative for abutment load estimation, field measurements indicate that actual abutment angles are a function of pillar and panel geometry, overburden properties and depth, Hill *et al.,* (2008). Also, over the last decade, the trend to wider longwall faces and (conversely) narrower room-and-pillar sections in deeper areas has challenged established design practices.

---

[1]*Technical Director, Golder Associates Pty Ltd, E-mail: davidhillmac@bigpond.com, Tel: 0417 472932*
[2]*Principal Geotechnical Engineer, Golder Associates Pty Ltd,*
[3]*Geotechnical Engineer, Golder Associates Pty Ltd,*
[4]*Principal Geotechnical Engineer, Golder Associates Pty Ltd,*

In recent years, considerable effort has been made both in the US and Australia with regard to expanding the abutment loading database and developing an improved understanding of the pillar loading environment. This paper examines some of the progress made and the implications thereof, with a focus on the derivation of more robust design methodologies.
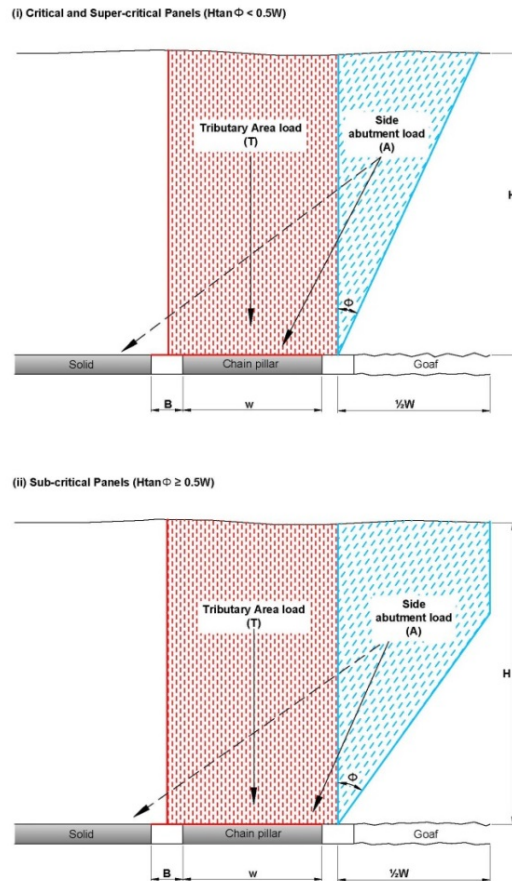
Figure 1: Schematic of side abutment loading model

THE EXPANDED DATABASE

A joint Australian and US longwall database has been compiled that incorporates the published work of Mark (1992), Colwell (1998) and Vandergrift and Conover (2010), as well as the outcomes of projects conducted by Golder Associates for industry clients from 2008 onwards. The data set is deliberately limited to measurements obtained from stress cells installed in the pillars, rather than the roof above the pillar, as the latter tend to show considerably more scatter, which is largely regarded as a function of the measurement technique.

The longwall database therefore covers:

- 29 sites,
- 6 coalfields,
- 13 seams,
- seam depths of 125m to 533m,
- roadway heights of 2.0 m to 3.6 m and
- panel widths of 105 m to 310 m (centres).

Most of the Australian data involves twin entry gate road systems, whereas the US data is from three and four entry systems. For the purpose of estimating an equivalent twin entry chain pillar dimension, the individual pillar widths for the multiple entry systems have been added together, plus the width of the intra-pillar entries, to arrive at an apparent combined pillar width 'w' for analytical purposes. This distance is considered a reasonable approximation of what the over-burden 'sees' around the extracted area. In

the multiple entry systems, goaf-side yield pillars are excluded from the analysis of maingate (i.e. side) abutment loading. Applying these criteria, apparent pillar width varies between 24 and 110 m in the side abutment loading database.

Figure 2 illustrates the frequency distribution for the abutment angle (φ) database. The abutment angle averages 14°, with a minimum of 4° and a maximum of 27°.
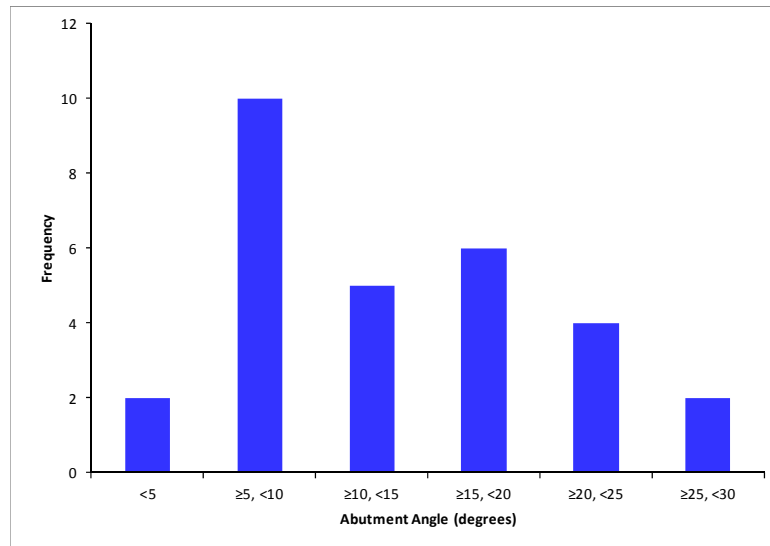
Figure 2: Frequency histogram for abutment angles in the expanded database

Figure 3 illustrates the variation in measured abutment angle versus depth (H). It can be seen that the measured abutment angle tends to reduce with increasing depth, although there is considerable scatter to the data. In particular, in the Western USA, as well as those areas of NSW in which depth exceeds 300m and the upper overburden is dominated by competent sandstone units, field studies strongly indicate that the measured abutment angle reduces as depth increases. A potential explanation is that traditional abutment angle models overstate the magnitude of abutment load at increasing depths of cover, which suggests that an increased proportion of the load is transferred elsewhere (i.e. to the goaf). Tulu and Heasley (2012**)** have suggested the relationship between abutment angle and depth summarised in Table 1.
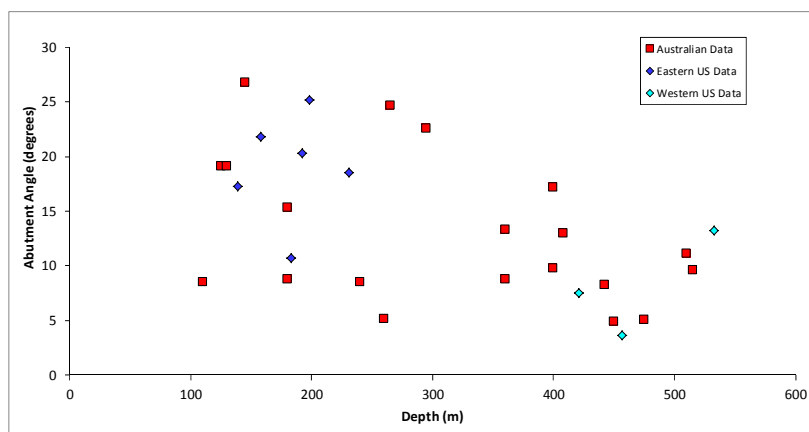
Figure 3: Variation in measured abutment angle versus depth

Table 1: Abutment angle concept according to Tulu and Heasley (2012)

Depth (H, in metres)	Abutment Angle (φ, degrees)
H ≤ 274	21
274 < H ≤ 625	$21 \times (H/274)^{-1.59}$

Figure 4 illustrates the variation in measured abutment angle versus chain pillar width (w). No correlation is apparent for pillar width in isolation. However, Figure 5 illustrates the variance in abutment angle for single side abutment loading versus chain pillar width to depth ratio; from this it can be seen that the measured abutment angle tends to reduce with reducing pillar width and increasing depth. The relationship is stronger than that with respect to depth alone. A possible explanation is that as chain pillar width and therefore stiffness reduces, the ability of the pillar to attract the side abutment load reduces and a greater proportion of this load is redistributed to larger, stiffer blocks of coal (i.e. the adjacent barrier or unmined longwall block). However, the measurement process usually includes an attempt to measure the component of load on the block side, as well as the pillar itself. It would seem that in deeper mines with stiffer overburden, the extent and proportion of the load re-distributed to the solid is greater than either can be measured or is suggested by widely applied stress distribution approximations, such as the abutment influence zone parameter (D) defined by Peng and Chiang (1984) and the associated square decay function for abutment stress defined by Mark (1992). In other words, some of the abutment load may go further afield, where it is unmeasured. There is some evidence for this in the deeper mines of the Western USA (Larson and Whyatt, 2012), as well as from one Australian mine at a depth of 400 m, viz:

- 75 m wide pillar: measured abutment angle 17°
- 25 m wide pillar: measured abutment angle 10°

However, at depths of <350 m, the available evidence suggests that the stress distribution defined by Mark (1992) remains a reasonable approximation.
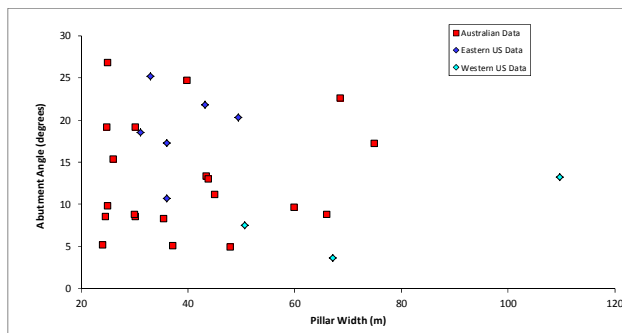
Figure 4: Variation in measured abutment angle versus chain pillar width
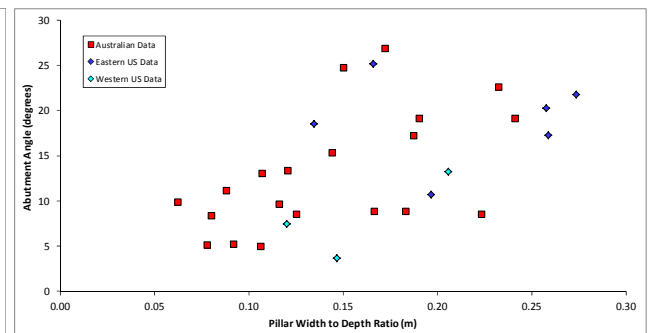
Figure 5: Variation in measured abutment angle versus chain pillar width to depth ratio

Figure 6 illustrates the variation in measured abutment angle versus panel width (W). Although no correlation is apparent, overburden stiffness and load transfer capabilities at a given depth are a function of panel width; increasing overburden "arching" or spanning would be expected at reducing panel width to depth ratios. Figure 7 confirms a weak trend of increasing abutment angle at increasing panel span to depth ratio; low abutment angles are generally associated with panels that would be considered "sub-critical" in subsidence terms (and especially at W/H ratios of <1). This is an important consideration in the Australian industry, where (as in the US) average longwall panel spans are progressively increasing. Also, in Australia at least, although depth may be increasing in the case of individual mines, the average longwall industry depth has remained at around 300 m for over 15 years. The implication is that an increasing proportion of Australian longwalls are migrating from sub-critical to super-critical loading environments.

The highly complementary nature of the US and Australian data is clearly evident from the plots; in particular, the Western US outcomes are highly consistent with deeper NSW experience.

The influence of various parameters on the abutment angle has been further assessed using Multiple Linear Regression (MLR). The general purpose of this statistical process is to determine a linear relationship between several predictor variables (dimensional parameters) and the response variable (abutment angle). A series of analyses were undertaken, from which it was ascertained that the abutment angle is best predicted by:

- depth (H)
- chain pillar width (w)
- panel span (W) to depth ratio (i.e. W/H)
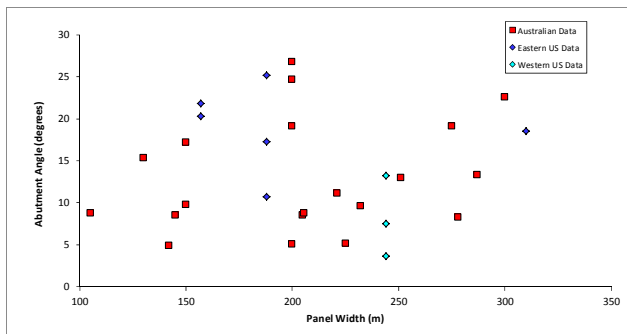
Figure 6: Variation in measured abutment angle versus panel width
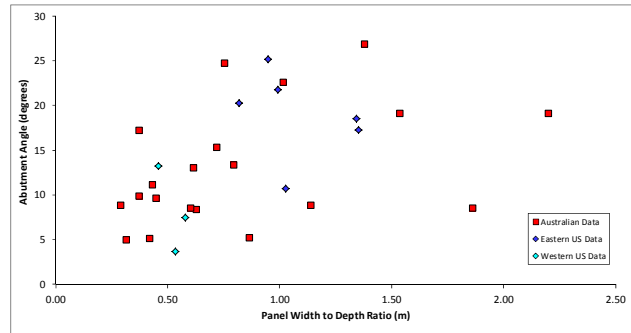
Figure 7: Variation in measured abutment angle versus panel width to depth ratio

Panel span on its own was found to be not statistically significant. The analysis was refined by removing the following cases from the data set:

- two cases in which multi-seam interaction is considered to have resulted in unusually low and otherwise unrepresentative abutment angles and
- two cases in which the spanning properties of the overburden again resulted in unusually low, unrepresentative abutment angles.

The resulting predictive formula is as follows:

Abutment angle, φ = 21.62 – 0.0221H + 0.0725w – 6.23C
Where C = Panel span criticality, defined by:
        C = 1, when W/H <0.75 and
        C = 0, when W/H ≥ 0.75

Figure 8 presents the measured and predicted abutment angles using the above formula for the sub-set of 25 cases from the database. The coefficient of determination for multiple regression (i.e. R^2 value) is favourable, at 0.65. The analysis indicates that:

- As depth increases, the abutment angle reduces (consistent with the Australian and US findings).
- As the panel width to depth ratio increases, the abutment angle increases.
- As pillar width increases, the abutment angle increases.
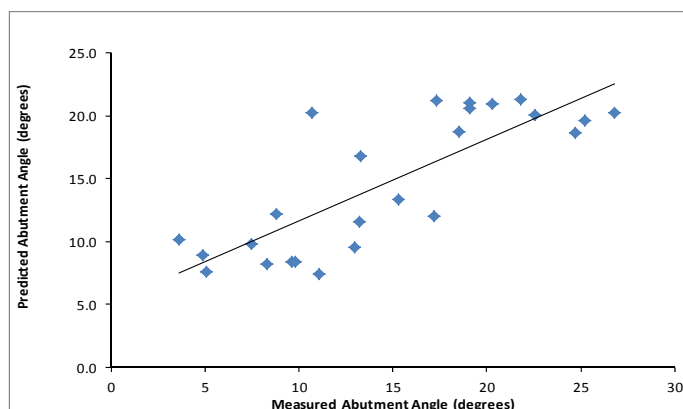
Figure 8: Predicted versus Measured Abutment Angle

This abutment angle formula and the associated concepts find application in:

- The design of chain pillars and associated gateroad support.
- Barrier pillar design.
- The design of total and partial pillar extraction systems.
- Subsidence analysis and control for partial extraction systems.

Other aspects of the database that are useful with respect to pillar and support design relate to the front and tailgate abutment loading factors. Specifically:

i)   The measured front abutment loading factor for pillars at the maingate corner of the longwall face ranges from 0.02 to 0.63, with a mean of 0.28 and a standard deviation of 0.16. Measured results are typically well below the factor of 0.5 that is commonly applied in the industry. This factor was found to be highly mine specific and not to relate strongly to the geometrical factors influencing the abutment angle.

ii) The measured tailgate abutment loading factor or "multiplier" for pillars at the tailgate corner of the longwall face ranges from 1.3 to 3.8, with a mean of 1.9 (1.7 ignoring one outlier). Measured results are typically higher than the factor of 1.5 commonly applied in the Australian industry. This factor was also found to be highly mine specific and not to relate strongly to the geometrical factors influencing the abutment angle.

STRESS MEASUREMENT CASE STUDIES

Apart from contributing to the increasing usefulness of the database as a whole, individual stress measurements provide invaluable data for enhanced design on a mine specific basis. This is illustrated by the following three examples from three contrasting geotechnical environments:

- Mine A: A gassy mine employing a three heading gateroad layout.
- Mine B: A deep mine utilising twin heading gateroads.
- Mine C: A moderately shallow multi-seam mine utilising twin heading gateroads.

Mine A

Figure 9 shows the pillar and stress cell array for Mine A, which was operating at a depth of 295m. Figure 10 illustrates the profiles for the changes in vertical stress associated with both front and side abutment loading.

From this information it was possible to determine that:

- The abutment angle was 23°.
- The ratio of front to side abutment loading was 0.3.

It is also possible to demonstrate, by coupling the stress measurement results to a broader review of the geotechnical environment that, with respect to the maintenance of tailgate serviceability, the chain pillars were over-designed (i.e. it would have been possible to reduce the pillar system width by up to 10 m).
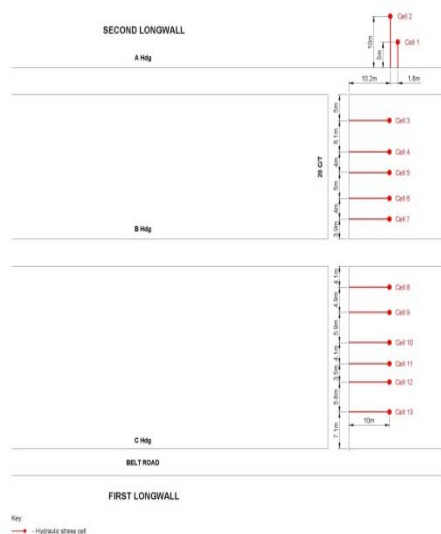
Figure 9: Mine 'A' Stress Cell
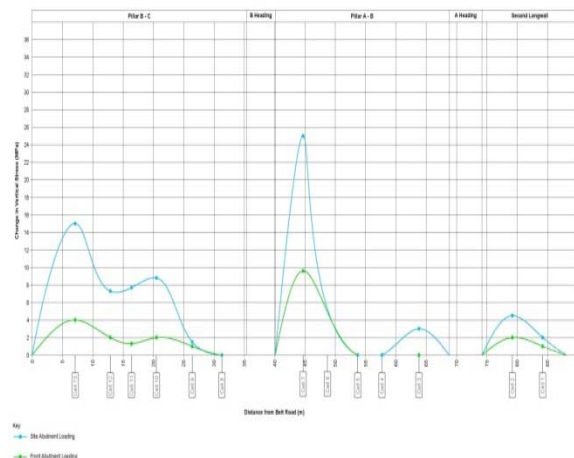
Figure 10: Mine 'A' Vertical Stress Changes due to Abutment Loading

Mine B

Figure 11 shows the pillar and stress cell layout for Mine B, which was operating at a depth of 510m. Figure 12 illustrates the profiles for the changes in vertical stress associated with front, side and tailgate abutment loading.

From this information it was possible to determine that:

- The abutment angle was 11°.
- The ratio of front to side abutment loading was 0.4.
- The ratio of tailgate to side abutment loading was 1.3.

Unusual features of the stress profile are the "triple hump" and the concentration of stress on the travel road side of the chain pillar during side abutment loading. This atypical profile was later effectively replicated by a second set of stress measurements in a subsequent gateroad.
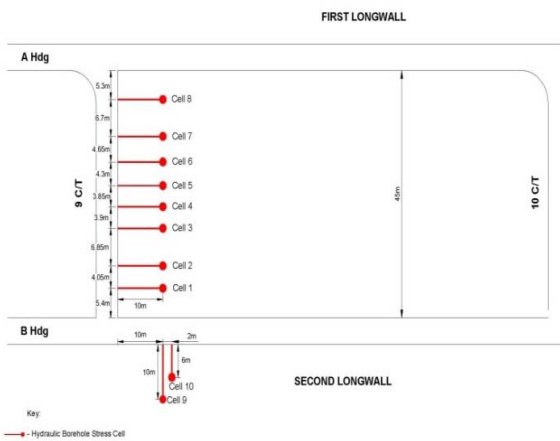
Figure 11: Mine 'B' stress cell array
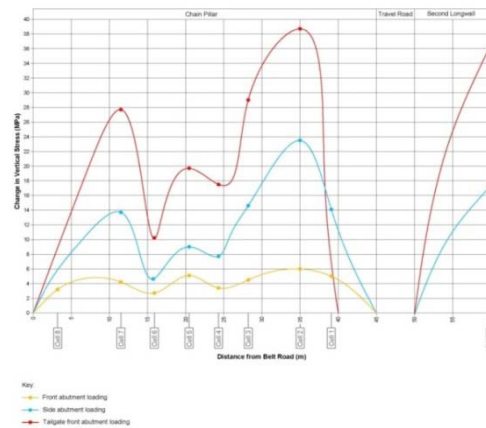
Figure 12: Mine 'B' vertical stress changes due to abutment loading

Mine C

Figure 13 shows the pillar and stress cell layout for Mine C, which was operating at a depth of 110 m. Figure 14 illustrates the profiles for the changes in vertical stress associated with front, side and tailgate abutment loading.

From this information it was possible to determine that:

- The abutment angle was 9°.
- The ratio of front to side abutment loading was 0.2.
- The ratio of tailgate to side abutment loading was 1.9.
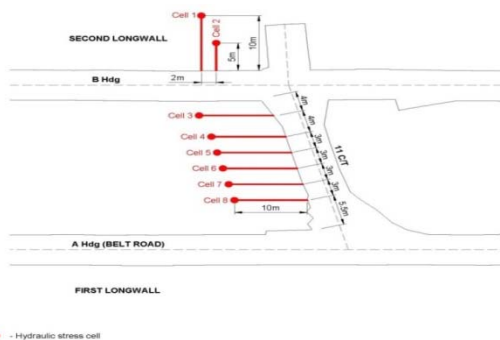
Figure 13: Mine 'C' stress cell array
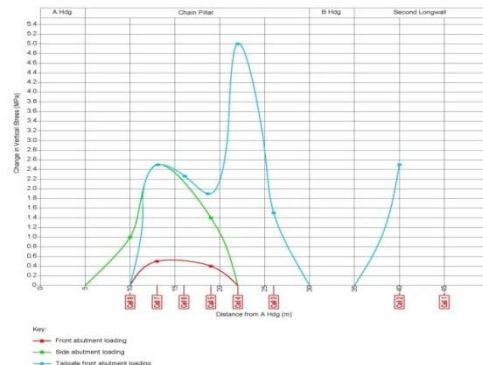
Figure 14: Mine 'C' vertical stress changes due to abutment loading

The low abutment angle and generally favourable loading environment is a direct function of the location of the monitoring site beneath an overlying longwall goaf. Similar to Mine A, it is again possible to

demonstrate, from the stress measurement and an assessment of the geotechnical environment that, with respect to the maintenance of tailgate serviceability, the chain pillars were significantly over-designed (i.e. it would have been possible to reduce the pillar system width by at least 5 m).

GAINING INFORMATION

Stress measurement is just one tool for the analysis of system performance. In this regard, the generation and application of complementary data sets has proven powerful for mining layout design, ground control and long-term stability analysis.   Examples of complementary approaches include:

i)   Monitoring pillar deformation using mapping, borescope and extensometry techniques. The information generated: (a) facilitates the definition of peripheral yield zones and therefore the pillar stress profile and abutment angle, (b) provides base data for rib support design, (c) enables the quantification of long-term pillar behaviour and (d) provides input for further analysis of pillar strength and performance.

ii)   Numerical modelling of pillar stress and ground deformation. For example, in the LaModel program, a coal mining specific software (Heasley *et al.,* 2010), it is possible to utilise the calculated or measured abutment angle in the analysis of stress and ground deformation. This involves the definition of the goaf material properties, in which the percent of overburden load applied to the goaf is inputted. This is a function of abutment angle, panel width and depth. The information generated can: (a) facilitate the assessment of long-term pillar stability, (b) contribute to the estimation of subsidence (and can be calibrated to actual subsidence results) and (c) assist in defining input material parameters for future mining layout optimisation.

CONCLUSIONS

This paper has examined some of the progress made in recent years with regard to understanding the vertical stress re-distribution around extraction panels and in particular the prediction of the abutment angle. The derived abutment angle formula is considered to be widely applicable and facilitates both improved pillar designs and the determination of associated ground support requirements. In most environments, site-specific stress measurement and related analyses represent a significant opportunity to further optimise mining layouts and ground support design.

REFERENCES

Colwell, M.G. 1998, Chain pillar esign (calibration of ALPS), *Final Report for ACARP Project C6036*.

Heasley, K A, Sears M M, Tulu I B, Calderon-Arteaga C and Jimison L. 2010, Calibrating the LaModel program for deep cover pillar retreat coal mining, *in Proceedings third International Workshop on Coal Pillar Mechanics and Design*, Morgantown, W. Va, pp 47-57.

Hill, D J, Canbulat, I, Thomas, R and van Wijk, J. 2008, Coal Pillar Loading Mechanisms and Progress in Pillar Design, *in proceedings 27th International Conference on Ground Control*, Morgantown, W. Va., pp 235-240,
http://icgcm.conferenceacademy.com/papers/detail.aspx?subdomain=icgcm&iid=36.

King, H J and Whittaker, B N. 1971, A Review of Current Knowledge on Roadway Behaviour, in p*roceedings* Symposium on Roadway Strata Control, *Institute of Mining and Metallurgy*, pp 73-87.

Larson, M and Whyatt, J. 2012. Load Transfer Distance Calibration of a Coal Panel Scale Model: A Case Study, *in proceedings 31st International Conference on Ground Control*, Morgantown, W. Va, pp 195-205.
http://icgcm.conferenceacademy.com/papers/detail.aspx?subdomain=ICGCM&iid=982.

Mark, C. 1992, Pillar Design Methods for Longwall Mining, *United States Bureau of Mines Information Circular 9247*, 53 pp.

Peng, S S and Chiang, H S. 1984, Longwall Mining. Wiley, 708 pp.

Tulu, I B and Heasley, K A. 2012, Investigating Abutment Load, *In proceedings 31st International Conference on Ground Control*, Morgantown, W. Va, pp 150-159,
http://icgcm.conferenceacademy.com/papers/detail.aspx?subdomain=ICGCM&iid=1007.

Vandergrift, T and Conover, D. 2010, Assessment of Gate Road Loading under Deep Western U.S. Conditions, *in Proceedings of the 3rd International Workshop on Coal Pillar Mechanics and Design*, Morgantown, W. Va, pp 38-46.

Wilson, A H. 1973, A Hypothesis Concerning Pillar Stability, *Mining Engineer (London)*, Vol. 131, pp. 409-417.

MINE SUBSIDENCE PREDICTIONS USING A MECHANISTIC MODELLING APPROACH

Detlef Bringemeier[1&2]

ABSTRACT: A practical, predictive method, based on closed form solutions for displacement and strain around longwall panels, is proposed to facilitate the assessment of subsidence and changes to ground conditions above longwall mining. The displacement discontinuity method is employed to simulate the displacement and strain field around a single longwall panel in a three-dimensional transversely isotropic medium. The analytical solutions are effectively combined and implemented in MATLAB language, which allows for deriving key information to subsidence predictions. Predictive accuracy, applicability and efficiency of the code are demonstrated using data from collieries in New South Wales. Close agreement was achieved between the key parameters maximum tensile strain, maximum tilt, maximum convex and minimum concave curvature derived by empirical methods, the proposed displacement discontinuity method and survey records. However, there is still scope for improvements in this approach and additional testing is recommended in order to further validate the proposed method and evaluate its potential for practical longwall mining impact and risk assessments.

INTRODUCTION

Longwall mining is the preferred mining method for coal resources in Australia if geological conditions are favourable and overburden to seam thickness ratios render coal extraction by open-cut methods uneconomical. One of the few drawbacks of the longwall mining method is the potential of mining induced ground movement interfering with aquifers, surface water sources and engineered structures, including transport ways, drainage and bridges.

In the Southern and Newcastle Coalfields, the operating mines are predominantly longwall operations extracting mostly gently dipping coal seams. Panels range between 163 m and 400 m in width and are up to 4065 m long. Vertical and horizontal displacement and tensile and compressive strain develop above, below and adjacent to the extracted panel due to the caving of the extracted coal cavity. This in turn alters the characteristics of the rock above and below the extracted seams and causes vertical and horizontal displacement at the ground surface. A variety of empirical and numerical techniques have been developed in an attempt to describe and quantify the observed changes at the ground surface above a completed panel or a panel undergoing extraction. In their review of mine subsidence prediction methods, Bahuguna, *et al.,* (1991) differentiate between (i) empirical techniques, (ii) influence functions, and (iii) theoretical modelling. Empirical techniques use observations to derive physically based correlation functions between observables (e.g. ground movement parameters) and mining parameters. The ground movement parameters are either single value parameters (e.g. maximum of an observable measured across or along the longitudinal centre line of a panel) or spatial parameters (e.g. profile functions). Methods using theoretical models are based on the application of stochastic or deterministic mechanics to relate rock mass behaviour to loading due to coal extraction and environmental influences. Theoretical models are based on a set of assumptions and the predictive performance of the model is strongly dependent on how well these assumptions are met by the system under investigation.

The aim of this paper is to present a mechanistic method to estimate ground displacement due to longwall extraction in a three-dimensional transversely isotropic medium. Computed results are compared with published data from the Southern and Newcastle Coalfields and results obtained with well-established empirical methods, demonstrating the validity and limitations of the proposed method.

DETERMINATION OF SUBSIDENCE AND THE STRESS FIELD AROUND A LONGWALL PANEL

Displacement Discontinuity approach

The caving of a longwall panel strip can as a first approximation be modelled as a discrete displacement along and normal to a rectangular roof and floor section with a uniform displacement small compared to

---

[1] *Golder Associates, 147 Coronation Drive, Milton, Queensland 4064, Australia, E-mail: dbringemeier@golder.com.edu*, Tel: *(+61) 7 3721 5400*
[2] *School of Civil Engineering, The University of Queensland, St Lucia, QLD 4072, Australia*

the panel width and depth. In this treatment it is assumed that the panel is horizontal and the ground surface can be represented by a traction-free plane surface of a three-dimensional transversely isotropic, elastic half-space with displacement and stress at equilibrium and zero at infinity. This problem requires the solution of a set of 15 coupled partial differential equations comprising three equations of equilibrium, six stress – strain relations and six strain – displacement relations. Using the displacement formulation, the set of equations can be reduced to three coupled second-order partial differential equations in terms of displacement. For a homogeneous transversely isotropic half-space, the equilibrium equations in terms of displacements can be further simplified by introducing potentials or harmonic displacement functions (Love, 1906).

The general solution of this problem for an infinite medium was first suggested by Elliot and Mott (1948) and Shield (1951) in the form of harmonic displacement functions Φ_1 and Φ_2 that represent the solutions of the system of partial differential equations

$$\left(\frac{\partial^2}{\partial x_1^2} + \frac{\partial^2}{\partial x_2^2} + \frac{\partial^2}{\partial(x_3^k)^2}\right)\Phi_k(x_1, x_2, x_3^k) = 0, \quad x_3^k = x_3/\sqrt{v_k} \quad \text{for} \quad k = 1,2 \tag{1}$$

where v_1 and v_2 are the roots of

$$c_{1111}c_{4444}v^2 + (c_{1313}(2c_{4444} + c_{1313}) - c_{1111}c_{3333})v + c_{3333}c_{4444} = 0 \ . \tag{2}$$

The displacement parallel to the Cartesian coordinates are expressed by the harmonic displacement functions

$$u_1 = \frac{\partial}{\partial x_1}(\phi_1 + \phi_2), \ u_2 = \frac{\partial}{\partial x_2}(\phi_1 + \phi_2), \text{and} \ u_3 = \frac{\partial}{\partial x_3}(q_1\phi_1 + q_2\phi_2) \tag{3}$$

with

$$\phi_i = \frac{1}{1+q_i}\Phi \quad \text{for} \ i = 1,2 \tag{4a}$$

$$q_i = (c_{1111}v_i - c_{4444})/(c_{1313} + c_{4444}) \quad i = 1,2 \tag{4b}$$

and c_{ijkl} are the components of the 4th order symmetric stiffness tensor with five independent parameters for a transversely isotropic material which are related to well-known engineering elastic moduli.
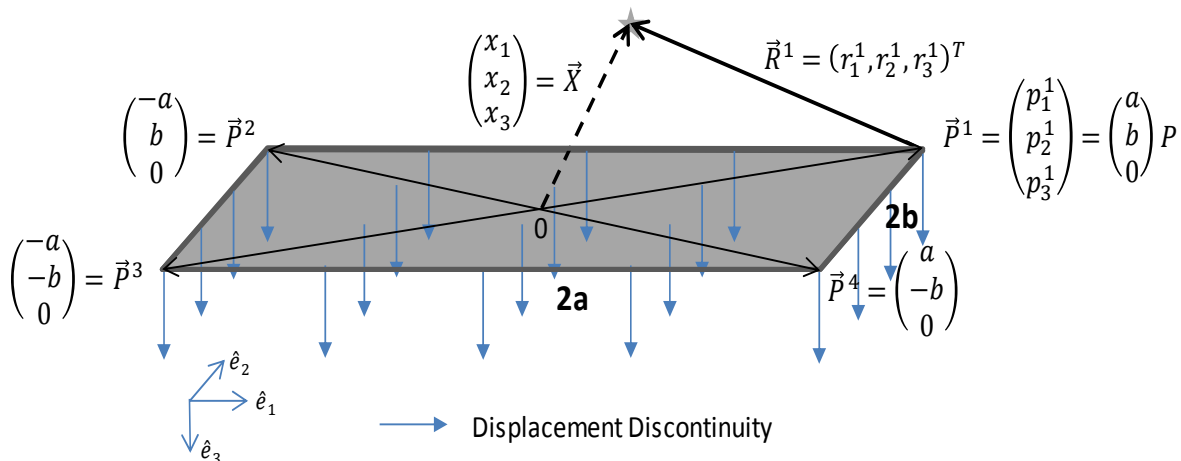
Figure 1: Representation of an extracted longwall panel using a Displacement Discontinuity

The explicit solution obtained by Berry and Sales (1962) for the derivatives of the displacement functions at any point $\vec{X} = (x_1, x_2, x_3)^T$ in an infinite space is proportional to the height T of the panel excavation and a function

$$\Phi = \frac{T}{4\pi}\frac{(1+q_1)(1+q_2)}{q_1-q_2}\sum_{i=1}^{4}(-1)^i\vec{R}^i \cdot \vec{F}^i \tag{5}$$

of the harmonic coordinate vector

$$\vec{R}^i = \left(r_1^i, r_2^i, r_3^i \right) \tag{6}$$

with

$$r_j^i = \left(x_j - p_j^i \right), \quad j = 1,2,3 \quad \text{and} \quad \left\| \vec{R}^i \right\| = R^i = \sqrt{\sum_{j=1}^{3} \left(r_j^i \right)^2}$$

and the function

$$\vec{F}^i = \left(\log\left(R^i - r_2^i \right), \quad \log\left(R^i - r_1^i \right), \quad \tan^{-1}\left(\frac{r_1^i r_2^i}{r_3^i R^i} \right) \right)^T . \tag{7}$$

Figure 1 presents an oblong shaped displacement discontinuity with corner points $\vec{P}^1 = (p_1^1, p_2^1, p_3^1)^T$, $\vec{P}^2, \vec{P}^3$ and $\vec{P}^4$. The stress field is derived by partial derivation of equations (3) and (5), and the strain – displacement and stress – strain relations.

It is noted that the presented solutions for the stress and displacement field are limited to real valued roots of equation (2) and do not extend to the case when the roots obtain complex conjugated values or become zero (isotropic material).

Berry and Sales (1962) extended the solution for an oblong shaped discontinuity in an infinite medium to a half-space with the discontinuity parallel to the traction free half-space boundary (e.g. panel extracted in a horizontal seam). They obtained a solution by mirroring the discontinuity and its properties at an infinite plane parallel to the discontinuity and thus creating a plane along which all shear stresses τ across that plane are equal but of opposite sign. Compressive and tensile stresses σ are continuous across this plane. The solution for the pair of displacement discontinuities is attained by exchanging $\Phi(x_1, x_2, x_3^k), k = 1,2$ in equation (4a) by the sum

$$\Phi\left(x_1, x_2, x_3^k + D^k \right) + \Phi\left(x_1, x_2, x_3^k - D^k \right) + \Phi^*\left(x_1, x_2, x_3^k \right), \quad k = 1,2 \tag{8a}$$

with D the distance of the panel to the half-space boundary. The symmetry of the solution ensures that on the half-space boundary $x_3 = 0$:

$$\sigma_{33}^l = \sigma_{33}^u, \quad \tau_{13}^l + \tau_{13}^u = 0, \quad \tau_{23}^l + \tau_{23}^u = 0$$

and the harmonic function

$$\Phi^*\left(x_1, x_2, x_3^k \right) = -\frac{2}{\alpha_1 - \alpha_2} \left(\alpha_1 \Phi\left(x_1, x_2, x_3^k - D^1 \right) - \alpha_2 \Phi\left(x_1, x_2, x_3^k - D^2 \right) \right), \quad k = 1,2 \tag{8b}$$

cancels out the remaining normal traction on z=0. The indices u and l are denoting the upper and lower half-space.

The displacement vector field at the half-space boundary, the z-component of such representing the ground surface subsidence above a mined panel, is found by means of equations (3), (4) and (8) with setting $x_3^k = 0$.

Transversely isotropic material description

Stratified inter- and overburden rocks typical for the Southern and Newcastle Coalfields and many other coal basins in Australia can in many cases be represented by an equivalent transversely isotropic medium. The linear stress-strain state is completely determined by the symmetric effective stiffness tensor $\hat{c}_{ijkl}$ with the components of the tensor derived by the method of asymptotic averaging (Vlasov *et al.*, 2003) and taking the form

$$\hat{c}_{ijkl} = \langle c_{ijkl} \rangle + \langle c_{ijm1} c_{m1n1}^{-1} \rangle \langle c_{n1p1}^{-1} \rangle^{-1} \langle c_{p1q1}^{-1} c_{q1kl} \rangle - \langle c_{ijm1} c_{m1n1}^{-1} c_{n1kl} \rangle \tag{9}$$

where $c_{ijkl} = \frac{E}{2(1+v)}\left[\frac{2v}{(1-2v)}\delta_{ij}\delta_{kl} + \delta_{ik}\delta_{jl} + \delta_{il}\delta_{jk}\right]$ are the components of the stiffness tensor of an isotropic, linear elastic material and δ_{ij} is the Kronecker delta with $\delta_{ij} = \begin{cases} 1 & i = j \\ 0 & i \neq j \end{cases}$. Summation with respect to repeating subscripts is implied here. The indices i,j,k,l,m,n,p,q X {1,2,3} are in conformity with the axes of the Cartesian coordinate system x_1, x_2, x_3 with x_1, x_2 parallel and x_3 oriented normal to the bedding planes. *E* and n are the Young's modulus and Poisson ratio, respectively. The c_{ijkl}^{-1} are the components of the inverse stiffness or compliance tensor and

$$\langle * \rangle = \frac{1}{B}\sum_{i=0}^{N}b_i(*), B = \sum_{i=0}^{N}b_i \qquad (10)$$

denotes the weighted average of the variable * with the layer thickness b_i representing the weights and B being the total thickness of the N layers composing the layered material.

There is a vast amount of data on the geomechanical properties of the Southern and Newcastle Coalfields sedimentary strata in public documents and geoengineering consulting reports. Some of the data relevant to this study has been collated and a summary is presented in Table 1.

Table 1: Typical material properties for selected stratigraphic units of the Southern and Newcastle Coalfields, NSW, Australia

	E/E_m [GPa]	υ [-]	C [MPa]	φ [°]	σ_T [MPa]	Thickness [m]
Hawkesbury Sst	14/7.3	0.29	9.7	37.25	3.58	0 – 187
Newport Formation	11.6/6.1	0.25	8.85	35.00	3.4	18 – 50
Bald Hill Cst	10.4/5.4	0.46	10.60	27.80	2.9	6 – 67
Bulgo Sst	18/9.4	0.23	17.72	35.4	6.55	90 – 180
Stanwell Park Cst	19.2/10	0.26	14.57	27.8	4.83	5 – 23
Scarborough Sst	20.6/10.7	0.23	13.25	40.35	7.18	16 – 40
Wombarra Shale	17/8.8	0.37	14.51	27.8	4.81	7 – 30
Coal Cliff Sst	23.8/12.4	0.22	19.4	33.3	7.87	10 – 20
Munmorah Conglomerate	19/9.9	*0.25*	5	42	8	15 – 120
Interbedding of Sst, Ust, Cst	6 – 50/13	*0.26*	n/a	n/a	n/a	17 – 36
Wallarah Seams	3/1.6	*0.3*	n/a	n/a	n/a	1.4 – 4.6
Awaba Tuff	16 – 18/8.8	*0.29*	n/a	15 – 20	n/a	0.5 – 18
Laminite	7/3.6	*0.26*	n/a	n/a	n/a	0.3 – 5
Teralba Conglomerate	21/10.9	0.25	5	42	8	10 – 18

Note: E – Young's Modulus, υ – Poisson's Ratio, c – Cohesion, φ – Friction Angle, σ_T – Tensile Strength, Sst – Sandstone, Ust – Mudstone, Cst – Claystone, n/a – not available
E_m – rock mass modulus assuming $E_m = E(0.02 + 1/(1 + e^{(60-GSI)/11}))$ and GSI of 60 for all strata
Italic – Inferred from tests results of similar material
Sources: Keilich (2009), Colin and Bryce (2013), Pells (2004), Ditton (2013)

The effective stiffness tensor for a transversely isotropic rock mass typical for the overburden of collieries in the Southern and Newcastle Coalfields is computed using equations (9), (10) and the thicknesses and material properties listed in Table 1. Components of the effective stiffness tensor are transformed back into moduli and Poisson ratios for comparison purpose and are summarised in Table 2. This data set forms the basis for ground displacement computation outlined in the following section.

Table 2: Set of rock engineering parameters derived for transversely isotropic overburden above longwall panels in the Southern and Newcastle Coalfields

Parameter Set	$E_\perp$ [GPa]	$E_\parallel$ [GPa]	$v_{\parallel,\perp}$ [-]	$v_{\parallel,\parallel}$ [-]	$G_\perp$ [GPa]
Southern – Newcastle Coalfields	1.38	0.17	0.14	0.30	0.46

Note: $E_\perp$ – Young's modulus across bedding planes, $E_\parallel$ - Young's modulus along bedding planes, $v_{\parallel,\perp}$– Poisson's ratio ps, $v_{\parallel,\parallel}$ - Poisson's ratio pp, $G_\perp$ - Shear modulus across bedding planes.

Comparison of ground movement parameters derived FROMempirical and the displacement discontinuity model

The development of a subsidence trough above an extracted longwall panel results in differential vertical (tilt and curvature) and horizontal displacements (strain). Tilt refers to the change in subsidence over a given horizontal distance and is defined in units of mm/m. Tilt indicates the magnitude of surface gradient change across and along a subsidence trough. Curvature refers to the change in tilt over a given horizontal distance and is defined in units of mm/m^2 or 1/km. The curvature indicates the magnitude of surface bending across and along a subsidence trough. The inverse of curvature is the radius of curvature or bending (Figure 2).
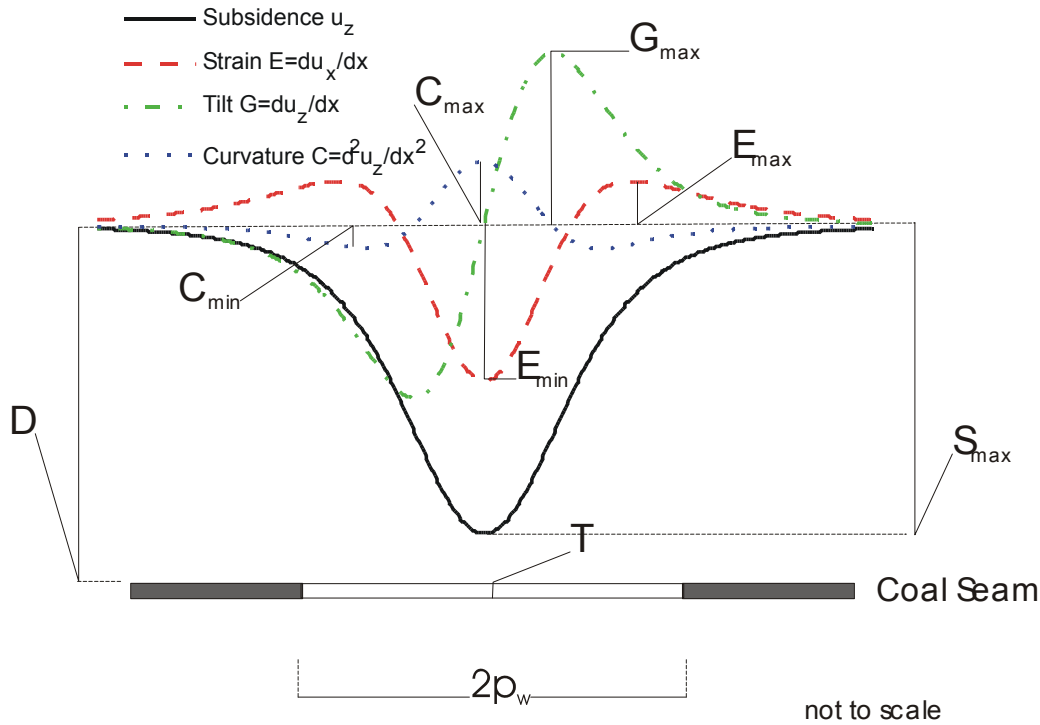
Figure 2: Subsidence and overburden distortion above an extracted longwall panel. Vertical scale strongly exaggerated. T: Extraction height of a panel, D: depth of panel, S$_{max}$: maximum subsidence and 2p$_w$: panel width

The validity of the displacement discontinuity model is exemplified by the ability to accurately resemble empirical relationships and ground movement parameter values obtained for the Southern and Newcastle Coalfields. In Figure 3 the computed maximum subsidence normalised by the panel extraction height is plotted against the panel width in terms of panel depth for a range of panel width to depth ratios typical for longwall mining in the Southern and Newcastle Coalfields. Data from both coal fields are well approximated for critical and super critical panels with width to depth ratios exceeding 0.8. For the lower width to depth range the model overestimates subsidence as a consequence of arching effects and partial closure typical for sub-critical panels, but not represented by the displacement discontinuity model. The large spread of data points can be partially attributed to variations in geomechanical parameters of the overburden, to changes in the depth to panel along the survey lines, to survey lines only partially crossing a panel and to the effects of multiple panel extraction.

In NCB (1975) linear correlations are established between the ratio of maximum subsidence, S_{max}, to depth of panel below ground surface, D, and observed (1) maximum convex and minimum concave strain, E_{max} and E_{min}; (2) maximum tilt G_{max} and (3) maximum convex and minimum concave curvature, C_{max} and C_{min}. The empirical relationships

$$K1 = \frac{E_{max}D}{1000S_{max}} \ , \qquad K2 = \frac{E_{min}D}{1000S_{max}}, K3 = \frac{G_{max}D}{1000S_{max}}, \quad K4 = \frac{C_{max}D}{1000E_{max}} \qquad (10\ a-d)$$

are based on data collected from British Coalfields.

Holla (1985) and Holla (1987) confirmed the linear relationships of equations (10 a) to (10 c) for subsidence parameters observed across longwall panels in the Southern and Newcastle Coalfields, respectively. More recent data are used in Holla and Barclay (2000) to derive a range of values for the proportionality factors of equations (10 a) to (10 c) with K1 ranging between 0.2 and 0.9, K2 between -0.9 and -1.5, K3 between 1 and 3 for panel width to depth ratios between 0.2 and 4. A value for K4 of 22 is reported in Keilich (2009) for the Southern Coalfield.
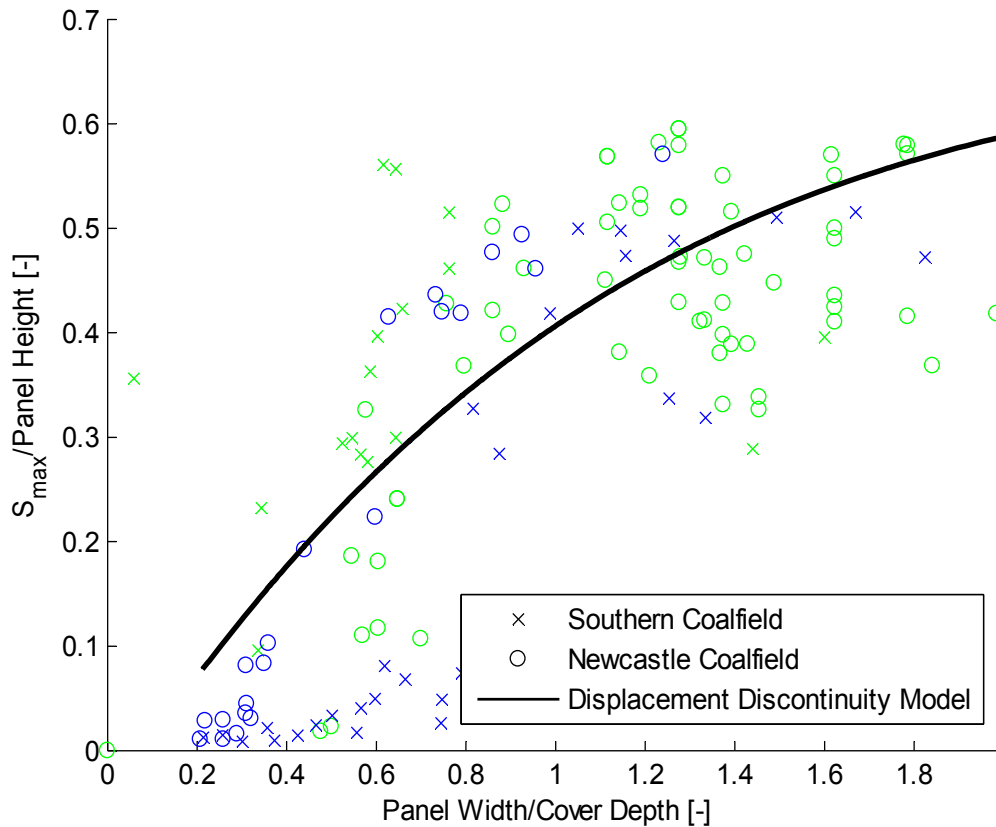
Figure 3:   Relationship between maximum subsidence and panel width in terms of depth. Color of markers represents different data sources: green - Ditton and Frith (2003), blue - Holla and Barclay (2000), red - this study)

The empirical relationships are tested with ground movement parameter values computed using the displacement discontinuity model described by equations (1) to (7) and a set of effective stiffness tensors derived above (Table). Both, the empirical linear and the mechanistic model relationships, are plotted in Figure 4 and Figure 5 together with subsidence parameter values obtained from subsidence monitoring of recent longwall mining and data reported in Ditton and Frith (2003).

(a)

(b)

Figure 4: Relationships between maximum tensile strain (a) and compressive strain (b) to maximum subsidence in terms of cover depth of longwall panel. Data sources: Ditton and Frith (2003) and collected field data
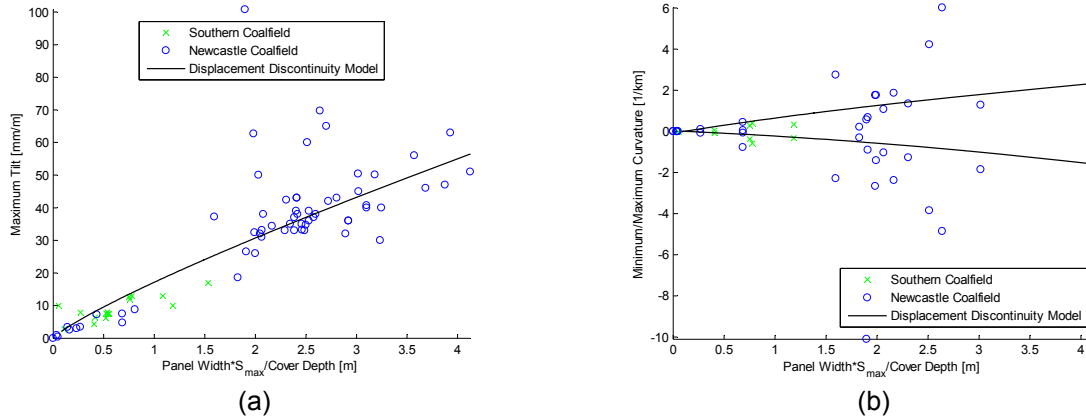
Figure 5: Relationships between maximum tilt (a), minimum and maximum curvature (b) to panel width and maximum subsidence in terms of cover depth for longwall panels with a panel width to cover depth ratio between 0.2 and 4. Data sources: Ditton and Frith (2003), Holla and Barclay (2000), and author's database

Solutions obtained from the displacement discontinuity model for a set of panel width to cover depth ratios between 0.2 and 4 are approximated using polynomial and potential functions to more easily compare the results with the empirical linear relationships of equations (10 a) to (10 d). The following non-linear approximation functions are a good fit, with a coefficient of determination R^2 close to 1 (R^2>0.98):

$$E_{max} = 376.9 \frac{S_{max}}{D}$$

(11a)

$$G_{max} = 29.8 \left(\frac{p_w S_{max}}{D} \right)^{0.8418}$$ (11b)

$$C_{max} = 0.0724 \left(\frac{p_w S_{max}}{D} \right)^3 - 0.3804 \left(\frac{p_w S_{max}}{D} \right)^2 + 1.6163 \left(\frac{p_w S_{max}}{D} \right) - 0.076$$ (11c)

$$C_{min} = -0.209 \left(\frac{p_w S_{max}}{D} \right)^2 - 0.4257 \left(\frac{p_w S_{max}}{D} \right) + 0.024$$ (11d)

The modelled relationship between maximum tensile strain and maximum subsidence in terms of cover depth is in close agreement with the empirical linear relationship and a K1 value of 0.38 was obtained. No such close agreement between the models is found for the maximum compressive strain with the model results plotting along a line for S_{max}/D below 0.0025 correlating well to data from the Southern Coalfield, but data points spreading more and more apart for S_{max}/D above 0.0025 with little correlation at values exceeding 0.01. Computed maximum tilt, maximum (convex) and minimum (concave) curvature do not correlate well with S_{max}/D as suggested by the empirical equations (10c) and (10d). However, when plotted against $p_w S_{max}/D$ computed as well as observed data points are in close agreement for maximum convex, minimum concave curvatures and maximum tilt.

CONCLUSIONS

As demonstrated by this study, the displacement discontinuity model of a single longwall panel in a transversely isotropic half-space can achieve results that are in close agreement with empirical model results and ground movement parameters obtain from monitoring data of the Southern and Newcastle Coalfields despite the simplicity of the mechanistic model. Differences between modelled and observed maximum subsidence in terms of panel height and maximum modelled and observed tilt are due to arching effects and partial closure typical for sub-critical panels, but not represented by the displacement discontinuity model.

The mechanistic method presented herein has the advantage over the empirical and influence functional methods in that it can be used for estimating ground movements due to panel extraction equally as for estimating subsurface stress and strain conditions. The method saves time, during repeated iterations of

the analytical solutions, making Monte-Carlo simulations for uncertainty assessment a feasible tool which would otherwise be impractical when used with numerical modelling (e.g. Flac3D, 3DEC). Last but not least the monitoring of ground displacement during extraction of a coal seam panel can be understood as a rock mechanical test and the displacement discontinuity model provides a means of inverse modelling for geomechanical parameter estimation of a large scale rock mass.   However, there is still scope for improvements in this approach and additional testing is recommended in order to further validate the proposed method and evaluate its potential for practical longwall mining impact and risk assessments.

REFERENCES

Bahuguna, P P, Srivastava, A M C and Saxena N C. 1991, A critical review of mine subsidence prediction methods, *Mining Science and Technology,* 15: 369-382.

Berry, D S and Sales, T W. 1962, An elastic treatment of ground movement due to mining – III three dimensional problem, transversely isotropic ground, *J. Mech. Phys. Solids*, 10: 73-83.

Colin, R W and Bryce, F J K. 2013, Background paper on New South Wales geology with a focus on basins containing coal seam gas resources, *Report issued to Office of the NSW Chief Scientist and Engineer by Unisearch Expert Opinion Services, UNSW Gobal Australia*, Sydney, 87 pp.

Ditton, S. 2013, Subsidence predictions and general impact assessment for the Mandalong Southern Extension Project, *Report prepared by DGS for Centennial Mandalong Pty Ltd, DGS Report No*, MAN-001/1, 12 August 2013

Ditton, S and Frith, R C. 2003, Review of industry subsidence data in relation to the impact of significant variations in overburden lithology and initial assessment of sub-surface fracturing on groundwater, *ACARP Project No. C10023*.

Elliot, H A and Mott N F. 1948, Three-dimensional Stress Distributions in Hexagonal Aeolotropic Crystals, *Mathematical Proceedings of the Cambridge Philosophical Society*, 44 (4): 522-533.

Holla, L. 1985, Mining Subsidence in New South Wales. 1. Surface Subsidence Prediction in the Southern Coalfield, *Department of Mineral Resources*, 32 pp.

Holla, L. 1987, Mining Subsidence in New South Wales. 2. Surface Subsidence Prediction in the Newcastle Coalfield, *Department of Mineral Resources*, 30 pp.

Holla, L and Barclay, E. 2000, Mine Subsidence in the Southern Coalfield, NSW, Australia, New South Wales, *Department of Mineral Resources*, 16 pp.

Keilich, W. 2009, Numerical modelling of mining subsidence, upsidence and valley closure using UDEC, PhD thesis, University of Wollongong, 355 pp.

Love, H. 1906, *A Treatise on the Mathematical Theory of Elasticity*, 551 pp (The University Press: Cambridge).

National Coal Board. 1975, *Subsidence Engineers' Handbook*, 2nd ed., 111 pp (National Coal Board: London).

Pells, P J N. 2004, Substance and Mass Properties for the design of Engineering Structures in the Hawkesbury Sandstone, *Australian Geomechanics*, 39:1 – 21.

Shield, R T. 1951, Notes on problems in hexagonal aeolotropic materials, *Mathematical Proceedings of the Cambridge Philosophical Society*, 47(2):401-409.

Vlasov, A N, Merzlyakov, V P and Ukhov, S B. 2003, Determination of deformation and strength properties of layered rock by asymptotic averaging, *Soil Mechanics and Foundation Engineering*, 40(6):197-205.

SYSTEMATIC APPROACH TO MITIGATE LONGWALL SUBSIDENCE INFLUENCES

Yi Luo

Abstract: The ground and surface subsidence process induced by longwall coal mining operations can cause adverse influences to subsurface and surface structures and water resources. Successful mitigation of these influences depends heavily on accurate assessment of the types, severities and locations of the subsidence-induced deformations and good knowledge of the structures. The most important step for mitigating subsidence influences is to accurately predict the dynamic and final movements and deformations in the area of interest. Based on the principle of influence function method, a series of subsidence prediction models have been developed for predicting dynamic and final surface and subsurface subsidence for longwall, room and pillar mining operations. The effects of inclined coal seam and steep surface terrains can also be considered the subsidence prediction. These prediction models have been validated with a large number of collected subsidence cases. With the accurately predicted ground deformations and good knowledge of structures, the types and severities of possible subsidence disturbances to the structures can be correctly assessed. For large and complicated structures, subsidence influences on structural stability, integrity and functionality have to be carefully considered. Once the causes and extents of the structural disturbances are identified, designing proper and cost-effective mitigation measures is often relatively easy. This systematic prediction-assessment-mitigation approach has been successfully employed in numerous applications.

INTRODUCTION

Subsidence associated with longwall mining operations generally has the potential to cause adverse effects to various surface and subsurface structures and water bodies. In order to cost-effectively reduce the severity of the subsidence influences, a systematic approach should be followed. The following three steps are involved in the approach: (1) accurate prediction of dynamic and final surface and subsurface movements (i.e., subsidence and horizontal displacement) and deformations (i.e., slope, strain, curvature, twisting and shearing), (2) accurate assessment of potential subsidence influences, and (3) properly designed and implemented subsidence mitigation measures.

In order to provide accurate subsidence prediction, mathematical and computer models have been developed for predicting dynamic (time-dependent) and final surface and subsurface subsidence associated with longwall mining operations. The developed subsidence prediction models have been calibrated and proven to be accurate innumerous cases of subsidence monitoring and structure mitigations. Various critical deformations have been derived and many assessment techniques have also been developed for assessing the potential and severity of subsidence influences to various surface structures. Techniques to mitigate the subsidence influences on various types of structures have also been developed and field tested. All the developed models and techniques have been used in a systematic way to predict, assess and mitigate longwall subsidence influences on surface structures.

Over the last two and half decades, this systematic approach has been improved and applied in mitigating: (1) over 300 residential structures ranging from simple trailers to large and complicated mansions as well structures on historic lists, (2) various buried water, gas, oil and sewage pipelines in varying pipeline material, sizes and constructions, (3) highways and railroads and their bridges, (4) various tower structures, (5) power substations, (6) reservoirs and dams, (7) investigation of various subsidence cases over inactive coal mines. In this paper, steps and techniques used in the systematic approach are presented.

SUBSIDENCE PREDICTIONS

The most important step for assessing and mitigating subsidence influences is to accurately predict the dynamic and final movements and deformations in the area of interest. Based on the principle of influence function method, a series of subsidence prediction models have been developed for predicting dynamic and final surface and subsurface subsidence for longwall and room and pillar mining

Department of Mining Engineering West Virginia University Morgantown, WV, USA, E-mail: tYi.luo@mail.wvu.edu

operations. Expanding the principle, models to consider effects of inclined coal seam and steep surface terrains have also been developed. These prediction models have been validated with a large number of collected subsidence cases.
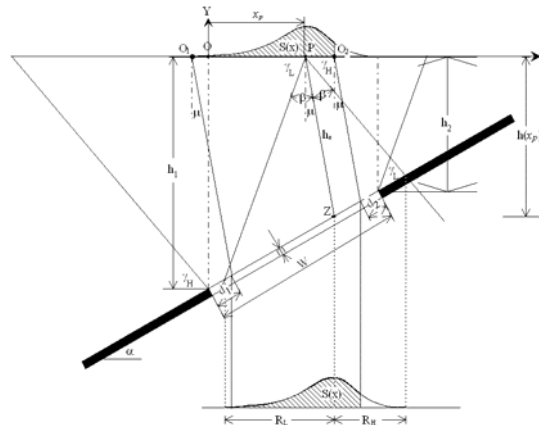
Final subsidence predictions

The principle of the influence function methods is used in developing mathematical models for predicting final surface and subsurface subsidence. The original influence function method (Knothe, 1957) is the backbone of the mathematical model for predicting final surface subsidence when both the extracted coal seam and surface are level or nearly level. It states that the extraction of an elemental area of an underground coal seam causes a surface point to subside in a particular manner. Generally, the point located directly above the extracted element receives the most subsidence. The farther the point is away from the extracted element, the less amount of influence is received. The mathematical function selected to represent the distribution of the subsidence influence caused by the elemental extraction is called the influence function. The final subsidence at a surface point is the result of all influences received at this point when the coal seam in the "mined area" has been extracted element by element. Mathematically, the final subsidence at a surface point is expressed as the integral of the influence function throughout the "mined area". The complete derivations of the mathematical expressions for the final surface movements and deformations have been presented elsewhere (Luo, 1989; Luo and Peng, 1989). In order to assure subsidence prediction accuracy, great effort has been made to monitor subsidence events and to collect subsidence cases from various sources. A set of final subsidence parameters have been derived from each of the collected cases and the empirical formulae have been developed for the parameters (Peng, *et al.*, 1995). The combination of the sound mathematical model and the reliable subsidence parameters result in a proven final subsidence prediction model.

The principle of the influence function method lays out a good foundation for expanding it into the development of prediction models for various application conditions. It is a well-known fact that the characteristics of surface subsidence in hilly terrains could be very different from that on level ground. The first expansion of the influence function method was the development of a comprehensive subsidence prediction model to consider the hilly surface terrains (Peng and Luo, 1988; Luo and Peng, 1999). In this model, the additional surface movements, other than that normal subsidence expected on level ground, occur along the interface between the topsoil and bedrock and within the topsoil zone. The intensity of the terrain effects on ground movements depends on slope angle, thickness, wetness and mechanical property of the soil zone.

Longwall mining in inclined coal seams has been a common practice in some major coal mining countries. The characteristics of the final subsidence basin induced by longwall operation in inclined coal seams are different from that caused by mining in a level coal seam. An influence function method is developed for the prediction of the final surface movements and deformations over a longwall panel extracted in an inclined coal seam (Luo and Cheng, 2009). The German experience and the findings from subsidence research in the US have been combined in developing an asymmetric influence function as shown in Figure 1. The degree of asymmetry of the influence function is dependent on the angle of the seam inclination. The determination of final subsidence is performed through a modified scheme of integrating the influence function between the inflection points.

The subsurface strata movements and deformations induced by the longwall subsidence process could affect the stability of subsurface mine structures, surface water bodies and subsurface aquifers and the emission and migration of methane. In order to understand such effects, subsurface subsidence prediction methods have been developed using the concept of influence function method. The first version was developed based on surface subsidence theory (Luo and Peng, 2000). This model can predict final subsurface subsidence but it could not take the variation of overburden stratification into consideration. This model was enhanced later (Luo and Qiu, 2012). In the enhancement, the overburden strata over a longwall gob are divided into a finite number of layers of equal thickness. The percent of the hard rock strata (i.e., sandstone and limestone) in each of the layers is calculated and used as an input. The subsidence on the top surface of a given layer can be determined in the following procedure: (1) transforming the overburden load above it into a uniform equivalent load on the layer; (2) defining the subsidence influence function at a prediction point using the equivalent load, layer thickness, percent of hard rock and vertical movement at the layer bottom directly under the prediction point; (3) integrating the influence function within a proper horizontal interval for the final subsidence on the top of the layer. Therefore, the influence function is no longer a fixed function as in the previous models but varies with location and strata composition. The source causing subsidence of the current layer is the magnitude and distribution of the vertical movement directly under the layer. This procedure is repeated from the

mining horizon, layer by layer upwards, until the ground surface is finally reached. Through this approach, the effects of the overburden stratification, especially the massive hard rock strata, on subsurface subsidence can be considered. In the subsurface subsidence prediction model, one new and useful deformation term, total strain, is also introduced and determined. The total strain reflects the volumetric change of the overburden strata at a given point.

Figure 1: Diagram showing relations for using influence function method to predict final surface subsidence over a longwall gob in inclined coal seam

Dynamic subsidence prediction

For most longwall mining operations, the time-dependent dynamic subsidence process can bring more disturbances to common structures than the final subsidence. Based on field subsidence monitoring, the dynamic subsidence process associated with longwall mining operations can be divided into four phases (Luo, 1989; Luo and Peng, 1992). The first three phases are shown in Figure 2 in which the surface subsidence profiles and the corresponding locations of the longwall face are plotted. The first dynamic subsidence phase is the subsidence initiation and development process in the initial stage of mining a longwall panel. This phase is characterised as having no or little surface subsidence until the longwall face has reached a subsidence-initiation distance and it is immediately followed by a sudden and rapid subsidence process (Figure 2a). It should be noted that the disturbance power associated with this phase is much stronger than any other dynamic subsidence phase. In shallow mines, large ground cracks could often occur at locations a short distance inside the panel setup entry. The second phase is the normal dynamic subsidence process in which the portion of the subsidence basin on the face side advances with the longwall face while it moves toward the recovery line of the panel as shown in Figure 2b. The normal subsidence phase is the simplest among the dynamic subsidence phases and the shape of the dynamic subsidence basin on the moving face side is milder than the final one on the setup entry side. The third is the residual subsidence phase occurring after the longwall face stops advancing. It is a transitional process for the ground to subside from its normal dynamic state to its final stage (Figure 2c). Most of these three dynamic subsidence phases last from 10 days to one month in US longwall operations before the final subsidence at a point is reached. The last phase is the long-term dynamic subsidence phase that could last for years (Luo, *et al.*, 1997; Luo and Peng, 2000). The causes for the long-term phase are re-compaction of the disturbed overburden strata and/or creep deformation of remnant mine structures. Generally, most of the long-term subsidence process is very minor and un-noticeable. However, the gradual failure of mine structures due to insufficient long-term stability (e.g., the chain pillar systems separating adjacent longwall panels) could induce significant long-term subsidence. Prediction methods have been developed for all these dynamic subsidence phases (Luo and Peng, 1992, 2000).

Based on the prediction methods, the following two subsidence prediction program packages have been developed.

Comprehensive and Integrated Subsidence Prediction Model (CISPM) is a computer program package for predicting surface the final and dynamic subsidence induced by underground mining operations conducted in a single coal seam. It predicts final subsidence basin for coal extraction in a longwall section of up to 10 panels, over an irregular (non-rectangular) underground opening (Luo and Peng, 1993), and the complete dynamic (time-dependent) subsidence process associated with longwall mining operations. It also provides services such as recommending subsidence parameters based on the site

specific geological and mining information, deducing the final subsidence parameters from collected subsidence data, processing and managing subsidence survey data. This program package has been successfully employed in numerous application cases for assessing and mitigating the subsidence influences on various surface structures and environment.

a. Initiation Phase   b. Normal Phase   c. Residual Phase
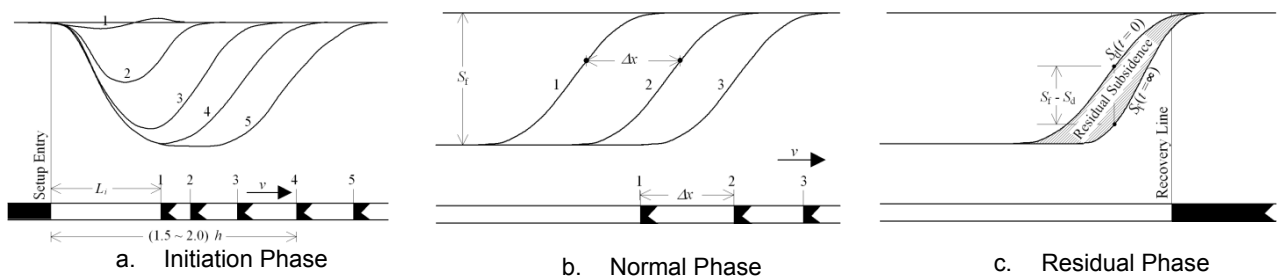
Figure 2: Dynamic Subsidence Phases Associated with Longwall Mining Operation

Subsidence prediction programs

Comprehensive and Integrated Subsidence Prediction Model – Multiple Seam (CISPM-MS) is a program for the prediction of the final surface movements and deformations caused by mining operations in multiple coal seams (Luo and Qiu, 2012). The operations can be conducted using longwall and/or room and pillar mining methods. In the prediction, the final surface movements and deformations at a surface point caused by the individual mining operations in multiple coal seams are summed. The effects of Multiple Seam Mining (MSM) interactions on the stability of remnant mine structures based on subsurface subsidence prediction are assessed. The additional subsidence caused by the failed mine structures due to MSM interactions in sufficiently large continuous areas is determined and included in the final surface subsidence.

ASSESSMENTS OF SUBSIDENCE INFLUENCES

As a caving method, longwall mining operations induce immediate surface subsidence that is generally capable of disturbing surface structures, surface and subsurface water bodies to varying degrees. For surface structures, a longwall subsidence event can cause structural integrity, stability and functionality problems.The severities of these subsidence disturbances depend on the magnitude of ground deformations, the characteristics of the structures and the natural surroundings. In order to gain a good knowledge of the structural and surrounding information, a careful site visit should be made to collect information such the geometry, materials, construction, strength and weaknesses and existing conditions of the structures. The ground condition (i.e., slope, approximate depth and wetness of the soil zone) should also be checked and documented. The distribution of expansive total strain (or called void intensity) in the overburden strata plays an important role in determining subsidence effects on surface and subsurface water bodies. Accurately assessing the types, severities and timing of subsidence influences provides hints for generating effective mitigation plans.

Critical surface deformations

For most of the common surface structures, it is the ground deformations that cause the problems. Based on extensive monitoring of structural responses to subsidence process, various critical deformations have been derived for various types of structures. A critical deformation is the minimum deformation to start a structural problem.

Subsidence-induced surface strain, especially tensile strain, is responsible for most of the integrity problems to the structural parts that have direct contact with the ground such as foundations, basement walls, and the lower part of building walls. The critical strains are:

- Cracks on soil surface: 1.2×10^{-2} m/m (ft/ft)
- Cracks on asphalt surface: 1.0×10^{-2} m/m (ft/ft)
- Cracks on concrete pavement: 2.0×10^{-3} m/m (ft/ft)
- Cracks on stone walls: 3.0×10^{-3} m/m (ft/ft)
- Cracks on brick and concrete-block walls: 2.0×10^{-3} m/m (ft/ft)

Curvature often is the second largest contributor to the integrity problems on the common structures, especially the super-structures. Curvature normally would have little effects on small structures. For typical residential structures, a curvature larger than 2.0×10^{-4} 1/m (6.0×10^{-5} 1/ft) could cause hairline cracks at building corners and joint lines and step cracks at the corners of doors and windows, etc.

Subsidence-induced surface slope could affect the stability of tall and slim structures such as chimneys, silos, towers. For residential structures, high slope (> 1%) could make them uncomfortable to live and could render their drainage systems unworkable. Compared to the permissible grade of 0.7% for railroad operation, the maximum subsidence-induced slope associated with longwall operations can easily disrupt normal railroad operation.

Residential and farm structures

For most residential and farm structures, the potential subsidence influences can be assessed by comparing the predicted deformations to the derived critical values while considering the dimensions, complexity, existing conditions, construction materials and methods. If a structure is located on or near long and steep sloping ground, the potential influences from the topography effects should also be assessed. Under certain conditions, the topography effects could be even stronger than those caused by subsidence alone. The assessments are normally conducted in two separate steps. The first step is to assess the potential influences caused by the predicted final surface deformations that will be permanently imposed on the surface structures. Final subsidence-induced problems normally occur in a zone along the panel edges. The second step is to assess the potential influences from the dynamic subsidence process. The structures located over the panel setup entry and the "central" portion of the panel will experience a significant time-dependent deformation process. The typical ground dynamic deformation process can be divided into two half stages. In the first half, a ground point will go through a process of increasing tension, maximum tension, decreasing tension and maximum slope. In the second half, the point will experience an increasing compression, maximum compression and decreasing compression process. Normally, convex curvature is accompanied with tensile strain while concave curvature goes with compressive strain. The first half of the dynamic subsidence is much more critical to common surface structures than the second half. In addition to the magnitudes of the maximum deformations, the locations from where the destructive deformations originate should also be identified.

Industrial and public structures

Industrial and public buildings include large workshops, telecommunication towers, power transmission towers and transformer stations, water towers or tanks, bridges, office and school buildings. For large structures with special purposes, the assessment of subsidence influences could be much more complicated than that for residential structures. These structures could be significantly different in structural designs and constructions as well as function tolerance limits. Accordingly, the assessment techniques for each type of structure could be different from the others. Therefore, in the stage of pre-mining site visit and information collection, detailed information about the structure and its performance limits should be obtained. Since most of these structures are large and inflexible, the subsidence-induced surface strains and curvatures are often fully capable of causing structural integrity failures such as cracks on and severe deformations of structural parts. Losing the intended structural functions is often the main concern for these structures. For example, telecommunication towers' long-distance signal relay function could be affected by subsidence-induced surface slope and differential horizontal displacement. The stability of tall structures with small bases during and after the subsidence process should be carefully assessed using the predicted subsidence-induced surface slope. Generally, most of the longwall subsidence events are unable to move the center of gravity of a tall structure out of its base. However, an inclined tall structure due to subsidence influence may have a reduced capacity to resist the force of strongest wind to be experienced and the stability under such condition should be assessed. The techniques to assess subsidence influences have been presented in other publications (Luo, *et al*., 2003, 2005; Luo, 2008).

Linear structures

Longwall subsidence could induce adverse influences to linear structures such as highways, power transmission lines, railroads, overland conveyors are buried pipelines. Among these linear structures, railroads, overland conveyors and buried pipelines are generally more prone to be adversely affected by longwall subsidence than the others because of the structural complexity and stringent performance tolerance limits. For highways, tensile strains higher than 2.0×10^{-3} and 1.0×10^{-2} m/m (ft/ft) could create cracks on concrete and asphalt pavements, respectively. High compressive strain (>3.0×10^{-3} m/m or

ft/ft) can create bumps on the asphalt pavements. For highways with a large gradient (e.g., >5%), the subsidence-induced slope could make driving unsafe if the speed limit is not lowered. For railroads, the subsidence-induced strain and curvature can affect the integrity problems to the railroad structures. The slope can easily affect the operability of rail traffic. Mine subsidence events can cause significant damages to highway and railroad bridges and affect the safety of their traffic (Luo and Peng, 1994). A subsidence event can induce significant additional stresses on buried pipelines. Methods to estimate stress distribution along buried pipelines have been recorded by (Peng and Luo, 1988; Luo, *et al*., 1997; Qiu and Luo, 2013). The methods have been developed and have been successfully applied to assess the subsidence influences to pipelines of various sizes, pipe materials, and transmitted media. Generally, the ground strain and curvature contribute the majority of the additional stresses on the pipeline.

Water bodies

Surface water bodies (i.e., streams, ponds, reservoirs) and subsurface aquifers could be impacted by longwall subsidence. The two significant subsidence influences to surface water bodies are dewatering and water pooling. To the subsurface aquifers, the influences could be temporary (able to recover some time after the subsidence event) and permanent water losses (Luo and Peng, 2010). In flat surface area or along steam valleys with gentle gradient, a longwall subsidence event can create surface water pools. The severity of other subsidence influences on surface and subsurface water bodies depend on the magnitude and distributions of the subsurface deformations, geological and hydrological system of the overburden strata. The subsurface subsidence prediction model provides a good tool for studies of the effects of longwall mining on the hydrological system. The subsurface expansive total strain (volumetric expansion of subsurface strata or void intensity) indicates the total voids in a unit volume of subsurface strata induced by the subsidence. Figure 3 shows that predicted distribution of subsurface total stain over a longwall gob. Apparently, expansive total strain is mainly concentrated in zones located a short distance inside the panel edges.

Since water loss would not occur in the continuous deformation zone in the overburden strata, the maximum void intensity at the upper limit of the fractured zone can be used as the critical value for assessing the subsidence influences on the subsurface hydrologic system. Based on the results of water drawdown tests in more than 200 boreholes in 27 Chinese coal mines (Liu, 1981) and subsurface subsidence prediction, the critical void intensity for significant water loss is determined to be 4.1×10^{-2} m/m (ft/ft). It indicates that when a block of rock expands 4.1% more than its original volume, the voids inside the deformed rock would allow a significant amount of water to flow through it. When a contiguous zone with void intensity higher than the critical value intersects with either a surface water body or an underground aquifer, significant water loss could occur through this zone into the longwall gob causing permanent loss of the water body.
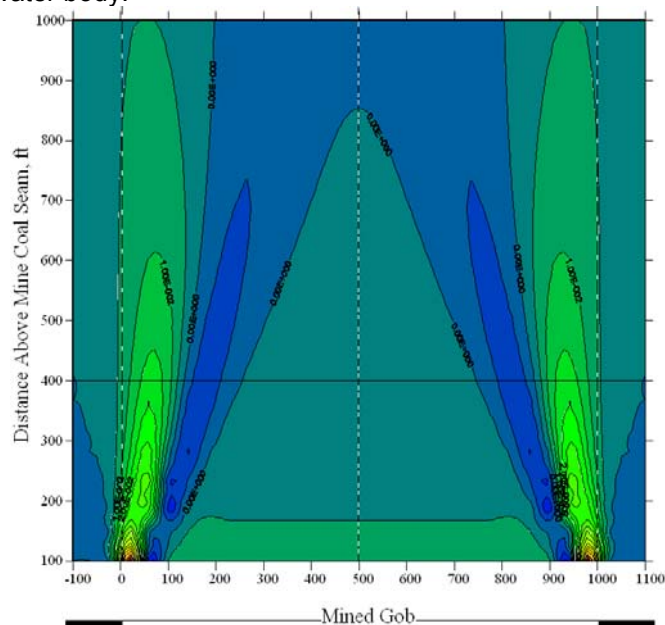
Figure 3: Predicted subsurface total strain over a longwall panel

In order to facilitate the quantitative evaluation of the water loss, subsidence-induced permeability in the overburden strata should be estimated. Under the influence of mine subsidence, the permeability at a given subsurface point (K) affected by subsidence is linked to the total strain (ε_t) by Equation 1. In the equation, K_o and ϕ_0 are the original permeability and porosity before subsidence. An example of using the subsurface subsidence prediction model in numerically assessing the effects of a longwall mining operation on a surface reservoir is shown in a publication (Qiu and Luo, 2013).

$$K = K_o \left(\frac{1 + \dfrac{\varepsilon_t}{\phi_0}}{1 + \varepsilon_t} \right)^3 \tag{1}$$

MITIGATION MEASURES

Various mitigation measures has been developed and applied to reduce subsidence influences on numerous surface structures and water bodies. Properly selected, designed and implemented mitigation measures can greatly reduce and even eliminate the anticipated subsidence influences.

Mitigation methods such as compensation trench, tension cable or rope, plane fitting, internal and external bracing are commonly and successfully employed to protect subsidence influences to common residential and farm structures. Properly designed and constructed compensation trenches can be used to reduce the severity of the subsidence-induced disturbances to structural parts having direct contact with ground such as structural foundation, basement walls and floor pavement. A well designed compensation trench creates a weak plane between the structure and the strain-generating ground as shown in Figure 4. The weak plane reduces the transmission of ground strain from the strain-generating ground to the structure and then the severity of the structural problems on the ground-contacting structural parts.

The tension cable method is suitable for structures that have relatively high compressive strength such as stone, concrete-block and brick structures or structural parts. The structure to be protected is wrapped with pre-tensioned steel wire cables at properly selected locations and with proper tensions (Figure 4). The tension cables can serve two purposes: (1) the tension forces applied by the cables place the structure into a compression state so that it is able to compensate some of the subsidence-induced final or dynamic tensile stresses, and (2) the rigidity of those structural parts is increased so that they can tolerate higher deformations transmitted to it. The tension cable method can also indirectly reduce the severity of the anticipated problems on the super-structures caused by dynamic and final surface curvature if the deformation on the structural part under the super-structure can be effectively controlled. For weaker wood structures, the tension rope method serves the same purposes as the tension cable.
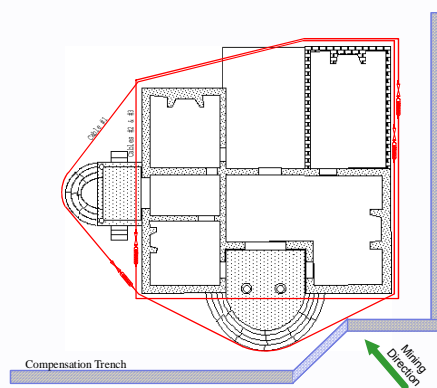
Figure 4: Mitigation Measures for a Historic House Located over the Central Portion of a Longwall Panel

The plane-fitting method (Luo and Peng, 1991) is a method to reduce the severity of disturbance to super-structure. It is particularly effective for structures that would experience a very intensive dynamic subsidence process such as those located over the central portion of subsidence basins over shallow

mines. Height adjustable devices are strategically placed under the super-structure and their heights are adjusted constantly according to the measured subsidence and a mathematical algorithm so that the super-structure is placed on a time-dependent inclined plane at any given time. By doing so, the protected structure is stress-free. In determining the desired inclined plane at a given time, the total amount of required adjustment should be minimised.

The external or internal bracing method is used to reinforce the weak spots (e.g., large doors, windows and indent parts.) of the structure. The bracing structures such as wood frames or steel beam should have good compression stiffness to resist any significant closure of these weak spots. Figure 4 shows an external bracing structure used to prevent potential closure of two wings of a U-shaped structure while tension cables were applied.

For large and linear industrial/public structures, the mitigation measures could vary considerably. In assessing subsidence influence on buried pipeline, it is found that the majority of the stress (>80%) on the pipeline is caused by strain transmitted to the pipeline (Luo, *et al*., 1997). Since the ground strain is transmitted to the buried pipeline through friction force, reducing the friction force between the burial soil and the pipeline will be the most effective way to reduce stresses on the pipeline. Uncovering the pipeline is the most effective way to reduce the friction force. In order to reduce the amount of the required mitigation work and to avoid unnecessary artificial disturbance to the buried pipelines, partial uncovering method has been proposed to uncover only the sections of pipelines where the estimated stresses exceed the permitted stress of the pipe steel. This partial uncovering method has been successfully employed in protecting numerous and varying types of buried pipelines.

Longwall subsidence can induce sufficient deformation that can cause structural damage to the railroads and affect the safety of rail traffic. In order to reduce the severity of such subsidence influence, it is ideal to lift the railroad track back to its original level as it is subsiding. However, it is often impractical to do so because of the limited window of time between railway traffic or the limited rail base space for placing the required additional ballast. A partial lifting method has been proposed and successfully employed to maintain the railroad operational under such limitations (Luo, *et al*., 2010). The essence of the partial lifting method is to raise the subsiding railroad track at a given time only a determined partial amount of the subsidence so that the rail tracks can be maintained on a smooth and operational profile. The required adjustment is made by adding ballast under the track. The application of this method requires a careful pre-mining planning based on the simulations of dynamic and final subsidence predictions. When implementing the method, a daily subsidence survey is required. The measured ground movements are used to generate an adjustment plan that can be made within the available window of time based on a special algorithm. The most recent application of this method was on a 2,400-m long section of railroad located over two longwall panels (top left photo in Figure 5). In this case, the railroad experienced a maximum subsidence of 1.524 m (5 ft). The coal trains were safely operated in two-hour intervals while it was subsiding. Figure 5 also shows some of the large and important structures that were affected by longwall subsidence and have been successfully protected with the systematic approach.
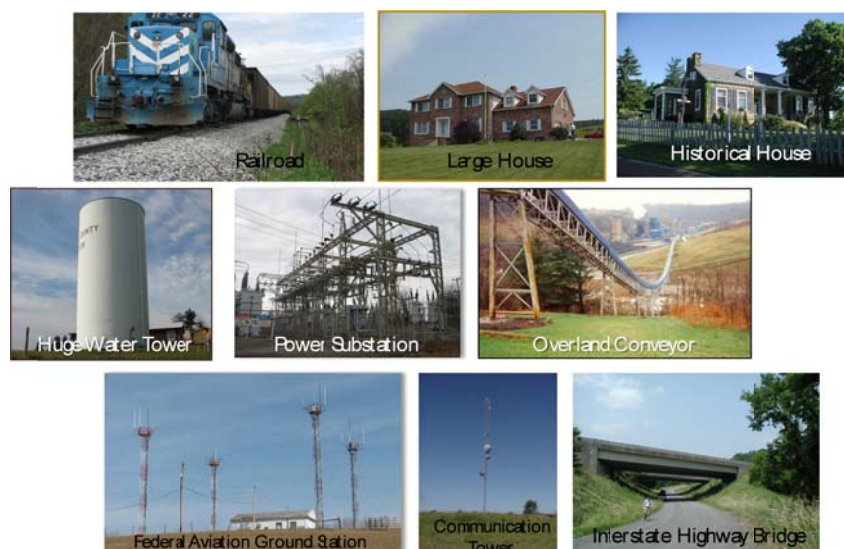

Figure 5: Examples of mitigated surface structures using the systematic approach

CONCLUSIONS

Longwall mining operations induce immediate and intensive surface and subsurface movements and deformations that could cause adverse effects to surface and subsurface structures and water bodies. A systematic approach, including accurate subsidence prediction, correct assessment and effective mitigation of the potential subsidence influences, has been developed and successfully applied to protect numerous surface structures over longwall mines. The application of this approach has been proven to be cost effective to the mining companies and helped to improve the public relations with local residents.

REFERENCES

Knothe, S. 1957, Observations of Surface Movements under Influence of Mining and Their Theoretical Interpretation, Leeds, s.n, pp 210-218.

Liu, T. 1981, Surface Movements, Overburden Failure and Its Applications, *Beijing, China: Coal Industry Publishing Co.*

Luo, Y. 1989, Integrated Computer Model for Predicting Surface Subsidence Due to Underground Coal Mining - CISPM (Ph.D. Dissertation), Morgantown: West Virginia University.

Luo, Y. 2008. Assessment and Mitigation of Subsidence Effects on a Tall Self-Supporting and Free-Standing Communication Tower, Morgantown, WV, s.n, pp 153-160.

Luo, Y and Cheng, J. 2009, An Influence Function Method Based Subsidence Prediction Program for Longwall Mining Operations in Inclined Coal Seams, *J. of Mining Science and Technology,* 19(9), pp. 592-598.

Luo, Y, Kimutis, R, Yang, K and Cheng, J. 2010, Mitigation of Longwall Subsidence Effects on Operating Railroad, Morgantown, WV, s.n, pp 89-96.

Luo, Y and Peng, S. 1989, *CISPM -- A Subsidence Prediction Model.* Morgantown, WV, USA, A.A. Balkema, Botterdam, Netherlands, pp 853-860.

Luo, Y and Peng, S. 1991, *Protecting a Subsidence Affected House -- A Case Study.* Lexington, KY, s.n., pp 297-300.

Luo, Y and Peng, S. 1992, *A Comprehensive Dynamic Subsidence Prediction Model for Longwall Operations.* Woolongong, Australia, s.n, pp 511-516.

Luo, Y and Peng, S. 1993, *Using Influence Function Method to Predict Surface Subsidence caused by High Extraction Room and Pillar Mining.* Calgary, Alberta, Canada, s.n, pp 342-353.

Luo, Y and Peng, S. 1994. *Monitoring Railroad Response to Mining Subsidence and Assessment of Subsidence Influence to Railroad -- A Case Study.* Morgantown, WV, s.n, pp 308-319.

Luo, Y and Peng, S. 1999, Integrated Approach for Predicting Mining Subsidence in Hilly Terrain. *Mining Engineering,* pp 100-104.

Luo, Y and Peng, S. 2000. Long-Term Subsidence associated with longwall mining – Its Causes, Magnitude and Developmen, *Mining Engineering,* Volume 10, pp 49-54.

Luo, Y and Peng, S. 2000, Long-Term Subsidence Associated with Longwall Mining – Its Causes, Magnitude and Development, *Mining Engineering,* Issue 10, pp 49-54.

Luo, Y and Peng, S. 2000, *Prediction of Subsurface Subsidence for Longwall Mining Operations,* Morgantown, WV, USA, s.n, pp 163-170.

Luo, Y and Peng, S. 2010, Subsurface Subsidence Prediction Model and Its Potential Applications in the Study of Longwall Subsidence Effects on Hydrologic System. *SME Transactions,* Volume 326, pp 458-465.

Luo, Y, Peng, S and Chen, H. 1997, *Long-Term Subsidence over Longwall Chain Pillar Systems and Its Effects on Surface Structure.* Morgantown, WV, s.n, pp 43-49.

Luo, Y, Peng, S and Chen, H. 1997, Protection of Pipelines Affected by Surface Subsidence. *SME Transactions,* Volume 302, pp 2202-2207.

Luo, Y, Peng, S and Chen, H. 1997, Protection of Pipelines Affected by Surface Subsidence. *SME Transactions,* Volume 302, pp 2202-2207.

Luo, Y, Peng, S and Kudlawiec, R. 2005, *Mitigating Longwall Subsidence Effects on a Large Industrial Building.* Morgantown, WV, s.n, pp 130 -136.

Luo, Y, Peng, S and Miller, B. 2003, *Influences of Longwall Subsidence on a Guyed Steel Tower – A Case Study.* Morgantown, WV, USA, s.n, pp 360-366.

Luo, Y and Qiu, B. 2012, *CISPM–MS: a Tool to Predict Surface Subsidence and to Study Interactions associated with Multi–seam Mining Operations.* Morgantown, WV, USA, s.n, pp 1-7.

Luo, Y and Qiu, B. 2012, Enhanced Subsurface Subsidence Prediction Model that Considers Overburden Stratification, *Mining Engineering,* 64(10), pp 78-84.

Peng, S and Luo, Y. 1988, Determination of Stress Field in Buried Thin Pipeline Resulting from Ground Subsidence Due to Longwall Mining, *Mining Science and Technology,* Volume 6, pp 205-216.

Peng, S and Luo, Y. 1988, Slope Stability Under Influence of Ground Subsidence Due to Longwall Mining. *Mining Science and Technology,* pp 89-95.

Peng, S, Luo, Y and Zhang, Z. 1995, Subsidence Parameters -- Their Definitions and Determination. *AIME-SME Transactions, Vol. 300,* pp 60-65.

Qiu, B and Luo, Y. 2013, *Applications of Subsurface Subsidence Model to Study Longwall Subsidence Influences on Overburden Hydrological System.* Charleston, WV, s.n.

Qiu, B and Luo, Y. 2013. *Improved Model to Assess Stress Condition on Buried Pipelines Affected by Mine Subsidence.* Montreal, Canada, s.n.

NUMERICAL SIMULATION OF SEISMIC DYNAMIC RESPONSE OF GROUND SURFACE ABOVE MINED-OUT AREA

Xiaoming Zhang[1], Xiaochen Yang[2], Zuo Wang[3] and Kyuro Sasaki[4]

ABSTRACT: Most coal mines are in the seismic intensity 7（12 degree evaluation or even higher in China. Large-scale mined-out spaces formed in the strata have been increased, because of excessive coal mining exploitation. The seismic response of mine surface will be different from other places because of the impact of the mined-out area on the seismic wave's propagation. This paper studies the seismic response acceleration, peak acceleration and displacement at the ground surface above unstable and compacted mined-out areas by FLAC3D numerical models for various conditions. The results of the numerical simulation are consistent with the surface seismic response of Zhaogezhuang Mine in the Tangshan earthquake, 1976. It has been shown that the seismic damage to the surface above the mined-out area especially to the surface above the boundary of the mined-out area was slightly less than those in other places at the ground surface, and the seismic damage to the surface which is 2-3 times the size of mined-out area's width, away from the mined-out area boundary was more severe than those in unexploited places. The surface area which is more than 4 times the size of the mined-out area's width away from the mined-out area boundary was not affected by seismic damage.

INTRODUCTION

The effect of underground structure such as roadway and chamber in coal mine on the seismic wave propagation is little because the size of them is smaller than the seismic wavelength. However, if the size of underground structure (such as large-scale mined-out area) and seismic wavelength are in the identical order of magnitude, the propagation of the seismic wave will be changed because of the mined-out area. A series of complex reflection and transmission are generated because of the different wave impedance in rock medium and the impact of mined-out area space .In addition, scattering will occur around irregular boundary of the mined-out area. These phenomena may generate large impacts on the dynamic seismic response at the ground surface. Previous studies have investigated the earthquake effect on the underground structure and the dynamic response of ground surface above shallow-buried chambers. This paper aimed to study the effect of deep mined-out area in coal mines on the dynamic response of the surface with the combined method of measured data and numerical simulation. The measured data about the dynamic response of ground surface in coal mine is deficient. In view of some detailed data of surface damage are recorded when a great earthquake happened in Tangshan city（China, 1976） where many collieries are located. This paper collected and studied the measured data of Zhaogezhuang Mine recorded by China Seismological Bureau in Tangshan to analysis the impact of the mined-out area on dynamic response of the ground surface. The measured displacement on the ground above the mined-out area and surrounding terrain which is near the mined-out area, and the destruction degree of the industrial square and civil buildings nearby is emphatically analysed. In addition, the seismic response of the ground surface above the mined-out area has been simulated by and analyzed by FLAC3D models for various conditions. The conclusions will give reference for the site selection of industrial and civil buildings near coal mines, stability of the buildings located near coal mines and coal mine reconstruction after earthquake.

DYNAMIC RESPONSE OF GROUND SURFACE IN ZHAOGEZHUANG MINE

Distribution of mine-out area

Zhaogezhuang Mine is located in Guye, northeast of Tangshan in Hebei province. The strike length of mine field is 9050 m and mining area is 31.55 km^2. The deep boundary of mine field is -1200 m around. The coal mine has mined ninth level when the earthquake happened in Tangshan, 1976. The mining

---
[1] *Institute of Engineering and Environment Liaoning Technical University, Huludao 125000, China. Email: xiaochen2024@163.com*
[2] *DFmc Technology Co., Ltd., Department of Communication Navigation, Dandong 118000, China*
[3] *College of Mining Engineering Liaoning Technical University, Fuxin 123000, China*
[4] *Kyushu University, Faculty of Engineering, Nishiku, Fukuoka 819-0385, Japan. Email: krsasaki@mine.kyushu-u.ac.jp*

depth is -735 m. The strike length is 4.5 km. The tendency length is 1.6 km. The mined-out area went up to 7.2 km^2 whose distribution is show in Figure 1.

Figure 1 shows the change rule of mined-out area distribution with time flow. The distribution arrangement of mined-out area is large because the coal mine has a long history of about one hundred years. At present, the mined-out area is about 10.02 km^2, of which east flank is 5.54 km^2 and west flank is 4.48 km^2.The mined-out area had gone up to 7.2 km^2 when the earthquake happened in Tangshan. This paper reports on the study by the seismic geological brigade of Chinese seismological bureau, comparing the local coordinates of the area based on the survey of surface deformation after the earthquake,. The surface deformation of the industrial square, surface above mined-out area, the surface above the mined-out area boundary and the village surface nearby are shown in Table 1.
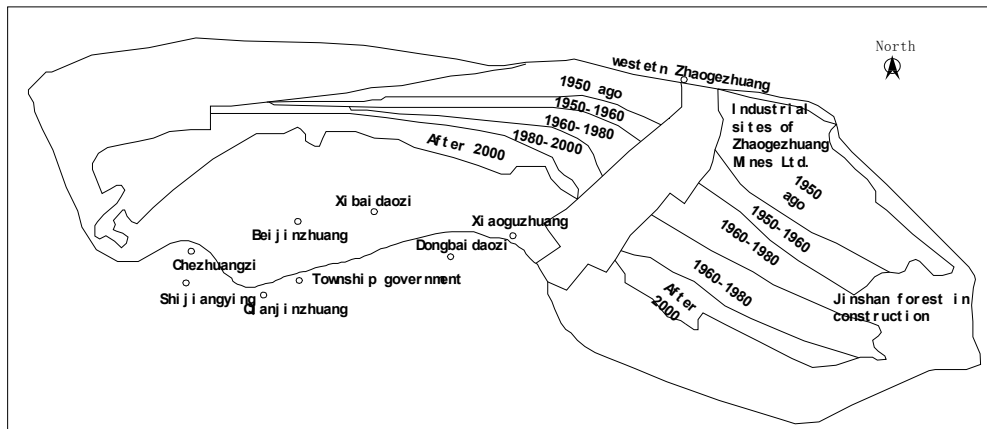
Figure 1: Distribution of mined-out area in Zhaogezhuang Mine

Displacement of surface and house collapse rate after earthquake

In order to analyze the influence of mined-out area on the dynamic response of the ground surface, this paper selects the surface deformation, houses collapsing rate of Zhaogezhuang Mine and the village nearby, which is based on seismic exploration value on surface deformation by Chinese seismological bureau.

Table 1: Surface destruction of Zhaogezhuang Mine and nearby

Ground surface above mined-out area	N39°33.318′, E118°6.846′	Surface Deformation，Horizontal displacement:36cm
Northern Industrial Square of Zhaogezhuang Mine	N39°36.418′, E118°11.834′	Ground crack and terrain scarp，Horizontal displacement:50cm
Southern Industrial Square of Zhaogezhuang Mine(mined-out area boundary)	N39°36.365′, E118°11.846′	Horizontal displacement:35cm
North of west Zhaogezhuang	N39°36.401′, E116°10.335′	Ground crack，2m fall in NW side，Horizontal displacement: 47cm
South of west Zhaogezhuang	N39°36.385′, E116°10.465′	1m fall in NW，Horizontal displacement: 38cm
Xiaoguzhuang	N39°36.105′, E118°11.643′	Ground crack，Horizontal displacement: 58cm
Qianjinzhuang	N39°35.505′, E118°9.193′	Horizontal displacement: 60cm，1m fall in NW

According to Table 1，the horizontal displacement of surface above mined-out area is 40 cm. The horizontal displacement of Industrial square boundary and southern surface of west Zhaogezhuang located in north flank boundary is 35 cm and 38 cm, respectively. However, the horizontal displacement of northern industrial square and northern surface of west Zhaogezhuang is 50 cm and 58 cm, respectively, which is significantly greater than the surface displacement in mined-out area boundary. The surface horizontal displacement of village further from mined-out area boundary is 58 cm and

60 cm, which is greater than the surface at mined-out area boundary, while is almost the same as horizontal displacement of other place in the mine field.

It can be concluded from Figure 2 that the surface horizontal displacement near mined-out area is small relatively. The displacement of other mine field and village far from mined-out area is similar which shows that dynamic influence of mined-out area on the ground surface will disappear with the increasing distance from the mined-out area. According to the Figure 3, the house collapsing rate at mined-out area boundary is 76% , which is less than the rate in other places and villages far from coal mine. The house damage amplitude of west Zhaogezhuang at mined-out area boundary is significantly smaller than the Xiaoguzhuang village. The earthquake makes the abscission in pool periphery wider, while not obvious. Light railway subgrade, which is used to deliver coal gangue beside the pond, slipped in the direction of the pond, while the degree of bend is slightly smaller than the track in other places.
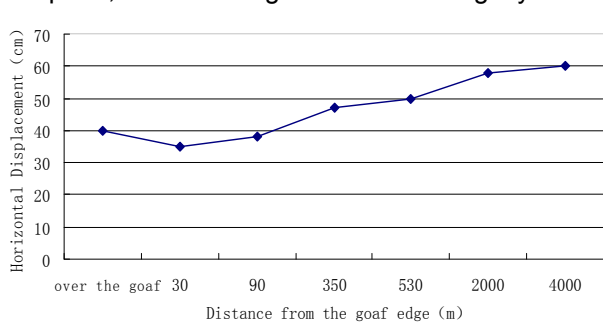
Figure 2: Horizontal displacement of surface near Zhaogezhuang Mine
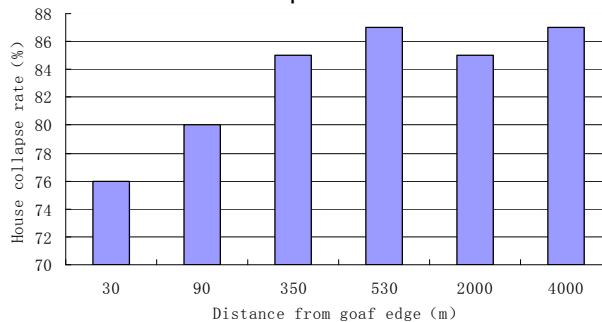
Figure 3: House collapse Rate of ground Zhaogezhuang Mine and near villages

NUMERICAL SIMULATION BY FLAC3D

Because of the FLAC3D is widely applied in rock mechanics and dynamic issues, this paper analyzes the seismic dynamic response of ground surface above mined-out area by FLAC3D.

Model of numerical simulation

The dimension of the model is 1600 m long in x direction, 430 m high in z direction and 100 m wide in y direction respectively. Since the effect in y direction is not considered, the model is simplified in quasi three dimension .Coal seam thickness is 4 m ,the mined-out area is set in the middle of the coal seam with 200 m long,100 m wide .The gangue height collapsed by roof is 3 m, the space not filled is 1 m. Elasto-plastic Constitutive Model and Mohr-Coulomb failure criterion are employed in this study. Elastic model is applied in gangue which is considered as support and space uses null model. Monitoring points from 1-9 are set on the ground surface in which point 1 is set above the mined-out area, point 2 is set above the boundary of the mined-out area, point 3 to 9 are set above the virgin areas . Properties of material used in calculation are the simplified rock parameter of Zhaogezhuang Mine. The model and monitoring points are presented in Figure 4.
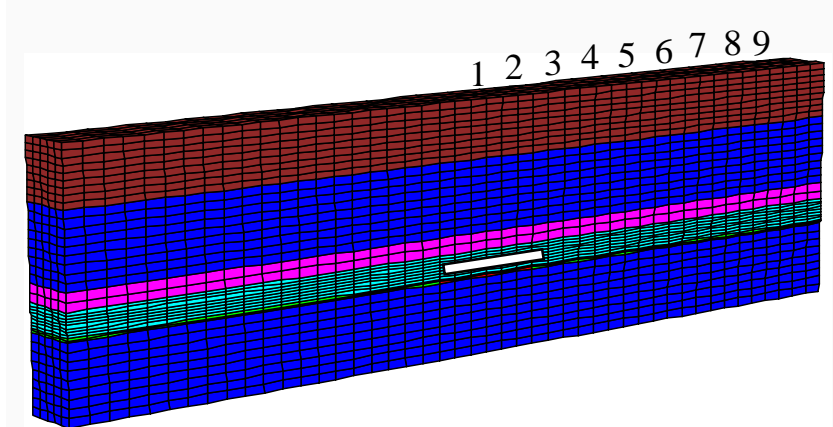
Figure 4: Mesh diagrams

Input waves and dynamic parameters

This paper adopts approximated acceleration waves of the Tangshan earthquake in E-W direction (Figure 5) and the peak value is 633.092 cm/s^2.The waves from 30s to 60 s are chosen in calculation. Acceleration spectrum shows that most of the power (approximately 95%) is made up of components of frequency 15 Hz (Figure 6).Therefore, cut-off-frequency is 15HZ and the dimension of the element is restrained as 10 m. The center frequency is defined as 0.6 Hz .For geological materials, damping commonly falls in the range of 2 to 5% of critical level. In the present study, 5% is chosen for calculation. The acceleration needs to be converted to stress when seismic wave is applied into the bottom of the model which is set as viscous boundary. Since S-wave is used in this paper, the acceleration-into-stress transformation formula is expressed as follows:

$$\sigma_s = -2v_S\sqrt{G\rho} \quad (1)$$

Where, v_S is the input shear particle velocity obtained by integration, ρ is the density of the base of the model, G is the shear modulus of the base of the model
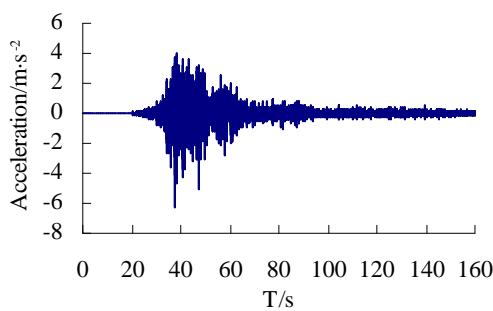
Figure 5: Seismic acceleration waves
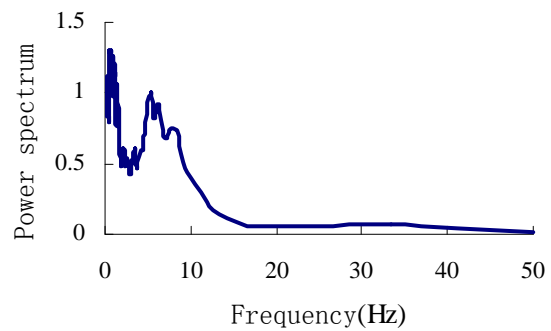
Figure 6: Plot of power spectrum versus frequency

NUMERICAL SIMULATION RESULTS AND DISCUSSION

Response acceleration of the ground surface

Figure 7 shows the acceleration-time curve of the monitoring points at the ground surface when mined-out area is 200m long and 350 m deep. It can be clearly shown that acceleration amplitude of the points above the mined-out area is smaller than those above the virgin coal seam. The peak accelerations of point 1 and point 2 are 6.47 m/s^2 and 5.56 m/s^2, respectively. It can be seen that the acceleration amplitude of point 2 which is above the boundary of mined-out area is smaller than that of point 1 above the mined-out area centre. The acceleration amplitudes of the point 3 to point 9 at the ground surface above the virgin coal seam are 7.08 m/s^2, 7.42 m/s^2, 7.54 m/s^2, 7.55 m/s^2, 7.67 m/s^2 , 7.19 m/s^2, 7.10 m/s^2 with the trend of increasing at first then decreasing. The acceleration amplitude of point 6 increases significantly, while point 8 and point 9 which is farther from the mined-out area shows the decreased trend. The peak acceleration of point 9 which is the farthest point from mined-out area is basically identical to the peak acceleration of the ground surface in the free-field condition.

(a) Point 1

(b) Point 2

(c) Point 4   **(d) Points 6**

(e) Point 8   **(f) Free-field**
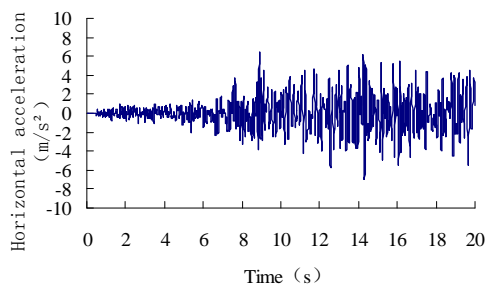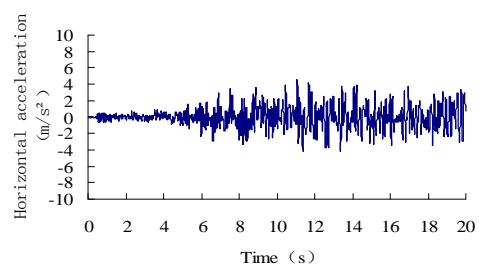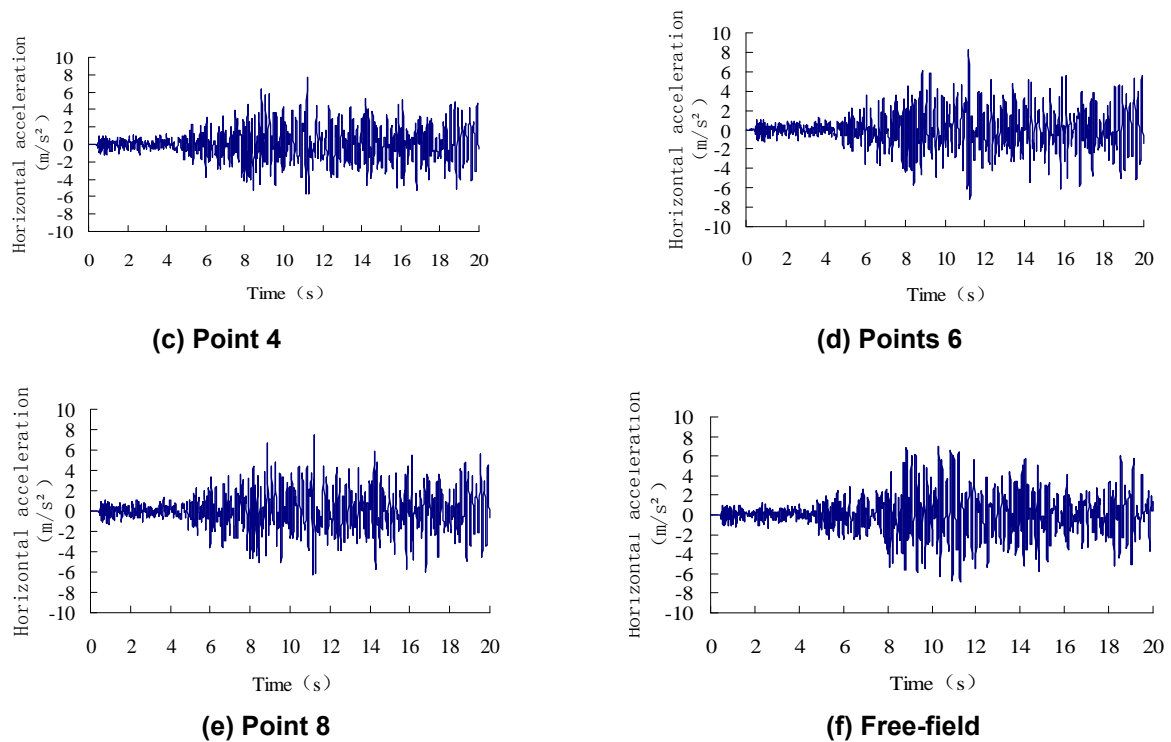
Figure 7: Response acceleration time-history curves of monitoring points

Peak acceleration of the ground surface at different depth of mined-out area

Figure 8 shows the peak acceleration of the monitoring points at the ground surface when the depth of mined-out area is 200 m, 250 m, 300 m, 350 m and 400 m.When the mined-out area is 200 m deep, the peak accelerations of point 1 to point 9 are 4.73m/s^2, 4.36 m/s^2, 5.73 m/s^2, 6.12 m/s^2, 6.62 m/s^2, 6.62 m/s^2, 6.27 m/s^2, 5.93 m/s^2, 6.44 m/s^2 which are all smaller than that of the ground surface in free-field conditions. It can be considered that the mined-out area which is 200m deep decrease the response acceleration at the ground surface. When the mined-out area is 250m deep, the peak acceleration values of point 1 to point 9 are all higher than those when the mined-out area is 200m deep, while they are still smaller than the peak acceleration of the surface points in free-field condition. When the mined-out area is 300m deep, the peak accelerations of point 1 to point 9 are 6.08 m/s^2, 5.55 m/s^2, 7.05 m/s^2, 7.13 m/s^2, 7.32 m/s^2, 7.56 m/s^2, 7.42 m/s^2, 6.85 m/s^2, 6.83 m/s^2 which get further increased .The peak accelerations of the points 1 and 2 are smaller than the surface points in free-field condition, while the values of points 5, 6, and 7 are higher than the free-field surface points. Finally, when the mined-out area depth reaches 350-400 m, the peak acceleration further increases and the trend of change is consistent with the values when mined-out area is 300 m deep.
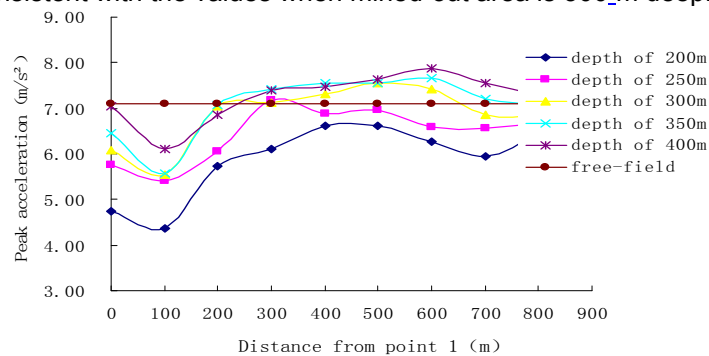
Figure 8: Peak acceleration of monitoring points at different depth of mined-out area

In general, the peak acceleration values of point 1 and point 2 become higher with the increasing mining depth, and they are lower than the peak acceleration of ground points in the free-field condition. It shows that the mined-out area reduces the response acceleration of the ground surface above it. When the mining depth reaches 300 m or deeper, the mined-out area magnifies the response acceleration of the

points above the virgin coal. However, the peak ground acceleration which is 4 times the mined-out area size away from the mined-out area boundary declines to the peak ground surface in the free-field condition.

Seismic displacement of ground surface

The Figure 9 shows that the surface displacement near the mined-out area will be different when an earthquake happens. The displacement values above the mined-out area are lower than thoseabove the virgin coal seam. The maximum displacement above the mined-out area, above the virgin coal seam, and the surface displacement in free-field are 0.260 m,0.280 m and 0.270 m which shows that the displacement values above the mined-out area becomes lower and the displacement above the virgin coal gets higher compared with the free-field surface displacement. When mining depth is 250m, 300 m and 350 m, the Figures show that the minimum displacement is at the point 1 with the values of 0.260 m, 0.260 m and 0.265 m. The maximum displacement is 0.28 m which is at 340 m, 450 m, and 550 m away from the mined-out area boundary. Therefore, the value and position of minimum displacement is little affected by mining depth with the value of 0.260 m above the centre of the mined-out area. The maximum displacement is 0.28 m which moves away from the mined-out area with the increasing mining depth.

From the results of the numerical simulation, the seismic response of the ground surface above the mined-out area is smaller than that away from the mined-out area, and the seismic response of the ground surface in a certain range above the virgin coal seam is larger than that of the area away from mined-out area. The analysis results above are consistent with the surface damage of Zhaogezhuang Mine in Tangshan earthquake.

(a) Depth of 250m

(b) Depth of 300m

(c) Depth of 350m

(d) Free field
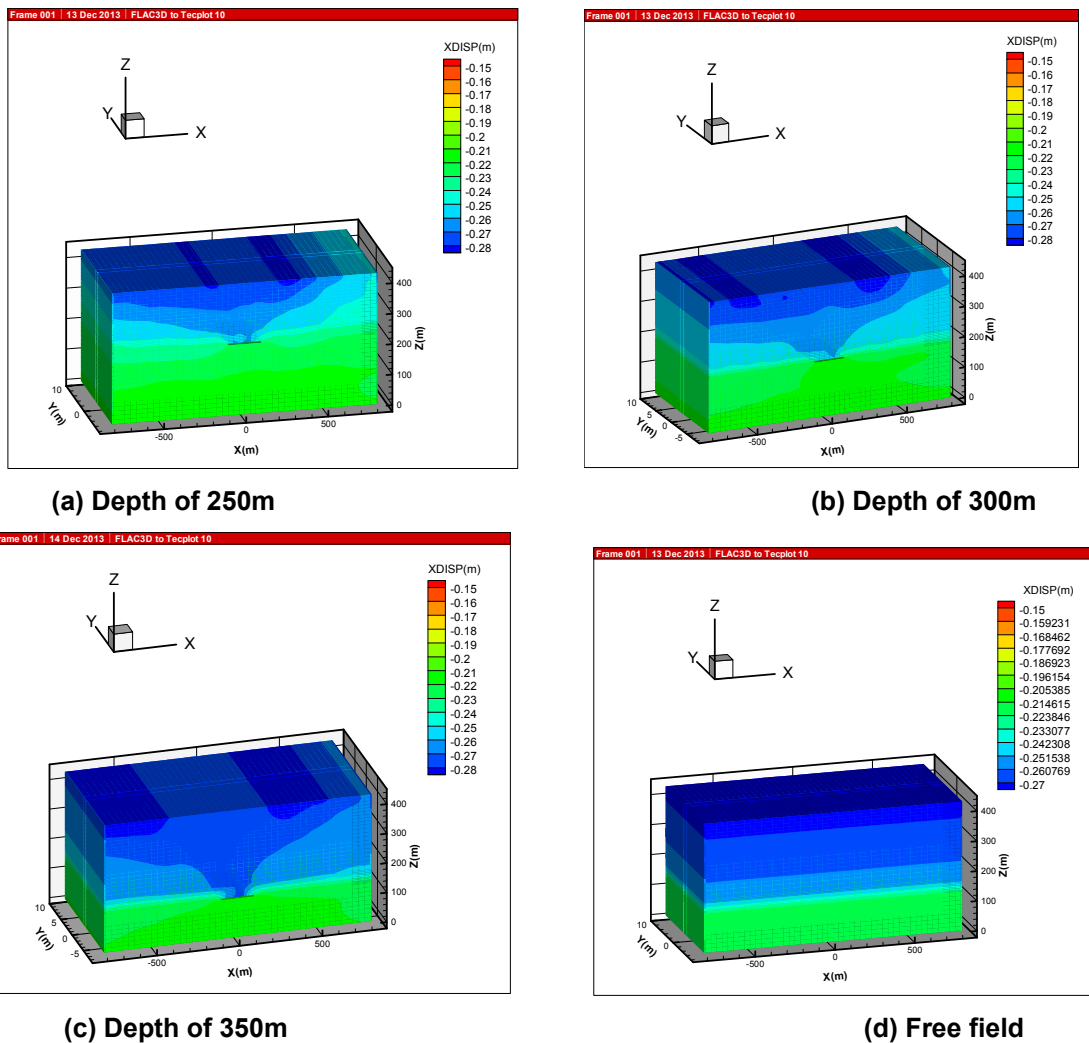
Figure 9: Contour band of surface displacement at different depth of mined-out area

CONCLUSIONS

This paper uses numerical simulation to analyse the seismic dynamic response of the ground surface of a coal mine. Some conclusions have been drawn as follow:

When unstable   mined-out area exists in the strata, the seismic damage at the ground surface which is above the mined-out area is about 10% less than that of the district which has no mined-out area in the strata, and the surface damage above the boundary of the mined-out area is the least with a 15% decline. When mined-out area is deep, the seismic damage of the ground surface, which is 2-3 times of the mined-out area size away from the mined-out area, becomes worse in comparison with no mined-out areas, and the increase amplitude of the damage is about 8%. The region at the ground surface which is greater than four times of the mined-out area size away from the mined-out area is not affected and the seismic damage in this region is consistent with the area without a mined-out area in the strata.

REFERENCES

Wang, L L. 1985, Foundation of Stress Wave, pp 105-112 (National Defence Industry: Beijing).

Li, H B, Ma, X D and Li J R. 2006, Study on influence factors of rock cavern displacement under earthquake, *Chinese Journal of Geotechnical Engineering*, 28(3): 358–362.

Summary of damage in Tangshan earthquake. 1978, (Earthquake Press: Beijing).

Itasca Consulting Group Inc. 2012, PFC user manual.

Developing a New Method to Identify the Source of Gas Emissions into Longwall and Goaf from Surrounding Strata

Abouna Saghafi[1], Kaydy Pinetown[2] and Hoda Javanmard[2]

ABSTRACT: During coal mining, strata is fractured and gas trapped in the roof and floor of coal seams travels into the workings. Depending on the extent and shape of fractured zones suitable gas drainage patterns are required to maximise the gas capture from strata but also to minimise the cost of operations. In this paper a new method to identify gas emitting zones/seams in the embedding strata and gas migration pathways is presented. The developed method was used in a coal mine in the Southern Coalfield of the Sydney Basin. Geochemical properties of gas trapped in coal seams above and below the mining horizon were analysed and compared with similar properties of gas collected from goaf areas. This study shows that using this method it is possible to identify the source of gas in goaf areas and thus determine the extent of fracturing in the strata around the mined seam.

INTRODUCTION

High gas emissions and gas surges into the coal face and goaf areas can occur rapidly due to changes in mine environmental and structural conditions. In addition to the gas released from the mined seam, much larger volumes of gas can also be released from other gas-bearing horizons in the strata above and below the mined coal seam (from fractured and de-stressed zones). Depending on the reservoir conditions and the geometry of the influenced zone, gas emitted into coal mines can be much larger than the gas contained within the mined seam. For example, Saghafi *et al*., (1997) studied the CH_4 emissions in gassy Australian underground mines and reported that the volumes of gas released from these mines exceeded the *in situ* CH_4 trapped in the mined seam by a factor of 4. Note that Kissell *et al*., (1973) reported that for US underground mines the volumes of gas released exceeded the *in situ* CH_4 by a factor of 7.

In order to maximise gas capture and reduce the cost of drilling the gas drainage engineer needs to know the extent of the mining-influenced zone and delineate the emissions zone. Suitable gas drainage patterns can then be designed to place gas boreholes in optimal locations and suitable angles.

One strategy for identifying possible gas migration pathways, particularly in caved areas (goaf) is to use a tracer gas such as sulphur hexafluoride SF_6. This tracer has been used to study gas and air paths in coal mines in various countries (Thimons *et al*., 1974; Vinson *et al.,* 1980). However, the use of this gas is problematic as it has the highest Global Warming Potential (GWP) of all greenhouse gases (GWP=~23,900) according to the Assessment Report on Climate Change (IPPC, 2007). SF_6 is also five times heavier than air, which leads to slow movement of this gas from its injection to the collection site for analysis.

In this study the properties of Coal Seam Gas (CSG) itself were used to identify the origin of goaf gas. For example, a component of the gas trapped in coal as an identifier of the coal seam containing that gas component can be used . An example is ethane (C_2H_6), which occurs naturally in coal. It can then be used to identify the emitting seams. However, this gas is only present in deeper seams. For this study a combination of molecular and carbon isotopic compositions of gas initially trapped in coal seams was used to identify the emitting zones/seams. The method makes it possible to identify the extent of the mining-influenced zone by comparing geochemical properties of gas accumulated in the goaf and coal face with gas desorbed from fresh cores from coal seams in the strata (delineation of mining influenced zone).

[1] *Visiting Professor, School of Civil, Mining & Environmental Engineering, University of Wollongong, NSW 2522, Australia, E-mail: abouna@uow.edu.au; abouna.saghafi@gmail.com*
[2] *CSIRO Energy Flagship, P.O. Box 52, North Ryde, NSW 1670, Australia, E-mail: kaydy.pinetown@csiro.au; hoda.javanmard@csiro.au*

STUDIED MINE AND METHOD OF INVESTIGATION

The studied mine was a longwall operation, located in the Southern Coalfield of the Sydney Basin.   Like most mines in this region no major coal seam is present in the overburden strata and all coal seams are located in underburden; in particular, three seams are located in the floor not far from the producing seam. These seams are likely to emit their gas into the coal face and goaf. These seams are located at ~10 m, ~20 m and at ~40 m below the producing seam. While the shallower seams (Seams 1 and 2) are likely to be influenced by mining, there were doubts about whether the deeper seam (Seam 3) was also influenced by mining and if so, whether the mining-induced fracturing would have allowed the escape of trapped gas from this deeper seam into the mining area and goaf. Note that high gas content levels have also been measured previously in the producing seam and other seams with various levels of carbon dioxide (CO_2) and methane (CH_4).   In Figure 1 a schematic of the mining geometry and location of potential gas emitting coal seams in the floor are shown.
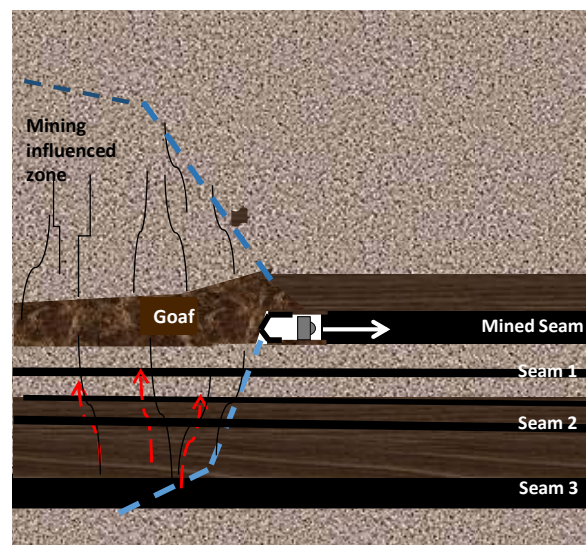
Figure 1: Schematic of mine operation and location of potential emitting seams in the floor strata based on mining induced fracture propagation

As mentioned in the previous section gas properties of coal seams ca be used as their identifiers. The selected attributes are gas molecular ratio in terms of CH_4 to CH_4+CO_2 and carbon isotope ratio. Note that the carbon atom has two stable isotopes: carbon 13 (^{13}C) and carbon 12 (^{12}C). The latter is by far the most abundant isotope of carbon accounting for 98% of these atoms. Carbon isotope ratio ($R = {}^{13}C/{}^{12}C$) is conventionally expressed in terms of a normalised differential ratio ($\delta^{13}C$). It quantifies the normalised difference between the $^{13}C/^{12}C$ ratio in the gas sample (R_g) and this ratio in a reference (R_r) material. The differential ratio of carbon isotopes for the target gas sample is then:

$$\delta^{13}C = 1000\frac{R_s - R_r}{R_r} \tag{1}$$

The differential ratio is increased by a factor of 1000 and is hence expressed as per mil (‰). For the carbon isotope the reference material is a carbonate called the Vienna Peedee Belemnite (VPDB). For VPDB the $^{13}C/^{12}C$ ratio is 0.0123 (For more details refer to Hoefs (1973).

This differential ratio is widely used for determination of the origin of coal seam gas in terms of its generation (biogenic or thermogenic gas, see for example, Smith *et al.,* (1992); Rice (1993); Smith and Pallasser (1996); Clayton (1998)).

The method of investigation developed for this study consisted of retrieving coal cores from surface exploration drilling into the sequences of coal seams below the floor of the mine (underburden). Coal cores were then measured for gas content in the field and the laboratory using the standard method (Australian Standard AS 3980-1999).   Gas desorbed from all stages of gas content testing (Q_1, Q_2 and Q_3 stages) were analysed for molecular composition (CH_4, CO_2 and N_2), however, carbon isotope composition analyses ($^{13}C/^{12}C$) were only applied to the gas desorbed during the Q_3 stage of gas

content testing. Simultaneously molecular and carbon isotope composition of gas collected from the goaf area was also analysed for molecular and isotope compositions.

RESULTS AND DISCUSSION

Two exploration boreholes were drilled across mined and under floor coal seams. Boreholes were drilled in two locations sufficiently away from active mining areas so that the virgin *in situ* conditions of gas initially trapped in the coal are preserved. From each borehole about eight fresh coal cores were retrieved, which were then measured for gas content and gas composition.

As discussed the molecular gas ratio (CH_4/CH_4+CO_2, %) was used as one of the identifiers of the seam. In Figure 2, the distribution of gas molecular composition against depth is shown. The depth of coal cores in this figure is not from the ground surface but from a datum level in the overburden of the mined seam. Note that in plotting this curve only the results of composition measurements for gas desorbed from Q_2 and Q_3 stages of gas content testing were used for this plot as gas collected at the Q_1 stage of gas content testing was prone to contamination and consequently associated with high errors of determination. The data show that CH_4 in the mixture increases with depth almost linearly, and therefore the molecular composition of desorbed gas is quite different for the underburden strata. Hence, for this sequence of coal seams and at this location, gas compositions for the seams in the strata are distinct, which justifies the use of gas composition as an identifier (attribute) of a coal seam in the sequence. The measured data showed that the CH_4/CH_4+CO_2 ratio for the mined seam and Seam 1 varied from 15 to 25%, for Seam 2 from 40 to 45% and for Seam 3 from 75 to 90%.

The carbon isotopic compositions of gases were measured using Gas Chromatography/Combustion/Isotope-Ratio Mass Spectrometry (GC-C-IRMS). The GC-C-IRMS system consists of a GC unit connected to a combustion device coupled via an open split to a mass spectrometer. Duplicate measurements are done on each of the gas components, i.e. on CO_2 and CH_4 components of coal seam gas. The results of measurements are shown in Figure 3, showing cross plots of the $\delta^{13}C$ values for the CO_2 component of the seam gas against these values for the CH_4 component of the seam gas. The data show that carbon isotope values are distinct for different seams in the sequence and hence isotope ratios can be used to identify emitting seams.
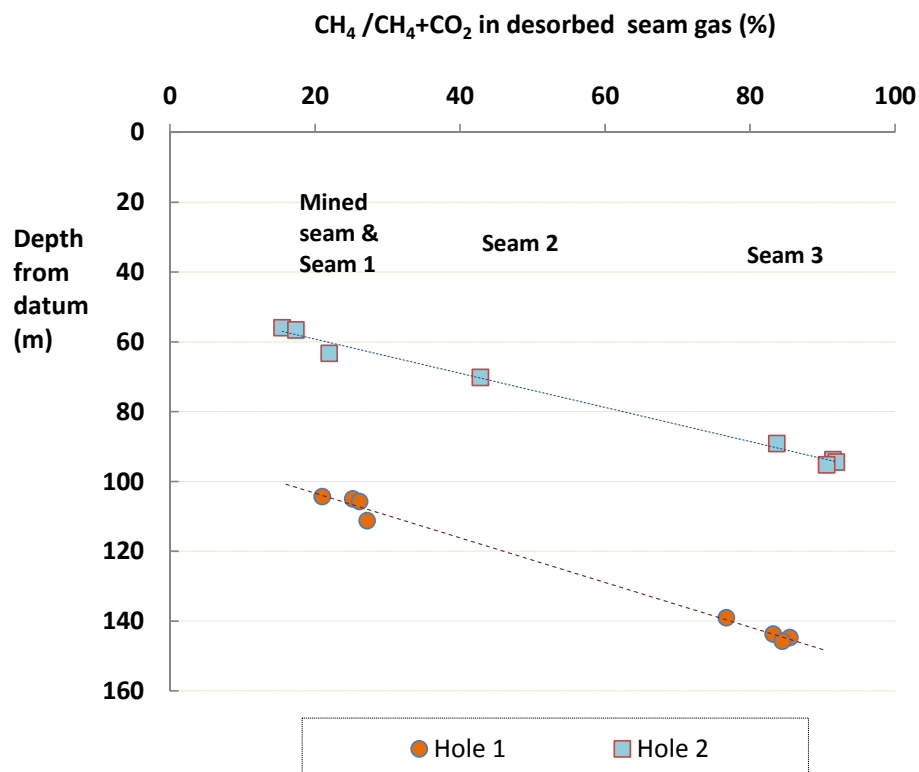
Figure 2: Molecular gas ratio (CH_4/CH_4+CO_2) of desorbed gas from cores from two boreholes drilled into strata not affected by mining
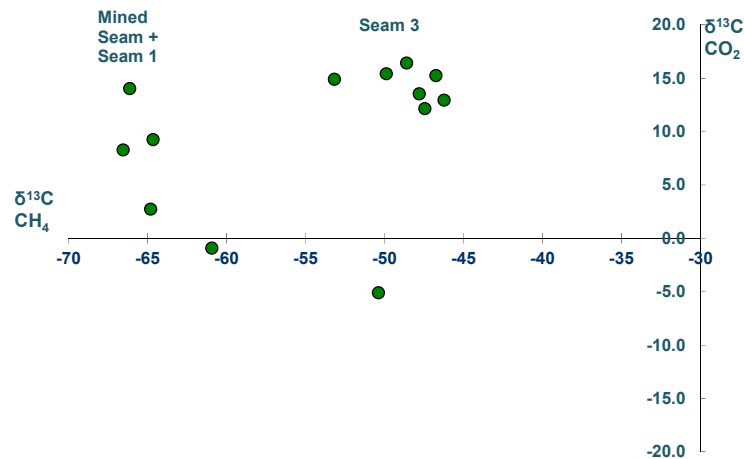
Figure 3: Cross plot of carbon isotope ratio for CO_2 and CH_4 for gas desorbed from coal samples for different seams

In order to determine whether any gas in the goaf is sourced from Seam 3, a number of gas samples were collected from the collar of a goaf drainage borehole and measured for molecular and carbon isotope compositions. The results showed that the ratio of CH_4/CH_4+CO_2 in the goaf was about 40%, $\delta^{13}C$ for CH_4 was about -61.5‰ and for CO_2 it was -6.4‰. Comparing these data with the data in Figures 2 and 3 suggests that gas emitted into goaf originated from the mined coal and from Seam 1.

CONCLUSIONS

A new method is described whereby geochemical properties of gas were described, namely molecular and isotopic composition, may be used to trace the source of gas emitted into goaf areas in underground coal mines. The method was applied to a participating mine in this study in the Sydney Basin. Results of the study showed that molecular composition and carbon isotope composition ($\delta^{13}C$) for gas initially trapped in coal seams in the sequence were markedly different. Thus, these values can be used as identifiers for the source of gas emitted into goaf areas.

Although the method is still in its trial stage, the preliminary use of the method shows that it could be effective in identifying the extent of the gas emissions zone in the underburden strata.

ACKNOWLEDGEMENTS

REFERENCES

Australian Standards. 1999, Guide to the determination of gas content of coal – Direct desorption method. Australian Standard 3980–1999, Standards Association of Australia, Sydney.

Clayton, J L. 1998, Geochemistry of coalbed gas- A review, *International Journal of Coal Geology*, 35, pp 159-173.

Hoefs, J. 1973, Stable isotope geochemistry, *Springer Verlag*, Berlin, 140p.

Intergovernmental Panel on Climate Change (IPCC). 2007, Fourth Assessment Report: Climate Change, Section 2.10.2: Direct Global Warming Potentials. Also available at: http://www.ipcc.ch/publications_and_data/ar4/wg1/en/ch2s2-10-2.html.

Kissell, F N, McCulloch, C M & Elder, C H. 1973, The direct method of determining methane content of coalbeds for ventilation design, *U.S. Department of the Interior, Bureau of Mines RI 7767, NTIS No. PB221628*.

Rice, D D. 1993, Composition and origins of coalbed gas, in: Law, B.E., Rice, D.D. Eds., Hydrocarbons from Coal, *AAPG Studies in Geology a38*, Tulsa, OK, pp 159–184.

Saghafi A, Williams D. J and Lama R D. 1997, Worldwide methane emissions from underground coal mining. *In: Ramani RV (Ed) Proceedings of the 6th International Mine Ventilation Congress*, Pittsburgh, PA, USA, pp 441—445.

Smith, J W and Pallasser, R J. 1996, Microbial origin of Australian coalbed methane. *AAPG 80 (6)*, 891-897.

Smith, J W, Pallasser, R J, Rigby, D. 1992, Mechanism of coalbed methane formation, *In; Beamish, B. and Gamson, P (eds) Symposium on coalbed methane research and development in Australia, James Cook University of North Queensland*, Townsville, Queensland, Australia, 63-73.

Vinson R P, Kissell F N, LaScola J C, Thimons E D. 1980, Face ventilation measurement with sulfur hexafluoride (SF_6), *US Bureau of Mines Report of Investigations RI 8473*, 16p.

Thimons E D, Bielicki, R J, Kissell, F N. 1974, Using sulfur hexafluoride as a gaseous tracer to study ventilation systems in mines, *US Bureau of Mines Report of Investigations RI 7916*, 22p.

STUDY OF PERMEABILITY OF COAL SAMPLES SUBJECTED TO CONFINING PRESSURES

Nazanin Nourifard[1], Lei Zhang[1&2], Naj Aziz[1] and Jan Nemcik[1]

ABSTRACT: Permeability is assessment of the ability of rock to transmit fluid flow through the rock body. It can be affected by rock structure due to the grain size, formation and the pressure or concentration gradient existing within and across it. Past studies focused on the relationship between permeability and axial stress on rock, and there has been limited research on the impact of circumferential stress and volumetric deformation on permeability. A programme of laboratory tests was conducted on coal samples to evaluate the permeability of coal under different confining pressures. A specialised permeability apparatus known as Multi-Functional Outburst Research Rig (MFORR), was used to study rock permeability under various confining pressures. Methane permeability tests on cylindrical coal samples were conducted at varying axial stress up to 3 MPa and confining CH_4 gas pressures between 0.2 MPa and 3 MPa. It was found that by increasing the confining gas pressure the permeability value decreased in elastic phase and maintained an almost constant value at gas pressures greater than 2 MPa. The results show that the permeability of coal sample under triaxial compression tend to decrease with the increase in stress.

INTRODUCTION

Permeability is one of the most important parameters that affect gas production rates and reservoir recovery of coal seams (Shi and Durucan, 2003; Wallace and Bruce, 1990). Coal is generally defined as a dual porosity rock, containing both macro pore and micro pore systems; the macro pore system consists of a naturally occurring network of fractures called cleats, serving as the primary pathways for gas transport. The micro porosity of coal is within the coal matrix blocks, surrounded and separated by cleats, consisting of large number of interconnected pores that serve as the storehouse for methane in adsorbed form (Mitra, *et al.*, 2012).

Permeability has a significant impact on the ability of a coal seam to produce gas. A recent study by Zhang (2012), examining factors contributing to effective drainage of gas from coal by Multi-Functional Outburst Research Rig (MFORR), found a significant lack of information on coal permeability in comparison with other parameters. Accordingly, research on coal permeability is ongoing, and this study forms a part of such endeavour to improve the knowledge about coal permeability and improve both the method and the apparatus assembly. The main issue is to choose a proper testing method, which fulfils the need for a better understanding of the permeability in permeable rock formations like coal and coarse grained rocks (Nourifard 2014).

EXPERIMENTAL PROCEDURE

Instrumentation

As the name suggests the MFORR enables studies to be carried out on coal/rock Uniaxial Compressive Strength (UCS); Tensile Strength (TS); the effect of gas pressure on coal/rock load bearing capacity; coal drillabilityand permeability and volumetrics changes under triaxial conditions. The equipment consists of the following components:

- The main apparatus support frame

- A precision drill

- A high pressure chamber which has a load cell for measuring the load applied to the samples of coal

- A pressure transducer for measuring the pressure inside the chamber

- Flow meters for measuring the gas flow rate

---

[1] *School of Civil, Mining and Environmental Engineering University of Wollongong, Wollongong, Australia, 2522, E-mail:naj@uow.edu.au*
[2] *CUMT*

- Two strain gauges for measuring the vertical and horizontal strains of the coal sample

- A universal socket for loading a sample of coal vertically into the gas pressure chamber

- A gas chromatograph (GC), and

- A data acquisition system
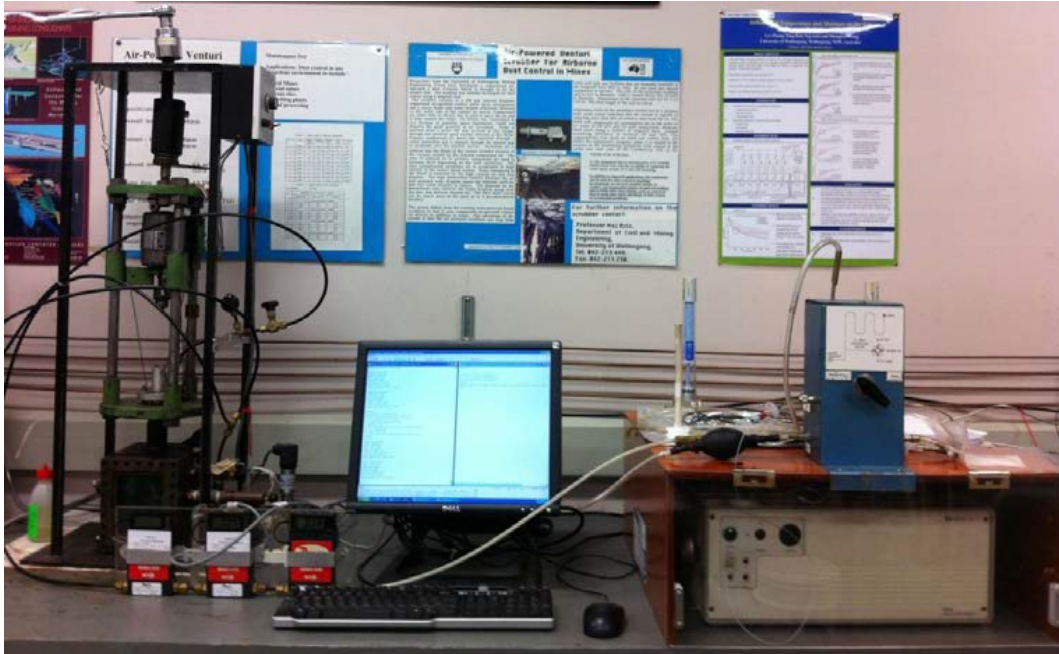
Figure 1: Multi-Function Outburst Research Rig with GC (Zhang, 2012)

The main frame of the apparatus is made of a sturdy steel structure, which houses the gas chamber and universal thrust connector. The gas pressure chamber is a hollow rectangular prism of cast iron with removable front and back viewing plates. The dimensions of the box are 110 mm x 110 mm x 140 mm. The viewing windows are made of 20 mm thick glass in a cast iron frame. Housed in the chamber is a 40 KN load cell capacity for monitoring the load applied.

Gas permeability tests were carried out on specially prepared coal samples 61 mm in diameter and 40 mm in height. The sample holding plates within the apparatus were widened from the initial diameter of 50 mm to 61 mm to accommodate larger diameter samples. A 3 mm diameter hole was drilled in the middle of each of the coal samples. Drilling was carried out perpendicular to coal bedding/layering to allow the pressurise gas to flow laterally through coal beddings. Before testing, both flat end-surfaces of the tested coal samples were sealed with thin rubber gasket pieces to ensure that the gas penetrated along the coal in a radial direction only into the central hole. Figure 2 shows the snapshot of one of the specimens ready to be tested, and Figure 3 shows coal sample sealed in triaxial pressure chamber and a general view of the MFORR
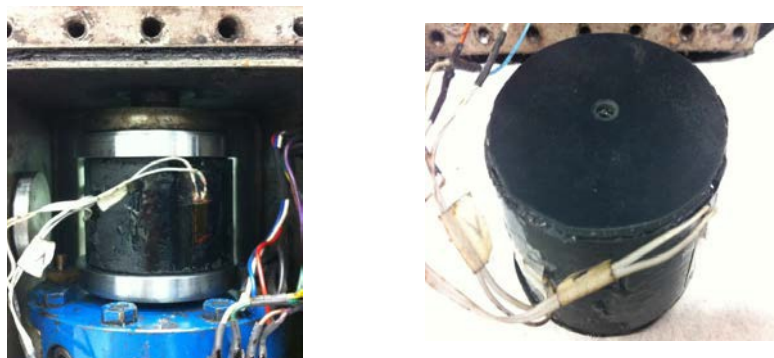
Figure 2: Coal samples for triaxial permeability test with MFOR
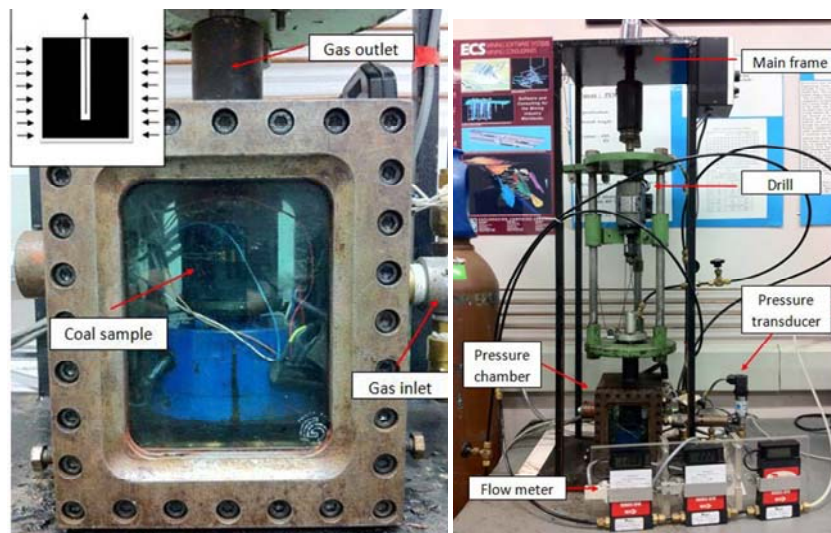
Figure 3: Coal specimen sealed in pressure chamber and Multi-Function Outburst Research Rig (MFORR)

The procedure for conducting each test consisted of mounting each tested sample in the pressure chamber. The loaded chamber was sealed, then vacuumed to remove air and subsequently re-pressurised to a predetermined level and maintained at that level. CH_4 gas was allowed to permeate the coal sample and flow out through the central hole. The released gas from the coal flowed through a measuring system consisting of a vacuum pressure sensor and gas flow meters with 0-2 L/min and 0-15 L/min measurement ranges.

The test sequence was followed in steps with varying vertical stress of 1, 2 and 3 MPa and gas pressure ranging from 0.2 MPa to 3 MPa. The load cell, flow meters, pressure transducer and strain gauges were connected to a computer through a data logger for data collection.

The permeability of the sample was calculated using the following Darcy's equation:

$$K = \frac{\mu Q \ln(\frac{r_0}{r_i})}{\pi L (P_1{}^2 - P_2{}^2)}$$

Where K is the permeability of coal, μ is viscosity of gas, Q is the flow rate of gas, L is the height of the sample, r_0 is the external radius of the sample and r_i, is the internal radius of the small centrally drilled hole, P_1 and P_2 are the absolute gas pressures inside and outside of chamber, respectively.

RESULTS AND DISCUSSION

Permeability analysis of coal specimens

Permeability values of all tests are shown inTable 1. The results were consistent for all tested coal samples. In general, the tests showed that the coal permeability decreases with increasing gas pressure and applied vertical load/stress. As the flow meter range was limited to 15 L/min maximum, in some of the coal permeability tests, coal permeability results could not be obtained above the measurement range of the flow meter. The consistent behaviour for all tested coal specimens indicated a reduction in permeability with increasing gas pressure. As the axial and confining stress increased, the gradual closure of pore and cleat within the coal reduced its permeability. When the vertical stress began to increase from 1 MPa to 2 MPa, the permeability of coal reduced significantly in all tested coal specimens. Test results indicate that the permeability values stay below 1 mD, when applied confining gas pressures exceed 0.5 MPa at the axial stress of 3 MPa. This is clearly shown in Figures 4 to 9. However, one sample, No 383413 (Figure 7) was very permeable even at the applied vertical stress of 3 MPa. High permeability values at 3 MPa vertical stress is attributed to the crack enlargement and possible sample strength failure in compression.

Table 1: permeability of tested samples in both perpendicular and parallel to beddings

Coal specimen	Permeability (mD) at 1 MPa axial load	Permeability (mD) at 2 MPa axial load	Permeability (mD) at 3 MPa axial load
383404	0.863	0.692	0.589
383408	27.142	13.326	0.700
383410	8.154	0.673	0.512
383413	25.091	14.017	10.121
383416	74.202	13.052	2.160
383418	254.466	51.522	-
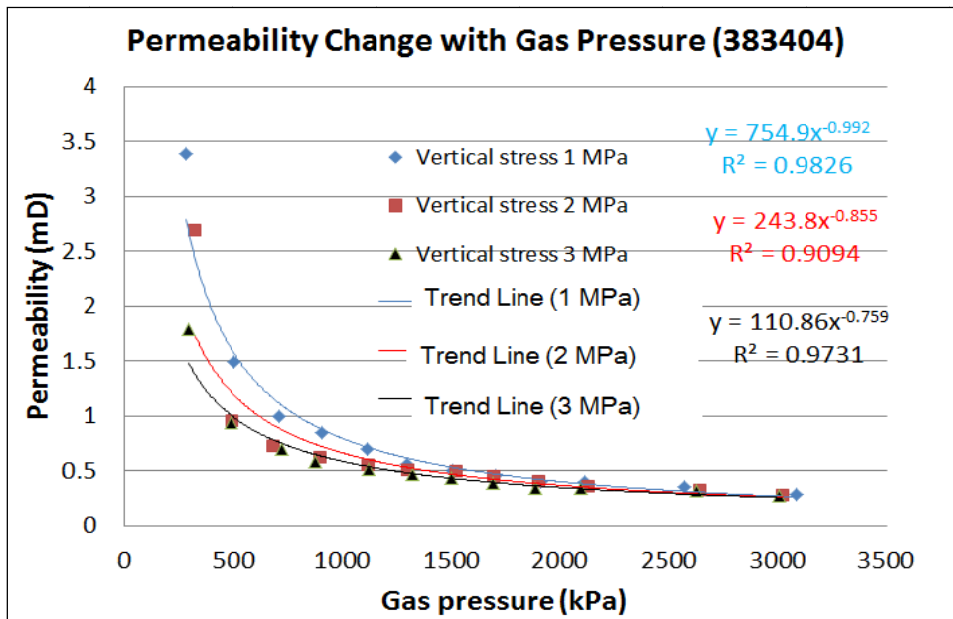
Figure 4: Permeability change for coal specimen no 383404
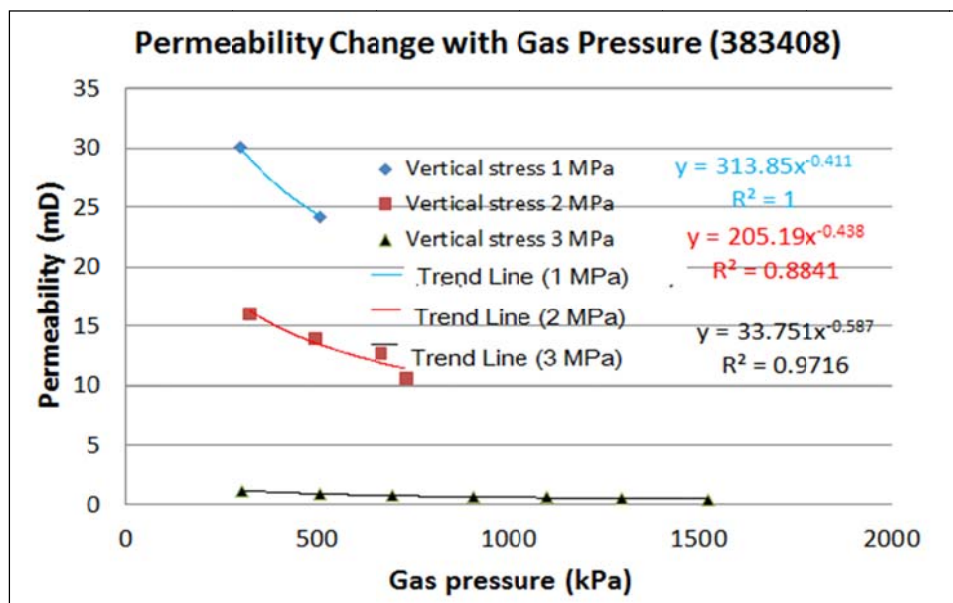
Figure 5: Permeability change for coal specimen no 383408
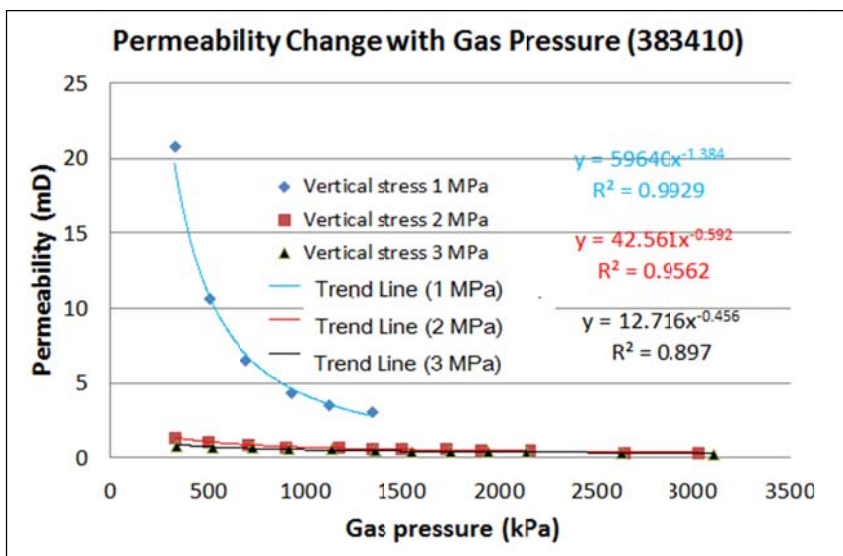
Figure 6: Permeability change for coal specimen no 383410
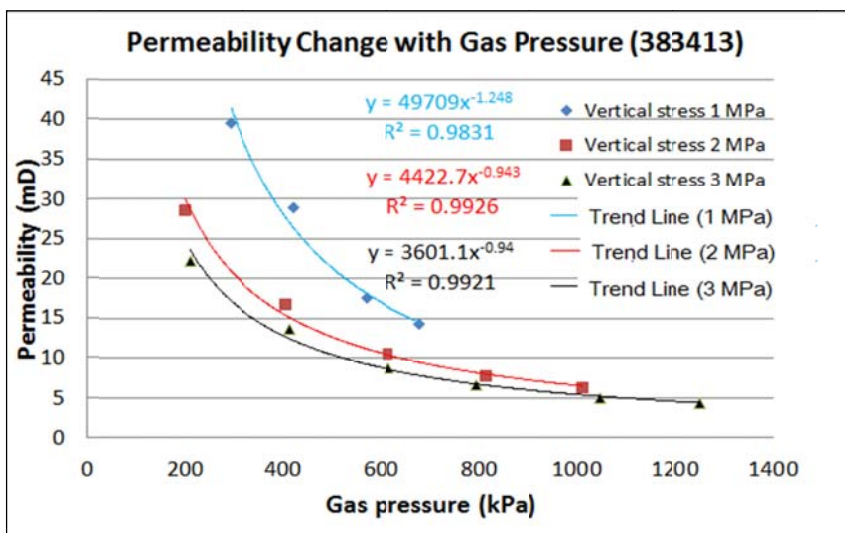
Figure 7: Permeability change for coal specimen no 383413
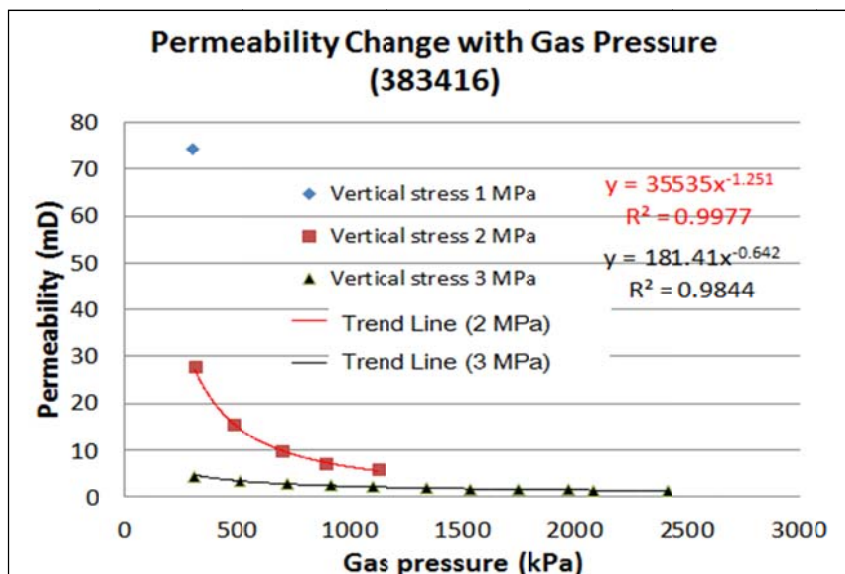
Figure 8: Permeability change for coal specimen no 383416

Permeability Change with Gas Pressure (383418)

$y = 2E+06x^{-1.686}$
$R^2 = 1$

$y = 385560x^{-1.557}$
$R^2 = 0.9919$

◆ Vertical stress 1 MPa
■ Vertical stress 2 MPa
— Trend Line (1 MPa)
— Trend Line (2 MPa)

Permeability (mD) — Gas pressure (kPa)
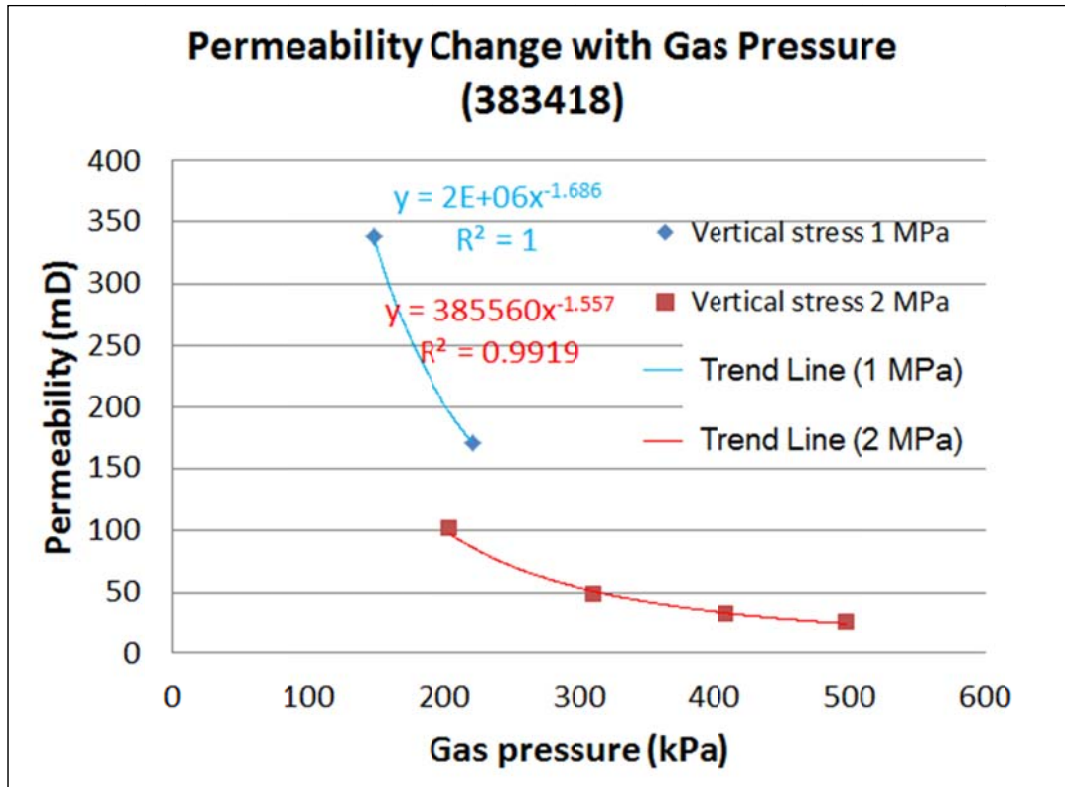
Figure 9: Permeability change for coal specimen no 383418

Examination of the vertically loaded coal samples subjected to the external gas pressure in the pressure chamber clearly showed that the permeability of coal specimens decreased with increased vertical load. There is no doubt that the introduction of methane contributed to the sorption of methane molecules in the coal matrix, which in turn swells the coal matrix and decreases it's the porosity.

A positive value of volumetric deformation indicates swelling and expansion of the tested specimens, and a negative value indicates shrinkage. The changes in horizontal strain were higher than the vertical strain. Lower vertical strain is due to axial loading of the sample.

The permeability changes can be analysed from three stages of the volumetric strain of tested coal specimens. During the first stage, the rock specimen is squeezed with the permeability decreasing rapidly at the beginning of the test. In the second stage, the specimen starts to swell, while in the last stage the samples continued to shrink with increasing axial load. The lowest permeability rate occurred at the last stage of the test at higher axial load and prior to coal failure at around 3 MPa.

Permeability classification of tested coal specimens

According to Palmer (2010) on of Coal Bed Methane (CBM) well completion, coal/rock permeability can be classified into the following categories as shown in Figure 10.

| Tight coal completions | Low-perm completions | High-perm completions | Ultra high-perm completions |

3 md   20 md   100 md
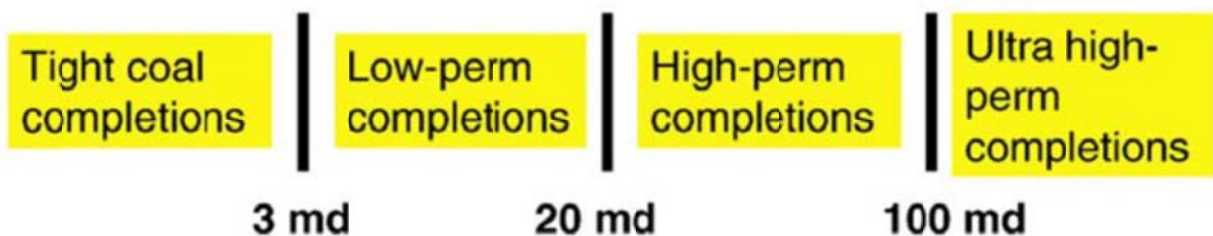
Figure 10: Permeability bands for CBM well completions (after Palmer, 2010)

According to Palmer (2010), the permeability of tested coal specimens can fall into the following classified categories as shown in Table 3, which shows the majority of tested specimens being considered as high permeability.

Table 2: Palmer permeability classification of the tested coal

Coal specimen no	Permeability (mD) On 2 MPa axial load average	Permeability (mD) On 3 MPa axial load average	Palmer classification
383404	0.692	0.589	Tight coal completions
383408	13.326	0.700	Tight coal completions to low permeability completions
383410	0.673	0.512	Tight coal completions
383413	14.017	10.121	low permeability completions
383416	13.052	2.160	Tight coal completions to low permeability completions
383418	51.522	-	High permeability

CONCLUSIONS

Through the study of permeability in coal samples under different confining pressures, the following conclusions have been made:

- Permeability rate of coals under triaxial compression varies by the type and nature of the matrix structure. In general, higher stress environment decreases the permeability.

- Coal sample permeability decreases with increasing gas pressure and at higher gas pressure, coal permeability stays stable and undergoes minor changes under vertical stress above 2 MPa.

- Strain gauge results from the MFORR test showed that coal samples experience negative volumetric changes or shrinkage with increased confinement pressures, both axially and laterally. The degree of the volumetric changes is found to be dependent on the level of the applied axial and lateral pressures.

- There is no simple linear relationship between the permeability and the volumetric change. The coal sample has different permeability behaviour that varies with volumetric changes.

REFERENCES

Aziz, N and Li, W. 1999, The effect of sorbed gas on the strength of coal – an experimental study, *Geotechnical and Geological Engineering*, 17(3-4), 387-402.

Mitra, Harpalani, Satya, Liu and Shimin. 2012, Laboratory measurement and modelling of coal permeability with continued methane production: Part 1- Laboratory results, *Fuel*, 94(0), 110-116.

Nourifard, N. 2014, Permeability of sandstone and coal samples subjected to confining pressure. MPhil thesis, University of Wollongong.

Palmer, I. 2010, Coalbed methane completions: A world view, *International Journal of Coal Geology* 82(3-4), 184-195.

Sereshki, F. 2005, Improving coal mine safety by identifying factors that influence the sudden release of gases in outburst prone zones, PhD thesis in University of Wollongong.

Shi, J, Q and Durucan, S. 2003, A disperse pore diffusion model for methane displacement desorption in coal by CO2 injection, *Fuel*, 82(10), 1219-1229.

Wallace, J and Bruce. 1990, Recovery of lotic macro invertebrate communities from disturbance, *Environmental Management*, 14(5), 605-620.

Zhang, L. 2012, Study of coal sorption characteristics and gas drainage in hard-to-drain seams, PhD thesis in University of Wollongong.

APPLICATION OF CONTINUOUS DRILLING TECHNOLOGIES IN COAL MINING

Scott Adam[1] and Joel Kok[2]

ABSTRACT: CRCMining's unique Tight Radius Drilling technology has recently demonstrated highly productive continuous drilling in a Bowen Basin coal formation. The system has been demonstrated to be economically deployable and reliably operable by drilling contractors. A detailed overview of the system is presented, including a summary of the technology status in terms of technical performance, system productivity and stimulation cost. Investigation of the application of continuous drilling technology is currently being extended to underground in-seam (cross panel) drilling and rapid roof bolt hole drilling for long tendon support. An update on these ACARP/CRCMining co-funded research initiatives is presented.

INTRODUCTION

Drilling is a critical element of almost every mining operation. It is interesting that the first rotary drill emerged in 1901, the first roller bit in 1909. Improvements in directional control through advanced borehole assemblies are a more recent innovation, but the fundamental concept of adding screwed sections of jointed drill rods still persists. Inherent constraints associated with the jointed drill string concept have become normalised and an absence of viable alternatives has forced industry to accept the intrinsic limitations, namely:

- Safety hazards associated with intense manual handling and man-machine interactions have persisted despite some attempts to introduce automation of aspects of the drill rod handling process, which are inevitably complex mechanical solutions not readily adaptable to the underground coal environment
- Drilling production inefficiency associated with frequent rod changes, both during drilling and extraction of the drill string
- Compromised formation properties in gas drainage holes due to 'skin effects' generally a result of the cutting action of mechanical drill bits, and the   rotary or sliding action of drill pipes in the hole
- Interruption (particularly in horizontal holes) to the wellbore circulation associated with frequent rod changes, resulting in settling of cuttings in the lateral and an increased risk of loss of drill string.
- Limitations in the integration of drilling into other mining processes due to the rigid requirement for a long drilling boom. For example the configuration options for a bolter miner are constrained by the dimensions of the drill mast which generally spans from the roof to the floor of the mining environment.

The inherent and unavoidable high safety risk and low productivity associated with conventional jointed rod drilling systems stand out as an example of hazards that the industry has been forced to accept due to an absence of an acceptable alternative technology. The ubiquitous nature of jointed drilling and its inherent constraints is of itself a barrier to realising alternative concepts which may offer step change performance improvement.

HISTORY OF CONTINUOUS DRILLING WITHIN CRCMINING

In 1994 CRCMining investigated application of high-pressure water jet assisted drilling technology using jointed drill pipes and conventional blade style drill bits. Recognising the benefit of continuous drilling, the CMTE researchers evolved the system into a self-propelled, pure water jet driven drilling tool

[1] *Program Leader – Underground Coal Research Program, CRCMining ,E-mail: s.adam@crcmining.com.au;Tel: 07 3365 5636*

[2] *Mechanical Engineer – Underground Coal Research program, CRCMining, E-mail: j.kok@crcmining.com.au*

deployed using a reel of flexible hose. In 1997, the water jet drilling technology was deployed into a pre-drilled vertical well to investigate the concept of radial drilling.

Today this expertise includes self-propelled water-jet cutting heads and associated mechanisms that can drill a borehole in a self-regulated manner whilst maintaining effective borehole diameter control. Applications of CRCMining's water jet drilling technology include:

1. **Tight Radius Drilling (TRD)** was developed to enable thick (>2m thickness) coal seams to be safely de-gassed from the surface in advance of the mining process.
2. **High Speed Cross Panel** drilling is an adaptation of the TRD system for underground in-seam application, mainly for the purpose of drilling de-gassing holes. It is also suitable for cross measure drainage holes.
3. **Continuous Cable Bolt Drilling** is being developed for continuous drilling of cable bolt holes for underground long-tendon roof support installation.

TIGHT RADIUS DRILLING

The current TRD deployment system uses a self-propelled, high pressure water drill head to create a radial pattern of horizontal boreholes (laterals) in the target coal seam (Figure 1). The system is deployed into a vertical well, which is prepared with an under-ream zone (1.8 m diameter) at each target horizon to accommodate the deployment whipstock that orientates the drilling tool from vertical to horizontal. Radial lengths in excess of 300 m have been achieved to date, with continuous drilling rates of over 240 m/hr observed in field conditions.
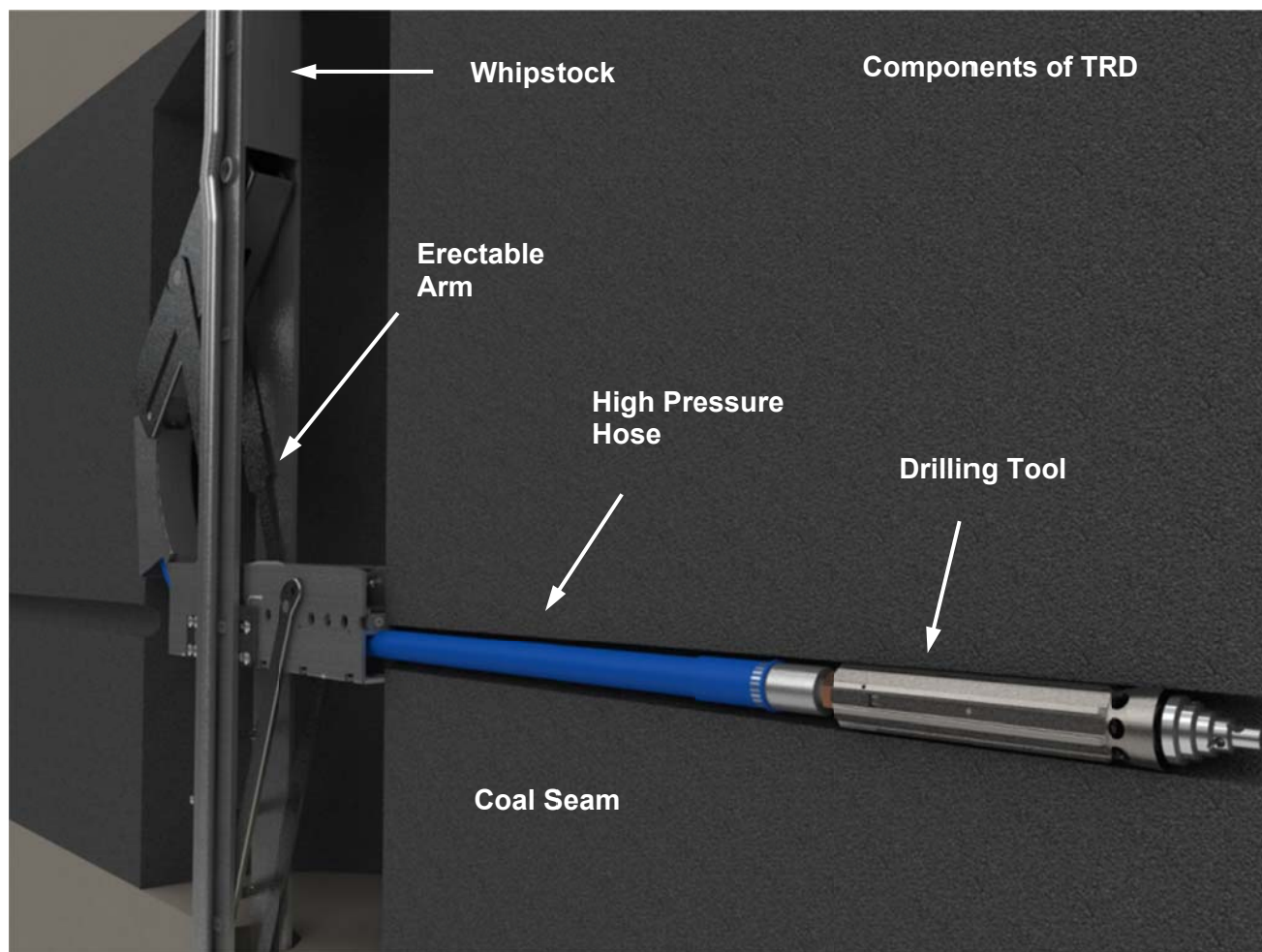
Figure 1: Continuous drilling offers a step change productivity increase and cost reduction to the mining industry. A flexible and continuous conduit is the key enabler
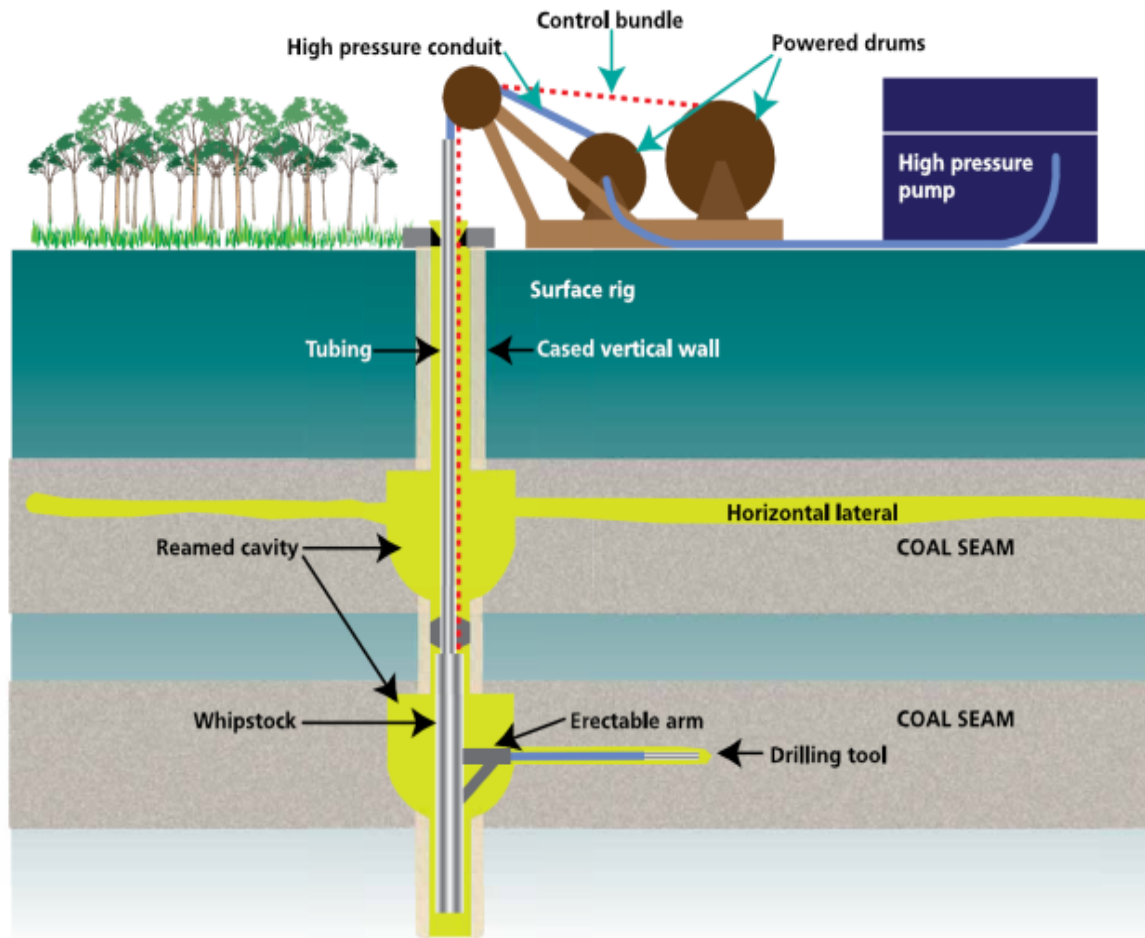
Figure 2: Tight Radius Drilling deploys a continuous water jet drilling too into the coal seam from a vertical well

CRCMining's water jet drilling technology has evolved to the point that it now reliably and rapidly forms a borehole of constant and regulated borehole diameter, an essential fundamental requirement for reliable drilling. Real time survey electronics in the drilling tool body constantly logs the borehole trajectory and reports the tool position to the surface drill controller in real time. Waterjet drilling systems are inherently remote controllable, with operators able to effectively control the system via computer interfaces. Drill advance is self-regulated and semi-automated. The continuous nature of waterjet drilling is highly compatible with automation and off site remote control of high skill drilling functions.

Seventeen years of development culminated in the first commercial deployment of TRD for the purpose of investigating broad scale degassing of a coal mine. In 2013, TRD was applied at BMC's South Walker Creek mine, proving that water jet drilling can be applied economically.

The system was operated by established service providers, executed under a commercial drilling contract, and achieved high productivity. This work has demonstrated proof of concept for the waterjet drilling method. Extensive patterns of radials were formed in the coal seam providing a large drainage area. All but three of the laterals were drilled without azimuthal steering.

With a peak productivity of 535 m total laterals drilled in just 6 hours, the vision for a 1000 m per shift drilling technology has been set as a reasonable target. Continuous drilling rates of between 2 and 4m/min were regularly demonstrated during this operation.

During this campaign, the steering concept was trialled briefly in three laterals, with promising results out to approximately 100 m lateral length. It is apparent that improvements in steering control and drilling tool geometry will increase the range, straightness and quality of waterjet drilling systems.
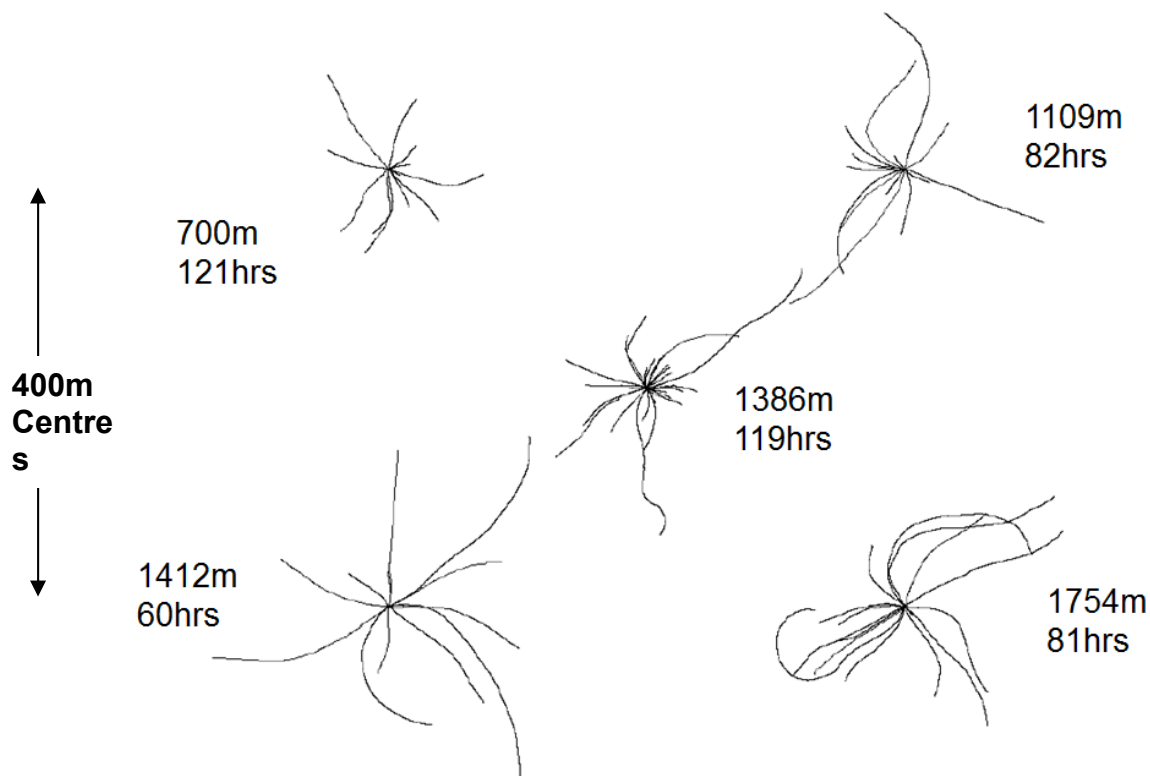
Figure 3: A five well pilot at BMC's South Walker Creek demonstrated commercial system performance
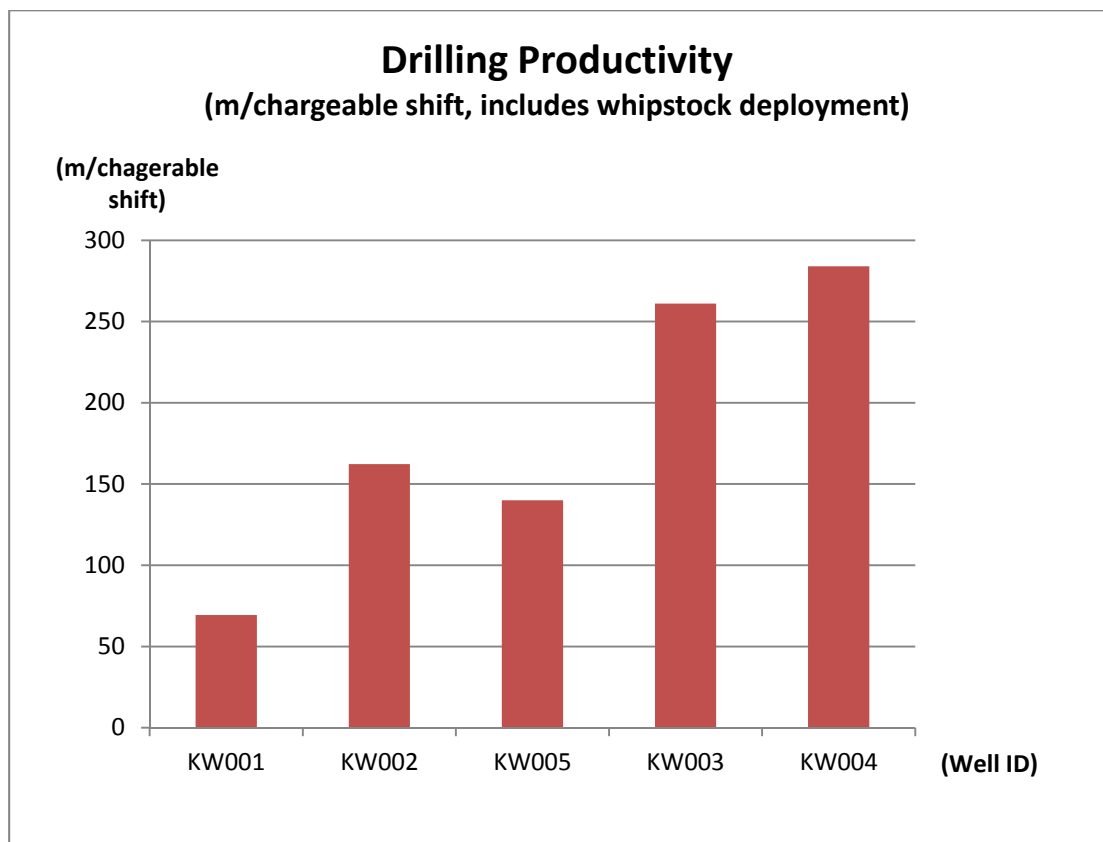
Figure 4: Drilling Productivity at South Walker Creek (in chronological order from left to right)
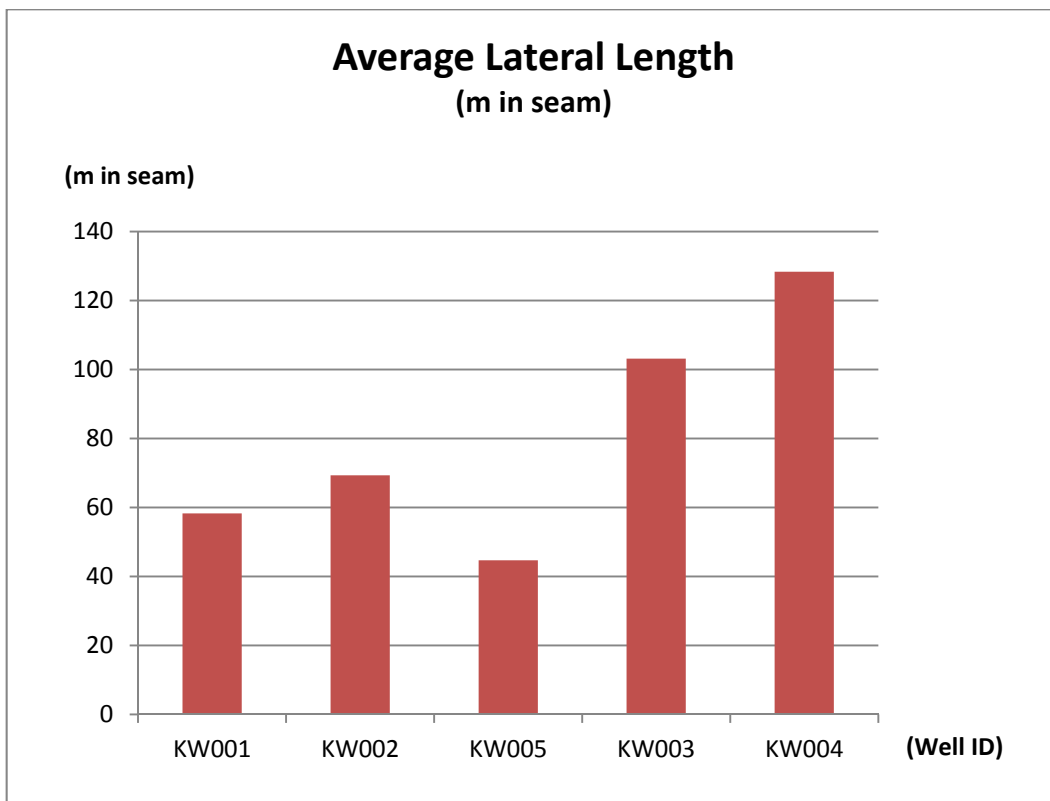
Figure 5: Average lateral length by well (in chronological order from left to right)
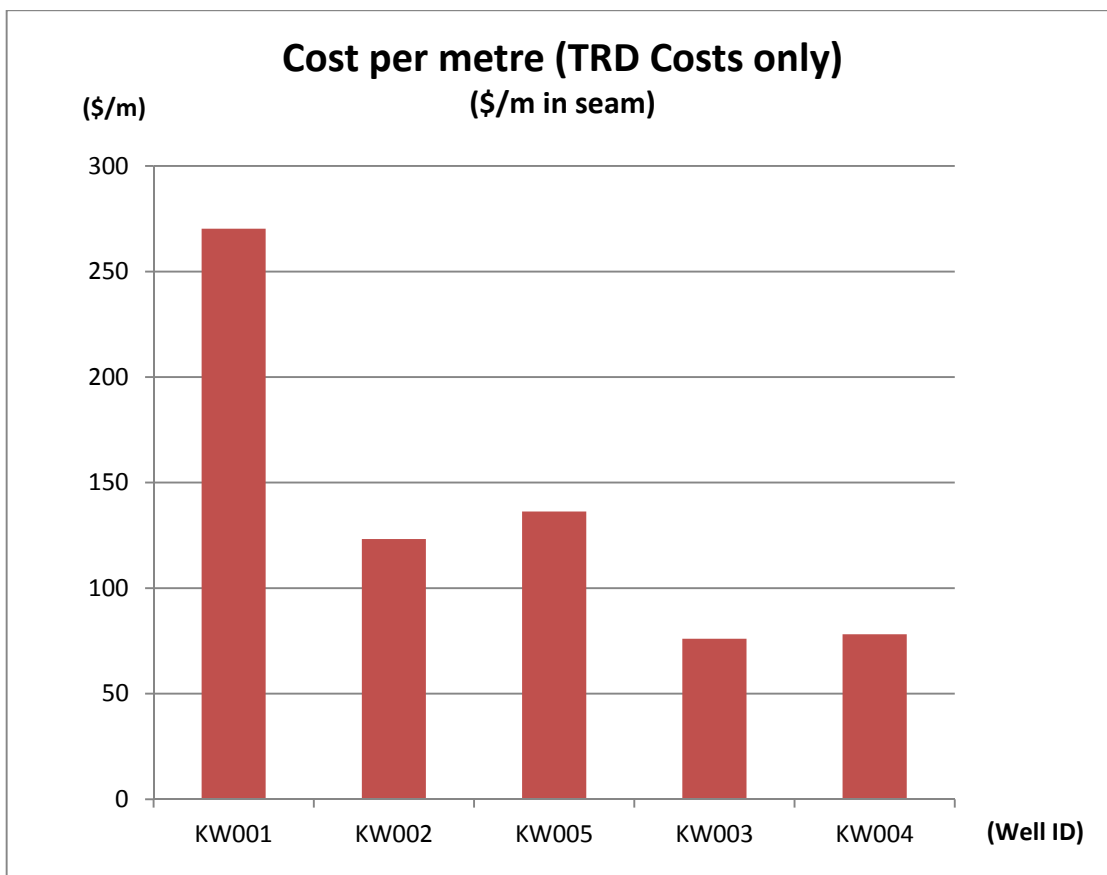
Figure 6: Cost per metre, per well (in chronological order from left to right)

HIGH SPEED CROSS PANEL (HSXP) DRILLING

Underground In-seam (UIS) drilling is carried out for three purposes in Australian coal mining: geological exploration, degasification of workings for mine safety, and greenhouse gas capture. Drilling across coal panels for the purpose of pre-mine gas drainage forms the bulk of UIS drilling activities. A survey of UIS drilling practises was recently completed by CRCMining for ACARP Project C17017[i] (Adam, *et al.,* 2013) and it was revealed that for the applications of cross panel and cross measure drilling, significant opportunity exists to improve the following:

- *Safety, by addressing inherent manual handling hazards associated with UIS drill rigs*
- *Rig utilisation productivity;* by addressing inherent inefficiencies of UIS drill rigs, such as frequent rod changes, slow pipe tripping cycles, slow average drilling rates. Current productivity is around 70-100m/shift. Currently, to drill a typical cross panel borehole drilling techniques take 4-6 shifts with two men crews
- *Reliability of borehole installation*, through adoption of continuous drilling practises (eliminating the need to stop circulation for the addition of jointed pipe.)

CRCMining's waterjet drilling technology has the potential to revolutionise drilling in coal mining applications. Rapid and continuous drilling eliminates man-machine manual handling hazards associated with conventional drilling, and will dramatically increase drilling productivity. The intrinsic simplicity of continuous drilling will enable future automation of the drilling cycle. In combination the advantages of continuous in-seam drilling will slash cost of pre-mine gas drainage whilst transforming the safety and productivity of the drilling function.

Development of a water jet drilling system for cross panel (UIS) applications was initiated in 1998, with ACARP funding. The results of this work are documented in ACARP Project Reports C7024[ii] (Dunn, *et al.,* 1999), and C8023[iii] (Dunn *et al*., 2001). This early work was aimed at the development of technical concepts and designs for a cross panel drilling system, and the manufacture and testing of such a system through a series of highwall drilling trials. In summary, specific technology development areas from this early work included:

- Demonstrating the concept of a continuous waterjet drill as a means of drilling horizontal in-seam drainage holes, with high penetration rates and with some long holes achieved.
- Preliminary investigations and development work on a suitable survey technology to track borehole trajectory.
- Investigations and development of concepts for effecting trajectory control (steering) of the drilling tool and
- Successful development of a prototype compact rig format with potential for underground application. The prototype rig carried 350 m of high pressure hose (Figure).

Figure 7: CRCMining's prototype HSXP rig with 350m hose capacity (2005)

The most recent HSXP trial was completed in 2005. The high speed cross panel system shared the same water-jet drilling technology as the TRD system. The drilling tools are the same. Improvements to the drill head technology including the cutting mechanism, survey electronics, wireless communications and steering techniques, have been successfully shared.

The 2005 trial showed that despite the successful development of a prototype drilling system, drill head cutting technology had at that time not yet matured sufficiently to provide reliable drilling performance. As a direct result, the drilling distance and quality were observed to be generally poor. The key observations from this project included (extract of a post-trial presentation):

From 2005; *"A means of strictly regulating hole diameter at all times is yet to be achieved*

- *Boreholes were calliper logged as consistently oversize (90 mm to 150 mm diameter)*
- *Inadequate flow rate for cuttings to stay entrained in flow due to large borehole diameter*
- *Build-up of cuttings in borehole increases the likelihood of 'boggy' drilling*
- *Appeared that bogging of hose due to accumulation of cuttings substantially increased friction on the hose and was ultimately a limiting factor for drilling depth and*
- *Drilling rate was erratic during testing (ranged from 0 to 5 m/min)"*

From this extract above, the key problem identified with the waterjet tools used in 2005 was their inability to regulate borehole diameter, from which a series of undesirable drilling conditions cascade. However, the lessons and the successful outcomes of the HSXP program did feed into the TRD project.

Since the last HSXP trial (2005), wherein the drilling results were poor due to immature drill head design, subsequent water jet drill technology improvements have resulted in drilling performance breakthroughs during the TRD trials at Broadmeadow Mine in 2010 and South Walker Creek in 2013 (These vastly improved drilling tools are yet to be trialed for HSXP).

The TRD breakthroughs described above have mitigated several key technical risks identified in the 2005 HSXP trials. A more recent technical risk review has identified the remaining key technical risks of;

- DRILLING RANGE - Reliably achieving 500 m long laterals to develop a cross panel fan pattern will require an improvement to the drilling system thrust/friction ratio.
- STEERING CONTROL and ACCURACY – Although survey electronics and the real-time wireless communications technology is established and proven from TRD, an improvement in steering control and survey accuracy is required to equal or exceed current UIS survey performance.
- BOREHOLE QUALITY - The drill head will require some tuning to match it to the UIS application to ensure high quality borehole creation is maintained at high penetration rates, in a variety of coal conditions, particularly friable, 'soft' coals.

An ACARP project is currently underway which seeks to address these remaining HSXP technical risks through a program of targeted, laboratory-based research, and a field validation trial at Peabody's Wambo underground mine in mid-2015.

This program of work aims to mitigate the remaining key technical risks, such that an investment in developing a commercial variant of the system would be a lower risk proposition for a commercializing entity.

CONTINUOUS CABLE BOLT DRILLING

Cable bolt or long tendon installations for roof support is considered to be a hazardous and highly unproductive (though necessary) geotechnical exercise, and presents a major bottleneck in the roadway development system in underground coal mining. Rock bolt drills themselves are considered to be higher risk equipment with operational risk mostly associated with rock falls, manual handling injuries, and incorrect operation of bolting machines (Burgess-Limerick 2010)[iv]. The evidence provides support for an improved and safer technique for cable bolt (6-8 m) drilling and installation systems so as to improve safety and productivity.

CRCMining is currently investigating a continuous cable bolt drilling system. The envisioned drilling system will use a high-pressure water jet cutting head deployed at the end of a flexible hose for

continuous drilling of holes of varying lengths. This essentially negates the need for manually adding / removing drill rods as part of the cable bolt installation process, reducing hazards associated with manual handling and poor productivity. The final embodiment of this technology is expected to have a small operational foot print. This technology is expected to provide a safer and more productive approach for this element of rapid roadway development.

The "Water-jet Cable Bolt Drill Investigation" project (ACARP C21018, Tadik *et al.,* 2013) showed promising potential forCRCMining's water-jet technology in drilling to cable-bolt hole quality requirements (namely in the areas of diameter control, straightness, hole depth, and borehole quality).

Figure 8: Current cable bolt drilling practice is manual-handling intensive

Key questions that this investigative project sought to answer included:

1. **Can water jets rapidly drill straight and smooth holes?** Drilling tests in 1.5 m long homogenous sandstone resulted in straight and consistent holes with tight diameter control. Penetration rates of 1.8 m/min were achieved at 90 MPa of water pressure.
2. **Can diameter control be maintained through bedding planes and spudding sections?** Drilling tests demonstrated that the water jet head was susceptible to produce slightly irregular diameter when the rock being encountered was inhomogeneous (i.e. of variable hardness such as that encountered when drilling through bedding layers). To achieve stricter diameter control in such instances, a modification to the drilling apparatus wasmade, and proved successful in providing good diameter control in inhomogeneous sandstone and also tested to be effective in preventing loss of control when spudding (during which the cutting head is susceptible to stalling).
3. **Can the tool drill up to 8 m by pushing the drilling tool with a hose?** Drill propulsion bytransmission of thrust force via the flexible high-pressure supply hose itself was investigated. (TRD drilling tools use rear-ward facing jets that give it propulsion). This thrust force transmission method and potential issues with longer holes (i.e. high friction, hose spiralling causing lock-up) was investigated and assessed to be effective,
4. **How much water is required?** During the course of the experimental program, highest drilling rates were achieved with an injection pressure of 90MPa (max capacity of CRCMining's high-pressure pump unit), with maximum water usage at approximately 100 litres/min. It is recognized that such consumption levels are at the high end of the range typical of current commercial rigs (generally below 50 litres per minute). Optimisation of the cutting head geometry and nozzle configuration has the potential to increase cutting efficiency (less water pressure / flow-rate required) while maintaining hole quality and productivity.

A second phase of this project is currently underway in which a field prototype will be developed and deployed to Wambo coal mine for field trials in 2015.

Figure 9: Prototype water jet cable bolt drill currently in development by CRCMining

The specific objectives of the second phase are:

1. Develop a field-deployable drilling tool prototype that embodies the key functionalities to meet hole quality requirements set by cable-bolt drilling application.
2. Optimise the cutting head design to improve drilling productivity and energy/water efficiency.
3. Field trial demonstration in a mine portal that assesses drilling tool's capability in drilling a minimum of 6 m – 8 m long holes in vertical-up and sub-vertical trajectories.
4. Assess and document issues related to water jet drilling in a mining environment.
5. If field trials are successful, proceed to OEM(s) engagement to initiate technology transfer.
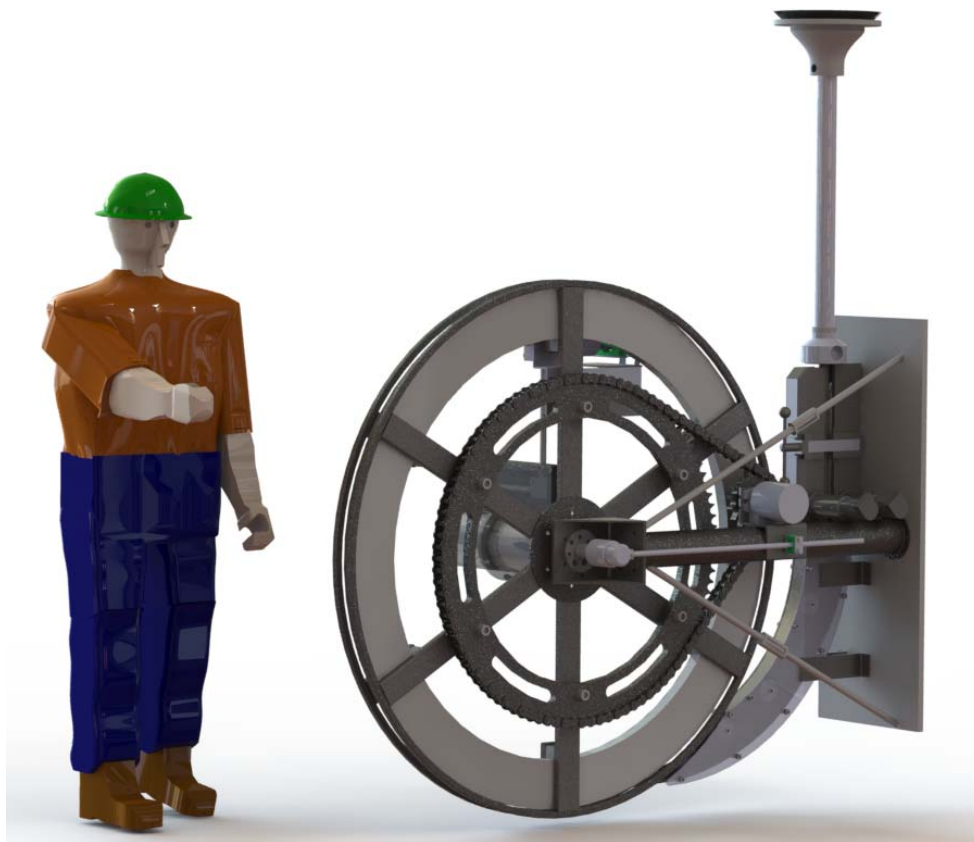
Figure 10: Concept deployment rig for the cable bolt drill tool

CONCLUSIONS

Continous drilling techniques have been shown to be effective and further work is being planned.

ACKNOWLEDGEMENTS

REFERENCES

Adam, S, Stockwell, M, Lever, P, Bewley, A, Prochon, E, Leonard, S and Cronin, J. 2013, Phase II-Tools to simplify the Coiled Tube Drilling System and Phase I – Coiled Tubing Drilling System Development – Risk Mitigation, *ACARP Project C17017*, February 2013.

Dunn, P, Stockwell, M, Adam, S, Hutchinson, I, Mason, I and Schultz, E. 1999, High Speed Cross Panel Drilling, *ACARP Project C7024*, November 1999.

Dunn, P, Stockwell, M, Adam, S, Hutchinson, I, Mason, I and Schultz, E. 2001, High Speed Cross Panel Drilling System, *ACARP Project C8023*, February 2001.

Burgess-Limerick. 2010, Reducing Injury Risks Associated with Underground Coal Mining Equipment, *ACARP Project C18012*, October 2010.

Tadic, D, Adam, S, and Kok, J. 2013, Water Jet Cable Bolt Drill Investigation, *ACARP Project C21018*, August 2013.

THE EFFECTIVENESS OF RAPID STONE DUST COMPLIANCE TESTING IN UNDERGROUND COAL

Dylan James Wedel[1], Bharath Belle[2] and Mehmet S Kizil[1]

ABSTRACT: The addition of stone (limestone) dust to roadway dust in an underground coal mine increases the Total Incombustible Content (TIC) to reduce the potential of the coal dust igniting and propagating an explosion. Coal dust explosions have been proven to be one of the most severe hazards in an underground coal mine hence as Queensland legislation requires the use of roadway stone dusting, the required levels of TIC are higher than other mining districts around the world which also employ other coal dust explosion barriers. Compliance testing currently involves Low Temperature Ashing (LTA) of representative samples with a turn around on results of up to two weeks. To minimise the time that the mine is potentially out of compliance and unsafe, the Coal Dust Explosibility Meter (CDEM) has been tested at a Queensland underground coal mine to determine its effectiveness, through 11 different calibration methods, in rapidly measuring the TIC of roadway dust samples. The key focus of the calibration methods was to explore the effectiveness of the CDEM at its designed threshold of 80% TIC, the use of an inbuilt methane content adjustment to replicate the Queensland legislative requirement of 85% TIC and the use of actual 85% TIC calibration samples. These calibration methods were replicated using both the manufacturer provided Pittsburgh coal dust and mine site specific coal dust for calibrating the CDEM. This paper provides the results of this investigation.

INTRODUCTION

Coal dust explosions present one of the most severe hazards in underground coal mining, however much has been learnt from past disasters, which has enabled the creation of the Department of Natural Resources and Mines, Queensland government Coal Mining Safety and Health Act (Qld,1999). Coal dust explosions are not as easily ignited as methane, however they are typically initiated by a methane explosion when dust is lifted into the air, increasing the strength of the explosion as it combusts. Stone dust in the form of limestone dust has been adopted globally as a means of increasing the incombustible content of roadway dust, rendering it inert to ignition and combustion if subject to a methane explosion. Frictional ignition has been identified as a potential means of coal dust ignition due to the increasing mechanisation in underground coal mines. This increased mechanisation has also resulted in a reduced coal particle size, which has been proven to require higher stone dusting quantities to render the roadway dust inert.

As the Coal Mining Safety and Health Regulation (DNRM, 2001) requires that incombustible contents of 70%, 80% and 85% are maintained in areas of the mine, compliance monitoring is part of an underground coal mine's legal obligation. Low Temperature Ashing (LTA) of roadway dust samples to determine the incombustible content, from the remains after combustion and the addition of the moisture content, has been accepted as the most accurate means of compliance testing. The colorimetric method involves human factor inaccuracies in sample preparation and visual competence during the comparison. The recently developed Coal Dust Explosibility Meter (CDEM), as detailed in Figure 1, exploits the different reflectance properties of coal and stone dust to compare dust samples to a reference sample of the desired incombustible content. Testing in USA underground coal mines has shown accuracies which challenge the colorimetric method and approach that of LTA (Harris *et al*., 2012).

Overview

In 1921, Queensland's worst mining disaster occurred at the Chillagoe Company's Mt Mulligan Mine in Far North Queensland, where 75 men were killed when a coal dust explosion engulfed the mine (QRC, 2007). A number of mine explosions have occurred since with varying degrees of coal dust ignition. Internationally, the increased number of casualties that are associated with coal dust explosions in

[1] *School of Mechanical and Mining Engineering, The University of Queensland, Brisbane, Queensland, Australia, Email: dylan.wedel@uqconnect.edu.au, Tel: 07 3365 3676*
[2] *University of Pretoria/Anglo American Metallurgical Coal, Brisbane, Queensland, Australia*

comparison to a methane explosion are illustrated by 1527 lives lost in the Honkeiko Colliery, China in 1942 (Cybulska, 1988).

Figure 1: CDEM Components (Harris *et al*., 2012)

COAL DUST EXPLOSIONS

Harris *et al.,* (2009) explained the reduction in coal dust size over the century was due to the higher mechanisation of coal mines and the reduction in conventional blasting, with factors such as continuous miners, longwall shearers, cutting speed and cutting depth each having varying effects on the fineness. Sapko, Cashdollar and Green (2007) tested large scale mixtures of Pittsburgh high volatile bituminous coal and stone dust for the propagation of an explosion, demonstrating in Figure 2 that the finer the coal dust, the higher the amount of stone dust required to inert the mixture.
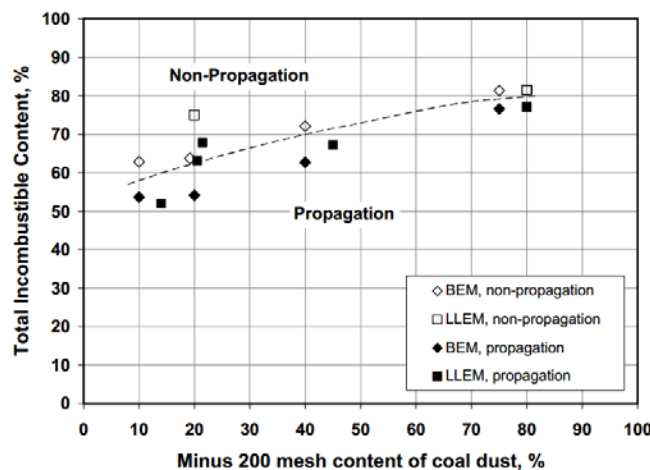
Figure 2: Effect of particle size of coal dust on the explosibility (Sapko, Cashdollar and Green, 2007)

Ignition Sources

Cybulska's (1988) study on major mine explosions concluded that the potential for a methane explosion is lower than a coal dust explosion due to the standards of ventilation and atmospheric sampling, minimising the accumulation of large pockets of methane. However, Cybulska (1988) points out that ignition of methane is easier than coal dust, hence it still provides a risk. Gillies and Jackson (1998) completed an analysis on the absolute flammability on a coal sample, as illustrated in Figure 3, demonstrating the impact that coal dust in the atmosphere has on the explosive limits of methane. The higher the coal dust concentration, the lower the explosive limit of the methane, promoting the importance of monitoring coal dust and methane concentrations together.

Du Plessis (1996) and Cain (2003) both describe that internationally, frictional ignition at the coal face has the highest potential for ignition of methane or coal dust. During Du Plessis' (1996) study of mine explosions, the increasing mechanisation of underground coal mining was responsible for 97% of explosions due to the resulting reduction in use of explosives for coal production.
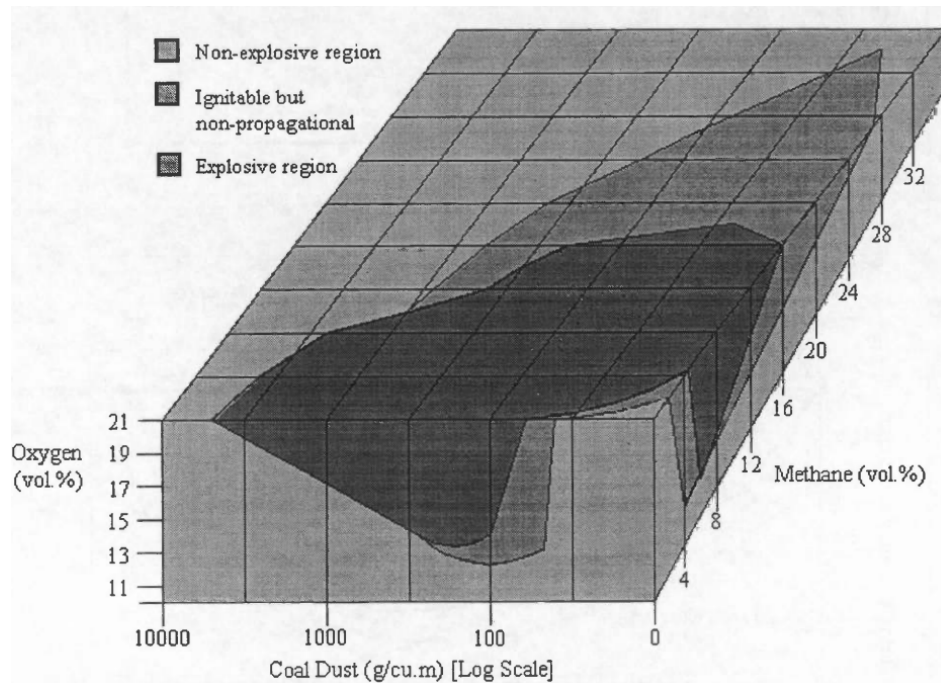
Figure 3: Absolute flammability limit surface for the coal sample (Gillies and Jackson, 1998)

Belle, Carey and Robertson (2012) describe that 70% of global frictional ignition events are initiated due to worn cutter picks and recommend a similar profile for pick replacement as Baker, Jones and Hardman (1981), as detailed in Figure 4.
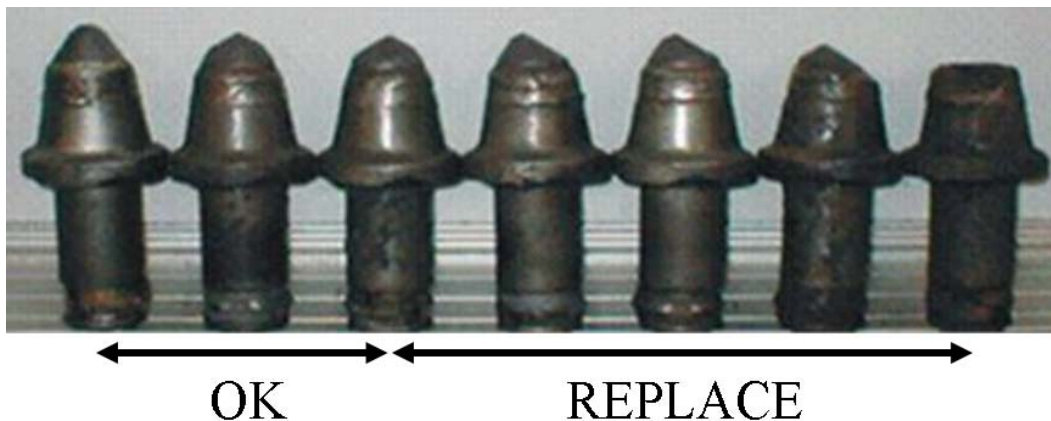
Figure 4: Cutting pick wear profiles (Belle, Carey and Robertson, 2012)

Suppression Methods

Stone dust, which is derived from limestone, gypsum or marble dust, increases the TIC of the roadway dust to the point where it is no longer explosible if subject to a potential ignition source (Jensen and O'Beirne, 1997). The addition of stone dust to the fine coal dust acts as a dilutant, heat sink and oxygen/gas obstruction (DNRM, 2003). Limestone dust has a very limited pulmonary risk hence is the most widely used substance for stone dusting (Hartman *et al.*, 1997). Coal Mining Safety and Health Regulation 2001 (QLD) (and USA coal mines) requires only the use of roadway stone dusting for coal dust explosion suppression, however elsewhere require coal dust explosion barriers to be installed in

underground coal mines (Cain, 2003). Queensland Coal Mining Safety and Health Regulation (DNRM, 2001) has a larger focus on roadway stone dusting with the highest legislative incombustible contents globally (DNRM, 2003).

Roadway dusting offers the advantages over other methods in that it does not affect ventilation resistance (like barriers hanging in the airstream), it provides protection throughout the mine (not just near the face like other barriers), is stirred up with the dust in the explosion front (does not require a pressure front to release it) and is simpler, safer and more cost effective to advance behind the production front than fixed barriers.

Passive stone dust barriers involve the placement of stone dust on lightweight boards which will be displaced by a pressure wave, allowing stone dust to fill the roadway (DME, 2002). This method engulfs the pressure front with stonedust, so any coal dust that is picked up is mixed with stone dust, inertising it prior to the flame front and effectively extinguishing the flame (Cain, 2003). These barriers require replacement of stone dust periodically as it is exposed to the atmosphere (coagulating and/or dispersing), they offer little protection for personnel inbye and require a specific range of conditions to deploy which are not always experienced during methane explosions and weak explosions. Triggered stone dust barriers are currently being developed so that the release of stone dust is determined by electrical sensors in the roadway or even integrated into continuous miners (Cain, 2003).

Bagged stone dust barriers, as shown in Figure 5, provide the same effect as stone dust being dispersed into the roadway upon impact of the pressure front (rupturing the bags).The key advantage of the bags is the longevity of the stone dust, as it is not exposed to the atmosphere, however if the explosion front lingers too far behind the triggering pressure front, there will not be stone dust in the airstream. Water barriers are closed troughs of up to 90 L which are suspended longways across the roadway and are composed of a material which is incombustible but will fail when subject to the pressure front, dumping a wall of water into the roadway, providing an alternative to stone dust barriers. Similarly, active on-board explosion suppression systems were tested in the Kloppersbos explosion tunnel (Belle and Du Plessis, 1999). These systems mounted on CM machines that detect the presence of a methane ignition by means of light sensors are employed in South African and Chinese coal mines. The electronic signals from the sensors trigger the suppression system which creates a barrier of flame-suppressing   material, thus containing the flame in the immediate vicinity of the ignition and so preventing further development and propagation of a coal dust/methane explosion.

Figure 5: Bagged stone dust barrier (Belle and Du Plessis, 1999)

Compliance Testing

DNRM (2003) recommends the stone dust compliance sample collection procedure of taking a uniform width and depth (not exceeding 5 mm) traverse strip sample from around the periphery of the roadway. Where spot samples are taken for weekly samples only, a representative area of the rib and floor should

be sampled to cover a total area greater than 0.1 m2 (DNRM, 2003). If there is any obstructions in the roadway such as conveyor belt structure, DNRM (2003) recommends sampling these surfaces as part of the strip or spot sample as they too have the potential to provide dust to propagate a coal dust explosion.

LTA is the analysis method which is employed in laboratories to accurately determine the TIC of the roadway dust sample (DNRM, 2003). Together the moisture content (through drying) and amount of incombustible material (through heating to burn off the coal) combines to give the incombustible content of the sample. The key advantage of the LTA method is the accuracy of the analysis, which far outweighs the accuracy of other testing methods as demonstrated by comparisons conducted by Harris *et al.,* (2008). Results from the laboratory are more costly than other methods and can take up to two weeks for quarterly stone dust samples to be returned, however weekly samples are turned around in a matter of days (Harris *et al.,* 2009).

The colorimetric method involves analysing the surface of a well-mixed homogenous sample of roadway dust, in comparison to predetermined reference samples at 70%, 80% and 85%, or compared to the greyscale of a digitally scanned sample. The digital colorimetric method involves sieving, drying and scanning reference samples of roadway dust with known TIC to established reference greyscales, then comparing those to scanned roadway dust samples (Kizil, Peterson and English, 2001; Peterson, 2001). The colorimetric method is a low cost (setup and ongoing testing) instant comparison of the roadway dust, albeit not required by Queensland Coal Mining Safety and Health Regulation 2001 (QLD, 2001) prior to sending for laboratory analysis, this practise offers the ability to enable immediate re-treatment of potentially non-compliant roadways. Peterson (2001) highlighted that sample discolouration; the visual ability of the tester to distinguish between the sample and reference colours; sufficient lightning, adequate drying to prepare the sample underground and consistency of the seam (relevance of reference samples) affect the accuracy of this method. In addition, supplied stone dust need not be typically 'white' in colour.

The CDEM, a hand held optical instrument for assessing coal dust incombustible content, has been created in collaboration between the Pittsburgh Research Laboratory of the National Institute for Occupation Safety and Health (NIOSH) and the Mine Safety and Health Administration (MSHA) (Sapko and Verakis, 2006). The CDEM produces either a green result which signifies the sample is compliant (lighter than the reference sample) or a red result which signifies a non-compliant sample (darker than the reference sample). In combination with a red result, it also estimates a range of the sample's TIC.

The CDEM employs an infrared light emitting diode, to focus a beam of infrared radiation onto the dust sample, with a silicon photodiode sensor, which measures the reflected light intensity. The reflected light intensity is then compared to the reference sample and the empirical normalised reflectance for Pittsburgh roadway dust samples, to determine if the sample is in compliance (Sapko and Verakis, 2006). Prior to the commercialisation of the product, Harris *et al.,* (2012) conducted a field study finding 75% of the 297 samples to pass and 25% to fail, the percentage of incorrect and correct readings are detailed in Table 1, with descriptions of the four criteria used to analyse CDEM effectiveness results.

Table 1: CDEM field study (after Harris *et al.,* 2012)

CDEM/LTA Comparison	Percentage (%)	Description
Disagreeing Red	9	Compliant samples that the CDEM falsely failed.
Disagreeing Green	1	Non-compliant samples that the CDEM falsely passed.
Agreeing Red	91	Non-compliant samples that the CDEM correctly failed.
Agreeing Green	99	Compliant samples that the CDEM correctly passed.

The two disagreeing values are low which proves this device to be promising, however the most concerning failure is the disagreeing green, which if the mine was to solely use the CDEM for compliance testing, these samples would have been considered compliant, even though they are actually non-compliant. Ideally this disagreeing value would be 0 with the optimum calibration standard, however there would not be a compliance issue if the disagreeing red was >0. The only issue with a disagreeing red sample would be that the cost and resource allocation employed to re-treat that roadway could be better utilised, saving costs and resource use.

CASE STUDY

Overview

Roadway dust samples were collected from a Queensland underground coal mine. The samples were well mixed, with a sieved sample taken from each for further testing using the LTA, CDEM and colorimetric methods. The results spanned 109 roadway dust samples, with each sample being tested with the CDEM three times for the 11 calibration methods to give 1199 averaged results. The colorimetric method and LTA results were a single result for each of the 109 samples. The 11 calibration methods include small variants on the seven detailed in the methodology due to variations in the reference samples' TIC and also due to the methane adjustment not equalling the desired 85%.

Calibration Methods

The calibration method detailed by the manufacturer is as follows (Sensidyne, 2013):

1. prepare a 50 mL sample of the provided Pittsburgh coal dust by passing through the molecular sieves (in the large tube) and sieve (in the funnel);
2. repeat step one with a 50 mL sample of stone dust from the mine;
3. repeat step one with a 50 mL mix of 20% Pittsburgh coal dust and 80% stone dust;
4. turn on CDEM;
5. attach reflectance calibration cup (standard cover) to base   and follow prompts on screen to complete calibration;
6. fill the small thimble sized cup with a representative sample from the dried and sieved coal dust and insert into the CDEM to complete the coal dust calibration; and
7. repeat step six with the stone dust and, mix of 20% Pittsburgh coal dust and 80% stone dust, to complete the entire calibration.

The key difference between calibration of the meter for use in United States of America (USA) and Australia is the TIC required by legislation being 80% and 85% respectively, providing the motivation for the analysis of these seven different calibration methods:

1. the manufacturer's standard (calibrated to Pittsburgh coal at 80% TIC with mine site specific stone dust) (Sensidyne, 2013);
2. the manufacturer's standard for Queensland (higher methane level to mimic the 85% TIC required by legislation) (Sensidyne, 2013);
3. the manufacturer's standard, air drying samples first (removing the use of the provided molecular sieves) (Wu, 2013);
4. calibrated to Pittsburgh coal at 85% TIC with mine site specific stone dust, using manufacturer's standard for sample drying;
5. calibrated to mine site specific coal at 80% TIC with mine site specific stone dust, using manufacturer's standard for sample drying;
6. calibrated to mine site specific coal at 80% TIC with mine site specific stone dust, using manufacturer's standard for sample drying and higher methane level to mimic the 85% TIC required by legislation; and
7. calibrated to mine site specific coal at 85% TIC with mine site specific stone dust, using manufacturer's standard for sample drying.

Results

Analysis of the CDEM data showed promising results with the CQ underground coal dust calibrations showing the lowest disagreements out of all the calibrations, as detailed in Table 2. Table 2 also includes the values derived from the two colorimetric tests which were conducted using the mine's colour templates for roadway dust samples with a known TIC of 80% and 85%. The two colorimetric methods both had low and no green disagreements, however there were many samples which were considered red disagreements.

Table 2: Percentage based on red and green result totals of CDEM and colorimetric calibration methods

Calibration Method (LTA %TIC)	Disagreement		Agreement	
	Red	Green	Red	Green
1 (80%)	85	2	15	98
2a (85.2%)	65	4	35	96
2b (84.8%)	65	4	35	96
3 (80%)	87	0	13	100
4 (85%)	67	2	33	98
5 (80%)	58	3	42	97
6a (84.8%)	38	8	63	92
6b (85.2%)	38	8	63	92
7a (89.7%)	61	3	39	97
7b (86%)	55	6	45	94
7c (85.1%)	25	11	75	89
Colorimetric (80%)	82	1	18	99
Colorimetric (85%)	60	0	40	100
Harris *et al.,* (2012) (80%)	9	1	91	99

The CDEM sample which provides the lowest disagreements is calibration method five (preference on lowest disagreeing green, then lowest disagreeing red) which is the calibration of the system to 80% using all mine site related references. Calibration method #3 offers no disagreeing green values, however this was a much smaller sample size due to the undried and dried samples showing a definitive result to begin with, hence further testing of the calibration method was discontinued. The CDEM and colorimetric method offer similar amounts of red disagreements, however both colorimetric methods have lower green disagreements. The all-important green disagreements are on average lower for the 80% calibration methods, potentially due to this being the upper limit the CDEM was designed for.

A comparison between the LTA and CDEM TIC results is displayed in Figure 6, however as the CDEM only displays TIC estimates between 70% and 80%, the data is situated within this zone. The green disagreements are those samples which lie to the left of the 1:1 line and the CDEM estimates them as 80% (top left quadrant). The red disagreements are highlighted in the bottom quadrant of Figure 6 as this is where the TIC determined by the CDEM is less than the LTA (which found the samples TIC >80%). The results where both are in agreement are the blue points lying in the remaining two quadrants. Figure 6 shows that the CDEM does not rank the TIC for the majority of samples higher than the LTA, hence providing an additional safety factor in the test results. Being too safe however is costly, in terms of re-treating roadways which may not require re-treatment following the return of LTA results.
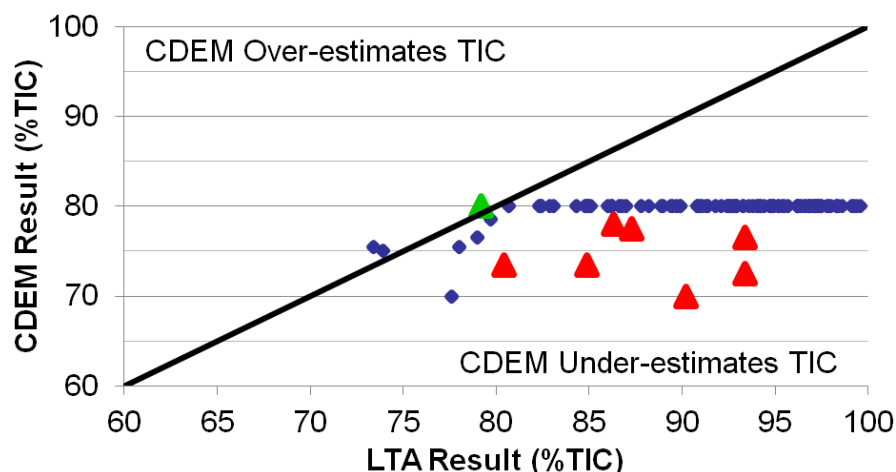
Figure 6: TIC correlation between averaged CDEM estimate and LTA result for calibration method five samples

To highlight the inability to replicate the results from Harris *et al*., (2012) field study of the CDEM, Figure 7 demonstrates the average results of testing at 80% TIC. The proportion of disagreements is substantially higher than the CDEM pre-commercialisation field study, disproving the effectiveness of the CDEM for rapid compliance testing for this particular mine site and set of samples.

The colorimetric methods offer little difference between the two reference levels in Table 2, however in comparison to the CDEM results in Figure 7, the average disagreements are slightly higher. The lower all-important green disagreements for the colorimetric method suggests the method may offer the potential of a higher accuracy (with minor adjustments), than the current CDEM calibration methods.
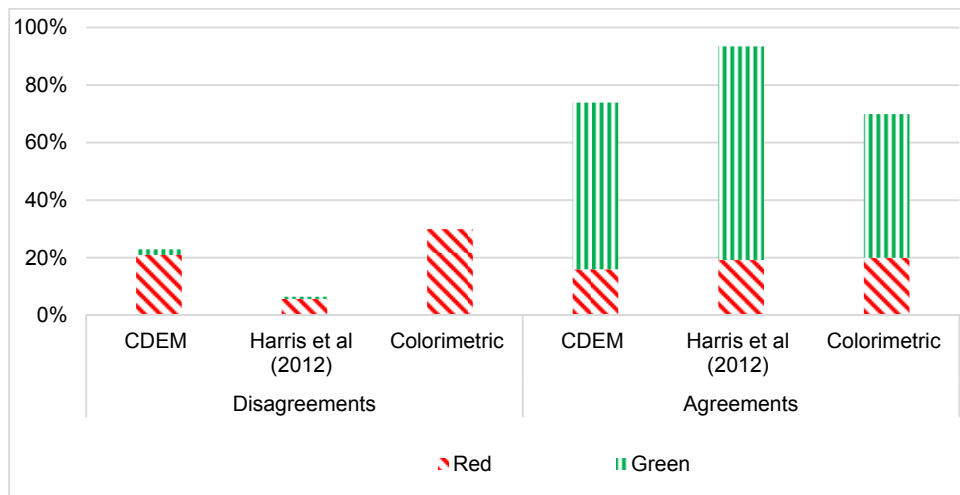
Figure 7: Average disagreements and agreements between CDEM, Harris *et al*., (2012) and colorimetric results with LTA for 80% TIC

ANALYSIS AND DISCUSSIONS

Calibration

The three calibration samples (80/85% TIC reference, coal and stone dusts) in combination with the initial reflectance calibration are the most critical variables in the process, as these define the accuracy of the CDEM in estimating TIC. The reference sample required by the manufacturer involves mixing the provided Pittsburgh coal dust with site specific stone dust. It can be seen in Table 2 that the calibration methods where the Pittsburgh coal dust was used as the reference sample (1, 2 and 4) experienced the highest number of disagreeing greens. As disagreeing greens are those which the CDEM would pass, even though they are non-compliant, this quite clearly disproves the effectiveness of the CDEM when used in CQ coals in accordance to the manufacturer's calibration methodology.

The TIC of the three reference samples developed for calibration method seven varied with 85.1%, 86% and 89.7%, and the effect this had on the accuracy of the CDEM is exemplified with the increasing number of green disagreements with the decreasing TIC. The green disagreements increase with decreasing TIC because the reference is becoming darker, but the samples are still not in compliance. It is of interest that the TIC of 89.7% offered the highest amount of red disagreements in calibration method seven, with 85.1% featuring the lowest number. The converse relationship between the red and green disagreements throughout the varying TICs in calibration method seven clearly demonstrates the fine line between what the CDEM estimates as compliant or non-compliant, hence the creation of a reference sample has a major impact on the CDEM effectiveness.

The 85% TIC reference sample should be prepared using coal dust and stone dust representative of the roadways that the CDEM is intended on being employed within for compliance testing. These samples should also follow the particle size distribution exemplified by the supplied Pittsburgh coal dust and be thoroughly mixed to ensure that the sample provides the appropriate surface area of 85% stone dust and 15% coal dust, when pressed against the CDEM probe. To further investigate the effectiveness of the device in its current state, if the initial reflectance calibration is replaced with an accurate site specific reference sample (the same used in the fourth calibration step), this would potentially align the CDEM with site specific parameters, potentially improving the effectiveness. This hypothesis is based on the

assumption that the reflectance calibration cup replicates the manufacturer's empirical reflectance for the 80% TIC sample using Pittsburgh coal dust.

Testing Methodology

Sapko and Verakis (2006) identified the impact that the moisture content of a sample has on the effectiveness of the CDEM in estimating TIC as detailed in Figure 8, however Wu (2013) recommended removing the use of the molecular sieves from the testing methodology, by leaving the 50 mL sample to dry overnight in an air conditioned room. This recommendation was tested in calibration method three with a small group of roadway dust samples finding that of the 48 samples, calibration method one and three agreed on 43 of the samples.
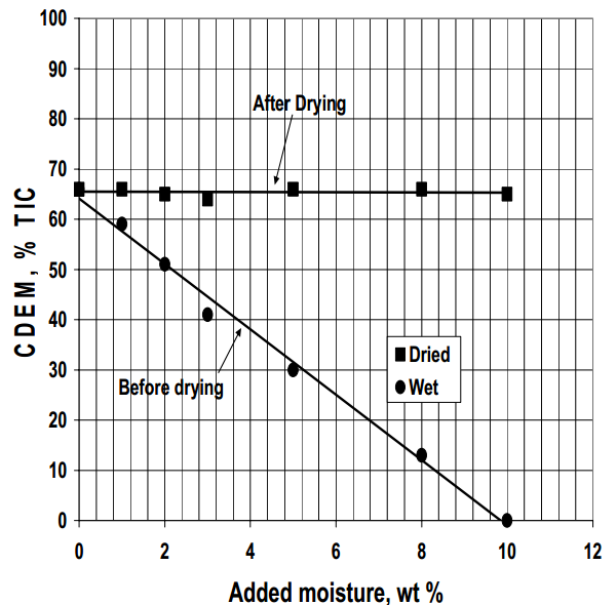
Figure 8: Effect of moisture on CDEM reading (Sapko and Verakis, 2006)

These results support molecular sieves being used on all samples to remove as much moisture as possible. The American Society for Testing and Materials (2008) has developed ASTM D4643 – 08 Standard Test Method for Determination of Water (Moisture) Content of Soil by Microwave Oven Heating which involves heating a small sample of a moist soil in the microwave for 3 minutes to remove all water. This method could be trialled for drying roadway dust samples prior to testing with the CDEM, more efficiently and less costly than molecular sieves.

Methane content adjustments used in calibration methods two and six can be compared to the actual 85% TIC calibration methods four and seven respectively. The actual 85% TIC reduces the disagreements, hence the methane content adjustments should not be used to mimic a TIC higher than 80% where there is the ability to mix an actual reference sample for the specific TIC.

Reflectance Algorithm

The CDEM calculates the normalised reflectance relative to the reference sample that is used to calibrate the meter, however the unit only accepts reference samples within a certain range of normalised reflectance either side of the empirical value found for the Pittsburgh coal dust. It would be of value to test the normalised reflectance from a series of samples which are close to the extinction limit (minimum TIC to prevent explosion) for the CQ underground mine, then having the value input as a single averaged value, rather than calibrating with a single sample, to potentially improve the CDEM effectiveness.

Intrinsic Safety

The CDEM has not been recognised in Queensland as intrinsically safe, as such the CDEM would need to be certified against International Electrotechnical Commission System for Certification to Standards Relating to Equipment for Use in Explosive Atmospheres (IECEx System) before being able to be used

in an underground coal mine (DNRM, 2014). Once certified, the CDEM would offer a less subjective means of preliminary testing in the low light conditions of an underground coal mine, as the colorimetric method requires good light for distinguishing between colours and the CDEM just displays the word green or red on the screen. This would allow for real time feedback during stone dusting.

Colorimetric Method

The data on a whole shows that similar accuracies are achievable from both the colorimetric and CDEM testing methods. Due to the lower cost and time involved with the colorimetric method, it is recommended that the CQ mine continues using the colorimetric method for preliminary testing (prior to LTA). To lower the number of disagreements, darker reference samples should be adopted for the colorimetric reference template. A safety factor should still be applied during colorimetric testing in the form of some compliant samples being slightly darker than the reference sample, to minimise the potential for any incompliant roadways being deemed safe. Adopting these actions will reduce time spent on using the CDEM with practically no change in accuracy and changing the colorimetric reference template will save large costs by reducing excessive stone dusting.

CONCLUSIONS

Testing in an underground coal mine has shown that the CDEM is not supported for use in its current equipment format in favour of the colorimetric method for preliminary compliance testing, as the accuracies achieved are lower than the manufacturer found during their testing. Adjustments of the reference samples of the colorimetric method to darker than they are currently, will allow the mine to achieve similar accuracies to the CDEM for a lower labour cost and adopting darker reference samples, the re-treatment of already compliant roadways will be reduced, hence reducing costs.

The CDEM proved to be more effective when calibrated using all mine site specific samples (coal dust, stone dust and 80%/85% reference sample) with the 80% TIC calibration offering the best results. The manufacturer's calibration method resulted in slightly lower green disagreements, than the mine site specific calibration methods, however it had significantly higher red disagreements, resulting in a higher cost for re-treatments. The single worst calibration method was one where the methane content was adjusted to mimic 85% TIC. The methane adjustment was found to be less effective than an actual TIC reference sample, hence when possible the methane adjustment should be avoided.

The air drying of samples was investigated as a cost reduction exercise by not using the manufacturer's molecular sieves for drying. The results however highlighted that this method is less effective than the molecular sieves. The effect of the reference sample for calibration on the accuracy of the results was found to be a result of the particle sizes of the coal dust featuring in the roadway dust samples. As the stone dust is typically regular in size throughout the mine, the resulting reflectance of roadway dust samples where different coal dust particle sizes is present, results in varied reflectance for the same TIC. It should be noted that the CDEM was only used on the surface for this study and not underground.

RECOMMENDATIONS

There are six key recommendations that have been derived from the findings of this study:

1. it is not recommended for immediate use of the CDEM as a preliminary testing method;
2. investigate improvement options for the current colorimetric method by updating the reference samples and developing different sets of reference samples for different operational zones of the mine (dependant of coal dust size) to reduce the additional costs of re-treating roadways that are actually compliant;
3. investigate the effectiveness of the CDEM in compliance testing in non-operational zones of the underground mine by developing different sets of reference samples for different operational zones of the mine (dependant of coal dust size) and replicating the testing that has been completed in this study to determine if the CDEM is more effective when calibrated with samples which are similar in composition to those being tested;
4. determine the normalised reflectance of the roadway dust at the extinction limit from a series of samples, so as to determine an average value that could be input into the CDEM as a reference rather than basing the calibration on a single reference sample or roadway dust;

5. adjust the programming of the CDEM to allow "developers or evaluators" to finely adjust calibration settings in an aim to improve the effectiveness of the meter;

6. complete the intrinsic safety certification on the CDEM upon fine tuning; and

7. investigate the use of the ASTM microwave drying method as an alternative to the use of the manufacturer's molecular sieves.

ACKNOWLEDGEMENTS

REFERENCES

American Society for Testing and Materials. 2008, ASTM D4643 – 08 Standard Test Method for Determination of Water (Moisture) Content of Soil by Microwave [online], Available from: < http://www.dot.nd.gov/manuals/materials/testingmanual/d4643.pdf > [Accessed: 29 August 2014].

Baker, R H, Jones, G J and Hardman, D R. 1981, An assessment of pick wear and its effect on continuous miner performance, *South African Chamber of Mines Res Org Report No 10/81*, 28 p (South African Chamber of Mines: Johannesburg).

Belle, B and Du Plessis J. 1999, Kloppersbos health and safety research in the South African coal industry, in *Proceedings International Conference on Mining - Challenges of the 21st Century*, New Delhi, pp 1-8 (CSIR Division of Mining Technology: Johannesburg).

Belle, B, Carey, D and Robertson, B. 2012, Prevention of frictional ignition in coal mines using chilled water sprays, in *Proceedings 12th Coal Operators' Conference*, Wollongong, pp 175-184 (University of Wollongong, Australasian Institute of Mining and Metallurgy and the Mine Managers Association of Australia: Wollongong).

Cain, P. 2003, The Use of Stone Dust to Control Coal Dust Explosions: A Review of International Practice, 100 p (rokdok: Lethbridge).

Cybulska, R. 1988, Propagation and Suppression of Colliery Explosions-with Particular Reference to Polish Conditions, *The AusIMM Bulletin and Proceedings*, 293(7):61-66.

DME. 2002, Department of Minerals and Energy, Republic of South Africa, Guideline for the Compilation of a Mandatory Code of Practice for the Prevention of Flammable Gas and Coal Dust Explosions in Collieries, 30 p (Department of Minerals and Energy: Sunnyside).

DNRM. 1999, Department of Natural Resources and Mines, Queensland Government, *Coal Mining Safety and Health Act 1999*, 2 March 2001.

DNRM. 2001, Department of Natural Resources and Mines, Queensland Government. *Coal Mining Safety and Health Regulation 2001*, 2 March 2001.

DNRM. 2003, Department of Natural Resources and Mines, Queensland Government. Quality of incombustible dust, sampling and analysis of roadway dust in underground coal mines, Coal Mining Safety and Health Act 1999, Recognised Standard – 05 [online]. Available from: < http://mines.industry.qld.gov.au/assets/inspectorate/recog_standard05.pdf > [Accessed: 30 December 2013].

DNRM. 2014, Department of Natural Resources and Mines, Queensland Government. Simtars: Testing, certification and calibration services [online]. Available from: < http://www.dnrm.qld.gov.au/mining/simtars/testing-cert-calibration-services > [Accessed: 29 August 2014].

Du Plessis, M. 1996, South African coal mine explosions, *in Proceedings QCO/DME Coal Industry Conference in Conjunction with Hazcoal Management*, Yeppoon, pp 127-134 (QCO/DME Coal Industry Safety Conference: Yeppoon).

Gillies, A D S and Jackson, S. 1998, Some investigations into the explosibility of mine dust laden atmospheres, *in Proceedings coal 98*, Wollongong, pp 626-640 (Australasian Institute of Mining and Metallurgy: Melbourne).

Harris, M L, Cashdollar, K L, Man, C and Thimons, E. 2009, *Mitigating coal dust explosions in modern underground coal mines*, 7 p (The National Institute for Occupational Safety and Health: Pittsburgh).

Harris, M L, Sapko, M J, Cashdollar, K L and Verakis, H C. 2008, Field evaluation of the Coal Dust Explosibility Meter (CDEM), *in Proceedings SME Annual Meeting*, Salt Lake City, pp 1-5 (Society for Mining, Metallurgy and Exploration: Eaglewood).

Harris, M L, Sapko, M J, Varley, F D and Weiss, E S. 2012, Coal Dust Explosibility Meter evaluation and recommendations for application [online], Available from: < http://www.cdc.gov/niosh/mining/UserFiles/works/pdfs/ic9529.pdf > [Accessed: 25 March 2014].

Hartman, H L, Mutmansky, J M, Ramani, R V and Wang, Y J. 1997, *Mine Ventilation and Air Conditioning (3rd Edition),* pp 95-101 (John Wiley & Sons, Inc.: New York).

Jensen, B and O'Beirne, T. 1997, The design and performance of underground explosion barriers – a review, *The AusIMM Proceedings*, 302(1):71-76.

Kizil, M S, Peterson, J and English, W. 2001, The effect of coal particle size on colorimetric analysis of roadway dust. Journal of Loss Prevention in the Process Industries, 14 5: 387-394.

Peterson, J. 2001, Colorimetric and density analysis of roadway dust, Bachelor of Engineering Undergraduate Thesis (unpublished), University of Queensland, Brisbane.

Peterson, J and Kizil, M S. 2001, Colorimetric and density analysis of roadway dust. In: , AusIMM Youth Congress. AusIMM Youth Congress, Brisbane, (21-26). 2-6 May 2001.

QRC. 2007, Make Safety their Monument, documentary, Queensland Resources Council, Brisbane, 19 January.

Sapko, M J, Cashdollar, K L and Green, G M. 2007, Coal Dust Particle Size Survey of U.S. Mines, *Journal of Loss Prevention in the Process Industries*, 20:616-620.

Sapko, M J and Verakis, H C. 2006, Technical development of the Coal Dust Explosibility Meter, in *Proceedings SME Annual Meeting*, St. Louis, USA, pp 1-5 (Society for Mining, Metallurgy and Exploration: Eaglewood).

Sapko, M J, Weiss, E S and Watson, R W. 1987, Explosibility of float coal dust distributed over a coal-rock dust substratum, *in Proceedings of the 22nd International Conference of Safety in Mines Research Institutes* (ed: D Guoquan), pp 459-468, (China Coal Industry Publishing House: Beijing).

Sensidyne. 2013, Coal Dust Explosibility Meter calibration and use, pp 1-4 (Sensidyne: St Petersburg).

Wu, H W. 2013, Personal communication, Mining Engineering and Mine Ventilation Consultant, Gillies Wu Mining Technolog.

EXPLOSION PREVENTION IN COAL MINE TBM DRIFTS-AN OPERATIONAL KNOWLEDGE SHARE

Bharath Belle[1] and Adam Foulstone[2]

ABSTRACT: Since the first record of a colliery explosion in Belgium, nearly 300 years ago, significant improvements have been achieved in the prevention of explosions in mines. However, based on the past surface TBM project safety statistics, gas explosion hazards are not unique to coal mines but also occur in TBM projects with 48 explosion fatalities recorded worldwide calling for continued diligence and improvements in explosion risk management. Success of TBM in civil engineering infrastructure in poor ground conditions resulted in consideration of its application to a coal mine in QLD. This paper provides a first time case study of TBM application in a coal mine drift development in identifying the explosion hazards and its management. The investigations were extensive with preliminary hazard identification from coal mining approach to application of various ventilation and explosion prevention controls. As in coal mine spontaneous combustion management, explosion hazard was managed by continuous nitrogen injection aimed at maintaining an explosive inert atmosphere in a highly inaccessible TBM pressurized chamber area. The background to hazard identification and control solutions including continuous nitrogen inertisation provided herein would enhance explosion management in both civil and mining TBM applications worldwide.

INTRODUCTION

A Tunnel Boring Machine (TBM) is typically used to develop roadway and utility tunnels with a circular cross section through a variety of sub surface ground as an alternate to drill and blast excavation methods (Figure 1). The following paragraphs describe TBM operational aspects to those unfamiliar such as in the coal mining industry. For soft subsurface ground conditions, as often encountered in coal mines with up to 7 bar of water pressure, Earth Pressure Balance (EPB) TBMs are used due to their ability to hold up soft ground by maintaining a hydrostatic balance between earth and pressure surrounding the excavation. The TBM (Figure 1) has two main components, i.e., shield which is in direct contact with the excavation face and the back-up system. The shield is essentially a steel skin that separates the interior of the TBM system from the ground. The back-up rolling system carries all the auxiliary elements that the TBM machinery requires for continuous advancement.

The front of the shield accommodates a cutter head that uses a combination of tungsten carbide cutting bits, and/or hard rock disc cutters (with sizes of 13 to 19 inches) which excavate the face as the cutting head rotates about its central axis. Depending on the ground conditions, additives such as bentonite, polymers and foam are injected from the cutter head to induce ground stability and smoother excavation conditions (Anglo, 2013). Advancement of the TBM face is by the action of thrust cylinders positioned at the rear section of the shield body which press axially against the tunnel liner to push the cutter head forward. The shield is divided into front and rear shield sections connected by hydraulic body frame components that allow for articulation. An erector arm, located at the rear body of the shield is used for installation of the concrete tunnel lining sections. The tunnel muck produced at the TBM's face is removed by a screw conveyor that feeds onto a transfer conveyor belt that in turn dumps it onto another conveyor for transport to surface.
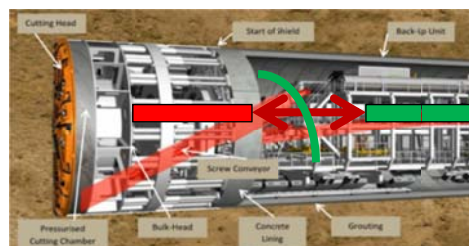

Figure 1: Overview of coal mine TBM with Explosion Risk Zoning

[1] *Anglo American Coal, Queensland, Australia/University of Pretoria, South Africa, E-mail: bharath.belle@angloamerican.com*, Tel: *+61 (7) 4841 0400*
[2] *464 Goonyella Road, Moranbah QLD 4744, Australia, E-mail: j.adam.foulstone@angloamerican.com*, Tel: *+61 (4) 08 153 531*

APPLICATION OF TBM IN COAL MINES

TBMs have been used in mining related projects since the 1950s. Subsurface geological risks typically distinguish these projects from typical civil engineering applications. There have been up to 24 TBM projects in mining worldwide, viz., Canada, Zambia, South Africa, USA, Norway, Germany, Mexico, Chile, Australia, Italy, China, and PNG. Based on the past mining experiences, it was noted by Brox (2013) that every tunnel project and site location is unique in terms of geology, access, terrain/cover, experience of candidate contractors and project completion demands.

During the 1970's and '80's, Robbins TBMs were used to access coal seams in a number of coal mines globally, i.e., Selby in the UK, three mines in Germany, the Donkin Morien Mine (under sea access) in Canada and Westcliff mine in NSW (Australia). The West Cliff Colliery Men and Materials Drift had 5 m diameter and was 1595 m long. It was built in 1975/6 with an average advance rate of 27.6 m/week. Documentation of these coal mining TBM applications did not convey any known occurrence of explosion hazards during development. Other known application of TBMs in the mining industry is the 8 km long Los Sulfatos exploration tunnel of 4.5 m diameter developed for Los Bronces mine at an elevation of 4000 m. Key reasons for its selection as a development method were flexibility to access the worksite, natural restrictions related to the portal installations and geotechnical and environmental considerations. The field review showed no known experiences of any methane gas intersections during the 8 km development (Belle, 2010) although a significant inflow of water had to be managed.

Success of TBM technology in establishing surface civil infrastructure and providing alternate means of rapid access in poor ground conditions, resulted in its consideration of its application at Grosvenor coal mine in QLD to establish the conveyor and men and material transport drift access roadway from the surface. The conveyor drift has a gradient of 1:6 with a length of 762 m and while the transport drift is a 993 m long and has a 1:8 gradient. Considering the geotechnical challenges, the TBM excavation method had to utilize EPB technology which is 135 m long and of 8.0 m diameter (Figure 1). For the first time, a TBM required addressing simultaneously ventilation, gas and cooling management elements, and other related mining hazards. The drift ventilation and gas management systems involved the supply and control of air using an intake and exhaust airway network to manage health and safety risks.

At the time of completing this paper, the TBM had finished the conveyor drift (Figure 6) with a total of 581 rings of 1.4 m length, at a distance of 813 meters from the tunnel opening at the surface. Currently, the TBM is planned to be moved to construct the people and materials drift, involving disassembling the front section of the machine underground. The machine was then retracted out the conveyor drift using heavy lift and transport equipment and face ventilation modified to force-exhaust system to manage the Goonyella Middle (GM) seam gas emissions. This conveyor drift was completed over a period of 5 months (Dec 20th to 15th May 2014).

With the ample knowledge on methane gas and its management in coal mines, it is a common practice in coal mines to continuously monitor and anticipate hazards that could result in explosions. Among various ventilation design factors, this paper will attempt to highlight the identification and management of methane and other gases in TBMs during drift development at Grosvenor from coal miner's perspective.

COAL MINE TBM EXPLOSION RISK ASSESSMENT

Coal mine explosion fatality statistics worldwide (Figure 2) demonstrate the need for eternal vigilance to prevent methane and coal dust explosions regardless of the level of gas emissions (Phillips, 2009). The mine explosion risks associated with TBM use was recognized by the mining team prior to start of the Grosvenor project. Copur *et al.,* (2012) captured the gas emissions and explosion risks associated with tunnelling globally (Table 1). Based on past TBM project safety statistics which recorded 48 explosion fatalities, gas explosion hazards are not unique to coal mines.

Key lessons from the past civil TBM project experiences (Copur *et al.,* 2002; Brox, 2013) in relation to ignition and explosion management are:

- Adequate knowledge and careful evaluations of technical and non-technical issues such as geology, access, sub-surface cover, fault zones and structures are required.
- Ensuring adequate background information on gas emissions from seams or strata for hydrocarbons.
- Need for skilled and experienced mining engineers.
- Use of gas measurement and control systems. The location and calibration of monitors at

strategic locations inside TBM's cutter head, shield, and segment erector section with automatic TBM shutdown system interlock features is required.

- Ignition prevention techniques such as grouting, pre-drainage, foam injection and sealed lining during the intersection of gassy water inflow conditions should be provided.
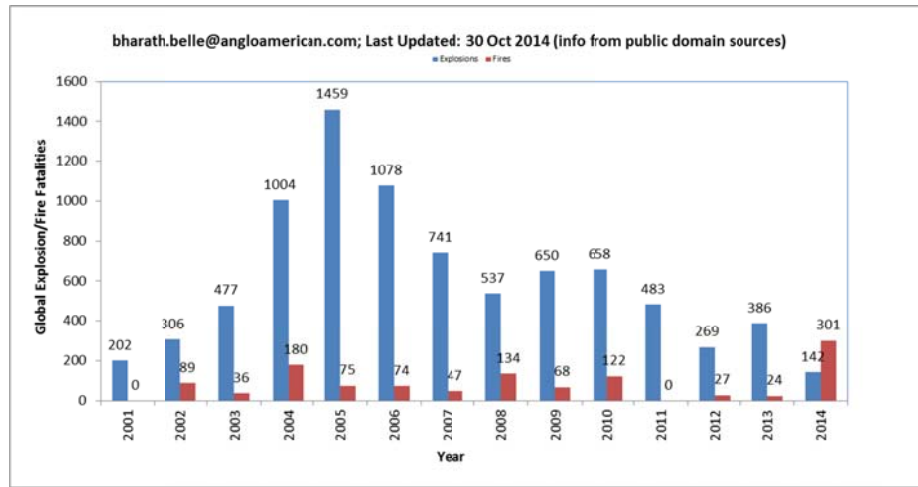
Figure 2: Global Mine Fires and Explosion Statistics (public domain sources)

Table 1: TBM encountered gases and explosion incidents worldwide (Source; Copur *et al.,* 2012)

Tunnel type	Country	Year	Length, km	Diameter, m	Fatalities, #
Los Angeles Water	USA	1971	8.85	6.8	17
Oil Field	Japan	1978	UN	UN	11
Water*	Georgia	1979	UN	UN	UN
Aqueduct	UK	1985	8.5	2.4	0
Waste Water	USA	1985	34	UN	0
Water	UK	1985	UN	UN	16
EPD-TBM	Japan	1993	UN	UN	4
Mill Creek	USA	2004	4.65	7.8	0
Electric Cable	Hong Kong	2004	UN	4.5	0
Zagros	Iran	2009	26	6.73	0
Hard rock	Spain	2010	UN	UN	0

*Whole team of workers; UN-Unknown

COAL MINE TBM EXPLOSION RISK ASSESSMENT

Safety and health risk assessment is inherent to coal mining operations in Australia and is entrenched in the local mining regulations. Considering the documented explosion risks associated with TBM operations, the risk assessment for Grosvenor coal mine involved key members of the mine technical and project team, TBM operator, contractors and the Queensland regulator. The majority of risk elements identified were in relation to the use of flameproof electric motors and intrinsically safe (IS) electric components to meet the compliance requirements as per the Queensland Coal Mining Health and Safety Act (Qld CMSHA) and Regulations (Qld CMSHR), Qld code of practice for Tunnelling and also the Australian Electrical Standards. A key hazard identified during consideration of the TBM for coal mining

application was the potential exposure to gasses during 10% of the tunnel length where the "P" seam coal measures would be encountered approximately 50 m above the target "GM" seam and when the TBM would be approaching the pit bottom (Figure 3) to be excavated within the GM seam horizon. This assumption was based on the information available from pre-drilled exploration boreholes. As shown in Figure 3, due to the presence of the water dam on the surface, no gas exploration holes could be drilled to a depth of between 400 m and 800 m. However, it was established that the P-seam follows over the TBM drift horizon towards the surface with methane gas anticipated during the drift development.
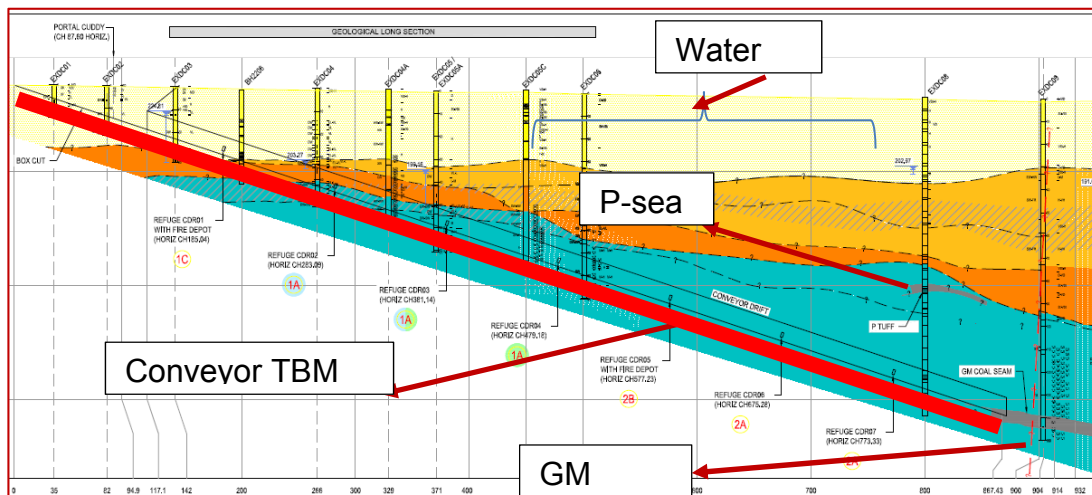
Figure 3: Geological long section profile along the conveyor TBM drift

The TBM risk assessment outcome ensured that the TBM incorporated relevant gas monitoring systems (shield area, cutter chamber, and screw conveyor discharge "stuffing box" assembly area) with automatic shutdown interlock feature should methane detected in any of these TBM sections. In addition, these measures incorporated the NERZ/ERZ requirements as legislated in the QLD Coal Mine Safety and Health Act (CMSHA) and Regulations (CMSHR, 2001).

TBM VENTILATION AND COOLING SYSTEM

Unlike the traditional continuous miner or road header machines in a coal face, the TBM face area at the front of the machine is sealed and potentially could contain a gas mix that may be liberated from the face area in the sealed chamber area. The EPB chamber and screw conveyor section are pressurised during excavation activities. The TBM exhaust ventilation design consisted of 2.0 m diameter steel duct continuously advanced using automated controls behind the TBM. The ducting was connected to a 150 kW surface centrifugal fan. The fan would induce adequate air flow to the face and tunnel. The exhaust ventilation system included a methane sensor to monitor the gas levels as in a typical mine shaft system. The steel duct was connected to a ribbed flexible ducting section to maintain a maximum draw-off distance of 2.0 m from the face during the cutting cycle. The ducting was positioned in such a way that any gas present near the screw conveyor or inbye the TBM area would be removed continuously from the face area. Figure 4 shows the typical ventilation circuit and the pressure-quantity survey results to be in compliance with the Qld CMH and S regulations, S342-S365 (McKew, 2014).
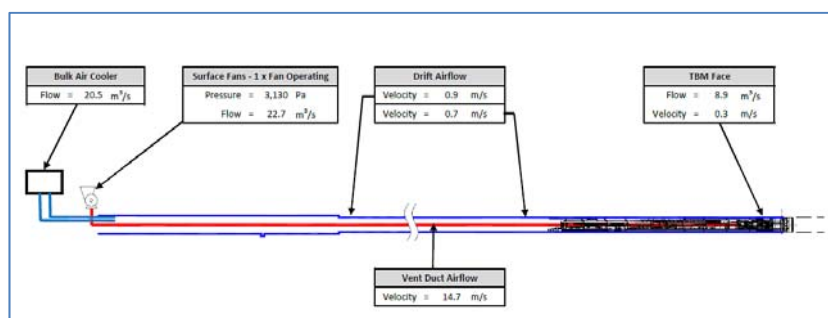
Figure 4: TBM Monthly ventilation survey results (McKew, 2014)

Figure 5 shows the TBM roadway temperature profile at the rear of the TBM area (behind the gantry 9 of the TBM, i.e., 100 m from the face). One of the observations made from the measured data is that there is a consistent Wet Bulb Temperature (WBT) difference between day and night. It is also noticed that the measured WBT during night shift is higher than the day shift WBT. This implies some type of data inaccuracy and points to the need for other, unbiased continuous real-time velocity and temperature monitors for underground use (Belle, 2014).

In addition to TBM heat load, steep geothermal gradient and very high surface ambient air temperatures (24°C WBT and 35°C DBT) in the Bowen Basin (Belle and Biffi, 2013) required the need for supplying cooled air during the TBM development to manage the thermal stress. This was achieved by a mobile surface Bulk Air Cooler (BAC) ducting at the drift entrance with a capacity of 15 to 20 m³/s of cooled air supplied at 10°C (Figure 6).
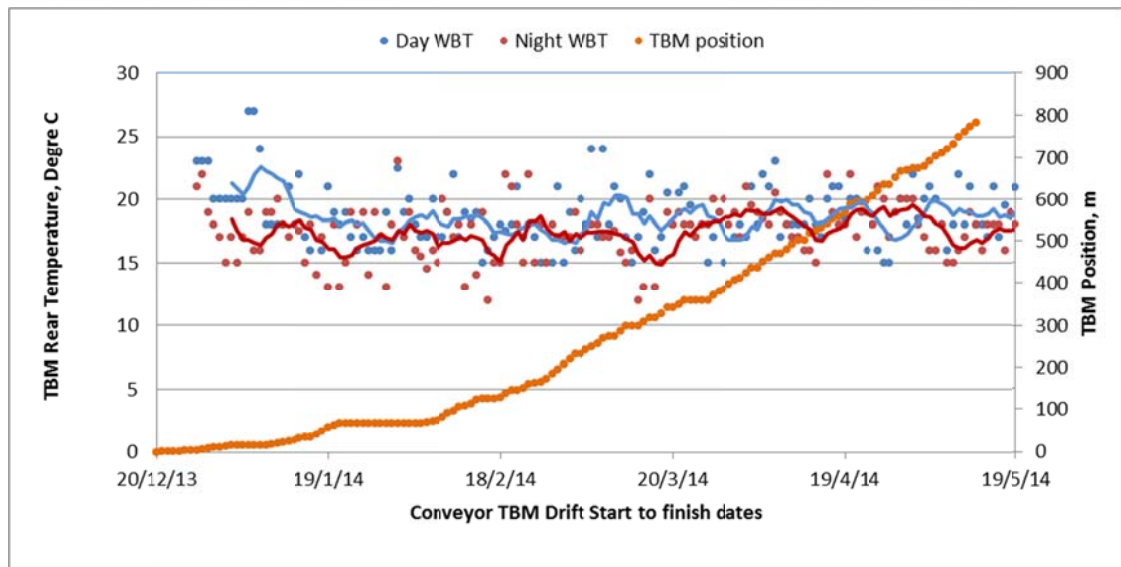
Figure 5: Use of BAC at surface conveyor drift on temperature profile in the TBM tunnel
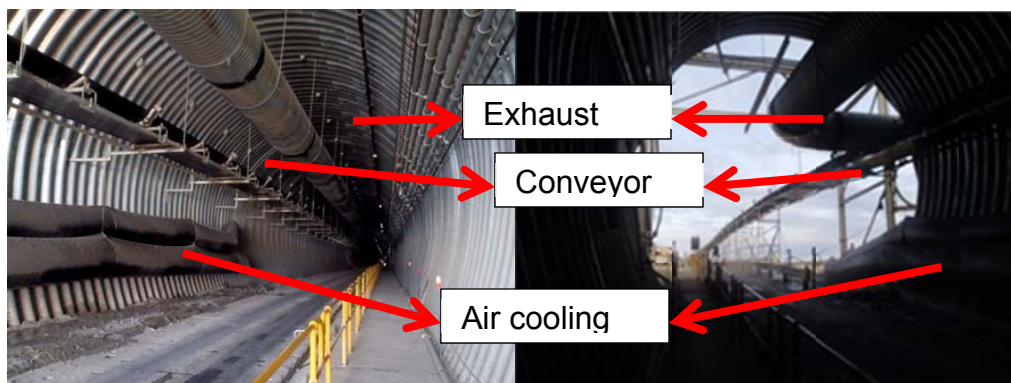
Figure 6: Completed conveyor drift development at Grosvenor coal mine

TBM METHANE EXPLOSION RISK CONTROLS-OPERATIONAL EXPERIENCES

In 2001, the Queensland legislation formalised the need for Explosion Risk Zones (ERZ) in underground mines that would allow for greater flexibility and continuous methane monitoring with alarms and relevant electrical power trip interlocks with the equipment. Section 286 requires the Site Senior Executive (SSE) to ensure that a risk assessment is carried out to identify the location and type of each ERZ at the mine. The zoning is risk based considering mining activities, absolute levels of methane in the general body (GB) and including foreseeable events and failure modes. The risk zones may be classified as one of ERZ0, ERZ1 and Negligible Explosion Risk Zone (NERZ). Section 287 of the Qld regulation defines ERZ0 as an underground mine, or any part of it, where the general body concentration of methane is known to be, or as identified by a risk assessment is likely to be, greater than 2%. To avoid any doubt, it is declared that, if the general body concentration of methane in a part of the mine that is defined as ERZ1 or NERZ becomes greater than 2%, then that part becomes an ERZ0.

Section 288(1) of the Queensland regulation defines ERZ1 as an underground mine, or any part of it, where the general body concentration of methane is known to range, or is shown by a risk assessment as likely to range, from 0.5% to 2%. In addition, Section 288 (2) defines each of the following places is an ERZ1-

(a) a workplace where coal or other material is being mined, other than by brushing in an outbye location;

(b) a place where the ventilation does not meet the requirements for ventilation mentioned in section 343 or 344;

(c) a place where connections, or repairs, to a methane drainage pipeline are being carried out;

(d) a place where holes are being drilled underground in the coal seam or adjacent strata for exploration or seam drainage;

(e) a place, in a panel, other than a longwall panel that is being extracted, inbye the panel's last completed cut-through;

(f) a goaf area;

(g) each place on the return air side of a place mentioned in paragraphs (a) to (f), unless the place is an ERZ0 under section 287;

(h) the part of a single entry drive with exhaust ventilation inbye the last fixed ventilation ducting in the drive.

Section 289(1) of the Queensland regulation defines negligible explosion risk zone (NERZ) as an underground mine, or any part of it, where the general body concentration of methane is known to be, or is identified by a risk assessment as likely to be, less than 0.5%. As in all coal mines, the TBM work area requires explosion risk zoning (ERZ) and is shown below in Figures 1 and 7.
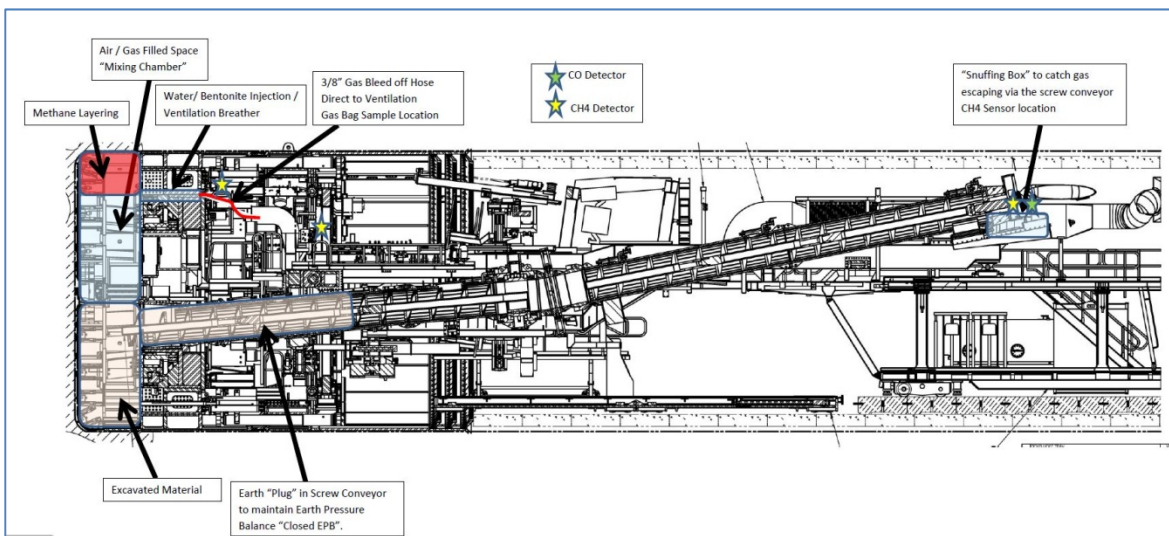
Figure 7: Gas monitoring stations on the TBM face area

The principal method of gas control from rib emissions during TBM development is the continued application of pre-cast concrete linings installed around the excavation's perimeter within the shield (but behind the bulk-head) as the TBM advances. Another gas control measure was provided by the use of the auxiliary face ventilation described above. The concrete lining is fully grouted as the shield advances, sealing the perimeter of the excavation from gas or water ingress. The section between the bulk-head and cutting face [cutting chamber] typically is an area where gas liberated from the surrounding strata is expected to be present. During EPB controlled development, the TBM machine is operated in "closed" mode where the TBM face area is sealed from the general tunnel environment with steel brushes packed with fibrous grease and pressurised with a combination of foaming agents, drilling muds and water. Closed mode operation is principally designed to control ground pressure acting to collapse the side walls of the excavation but also isolates any resultant gas from the general body.

One of the positive attributes of coal mining and welfare of its workers is the constant vigilance in identifying the health and safety hazards through continuous and regular monitoring and inspections.

There were a number of operational experiences related to identifying the methane hazard and its management that were previously not well understood or documented in the TBM applications in civil or mining projects. The gas monitoring system that was implemented while the TBM was cutting the stone strata was complemented with deputy's hand held multi-gas detectors, a regular bag sample regime and the real-time gas sensors present at the face area and at the screw conveyor duct exit. The Carbon Monoxide (CO) limit at conveyor was set at 10 ppm alarm and 30 ppm power trip.

As normally done in coal mines, bag samples collected from the TBM area were analysed using the Gas Chromatograph (GC) at a nearby operating coal mine. The early bag sample results from TBM samples showed that hydrogen was generally present in concentrations around 1,000 ppm, even when CO and ethylene were negligible. Based on coal mining experience, there was no reason for concern initially since the regular presence of hydrogen; CO and ethylene indicate any spontaneous combustion of carbonaceous material in the strata. As part of the routine bag sampling and analyses (11th March 2014), elevated levels of CO, CO_2, hydrogen, and ethylene in abnormal proportions were encountered while the TBM was cutting in the stone zone (~ 300 m from the surface). Initially, the measured gas levels were reasoned to result from the presence of a range of greases used to positively pressurize the cutter bearings of the TBM. The bag samples collected at the face area and screw conveyor indicated that CH_4 was found in the face area (< 2 %) and very low levels of methane (~0.1%) were detected where face/muck removal by the screw conveyor at the snuffing box. Similarly, the levels measured at the exhaust fan on the surface were ~0.1 % to 0.16% in 25 m^3/s of air (i.e., 40 l/s of methane). In order to better understand the phenomena, a bag sample strategy was implemented to collect samples at 3 am and 3 pm each day with results in relation to the TBM advance rate and its location shown in Figures 8 and 9.
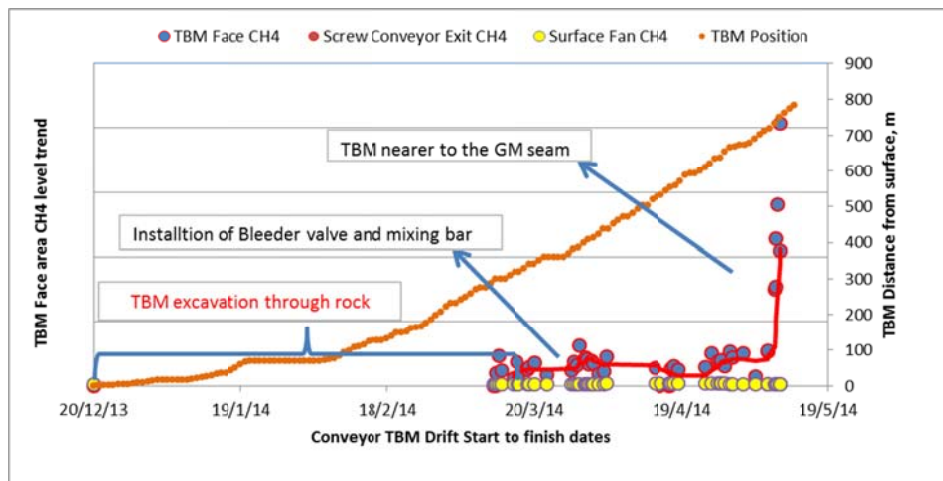
Figure 8: Measured methane levels in bag samples from the TBM shield area
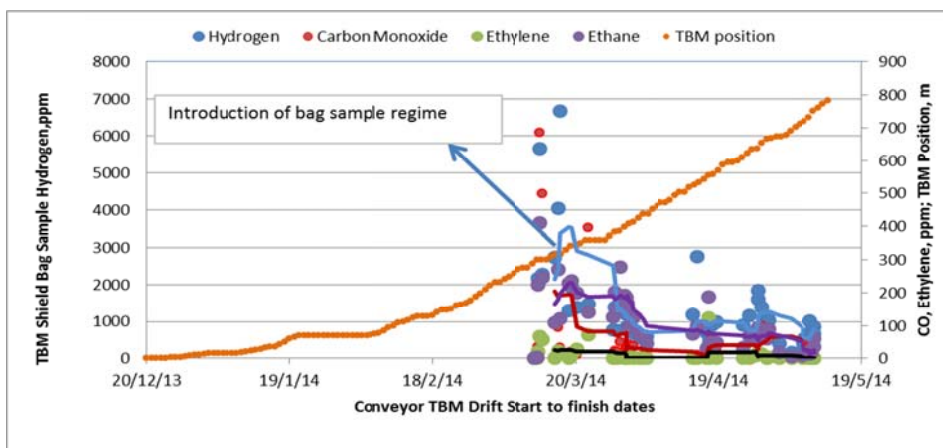
Figure 9: Measured sponcom indicator gases in bag samples from the TBM shield area

An immediate investigation was initiated upon detecting elevated levels of methane and other gases from bag samples. As part of the investigation, the TBM was stopped for visual observations the shield face

area. Seized cutter head discs were found contributing to heat generation and resulting in increased temperature that resulted in additional grease usage (Figure 10).

Figure 10: Typical coal lenses (Left) and cutting face (right) of a TBM with specs of coal.

Based on the gas detection and elimination process, it was concluded that there are two separate and distinct gas sources occurring at the TBM face area, i.e., methane release from carbonaceous rocks and other hydrocarbons suspected to be emanating from hydrocarbon based chemicals used in the rock cutting and support process in the TBM face area enclosure.

With the introduction of the bag sample regime data and field observations, the following methane and hydrocarbon management controls were attempted:

- A mixing bar was fitted to the cutter head to create a turbulent airflow within the cutter chamber to assist in gas mixing and prompt dilution and to prevent regrinding in order to reduce the heat and production of hydrocarbons. In order to manage the risk at the enclosed face where a possible layer of methane (< 2%) may be present, positive ventilation was seen as a control. However, the application of positive ventilation of the cutter head was not possible due to the sealed enclosure head and other operational risk assessment outcomes. A sample hose at the bulk head area was introduced to bleed air in an attempt to reduce the methane layering (Figure 11).
- In order to eliminate the presence of voids inside the TBM's pressurized cutting chamber, the quantity of the injected bentonite and foam mixture was increased. This control resulted in increased muck temperature. Alternatively, bentonite use was reduced and foam quantity was increased to reduce the operating temperature (Figure 12). At this stage, it was noted that the cutting strata was a mixture of hard and soft layers interspersed with carbonaceous pockets.
- Considering the presence of other hydrocarbons, the thrust pressure and cutting rate were reduced to minimize the muck operating temperature in conjunction with the introduction of a muck heat Trigger Action Response Plan (TARP) with additional foam/fluid mix. Reduced thrust pressure of the EPB-TBM and implementation of muck heat TARP to 45 °C further reduced the generation of hydrocarbon products.
- Lastly, as used in coal mine spontaneous combustion management and goaf seal management, continuous low temperature enabled Floxal nitrogen to be introduced, instead of compressed air for the generation of foam designed to minimise void creation. This resulted in the generation of an inert atmosphere in the face area and reduced heat generation that otherwise would have stimulated hydrocarbon generation.

Figure 11: Methane sampling/bleed hose (left) behind the cutter bulkhead (right)
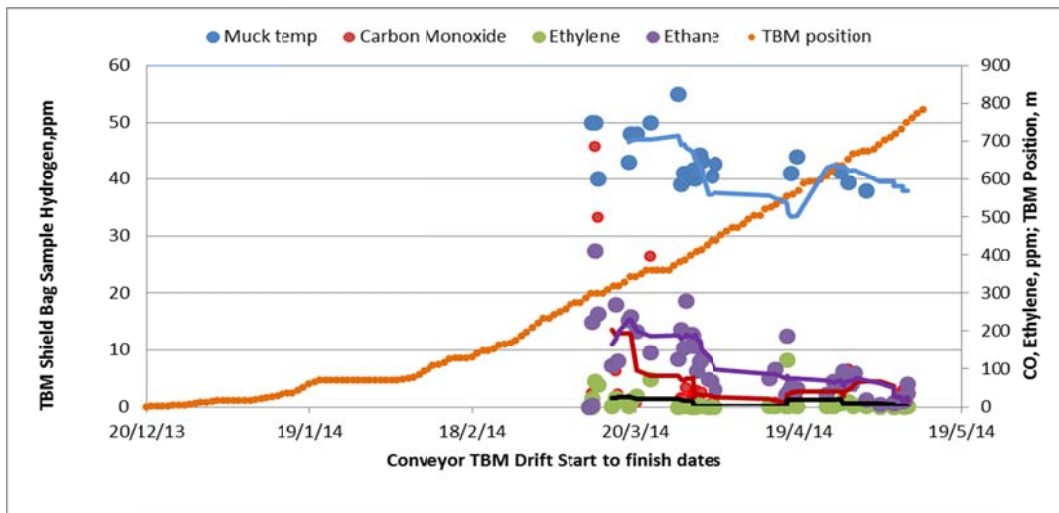
Figure 12: Influence of muck temperature and nitrogen injection to TBM shield area

Figures 13 and 14 shows the influence of injecting of nitrogen through the existing *in-situ* Bentonite line directly into the cutter chamber to create an inert atmosphere. Purging of the cutter chamber was introduced after cutter inspections to ensure an inert atmosphere is provided prior to rotating the cutter head. After the introduction of nitrogen, the methane gas from the carbonaceous material present in the EPB-TBM face area behaved as an inert blend as opposed to an explosive one. This resulted in a decrease in the magnitude of hazardous gas spikes without affecting the generation of the spontaneous combustion indicator gases. It was speculated that the methane is most likely to have come from strata, although coal seam was not intersected. Other benefits of injecting nitrogen gas at low temperature was the reduction of the overall muck temperatures to below 45°C which otherwise would have resulted in more carbon monoxide being generated and other chemical odours being detected. In summary, based on the results, it was noted that the likely source of carbon monoxide and ethylene is different from that producing hydrogen. The presence of high levels of hydrogen identified initially at the start of the drift could not be explained.

As noted from Figure 8, when the TBM approached the GM seam, the gas levels at the face area increased due to the formation of a gas sink. In addition, with the retraction of the TBM face area, and due to the buoyancy effect of the gas in the TBM decline, the ventilation system had to be altered with a force ducting to provide adequate dilution and eliminate the formation of explosive gas mixtures. Although high gas levels were observed at the TBM-EPB chamber area, the highest measured gas level from the surface fan was 0.11% of methane. While there may be multitudes of ratios that would indicate coal heating, a simple CO/O2 deficiency ratio of < 0.01 of the bag sample results disproved any existence or initiation of coal heating contributing to the measured sponcom indicator gases.
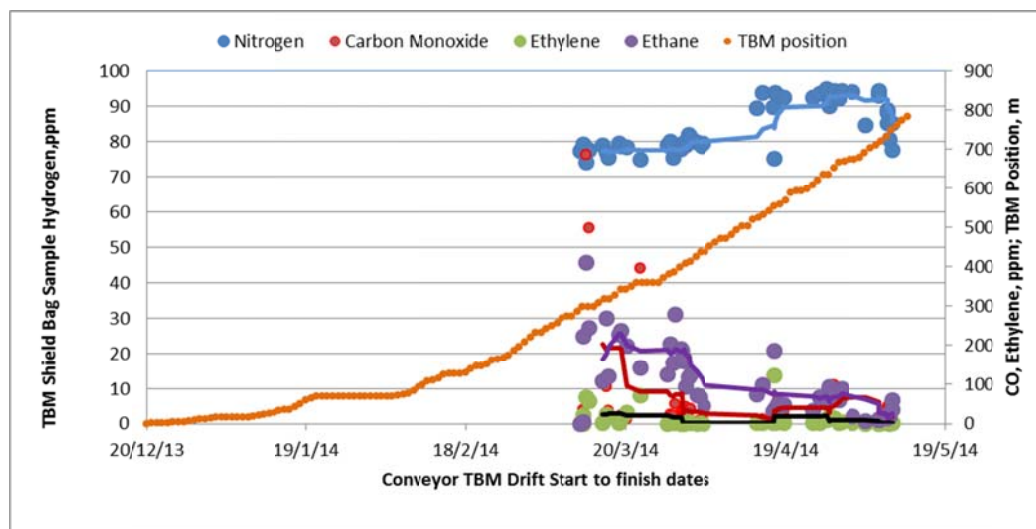
Figure 13: Influence of Floxal nitrogen to TBM shield area to create inert atmosphere
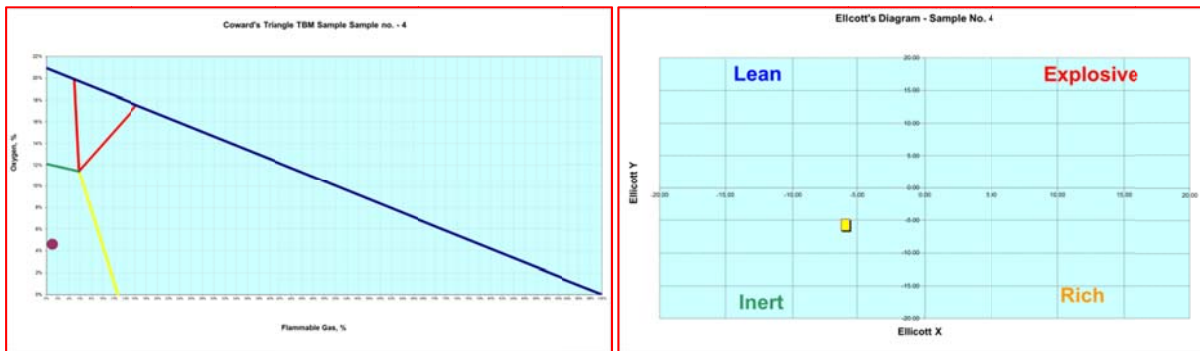
Figure 14: Cowards triangle and Ellicott's diagram indicating TBM face inert atmosphere

LABORATORY INVESTIGATIONS OF TBM FLUIDS FOR METHANE SOURCES

Based on the measured gas levels obtained from the bag samples taken at the TBM face area, it was decided to identify through laboratory means, whether hydrogen, ethylene, carbon monoxide, ethane and methane are liberated from the heating of chemical fluids used in the operation of the EPB-TBM. Furthermore, after the implementation of nitrogen inertisation as part of the explosion risk management process, laboratory testing was carried out to distinguish between oxidation and thermal degradation of products used in the TBM. The five samples submitted for testing were; foam, polymer foam additive, grease, sealed bearing oil and wear indicator oil. Laboratory testing on the five samples was conducted at SIMTARS by heating each of the samples (except foam) incrementally up to at least 250°C in both nitrogen and normal air flow (Brady, 2014). Out of the five samples tested the most likely product contributing to the elevated hydrogen is the foam. Although not as high as those measured in samples collected from the TBM similar concentrations were measured in samples from both nitrogen and air tests up to ~150°C. Most of the other products tested would produce carbon monoxide and ethylene if heated above 200°C accounting for spikes of these components at various times. Figure 15a to 15e show the generated gas level data from chemical products used in TBM shield area along with the spontaneous combustion indicator gases of four Grosvenor coal samples (i.e., carbon monoxide, hydrogen, ethylene, methane and ethane). The results indicate that at the various temperature conditions of the muck in the TBM face area, the measured gas levels in the face area of the TBM are not as the result of spontaneous combustion activity of any carbonaceous strata material.
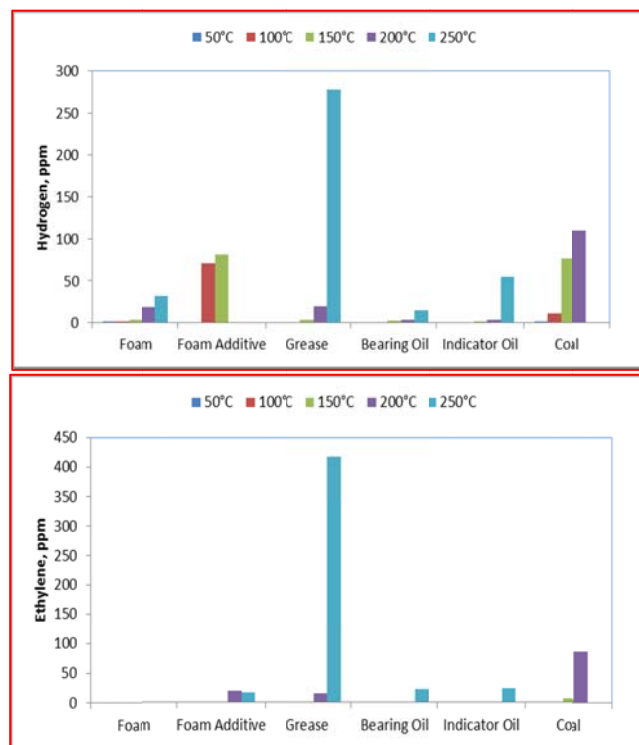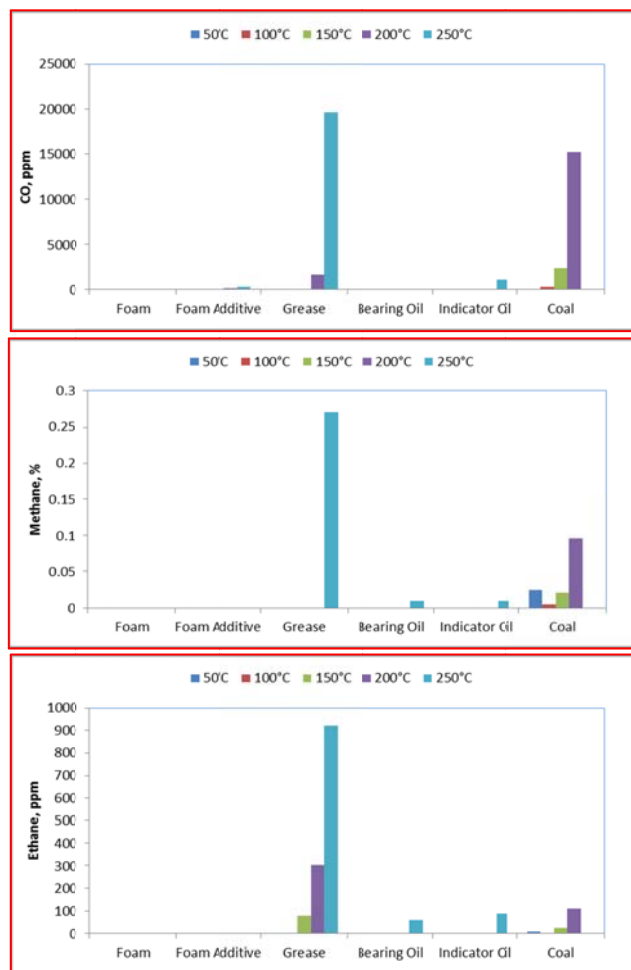
Figure 15: Comparison of generation of gases from chemicals used in TBM face area-Hydrogen (top left-15a), Ethylene (top right-15b), CO (middle-Left-15c), methane (middle-right-15d) and ethane (bottom-15e) at various temperatures

Similarly, from the laboratory test results of heating individual chemical components used in the TBM, it was concluded that it is unlikely the methane measured in the TBM samples came from any of the products analysed. The measured value of 0.27 % in grease appears to be an anomaly, as it was the only measured methane at various temperature conditions (Figure 15d). The laboratory test results of generated gases have indicated that hydrogen; ethylene, carbon monoxide and ethane gases are generated even while being purged with nitrogen with noticeable odours generated when heated above 200°C. These odours were noticed by the TBM operators during the TBM conveyor drift development. Amongst the five chemicals tested, the grease was found to be the primary contributor towards the significant volumes of hydrogen, ethylene, and CO at higher temperatures. However, it is important to note that any interaction effects of these chemicals that may have resulted in the generation of methane or other gases was not studied and cannot be discounted at this stage. Amongst the other gases recorded, the reasons behind the significantly higher measured levels of hydrogen prior to nitrogen injection and temperature control of the muck in the TBM face area were not clear. Therefore, it has been planned to introduce the bag sample regime from the beginning of the men and material drift development. While continuous nitrogen injection has definitely assisted the temperature control and maintaining inert mixture of the explosive gas (Figure 14), it had minimized the chance of methane ignition in the TBM face area.

CONCLUSIONS AND WAY FORWARD-GLOBAL TBM APPLICATION

The application of the EPB-TBM in the development of the conveyor drift (813 m in length) was safely completed with success with significant learnings in the methane and other hazardous gas identification and its effective methane explosion risk management. At the time of completion of this paper, the men and material drift development using the same TBM has been initiated. In summary, following

conclusions that are applicable to a coal mine or other civil TBM projects in managing the explosion risks have been made:

- For the first time in the application of TBM development in coal mines, the operational experience has suggested that methane and other spontaneous combustion gases will continue to be present as potential explosion hazards.
- The chemicals used in the muck management and stability of the EPB-TBM face area may also generate levels of spontaneous combustion indicator gases at elevated muck temperatures suggesting that maintaining a low muck temperature would be beneficial in managing harmful gas generation.
- Application of continuous nitrogen inertisation as spontaneous combustion and explosion management was successful in managing the explosive gases present at the EPB-TBM face area.
- Continuous monitoring and maintaining a well-established gas bag sample regime and controls including the TARPs for various gases and ventilation controls must be continued in managing the potential explosion risks.
- Considering the recorded 48 fatalities in the last 45 years due to gas explosions in the tunnelling industry, civil engineering tunneling projects must apply Qld NERZ/ER1/ERZ0 explosion risk zoning; hazard monitoring practices using continuous monitoring systems; bag sample regime and the use of TARPs for risk management, and the use of nitrogen inertisation to maintain inert atmosphere in the TBM face area.
- Ensuring relevant operator skills with adequate coal mine ventilation, gas and heat management experience is valuable for the global TBM industry in eliminating explosion risks in the future TBM projects.

ACKNOWLEDGEMENTS

REFERENCES

Anglo American. 2013, *Internal TBM Application Document*.

Belle, B. 2010, Los Bronces Safety Risk Review, Anglo American plc.

Belle, B and Biffi, M. 2010, Cooling pathways for deep Australian longwall coal mines of the future, *Mine Ventilation Conference Proceedings*, Adelaide, Australia, pp 94-104.

Belle, B. 2014, Underground Mine Ventilation Air Methane (VAM) Monitoring – An Australian Journey towards achieving 'accuracy', *Proceedings of the Coal Operator's Conference*, Wollongong, Australia.

Brady, D. 2014, Grosvenor TARP Trigger Review Report, *Anglo American Internal Document*, Australia.

Brox, D. 2013, Technical considerations for TBM tunneling for mining projects, Society for Mining, *Metallurgy, and Exploration transactions*, USA, Vol. 334, pp 498-505.

Copur, H, Cinar, M, Okten, G and Bilgin, N. 2012, A case study on the methane explosion in the excavation chamber of an EPB-TBM and lessons learnt including some recent accidents, *Tunneling and Underground Space Technology*, 27 (2012) 159–167, http://www.legislation.qld.gov.au/LEGISLTN/CURRENT/C/CoalMinSHR01.pdf.

McKew. 2014, Grosvenor Ventilation Survey report, *Anglo American Coal*, Australia.

Phillips, H. 2009, MVS Symposium, South Africa.

CHANGES IN CUTTER PERFORMANCE WITH TOOL WEAR

Esmat Sarwary and Paul Hagan

ABSTRACT: Mechanical excavators such as shearers, road-headers, and continuous miners that utilise conical picks are increasingly being used in civil construction and mining. Their application has broadened to include stronger and more abrasive rock types that result in higher wear rates and considerably shorter life span. This results in a bottleneck resulting in lower utilization and lower productivity. An understanding of the factors that cause high wear rates is crucial in the selection and design of an excavator, selection of cutter tools, and definition of optimum cutting geometry. All these parameters can contribute to major cost savings for companies using mechanical excavators. This paper explores how tool wear affects the cutting performance of a point attack pick with changes in the depth of cut. Linear rock cutting tests were performed using samples of Gosford Sandstone and Gambier Limestone at a constant speed of 0.06 m/s and pick attack angle of 55°. The rock samples were cut at depths ranging between 5 mm and 20 mm using a standard conical pick having tip angles of 70°, 90° 100° and 110°. The cutting forces and normal forces, specific energy, and yield were correlated against depth of cut. The results reveal that for each rock type, the specific energy increases at a decreasing rate with pick wear, confirming cutting efficiency decreases with increasing pick wear whereby a slight increase in pick wear resulted in a significant reduction in cutting efficiency. There was a near two to threefold decrease in efficiency between a sharp pick and worn out pick. The cutting and normal forces were also found to increase at a decreasing rate with pick wear.

INTRODUCTION

Most mechanical rock cutting machines in coal mining use tungsten-carbide conical picks, mounted on a cutting head to fracture the rock *in situ* prior to its removal and further processing (Lloyd, 1985). As theory relating to the mechanical excavation of rock has emerged and evolved over time, so too has the utilisation of these machines, often replacing traditional drill and blast methods, resulting in an increase in safety performance and a reduction in operating cost. As a consequence, laboratory-scale rock cutting facilities such as the Portable Linear Rock Cutting Machine (PLCM) in the Machine Cuttability Research (MCR) facility within the School of Mining Engineering at UNSW Australia are able to provide data for machine selection, design, and performance prediction for a given rock formation (Balci and Bilgin, 2006; Jacobs and Hagan, 2007; Langham-Williams and Hagan, 2014).

Normal force measured by the PLCM can be used to estimate the effective mass and thrust required of an excavator. This is a crucial parameter as it provides an insight into the range of necessary forces provided by the excavator in order for the cutter to effectively penetrate the rock and maintain the cutting depth. Furthermore, the cutting force measured by the PLCM is crucial to evaluating the energy requirements for excavating the rock. Cutting force is used to calculate the specific energy requirements, defined as the amount of energy required in excavating a unit volume of rock. Specific energy is a direct measure of cutting efficiency. Lower specific energy correlates to more material being produced by a given machine; therefore, lower specific energy indicates an increase in cutting efficiency (Roxborough, 2009).

Despite picks being typically constructed from tungsten carbide due to its hardness, thermal resistance, high compressive strength and high impact resistance; they are still susceptible to wear (Hudson *et al.*, 1993). There are several mechanics of wear, such as frictional wear, abrasive wear, microfracturing, thermal fatigue, impact damage, and chemical erosion, all of which contribute to tool wear. The consequence of wear on the cutting is familiar in the mining and tunnelling industry, since the performance of the machine deteriorates significantly as the tools become blunt. The mining output will fall, repairable dust production will rise, and the risk of incendive sparking increases (Roxborough, 2009).

PROJECT OBJECTIVES

The objective of this project was to determine how tool wear of a point attack pick impacts on cutting performance in two different rock types. Cutting tests were undertaken in a combination of a pick of differing tool angles and at differing depths of cut. Changes in cutting performance were assessed in

School of Mining Engineering, UNSW Australia, Sydney, NSW 2052, Australia, E-mail:p.hagan@unsw.edu.au

terms of changes in:
- Cutting force, F_C
- Normal force, F_N
- Specific Energy, SE, and
- Yield, Q

METHODOLOGY

The research involved tests conducted using the newly installed the newly commissioned PLCM as shown in Figure 1. The linear rock cutting tests were performed using blocks of Gosford Sandstone and Gambier Limestone at a constant cutting speed of 0.06 m/s and attack angle of 55°. Tests were undertaken at depths ranging from 5 mm to 20 mm with conical picks at four different pick angles. A data acquisition system was used to record the cutter forces measured by a triaxial dynamometer during linear rock cutting tests.
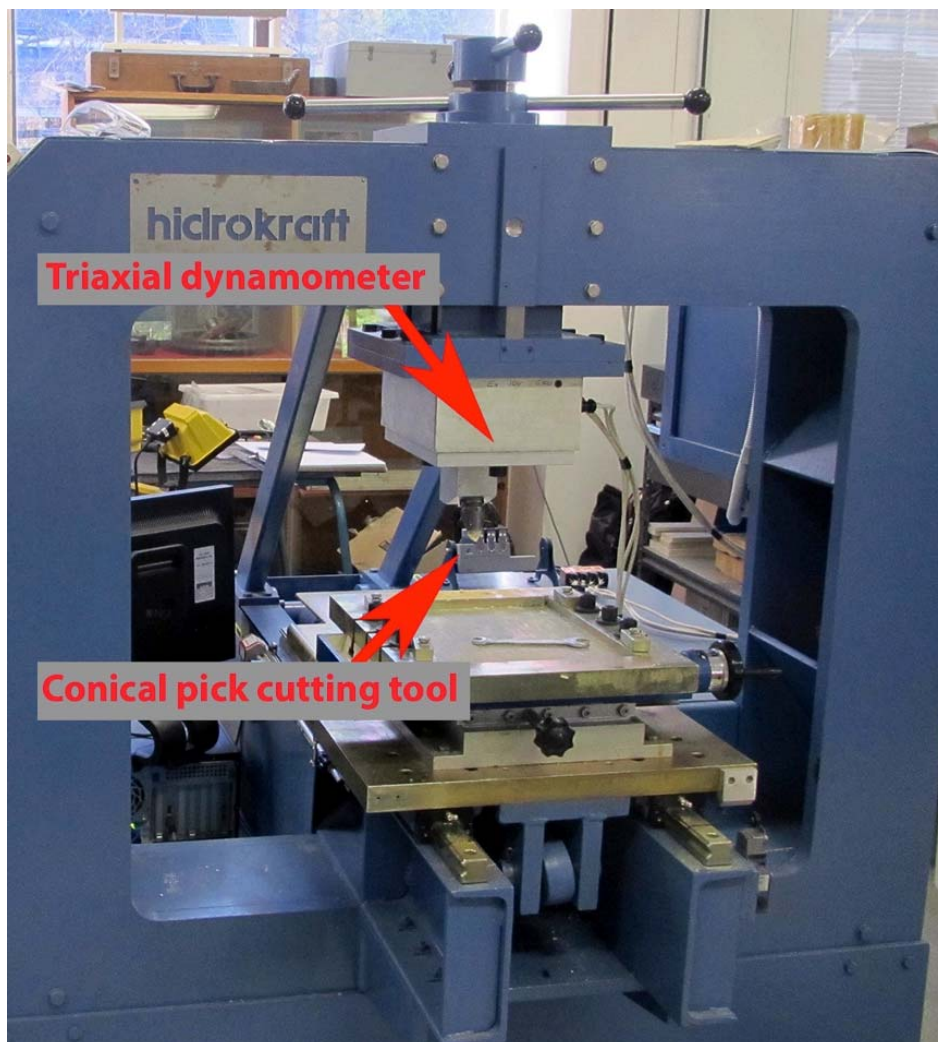
Figure 1: Portable Rock Cutting Machine in the Machine Cuttability Research facility at UNSW

Sample preparation

Blocks of test samples having dimensions of 260 × 180 × 100 mm were set in plaster within a small steel box frame to provide the necessary confinement during testing, as depicted in Figure 2. The preparation of the plaster involved mixing with water at a ratio of 5:3.25 (that is 5 kg of powder to 3.25 kg of water).

The samples were cured for at least 24 hrs prior to any testing to ensure the plaster had hardened sufficiently.
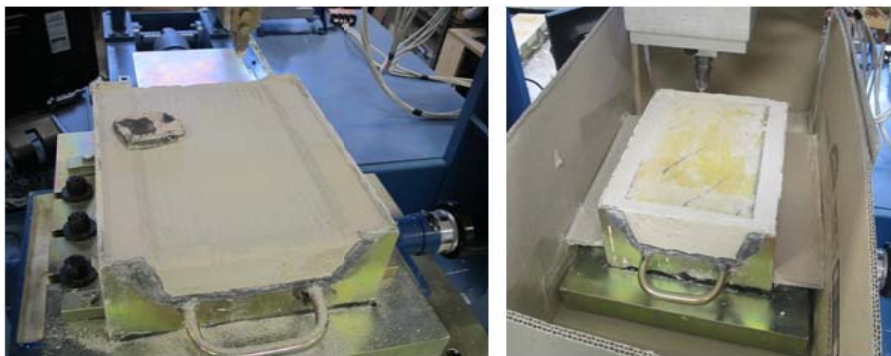
Figure 2: Method of securing the blocks of rock samples for cutting tests

Preparation of test picks

New Sandvik conical picks with short-tailed 25 mm shank were machined to provide four different pick tip angles of 70°, 90° 100° and 110° representing a pick at various states of wear. An illustration of the pick used in the tests is shown in Figure 3 with dimensions provided in Table 1.
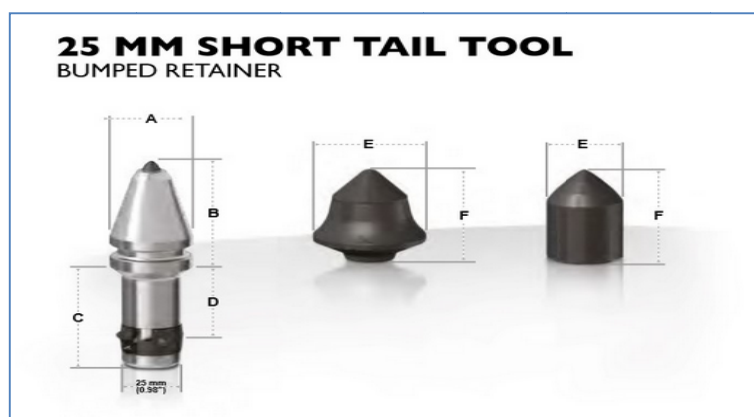
Figure 3: The short tail pick used in the tests (Sandvik Mining, 2013)

Table 1: Specifications of 25 mm Short Tail Pick

Product Code	Dimensions (mm)					
	A	*B*	*C*	*D*	*E*	*F*
P9QA-2560-3562	35	58	58	42	12	19

(Source: Sandvik Mining, 2013)

The pick holder system was designed with a fixed insert as shown in Figure 4. The design allowed the pick to be mounted at an attack angle of 55°. According to Mostafavi *et al.,* (2006) this is within the range of angles when mounting picks on continuous miners, road-headers, and shearers.
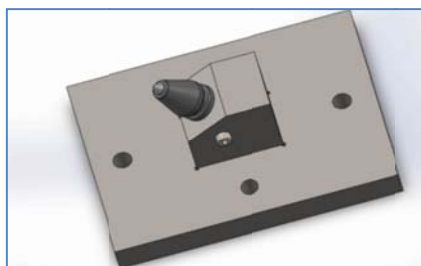
Figure 4: Design of conical tool holding unit that is mounted directly on the dynamometer

Data analysis

The cutting (F_C) and normal (F_N), forces were measured using the integrated triaxial dynamometer. The length of the cut was measured using a Linear Variable Displacement Transducer (LVDT). The LabView software package was used for real time monitoring and recording of the forces and displacement.

The force values in conjunction with mass of collected debris were used to calculate the specific energy and yield based on the following formulas:

$$Q = (m / \rho) / l \tag{1}$$

where:
Q: yield (m^3/km)
ρ: density of the rock (kg/m^3)
m: weight of the debris collected (kg)
l: length of cut (km)

$$SE = Fc / Q \tag{2}$$

where:
SE: Specific energy (MJ/m^3),
Fc = cutting force (kN)

Strength and density of test samples

Compressive strength tests were conducted on specimens of Gambier Limestone, in accordance with the ISRM suggested method for uniaxial compressive strength determination (Brown, 1981).

The testing procedure involved six limestone rock specimens with a diameter and length of 52 mm and 104 mm respectively using an MTS universal test machine. The tests were conducted at a constant displacement rate of 0.003 mm/sec. The strength of the Gosford Sandstone was earlier determined by Masoumi (2013).

Nine core samples were weighed and the diameter and length of each sample recorded. Sufian and Russell (cited in Masoumi, 2013) conducted an X-ray CT scan on Gosford Sandstone. By using a resolution of 5 μm they calculated the porosity to be approximately 18.5% with density of 2.5 × 103 kg/m3. Table 2 summaries the strength and density of the two of rock types. As shown in Table 2, there is over a ten-fold difference in strength and near doubling in rock density between the sandstone and limestone samples.

Table 2: Strength and density of Gosford Sandstone and Gambier Limestone samples

Rock type	UCS (MPa)	Density (t/m^3)
Gosford Sandstone	52.3	2.5
Gambier Limestone	5.0	1.4

RESULTS

A series of cutting tests were conducted in the sandstone and limestone with typical results as shown in Figure 5.

The results of the cutting and normal forces, specific energy, and yield were correlated against picks at different tool angles representing various states of wear. Figures 6 and 7 show the effects of pick wear on cutting and normal force for the two rock types. The trends in each of the graphs indicate cutting and normal force increase with pick wear. The magnitude of forces is much greater for Gosford Sandstone compared to Gambier Limestone, nearly three times greater for cutting force and six times greater for normal force. This is in line with the sandstone's much greater strength and density. It is also evident that

the magnitude of cutting force for both types of rock is greater than the magnitude of normal force. Cutting force is also approximately 1.6 times greater than the normal force for sandstone and 2.8 times greater for limestone.

Figure 5: Cutting with a pick tip angle of 70˚ at 15mm depth of cut in Gosford Sandstone (left) and Gambier Limestone (right)
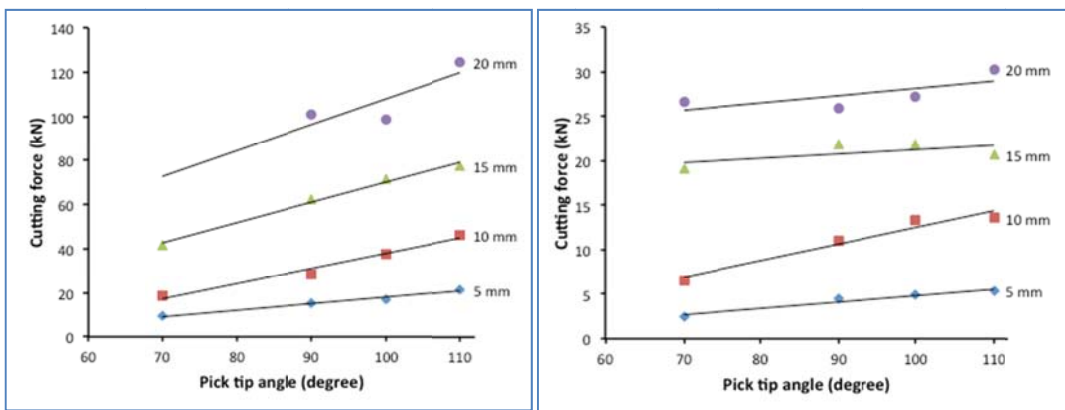
Figure 6: Effect of wear on cutting force at varying depths of cut for Gosford Sandstone (left) and Gambier Limestone (right)
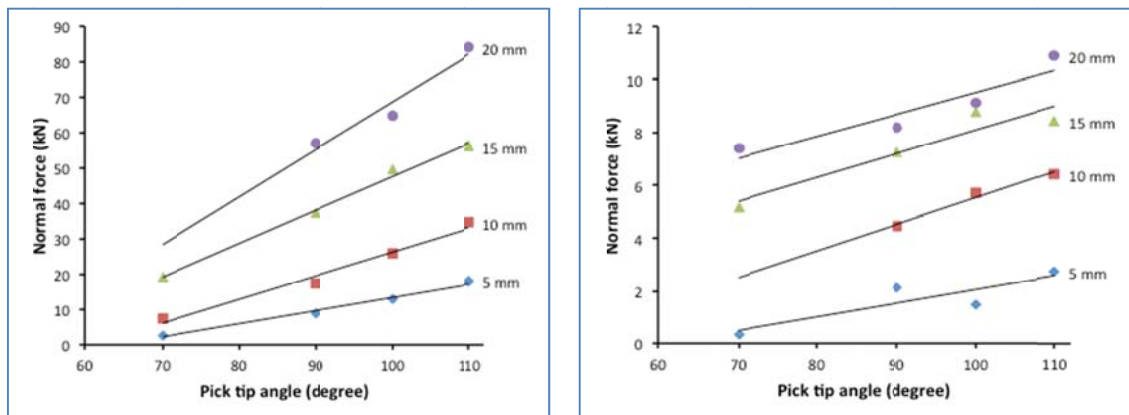
Figure 7: Effect of wear on normal force at varying depths of cut for Gosford Sandstone (left) and Gambier Limestone (right)

Table 3 shows the variation in cutting force and normal force with tool angle at increasing depths of cut in the two rock samples. In the case of sandstone, the gradient increases with depth of cut indicating the impact of wear increases with depth of cut. The gradients are of similar magnitude level for cutting force

and normal force.

The situation is not as consistent for the softer limestone whereby there is little significant change in gradient with depth and the values for cutting and normal force are again comparable. Earlier work has found that increasing wear usually has a much more deleterious effect on normal force than on cutting force (Roxborough, 2009). The consequence of this effect is that machines, such as continuous miners and road-headers, become thrust limited rather than torque limited with increasing wear.

Table 3: Variation in forces with tool angle and depth of cut

Rock type	Depth of cut (mm)	Cutting force gradient (kN/deg)	Normal force gradient (kN/deg)	Ratio C:N
Sandstone	5	0.30	0.37	1.5
	10	0.69	0.67	1.6
	15	0.92	0.95	1.6
	20	1.18	1.34	1.7
Limestone	5	0.07	0.05	2.7
	10	0.19	0.10	2.3
	15	0.05	0.09	2.9
	20	0.08	0.08	3.2

Figure 8 shows specific energy increase with pick tip angle and hence wear. Hence as would be expected cutting efficiency decreases with increasing wear. Also specific energy decreases with increasing depth of cut and hence cutting efficiency increases with increasing depth of cut
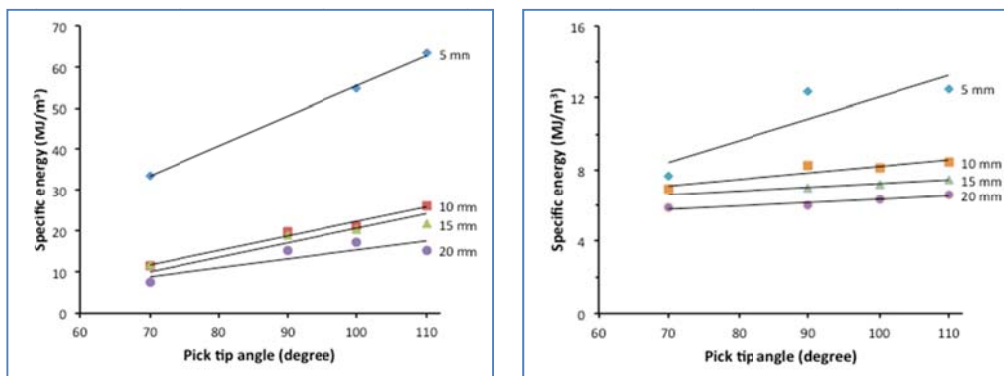
Figure 8: Effect of wear on specific energy for Gosford Sandstone (left) and Gambier Limestone (right)

The increase in normal force required to successfully achieve pick penetration will result in the machine becoming thrust limited, consequently leading to eventual stalling.

Although the general trend indicates that wear has a negative impact on cutting efficiency, there are some outlier results. Closer analysis of the result reveal that cutting sandstone with pick tip angle of 110° at 20 mm depth of cut results in a slightly lower specific energy compared to cutting with pick tip angle of 90° and 100° which represent a slightly less worn out pick. A possible explanation is that not only the groove cut with a 110° pick tip angle is wider but it has been able to achieve the same penetration depth as a sharp pick under the same constant thrust force provided by the PLCM, resulting in greater yield which consequently would have yielded a lower efficiency. These variations may also be due to differences in microfractures, grain size distribution, and varying joint structure within the different rock samples, suggesting that the rocks tested are not perfectly homogenous. There are also similar outliers observed when cutting sandstone with a pick tip angle of 90° and cutting limestone at a pick tip angle of 110° at 5 mm depth of cut which suggests that it is more efficient to cut with a more worn out pick.

From Figure 8, it is evident that the trend indicates that it is more cost effective because it requires less

energy to excavate Gambier Limestone than Gosford Sandstone. However, whether it is more efficient to mine the two different types of rock would require further exploration. It is further observed that wear has a dramatic effect on cutting efficiency at shallow depths of cut and higher specific energy, but at the deeper depths of cut, such as 15 mm and 20 mm, a more worn out pick (φ = 110°) has little effect on cutting efficiency. This indicates that a slightly more worn pick will perform just as well at a higher depth of cut.

Table 4 shows the percentage decrease in specific energy from 5 mm to 10 mm depth of cut for both limestone and sandstone. The data outlined in the table shows that a specific mechanical excavator capable of mining both limestone (soft rock) and sandstone (hard rock) will have a higher efficiency when mining sandstone compared to limestone as depth of cut increases, given that all other conditions are constant. This is due to the percentage drop in specific energy when transitioning from a 5 mm depth of cut to 10 mm being significantly higher in sandstone regardless of pick's state of wear. This trend concerns the brittleness of the rock, which is a function of compressive and tensile strength of the rock (Goktan and Yilmaz, 2005). Generally, if the tensile strength of the rock is similar, a higher compressive strength value means that the rock would be more brittle (Goktan and Yilmaz, 2005). Since the strength of Gosford Sandstone is 50.3 MPa, it is more brittle compared to the Gambier limestone of 5.0 MPa. In this case, when a pick penetrates the rock at the same depth of cut, the ease with which fractures propagate with sandstone is higher compared to limestone, thus resulting in more rock fragments. This is consistent with experimental results for this research project. More fragments indicate a higher yield, given that other parameters are constant, which leads to a lower specific energy.

Table 5: Variation in specific energy with tool angle

Rock type	Tip angle (degrees)	Reduction in specific energy (%)
Limestone	70	9
	90	33
	100	49
	110	32
Sandstone	70	58
	90	23
	100	61
	110	58

CONCLUSIONS

A series of rock cutting tests was conducted with two rock types of different strengths and picks with four levels of pick tip angle to simulate wear of the pick cutting tool. It was found that cutting and normal force increased with pick tip angle and hence with pick wear but the rates of increase varied between the two rocks types. As the depth of cut increased there was a rise in the forces. In the weaker Gambier Limestone, there was little change in the effect of wear on the rate of increase in forces with depth of cut. Whereas for the stronger Gosford Sandstone, the effect of wear on forces was more enhanced and this was compounded at larger depth of cut. Mirroring the difference in compressive strength between the two rock types, there was a near three-fold difference in cutting forces and six-fold difference in normal between the two rock types.

Specific energy also increased with wear, indicating that cutting efficiency decreased with pick wear. A two to threefold increase in specific energy was observed between a sharp pick (70°) and a mostly worn pick (110°). The percentage drop in specific energy transitioning from a 5 mm to 10 mm depth of cut in sandstone is always higher, regardless of the pick's state of wear. This suggests that mechanical excavators capable of mining both limestone (weak rock) and sandstone (strong rock) will have a higher efficiency when mining sandstone compared to limestone, given all other conditions held constant

ACKNOWLEDGEMENTS

REFERENCES

Balci, C and Bilgin, N. 2006, Correlative study of linear small and full-scale rock cutting tests to select mechanized excavation machines, *International Journal of Rock Mechanics & Mining Science*, pp 468-476.

Brown, E T. 1981, *Rock Characterisation Testing and Monitoring: ISRM Suggested Methods*, pp 111-137 (Pergamon Press: Oxford).

Goktan, R M and Yilmaz, N G. 2005, A new methodology for the analysis of the relationship between rock brittleness index and drag pick cutting efficiency, *Journal of The South African Institute of Mining and Metallurgy*, pp 727-733.

Hudson, J, Brown, E T, Fairhurst, C and Hoek, E. 1993, *Comprehensive Rock Engineering*, Volume 3, pp 155-175 (Pergamon Press: New York).

Jacobs N and Hagan P. 2009, The effect of stylus hardness and some test parameters on CERCHAR Abrasivity Index, in *Proceedings 43rd US Rock Mechanics Symposium*, Asheville, NC, USA, June.

Langham-Williams J and Hagan P. 2014, An assessment of the correlation between the strength and cuttability of rock, *in Coal 2014: Proceedings 14th Underground Coal Operators' Conference,* University of Wollongong, Feb, (eds: N Aziz, B Kininmonth, J Nemcik and T Ren) 12-14 February (Australasian Institute of Mining and Metallurgy.

Lloyd, M J A. 1985, An investigation into the effect of the angle of attack on the cutting performance of a point attack cutting pick, Honours thesis (unpublished), University of New South Wales, Sydney.

Masoumi, H. 2013, Investigation into the mechanical behaviour of intact rock at different sizes, Doctor of Philosophy thesis (unpublished), University of New South Wales, Sydney.

Mostafavi, S, Yao, Q Y, Zhang, L C, Li, X S, Lunn, J and Melmeth, C. 2006, Effect of attack angle on the pick performance in linear rock cutting, in *Proceeding 45th US Rock Mechanics/Geomechanics Symposium*, San Francisco, California, pp 11-14 (American Rock Mechanics Association: California).

Roxborough, F F. 1987, The role of some basic rock properties in assessing cuttability, in *Proceedings of Seminar on Tunnels: Wholly Engineered Structures*, Sydney, (Institute of Engineers Australia/AFCC: Canberra).

Roxborough, F F. 2009, Principles of machine mining, *Monograph 12 - Australasian Coal Mining Practice*, Chp 11. (AusIMM: Melbourne).

Sandvik Mining. 2013, Mining tools [online], Available from < www.miningandconstruction.sandvick.com/sandvick> [Accessed: 18 of March 2014].

Lessons From the Operational Use of the GAG Jet Engine at Mine Sites

Martin Watkinson[1], Ken Liddell[2], Sean Muller[3] and Clive Hanrahan[4]

ABSTRACT: Rio Tinto Coal Australia (RTCA), Queensland Mines Rescue Service (QMRS) and Simtars conducted a partial inertisation of an underground coal mine using the GAG-3A engine in February 2014. This was an ACARP funded project No C23006. This project monitored the environmental conditions and the flow of inert GAG gases into and around the mine. Observations were made by a variety of remote sensing technologies and by direct measurements as well as observations made by mines rescue personnel in the inertised area. This paper documents methodology, observations and the outcomes including a review of previous inertisations. This project proved that the GAG is a reliable and effective inertisation system. It demonstrated the critical requirement for effective sealing of GAG docking points. It is not envisaged that the GAG could be deployed where there is an expectation that mine personnel could be in the vicinity as temperatures of 90°C were measured. Mine infrastructure and strata in zones close to the GAG docking station were detrimentally affected by prolonged exposure to the high humidity and temperature.

INTRODUCTION

Rio Tinto Coal Australia (RTCA) Kestrel North Mine is located 50 km NE of Emerald in Queensland. The mine was accessed by two cross measure drifts, one for the conveyor and one for men and materials. Rope haulage was installed in both drift for man transport and materials transport. Several shafts were sunk as part of the mine development.

Kestrel North Mine was in the process of being closed due to exhaustion of the economical coal reserves and was been made available for the trial. It was initially planned that a week would be dedicated to trialling and monitoring inertisation with the mine being re-ventilated and additional instrumentation moved/installed as required. Operational issues with the water table required a revised scope where inertisation would be monitored on two separate days. This was ACARP funded Project C23006 (Watkinson *et al.,* 2014).

GORNICZY AGREGAT GASNICZY (GAG) SYSTEM

The GAG jet engine system itself is a custom designed zero-thrust jet engine with after-burner; coupled with an extension duct where water is injected into the hot exhaust gases. The system is mounted on a trailer to enable rapid deployment and operation by Queensland Mines Rescue Service QMRS (See Figure 1).

Figure 1: Section of the GAG system showing water injection mechanism

This combination of cooled, jet engine exhaust and water vapour is then introduced into the mine to establish an inert atmosphere.

[1] *Executive Mining Engineer, Simtars, E-mail: martin.watkinson@simtars.com.au, Tel: +61 73810 6386*
[2] *Director Mining Research, Simtars, E-mail: ken.liddell@simtars.com.au, Tel:+61 738106321*
[3] *Analytical Chemist, Simtars, E-mail sean.Muller@simtars.com.au, Tel:+61 73910 6338*
[4] *GAG Operations manager, QMRS, E-mail: chanrahan@qmrs.com.au, Tel: +61 74958 2244*

The GAG consumes 1800 litres of A1 jet fuel/hr and can produce around 25m3/s of jet exhaust product and water vapour. The untreated exhaust gases are very hot as they exit the engine afterburner so they are then cooled by the injection of water at a rate of 600L/minute. The resultant temperature of the inertisation gases is close to 90°C. Further cooling of the gases occurs as they pass into the mine which results in water condensing out of the vapour phase. This water vapour loss results in a net volume flow rate of inert gas of around 7m3/s.

The composition of the GAG exhaust gases range between these values in normal operation:

- O2   0.5-5%;
- CO2   10-16%;
- N2 & water vapour   79.5-84.5%.
- H2   20-200 ppm
- CO   up to 300 ppm).

KESTREL INERTISATION

All elements of the intended inertisation process were risk assessed and detailed procedures put in place to cover the operation. The "target" of the inertisation was the 311LW block. The planned inertisation circuit was the 1km length of the cross measure conveyor drift to 3CT; the belt road 2km towards LW311; then back around the return to the up-cast shaft, as indicated in Figure 2. The entire route was approximately 5.4km in length the approximate volume to be inertised was around 81,000m3. RTCA teams prepared stoppings and sealed access doors as necessary ahead of the exercise in order to minimise leakage.

On Day 1 a ventilation rate of10 m3/s was established in the GAG circuit with around 30 m3/s being delivered into the vehicle roadways. This enabled QMRS personnel to be underground and enter the GAG circuit under Compressed Air Breathing Apparatus (CABA) at predetermined Look Points (LP). On Day 2 there was no mine ventilation thus no underground observers were in place.
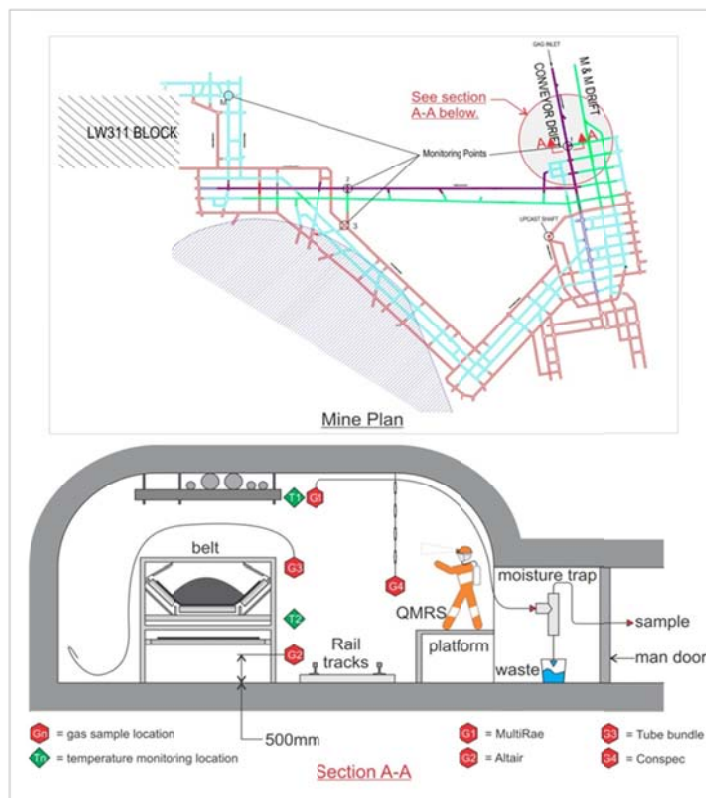
Figure 2: Inertisation Layout, Monitoring Point locations and LP1 test set up

Monitoring

A wide scope of monitoring activities were implemented, in particular as it was possible to have personnel stationed in ventilated areas adjacent to the 3 points in the GAG circuit (look points 1 to 3). During the inertisation these personnel were able to enter the GAG circuit under CABA and following QMRS protocol, to make environmental observations augmented by additional gas and temperature monitoring at other inaccessible positions. The broad scope of the monitoring aims is shown in Figure 3. The scope was achieved by monitoring temperatures, gas levels, relative humidity, air flow, visibility and physical inspections of the mine infrastructure.
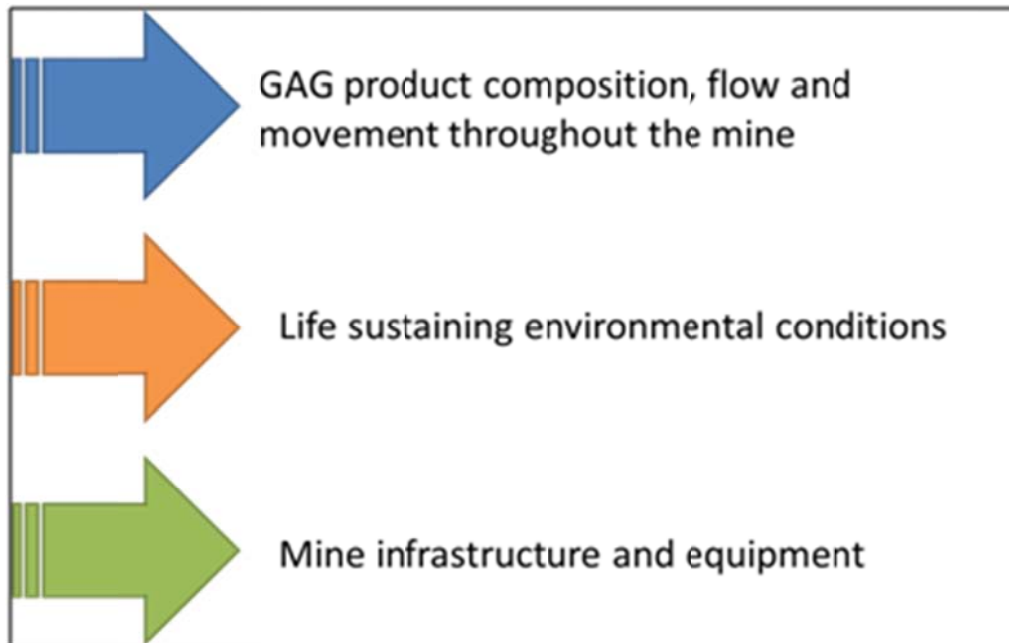
Figure 3: Scope of the monitoring during the inertisation at Kestrel North

Gas monitoring

Gas monitoring was conducted using a variety of techniques, which included the mine's tube bundle and real time systems. Additional sampling was set up at each LP. Queensland Mines rescue used XAM7000 hand held gas detectors to monitor gas concentrations during their inspections of the zone being inertised.

Temperature

Temperature in the drift was monitored continuously over a range of 0-400m, in 1m intervals. This was achieved by the use of a SensorNet Distributed Temperature Sensor (DTS) system. The DTS is a laser and fibre optic based device that can measure temperature at 1m intervals over distances of 10 km. Thermocouples were used at each LP at the roof and floor level. The primary concern was to ensure the safety of the QMRS personnel and that they did not enter the conveyor drift if the atmosphere presented them with unmanageable risks. Monitoring was established to give the underground crew live gas and temperature readings from inside the inertisation circuit.

Monitoring at LP1 consisted of:

- Two thermocouple positions.
- MultiRAE gas analyser sampling through water traps.
- Tube bundle point (in the drift).
- Conspec real time oxygen and carbon dioxide sensors (in the drift).
- Altair gas detector measuring in situ, (50cm off the ground under the conveyor).

Additional observations carried out by QMRS personnel at all 3 LPs included:

- Visibility.
- Relative humidity.
- Gas concentrations.
- Taking bag samples for subsequent gas chromatograph analysis.

Note: At LP1 the Real Time (RT) system provided data on carbon monoxide and oxygen for just 2 hours.

Day 1 Inertisation

Temperature distribution in the drift is shown in Figure 4.
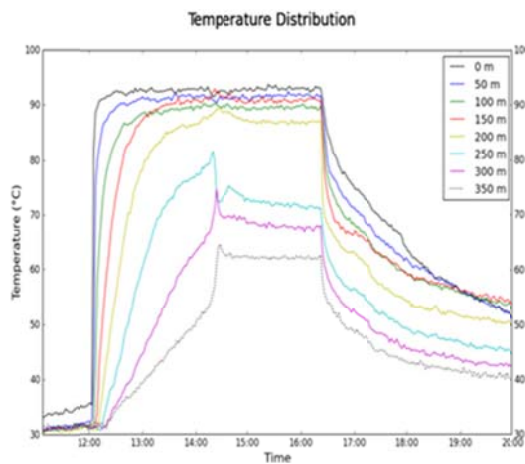
Figure 4: Temperature distributions in the conveyor drift
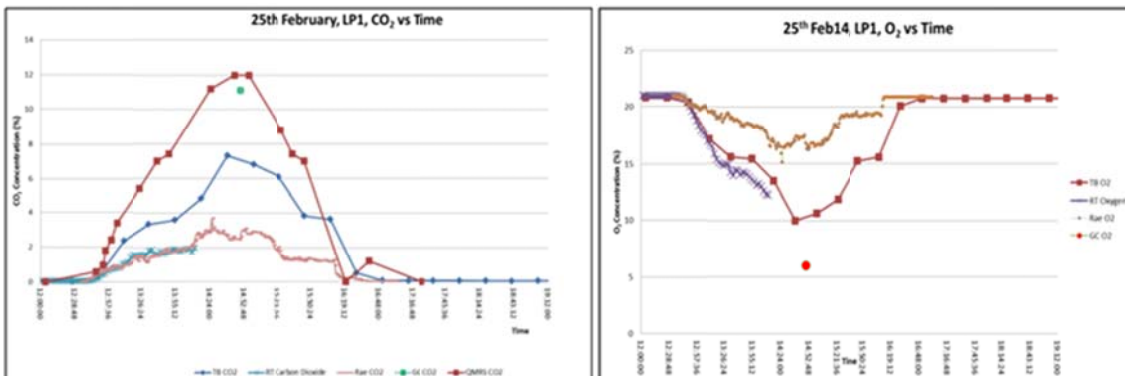
Figure 5: CO2 and O2 measurements at LP1 on Day 1
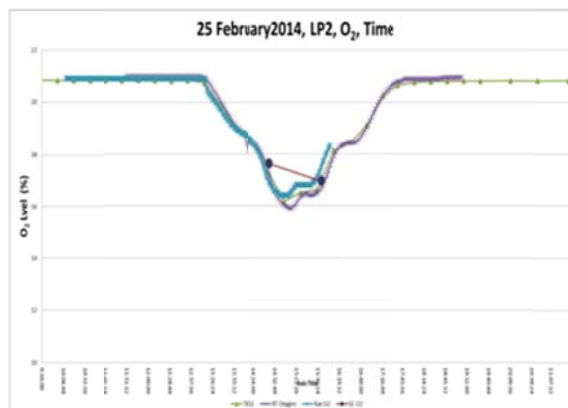
Figure 6: Oxygen level results at LP2

LP3 gas monitoring results

Very little GAG product made it to LP3.

The maximum (minimum for O_2) gas levels measured at LP3 were:

- CO 13.4 ppm
- CO2 0.73%
- O2 dropped by 1% from the baseline levels

Day 1 - concluding observations

- The leakage around the conveyor drift door was substantial and adversely impacted the process of inertising the mine. In preparation for the second inertisation event, RTCA staff provided additional sealing around and behind the conveyor door
- The inertisation run on day 1 was curtailed due to the break in the compressed air line, which rendered any further attempt at inertisation futile.
- Comparative gas measurements at LP1 showed a wide variation between instruments. See figure 5

  o This could be due to layering of the GAG product as it emerged from the conveyor drift at pit bottom

  o Further investigation into layering is necessary

- The CO levels at LP1 were much higher than measured by gas monitoring at the GAG. An additional tube bundle line was installed in the conveyor drift; close to the GAG inlet position to verify readings.
- The real time monitoring system at LP1 failed after 2 hr. See figure 5
- Despite the leakage at the surface, the zone around LP1 (1km from the portal) had an inert atmosphere (less than 10% oxygen) after 2 hr and 45 min. At LP2 the oxygen level fell to 16% see Figure 6
- Visibility remained good 1 km from the GAG inlet.
- Temperatures close to the GAG reached 93°C, but remained at ambient in the mine.
- After the conveyor drift had cooled the surface roller door was opened and inspection showed deterioration of exposed rock/coal areas and buckling of the steel rail track in places.

Day 2 - concluding observations

- There was no mine ventilation on day 2, but natural ventilation paths allowed the inertisation to take place and the GAG gases were delivered much more effectively than on day 1 due to the improvements of the conveyor drift portal door seal.
- Leakage through an open door at 3CT reduced the impact of inbye inertisation however; the process was unaffected up to LP1 as seen from the progress of temperature gradients in the drift and with GAG product migration.
- Maximum temperatures in the conveyor drift reached the same levels as on day 1, i.e. close to 90°C as shown in Figure 7.
- A low oxygen atmosphere (less than 5%) was achieved after 2 hrs and 19 min (Figure 8).

The main visual observations in the conveyor drift were that the rail tracks had buckled and split in places due to the 90°C heat and the lack of rail expansion joints (Figure 9). Surface areas of the drift had deteriorated following exposure to the GAG product. Shotcrete areas had fared better, but exposed rock and coal were spalling and in places had fallen away.

Temperature Distribution
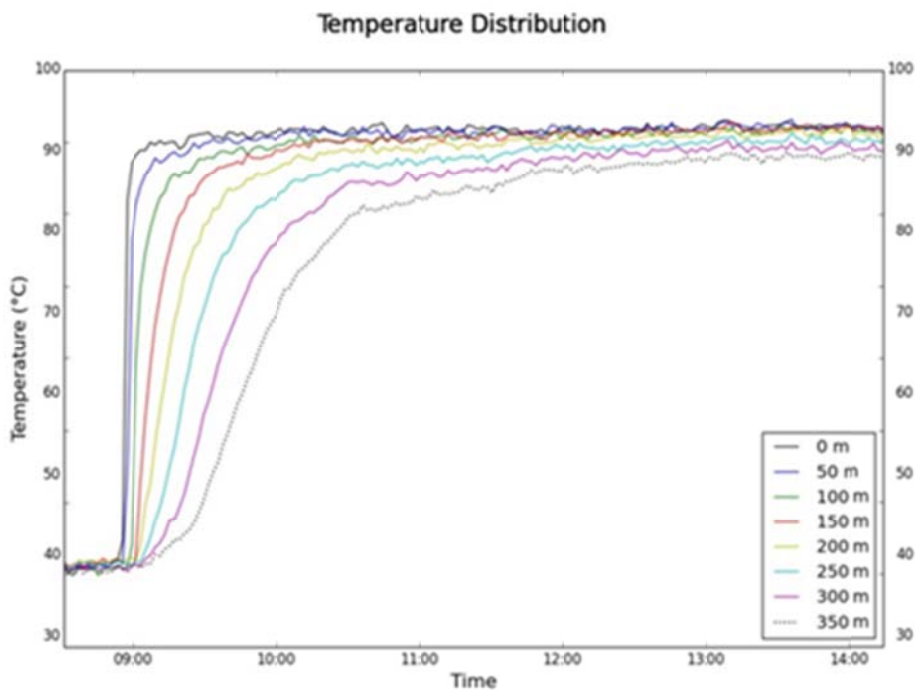
Figure 7: Temperature distributions in the conveyor drift during Day 2
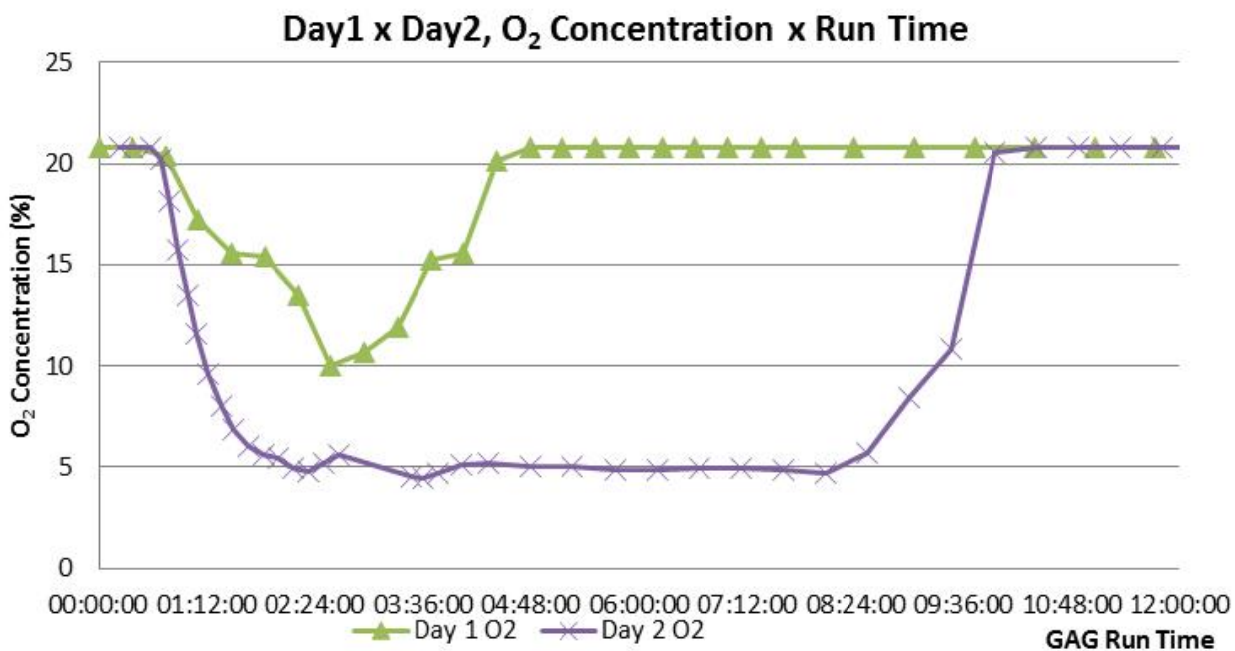
Figure 8: Oxygen percentages at LP 1, Day 1 & Day 2

Figure 9: Damage to dolly-car rail & spalling in the conveyor drift

OTHER INERTISATIONS

Kestrel North Mine – August 2013

In August 2013 the RTCA decided to seal and inertise an area of the mine in bye of 12CT in the 300 series longwalls to protect the 311LW block to enable coal production to continue for as long as possible. (Kachel, J, 2013). The area to be sealed would contain a void of over 200,000 m3. All adjacent goafs were inert.

In preparation for the inertisation, substantial preparatory works were carried out to direct the GAG product to the 313 area and to allow continued coal production elsewhere in the mine, without putting personnel at risk of exposure to potential high temperatures or GAG gases.   The progress of the GAG gases was monitored using the tube bundle system.

Observations

- Introduction of GAG gases down a shaft worked well.
- Real time sensors are needed during a GAG operation as the tube bundle delay times were in excess of 60 minutes. So the tube bundle system couldn't be used to control the process.
- The inertisation route split into 3 roadways and may have resulted in excess dilution rather than a displacement of the fresh air out of the area to be sealed.
- Gas samples from the GAG jet system, tube bundle, gas chromatograph and real time were similar.
- GAG output temperatures were higher than anticipated.
- The target of <5% O2 in the sealed area wasn't achieved. (13% was achieved)
- Some equipment in the mine was damaged from high temperatures. This included pogo sticks, guide cones on the escape routes and the real time telemetry equipment.
- Some rib spall occurred
- Stone dust was washed away
- After shut down, underground crews couldn't access the zone for over 5 hours

Collinsville, 1997

Surface and underground trials of the GAG-3A jet inertisation device were held at the Collinsville No 2 underground coal mine from 7th April to 18th April 1997. (Bell, *et al*., 1997)

The test criteria for the trial were developed by the Moura Task Group 5 Committee. This committee was tasked with investigation of inertisation and sealing strategies in underground coal mines.

- Output flow rates during the trial were measured at 19 m3/s (against a target of 20-25 m3/s).
- The GAG output was stable around 90°C, oxygen 6-8%, carbon dioxide 8-10%
- Control of ventilation was a major priority
- Limited stratification of the GAG gases showed that it tended to move closer to the roof than the floor.
- Simtars concluded that the GAG-3A system is a good solution to inertise an underground coal mine.
- It is not considered a universal solution

Goede Hoop Colliery South Africa, 2005

A fire was detected on 10 April 2005 in Goede Hoop Colliery in South Africa.   The mine is a bord and pillar mine and the fire was detected near a downcast shaft some 12 km from the main intakes of the mine. Underground seals were built to isolate the fire area. An evaluation of inertisation capability was undertaken and the Steamexfire fire unit selected on availability and weight for transport.   The unit was

run from 21 April 2005 to 6 May 2005. Initial use introduced 14-18% oxygen underground due to the settings on the unit. One working section and associated equipment became trapped in the fire area. The area was not recovered after the inertisation. The inertisation process pressurized the affected area to maximum of 6.5 inches of water gauge (1.6 Kpa). The system ran for a total of 191.5 hours. The estimated volume of the product inserted into the fire affected area was approximately 17.2M m3. This is three times more than the estimated volume to fill the workings of 6M m3. (Romanski M 2005)

Svea Nord Norway, 2005

Little is known of the operation at Save Nord other than what is provided in the 2005 Store Norske Spitsbergen Grubekompani annual report: "On the night of 30th July 2005, a plastic pipe in the C drift of main drift 3 caught fire. The pipe had been welded to its full 1.3 km length only a few hours earlier by a specialist contractor. The mine was quickly evacuated, and in a few hours the fire was ablaze along the entire length of the pipe. After a month of inertisation with the steamexfire unit the mine was recovered in February 2006. Production was resumed on 1st April 2006.

Pike River

A bespoke docking device created form an old shipping container and placed into the mine opening. The area around was sealed with shotcrete and PUR. Despite several issues with leakage, the mine was successfully inertised and the fire brought under control. This was a single entry and the fire was approximately 2.4 Km from the portal with the vent at the upcast shaft.

Blair Athol

Underground mine fires in old mine workings at an open cut mine were brought under control by using the GAG to fill the mine with inert gas then keeping it topped up using the Tomlinson Boiler. In preparation the open roadways in the high wall were plugged with inter-burden and clay to create a seal. This was an ongoing issue and over $1 million was spent on diesel for the Tomlinson boiler. The GAG was instrumental in bringing the situation under control by the flooding the fire zones with inert gas.

Loveridge

On the afternoon shift of Friday 13th February 2003 coal cars loaded with garbage gathered from the operating sections and throughout the mine was brought to the slope bottom in order to be sent out of the mine for dumping. One of the cars caught fire. The fire was thought to have been extinguished, using several fire extinguishers. Within a short time the fire had flared up again. The decision was made to pull the cars out of the mine to the surface via the slope track. Whilst undertaking this task several adverse events took place that prevented the cars from being sent out via the slope track. The fire then spread from car to car and subsequently out of control. The mine was sealed and the GAG was selected for the inertisation process. There were issues with the sealing of the belt drift and leakage up to 30% of the GAG product was being lost. The GAG operated for a period of 13 days and a maximum back pressure of around 2.2kPa was measured. An inert atmosphere was established over 14km from the GAG docking station. The fire was extinguished and the mine recovered successfully (Parkin, 2003).

Newland Southern Underground

The Newlands Southern underground mine was inertised using the GAG placed at the fan shaft. Little is known of the outcomes other than there was a failure of the shaft collar some 6 months after the GAG had been used and the failure was attributed to the hot GAG gases.

Southland

The GAG was deployed to the Southland mine fire in 2003. The use was suspended and the full benefit of the GAG was not realised due to the mine not being sealed and the GAG product being diluted. The GAG was run 27 to 29 December 2003. The main fan stopped on 29th December and the mine was sealed and left to naturally inertise up to 27 January 2014 (Haynes PJ, Davis J Southland).

Carborough Downs

There was a spontaneous combustion identified in a longwall goaf an attempt was made to use the GAG for inertisation , however due to the fact the mine was not completely sealed and no direct control over the

ventilation circuit little or no GAG product made it to the longwall. The heating was brought under control by nitrogen foam injection

CONCLUSIONS

It has been demonstrated that the GAG is an effective tool for whole-mine inertisation. There are clear outcomes, namely:

- Successful deployment of the GAG depends on the mine being effectively sealed.
- It is likely to take many days for the GAG to inertise a typical longwall mine in Australia.
- Attempting to direct the GAG product to a specific, remote location underground is not practical without pre-existing infrastructure.
- The integrity and position of normal mine ventilation control devices doors/stopping regulators can have a major influence on the spread of the GAG gas through the mine
- GAG temperatures rise to a maximum of 90°C.
- Temperatures would rise quickly to levels that would not permit men to survive if they were close to the GAG docking station.
- Areas of rock or coal in the roof and rib that become exposed to high temperatures and humidity can be expected to experience deterioration.
- In the event of an underground emergency access to the portal will be restricted.
- Strategically located tube bundle sampling locations appear to be the optimum solution for monitoring the spread of the GAG gas underground.
- The GAG gas can contain up to 300 ppm of carbon monoxide and 200 ppm of hydrogen.

REFERNCES

Bell, S. Humphries, D. Harrison, P. Hester ,C and Torlach, J. 1997, Practical demonstration and evaluation of jet engine inertisation techniques, (C6019), *Brisbane: ACARP*.

Brady J.P. 1997, Sealing, monitoring and low flow goaf inertisation (C6002), *Brisbane: ACARP*.

Haynes PJ and Davis J, Southland Colliery: Longwall Relocation SL3 to SL4 and Spontaneous Combustion Event.

Kachel, J. 2013, Kestrel North Inertisation, Kestrel Internal Powerpoint presentation.

Parkin, R. 2003, Inertisation of Loveridge No.22 coal mine by Queensland Mines Rescue Service, Qld, *Mining Industry Health and Safety Conference*, August 2003, Townsville.

Romanski M. 2005, Goede Hoop Colliery Mine Fire Global SteamExfire Inertisation Services report, April/May 2005.

Store Norske Spitsbergen Grubekompani. 2005, Annual Report.

Watkinson, M. Liddell, K. Muller, S. Gido, M and Nissen J. 2014, A practical research study into the environmental and physical impacts during an underground mine inertisation with the GAG jet *(C23006) Brisbane ACARP*.

Contrast in Self-Heating Rate Behaviour for Coals of Similar Rank

Basil Beamish and Jan Theiler

ABSTRACT: Adiabatic oven testing of seven coal samples with a similar rank has been conducted, which demonstrates differences in their self-heating rate behaviours under the mine settings that they are found in. This has been achieved using a new benchmarking adiabatic test that provides an accurate means of establishing if a coal can reach thermal runaway and in what minimum timeframe. Four of the samples reached thermal runaway, but there was a considerable range in the time taken. The shape of the self-heating rate curves also showed a degree of variation. One of the samples displayed gradual self-heating over the duration of the test and would have reached thermal runaway eventually. The other two samples initially self-heated and reached a maximum temperature before the heat loss mechanism from moisture evaporation dominated and the coal temperature steadily decreased. One of these samples was retested at a lower moisture state and was able to reach thermal runaway. These results confirm the importance of testing samples to assess the risk of developing a spontaneous combustion event.

INTRODUCTION

Adiabatic oven testing has been used routinely by Australian and New Zealand coal mine operations since the early 1980's to rate the propensity of coal to spontaneously combust (Humphreys *et al.*, 1981). A relative rating scale has been applied to the R_{70} initial self-heating rate parameter normally obtained from these tests (Beamish and Beamish, 2012). This intrinsic spontaneous combustion propensity rating enables an assessment to be made of the possible risk of a spontaneous combustion event developing; however it does not provide an indication of the timeframe in which this can occur. More recently adiabatic oven testing has been applied to benchmark the time taken to reach thermal runaway (Beamish and Beamish, 2010, 2011, 2012).

R_{70} values are strongly rank dependent (Beamish and Arisoy, 2008a,b; Beamish and Beamish, 2012), with low rank coals having high R_{70} values (up to 99 °C/h for lignite) and high rank coals having low R_{70} values (less than 0.5 °C/h for medium and low volatile bituminous coals). Other coal properties such as mineral matter and coal type (dull or bright) can also affect the R_{70} value (Beamish and Blazak, 2005; Beamish and Clarkson, 2006; Beamish and Sainsbury, 2008). This paper presents examples of the self-heating behaviour of coals with a similar rank that shows considerable contrast in self-heating rates under moist adiabatic conditions.

COAL SAMPLES AND ADIABATIC TESTING

Seven coal samples of similar rank from Queensland (five samples) and New South Wales (two samples) were tested in an adiabatic oven to establish their R_{70} values and to benchmark the time taken to reach thermal runaway under conditions more closely resembling those of the mine site. The R_{70} testing procedure is described by Beamish (2005) and essentially involves testing a dried, crushed coal sample under adiabatic conditions from a fixed starting temperature of 40 °C. The benchmarking procedure, known as SponComSIM™ testing, uses the coal in its as-mined moisture state and a starting temperature that reflects the site-specific conditions. The results obtained provide both an indication of the time taken to reach thermal runaway and the characteristic behaviour of the coal as self-heating progresses. This can be compared against case history coals of known self-heating behaviour.

The coal quality details of the samples are contained in Table 1 and their similarity in coal rank is demonstrated on a Suggate rank plot (Suggate, 2000) shown in Figure 1. The Suggate rank number for the samples ranges from 11.0 to 11.5 and the samples are considered to be high volatile bituminous under the ASTM classification scheme. There is a difference in coal type from high vitrinite (QLD1 and QLD4 plotting within the New Zealand coal band) to low-medium vitrinite (QLD2, QLD3, QLD5, NSW1 and NSW2 plotting below the New Zealand coal band). Three of the Queensland samples (QLD3, QLD4 and QLD5) are from the one seam and the other two samples (QLD1 and QLD2) come from different

mining locations. The two New South Wales samples are from the same seam with NSW1 collected from the upper part of the seam and NSW2 collected from the lower part of the seam. All of these coals are mined for thermal coal markets.

Table 1: Coal quality data for Queensland and New South Wales coal samples

Sample	R_{70} (°C/h)	Moisture content (%, ar)	Ash content (%, db)	Sulphur content (%, db)	Volatile matter (%, dmmf)	Calorific value (Btu/lb, mmmf)	ASTM rank
Queensland coals							
QLD1	2.74	7.3	8.7	0.31	40.2	13666	hvBb
QLD2	3.42	8.8	13.8	0.26	28.2	13567	hvBb
QLD3	7.35	10.0	4.6	0.33	31.3	13040	hvBb
QLD4	7.78	8.0	2.4	0.62	40.7	13346	hvBb
QLD5	6.34	12.0	4.2	0.57	36.7	12858	hvBb
New South Wales coals							
NSW1	6.76	9.1	9.1	0.38	27.8	13277	hvBb
NSW2	4.18	8.1	7.9	0.36	30.0	13541	hvBb
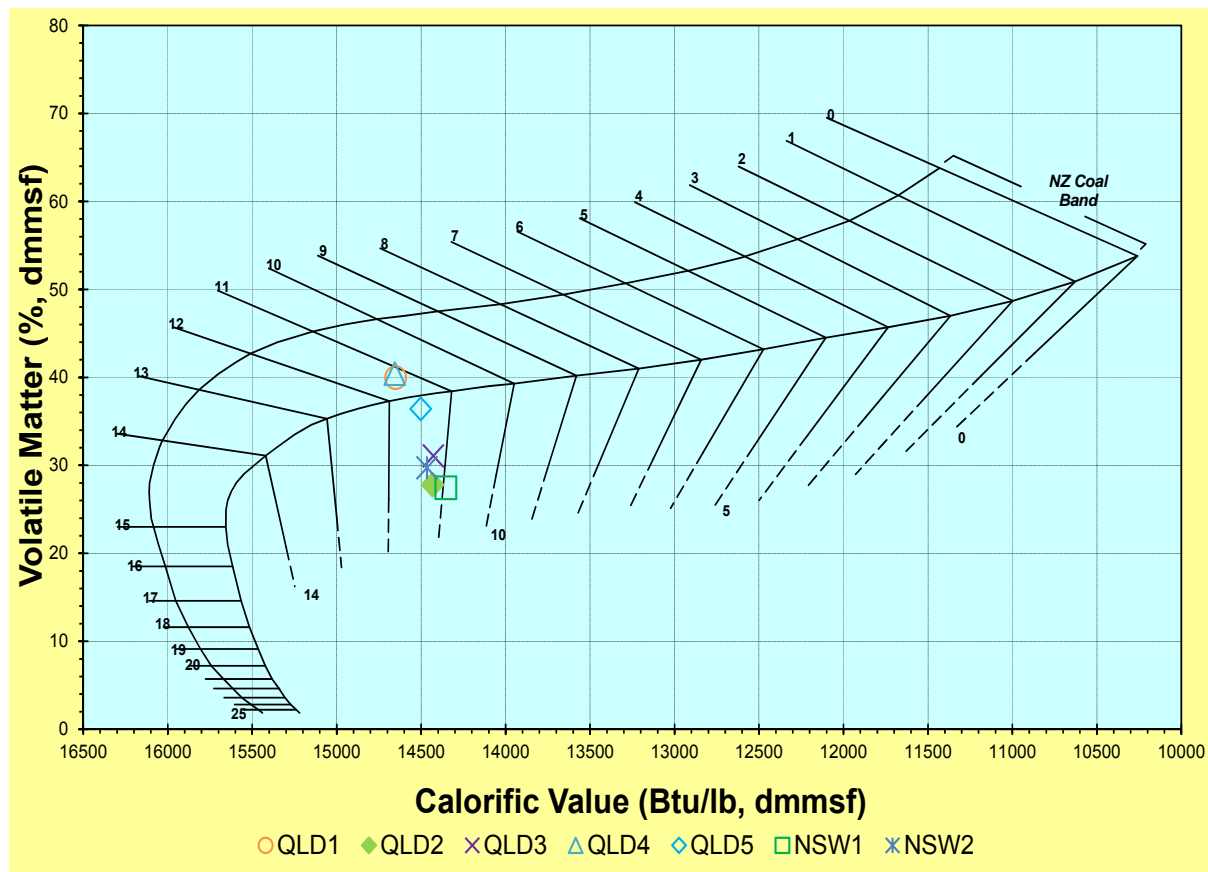
Figure 1: Suggate rank plot of coal samples used in adiabatic testing

ADIABATIC TESTING RESULTS AND DISCUSSION

R$_{70}$ values

The R$_{70}$ self-heating rate curves for all the samples are shown in Figure 2. The Queensland samples show a range of R$_{70}$ values from 2.74 °C/h to 7.78 °C/h, which rates these coals as having a high to very high intrinsic spontaneous combustion propensity for Queensland conditions (Beamish and Beamish, 2012). The New South Wales samples have a narrower range and rate this coal seam as having a high intrinsic spontaneous combustion propensity based on New South Wales conditions (Beamish and Beamish, 2012). The lower R$_{70}$ values for the QLD1 and QLD2 samples may be related to a combination of higher ash contents and a slightly elevated rank compared to the other Queensland samples. The difference in the R$_{70}$ values of the New South Wales samples may be related to a subtle difference in the mineral matter assemblage present in each sample. The lower part of the seam is believed to contain the mineral Dawsonite, similar to other seams in this region (Zhao *et al.*, 2014), which may be acting as a natural block to oxygen availability to reactive sites.
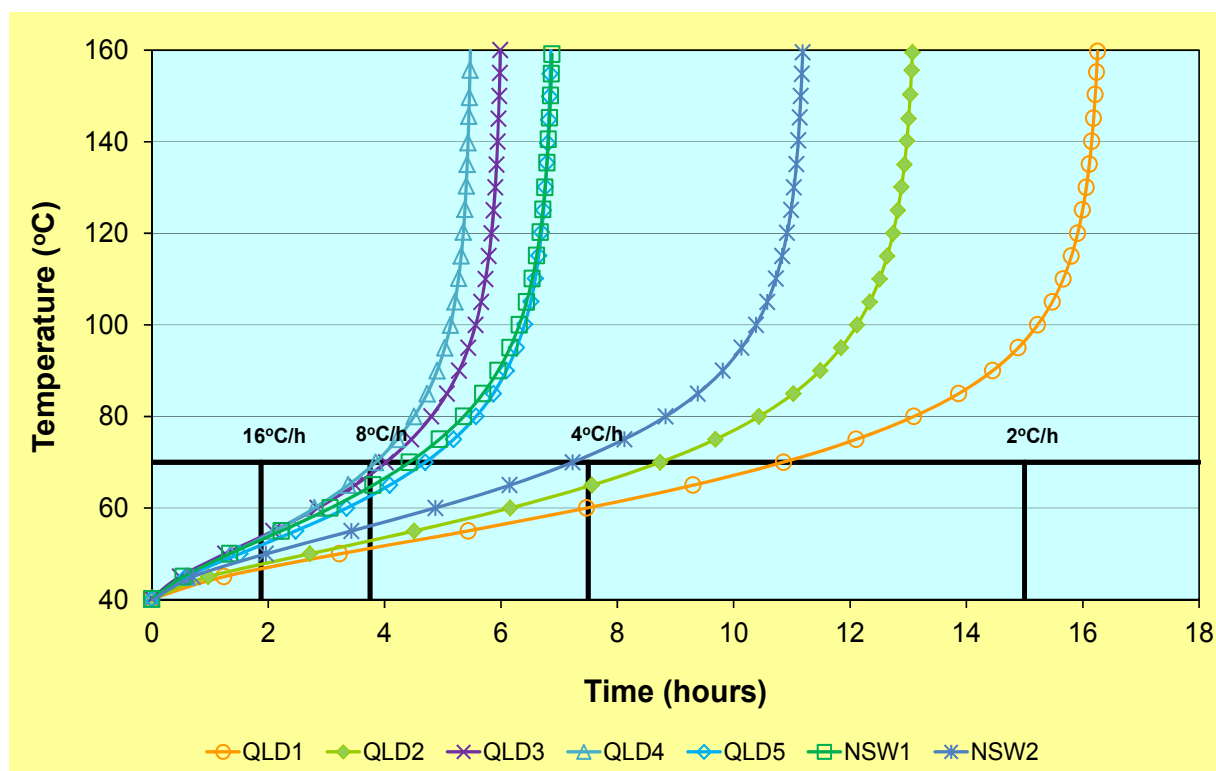
Figure 2: Adiabatic self-heating curves for a range of Queensland and New South Wales high volatile bituminous coals under dry conditions

Self-heating performance

The SponComSIM™ test results are shown in Figure 3. Despite the similarity in coal rank of the samples there is a clear set of contrasting behaviours displayed by the coals under these test conditions. Not all of the samples reached thermal runaway.

Sample QLD1, which has the lowest moisture content of the samples and the lowest R$_{70}$ value gradually self-heats to thermal runaway (Figure 3), and the shape of the self-heating curve is similar to the R$_{70}$ self-heating rate curve (Figure 2). The main difference is that it takes 136 hours to reach 160 °C compared with 16 hours in the dry state used for the R$_{70}$ test.

Sample QLD2 has a higher R$_{70}$ value than sample QLD1, but it also has a higher moisture content (8.8% cf 7.3%). In this case the increased moisture content of the coal is sufficient to provide a higher heat loss from moisture evaporation as the coal temperature increases from the oxidation reaction. Consequently, the coal initially self-heats to a maximum temperature of 53 °C before the heat loss from moisture evaporation exceeds the heat gained from coal oxidation and subsequently the temperature of the coal

decreases (Figure 3). This result emphasises the importance of this heat balance mechanism in governing whether an intrinsically reactive coal can reach thermal runaway.
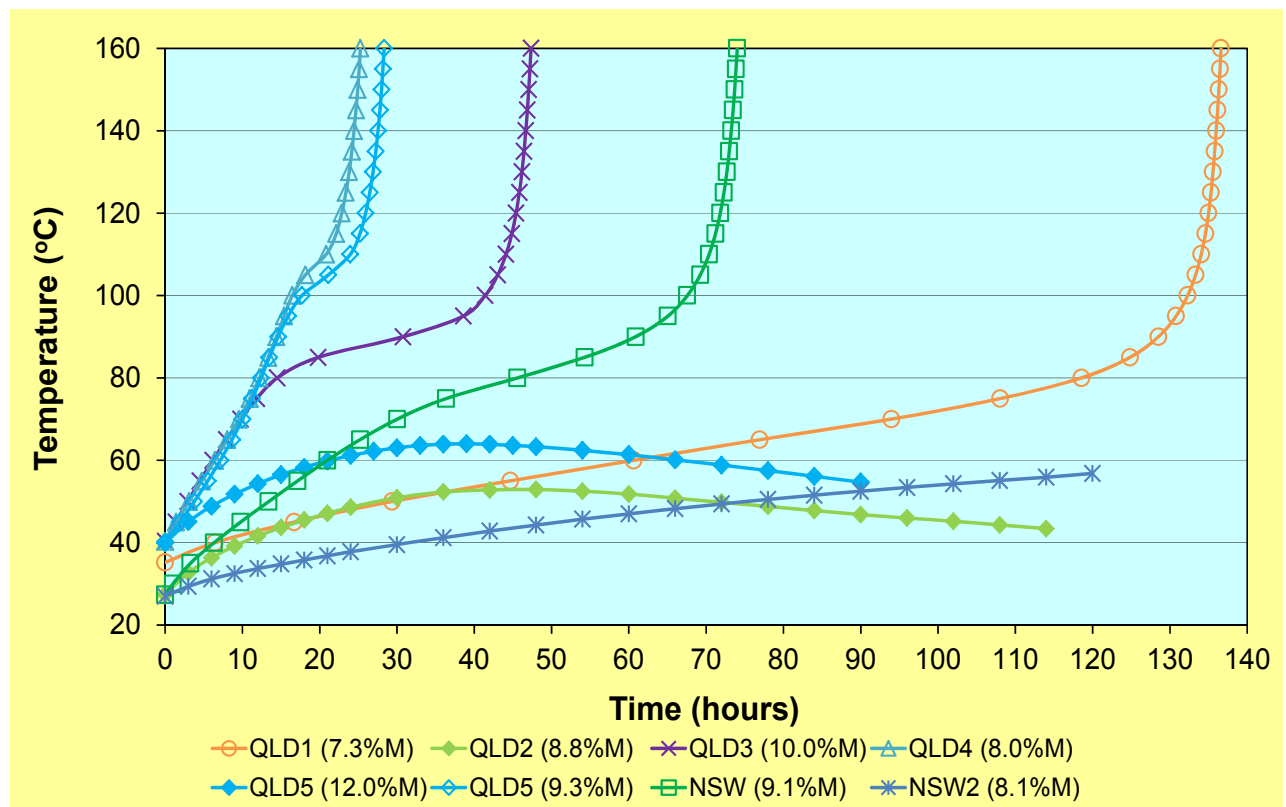
Figure 3: Adiabatic self-heating curves for a range of Queensland and New South Wales high volatile bituminous coals under moist conditions

This heat balance mechanism is further demonstrated by the self-heating performance of the QLD3, QLD4 and QLD5 coal samples. All three samples are identified as very reactive from the R_{70} test results, but it is clear that the time to thermal runaway under normal mine conditions is strongly modified by the moisture content present in the coal. In this case QLD4 reaches thermal runaway in the shortest time due to having the lowest moisture content (8.0%) and QLD5, which has the highest moisture content (12.0%) does not reach thermal runaway at all (Figure 3). Instead QLD5 displays a similar self-heating curve to QLD2 and reaches a maximum temperature of 64 °C before the heat loss from moisture evaporation exceeds the heat gained from coal oxidation and subsequently the temperature of the coal decreases. A replicate sample of QLD5 was tested at a lower moisture content of 9.3% to confirm the influence of the moisture on the coal self-heating performance. This result is shown in Figure 3 and it can be seen that the self-heating curve falls between QLD3 and QLD4, consistent with the moisture content difference between the samples.

Sample QLD3 shows a noticeable inflection in the self-heating curve once the coal temperature exceeds 80 °C. This is referred to as a moisture shoulder and is the result of the on-going heat balance response between heat loss from moisture evaporation and heat gain from coal oxidation. As the coal dries out more reactive sites become available for the oxidation reaction to continue and in this case it appears that once the coal temperature exceeds 100 °C the coal temperature rapidly progresses to thermal runaway.

The intrinsic coal reactivity of NSW1 is just over 50% higher than NSW2 as shown by the difference in their R_{70} values (Table 1). This difference is sufficient for NSW1 to reach thermal runaway in a shorter timeframe than NSW2 despite having 1% more moisture content. There also appears to be a fundamental difference between the self-heating response of NSW1 and QLD3. Despite having a higher moisture content QLD3 reaches thermal runaway in a shorter timeframe than NSW1. This may be due to subtle differences in the pore structure of the two coals as a result of their different basinal histories both during and after coalification. Reactive sites may be more readily available in the QLD3 sample than in the NSW1 sample.

CONCLUSION

Coal self-heating performance is not a simple predictable behaviour. There are many competing influences and mechanisms taking place that can moderate whether a spontaneous combustion event can take place. The overall outcome is governed by the heat balance, which is a function of the interaction between coal intrinsic properties and site-specific extrinsic factors. Coals of quite similar rank can display contrasting self-heating behaviours due to these parameters. This has been demonstrated from adiabatic oven testing of thermal coals from Queensland and New South Wales. Essentially, one of the key controls identified by this testing is the importance of the interaction that takes place between the moisture in the coal and intrinsic oxidation reaction rate.

Higher moisture content coals display an inflection in the self-heating rate curve due to the competing effects of heat loss from moisture evaporation and heat gain from coal oxidation. This prolongs the time taken to reach thermal runaway and is an important feature of coal self-heating performance that needs to be identified. In some cases the heat loss mechanism from moisture evaporation is sufficient to overcome the heat gain from oxidation and results in the coal losing temperature and therefore it is not able to achieve thermal runaway in a practical timeframe or not at all.

ACKNOWLEDGEMENTS

REFERENCES

Beamish, B B. 2005, Comparison of the R_{70} self-heating rate of New Zealand and Australian coals to Suggate rank parameter, *International Journal of Coal Geology*, 64(1-2):139-144.

Beamish, B B and Arisoy, A. 2008a, Effect of intrinsic coal properties on self-heating rates, in *Proceedings 12th US/North American Mine Ventilation Symposium (ed: K G Wallace Jr)*, pp 149-153 (The Society of Mining, Metallurgy and Exploration Inc., Littleton, USA).

Beamish, B B and Arisoy, A. 2008b, Effect of mineral matter on coal self-heating rate, *Fuel*, 87:125-130.

Beamish, B and Beamish, R. 2012, Testing and sampling requirements for input to spontaneous combustion risk assessment, in *Proceedings of the Australian Mine Ventilation Conference (eds: B Beamish and D Chalmers)*, pp 15-21 (The Australasian Institute of Mining and Metallurgy: Melbourne).

Beamish, B and Beamish, R. 2011, Experience with using a moist coal adiabatic oven testing method for spontaneous combustion assessment, *in Proceedings 11th Coal Operators' Conference (ed: N Aziz)*, pp 380-384 (University of Wollongong and The Australasian Institute of Mining and Metallurgy).

Beamish, B and Beamish, R. 2010, Benchmarking moist coal adiabatic oven testing, *in Proceedings 10th Coal Operators' Conference (ed: N Aziz)*, pp 264-268 (University of Wollongong and The Australasian Institute of Mining and Metallurgy).

Beamish, B B and Blazak, D G. 2005, Relationship between ash content and R_{70} self-heating rate of Callide coal, *International Journal of Coal Geology*, 64(1-2):126-132.

Beamish, B and Clarkson, F. 2006, Self-heating rates of Sydney Basin coals – The emerging picture, *in Proceedings of the 36th Sydney Basin Symposium*, pp 1-8 (University of Wollongong).

Beamish, B B and Sainsbury, W. 2008, Development of a site specific self-heating rate prediction equation for a high volatile bituminous coal, *in Proceedings 8th Coal Operator's Conference (ed: N Aziz)*, pp 161-165, (University of Wollongong and The Australasian Institute of Mining and Metallurgy).

Humphreys, D, Rowlands, D and Cudmore, J F. 1981, Spontaneous combustion of some Queensland coals, in *Proceedings of Ignitions, Explosions and Fires in Coal Mines Symposium*, pp 5-1 - 5-19 (The AusIMM Illawarra Branch).

Suggate, R P. 2000, The Rank (Sr) scale: its basis and its application as a maturity index for all coals, *New Zealand Journal of Geology and Geophysics*, 43:521-553.

Zhao, L, Ward, C R, French, D and Graham, I T. 2014, Mineralogy and major-element geochemistry of the lower Permian Greta Seam, Sydney Basin, Australia, *Australian Journal of Earth Sciences*, 61(3):375-395.

THE HAZELWOOD MINE FIRE 2014

David Cliff

ABSTRACT: On 9 February 2014 a fire began in the open cut brown coal mine at Hazelwood near Morwell in Victoria. This fire burnt for 45 days before it was extinguished. The fire necessitated the evacuation of parts of Morwell and required a major coordinated fire-fighting effort. The severity of the fire and the impact upon the local community caused the Victorian Government to institute a Board of Inquiry (Teague *et al.,* 2014). This paper discusses the information presented to the Board of Inquiry into this fire and the conclusions and recommendation of the Inquiry, focussing on what caused the fire and what could be done to prevent a recurrence. This paper draws heavily on the Board's published report of over 430 pages (Teague *et al.,* 2014) and is the source of the information unless otherwise stated.

INTRODUCTION

The Latrobe Valley coal reserves are unique and are characterised by a relatively thin layer of soil and clay overburden covering massive coal seams that are on average 100 metres thick. This makes accessing the vast brown coal reserves in the Latrobe Valley relatively easy compared with elsewhere in the world.

The Hazelwood Mine provides approximately 25 per cent of Victoria's baseline electricity supply. Coal was first discovered at Morwell were discovered in the late nineteenth century by the Great Morwell Coal Mining Company. The State Electricity Commission of Victoria (SECV) acquired the Hazelwood mine site in 1924. The SECV established the Hazelwood mine, then known as the Morwell Open Cut in 1949, in order to supply brown coal to the adjoining briquette works, to supply the increase in power demands post world war two. Mining operations initially commenced in 1955 in what is now known as the east field, bounded at the north by the northern batters.

The Hazelwood mine was further developed from the late 1950s. Between 1964 and 1971, the Hazelwood Power Station was built and demand for coal from the Hazelwood mine increased dramatically. The Hazelwood pondage was constructed in the early 1970s to establish a supply of cooling water for the Hazelwood Power Station. Mining of the east field continued until about 1980. The Hazelwood mine then expanded to the south-west, then to the south-east and then west again, where the operational area of the mine is now situated. Under the current proposed mining schedule, mining at the Hazelwood mine will continue to the west and then to the north before the anticipated closure of the mine in 2031.

The Victorian Government privatised the SECV in the early to mid-1990s, and its power stations were sold separately to overseas interests.

The Hazelwood mine, including the land on which it operates, is owned by the Hazelwood Power Partnership. Since 7 June 2013, the four partners have been subsidiaries of International Power (Australia) Holdings Pty Ltd. This company is in turn jointly owned by subsidiaries of GDF Suez S.A. (72 per cent ownership) and Mitsui & Co Ltd (28 per cent ownership). GDF Suez S.A. is a global energy company with corporate headquarters in France.

Fire is a well-known occurrence in mines in the Latrobe Valley, and there have been a number of fires in the past ten years at the Hazelwood mine, most recently in 2005, 2006 and 2008. On each of these occasions the fire initiated in a single location, rapidly increased in size, fanned by strong winds and took a number of days to extinguish (Potter, 2008).

THE MINE

The Latrobe Valley currently contains three huge open cut brown coal mines. Open cut brown coal mines are particularly vulnerable to fire.   Laboratory reactivity tests place the coal in the exceptionally high category (Beamish and Arisoy, 2008) due to its low rank. The coal is only stable when wet (inherent moisture is about 60 % by weight). If the coal was dried, any fire initiated in the coal would spread quickly and be difficult to extinguish. The coal is not stockpiled but burnt as soon as possible after being

The University of Queensland, School of Mechanical and Mining, Email:d.cliff@mishc.uq.edu.au, Tel: 0401993760

mined. Hazelwood open cut mine is shown in figure 1. The mine stretches approximately 5km from west to east and about 2.5 km from south to north at the widest point. The area being extracted is located in the south west of the pit.

Figure 1: Aerial view of the mine (**Teague *et al.,* 2014**)

THE EVENT

Victoria experienced one of its hottest and driest summers on record in 2014. In mid-January 2014, Melbourne endured its most prolonged heatwave since 1908, with four consecutive days over 40°C. Between 7 and 9 February 2014, emergency services and firefighting resources were committed to responding to multiple significant fires across the State and within the Latrobe Valley. The Fire Services Commissioner and the Chief Health Officer made several announcements warning the community about the potential for extreme weather conditions and associated fire and health risks. On 9 February 2014, the entire State of Victoria was facing the most extreme weather conditions since Black Saturday.

This weather had the effect of drying out the abandoned areas of the mine leaving the exposed batters in the north and east in a reactive state. The predominant wind at this time came from the north-west/south-west that would tend to fan any fire along the exposed batters and the abandoned area of the mine.

The Hazelwood mine fire that began on 9 February 2014 was the largest and longest burning mine fire that has occurred in the Latrobe Valley to date. The fire was not a spontaneous combustion event. The fire was probably caused by embers spotting into the Hazelwood mine from bushfires burning in close proximity to the mine. The mine fire burned for 45 days and sent smoke and ash over the town of Morwell and surrounding areas for much of that time.

The Hazelwood mine fire was not only a major complex fire emergency but also posed a serious public health emergency.

The impact of the Hazelwood mine fire on the Latrobe Valley community has been significant. People have been affected in many ways. First and foremost, the community has experienced adverse health effects and may be affected for an indeterminate period into the future.

In addition there have been significant financial impacts on many people, including medical costs, veterinary costs, time taken off work, relocation from their homes and cleaning their homes. Local businesses have suffered a downturn in business, and the costs of cleaning their businesses. There is also the possible decrease in property values.

It is impossible to quantify the cost of the Hazelwood mine fire, but the Board of Inquiry estimated the total cost borne by the Victorian Government, the local community and the operator of the Hazelwood mine, GDF Suez, exceeds $100 million.

During the Inquiry, the State and GDF Suez expressed a commitment to undertake numerous additional actions in response to the Hazelwood mine fire. The Board of Inquiry made 18 recommendations to the State and GDF Suez, which have been drafted taking into account the feasibility of implementation, as well as the issues raised by the Latrobe Valley community.

THE SOURCE OF THE FIRE

The Hazelwood mine fire was not just one fire, it started as a series of smaller fires that ignited in the northern, eastern and south-eastern batters and floor of the Hazelwood mine on 9 February 2014.

There is difficulty in determining with precision which of the external fires was responsible for the spotting of embers into the mine. On the evidence provided, spotting from the Hernes Oak fire was the more likely cause of the Hazelwood mine fire, while spotting from the Driffield fire may have also contributed. Both the Hernes Oak fire and the Driffield fire are regarded by Victoria Police as suspicious and both are the subject of ongoing investigation.

The probability of embers spotting into the Hazelwood mine was supported by clear evidence from several mine employees, contemporaneous photographs and video, expert evidence and computer simulations of likely fire behaviour on 9 February 2014. Figure 2 shows possible fire sources and area of the mine affected.

Figure 2: Possible sources of the fire and areas of the mine that burnt (Teauge *et al.,* 2014)

RECOMMENDATIONS OF THE INQUIRY AND COMMENTS

The discussion on the causes of the fire and what can be done to minimise the potential for a repeat

including mitigating any potential consequences is best framed in terms of the recommendations of the Board of Inquiry.

The recommendations of the inquiry focus in two different areas: the State and GDF Suez, the operator of the mine. The term 'State' is used broadly in the recommendations to refer to the Victorian Government, the Victorian public service, and public entities such as Emergency Management Victoria, the Country Fire Authority, the Environment Protection Authority and the Victorian WorkCover Authority. Recommendations relevant to the State are generally not prescriptive in terms of the entity tasked with implementation.

The first recommendation relates to mandating a plan to implement the recommendations of the Inquiry and the commitments made by GDF SUEZ, and to report on the progress made in their implementation.

Recommendation 1

The State empowers and require the Auditor-General or another appropriate agency, to:

- oversee the implementation of these recommendations and the commitments made by the State and GDF Suez during this Inquiry; and
- report publicly every year for the next three years on the progress made in implementing recommendations and commitments.

The next two recommendations relate to the need to improve the rapidity and complexity of the response to an incident by external agencies. It is interesting to note that most Queensland coal mines operate emergency response plans based upon the Australasian Inter-service Incident Management System and it is the model recommended by the Mines Rescue Service of New South Wales.

Recommendation 2

The State establish, for any future incident, integrated incident management teams with GDF Suez and other Victorian essential industry providers, to:

- require that emergency services personnel work with GDF Suez and other appropriate essential industry providers; and
- implement the Australasian Inter-service Incident Management System.

Recommendation 3

The State enact legislation, to:

- require Integrated Fire Management Planning; and
- authorise the Emergency Management Commissioner to develop and implement regional and municipal fire management plans.

The next recommendation enhances the capacity of the legislation to consider the potential impacts of fire on the adjacent community, and the capacity of the government to monitor compliance with this.

Recommendation 4

The State:

- bring forward the commencement date of s.16 of the Mineral Resources (Sustainable Development) Amendment Act 2014 (Vic), to facilitate the requirement that approved work plans specifically address fire prevention, mitigation and suppression; and
- acquire the expertise necessary to monitor and enforce compliance with fire risk measures adopted by the Victorian coal mining industry under both the mine licensing and occupational health and safety regimes.

One of the major issues identified was the time taken to assess the potential health impact of the smoke from the fire on the population of Morwell. In particular the capacity to assess the potential health impacts from fine particles sub 2.5 micrometres in diameter (PM $_{2.5}$) was recognised as being inadequate. The Victorian EPA was not equipped to respond to the monitoring requirements of such a

fire. Further, it was recognised that more work was needed to quantify the potential health impacts and to try to establish a full national ambient air quality standard for $PM_{2.5}$ rather than the current advisory standard. The potential exposure of fire fighters to carbon monoxide from the fire was also a concern to the Inquiry. Due to the level of uncertainty of the potential health impacts on the local population the Inquiry recommended a long-term health study of the residents.

Recommendation 5

The State equip itself to undertake rapid air quality monitoring in any location in Victoria, to:

- collect all relevant data, including data on $PM_{2.5}$, carbon monoxide and ozone; and
- ensure this data is used to inform decision-making within 24 hours of the incident occurring.

Recommendation 6

The State take the lead in advocating for a national compliance standard for $PM_{2.5}$.

Recommendation 7

The State review and revise the community carbon monoxide response protocol and the firefighter carbon monoxide response protocol, to:

- ensure both protocols are consistent with each other;
- ensure both protocols include assessment methods and trigger points for specific responses;
- ensure GDF Suez and other appropriate essential industry providers are required to adopt and apply the firefighter carbon monoxide protocol; and
- inform all firefighters about the dangers of carbon monoxide poisoning, and in particular
- highlight the increased risks for those with health conditions and those who are pregnant.

Recommendation 8

The State review and revise the Bushfire Smoke Protocol and the PM2.5 Health Protection Protocol, to:

- ensure both protocols are consistent with each other; and
- ensure both protocols include assessment methods and trigger points for specific responses.

Recommendation 9

The State develop and widely disseminate an integrated State Smoke Guide, to:

- incorporate the proposed State Smoke Plan for the management of public health impacts from large scale, extended smoke events;
- include updated Bushfire Smoke, carbon monoxide and $PM_{2.5}$ protocols; and
- provide practical advice and support materials to employers, communities and individuals on how to minimise the harmful effects of smoke.

Recommendation 10

The State should continue the long-term health study, and:

- extend the study to at least 20 years;
- appoint an independent board, which includes Latrobe Valley community representatives, to govern the study; and
- direct that the independent board publish regular progress reports.

Communications during the fire came under close scrutiny and there were a number of instances where inadequate communications occurred between the various emergency response agencies and also by the agencies with the public. Appropriate risk communication with the public is difficult to achieve and relates not just to information but establishing and maintaining trust so that the information is accepted.

Recommendation 11

The State review and revise its communication strategy, to:

- ensure all emergency response agencies have, or have access to, the capability and resources needed for effective and rapid public communications during an emergency; and
- ensure, where appropriate, that private operators of essential infrastructure are included in the coordination of public communications during an emergency concerning that infrastructure.

Recommendation 12

The State, led by Emergency Management Victoria, develop a community engagement model for emergency management to ensure all State agencies and local governments engage with communities and already identified trusted networks as an integral component of emergency management planning.

The remaining recommendations relate to improving the capacity of the mine operator to prevent and control such an event in the future. Some of the recommendations relate to improved capacity in terms of preparedness and equipment redundancy whilst others relate to improved planning and risk assessment and control.

Recommendation 13

GDF Suez revise its Emergency Response Plan, to:

- require an increased state of readiness on days of Total Fire Ban;
- require pre-establishment of an Emergency Command Centre;
- require pre-positioning of an accredited Incident Controller as Emergency Commander; and
- require any persons nominated as Emergency Commander to have incident controller accreditation and proficiency in the use of the Australasian Inter-service Incident Management System.

Recommendation 14

GDF Suez establish enhanced back-up power supply arrangements that do not depend wholly on mains power, to:

- ensure that the Emergency Command Centre can continue to operate if mains power is lost; and
- ensure that the reticulated fire services water system can operate with minimal disruption if mains power is lost.

Recommendation 15

GDF Suez:

- conduct, assisted by an independent consultant, a risk assessment of the likelihood and consequences of fire in the worked out areas of the Hazelwood mine, and an assessment of the most effective fire protection for the exposed coal surfaces;
- prepare an implementation plan that ensures the most effective and reasonably practicable controls are in place to eliminate or reduce the risk of fire; and
- implement the plan.

Recommendation 16

GDF Suez:

- review its 'Mine Fire Service Policy and Code of Practice' so that it reflects industry best practice and ensures that, by taking a risk management approach, it is suitable for fire prevention, mitigation and suppression in all parts of the Hazelwood mine; and
- incorporate the revised 'Mine Fire Service Policy and Code of Practice' into the approved work plan for the Hazelwood mine.

Recommendation 17

GDF Suez adopt and apply the firefighter carbon monoxide response protocol.
Recommendation 18

GDF Suez improve its crisis management communication strategy for the Hazelwood mine in line with international best practice.

CONCLUSION

The fire in the open cut at Hazelwood in February 2014 caused major disruption to the local community as well as major costs to the state. The Board of Inquiry established to inquire into the incident found that there were major deficiencies in the way the fire was treated. The Board of Inquiry did not accept the position of the mine operator that the fire was not reasonably predictable – a "Perfect Storm". It found that more should have been done to prevent such an occurrence.

REFERENCES

Beamish B B and Arisoy A. 2008, Effect of intrinsic coal properties on self-heating rates, *12th North American Mine Ventilation Symposium*, pp 149 -153.

MRSDA. 2014, Mineral Resources (Sustainable Development) Amendment Act 2014, Victoria, assented 25 February 2014.

Potter, M. 2008, Understanding the CFA's role in effective emergency prevention and response techniques for the coal industry, *IQPC Emergency Response Conference*, February, Brisbane.

Teague B Hon, Catford J and Petering S. 2014, Hazelwood Mine Fire Inquiry report 2014, *Hazelwood Mine Fire Inquiry*, Victorian Government Printer.

TRANSLATING ROAD SAFETY RESEARCH ON NIGHT-TIME VISIBILITY TO THE CONTEXT OF MINING

Joanne Wood[1], David Cliff[2] and R Burgess-Limerick[3]

ABSTRACT: In recent years a significant amount of research has been undertaken in collision avoidance and personnel location technology in order to reduce the number of incidents involving pedestrians and mobile plant equipment which are a high risk in underground coal mines. Improving the visibility of pedestrians to drivers would potentially reduce the likelihood of these incidents. In the road safety context, a variety of approaches have been used to make pedestrians more conspicuous to drivers at night (including vehicle and roadway lighting technologies and night vision enhancement systems). However, emerging research from our group and others has demonstrated that clothing incorporating retroreflective markers on the movable joints as well as the torso can provide highly significant improvements in pedestrian visibility in reduced illumination. Importantly, retroreflective markers are most effective when positioned on the moveable joints creating a sensation of "biological motion". Based only on the motion of points on the moveable joints of an otherwise invisible body, observers can quickly recognize a walking human form, and even correctly judge characteristics such as gender and weight. An important and as yet unexplored question is whether the benefits of these retroreflective clothing configurations translate to the context of mining where workers are operating under low light conditions. Given that the benefits of biomotion clothing are effective for both young and older drivers, as well as those with various eye conditions common in those >50 years reinforces their potential application in the mining industry which employs many workers in this age bracket. This paper will summarise the visibility benefits of retroreflective markers in a biomotion configuration for the mining industry, highlighting that this form of clothing has the potential to be an affordable and convenient way to provide a sizeable safety benefit. It does not involve modifications to vehicles, drivers, or infrastructure. Instead, adding biomotion markings to standard retroreflective vests can enhance the night-time conspicuity of mining workers by capitalising on perceptual capabilities that have already been well documented.

INTRODUCTION

The problem

Collisions between mine vehicles and other vehicles, personnel and infrastructure continue to be one of the main causes of fatal accidents in the mining industry, with reports that among the 112 fatalities that occurred in the mining, exploration and extraction industries in Australia during 1998 - 2008, vehicle collisions accounted for ~28% and claimed the lives of 31 people (Kizil *et al.,* 2011).

Collisions between pedestrians and mining equipment are a particularly high risk in underground mines, although interactions between pedestrians and vehicles also occur at surface mines.

Consequently, there has been a significant amount of research undertaken in collision avoidance and personnel location technology in order to reduce the relatively high number of incidents involving pedestrians and mobile plant equipment, given the unacceptably high risk they represent in underground coal mines. Improving the visibility of pedestrians to drivers would potentially reduce the likelihood of these incidents.

Improving pedestrian visibility

In the context of road safety, a variety of approaches have been used to make pedestrians more conspicuous to drivers at night, these have included vehicle and roadway lighting technologies and night vision enhancement systems. This has been a particular focus given that crash statistics indicate that

---

[1] *School Cal Optometry and Vision Science and Institute of Health and Biomedical Innovation Queensland University of Technology Victoria Park Rd, Kelvin Grove Q 4059, E-mail: j.wood@qut.edu.au, Tel: +61 7 3138 5701*
[2] *Sustainable Minerals Institute, The University of Queensland, St Lucia QLD 4072, E-mail: d.cliff@mishc.uq.edu.au, Tel: +61 7 3346 4086*
[3] *Sustainable Minerals Institute, The University of Queensland, St Lucia QLD 4072, E-mail: r.burgesslimerick@uq.edu.au, Tel: +61 7 73346 4084*

when adjusted for mileage, the night-time fatality rate is two to four times higher than that for daytime (NHTSA, 2005) and night-time crashes are more severe than those occurring in the day (Plainis *et al.,* 2006). The night-time elevation in road safety risk is even greater for collisions between vehicles and pedestrians who are up to seven times more vulnerable to a fatal collision at night than in the day (Sullivan and Flannagan, 2002).

Although multiple factors, including alcohol and fatigue, may contribute to the elevated night-time fatality rate, the basic difference between night and daytime driving is the reduction in illumination at night. The increase in crash rates, particularly collisions with pedestrians, cyclists, and other low-contrast obstacles during night-time driving, has been largely attributed to poor visibility (Owens and Sivak, 1996).   It has also been suggested that even the low illumination levels available from a full moon can have a positive effect on pedestrian fatalities. For example, pedestrian fatalities were 22% lower on nights with a full moon than on moonless nights (Sivak *et al.,* 2007). The problems of poor visibility at night are further compounded by drivers' misjudgment of their own visual limitations, where drivers' confidence appears to be largely based upon their lane-keeping ability at night, which is relatively unimpaired compared to the significant loss in 'focal' vision evident under low light conditions (Owens and Tyrrell, 1999, Owens, 2003).

An important challenge is to better understand the problems involved in driving under reduced light levels where there has been only limited research, despite the risk to safety, particularly for vulnerable road users such as pedestrians. In addition, there has been a widespread emergence of night vision systems and other devices which are believed to assist in night-time driving, including near and far infrared night vision systems (Tsimhoni *et al.,* 2004) and adaptive headlights. These interventions require rigorous evaluation and validation under as realistic driving conditions as possible to ensure that they actually do provide tangible safety benefits for all road users.

Research from our group and others has clearly demonstrated that clothing incorporating retroreflective markers positioned on the moveable joints that create a sensation of "biological motion" has potential benefits for improving night-time visibility. Biological motion is a compelling visual phenomenon, where based only on the motion of point-lights on the moveable joints of an otherwise invisible body, observers can quickly recognize a range of features of the moving human form (Blake and Shiffrar, 2007).

Biological motion

The effect of biological motion was first demonstrated more than four decades ago (Johansson, 1973), as an extension of psychophysical research into motion perception, where the moving point-lights on the joints of a moving person were sufficient to perceive a human form. Since that time there has been an extensive body of research that has demonstrated that such point-light walkers are able to convey information about gender (Kozlowski and Cutting, 1977), identity of walkers (Troje *et al.,* 2005), emotions (Roether *et al.,* 2008), and even to the estimation of the weight of lifted objects (Bingham, 1993).

Research to improve night-time conspicuity of pedestrians

Our research has demonstrated that clothing that incorporates retroreflective markers on the moveable joints (ankles, knees, shoulders, waist, elbows and wrists) which are illuminated by oncoming headlights produce similar visibility benefits to that of the biological motion effect of point-light walkers (Figure 1).
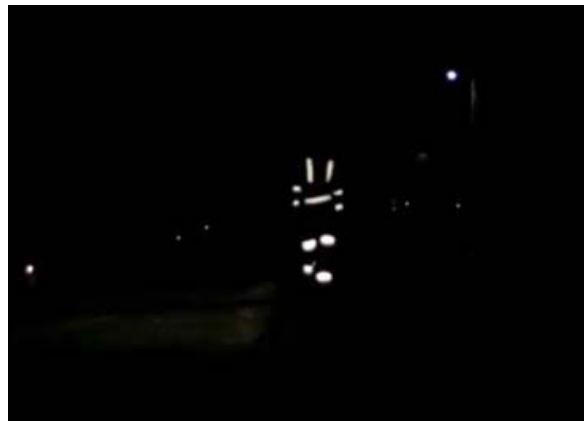

Figure 1: Example of biomotion clothing for improving pedestrian conspicuity at night

Our studies have demonstrated that retroreflective strips positioned in the full biomotion pattern provide substantial advantages for improving pedestrian visibility over and above that of retroreflective material positioned on the torso, such as retroreflective vests. In one of our closed road studies, for example, drivers using low beam headlights recognised a pedestrian walking while wearing biomotion markers at a distance that was 3.4 times greater than when the same pedestrian wore a vest that included an equal amount of retroreflective material (148m compared to 43m) (Wood *et al.,* 2005). Importantly, these studies clearly demonstrate that it is the configuration and not the amount of retroreflective material that determines pedestrian conspicuity. Our other research has also shown that the visibility advantages of biomotion configurations are relatively robust to the effects of driver age (Wood *et al.,* 2005, Owens *et al.,* 2007, Wood *et al.,* 2014a), visual impairment (Wood *et al.,* 2012a, Wood *et al.,* 2010), headlight glare (Wood *et al.,* 2012a) and the visual clutter surrounding the pedestrian (Tyrrell *et al.,* 2009). Field studies at real road worker sites have also demonstrated improvements in perceived conspicuity of roadworkers (Wood *et al.,* 2011), which are reflected in recent closed road studies (Wood *et al.,* 2014b). We have also demonstrated that an adapted form of biomotion markers attached to the ankles and knees have significant benefits for improving bicyclist conspicuity, over and above that of a standard retroreflective cycling vest (Wood *et al.,* 2012b).

Previous research has also demonstrated that a key element of the visibility problem of vulnerable road users, including pedestrians and cyclists, is their failure to appreciate the extent of the problem and their tendency to overestimate their own visibility to oncoming drivers (Tyrrell *et al.,* 2004b, Wood *et al.,* 2013). In the only study that sought to alter pedestrians' estimates of their own visibility, it was demonstrated that a lecture-based delivery of information on night-time visibility effectively changed subsequent judgments of visibility by pedestrians in an on-road situation (Tyrrell *et al.,* 2004a). This research provides reason for optimism about translating the findings from our research into safety benefits for workers over and above the benefits gained by using biomotion. We have recently developed a video-based intervention that similarly outlines the problems of the conspicuity of pedestrians under low light levels, highlighting the need to be aware of difficulties that drivers have in seeing pedestrians at night-time, particularly older drivers and those with visual impairment, and the utility and value of biomotion markings in relation to other clothing configurations. There is potential application for effective and easily implementable interventions like this in the context of mining organisations, which have the potential to change both knowledge and behaviour of workers with ultimate benefits for workplace safety.

Low illumination levels are a constant hazard associated with underground mines, and are also associated with night-time operations at surface mines. The importance of retroreflective markings on clothing is recognized by the mining industry and is a standard on all sites. Some sites also mandate reflective strips on upper and lower body. The location of these retroreflective markings to coincide with the anatomical joints in the biomotion pattern constitutes a relatively low-cost modification to these standards.

CONCLUSIONS

The adoption of retroreflective markers in a biomotion configuration has the potential to be an affordable and practical way to provide a sizeable safety benefit in the mining context. It does not involve modifications to vehicles, drivers, or infrastructure; instead, adding biomotion markings to standard vests can enhance the night-time conspicuity of workers by capitalising on perceptual capabilities that are already well established.

REFERENCES

Bingham, G P. 1993, Scaling judgments of lifted weight: Lifter size and the role of the standard, *Ecological Psychology, 5***,** 31-64.

Blake, R and Shiffrar, M. 2007, Perception of human motion, *Annual Review of Psychology, 58***,** 47-73.

Johansson, G. 1973, Visual perception of biological motion and a model for its analysis, *Perception & Psychophysics, 14***,** 201-211.

KIZIL, G. V, BYE, A and JOY, J. 2011, Development and Application of Risk-Cost-Benefit (RCB) Decision Support Framework and Analytical Tools, RCBGEN and RCEMETHOD, for the Minerals Industry, *Technical Report, ACARP 17014*.

Kozlowski, L T and Cutting, J, 1977. Recognizing the sex of a walker from a dynamic point-light display. *Perception and Psychophysics, 21***,** 575-580.

Nhtsa. 2005, *Motor Vehicle Traffic Crash Fatality Counts and Injury Estimates for 2004* [Online]. Washington, D.C. Available: http://www.nhtsa.dot.gov.

Owens, D. A. 2003, Twilight Vision and Road Safety: Seeing More Than we Notice but Less Than We Think. *In: IN J.T. ANDRE, D. A. O., & L.O. HARVEY (EDS.) (ed.) Visual Perception: The Influence of H.W. Leibowitz*, Washington, D.C: American Psychological Association.

Owens, D A and Sivak, M. 1996, Differentiation of visibility and alcohol as contributors to twilight road fatalities, *Human Factors,* 38**,** 680-689.

Owens, D A and Tyrrell, R A. 1999, Effects of luminance, blur, and age on nighttime visual guidance: A test of the selective degradation hypothesis, *Journal of Experimental Psychology:Applied,* 5**,** 115-128.

Owens, D A. Wood, J M and Owens, J. M. 2007, Effects of age and illumination on night driving: A road test. *Human Factors,* 49**,** 1115-1131.

Plainis, S, Murray, I J and Pallikaris, I G, 2006. Road traffic casualties: understanding the night-time death toll, *Injury Prevention,* 12**,** 125-138.

Roether, C L, Omlor, L and Giese, M A. 2008, Lateral asymmetry of bodily emotion expression. *Current Biology,* 18**,** R329-30.

Sivak, M, Schoettle, B and Tsimhoni, O. 2007, Moon phases and nighttime road crashes involving pedestrians, *Ann Arbor, MI: University of Michigan Transport Research Institute*.

Sullivan, J M and Flannagan, M J. 2002, The role of ambient light level in fatal crashes: inferences from daylight saving time transitions, *Accident Analysis & Prevention,* 34**,** 487-498.

Troje, N F, Westhoff, C and Lavrov, M. 2005, Person identification from biological motion: effects of structural and kinematic cues, *Perception & Psychophysics,* 67**,** 667-75.

Tsimhoni, O, Bargman, J, Minoda, T and Flannagain, M J. 2004, Pedestrian detection with near and far infrared night vision enhancement, *Ann Arbor, MI: University of Michigan Transport Research Institute*.

Tyrrell, R A, Patton, C W and Brooks, J O. 2004a, Educational interventions successfully reduce pedestrians' overestimates of their own nighttime visibility, *Human Factors,* 46**,** 170-182.

Tyrrell, R A, Wood, J M and Carberry, T P. 2004b, On-road measures of pedestrians' estimates of their own nighttime conspicuity, *Journal of Safety Research,* 35**,** 483-490.

Tyrrell, R A, Wood, J M, Chaparro, A, Carberry, T P, Chu, B S and Marszalek, R P. 2009, Seeing pedestrians at night: visual clutter does not mask biological motion, *Accident Analysis & Prevention,* 41**,** 506-12.

Wood, J, Chaparro, A, Carberry, T and Chu, B. S. 2010, Effect of simulated visual impairment on nighttime driving performance, *Optometry & Vision Science,* 87**,** 379-86.

Wood, J M, Lacherez, P and Tyrrell, R A. 2014a, Seeing pedestrians at night: effect of driver age and visual abilities, *Ophthalmic & Physiological Optics,* 34**,** 452-8.

Wood, J M, Marszalek, R, Lacherez, P and Tyrrell, R A. 2014b, Configuring retroreflective markings to enhance the night-time conspicuity of road workers, *Accident Analysis & Prevention,* 70**,** 209-14.

Wood, J M, Tyrrell, R A and Carberry, T P. 2005, Limitations in drivers' ability to recognize pedestrians at night, *Human Factors,* 47**,** 644-653.

Wood, J M, Tyrrell, R A, Chaparro, A, Marszalek, R P, Carberry, T P and Chu, B S. 2012a, Even moderate visual impairments degrade drivers' ability to see pedestrians at night, *Investigative Ophthalmology & Visual Science,* 53**,** 2586-92.

Wood, J M, Tyrrell, R A, Marszalek, R, Lacherez, P and Carberry, T. 2013, Bicyclists overestimate their own night-time conspicuity and underestimate the benefits of retroreflective markers on the moveable joints, *Accident Analysis & Prevention,* 55**,** 48-53.

Wood, J M, Tyrrell, R A, Marszalek, R, Lacherez, P, Carberry, T and Chu, B S. 2012b, Using reflective clothing to enhance the conspicuity of bicyclists at night, *Accident Analysis & Prevention,* 45**,** 726-30.

Wood, J M, Tyrrell, R A, Marszalek, R, Lacherez, P, Chaparro, A and Britt, T W. 2011, Using biological motion to enhance the conspicuity of roadway workers, *Accident Analysis & Prevention,* 43**,** 1036-41.

CAUSES OF DYNAMIC OVERBREAK AND CONTROL MEASURES TAKEN AT THE ALBORZ TUNNEL, IRAN

Mohammad Farouq Hossaini[1], Mohammad Mohammadi[2], Nabiollah Hajiantilaki[2] and Alireza Tavallaie[2]

ABSTRACT: Drilling and blasting is widely used in underground excavation projects, where the amount of damage to the surrounding rock mass is crucially important, due to its impact on the safety of working environment and operational costs,. The causes of overbreak in the Alborz Tunnel of Iran are evaluted. In this regard, ten rounds of presplitting and 11 rounds of smooth blasting methods were carried out to determine the dominancy of ground condition over the blasting pattern characteristics. Further study was undertaken to identify the most important parameters of ground condition affecting the overbreak area. These parameters include; joint condition, spacing, orientation, RQD and type of rock mass. As the characteristics of the blasting pattern have very little effect on the amount of overbreak, the smooth blasting technique was chosen for the future operations where the current ground condition is going to be dealt with for about 500 meters of length, based on the data acquired from the Alborz Exploratory Tunnel. Results of this investigation helped to solve disputes between contractors and clients over the issue of permissible overbreak.

INTRODUCTION

Overbreak is the result of damage to surrounding rock mass, which can be quantified as the extra cost involved in additional removal of muckpile and the application of extra support. Overbreak either occurs immediately after blasting or within time durations, which are dynamic and quasi-static type respectively (Mandal and Singh, 2009).

As an undesirable phenomenon in underground construction practices, overbreak can occur due to the effect of the ground conditions and the nature of excavation operations (Ibarra *et al*., 1996). However, the factors influencing the smoothness and softness of the perimeter can be classified into four categories namely: drilling accuracy, perimeter hole spacing and loading (charging), treatment of first-row-in holes and geology (McKown, 1984). A summary of factors affecting overbreak is depicted in Figure 1. The occurrence of excessive overbreak can incur an additional cost for controlling the percent of overbreak, which is crucially important in any underground excavation project. Thus, during this investigation, smooth and presplitting methods of blasting were carried out to minimize the overbreak percentage in the Alborz Tunnel of Iran. The nature of overbreak after carrying these different blasting patterns was analyzed and decisions made towards the causes of dynamic overbreak.
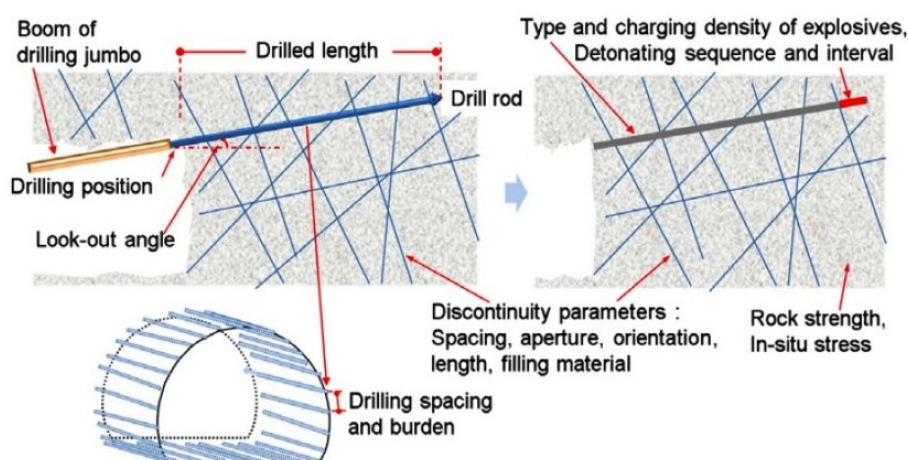
Figure 1: Summary of the causes of overbreak (Kim and Moon, 2013)

[1] *School of Mining Engineering, University College of Engineering, University of Tehran, Tehran, Iran, Email:* *mfarogh@ut.ac.ir*
[2] *General Mechanic Co., Tehran, Iran*

Case study

The Albroz Tunnel is the largest one with an approximate length of 6400 to be excavated along the Tehran-Shomal freeway in Iran. The rock mass type blasted during this study was Tuff. A combination of black and grey Tuffs comprise the face of the excavation, where the uniaxial compressive strength of rock material for both types varies from 70 to 120 MPa. The thickness of alternative Tuff layers differs from 60 to 600 mm and the orientation of these layers with regard to the tunnel axis is fair as reported by Wickham *et al.,* (1972). Three different joint sets exist in addition to bedding surfaces. The characteristics of these discontinuity sets are presented in Table 1. The geomechanical evaluation of Tuffs of the Alborz region of Iran is reported by Yassaghi *et al.,* (2005). A schematic view of the alternation of black and grey Tuffs is displayed in Figure 2.

Table 1: Properties and condition of discontinuities of the rock mass under investigation

System	Type	dip/dip direction	Roughness		Spacing (cm)
I	Bedding	15/244	Smooth	undulating	6 - 50
II	Joint	65/090-086	Smooth	planar	35 - 45
III	Joint	78/140	Slightly Rough	planar	20 - 25
IV	Joint	84/183	Slightly Rough	planar	15 - 18
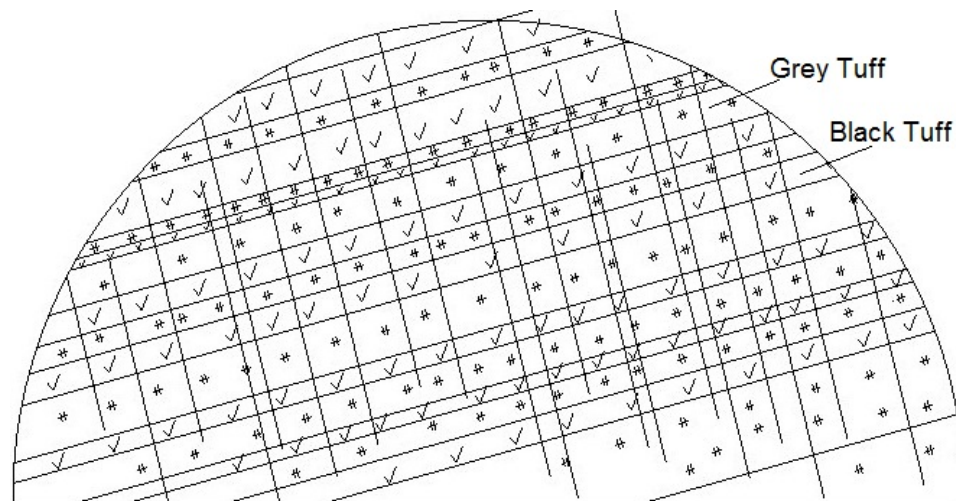
Figure 2: bedding condition in the face of excavation (schematic view)

Blasting practices in the alborz tunnel

As the characteristics of contour holes have a great influence on the results of blasting with respect to overbreak and underbreak, the presplitting and smooth blasting methods of controlled blasting were carried out in the Alborz Tunnel to acquire the intended tunnel profile with minimum possible overbreak. The characteristics of contour holes in the blasting patterns for both presplitting and smooth blasting are presented in Table 2. The implementation of these blasting patterns was strictly supervised in both drilling and charging stages ensure the accurate execution of designed patterns for 21 blasting rounds. However, the results of blasting did not cause any noticeable changes in the amount and nature of the overbreak due to the orientation of bedding with the tunnel axis. The acquired tunnel profile after each blasting round (either by pre-splitting or by smooth blasting) was as depicted in Figure 3, obtained via electronic surveying. Figure 4 shows the charging process and post blast profile of the tunnel. The dominancy of ground condition over the blasting pattern condition was concluded as a result of performing different controlled blasting methods. Therefore, it should be noticed in the definition of permissible overbreak for this section of the Alborz Tunnel, to consider the right values of constants to represent the ground condition, as suggested by Ibbara *et al.,* (1972). The difference in the amount of overbreak in right and left sections of the tunnel profile shows the effect and dominancy of ground condition over blasting pattern characteristics. The mechanism of overbreak in right section is due to sliding whereas it is due to block failure in left part. Due to the dominancy of ground condition on the overbreak the smooth blasting method is preferred compared to pre-splitting as it needs less drilling holes.

Table 2: Characteristics of contour zone in presplitting and smooth blasting methods performed in the Alborz Tunnel

Blasting method	Spacing (cm)	Charge density in drill holes (kg/m)	Hole diameter (mm)	Charge diameter (mm)	Powder factor of contour zone (kg/m^3)
Presplitting	50	0.24	51	27	0.44
Smooth blasting	70	0.2	51	27	0.28
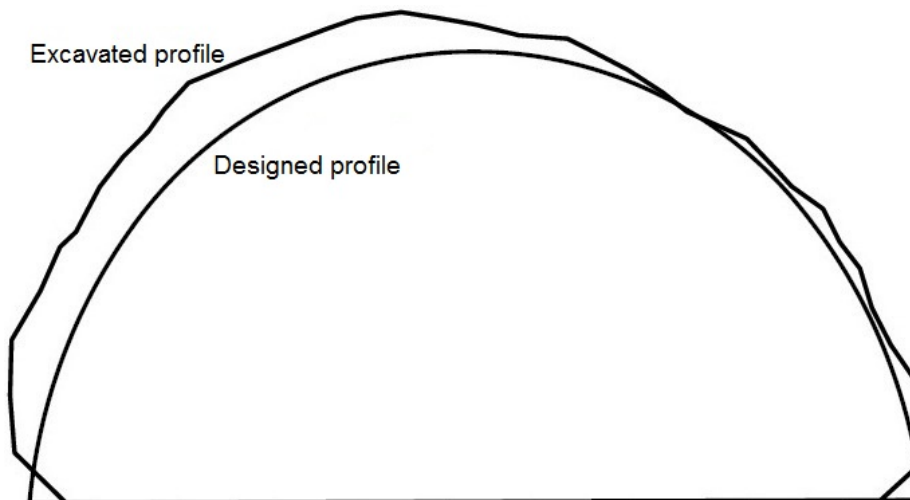
Figure 3: Overbreak of blasting rounds in the Alborz Tunnel

Geological causes of overbreak

The results of the presplitting and smooth blasting techniques revealed the dominancy of geological conditions over blasting patterns on overbreak occurrence in the study area. Therefore, a further study was carried out to determine specific causes of overbreak related to geological conditions which can be of great importance in future uses of presplitting and smooth blasting techniques in the Alborz Tunnel as well as any other tunneling cases.

Figure 4: Charging process and resulted profile after blasting

A wide range of research has been carried out to obtain a reliable method for determination of the amount of damage and overbreak on the surrounding rock mass caused as a result of blasting. Almost all parameters, used for determination of damage level to surrounding rock mass, are related to ground condition, showing the importance of geological features as the main cause of overbreak. Some of

these parameters include Peak Particle Velocity (PPV), rock density, P-wave velocity, dynamic tensile strength of rock, site quality constant, Young's modulus, uniaxial tensile strength of rock, joint orientation and rock mass strength (Langefors and Kihlström, 1967; Holmberg and Persson, 1979; McKenzie, 1994; Yu and Vongpaisals, 1996; Innaurato *et al*., 1998; Johansen and Mathiesen, 2000). Jointing is the most critical aspect of stability and damage level to the surrounding rock mass and thus the stability of underground structure should be considered in terms of joint condition, spacing and orientation (Cunningham and Goetzsche, 1990). The following are some likely results of some investigations on the causes of overbreak in underground blasting, in cases with ground condition similar to the Albroz Tunnel.

- Excessive overbreak can occur where open joints containing gouge are encountered (Cunningham and Goetzsche, 1990).Filled open joints are present in parts of the Alborz Tunnel under investigation.
- Noticeable overbreak even in case of low values of powder factor and high advance per blast can occur in weak and fair rocks (Chakraborty *et al.,* 1994). The rock mass under this investigation is categorized as fair rock mass.
- The surrounding rock mass will be prone to excessive overbreak as the result of blasting if the Rock Quality Designation (RQD) index of rock mass is lower than 70% (Cunningham and Goetzsche, 1990). The RQD of the surrounding rock mass in this study is 60%.
- The excavation profile can be controlled by joint orientation to such a degree that it can be worthwhile to either change the design profile, or alter the position or orientation of the excavation. This would be of great importance if the plane runs diagonally across the tunnel and parallel to it (Cunningham and Goetzsche, 1990). Almost the same situation is present in the area covered by this study.
- Joint orientation of 60° to 90°, preserving the intended shape of the tunnel would be very difficult. The situation probably will be beyond blasting control for joint angles less than 15° (Cunningham and Goetzsche, 1990). Joint angle is less than 15° in the area under this investigation.
- Perimeter problems can be expected in the jointed rock mass, where the drilling pattern is wider than the joint spacing (Cunningham and Goetzsche, 1990). Due to very small spacing of the beddings and joint sets, the drilling pattern was wider than the joint spacing in the area of this study.

The quality of surrounding rock mass is therefore determined as the most dominant affecting parameter on the percent of overbreak in the study area. The same condition of surrounding rock mass in the Alborz Tunnel is going to be dealt with for about another 500 m based on the geological maps obtained from the Alborz Exploratory Tunnel. Thus, the obtained results from this research can be very helpful in dealing with blasting pattern design, overbreak considerations and disputes between the contractor and client over the issue of permissible overbreak.

RESULTS AND CONCLUSIONS

Different causes affecting overbreak were analyzed in the Alborz Tunnel using controlled methods of presplitting and smooth blasting. Two blasting methods were carried out for 21 rounds of blasting (10 rounds of presplitting and 11 rounds of smooth blasting) the results of which are as follows:

- The excavated profile after each blasting round was almost the same as other rounds of blasting for both presplitting and smooth blasting methods showing that the nature of blasting patterns have very little influence on the percent of overbreak due to dominancy of the ground condition.
- The differences between the nature of overbreak in the right and left parts of the cross section occurred as aconsequence of bedding orientation with regard to tunnel axis. These states of overbreak also proved the dominancy of ground condition over the blasting pattern characteristics.

- As there is no considerable change in the percent of overbreak, the smooth blasting method was chosen to be carried out in the blasting patterns due to its lower drilling requirements compared to presplitting method.
- Joint condition, orientation, spacing, RQD and rock mass type, as the factors defining ground condition, were determined to be the most important factors influencing the results of blasting as follows:

1. Joint condition: Open joint sets were encountered.
2. Joint orientation: The angle of discontinuity sets with regard to tunnel axis was less than 15°
3. Joint spacing: Very small joint spacing led to a condition where the drilling patterns were wider than joint spacing.
4. RQD: was less than 70 %
5. Rock mass type: the strip surrounding rock mass caused noticeable overbreak even with low values of powder factor.

As the current condition of ground is going to be dealt with for about another 500 m of length, the results of this investigation will be very helpful in determination of permissible overbreak and solution of disputes between the contractor and the client.

REFERENCES

Chakraborty, A, Jethwa, J and Paithankar, A. 1994, Effects of joint orientation and rock mass quality on tunnel blasting*, Engineering geology*, 37(3):247-262.

Cunningham, C and Goetzsche, A. 1990, The specification of blast damage limitations in tunnelling contracts, *Tunneling and Underground Space Technology*, 5(3):193-198.

Holmberg, R and Persson, P A. 1979, Design of tunnel perimeter blasthole patterns to prevent rock damage, *Proceedings*, *Tunneling*.

Ibarra, J, Maerz, N and Franklin, J. 1996, Overbreak and underbreak in underground openings part 2: causes and implications, *Geotechnical & Geological Engineering*, 14(4):325-340.

Innaurato, N, Mancini, R and Cardu, M. 1998, On the influence of rock mass quality on the quality of blasting work in tunnel driving, *Tunneling and Underground Space Technology*, 13(1):81-89.

Johansen, J and Mathiesen, C. 2000, Modern trends in tunneling and blast design, *Taylor & Francis Group*.

Kim, Y, Moon and H K. 2013, Application of the guideline for overbreak control in granitic rock masses in Korean tunnels, *Tunneling and Underground Space Technology*, 35:67-77.

Langefors, U and Kihlström, B. 1967, The modern technique of rock blasting, *Wiley*.

Mandal, S K and Singh, M M. 2009, Evaluating extent and causes of overbreak in tunnels, *Tunneling and Underground Space Technology*, 24(1):22-36.

McKenzie, C. 1994, Blasting for Engineers, *Blastronics Pty. Ltd*., Brisbane, Australia.

McKown, A F. 1984, Some aspects of design and evaluation of perimeter control blasting in fractured and weathered rock, *Proceedings Tenth Conference Explosives and Blasting Technique*, SEE, Montville, OH, pp.120-151.

Wickham, G E, Tiedemann, H R and Skinner, E H. 1972, Support determination based on geologic predictions, *proc. Rapid Excav. Tunneling Conf.,* AIME, New York, pp. 43 – 64.

Yassaghi, A, Salari-Rad, H and Kanani-Moghadam, H. 2005, Geomechanical evaluations of Karaj tuffs for rock tunneling in Tehran-Shomal Freeway, Iran, *Engineering Geology 77*, pp. 83-98.

Yu, T and Vongpaisals, S. 1996, New blast damage criteria for underground blasting, *CIM bulletin*, 89(998):139-145.

MONETARY SAVINGS OPPORTUNITIES OF ELECTRONIC BLAST INITIATION SYSTEMS

Edward Hay and Saiied Mostafa Aminossadati

ABSTRACT: There are several blast initiation systems available on the market; these form a large component of the performance of each blast. Each available system has its own advantages and disadvantages which can affect the fragmentation of each blast, which in turn can affect downstream processes such as digging and hauling of material. This study was conducted to determine if there were monetary savings opportunities due to an increase in fragmentation (and hence downstream productivity) due to the use of an electronic blast initiation system over a pyrotechnic blast initiation system. It was completed using data collected from an open cut metallurgical coal mine in Queensland that agreed to be used as a case study. Statistical analysis of data was completed in order to identify if downstream productivity had increased, with the results from this being used to calculate potential savings opportunities. The results of this study suggest that there are increases in productivity during loading and hauling, which lead to significant savings opportunities when using an electronic blast initiation system.

INTRODUCTION

Most operating mines require a blasting system that is consistently capable of performing each required blast to specification. A large component of achieving this is the blast initiation system. Generally, blasts are initiated using a traditional pyrotechnic system; however these blasts are limited to the set of timings available for both surface connectors and downhole lines, and are also subject to the inherent inaccuracies of pyrotechnic elements (Combrinck and Strong, 2007). Due to these timing limitations and inaccuracies, blasthole interaction is often not at the optimal level to achieve the best fragmentation and, as a result of this, downstream processes such as digging productivity are negatively affected (Sullivan, 2003).In order to combat these issues with pyrotechnic systems, an electronic initiation system can be used. Electronic detonators have been in development for over four decades, yet have only been commercially acceptable within the last ten years. During this time, the benefits of them have become evident in both safety and productivity aspects of mines. From a safety perspective, the use of inert wires removes the inherent risk associated with pyrotechnic connections, while two way communications between a programming unit and each detonator aids in the identification of faults before they become a major event. Potential improvements to productivity stem from the increased control over blast induced forces in the strata that allow for better fragmentation which can decrease digging cycle times, and increases in loading fill factors (Cardu, 2013).

This project was completed using an open cut metallurgical coal mining site in Queensland as a case study site. The site had been using a pyrotechnic blast initiation system, using shock tube connectors. The price of metallurgical coal rose dramatically in 2011 (MCI, 2014), which provided larger revenue for the sites coal. Using this additional income, the site started investigating the use of a more expensive electronic blast initiation system. When the metallurgical coal price dropped in 2013 (MCI, 2014), many mine managers and accountants recommended reverting to the use of a pyrotechnic system as these systems are cheaper than electronic systems. Fortunately operations managers on site identified that there appeared to be an increase I productivity when using the electronic system. They thought that it could lead to savings in downstream processes, but these needed to be quantified in order to provide reason for the continued use of the electronic blast initiation system.

BLASTING CONCEPTS

Explosive detonation and rock interaction

When an explosive charge that is contained within a blasthole is detonated, there is a series of stress waves that move out radially, as well as the creation of gasses that are under extreme pressure. Primary breakage is due to the stress waves, with secondary breakage processes attributed to the gasses and indirect tensile stresses. The interaction between detonated explosives, and their associated breakage mechanisms, and a rock mass is a complex system that consists of three predominant zones. These

School of Mechanical and Mining Engineering, The University of Queensland, Qld 4072. E-mail: edward.hay@uqconnect.edu.au

zones, from the centre out, are: the crushed zone, cracked zone, and the radial fracture zone, as seen in Figure 1. The crushed zone is the region that immediately surrounds the Blasthole cavity. Blast induced stresses that exceed the Ultimate Compressive Strength (UCS) of the rock mass in this region are responsible for the intense crushing and pulverizing of the rock. The cracked zone is the area surrounding the blasthole, but outside the crushed zone. Blast induced stresses in this region are now below that of the rock mass UCS, although some crushing may occur in this region where the rock mass has inherent compressive weaknesses. The major characteristic breakage in this zone is due to elasto-plastic behavior of the rock mass, combined with rapidly expanding gasses creating cracks propagating outwards from the edge of the crushed zone.

The zone of radial fracturing is the area surrounding the cracked zone. Although blast induced stresses are now not large enough to cause crushing of the rock, they still act to push the material radially out. This movement results in the rock mass being subject to tensile stresses that are tangential to the direction of stress wave propagation. As the tensile strength of rock is considerably lower than its UCS, these small tensile stresses are all that are required to further fractures that formed in the cracked zone (Fairhurst and Kutter, 1971).
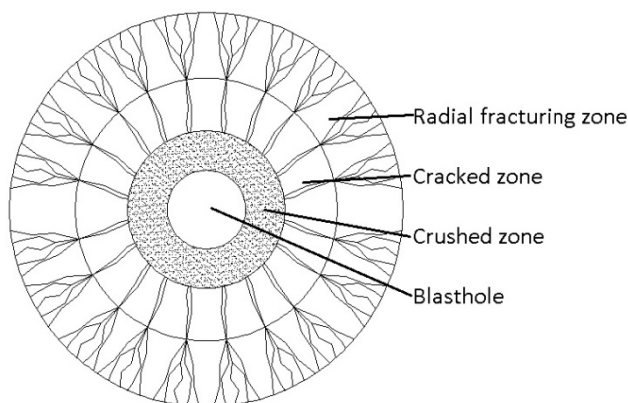
Figure 1: Zones of breakage around a blasthole

Blasthole interaction and timing

Blastholes breakage processes are able to interact in two predominant ways, these being between two or more holes in the same row (inter-hole), or between two or more holes that are in different rows that line up (inter-row). In order for blasts to fragment properly, a free-face must be available for material to move towards.

Interaction between blastholes can act to improve or hinder fragmentation of a blast as a whole. For optimal fragmentation results, the entire blast should be initiated on a hole-by-hole basis as seen in Figure 2. In doing this, the benefits of both inter-hole and inter-row interactions are exploited, as well a dynamic free face being provided to each blasthole by the blastholes before it (Orica, 2013).
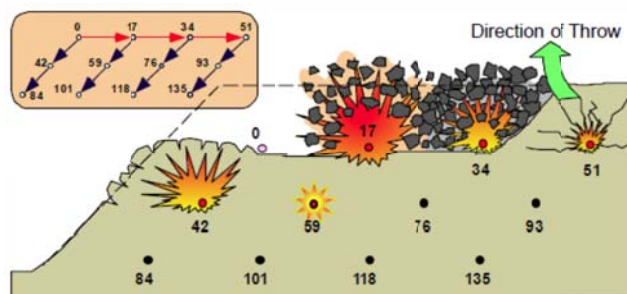
Figure 2: Multi-row blast initiated on a hole-by-hole basic (Orica, 2013)

Stagg and Nutting (1987) suggested that delays between 3-56 ms/m of burden or spacing were appropriate to achieve the desired fragmentation. This however does not specify what range the inter-hole and inter-row timing delays should be, providing an area for inaccuracy. Orica (1998) suggested separate ranges for inter-hole and inter-hole timings. These recommendations are 2-5 ms/m for inter-hole, and 10-25 ms/m for inter-row. The optimal timing for any given blast is the one that

produces the best overall fragmentation that cannot be further improved without significantly increasing the powder factor.

Fragmentation, diggability and fill factors

The three statistical Key Performance Indicators (KPI) for this study (loads/operating hour involving loose Cubic Meters (LCM) and loading rate, and LCM and operating hours are each related to the fragmentation and fill factors. As rock is blasted in order to excavate it, it is broken down into smaller fragments. The more a material is broken down, the more fragmented it is. This means that as fragmentation increases, particle size decreases. It was thought that this decrease in particle size may do two things for the machines digging the material. The first is making it easier for the loaders bucket to penetrate into the material, increasing the rate at which loads can be completed, thus increasing the loads completed in each operating hour. The second is increasing the amount of material in the bucket as with smaller particles, there are fewer voids left in the bucket, thus increasing the fill factor which directly relates to LCM's per load.

It has been suggested by Cardu (2013) that when compared to a pyrotechnic initiation system, an electronic system can provide a decrease in mean particle size of 25 %. Similar work by Sullivan (2003) found that 11 % more material passed through the required passing size. Each of these studies show that using electronic detonators can increase the fragmentation of a blast. Martin and Miller (2007) took this analysis one step further and found that when using an electronic initiation system in a quarrying application, operating costs were decreased by 13 %, suggesting that savings opportunities exist in an operation when lauding and hauling rock material.

BLASTING TECHNOLOGIES USED

Bulk explosives and primers

There are several variations of bulk explosive that can be used to load blastholes. The most common bulk explosive used in the mining industry is Ammonium Nitrate Fuel Oil (ANFO), although each product has situations where they are more suitable over other options (University of Queensland, 1996). Nielson and Kristiansen (1996) suggest that when selecting a bulk explosive for a blast, it is desirable to use the explosive which has the highest velocity of detonation to provide the highest fragmentation, provided the powder factor is not changing. However, financial analysis may show that this is not the most optimum explosive for the blast.

Although bulk explosives provide the energy required to induce rock breakage, they are not sensitive enough to be initiated by detonation cord or a detonator alone. In order to initiate bulk explosives, a primer is used. Primers are a packaged source of high explosive that can be initiated by a detonator, and provide sufficient energy and shock to initiate a bulk explosive (Coundouris and Scott, 2009). The optimum bulk explosive and primer were selected for each blast at the case study site during the period from which data was used. For each blast examined for this study, a site sensitized emulsion, and identical primers were used.

Detonation system

Before the case study site started trialing electronic blast initiation systems, they were using a shock tube initiated pyrotechnic delay system. Central to both pyrotechnic and electronic systems are the detonators that are used in blastholes. Figure 3 shows the internal structure of the two types of detonators used at the case study site during the trial period.

Though both types of detonators will provide the energy required to initiate the primer, and hence the bulk explosive, there is one fundamental difference that provides the basis for this study. This difference is how the timing delay is achieved within each detonator. The shock tube initiated detonators that form the centre of a pyrotechnic initiation system use a pyrotechnic element that burns at a certain rate to provide the timing delay. This timing method has inaccuracies of up to 1.0 %, meaning that detonators may not detonate at the exact timing delay required. The electronic detonators that form the centre of an electronic initiation system have an internal digital delay timer. This timing method reduces timing inaccuracies to 0.1 %, meaning there is less difference between the design delay time, and the actual delay time. This increase in accuracy of timing means that when using an electronic system, the timing of the blast will be more accurate, which should lead to an increase in fragmentation. Another way that

electronic initiation systems achieve increased fragmentation is through the available range of timing delays. Pyrotechnic systems are only available at set delay times for detonators and downhole connectors; electronic detonators however can be individually programmed exactly to any value between 0 - 15,000 ms (Cardu and Giraudi, 2013).
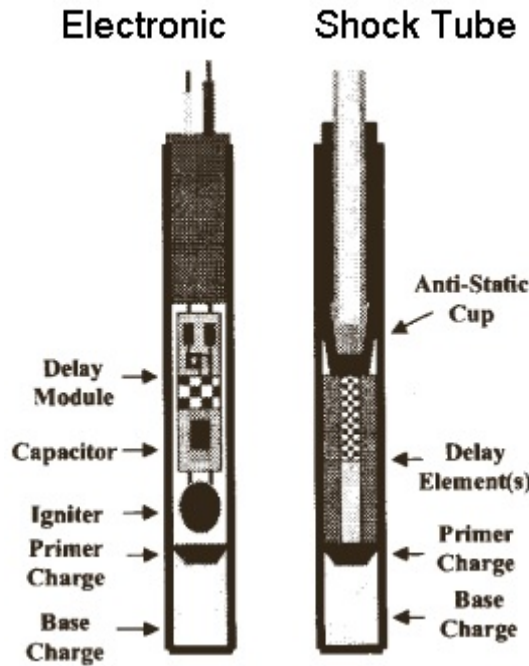
Figure 3: Detonators used on-site during the trial period (adapted from Coundouris and Scott, 2009)

COMPARISON CALCULATIONS

Data collection

Initially, pairs of blasts were to be identified that were in either adjacent blocks in the same strip, or the same block location in adjacent strips as shown in Figure 4. This would have ensured that geological differences were minimal in order to retain some level of consistency for the comparison.
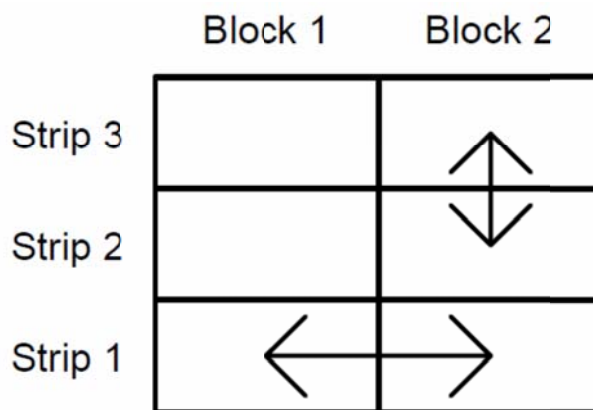
Figure 4: Ideal blast locations for comparison

Due to the guidelines on-site as to which initiation system to use for each blast, no such pairs could be identified. In the absence of such pairs, an alternative approach was implemented. This approach saw blasts with complete sets of dig data that were initiated using either of the two systems during the trial period (January 2012 – December 2013) being compared. These blasts were identified through the case study sites internal reporting software. Once these blasts had been found, the reporting software was then used to access dig data. The dig data reports contained the following information:

- Date of shift;
- Night/day shift;
- Loader, loader availability, loader utilization;
- Shift operating hours;
- Shift operating delays and standby times;
- Scheduled and unscheduled time losses;
- Volume of overburden moved in shift; and
- Number of loads completed in shift.

This data was extracted and record for each of the three excavation fleets used on-site for both pyrotechnically and electronically initiated blasts. These are 30 m^3 loaders with three pass matched trucks, 34 m^3 loaders with three pass matched trucks, and 60 m^3 loaders with two pass matched trucks. This created six sets of data, which were then normalized in order to remove any errors from loaders occasionally working on the border between two blasts on the same shift, resulting in material being moved that was not to be included in the analysis.

Data analysis and KPI calculations

Equations 1, 2 and 3 shows how the three KPI's of the study were calculated. Once these values had been worked out for all data points, a strict outlier removal was conducted. A data point was considered an outlier if it was outside the range defined by Equation 4.

$$\frac{Truck\ loads}{Operating\ hours\ on\ shift} = \frac{Loads}{Operating\ hour} \qquad (1)$$

$$\frac{Volume\ of\ overburden\ moved\ on\ shift}{Truck\ loads\ on\ shift} = \frac{LCM}{Load} \qquad (2)$$

$$\frac{(Loads/Operating\ hour)\ on\ shift}{(LCM/Load)\ on\ shift} = \frac{LCM}{Operating\ hour} \qquad (3)$$

$$X < Q1 - (1.5 * IQR)\ Or\ X > Q3 + (1.5 * IQR) \qquad (4)$$

Where:

- X is the data point in question;
- Q1 is the first quartile of the data set;
- Q3 is the third quartile of the data set; and
- IQR is the interquartile range (i.e. Q3-Q1)

Once outliers were removed, key statistical values for each data set were calculated, these were the minimum, median, maximum, average and variance.

AU$/LCM calculations

Equations 5, 6 and 7 were used to calculate the total cost of loading and hauling one LCM of overburden. These calculations were completed using operating costs that were supplied by the case study site which can be seen in Table 1.

$$\frac{Loader\ hourly\ operating\ cost\ (AU\$/hour)}{Average\ LCM/operating\ hour} = Loader\ \frac{AU\$}{LCM} \qquad (5)$$

$$\frac{Truck\ hourly\ operating\ cost\ (AU\$/hour)/average\ truck\ loads\ per\ hour}{Average\ LCM/load} \qquad (6)$$

$$= Trucking \; \frac{AU\$}{LCM}$$

$$(Loader \; AU\$/LCM) + (Trucking \; AU\$/LCM) = Total \; \frac{AU\$}{LCM} \qquad (7)$$

These calculations done for each of the six data sets, provide costs for each loader fleet for both pyrotechnical and electronic blasts. Equation 8 shows how the difference between these two costs provides the savings the result from the use of an electronic system.

$$\left(Electronic \; \frac{AU\$}{LCM}\right) - \left(Pyrotechnic \; \frac{AU\$}{LCM}\right) = \frac{AU\$ \; savings}{LCM} \qquad (8)$$

Table 1: Operating costs of on-site equipment

	30 m^3 fleet	34 m^3 fleet	60 m^3 fleet
Loader op. cost (AU$/op. hour)	1099.00	973.00	746.00
Truck op. cost (AU$/op. hour)	288.00	374.00	374.00

Savings opportunities calculations

Once savings possible for each LCM moved were calculated, a calculation was required to identify if these savings were enough to offset the additional upfront cost of using an electronic initiation system. In order to do this, a conceptual blast was designed that resembled a typical overburden shot at the case study site. This conceptual shot had the following parameters:

- 478 holes;

- Three detonators/hole;

- 34 m average hole length;

- 270 mm hole diameter;

- 8.6 m burden;

- 10.7 m spacing; and

- 1.7 million LCM

Using this information, and the values in Table 2, two factors could be calculated: the additional cost for using an electronic initiation system, and the total savings for the blast for each loader fleet. Equation 9 shows how the savings for the blast were calculated for each of the three loader fleets.

$$\frac{AU\$ \; savings}{LCM} * Blast \; volume = Total \; AU\$ \; savings \; for \; blast \qquad (9)$$

For the conceptual blast, it is assumed that all loading practices remain the same, and the time spent to load is the same, meaning that the only difference in cost is that of the detonators and associated connections for each initiation system. It is important to note that the values in Table 2 include the detonator and associated surface connections for each detonator in the blast.

Table 2: Cost of implementing each initiation system

Electronic system (AU$/detonator)	Pyrotechnic system (AU$/detonator)
44.31	25.12

Equation 10 was used to calculate the total cost for each initiation system if it were to be used on the conceptual blast. Once total initiation costs were calculated, the difference in initiation costs were calculated using Equation 11. This represents the additional cost due to using an electronic initiation system. Once the additional cost for using an electronic system was identified, Equation 12 was used to identify the net savings opportunity for the conceptual blast.

$$Total\ initiation\ cost = Number\ of\ holes * Detonators\ per\ hole * Cost\ per\ detonator \qquad (10)$$

$$Difference\ in\ inititation\ cost$$
$$= Cost\ for\ electronic\ initiation - Cost\ for\ pyrotechnic\ initiation \qquad (11)$$

$$Net\ savings = Total\ savings\ for\ blast - Additional\ electronic\ cost \qquad (12)$$

RESULTS

Statistical Results

Each loading fleet has two data sets, one for blasts initiated using a pyrotechnic system, and one for blasts initiated using an electronic system. Each of these data sets has three KPI's analysed, providing nine groups of data for comparison. It can be seen in Tables 3, 4 and 5 that every data comparison pair, the average values for electronic blasts are higher. This shows that there is an increase in fragmentation, providing increases in diggability which results in higher downstream productivity. It is worth noting that for a large portion of the data comparison pairs that the variance is lower, meaning that these higher values are being achieved more consistently. For the pairs where the electronic blasts have higher variance, the minimum and maximum are both higher than that of the pyrotechnic blasts, meaning that they are digging at less consistent rates, but are still outperforming the pyrotechnic blasts.

Table 3: Key statistical results for 30 m³ loader fleet

	Loads/op. hour		LCM/load		LCM/op. hour	
	Av.	Var.	Av.	Var.	Av.	Var.
Pyro.	22.72	21.53	89.79	0.07	2,042	167,690
Elec.	23.61	2.69	90.61	0.19	2,140	24,211

Table 4: Key statistical results for 34 m³ loader fleet

	Loads/op. hour		LCM/load		LCM/op. hour	
	Av.	Var.	Av.	Var.	Av.	Var.
Pyro.	18.87	2.66	103.63	73.44	1953	50,073
Elec.	20.58	4.29	109.10	102.01	2,240	73,690

Table 5: Key statistical results for 60 m³ loader fleet

	Loads/op. hour		LCM/load		LCM/op. hour	
	Av.	Var.	Av.	Var.	Av.	Var.
Pyro.	30.52	10.37	121.58	19.27	3,745	126,522
Elec.	30.83	11.83	130.69	15.76	3,998	103,961

AU$/LCM results

Figure 5 shows that due to the increase in fragmentation, and hence downstream productivity, there are savings available, on an AU$/LCM basis, through the use of an electronic blast initiation system.

Savings results

The difference in cost to load the conceptual blast with an electronic initiation system was calculated to be AU$27,524. It can be seen in Table 6 that even with the additional cost of using an electronic system, substantial savings opportunities are available for each loader fleet and associated trucks.
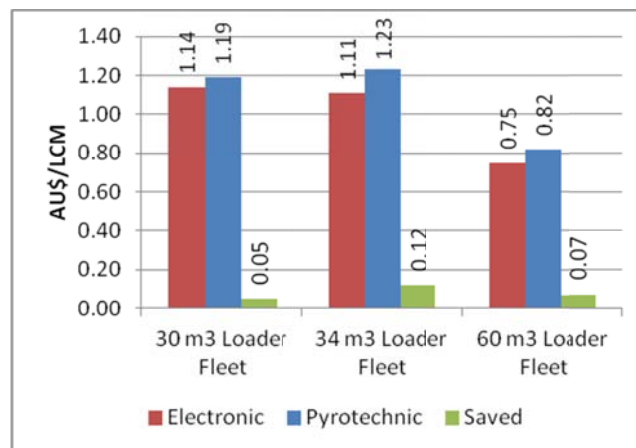
Figure 5: AU$/LCM saving opportunities for each loader fleet

Table 6: Net savings when using an electronic blast initiation system

	30 m^3 fleet	34 m^3 fleet	60 m^3 fleet
Total AU$ saved	85,757	205,817	120,059
Electronic AU$ difference	27,524	27,524	27,524
Net AU$ saved	58,233	178,293	92,535

CONCLUSIONS

This study was completed in order to identify if savings opportunities existed due to an increase in fragmentation through the use of an electronic blast initiation system at an open cut coal mine in Queensland.

Through completing statistical analysis, it was found that there was an increase in both the number of loads per operating hour, and material in each load by 1.0-9.1 % and 0.9-7.5 % respectively. These increases translated to an overall increase in material moved per operating hour by 4.7-14.7 %. These findings are consistent with those suggested by Cardu (2013) and Sullivan (2003).

Through this production increase, it was found that the case study site was saving AU$0.05, AU$0.12 and AU$0.07 on each LCM moved for each of the 30 m^3, 34 m^3 and 60 m^3 respectively. These savings translate directly into savings opportunities of AU$58,233, AU$178,293 and AU$92,535 for the conceptual blast. This finding is consistent with that found by Martin and Miller (2007).

Through the completion of this study, it has been found that the use of an electronic blast initiation system over a pyrotechnic blast initiation system increases both fragmentation and downstream productivity (overburden loading and hauling) significantly enough that substantial savings opportunities exist.

ACKNOWLEDGEMENTS

REFERENCES

Cardu, M. 2013, A review of the benefits of electronic detonators, Rem: Revista Escola de Minas, 66 (3), pp. 375-382.

Cardu, M and Giraudi, M. 2013, A review of benefits of electronic detonators [online], Available from: <http://www.cbmina.org.br/media/palestra_6/T39.pdf> [Accessed 1 October 2014].

Combrinck, S and Strong, N. 2007, Use of electronic detonators at Cracow gold mine, *in Proceedings World Gold Conference*, pp 41-46 (Cairns).

Coundouris, S and Scott, A. 2009, Initiation systems, in Learning guide rock breakage, *Rock blasting*

module *(Ed: I Onederra, D Chalmers and C Workman-Davies) pp 57-70 (Mining Education Australia)*.

Fairhurst, C and Kutter, H K. 1971, On the fracture process in blasting, *International Journal of Rock Mechanics and Mining Science*, 8(3):189-202.

Martin, D and Miller, D. 2007, A review of the benefits being delivered using electronic delay detonators in the quarry industry, *paper presented to The Institute of Quarrying Australia 50th National Conference*, Hobart, October 2007.

Metals Consulting International. 2014, Metallurgical coal prices [online], Available from: <www.steelonthenet.com/files/metallurgical-coal.html> [Accessed 1 September 2014].

Nielson, K and Kristiansen, J. 1996, Blasting-Crushing-Grinding: Optimisation of an integrated comminution system, *in Proceedings FRAGBLAST 5 – Fragmentation by Blasting,* pp 267-277 (Montreal, Canada).

Orica. 1998, Safe and Efficient Blasting in Open Cut Mines, Orica Australia Operations, p 138.

Orica. 2013, Tutorial 4: Blast timing principles, *in Rock breakage Course DVD* (Ed: I Onederra, D Chalmers and C Workman-Davies) (Mining Education Australia).

Stagg, M S and Nutting, M J. 1987, Influence of blast delay time on rock fragmentation: one tenth-scale tests, *BuMines IC 9135*, Chicago, Illanois, pp 79-95b.

Sullivan, R. 2003, Using electronic Detonators to improve fragmentation, diggability and crusher throughput, *in Proceedings Fifth Large Open Pit Mining Conference*, pp 199-202 (Kalgoorlie).

University of Queensland. 1996, Explosives selection, *in JKMRC Monograph No.1 (Ed: A Scott)*, pp 146-179 (University of Queensland: Brisbane).

Changes in Drilling Performance and Dust Suppression With the Use of a Water Separator Sub

Brianna Millgate and Paul Hagan

ABSTRACT: Drill and blast is a key excavation process in open pit mining systems. Rock fragmentation due to drilling results in the production of fine dust particles that can be detrimental to the environment. There are different methods to manage the dust make often based on some form of "wet" drilling which can cause further issues. The water separator sub is a device aimed at overcoming some of these issues. This paper outlines a study undertaken of the effect of a water separator sub on drill performance and dust suppression. The study involved collecting dust measurements through a real time dust monitor, and analysing drill performance data from a mine site, in particular drill penetration rate data and bit life.

INTRODUCTION

Depending on the type of rock being drilled, drilling can be a source of harmful dust that is detrimental to human health (Kalestone Environmental, 2011). Current dust suppression techniques have pitfalls in terms of productivity, health and safety and environmental sustainability.

The water separator sub shown in Figure 1 is a device that replaces the bit sub in the drill string. It is designed so the combination of water and compressed air that is directed down through the centre of the drill string takes a sudden sharp turn before the drill bit. Due to the higher inertia of water particles, the water is unable to negotiate the turn and is physically separated from the air (USBM, 1988). The air continues its flow and makes it way through the U-turn flowing through slots to the bit. The water accumulates in a small reservoir and the air pressure forces it to be ejected out of weep holes located above the bit as a fine spray as shown in Figure 2 (NIOSH, 2012). The compressed air that exits the drill bit forces the fragmented drill cuttings up the hole and then mixes it with the water spray carrying the wetted material to the surface (Listak and Reed, 2007).
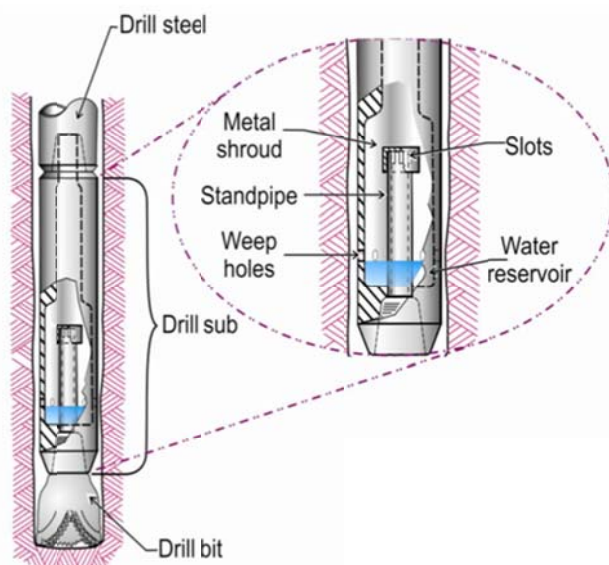
Figure 1: Schematic of water separator sub in a blasthole (NIOSH, 2012) (left) and, installation of the sub (right)

The water separator sub has the potential to utilise the advantages of wet drilling in terms of dust suppression. This contributes to sustainability of the mining industry by allowing drilling operations to occur, without posing a threat to human health and the environment. Minimising dust also benefits a mining operation's social license to operate. Dust can be irritating and worrying to surrounding

communities, even if the particular dust particles are not harmful. It can result in complaints and resistance from communities to any future development or extension of operations. Dust can also be extremely problematic for visibility. It can cause operations to be halted, resulting in lost production. Suppressing dust at drilling operations will help reduce dust make at a mine site and contribute to ensuring production is maintained.

Figure 2: Water spray from weep holes in side of the sub above the drill bit

The water separator sub also has the potential to lower drill bit costs. Preventing water from coming into contact with the drill bit can extend bit life by preventing corrosion and premature bit wear that is associated with standard wet drilling. If drill bit life is extended, bits do not need to be replaced as often reducing downtime and therefore lowering costs. This contributes to sustainability as companies are always looking for ways to lower operating costs in order to mine economically in deep pits and in tough markets.

METHODOLOGY

The project involved a field study at an openpit coalmine operating in the Hunter Valley of Australia. Data related to bit life and penetration rate and, measurements of dust levels were analysed over a period of several months before and after a water separator sub was installed.

RESULTS

Dust levels

Dust monitoring was conducted to compare the effect of wet drilling on dust suppression with and without use of the water separation over a six-day period. A Dust Trak II Aerosol Monitor mounted on the surface near to the drillhole collar as shown in Figure 3 was used in the study. The unit utilises a light-scattering laser photometer to provide real-time aerosol mass readings every 30 seconds and reports the instantaneous dust concentration in air in units of mg/m^3. Figure 4 shows a plot comparing the dust readings for the same time period for the three days before and after sub installation that indicates there were more instances of high peaks readings before sub installation.

Figure 3: Dust monitor in use during drilling operations
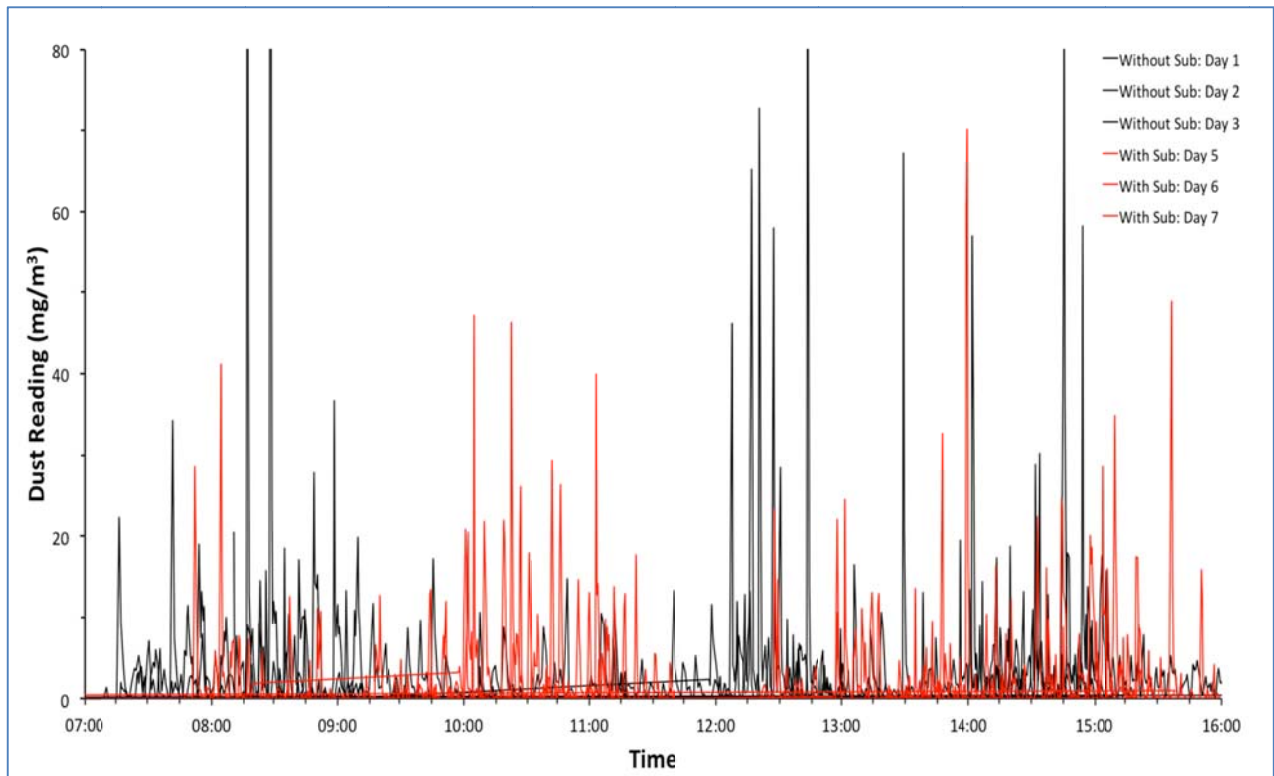
Figure 4: Variation in dust readings before and after sub installation

Table 1 shows a summary of the mean and maximum readings on each day of monitoring. While use of the water separator sub in wet drilling resulted in a slight reduction in the mean daily dust readings of 12%, there was a near halving in the maximum daily dust readings.

Table 1: Comparison of dust readings over a six-day period

	Day	Dust reading (mg/m^3)	
		mean	*maximum*
no water separator	1	1.99	65.3
	2	4.24	159.0
	3	2.08	98.6
	mean	**2.77**	**107.6**
water separator installed	5	3.65	70.3
	6	1.16	49.1
	7	2.48	35.0
	mean	**2.43**	**51.5**

On Day 4, dust monitoring commenced at 8:00 am with wet drilling prior to installation of the water separation and continued until the water separator was installed at approximately 9:30 am. Dust monitoring then continued until 3:30 pm, utilising water separated wet drilling. There was a noticeable reduction in the dust levels after the sub installation with more consistent and fewer peaks in dust make post installation as shown in Figure 5.The results in Table 2 compare the mean, minimum and maximum readings before and after the sub was installed.

The significance of this data set is that it applies to the same set of conditions in terms of rock type, drill machine, drill bit, operator and weather conditions. As the data indicates there was a reduction in the mean reading by 0.81 mg/m^3 or 25%, the minimum reading decreased by 0.027 mg/m^3 or 47%, and the maximum reading decreased significantly by 17.9 mg/m^3 or 37%. This shows that on this day with all other variables being the same, use of the water separatorsub increased the effectiveness of wet drilling in reducing dust make.
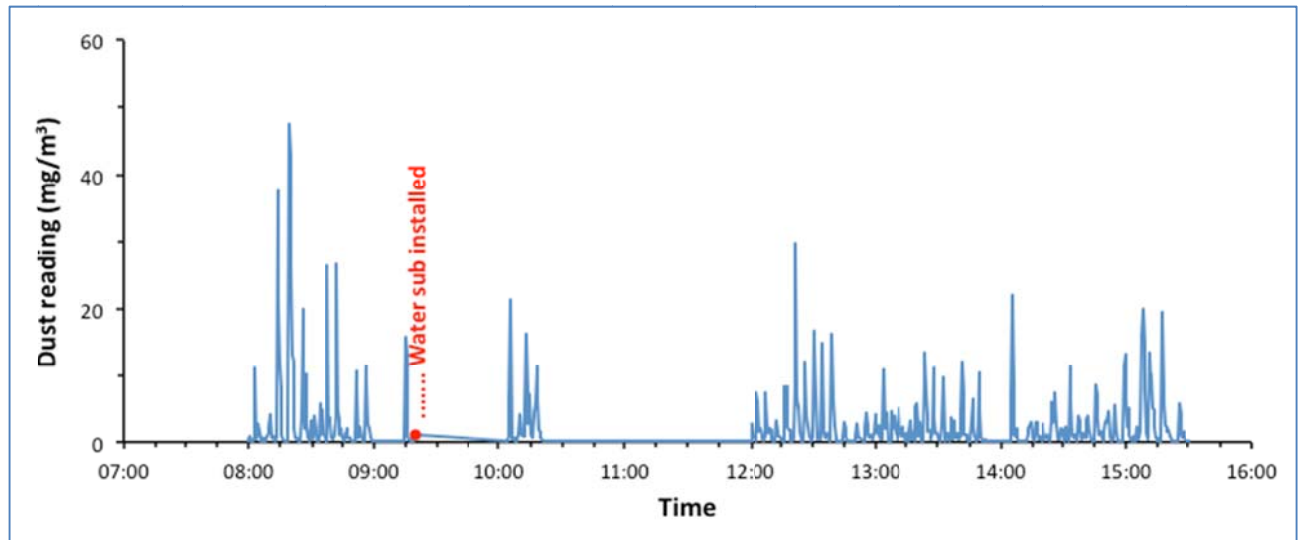
Figure 5: Variation in dust readings before and after sub installation on Day 4

Table 2: Effect of water separator installation on dust make

	Dust reading (mg/m³)		
	mean	*minimum*	*maximum*
before installation	3.19	0.057	47.6
after installation	2.38	0.03	29.7
percentage change	25%	47%	37%

Dust monitoring limitations

While it was planned to maintain similar conditions with the water separator sub during the study, in reality a number of changes occurred and differences in operating conditions that may have impacted on the measurements.

First, the drill rig used in the study was fitted with a dust curtain and collection system. It was observed that there were differences between drill operators in the use of this system.

Second, the water flow rate was not fixed but varied by the operator depending on the ground conditions and the amount of visible dust present.

Third, the drill rig was moved between drill sites after three days into the study. It was initially planned that the drill rig would remain in the same location for the duration of testing, however due to scheduling changes, drilling was completed prematurely and the rig relocated. This is likely to have introduced differences in geological ground conditions. This factor does not apply to the data in Table 2. Finally, weather conditions such as temperature, wind and humidity can also affect the amount of dust generation. Dry, hot and windy days will see an increase in the amount of dust present in the air. It was observed during the period of study that drilling operations occurred on fine, sunny days with minimal wind. Even so any small gust of wind may have affected the readings depending on the location of the dust monitor and wind direction. For example, if a wind gust was in the direction of the dust monitor it may have temporarily resulted in a higher measurement, conversely if the wind gust was away from the dust monitor it would have reduced the dust measurement.

Drill penetration rate

The mean daily drill penetration rate per shift was analysed over a nine month period prior to installation of the water separator sub and six months post installation. Histograms of the respective performance are shown in Figure 6 and various statistics summarised in Table 3. A comparison of the results for both cases shows there were reductions of 10.4% and 8.8% in the median and mean penetration rates respectively. The use of the water separator sub had been expected to increased penetration rate by

removing water from the point of rock breakage, however the data indicates the opposite seemed to have occurred.
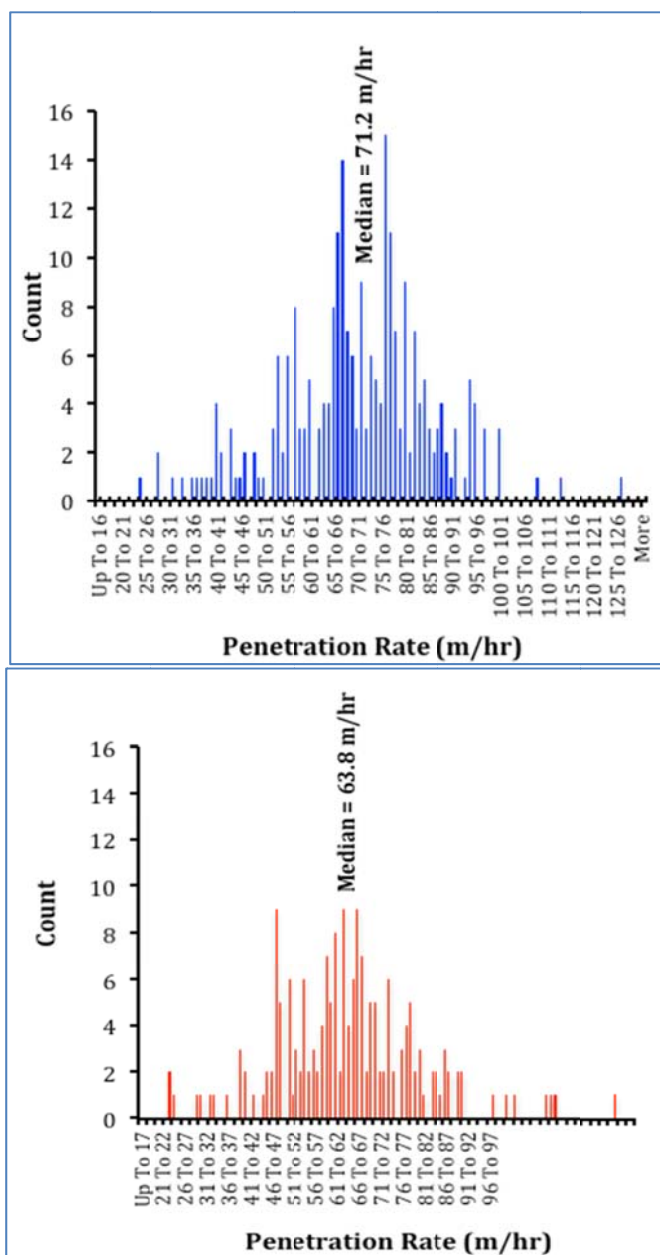
Figure 6: Mean daily drill penetration rate before sub installation (left) and after sub installation (right)

Table 3: Comparison of the drill bit penetration rate before and after sub installation

	Daily penetration rate (m/hr)		
	median	*mean*	*s.d.*
before installation	71.2	70.4	16.9
after installation	63.8	64.2	16.4
percentage change	10.4%	8.8%	–

Penetration rate data limitations

A problem in analysing penetration rate data is that it is reliant on operator efficiency. Each operator's experience and drilling performance will influence penetration rates. This factor could have accounted for

some variance in the results. On the other hand, considering the size of the two data sets, this is less likely to be a contributing factor. Nevertheless during the period of study, a number of new drillers were employed and, due to the large number of operators at the mine as well as the number of drill rigs, there may have been differences in the actual operators between the two periods.

Another issue is variation in ground conditions. Numerous drill sites can result in variations in the material properties of the overburden material. Factors such as strength, hardness and abrasivity of the rock and moisture content all present the potential to alter penetration rates.

Drill bit life

Bit life was examined over similar periods as penetration rate before and after installation of the water separator sub. The data analysed for drill bit life was based on the metres drilled per bit from the time a bit was first mounted to being dismounted. This was chosen as simply measuring the period during which a bit was used and does not take into account time delays for crib breaks or maintenance, nor does it consider lower penetration rates due to harder rock beds. Table 4 shows a comparison of the mean, minimum and maximum metres drilled per bit before and after sub installation. The mean bit life was found to have increased significantly by 58% after the water separator sub was installed. The improvements in the minimum and maximum values were 78% and 71% respectively.

Table 4: Comparison of the drill bit life before and after water sub installation

	Number of bits	*Bit life (m/bit)*		
		mean	*minimum*	*maximum*
before installation	13	13,326	6,743	26,230
after installation	8	21,060	12,039	44,854
percentage change		58%	78%	71%

Drill bit life limitations

A limitation on the reliability of the data is the variation in ground conditions. As is the case for penetration rate, drilling operations would have occurred between locations in the pit resulting in different drilling conditions with changes in rock strength, hardness and abrasivity.

Another factor that may have impacted on bit life is the operator decisions on what constitutes a worn-out drill bit. Although there are strict guidelines on what constitutes a worn bit, if a bit was used past its optimum point then it would have skewed the results towards appearing to have improved drill bit life and conversely if changed too early.

CONCLUSION

The impact of a water separator sub was examined in terms of changes in dust make, drill penetration rate and drill bit life. Water is injected into the compressed air line that is used to bail rock fragments from the bit face in order to reduce the amount of fine dust produced at the drillhole collar. Over a three-day period both before and after installation of the sub, there was little significant change in the measured dust levels. As the drill rig was moved before and after installation this may have consequently resulted in changes in drilling conditions and may have masked any improvements. Interestingly, a 25% reduction in dust make was measured post installation on the actual day the sub was installed. It is recommended that a further study be undertaken over a much longer time period to confirm the impact on dust levels.

The average daily drill bit penetration rate and bit life were analysed over a nine-month period before installation of the sub and a six-month period after installation. It was found that there was a reduction in the median and mean penetration rates by 10.4% and 8.8% respectively. Conversely, the sub had a marked beneficial effect of increasing bit life over the period studied of 25%.

Overall, while installation of the water separator sub was not found to have had any significant impact in the measured dust levels on the surface near the drillhole collar, it had a slight detrimental impact on penetration rate while it had led to a significant improvement in extending bit life.

REFERENCES

Kalestone Environmental. 2011, NSW Coal Mining Benchmarking Study: international best practice measures to prevent or minimize emissions of particulate matter from coal mining [online]. Available from: <www.epa.nsw.gov.au> [Accessed: 15 May 2014].

Listak J and Reed W. 2007, Water separator shows potential for reducing respirable dust generated on small-diameter rotary blasthole drills, *International Journal of Mining, Reclamation and Environment,* 21(3):160–172.

National Institute of Occupational Safety and Health (NIOSH). 2012, *Dust Control Handbook for Industrial Minerals Mining and Processing,* pp. 79-108 (Department of Health and Human Services: Pittsburgh).

United States Bureau of Mines (USBM). 1988, Impact of drill stem water separation on dust control for surface coal mines. US Bureau of Mines Technology 308 p1-2.

Simulation of Payload Variance Effects on Truck Bunching to Minimise Energy Consumption and Greenhouse Gas Emissions

Ali Soofastaei, Saiied Mostafa Aminossadati, Mehmet Siddik Kizil and Peter Knights

ABSTRACT: Data collected from truck payload management systems at various surface mines shows that the payload variance is significant and must be considered in analysing the mine productivity, energy consumption and greenhouse gas emissions. Payload variance, causes significant differences in gross vehicle weights. Heavily loaded trucks travel slower up ramps than lightly loaded trucks. Faster trucks are slowed by the presence of slower trucks, resulting in 'bunching', production losses and increasing fuel consumptions. This paper simulates the truck bunching phenomena in large surface mines to improve truck and shovel systems' efficiency, minimise energy consumption and reduce greenhouse gas emissions. The study concentrated on completing a practical simulation model based on a discrete event method which is most commonly used in this field of research in other industries. The rate of greenhouse gas emissions corresponding to diesel consumption by haul trucks is calculated according to global warming potential guidelines. The simulation model has been validated by a dataset collected from a large surface mine in Arizona state, USA. The results have shown that there is a good agreement between the actual and estimated values of investigated parameters. The validated model has been utilised in a real mine site in central Queensland, Australia as a case study. The focus of this case study has been on the relationship between the trucks bunching due to payload variance with average cycle time, average hauled mine materials, fuel consumption and greenhouse gas emissions. The results have indicated that there is a non-linear correlation between the payload variance and the mentioned parameters. In this case study, the simulation results indicate that a reduction of up to 15 minutes on average cycle time is possible if the standard deviation of payload is reduced from 30 down to 5 tonnes. By reducing the payload variance, the average of hauled mine materials can be increased up to 35 kt per day. Moreover, the fuel consumption and greenhouse gas emissions can be reduced dramatically by reducing the payload variance.

INTRODUCTION

Improving the efficiency of haulage systems is one of the great challenges in mining engineering and is the subject of many research projects undertaken in the mining industry (Ercelebi and Bascetin, 2009; Limsiri, 2011).The main effective parameters on material transport when the truck and shovel system is used in surface mines are mine planning, road condition, truck and shovel matching, swell factors, shovel and truck driver's ability, weather condition, payload distribution and payload variance (Raj, Vardhan and Rao, 2009). Based on the literature, among all the above mentioned parameters, truck payload variance is one of the most important parameters in this field (Schexnayder, Weber and Brooks, 1999). The main source of the payload variance in truck and shovel mine operation is the loading process. Loading is a stochastic process and excavator performance is dependent on factors such as swell factor, material density and particle size distribution (Singh and Narendrula, 2006). Variation of these factors causes variation of bucket and consequently truck payloads, affecting productivity. Reducing truck payload variance in surface mining operations improves productivity by reducing bunching effects and machine wear from overloaded trucks (Paton, 2009).In large surface mines having long ramps, bi-directional traffic and restrictions on haul road widths negate the possibility of overtaking. Overloaded trucks are slower up ramp in comparison to under-loaded trucks. Thus faster trucks can be delayed behind slower trucks in a phenomenon known as truck bunching (Knights and Paton, 2010). This is a source of considerable productivity loss for truck haulage systems in large surface mines. There are some investigations about the payload variance simulation and the effect of this event on other mining operation parameters. The study conducted by Hewavisenthi, Lever and Tadic(2011) is concerned with using a Mont-Carlo simulation to study the effect of bulk density, fill factor, bucket size and a number of loading passes on the long term payload distribution of earthmoving systems. The focus of their study is on simulation of payload distribution and variance in large surface mines. The study conducted by Knights and Paton(2010) is concerned with the truck bunching due to load variance.

This study was conducted to provide an analysis of the effect of load variance on truck bunching. Webb(2008) investigated the effect of different bucket load sizes on truck cycle times and the inherent costs. The research project being undertaken will focus primarily on the effect of load variance on truck bunching. The payload variance not only affects the production rate, but also it is an important parameter in the analysis of energy consumption and gas emissions.

The trucks utilised in the haulage operations of surface mines use a great amount of energy (DOE, 2002) and this has encouraged truck manufacturers and major mining corporations to carry out a number of research projects on the energy efficiency of haul trucks (EEO, 2012).There are many factors that affect the rate of fuel consumption for haul trucks such as payload, truck velocity, haul road condition, road design, traffic layout, fuel quality, weather conditions and driver skill(Cetin, 2004). A review of the literature indicates that understanding of energy efficiency of a haul truck is not limited to the analysis of vehicle-specific parameters; and mining companies can often find greater energy saving opportunities by expanding the analysis to include other effective factors such as payload distribution and payload variance (White and Olson, 1992).

This paper aims to present a new simulation model based on the discrete event methods to investigate the effect of truck bunching due to payload variance on average cycle time, the rate of loading materials, fuel consumption and greenhouse gas emissions.

PAYLOAD VARIANCE

Loading performance depends on different factors such as bench geometry, blast design, muckpile fragmentation, operators' efficiency, weather conditions, utilisation of trucks and shovels, mine planning and mine equipment selection (Schexnayder, Weber and Brooks, 1999; Hewavisenthi, Lever and Tadic, 2011). In addition, for loading a truck in an effective manner, the shovel operator must also strive to load the truck with an optimal payload. The optimal payload can be defined in different ways, but it is always designed so that the haul truck will carry the greatest amount of material with lowest payload variance (Knights and Paton, 2010). The payload variance can be illustrated by carrying a different amount of overburden or ore by the same trucks in each cycle. The range of payload variance can be defined based on the capacity and power of the truck. The increase of payload variance decreases the accuracy of the maintenance program. This is because the rate of equipment wear and tear is not predictable when the mine fleet faces a large payload variance (Paton, 2009). Minimising the variation of particle size distribution, swell factors, material density and fill factor can decrease the payload variance but it must be noted that some of the mentioned parameters are not controllable. Hence, the pertinent methods to minimise the payload variance are real-time truck and shovel payload measurement, better fragmentation through optimised blasting and improvement of truck-shovel matching. The payload variance can be shown by variance of standard deviation (σ). Standard deviation measures the amount of variation from the average. A low standard deviation indicates that the data points tend to be very close to the mean; a high standard deviation indicates that the data points are spread out over a large range of values. This parameter can be calculated by Equation 1.

$$\sigma = \sqrt{\frac{1}{N}\sum_{i=1}^{N}(x_i - \mu)^2} \tag{1}$$

Where N is the number of available data for each parameter, i is a counter of data, x is the value of parameter and μ can be calculated by Equation 2.

$$\mu = \frac{1}{N}\sum_{i=1}^{N}x_i \tag{2}$$

Figure 1 shows the different kinds of normal payload distribution (the best estimation function for payload distribution) based on the difference σ for one type of the mostly used truck in surface mines (CAT 793D).

The GVW is the total weight of empty truck and payload. Based on the CAT 793D technical specifications, the range of Gross Vehicle Weight GVW () variation is between 165 tonnes (empty truck) and 385 tonnes (maximum payload). Hence, the maximum σ for this truck can be defined as 30; that is

because for higher standard deviations, the minimum GVW is less than the weight of empty truck and the maximum GVW is more than the maximum capacity of truck.
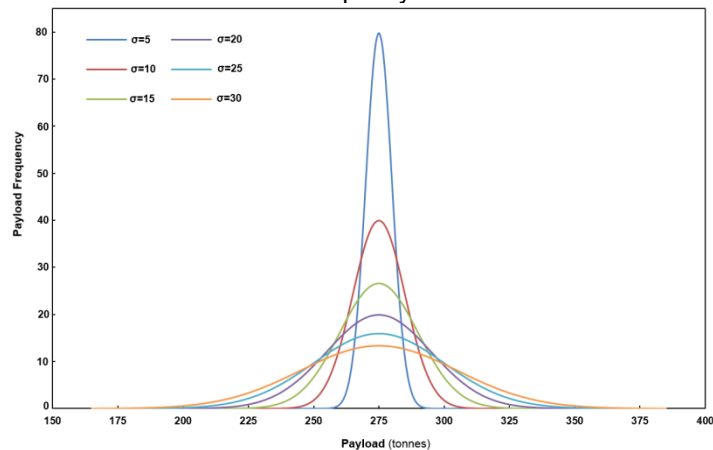

Figure 1:Normal payload distribution for difference standard deviations (σ) (CAT 793D)

Simulation Models

Based on the condition of truck and shovel mining operation in surface mines, the best simulation for this event can be by discrete event methods. Discrete event simulation can be used to model systems which exhibit changes in state variables at a discrete set of points in time(Banks *et al.*, 2010).The models can be static or dynamic. Static models represent a system at a specific time, while dynamic models represent a system as it evolves over a period of time (Byoung and Donghun, 2013). A mining operation is a dynamic system which is very difficult to model using analytical methods. There are different kinds of discrete simulation models used for modelling the systems in industrial projects. In this study, some of the most popular models have been investigated and a new model to simulate the truck bunching event in surface mining operation has been developed.

The first investigated model is AutoMod. This model is a simulation system which is designed for use in material movement systems developed by Applied Materials, USA(Muller, 2011). It can be used for simulation of truck haulage circuits and transport circuits, conveyors, load dumping and retrieval, cranes and robots. Simulations with AutoMod have the ability for simulation of complex movement with stochastic inputs.

The second studied model is SIMUL8. This model is a graphically oriented simulation package developed by the SIMUL8 Corporation (Concannon, Hunter and Tremble, 2003). This software is a discrete event simulation package, meaning it simply executes tasks in queue based on time, which then triggers the activity of new tasks. SIMUL8 can be used in simulation of multiple haulage systems, but is more effective at single circuit simulations.

The third analysed model is GPSS/H. This model was released in 1977 by Wolverine Software Corporation who still develop and sell this model today (Stout *et al.*, 2013). GPSS/H is stochastic in nature, such that it can execute Monte Carlo style randomisation to apply statistical distributions. GPSS/H is particularly adept at simulating queuing and bunching.

The fourth observed model in this project is WITNESS. This model is a discrete event simulation suite developed by Lanner (Paton, 2009). Witness is capable of producing haulage system simulations in a dynamic animated computer model.

The last but not least inspected model is Arena. This model is a simulation software package developed by Rockwell Automation based on the SIMAN programming language (Kamrani, Hashemi and Rahimpour, 2014). SIMAN is a Discrete Event Simulation package which can be used in a process or event scheduling mode. SIMAN is most commonly used in conjunction with Arena in the industry today. The ARENA system can produce scale models of circuits and other simulations.

<div align="center">**TRUCK BUNCHING MODEL**</div>

Developed algorithm

Hauling operations in surface mines consist of different kinds of components. These components are loading, hauling, manoeuvring, dumping, returning and spotting (see Figure 2).
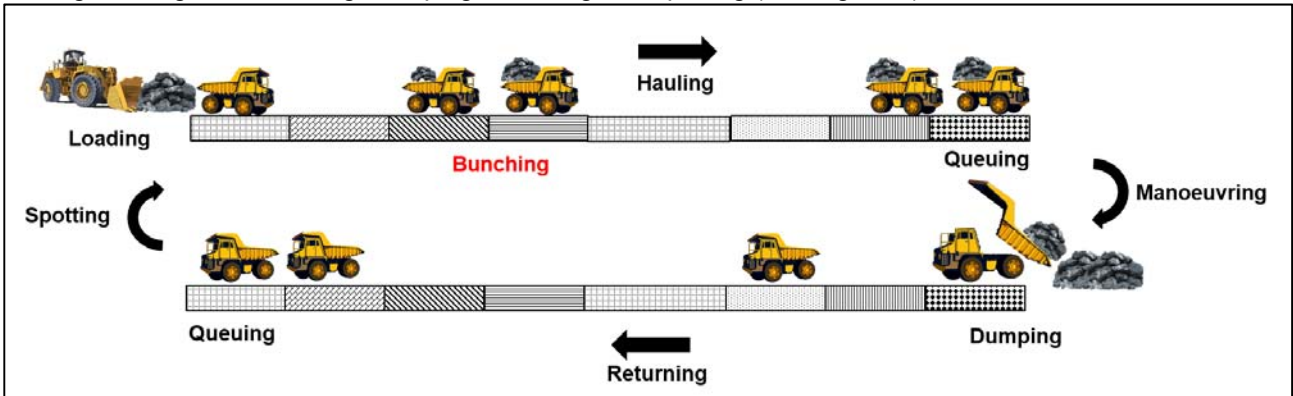
<div align="center">**Figure 2: Schematic of hauling operation in surface mines**</div>

In the standard hauling operation loading time is the time taken to load the truck, hauling and returning time are traveling time for each truck between loading zone and dumping area. Spotting time is the time during which the loading unit has the bucket in place to dump, but is waiting for the truck to move into position. Spotting time will depend on the truck driver's ability and the loading system. Double-side loading should almost eliminate spot time. Dumping time is the time taken for the truck to manoeuvre and dump its payload either at a crusher or dump.

Based on the above mentioned hauling operation components, four main times can be defined; fixed time, travel time, wait time and cycle time.

Fixed time is the sum of loading, spotting and dumping time. It is called 'fixed' because it is essentially invariable for a truck and loading unit combination. Travel time is the time taken to haul and return the payload. Wait time is the time the truck must wait before being served by the loading unit, waiting in a queue for dumping and the waiting in a line behind the overloaded trucks in large surface mines (truck bunching). Cycle time is the round trip time for the truck. It is the sum of fixed, travel and wait time.
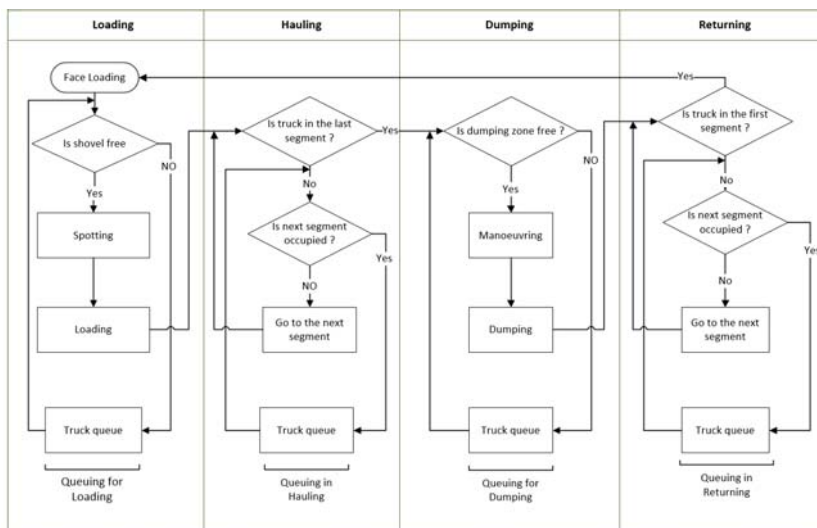
<div align="center">**Figure 3: Truck bunching algorithm**</div>

Figure 3 illustrates the proposed algorithm to complete a discrete event model in this project. This algorithm consists of four main subroutines to cover all processes in the hauling operation. These main components are loading, hauling, dumping and returning. Based on the developed model, each component has a waiting time.

Payload distribution and variance simulation

A main part of the truck bunching model is simulating the payload distribution and variance. In this study, a simulation model was designed to estimate the distribution of truck and bucket payloads based on variations of input parameters. These parameters are bucket size, number of loader passes (to fill the truck tray), distribution of bucket bulk density and distribution of bucket fill factor.

This simulation was implemented as a MATLAB workbook and a commercially available Monte-Carlo simulation engine was used to run the simulation. In this model the truck payload is calculated by Equation 3.

$$m_k = \rho_k \sum_{q=1}^{p} v_b f_q \tag{3}$$

Where m_k is truck payload (for the kth truck), V_b is bucket rated capacity, f_q is fill factor, ρ_k is bucket density (one value for all of the passes in one truck), q is bucket pass and p is the maximum bucket pass to fill the truck tray. In this simulation bucket bulk density (ρ_k) and fill factor (f_q) are randomly selected by the Mont-Carlo simulation engine.

Decision variables

In completed discrete event model three decision variables have been defined. These variables are u_k, s_k and $n_{i,k}$.

$$u_k = \begin{cases} 1 & \text{If } Truck_k \text{ is in first segment} \\ 0 & \text{Otherwise} \end{cases} \tag{4}$$

$$s_k = \begin{cases} 1 & \text{If } Truck_k \text{ is in last segment} \\ 0 & \text{Otherwise} \end{cases} \tag{5}$$

$$n_{i,k} = \begin{cases} 1 & \text{If } V_{i,k} > V_{i,(k-1)} \\ 0 & \text{Otherwise} \end{cases} \tag{6}$$

To create a practical model, it is necessary to define some functions based on the above mentioned decision variables.

Objective functions

In this section, the objective functions for cycle time and traveling time have been presented in Equation 7 and Equation 8.

$$(\text{Cycle Time})_k = t_S + t_L + \sum_i t_{(T)_i} + t_M + t_D + (t_S + t_L)W_{okj}u_k + (t_M + t_D)W_{Lkj}s_k \tag{7}$$

Where:

t_s :   Spotting time;

t_L :   Loading time;

t_T :   Travel time;

t_M :   Manoeuvring time;

t_D :   Dumping time;

W_{0kj} :   Number of trucks at queue in front of truck k at time j in the first segment;

W_{Lkj} :   Number of trucks at queue in front of truck k at time j in the last segment;

u_{k} : First decision variables; and

s_k : Second decision variables.

$$t_{(T)_{i,k}} = \sum_i \frac{2X_i(V_{(i+1),(k-1)} - V_{(i-1),k})}{V_{(i+1),(k-1)}^2 - V_{(i-1),k}^2} n_{i,k} + \frac{2X_i(V_{i,k} - V_{(i-1),k})}{V_{i,k}^2 - V_{(i-1),k}^2}(1 - n_{i,k}) \tag{8}$$

Where:

$t_{(T)i,k}$:   Travel time for truck k in segment i;

X_i : The length of segment i;

$V_{i,k}$: The velocity of truck k in segment i;

$V_{(i-1),k}$:   The velocity of truck k in segment i-1; and

$n_{i,k}$: Decision variable.

The effect of truck bunching on hauled mine materials in each shift can be estimated by Equation 9.

$$\text{Hauled min e materials} = \sum_{r}\sum_{k} \text{payload}_{k,r} / \text{shift time}$$

(9)

Where:

Payload $_{k,r}$:The payload of truck k in cycle r.

Fuel Consumption simulation

Haul truck fuel consumption is a function of various parameters. The key parameters that affect the energy consumption of haul trucks include the payload management, the model of the truck, the grade resistance and the rolling resistance, according to a study conducted by the Department of Resources, Energy and Tourism(EEO, 2012). In the present study, the effects of the GVW, the truck velocity and the Total Resistance (TR) on the energy consumption of the haul trucks were examined. The TR is equal to the sum of the Rolling Resistance (RR) and the Grade Resistance (GR) when the truck is moving against the grade of the haul road.

$$TR = RR + GR$$

(10)

Figure 4 presents a schematic diagram of a typical haul truck and the key factors that affect the performance of the truck such as the GVW, RR, gradient, friction force and Rimpull Force (RF).
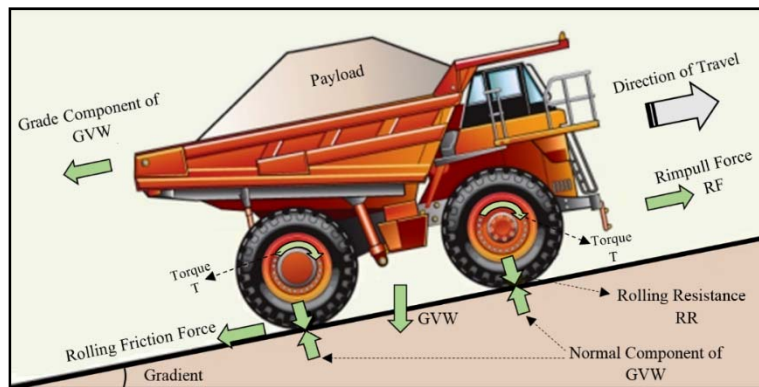
Figure 4: A schematic diagram of a typical haul truck

RF is the force available between the tyre and the ground to propel the machine. It is related to the Torque (T) that the machine is capable of exerting at the point of contact between its tyres and the ground and the truck wheel radius (r).

$$RF = \frac{T}{r}$$

(11)

The truck fuel consumption can be calculated from Equation 3(Filas, 2002):

$$FC = \frac{SFC}{FD} (LF. P)$$

(12)

Where SFC is the engine specific fuel consumption at full power (0.213–0.268 kg/kw.hr) and FD is the fuel density (0.85 kg/L for diesel). The simplified version of Equation 3 is presented by Runge(2005):

$$FC = 0.3 (LF. P)$$

(13)

Where LF is the engine load factor and is defined as the ratio of average payload to the maximum load in an operating cycle(Kecojevic and Komljenovic, 2011). P is the truck power (kW). For the best performance of the truck operation, P is determined by:

$$P = \frac{1}{3.6}(RF.V)$$ (14)

Where the RF is calculated by the product of Rimpull (R) and the gravitational acceleration (g). V is calculated by Equation 15.

$$V = a - b \times \exp(-c \times R^d)$$ (15)

Where a= 53.867, b= 54.906, c= 37.979 and d= -1.309.

In this paper, DataThief 5.6 and Curve Expert 2.1 were used to find an equation for R as a function of TR and GVW based on the Rimpull-Speed-Grade ability curve.

$$R = 0.183\,GVW\,(0.006 + 0.053\,TR)$$ (16)

The developed model, in this project, can simulate the fuel consumption by haul trucks based on the above mentioned formulas.

Greenhouse gas emissions

Diesel engines emit both Greenhouse Gases (GHG_S) and Non-Greenhouse Gases ($NGHG_S$) into the environment(Aziz and Kecojevic, 2008). Total GHG emissions are calculated according to the Global Warming Potential (GWP) and expressed in CO_2 equivalent or CO_2 - e.
The following equation can be used to determine the haul truck diesel engine GHG_S emissions(ANGA, 2013).

$$GHG_{Emissions} = (CO_2 - e) = FC \times EF$$ (17)

Where FC is the quantity of fuel consumed (kL) and EF is the emission factor. The emission factor for haul truck diesel engines is 2.7 t.

Model Validation

Model validation is a main part of this project. To validate the developed model a dataset collected from a large open pit mine in the central part of Arizona State, USA has been applied. This dataset included measuring loader payloads, truck payloads, bucket bulk density, fill factors and swell factors (Table 1).

Table 1: A sample of data collected for model validation

NO	Average Loader Payload (tonne/pass)	Truck Payload (tonne)	Average Bucket Bulk Density (tonne/m³)	Loader Bucket Fill Factor	Average Swell Factor
1	47.23	218.21	2.01	0.937	1.25
2	45.12	217.46	1.98	0.978	1.22
3	38.14	209.42	1.96	0.919	1.18
4	42.15	210.36	2.03	0.954	1.27
5	46.58	216.78	2.14	0.984	1.19
6	47.56	217.96	1.86	0.927	1.26
7	39.87	218.04	2.07	0.946	1.24
8	38.47	218.43	2.18	0.992	1.25
9	42.58	217.69	2.05	0.957	1.20
10	40.59	216.97	1.99	0.939	1.25

In this mine, the volume of material loaded into the bucket was determined by comparing loaded and empty laser scan profiles of the buckets. Fill factors were calculated by dividing the material volume by the rated volume of the bucket and bulk densities were calculated by dividing the payload by the loaded volume. On-board payload monitoring systems were used to measure payloads. The validation of model has been completed for average cycle time and the average of mine material hauled by one type of truck (CAT 793D) after truck bunching. The test results of the developed model are shown in Figure 5.
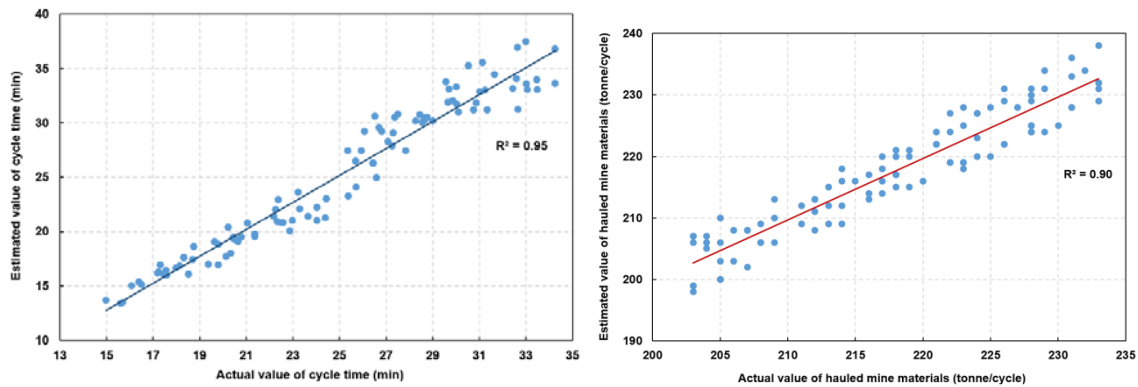
Figures 5a & 5b: Comparison of actual values of cycle time and hauled materials with model outputs

The results indicate good agreement between the actual and estimated values of average cycle time and average hauled mine materials.

CASE STUDY

In this project, a real mine site dataset that was collected from a large surface mine in central Queensland, Australia has been analysed. In this case study, Talpac^{TM} and MATLAB software have been used to develop the model. The effect of truck bunching due to payload variance on average cycle time and average hauled materials are illustrated in Figure 6. In this figure, the standard deviation indicates the payload variance changes from 5 to 30.
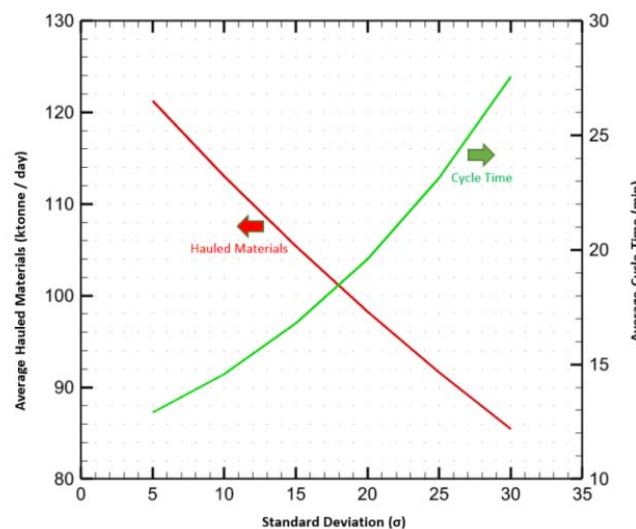
Figure 6: The effect of payload variance on average cycle time and average hauled materials

Figure 6 demonstrates that, there is a non-linear relationship between standard deviation and average cycle time in the fleet. This figure also illustrates the relationship between the standard deviation (σ) and average hauled materials. Finding the best correlation between the standard deviation and average hauled materials can be very important in calculation of the effect of truck bunching due to payload variance on productivity and production cost. Hence, the following equation has been developed to estimate the hauled mine materials based on the payload variance.

$$\text{Hauled Materilas} = 130 \times \exp(-0.014\sigma) \tag{18}$$

The effect of payload variance on haul truck fuel consumption in different haul road conditions is illustrated in Figure 7. In this figure, the total resistance has been changed from 5% to 30% and the payload standard deviation is varied between 0 and 30. It is noted that, to have a better understanding, a fuel consumption index (FC_{Index}) has been defined. This index presents the quantity of fuel used by a haul truck to move one tonne of mine material (Ore or Overburden) in an hour.
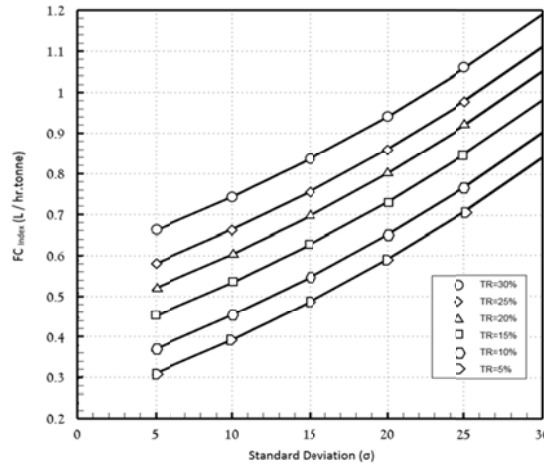
Figure 7: The effect of payload variance on haul truck fuel consumption in different haul road conditions (TR= Total Resistance)

Figure 7 demonstrates that there is a non-linear relationship between the standard deviation and the fuel consumption for all haul road total resistance. Moreover, the FC_{Index} rises with increasing the total resistance.

The variation of CO_2-e with standard deviation for CAT 793D is presented by CO_2-e_{Index} in Table 2. In this table CO_2-e_{Index} presents the amount of GHG emission generated by truck to haul one tonne of ore or overburden in an hour.

Table 2: The variance of CO_2-e $_{Index}$ (kg/hr. tonne) with standard deviation (CAT 793D)

σ \ TR	5%	10%	15%	20%	25%	30%
5	0.83	0.99	1.21	1.40	1.56	1.78
10	1.06	1.22	1.43	1.62	1.78	2.00
15	1.31	1.47	1.68	1.87	2.04	2.25
20	1.59	1.75	1.97	2.16	2.32	2.53
25	1.91	2.07	2.29	2.47	2.64	2.85
30	2.27	2.43	2.64	2.83	2.99	3.21

Based on the tabulated results, it is obvious that there is a non-linear relationship between the CO_2-e_{Index} and the standard deviation for each haul road total resistance. The minimum greenhouse gas is emitted for the minimum total resistance (TR=5%) when the standard deviation has been zero (σ=0) and the maximum pollution is generated for the maximum total resistance and standard deviation (TR=30% and σ=30).

CONCLUSIONS

This paper aimed to develop a discrete event model to simulate the effect of payload variance on truck bunching to minimise energy consumption and greenhouse gas emissions. There is a significant payload variance in the loading process in surface mines. The main reason for truck bunching in this type of mine is the variance of payload. In this paper, an innovative simulation model was developed to investigate the effects of payload variance on truck bunching, mine operation efficiency, decreasing the fuel consumption and reducing greenhouse gas emissions by haul trucks. To validate the developed

model a dataset collected from a large surface mine in the central part of Arizona State, USA was used. Validation of the model was completed for the cycle time and the hauled mine materials by one type of truck (CAT 793D) after truck bunching. The results indicated a good agreement between the actual and estimated values of cycle time and hauled mine materials. The model was utilised in a real mine site in Australia as a case study. The results of this project showed that there is a non-linear relationship between standard deviation and cycle time in the fleet. In this case study, a correlation between the standard deviation and hauled mine materials was developed and the effects of truck bunching due to payload variance on energy consumption and greenhouse gas emission were studied.

ACKNOWLEDGMENTS

REFERENCES

ANGA, 2013. *National greenhouse accounts factor.s*

Aziz, N and Kecojevic, V. 2008, The CO2 footprint of the US mining industry and the potential costs of CO2 legislation, *The International Journal of Mineral Resources Engineering*, 1(2):111-129.

Banks, J, Carson, J, Nelson, B and Nicol, D. 2010, *Discrete event System simulation', Pearson Education*New Jersey, USA).

Byoung, K and Donghun, K. 2013, *Modeling and Simulation of Discrete-Event Systems* (John Wiley and Sons, Inc: New York, USA).

Cetin, N. 2004, Open-pit truck/shovel haulage system simulation, Middle east technical university.

K H Concannon, Hunter, K I and Tremble, J M, 2003, *Simul8-planner simulation-based planning and scheduling.*

DOE. 2002, *Energy and environmental profile of the US mining indusdry*.

EEO. 2012, *Analyses of diesel use for mine haul and transport operations, Australia*.

Ercelebi, S and Bascetin, A. 2009, Optimization of shovel-truck system for surface mining, *The Journal of The Southern African Institute of Mining and Metallurgy*, 109:433-439.

Filas, L. 2002, *Excavation, loading, and material transport*.

R Hewavisenthi, Lever, P and Tadic, D, 2011. *A Monte Carlo simulation for predicting truck payload distribution*

Kamrani, M, Hashemi, S M and Rahimpour, S. 2014, Traffic simulation of two adjacent unsignalized T-junctions during rush hours using Arena software, *Simulation Modelling Practice and Theory*, 49:167-179.

Kecojevic V and komljenovic, D. 2011, Impact of bulldozer's engine load factor on fuel consumption, CO2 emission and cost, *American Journal of Environmental Sciences*, 7:125-131.

Knights P and Paton, S. 2010, *Payload variance effects on truck bunching*.

Limsiri, C. 2011, Optimization of loader-hauler fleet selection, *European Journal of Scientific Research*, 56(2):266-271.

Muller, D. 2011, *Automod™ - Providing simulation solutions for over 25 years*.

Paton, S. 2009, Truck bunching due to load variance, The University of Queensland, Australia.

Raj, M, Vardhan, H and Rao, Y. 2009, Production optimization using simulation models in mines: a critical review, *International Journal of Operational Research*, 6(3):330-359.

Runge, I. 2005, *Mining economics and strategy*, 3 ed (Littleton Co: USA).

Schexnayder, C, Weber, L and Brooks, T. 1999, Effect of truck payload weight on production, *Jurnal of Construction Engineering and Management*, 125:1-7.

Singh, S and Narendrula, R. 2006, *Productivity indicators for loading equipment*.

Stout, C E, Conrad, P W, Todd, C S, Rosenthal and SKnudsen, H P. 2013, Simulation of a large multiple pit mining operation using GPSS/H, *International Journal of Mining and Mineral Engineering*, 4(4):278-295.

Webb, B. 2008, Effects of bucket load distribution on performance, The University of Queensland, Australia.

White J and Olson, J. 1992, *On improving truck/shovel productivity in open pit mines*.

DEVELOPMENT AND IMPLEMENTATION OF A GEOTECHNICAL DATABASE MANAGEMENT SYSTEM

Sean Keen[1], Alex Hossack[2] and Mehmet S Kizil[1]

ABSTRACT: Geotechnical Engineering is classified by many mining companies as the highest corporate, investor and operational risk associated with the development and successful exploitation of a mineral resource. Given the shift in culture towards geotechnical engineering and the influx of new exploration projects, the quantity and complexity of geotechnical data is increasing at exponential rates. Unfortunately, in some cases, data management techniques have lagged behind data capture processes, resulting in relatively primitive technologies to store highly sensitive and costly data. Under these primitive systems, there is no quantifiable handling on the quantity or quality of geotechnical data. The rollover effects of poor data management standards are significant and in severe cases, areas require redrilling or revaluation to capture lost data. The aim of this project was to capture, extract and upload geotechnical data into an easily accessible, single source geotechnical database. Using Rio Tinto Coal Australia (RTCA) as a case study, the project formed a framework for future database implementations by outlining the systematic project progression from data extraction to population and application of the database. By providing a single source database, frequent engineering tasks at RTCA were automated which significantly increased engineering efficiency and accuracy. Additionally, comprehensive Quality Assurance and Quality Control (QAQC) checks improved overall data integrity, resulting in enhanced data confidence.

INTRODUCTION

Geotechnical engineering is a relatively young field of expertise in the resource industry (Harrison and Hudson, 2007). In its most simplistic form, geotechnical engineering involves the acquisition of geological, structural, hydrogeological and geomechanical data to feed a geotechnical model (Hanson, Thomas and Gallagher, 2005). This geotechnical model forms the basis of decisions surrounding pit geometry, slope and batter angles, mining method and equipment selection and plays a factor in virtually all other strategic planning decisions (MOSHAB, 1997). Due to the inherently anisotropic and inhomogeneous geological makeup of resource deposits, huge data sets are required to accurately depict geotechnical behaviour over a single mine site. These data sets require extensive exploration drilling programs and subsequent laboratory and geophysical analysis of the samples (Hanson, Thomas and Gallagher, 2005). The extensive coring and drilling involved to obtain geotechnical data incurs enormous capital and operational costs to companies, rendering any subsequent datasets extremely valuable.

Rio Tinto Coal Australia (RTCA)'s Orebody Knowledge (OBK) team is responsible for the collection and management of geotechnical data for Rio Tinto's five coal mines and nine exploration projects in New South Wales and Queensland. Presently, the data captured from field and laboratory investigations are kept in servers, archives and libraries. Under the current system, there is no quantifiable handling on the quantity or quality of geotechnical data, resulting in significant and costly rollover effects. The Geotechnical Database Management System (GDMS) is designed to capture and update the existing geotechnical database with relevant information from RTCA archives, servers and libraries. Relevant information will be extracted from digitised and electronic documents and uploaded into the database system. At a minimal cost to RTCA, the new database will aim to collate all existing data into a single database and provide secure storage of highly valued information. The database will undergo a strict validation process prior to and following the population of the database to ensure the entries fall within acceptable limits, do not contain errors and allow for effective modelling.

Implementing a geotechnical database, at a minimal cost, has huge cost benefits for Rio Tinto. By securing the geotechnical data into a readily available database management system the risk of losing and/or corrupting data is almost negligible. By removing this risk, the need to redrill or revaluate areas would be extremely rare. Furthermore, by creating a single source database, engineering efficiency will increase significantly and allow for superior geological and geotechnical models. By reporting the pitfalls

[1] *School of Mechanical and Mining Engineering, The University of Queensland, Queensland, Australia, E-mail:* m.kizil@uq.edu.au
[2] *Rio Tinto Coal Australia, 123 Albert Street, Brisbane QLD 4000; Tel (H) +61 07 38787612 +M: 0450 906 307*

and inefficiencies of the project and outlining recommendations, the process can be streamlined and a framework for future projects can be drafted. Figure 1 shows the slope failure occurred at Bingham Canyon mine in 2013. Such events may be detected earlier and be avoided with the availability of better geological and geotechnical models.

Figure 1: Slope instability causing landslide, Bingham Canyon (Pankow *et al.,* 2013)

Following the implementation of the database, the system will be used to source a drill and blast fragmentation model with geotechnical data for RTCA's open cut mines. The model will output fragmentation distributions based on the information provided by a live link to the database. The model will serve as a useful tool for site drill and blast engineers and demonstrate the benefits of the database to disciplines outside the realms of geotechnical engineering.

GEOTECHNICAL DATA IN MINING

Before a geotechnical database can be scoped and implemented, the geotechnical data required for the database must be identified. For population and implementation purposes, simply identifying the parameters is not enough. For a database to undergo a population and implementation stage with rigorous validation, the data and the format of the data needs to be understood. Additionally, crucial metadata – data relationships must be recognised to ensure data within the database retains fundamental explanatory information.

Geomechanical Data

Geomechanical data aims to quantify the intrinsic strength of rock specimens gathered through field sampling. The data gathered from geomechanical testing forms the essential inputs for numerical and empirical design tools (Hadjigeorgiou, 2012). These design tools identify areas within a mine that are susceptible to instability or require increased support and reinforcement infrastructure. Hoek (1994) cautioned that inadequate emphasis placed on the collection of geomechanical data can result in data limited models and designs. With limited data, highly advanced and technical models cannot operate at desired accuracy levels. Hence, any design modelling requires significant quantities of geomechanical data to accurately gauge the strength of the geological formation. Unfortunately the process to acquire and test specimens for geomechanical data is costly though any subsequent data is highly valuable.

Field Test Data

Field data refers to the information captured on site through manual and automated logging as well as *in-situ* tests not specifically related to hydrogeological data. The majority of field data is captured during exploration drilling where geologists and geotechnical engineers log information regarding the extracted core (Harrison and Hudson, 2007). The highly manual task produces detailed logs of grain size, lithology, defects, strength and overall appearance of rock mass down-hole. These logs form the basis of geological models and rock domain classifications. The labour intensive process has a high risk of human error and the logs depend heavily on the skill of the geologist or geotechnical engineer. When

establishing a database, terminology standardisation is paramount to ensure consistency across logs and to support electronic data validation processes.

Hydrogeology Data

Hydrogeology is a broad term used to describe issues related to ground and surface water. Atkinson, Dow and Brom (1984) postulated that ground water issues in mining operations take two general forms:

1. Engineering associated challenges relating to seepage forces, water inflow, piping and slaking; and
2. Environmental controls identifying the effect of mining on the water table, water quality and nearby water resources.

The data formats vary greatly for different hydrogeological tests, however the testing can usually be classified as either monitoring or discrete in-situ testing. Water levels, quality readings, seepage rates and hydraulic forces can all be measured continuously under monitoring type scenarios or as a discrete measurement.

Geotechnical Monitoring Data

Monitoring data is associated with the surveillance of engineering structures, either visually or through instrumentation. Brady and Brown (2004) proposed monitoring data, in a geotechnical context, is carried out for one of four main reasons:

1. To record the variation in geotechnical parameters such as water table level and seismic activity;
2. To ensure safety during development and operations by alerting management to excessive ground deformations, groundwater pressures and loads;
3. To control and ensure the stability of ground reinforcements and remedial works; and
4. To check the validity of assumptions, conceptual models and rock mass properties.

Although monitoring data is cheap to acquire, the time dependent and non-repeatable nature of the data renders the information extremely valuable. Additionally, the continuous data capture associated with monitoring means the subsequent data is significant in quantity.

Legacy Data

Legacy data is defined as information that is 'inactive' – stored in physical or electronic format and is not currently understood, used or managed (Perez *et al.,* 2002). Companies dealing with existing geotechnical information in a legacy format are required to undergo a process of inventory, extraction and migration of the data. This process fosters successful population of the geotechnical database utilising structured QAQC processes.

GEOTECHNICAL DATA MANAGEMENT

Companies and contractors that deal with large sets of geological and geotechnical data often struggle with storing, recalling and manipulating data in an accurate and efficient manner. Data management tools are available, however the quality of these tools vary, as does the quality of the data stored within them. Many systems lack the proper validation, interrogation and querying capabilities required to maintain an effective and accurate database. Bad experiences and rudimentary thinking has resulted in companies storing data in excel spreadsheets or in poorly organised servers and archives (Caronna, 2010). In some veteran departments, the use of paper-based reports is common practice which is becoming increasingly impractical as projects become larger and more advanced (Caronna, 2010).

An advantage of a GDMS is the ease in which data can be viewed, filtered and manipulated. Furthermore, through business rules, data validation and thorough QAQC processes the risk of inaccurate information is greatly reduced. A properly designed database will only require data to be entered once, eliminating the need for re-entry and reformatting. A study performed by Goldin *et al.,* (2008) showed on average 1.24% of data entries in excel are entered incorrectly; the error then compounds every time the data is re-entered. The 'single entry multi-use' set up of a well-designed

database reduces human transcription errors which is a major source of inaccuracy for companies dealing with large quantities of geotechnical data (Antoljak and Caronna, 2012).

Reportbase vs Database

Understanding the importance of a GDMS is an important first step to successful data management, however, the development of a database system is not as intuitive as it may seem. Caronna (2006) discussed a common pitfall that geotechnical engineering firms encountered during the implementation of a GDMS. Caronna used the term 'reportbase' to describe databases designed for the sole purpose of generating specific reports. Companies that followed this line of thinking created a disparity between the raw data and the formatted information within the database. This was a result of the extensive use of computer aided design (CAD) software, excel and word programs to enter data into the database, creating formatted information for specific reporting needs. This approach to database implementation limited the usability and functionality of the data.

The defining characteristic of a reportbase, as outlined by Caronna (2006), is the structure of the database mimicking a one-to-one image of the desired report. The advantage of this layout revolves around the simplicity of setup, the ease of use and the uncomplicated table arrangement. Despite the simplicity, data in this form had limited to no reusability, no electronic validation and limited automation.

Caronna (2006) described that a database, in its truest form, contains data free from the constraints of formatting, where each individual parameter is captured in its own field. The unformatted, but controlled layout allows data to be easily queried and manipulated into reports, graphs and tables for a broad range of functionalities. The configuration of the database tables does require a reporting engine and increased querying capabilities to manipulate the data into the desired format. The higher database complexity requires increased design work and generally an increased implementation cost (Caronna, 2006). The increased complexity and cost of the database is more than offset by the advantages of this configuration, most notably:

- Database contains data, not formatted information;
- Data reusability;
- Improved querying functionality;
- Electronic validation;
- Enforced standardisation of data descriptions; and
- Electronic data capture.

Quality Assurance and Quality Control

QAQC of data is an essential process to ensure the integrity and accuracy of any database. An effective QAQC system identifies the key errors associated with the data and employs controls and risk management techniques to mitigate or fully eliminate the issue, with the ultimate goal to perform modelling or design work without unacceptable influence of inaccurate entries. The key errors associated with geotechnical data are not attributable to one source and an effective system takes into account a broad range of possible errors, most notably (Baecher, 1987):

- Human incompetency/error;
- Sample degradation;
- Data tampering;
- Laboratory errors;
- Mislabelled information;
- Unrepresentative values; and
- Data entry errors.

Extensive literature regarding QAQC processes is widely published in both print and electronic formats. A brief summary of important QAQC practices for geotechnical data management are outlined in Figure 2.

CASE STUDY

A database management system was created using data collected from all existing RTCA mines and development projects. The sites are located in the Bowen Basin in Queensland and the Hunter Valley in New South Wales. The geographic spread of sites and complexity of the legacy data provided a good basis for determining a robust system for the development of a database management system. The

creation of the database was conducted in successive stages, which allowed the process to be broken down and successfully managed throughout the entirety of the project. The eight stages were:

- Data collation;
  - Business rules
  - Data inventory;
  - Data extraction;
  - Database scoping study;
  - Database implementation;
  - User acceptance testing; and
  - Data migration.

Data tracking	• Monitor changes. • Promote accountability.
Data licensing	• Limit manager licenses with data manipulation capabilities.
Data confidence	• Data prioritisation to categorise data entry. • Database search only retrieves information with highest priroitisation. • Ability to superseed previous entries without deleting.
Duplicate data	• Dupllicate data tracking to ensure repeated data is elminated. • Compare incoming data to existing data entries.
Required fields	• Assigning required fields alleviates the threat of unusable data due to missing metadat. • Ensures all mandatory fields contain data.
Referential integrity	• Assess and interrogate data by setting up relationships between data types (i.e. lithology vs density and UCS vs derived sonic UCS).

Figure 2: Important QAQC processes for a GDMS

Data Collation

Data collation was performed progressively through March to May 2014, where all pertinent geotechnical information was compiled onto a single server. The majority of the geotechnical data existed on site specific servers and within existing repositories on the RTCA Brisbane corporate server. A total of 64,334 electronic geotechnical data files were collated and sorted into corresponding project codes over a period of ten weeks. The Rio Tinto archives were also searched to retrieve any applicable information utilising key search words i.e. geotechnical, groundwater and geomechanical. In total, 947 files in hardcopy format were scanned and the subsequent electronic files collated and sorted according to site.

Business Rules

Individual business rules were created for all possible geotechnical parameters and their related units to ensure inventoried and extracted datum was entered under the correct heading and followed accepted data values. Additionally, dictionary codes and reference tables were created for some fields to ensure standardisation of terms throughout the database. By reducing the spread of possible entries and enforcing consistency, the database had dramatically improved querying and reporting capabilities.

Data Inventory

The physical data inventory process was outsourced. The data inventory process began on the 15th of April and concluded on the 11th of July. During the process 11,004 files were inventoried, with weekly deliveries of ~2000 reports over the three month period. The data inventory process created a detailed list of files and the information contained within each data file. Data types were prioritised based on necessity and strategic impact to the business. Interoperability of data types was also a significant driver

in the selection of inventoried files. The process was controlled using inventory headings and a thorough QAQC process.

Data inventory headings were created to act as a template for the inventory process. Geotechnical data types were classified into 44 umbrella headings which represented the column headers for the inventory sheet. When a data file contained relevant geotechnical information, a Y was scribed underneath the corresponding column header, to signify this type of data existed within the file. Each new data file was captured on a new row in the data inventory sheet. In the case where multiple boreholes exist within the one data file, each new borehole was captured on a new row under the same file name. All inventoried files were subject to stringent QAQC checks by the inventory team and once the delivery had been made to RTCA.
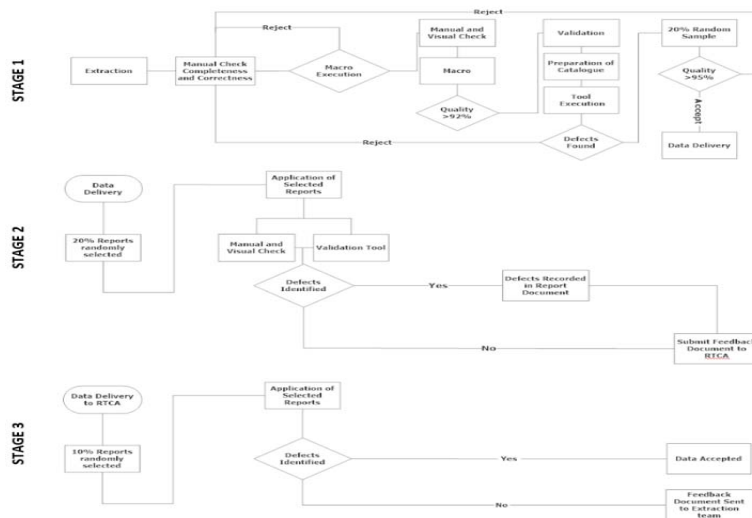
Data Extraction

The data extraction phase aimed to extract all relevant geotechnical information from selected files under data extraction headings. Similarly to data inventory, the extraction process was outsourced, however, duplicate files were identified during the inventory stage, and as such not all inventoried files required extraction. The data extraction process began on the 2nd of July and is expected to conclude on the 16th of January. During the process 6,401 files are scheduled for extraction, with fortnightly deliveries of ~500 reports over the seven month period. Like the inventory process, data extraction was controlled using extraction headings and a comprehensive QAQC process.

A total of 541 headings were created, each tasked with capturing a particular piece of data. The extraction headings acted as column headers and the relevant data was entered into the corresponding column. Each new data file was entered on a new sheet and files with more than one borehole or files containing numerous datasets were entered on separate rows. Additionally, the extraction heading sheets were used as a template for the legacy importer objects, successfully eliminating the need for further data manipulation.

The manual nature of data extraction can lead to extensive human transcription errors within the geotechnical data. Three QAQC stages were implemented during data extraction to ensure data integrity was maintained, the full QAQC flowchart is summarised in Figure 3. Maskell (2014) outlined the first stage of quality control used for the extraction of RTCA's legacy data, identifying five QAQC checks throughout the extraction phase, these are:

1. Manual check for completeness and correctness of data;
2. Quality control check of 100% of the extracted data (quality must exceed 92%);
3. Electronic validation of data (0% defect tolerance);
4. Quality assurance check of 20% data sample (quality must exceed 95%); and
5. Electronic validation against business rules (0% defect tolerance).

Figure 3: Data extraction QAQC flowchart

Should any of the data checks fail, the data flows back through the process to fix inaccurate data and remove defects. The process ensures not only data accuracy, it fosters data totality by certifying all relevant data is captured. During the extraction of RTCA legacy data, 20% of the personnel allocated to data extraction were exclusively assigned to QAQC to ensure the process was thorough.

When data passed the QAQC checks, the files progressed to a separate team of analysts to perform quality assurance on an additional 20% of randomly selected files forming stage 2 of the QAQC pocess. The extracted data was cross referenced against the business rules and specification documents to ensure accuracy. If defects were present, a feedback document was constructed and sent to RTCA with the extracted files. If the defects proved to be a systemic issue, the data was typically recirculated through the entire extraction process.

The data packages sent to RTCA were subject to a final QAQC process undertaken by the OBK team. Of the extracted files, 10% were randomly selected and checked to ensure all data was captured and accurate. Files containing errors were corrected and feedback was provided to ensure accuracy was maintained. If errors were unacceptably high, the batch would require re-extraction.

Database Scoping Study

Prior to implementation of the database, a scoping study was conducted to personalise the database to RTCA's specific customary requirements. The scoping study outlined the most effective workflow for the database implementation to satisfy the habitual necessities of the RTCA legacy data and the required outputs. The solution of the scoping study addressed three fundamental aspects of the technical deployment:

1. People – the roles required to run the system;
2. Process – workflow and practices to optimise data management; and
3. Technology – technological components that the implementation will be based upon.

Database Implementation

The implementation process was undertaken after the completion of the scoping study, ensuring the key attributes outlined within the scope were included to produce the proposed workflow. A relational database structure was chosen for the GDMS using a process known as data normalising. Under a relational database system, data is identified and placed in relevant tables with strict rules governing duplication of data through identification of uniqueness. Data uniqueness was controlled by primary keys which consist of one or more fields in a table. A primary key is completely unique to a data entry and cannot be repeated in any other data set. For example, when describing collar data, the hole ID and project code fields were used as the primary keys, as no two boreholes have the same entries for these two fields. Any primary key consisting of two or more fields are referred to as composite keys.

Given that relational databases place data in separate tables, it is also important that correlated data in separate tables be linked together using a derived relationship. A derived relationship links data to metadata or dependant data, forming a parent – child table relationship. This relationship is defined using a foreign key which enforces referential constraint by referencing a key field in the child table which relates it to the parent table. By normalising data into parent – child relationships, data integrity is enforced and the possibility of redundant data is eliminated.

User Acceptance Testing

Database acceptance testing was carried out during the implementation of the database, to ensure objects within the database were up to standard. During testing the functionality, layout and aesthetics were evaluated, and were only accepted into the database once approval was granted. User acceptance testing was also carried out after the completion of the database implementation phase and during data migration to ensure objects were fit for purpose and to minimise or altogether mitigate start up issues.

Data Migration

The migration of the RTCA legacy data was the first step involved in populating the database. Using the extraction sheets completed by Cyient, the data was transferred into the database using the legacy template importers. Given the age and complexity of the data, a number of issues were encountered during the migration phase of the project which are summarised in Figure 4.

The legacy template importers were created to support the populated extraction sheets. Creating importers that could populate the database without further data manipulation offered significant costs benefits and reduced the likelihood of human transcription errors. An importer was created for every extraction sheet, which was capable of reading multiple rows of data from the CSV file.

Additionally, fourteen import objects were built for the project, tasked with identifying and performing a defined expression on the data, and subsequently writing it into the database. Import objects differed to the legacy template importers, in this case, the data being loaded does not follow the extraction sheet template.

Inconsistent datum's	• Different coordinate systems used for data given the age and geographical spread of information.
Missing collar data	• Lare amounts of data exisiting without relevant collar or coordinate information. • Coordinate information was recovered from previous systems.
Continuation in lithology files	• Lithology files used continuation, where the same interval was split over multiple rows. • Required altercation to existing importer.
Data truncation	• In some cases data was too long and required truncation to fit within specified character limits.
Undefined lithology codes	• Lithology codes that were not defined in the dictionary codes.
Discrepancies between data	• Drilling times (start times later than end times). • Different logged depths for geophysics, geotechnical logs and lithology logs for same hole.

Figure 4: Legacy data issues discovered during data migration

Generally, data entered through an import object is computer generated with numerous entries in a set form i.e. geophysical LAS files. Extracting and manually writing this information into the legacy template would be time consuming and inefficient. Therefore, import objects were created to read the data from the original file type, as such the data must follow a predetermined template which can be viewed in the individual importer objects.

Finally, data entry tools were used for data types that could not be entered via importers, or for entries where importers were inefficient. Each data entry tool was strategically designed to incorporate validation rules to ensure data integrity was maintained.

Database Outputs

With the database successfully populated, the functionality of a relational database now becomes an issue for querying and viewing data. Whilst code and relational tables provide an efficient mechanism for storing site specific attributes, information presented in this format is not intuitive or easy to comprehend. To aid viewing, the database is 'flattened' so that field names appear as column headers and their values appear in the associated column. The GDMS database provides the means to flatten using a feature known as compound definitions. Compound definitions create a view accessible through user specified filters. Data accessible through compound definitions are not stored in the database as a distinct object, rather a 'SELECT' statement which is triggered by the user forming the view.

In the GDMS Project, views were created through a separate program to the core database. The program incorporates an intuitive 'drag-and-drop' functionality with inbuilt filters to mould a table to specific requirements and purposes. For specific data outputs that are frequently required, a form object within the database workspace can be created.

DATABASE APPLICATION – FRAGMENTATION MODEL

Fragmentation models are an important feature of drill and blast designs. The model acts as a cheap tool for engineers to evaluate and compare outputs from different blast designs. All models require input relating to bench parameters (spacing, burden and hole diameter) and explosive properties, the somewhat uncontrollable error in models originates from the input of geotechnical and geological data. Rock mass by its very nature is inhomogeneous and anisotropic, hence assigning a global value for faults, joint spacing, UCS and other properties is a necessary, and all be it, inaccurate assumption (Kanchibolta, Morrell and Valery, 1999).

Fragmentation models can be generalised into two main categories; empirical models and numerical models. Numerical models follow a mechanistic approach, tracking the physics of detonation in well-defined rock mass for specific blast geometries. This type of model requires very specific and detailed data regarding detonation, the rock mass and the end result. Empirical methods offer a more generalised model which is more suitable for daily blast design. The Kuz-Ram empirical model is one of the most established simulation, used for its simplicity for garnering data, simple calculations and clear outputs (Cunningham, 2005). The Kuz-Ram algorithms are easily incorporated into spreadsheets for ease of modelling, Figure 5 is an Excel fragmentation model created for RTCA.
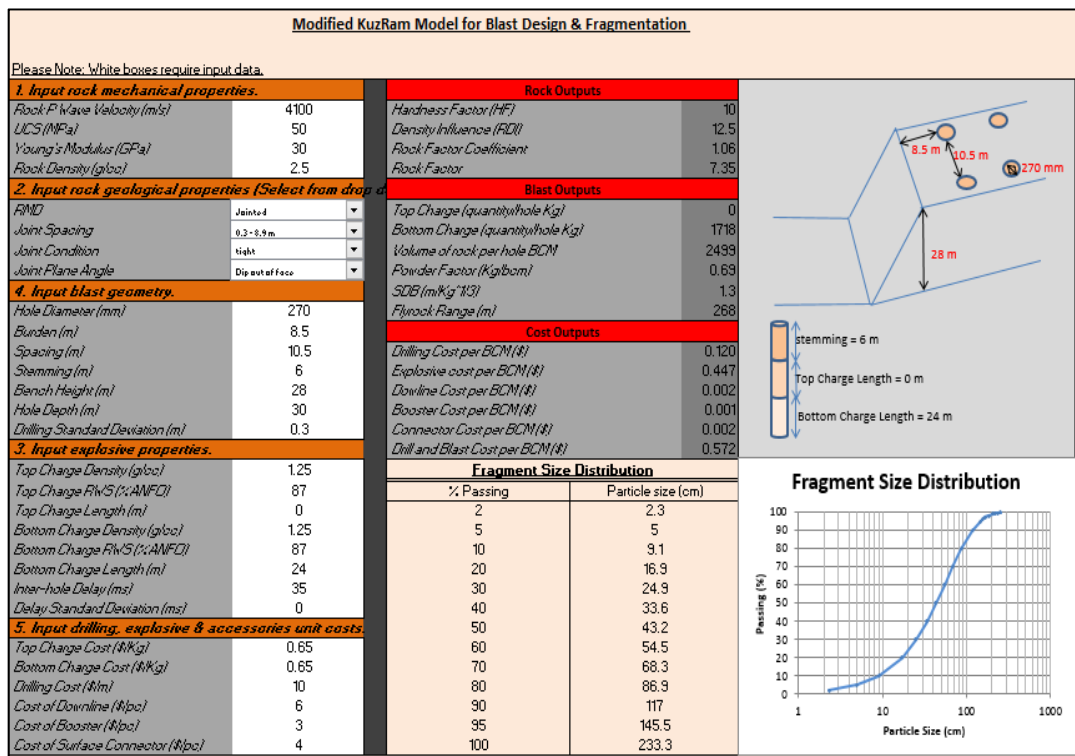
Figure 5: RTCA Kuz-Ram fragmentation Model

Advantages of a Fragmentation Model

Drilling and blasting of a rock mass is used to condition rock and ore for extraction and is the first phase of the comminution process. The Run Of Mine (ROM) fragmentation is considered ideal, from an operations stand point, if the dig rates and haul requirements are satisfied. For this reason drill and blast engineers design blasts to meet the minimum fragmentation requirements of the operation. Although this approach maximises mining productivity relative to operational expenditure, it ignores the potential impact of downstream processing and the productivity of production equipment (Kanchibolta, Morrell and Valery, 1999).

A study conducted by Doktan (2001) reviewed the effects of blast fragmentation on truck and shovel fleet performance. The study showed better fragmentation resulted in the following operational improvements:

- Increased digability (up to 35%);

- Higher bucket payload (reduced void ratio and increased fill factor);
- Higher truck payload; and
- Reduced maintenance requirements on truck and shovel fleet.

Given the importance of proper fragmentation, the use of a fragmentation model can represent significant production and fiscal advantages to a business.

Creating a Live Link between the GDMS and the Fragmentation model

Even with inherent errors, the advantages of fragmentation models are considerable, however these models are often put in the too hard basket and dismissed.   The ability of drill and blast engineers to acquire the correct geotechnical information to accurately model a blast design is the most time consuming component of the process. Finding the information for a blast at a specific location can be a struggle and the data is often incomplete and inaccurate. When mines have multiple blasts a day, it is understandable that many sites do not utilise fragmentation models.

A Kuz-Ram script was created during the database implementation to query relevant geotechnical information for the fragmentation simulation. The algorithm queried two key types of geotechnical information to fulfil the requirements of the model, that is, geomechanical data and structural properties. Given the significant quantity of relevant information in the database, filtering the results for the blast zone was crucial. By outlining the coordinates of the blast through Easting, Northing and RL ranges the data was restricted to the blast horizon, limiting the geotechnical data to the most pertinent entries.

The RTCA geotechnical database system was linked to the Excel fragmentation model through an SQL database connection. The generated data could be dumped into the fragmentation model from any computer with access to the RTCA server and a current installation of SQL. Assuming the blast geometry and explosive data had previously been entered into the model, by refreshing the excel sheet a fragmentation distribution, drill and blast cost per BCM, peak particle velocity at nearest structure, and flyrock range was immediately generated using the updated geotechnical data.

CONCLUSIONS

The aim of this project was to capture, extract and upload RTCA's geotechnical data into an easily accessible, single source geotechnical database. At a minimal cost to RTCA, the database system aimed to increase data security and accuracy; allowing for more efficient engineering processes.

The GDMS at RTCA was used as a case study to document a systematic database implementation process from start to finish. The inventory and extraction processes were analysed, with significant emphasis placed on the development of specific business rules to ensure data integrity and totality was maintained. Furthermore, the manual nature of the data extraction process demanded intense QAQC procedures to limit human transcription errors. Three separate QAQC workflows were implemented to ensure the data was extracted correctly, involving re-extraction of random data samples to ensure quality and running data through macros against business rules to limit defects.

The database scope and implementation process was discussed, identifying a relational database as the most suitable structure given the variety and complexity of the RTCA legacy data. Primary keys and foreign keys were established throughout each table to remove redundant and duplicate data and ensure correlated data could be linked by forming derived relationships. Importer objects were developed and analysed to outline the data migration process and the strict validation procedures associated with these objects.

Finally, the advantages of creating a live link between the geotechnical database and a blast fragmentation model were discussed. By querying the database for geomechanical and structural information within the blast coordinates; accurate and up-to-date geotechnical data can be fed into the model. The model was developed to create a cost effective comparative tool to compare blast outputs for varying blast geometries and explosives.

ACKNOWLEDGMENTS

Sjoberg and Sabine Stam for their constant guidance, geotechnical expertise and willingness to assist in the project.

REFERENCES

Antoljak, S and Caronna, S. 2012, Subsurface databases in geoenvironmental engineering, *Chemical Engineering Transaction*, 28:97-102.

Atkinson, T, Dow, R and Brom, R. 1984, A review of hydrological investigation for deep coal mines, with special reference to petrophysical methods, *International Journal of Mine Water*, 3(3):19-34.

Baecher, G. 1987, Error analysis for geotechnical engineering [online], Nexus Associates. Available from:
<http://pm.umd.edu/files/public/water_library/1987/Report_Error%20Analysis%20ffo%20Geotechnical%20Engineering_Sep%201987_Baecher.pdf> [Accessed 4th May 2014].

Brady, B and Brown, E. 2004, Rock Mechanics for Underground Mining, pp 85-120 (*Springer: Delhi*).

Caronna, S. 2006, The comparative value of geotechnical databases vs. reportbases, *in Proceedings Geotechnical Engineering in the Information Technology Age*, pp 145-149 (GINT Software: Atlanta).

Caronna, S. 2010, Fundamentals of geotechnical database management, *Geotechnical News*, 28(2):37-40.

Cunningham, C. 2005, The Kuz-Ram fragmentation model 20 years on, *in Proceedings European Federation of Explosives Engineers*, pp 201-210 (ISBN: Brighton).

Doktan, M. 2001, Impact of blast fragmentation on truck shovel fleet performance, *in Proceedings 17th International Mining Congress and Exhibition of Turkey*, pp 375-380 (IMCET: Turkey).

Goldin, S, Parks, D, Skeate, R and Wahi, M. 2008, Reducing errors from electronic transcription of data collected on paper forms: a research data case study, *Journal of the American Medical Informatics Association*, 15(3):386-389.

Hadjigeorgiou, J. 2012, Where does the data come from [online], Lassonde Institute of Mining. Available from: <http://www.acg.uwa.edu.au/__data/page/2139/DHS12_Hadjigeorgiou_keynote.pdp> [Accessed: 8th May 2014].

Hanson, C, Thomas, D and Gallagher, B. 2005, The value of early geotechnical assessment in mine planning [online], University of Wollongong. Available from:
<http://ro.uow.edu.au/cgi/viewcontent.cgi?article=1064&context=coal> [Accessed: 10th March 2014].

Harrison, J and Hudson, J. 2007, Engineering Rock Mechanics, pp 1-9 (Pergamon: Oxford)

Hoek, E, 1994, *The challenge of input data for rock engineering, ISRM News Journal*, 2(2):23-24

Kanchibolta, S, Morrell, S and Valery, W, 1999. Modelling fines in blast fragmentation and its impact on crushing and grinding, *in Proceedings a Conference on Rock breaking*, pp 137-144 (AusIMM: Kalgoorlie).

Maskell, J. 2014, Personal communication, 16 May.

MOSHAB. 1997, Geotechnical considerations in underground mines [online]. Available from: <http://www.dmp.wa.gov.au/documents/Factsheets/MSH_G_GeotechnicalConsiderationsUGGeote.pdf> [Accessed: 11 March 2014}.

Pankow, K, Moore, J, Hale, M, Koper, K, Kubacki, T, Whidden, K and McCarter, M. 2013, Massive landslide at Utah copper mine generates wealth of geophysical data, *GSA Today*, 24(1):4-9.

Perez, J, Ramos, I, Anaya, V, Cubel, J, Dominguez, F, Boronat, A and Carsi, J. 2002, Data reverse engineering of legacy databases to object orientated conceptual schemas [online], *Theoretical Computer Science*, Available from:
<http://citeseerx.ist.psu.edu/viewdoc/download?doi=10.1.1.99.6293&rep=rep1&tyty=pdf> [Accessed: 8th May 2004].

THE APPLICATION OF HOSE MANAGEMENT IN MINING

Paulo Roberto Pereira

ABSTRACT: In a surface mining operation the unscheduled downtime due to hose can reach up to 37% of the entire unscheduled downtime for a prime mover hydraulic shovel. Reliability Based Maintenance Programs are more effective at improving fleet availability and Total Cost of Ownership. In this regard, correct process management is a fundamental building block of any successful machine reliability centered maintenance program. This can be expressed as well as the correct management of the application of the machine components, the quality and capability of the human resources involved, the comparative acquisition costs of those components and more importantly the comparative operational performance of those components. The main objective is to quantify the economic value that a reliability centered component maintenance program will bring to the operation in increased safety, machine availability and productivity, environmental compliance and total cost of ownership. This paper will present what this program, called Hose Management Program, looks like for flexible hose assemblies, its applications and the value that it has brought to some mine operators around the world.

RELIABILITY CENTERED MAINTENANCE – AN OVERVIEW

Reliability Centered Maintenance (RCM) is a process to ensure that assets continue to do what their users require in their present operating context (Moubray, 1997).

It is generally used to achieve improvements in fields such as the establishment of safe minimum levels of maintenance, changes to operating procedures and strategies and the establishment of capital maintenance regimes and plans. Successful implementation of RCM will lead to increase in cost effectiveness, machine uptime, and a greater understanding of the level of risk that the organization is managing.

John Moubray (1977), characterized Reliability-centered Maintenance as a process to establish the safe minimum levels of maintenance.

Reliability centered maintenance is an engineering framework that enables the definition of a complete maintenance regime. It regards maintenance as the means to maintain the functions a user may require of machinery in a defined operating context. As a discipline it enables machinery stakeholders to monitor, assess and recommend the working regime of their physical assets. This is embodied in the initial part of the RCM process which is to identify the operating context of the machinery, and write a Failure Mode Effects and Criticality Analysis (FMECA). The second part of the analysis is to apply the "RCM logic", which helps determine the appropriate maintenance tasks for the identified failure modes in the FMECA. Once the logic is complete for all elements in the FMECA, the resulting list of maintenance is "packaged", so that the periodicities of the tasks are rationalized to be called up in work packages; it is important not to destroy the applicability of maintenance in this phase. Lastly, RCM is kept live throughout the "in-service" life of machinery, where the effectiveness of the maintenance is kept under constant review and adjusted in light of the experience gained.

RCM can be used to create a cost-effective maintenance strategy to address dominant causes of equipment failure. It is a systematic approach to defining a routine maintenance program composed of cost-effective tasks that preserve important functions.

The important functions (of a piece of equipment) to preserve with routine maintenance are identified, their dominant failure modes and causes determined and the consequences of failure ascertained. Levels of criticality are assigned to the consequences of failure. Maintenance tasks are selected that address the dominant failure causes. This process directly addresses maintenance preventable failures. Failures caused by unlikely events such as non-predictable acts of nature will usually receive no action provided their risk (combination of severity and frequency) is trivial (or at least tolerable). When the risk of such failures is very high, RCM helps the user to consider changing something which will reduce the risk to a tolerable level.

Gates Corporation, Englewood, Colorado, USA, E. mail: pp3456@gates.com Tel: +1 303 513 7354

The result is a maintenance program that focuses scarce economic resources on those items that would cause the most disruption if they were to fail. For mobile equipment failure of certain components will always be severe enough to cause that piece of equipment to be down often in an unscheduled basis. Therefore, there is an immediate detrimental impact (severe) to the performance of that equipment and by extension to the operation in which that equipment is involved. This is true for hose assemblies on any piece of equipment

RCM emphasizes the use of Predictive Maintenance (PdM) techniques in addition to traditional preventive measures. By establishing testing parameters for component it is possible to define "useful lives" for items which not necessarily means their ultimate life but the recommended durability of that component in a lab setting. By combining this durability with the ability to monitor the lab parameters in the field a "predictive" replacement schedule can be produced by the maintenance personnel

RELIABILITY CENTERED MAINTENANCE - EVOLUTION

Since the 1930's, the evolution of maintenance can be traced through three generations. RCM is rapidly becoming a cornerstone of the Third Generation, but this generation can only be put in perspective in the light of the First and Second Generations.

The First Generation

The First Generation covers the period up to World War II. In those days industry was not very highly mechanized, so downtime did not matter much. This meant that the prevention of equipment failure was not a very high priority in the minds of most managers. At the same time, most equipment was simple and much of it was over-designed. This made it reliable and easy to repair. As a result, there was no need for systematic maintenance of any sort beyond simple cleaning, servicing and lubrication routines. The need for skills was also lower than it is today.

The Second Generation

Things changed dramatically during World War II. Wartime pressures increased the demand for goods of all kinds while the supply of industrial manpower dropped sharply. This led to increased mechanization. By the 1950's machines of all types were more numerous and more complex. Industry was beginning to depend on them.

As this dependence grew, downtime came into sharper focus. This led to the idea that equipment failures could and should be prevented, which led in turn to the concept of preventive maintenance. In the 1960's, this consisted mainly of equipment overhauls done at fixed intervals.

The cost of maintenance also started to rise sharply relative to other operating costs. This led to the growth of maintenance planning and control systems. These have helped greatly to bring maintenance under control, and are now an established part of the practice of maintenance.

Finally, the amount of capital tied up in fixed assets together with a sharp increase in the cost of that capital led people to start seeking ways in which they could maximize the life of the assets.

The Third Generation

Since the mid-seventies, the process of change in industry has gathered even greater momentum. The changes can be classified under the headings of new expectations and new techniques.

Evolution of Maintenance Expectations as shown in Figure 1.

New techniques

There has been explosive growth in new maintenance concepts and techniques. Hundreds have been developed over the past fifteen years, and more are emerging every week.

Figure 2 shows how the classical emphasis on overhauls and administrative systems has grown to include many new developments in a number of different fields.
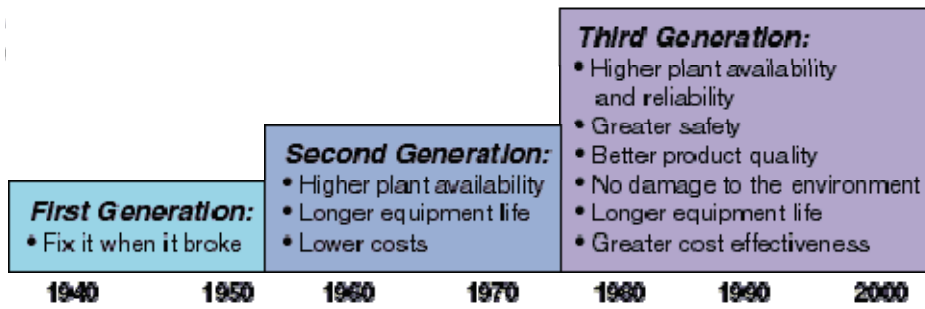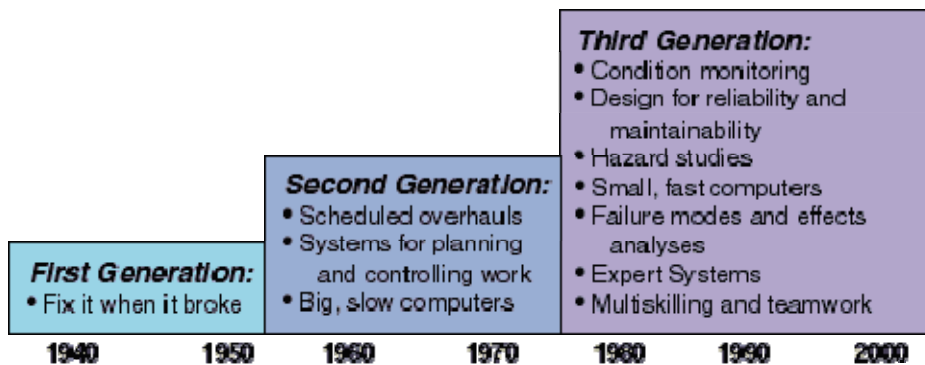
Figure 1: Evolution of maintenance expectations

Figure 2: Evolution of maintenance technologies

The new developments include:

- decision support tools, such as hazard studies, failure modes and effects analyses and expert systems
- new maintenance techniques, such as condition monitoring
- designing equipment with a much greater emphasis on reliability and maintainability
- a major shift in organizational thinking towards participation, team-working and flexibility.

A major challenge facing maintenance people nowadays is not only to learn what these techniques are, but to decide which are worthwhile and which are not in their own organizations. If we make the right choices, it is possible to improve asset performance and at the same time contain and even reduce the cost of maintenance. If we make the wrong choices, new problems are created while existing problems only get worse.

The challenges facing maintenance

In a nutshell, the key challenges facing modem maintenance managers can be summarized as follows:

"To select the most appropriate techniques to deal with each type of failure process in order to fulfill all the expectations of the owners of the assets, the users of the assets and of society as a whole in the most cost-effective and enduring fashion with the active support and co-operation of all the people involved."

RCM provides a framework which enables users to respond to these challenges, quickly and simply. It does so because it never loses sight of the fact that maintenance is about physical assets. If these assets did not exist, the maintenance function itself would not exist. So RCM starts with a comprehensive, zero-based review of the maintenance requirements of each, asset in its operating context.
All too often, these requirements are taken for granted. This results in the development of organization structures, the deployment of resources and the implementation of systems on the basis of incomplete or incorrect assumptions about the real needs of the assets. On the other hand, if these requirements are defined correctly in the light of modem thinking, it is possible to achieve quite remarkable step changes in maintenance efficiency and effectiveness.

Hose Assemblies and RCM – The need for a Hose Management Program

The Hose Management Program seeks to address the third generation of Maintenance Expectations as listed in Figure 1 with the following techniques:

a) Condition monitoring, where hose condition both external and internal are closely monitored
b) VEVA (Value Engineering/Value Analysis) for greater system reliability and maintainability
c) Hazard studies enabled by systematic inspections, tracking, condition monitoring and engineering analysis of the data collected
d) Root cause and effects analysis supported by the build-up of experience and investigation of failures. This will also help establish a site specific standard of systems criticality and a reliability based hose replacement
e) Expert systems that support traceability of hose assemblies
f) Multiskilling and team work between end user and supplier team which are crucial for the successful implementation of the program

To extend on the above and explain the hose assembly performance relationship to RCM and the need for a well designed and implemented Hose Management Program the 7 RCM Expectations above as they pertain to Hose Assemblies are discussed as follows:

1) What is the item supposed to do and what are its associated performance standards?
   Hose assemblies convey power through the dynamic action of pressurized hydraulic fluids which enable a piece of machinery to perform its basic operating functions of loading, ripping, digging, hauling, drilling or grading. The performance standards are derived from the various industry bodies that establish standards for hose assemblies such SAE, ISO, DIN and MDG 41 to name a few.
2) In what ways can it fail to provide the required functions?
   Hose assemblies can fail in several ways depending on the application in which they are installed. They can fail by internal effects such as manufacturing defects, poorly designed hose / coupling interface, continuous pressure impulse spikes above working pressure, temperature spikes and by external effects such as poor crimping, twisting, external cover abrasion, cuts, or gouges. The program tracks hose assemblies from cradle to grave thereby identifying when the hose fails and what was the failure mode.
3) What are the events that cause each failure?
   Many events cause these failures but most are related to manufacturing processes, crimping practices, installation practices and engineering practice. Analysis of each failure will help to recommend the right product that will ensure from the beginning the highest possible reliability for a particular hose assembly.
4) What happens when each failure occurs?
   Usually, when a hose assembly fails on a piece of mining equipment the equipment is out of service immediately after the failure. Although the frequency will vary, from a mining operator's perspective the severity is high and immediate. Additional risks that are involved are severe injury to the operator and potential complete loss of the piece of equipment due to a fire for example. In addition, the environmental consequences of a failure might be severe depending on which hose assembly fails. Usually, the cost of the hose assembly that fails pales in comparison with all the other costs that are involved with a failure
5) In what way does each failure matter?
   Each failure matters because it will affect to a greater or lesser extent the profitability pyramid of a mining operations described in Figure 3:

Every one of the sub-pyramids can have an economic value associated with them and in conjunction changes in them will lead to incremental positive or negative cash flows in a given mining operation.

1) What systematic task can be performed proactively to prevent, or to diminish to a satisfactory degree, the consequences of the failure?
   The most proactive action an operator can take to prevent or diminish to a satisfactory degree the consequences of failure is to take an Applications Engineering approach. This approach involves studying the hydraulic system on the machine and prescribing the right hose assembly component for that application. In addition, Application Engineering helps with the serviceability of the machine when it comes the time for Hose Assembly fabrication, replacement while also helping with the cost of the machine's Bill of Materials
2) What must be done if a suitable preventive task cannot be found?

Time and answers to questions 1 through 6 will help build a database of well documented cases that will help the user to establish maintenance principles and a body of maintenance tasks (preventative and/or predictive) where correct remediation is not immediately obvious. So, this body of information is the essence of the Hose Management Program.

Figure 3: Profitability pyramid

Key Components of the Hose Management Program

1) Key performance Indicators to be determined at the beginning of the implementation of the program
2) High performance products that will enable a significant reduction in undesired outcomes
3) Product application engineering analysis that will optimize hydraulic systems
4) Hose assembly tagging and tracking to track the lifecycle of every hose assembly
5) Internal Condition Monitoring and engineering analysis of selected hydraulic circuits
6) External Condition Monitoring of hose assembly conditions
7) Risk analysis based on hose assembly function and location on a given piece of equipment
8) Reliability Based Replacement Alerts based on condition monitoring

APPLICATIONS OF THE HOSE MANAGEMENT PROGRAM

By applying some or all of the components of the Reliability Based Hose Management program as described above it has been possible to produce the following results at several different types of mining operations described in Figure 4:

Mine Type	Area of Improvement	Equipment Type	Quantifiable Improvement After Hose Management
UG Hard Rock Mine	Mean Time Between Failures	One boom Jumbo	206% Improvement
UG Hard Rock Mine	Mean Time Between Failures	One boom Jumbo	240% Improvement
UG Room and Pillar Coal Mine	Total Cost of Ownership	Continuous Miner	Reduction in Hose and couplings expense
Aggregates Mine	Mean Time Between Failures	Mining Fleet	33% Increase in Fleet Availability
Surface Coal Mine	Total Cost of Ownership	Large Hydraulic Shovel Boom Hoses	Reduction in Hose Acquisition Cost
Surface Coal Mine	Mean Time Between Failures	Hydraulic Shovel Boom Hoses	20% to 40% longer life.
Mining OEM	BOM, Assembly Time	Haul Truck	Reduction in the BOM Cost

Figure 4: Hose management field examples

Relation between the cost of a hose assembly and the cost of downtime

An idea of the relationship between the cost of downtime for selected mining operations and the cost of a hose assembly on a given machine are presented in two examples shown in Figure 5

Surface Gold Mine Heap Leach
- **Cost of Hose Assembly: up to $840.00**
- **Content per Machine: up to $25,000**
- **Lost production per hour of downtime on a prime mover: $77,000/Hr**
- **Spot Gold Price at 1,300/oz**

Surface Coal Mine
- **Cost of Hose Assembly: up to $1,100.00**
- **Content per Machine: up to $40,000**
- **Lost production per hour of downtime on a prime mover: $27,000/Hr**
- **Spot Price of Coal at $7.53/metric ton**

Figure 5: Relative values of downtime, content per machine and hose assembly pricing

CONCLUSIONS

The paper discusses Reliability Based Maintenance applied to Hose Assemblies and shows the results produced by applying one or more components of a Reliability Based Hose Management Program in several mining operations around the world departing from a time based maintenance program to a

condition based maintenance program. This new approach in hose assembly maintenance has shown significant improvement in Mean Time Between Failures, Reduction in the Total Cost of Ownership and improvement in Mobile equipment Fleet availability. The main factors determining the success of mining operations were discussed and it is shown that the acquisition cost of a hose assembly is insignificant compared to the value of downtime of a major piece of equipment in any mining operation.

REFERENCE

Moubray, J. 1977, Reliability Centered Maintenance, 2nd Edition, Published, April 1997, *by Industrial Press*, ISBN: 0831130784.

STRENGTH PROPERTIES OF FIBRE GLASS DOWELS USED FOR STRATA REINFORCEMENT IN COAL MINES

David Gilbert, Ali Mirza, Xuwei Li, Haleh Rasekh, Naj Aziz and Jan Nemcik

ABSTRACT: Glass-Reinforced Polymer (GRP) bolts, commonly known as Fibre Glass (FG) dowels are increasingly applied for strata reinforcement in mines. The most popular dowels used in coal mines are the 22 mm diameter fully threaded type. A series of tests were undertaken to evaluate various strength properties of FG dowels. These include tensile failure tests by the double-embedment method, single and double guillotine shear tests, double shear tests in concrete medium and punch shear tests. Punch shear tests were used to evaluate the dowel shear strength parallel and perpendicular to the fibre glass strands or elements direction of extrusion. The study found that the tensile strength of the 22 mm diameter fibre glass dowels was in the order of 30 t. In the shear testing, the peak shear load was influence by the encapsulation grout type and the level of fibre glass axial pre-tension. Also, there was a nearly fivefold difference in the shear strength value of fibre glass dowels tested parallel as against perpendicular to the dowel axis.

INTRODUCTION

Glass-Reinforced Polymer (GRP) bolts, commonly known as Fibre Glass (FG) dowels are increasingly used in Australian coal mines as a mean of rib support in heading development and for coal face equipment recovery. The increased mechanisation of coal winning particularly by longwall mining necessitated the use of non-metallic rib dowels for rib support, where extraction includes cutting of bolts. FG dowels are made by pultrusion, a process that combines extrusion and pulling of molten or curable resin and continuous fibres usually arranged in unidirectional layers, through a die of a desired structural shape ("pull" and "extrusion"). FG dowels are made of glass strands pulled through a saturated thermo set resin and heated (Lowenstein, 1973). Presently FG dowels used in coal mines rib support have continuous rope thread profiles providing deformations for high bond strength with resin and rock. Other factors contributing to the increased application of polymeric dowels, as elements of support instead of steel, include:

- Improvement in the strength properties of the non-steel based dowels. The ultimate tensile strength of presently made 22 mm diameter dowels can range between 57 - 85 % of steel rebar of the same diameter.
- Easy and safe handleability of the non-steel dowels particularly FG ,
- Lightweight, fire resistant and easy to handle,
- FG dowels are relatively cheap,
- Cuttable, longer lasting and can be supplied a greater length.

Presently, there are two types of GRP bolts in the market, they are plastic and FG dowels, however, FG dowel is characterised as having lower yield deformation against shearing, and can twist on torqueing. Properties and characteristics of polymeric bolts are variable depending on the chemistry of the product, dowel diameter, solid or hollow core, surface profile shape and composition. FG dowels are used as rib support dowels. Dowels of the same core diameter can vary in length, identified by dowel colour and colour coding. Typical dowel lengths with colour coding include dowel length 1.2 m (blue), 1.5m (orange), 1.8m (red) and 2.1 m (green).

Procedures used for evaluating strength integrity of dowels are based on Australian and various international standards. These include American Standards of Testing Materials (ASTM. C-759, 1991), The British Standard (BS 7861- Parts 1 and 2, 1996), International Standard ISO 10406-1 (2008), South African Standard, SANS1534 (2004) and others. In general, many well-known standards are invariably interrelated; however, the suitability of any particular standard, for testing the given property of the dowel, will depend on the purpose of the dowel use and host medium properties. The current reporting

School of Civil, Mining and Environmental Engineering, University of Wollongong, NSW, Australia. E-mail: naj@uow.edu.au,
Tel: +61 242213449

of the shear strength of dowels is normally based on guillotine testing of the FG rod in steel apparatus. Guillotining of the GRP dowels in steel shear apparatus yields lower shear values and is a desirable test. It is important that the shear strength of dowels must be determined based on simulated ground conditions, and therefore it is logical to test dowels in rock or cementitious medium of concrete. Accordingly there is a need for establishing a credible testing methodology and procedures of marketed dowels. The double shear testing of dowels in concrete blocks represents a novel approach to simulating the shear behaviour of dowel in rock formation *in situ.*   This paper discusses tensile and shear strength characteristic of 22 mm core diameter FG dowels, which are used in Australia coal mines.

TENSILE STRENGTH PROPERTIES

Eight FG solid core dowels were tested for failure. Each 500 mm long dowel section was double embedded in 150 mm length steel tubes and pull tested to failure. Oil based standard J-LOK resin was used to install the dowels in steel tubes. FG dowels were pull-tested in a 50 t Instron universal testing machine. The elongation of the 110 mm length of the middle section was monitored using an accurate extensometer as shown in Figure 1 and b. Monitoring of the bolt section elongation was necessary in order to eliminate any displacement of bolt ends between the jaws of the test machine or the encapsulated bolt ends in the steel tubes being displaced.

To alleviate the concern of the possible influence of short lengths of tested samples end in steel tubes on test values, tests were also made on 1.2 m long dowels with ends being embedded in 450 mm long steel tubes as shown in Figure 1b. Solid threaded bars were connected to the end of each embedded encapsulation tube, to enable anchoring/clamping of the dowel and tube assembly to the jaws of the testing machine. The internal lining of embedded tubes was threaded with 2 mm threads and in accordance with recognised test standards such as ISO-10 406-1:2008. Figure 2 show short and long encapsulated dowels before and after testing. Figure 3 shows the load displacement of both short and long dowel test results. The pull test results revealed that end encapsulation of the dowels had no significant influence on the outcome of strength test results. The average displacement of the short encapsulated bolt at yield strength is in the order of 6%; however the displacement amount at yield strength appears to be significantly longer at around 9%. More tests are needed to verify this finding.

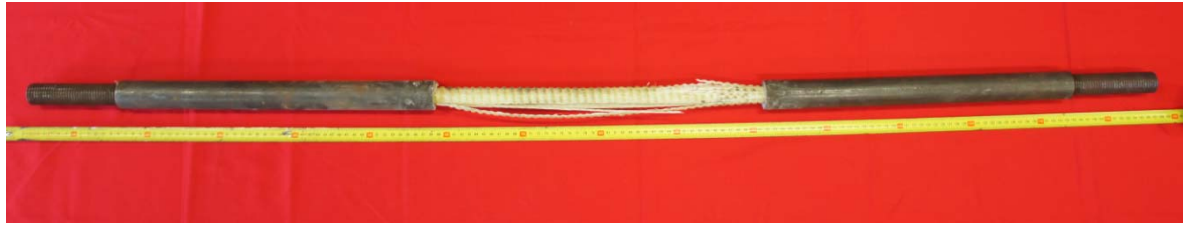(a)   500 mm long dowel section   (b) 1200 mm long dowel

Figure 1: Fibre glass bolt tested for tensile failure with extensometer

(a) Intact 500 mm long dowels with short end encapsulation   (b) post-test 500 mm long shor
     samples

(c)   Post-test 1.2 mm long test sample
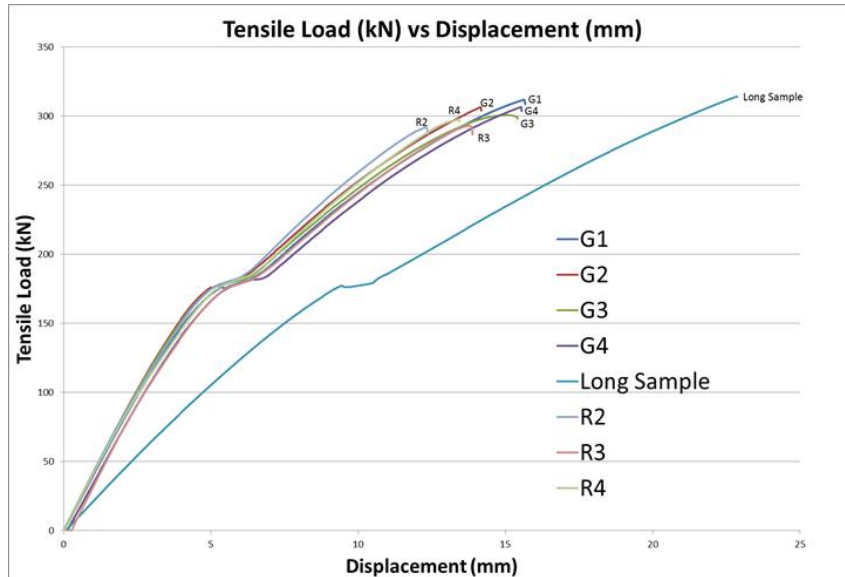**Figure 2: FG dowels prior to and post tensile failure testing**

Figure 3: Tensile load versus displacement of 500 mm long and 1.2 m long dowels

SHEAR TESTING OF DOWELS

Single shear guillotine test

Figure 4 shows the single shear apparatus used for shear testing of FG dowels. Commonly known as guillotine and is in compliance with the British Standard 7861 (2009), the instrument allows direct shearing of dowels and steel rebar to failure. Figure 5 shows examples of tested samples. Figure 6 shows load-displacement graphs of single shearing tests of only six, 300 mm long dowel sections. Details of the test results are also shown in Table 1. The average value of the shear strength was 133.51 MPa. The cut face surface of all ten tested dowels was identically stepped at mid face as is obvious in Figure 5. This may be attributed to the possibility of (a) the lateral incremental side movement of the dowel side during the shearing process, as the dowel sample was not grouted to its housing or held tight against the shearing apparatus and (2) the structural composition of the strands lay binding resin.

Figure 4: Single shear guillotine apparatus

Figure 5: Single sheared failed 22 mm diameter dowels

Table 1- Single shear results for ten dowels

Sample	Displacement (mm)	Peak Load (kN)	Shear Stress (MPa)
1	7.25	49.48	130.16
2	8.55	46.59	122.57
3	7.13	48.26	126.96
4	7.35	51.35	135.09
5	7.94	52.74	138.73
6	8.40	49.83	131.08
7	8.26	52.67	138.56
8	8.28	53.26	140.11
9	7.76	50.32	132.39
10	7.64	52.99	139.41
	Ave	**50.75**	**133.51**
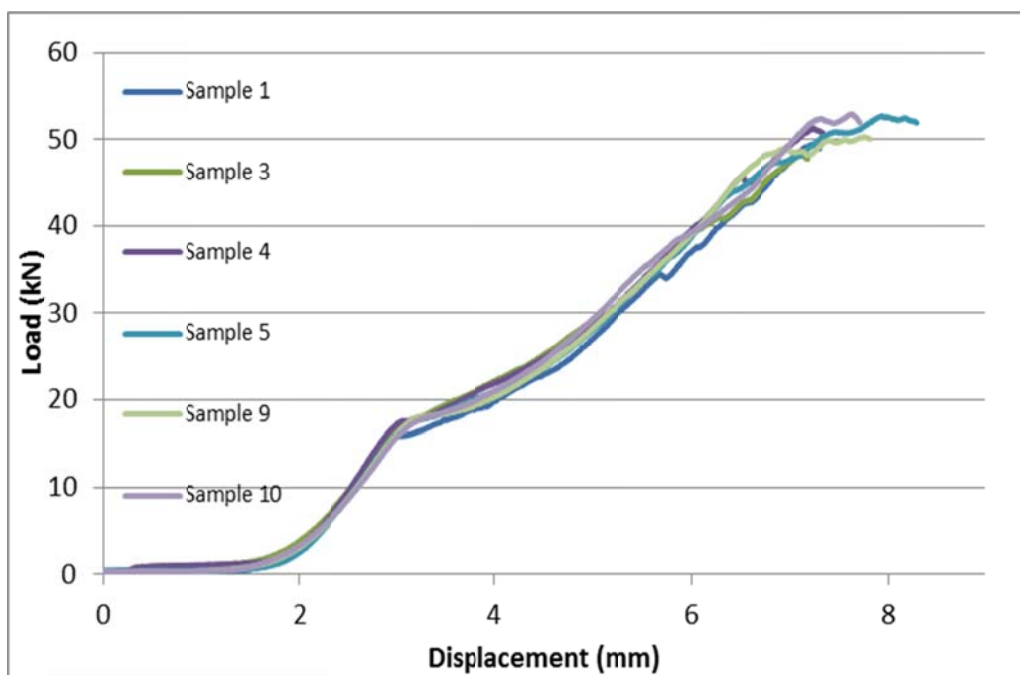
Figure 6: Shear load displacement graphs of single shear testing

Double shear Guillotine test in steel frame

The purpose of this section was to assess the single shear strength capacity of fibreglass dowels using a double Shear Testing Apparatus, which is conveniently named as Double Shear Guillotine test. The test produces steel on dowel interaction, whereas in *in situ* it would be the strata on grout on dowel interaction. However this test was carried out to compare test results with the single shear strength values using the single shear method.

Figure 7 shows the double shear test apparatus used for the study. It consists of two steel pieces. The bottom piece or 'U' shaped piece measured 143 mm x 83 mm x 70 mm. The top piece or 'T' shaped piece is inserted into the 'U' shaped piece. It measures 131 mm x 92 mm x 70 mm. The dowel was inserted through the middle of the combined apparatus and sheared up to a maximum depth of 30 mm. Each tested dowel rod cut into 300 mm specimen length. The shear testing was carried out using the 500 kN capacity Instron Universal Testing Machine, at a rate of 1mm/min.

Figure 7: Double shear guillotine apparatus set up

The shear strength of the dowel was determined using;

$$\tau = \frac{F}{2A} = \frac{2\ Peak\ load}{\pi D^2} \tag{1}$$

Where:

τ = shear strength
F = Peak load at failure
A = dowel cross sectional area
D = Dowel Diameter

Table 2 shows the results of double shear guillotine test, four dowel sections were tested and the average failure load and shear strength of the dowels were 50.48 kN and 123.79 MPa respectively. These results compare favourably with the single shear test results as reported in Table 1. The pattern of the shear failures was similar to the single shear test, but less pronounced as is shown in Figure 8.

Table 2: Double shear guillotine test results

Sample	Peak shear Load (kN)	Single face Peak Load (kN)	Shear Stress (single face) (MPa)
1	103.77	51.88	136.49
2	98.03	49.01	128.94
3	111.04	55.52	146.06
4	90.99	45.50	119.69
Average		50.48	132.79

Figure 8: failure pattern of dowels in guillotine

Double shear test in concrete

Double shear strength of fibre glass dowels was investigated in three piece concrete blocks consisting of a 300 mm long prism block, sandwiched between two 150 mm side cubes. 40 MPa, Uniaxial Compressive Strength (UCS) mortar blocks were prepared with sand: cement ratio of 3:1. Once mixed the mortar was poured into the internally greased marine plywood mould, measuring 150 mm x 150 mm x 600 mm. The mould was divided into three compartments separated by two metal plates. A plastic conduit, 20 mm in diameter was set through the centre of the mould lengthways to create a hole for FG dowel installation. The cast mortar blocks were left for 24 hours to set and harden. The set blocks were then removed from the mould assembly and kept in a moist environment for a period of 30 days to cure. The central hole of the mortar block was then reamed rifle-shaped to 27 mm diameter, ready for the installation of the dowel with cement grout. The strength of the concrete blocks was determined from testing of the representative 100 mm diameter cylindrical concrete specimens, cast at the time of concrete preparation and pouring.

Two different cementitious grouts were used when installing and encapsulating FG dowels in concrete blocks; (a) Jennchem Top-Down 80 grout (TD80) and (b) Jennchem Bottom-Up 100 grout (BU100). The strength of both grouts varied depending on the product composition and water content. In this study the level of water for each grout was maintained constant at six litres per bag. The FG concrete assembly was left for a minimum of seven days before being tested.

A total of 11 tests were conducted in this study. Dowels for each category of grout used were pretensioned to various loads up to 22.50 kN and then tested for shear. An attempt to apply pretension load of 25 kN was not possible as extra load torque applied to the dowel nuts caused the dowel ends to twist, leading to lower shear loads.The applied axial tension load due to subsequent shearing load, were monitored using two 30 t capacity load cells shown in the assembled setup in Figure 9. A 50 t capacity Instron universal testing machine was used for shearing study. Clearly there are variations to the shear

strength properties of the FG dowels based on the level of pretension loads and grout type as shown in Table 2 and Figure 8 t was found that;

a) The shear values of dowels were higher with increased pretension loads.
b) Increased pretension loads greater than 22.5 kN caused dowel ends to twist   thus affecting double shear strength values as is evident from the lower value shear load of   the dowel pre-tensioned at 25 kN,
c) Shear load values of dowels are affected by the grout type, with average shear values obtained from FG dowels tested with grout TD80 being higher than test results with BU100 grout, despite the fact that BU100   grout has relatively superior strength in comparison with TD80 grout.
d) The shear value of each tested dowel was determined taking into consideration the shear strength contribution from 150 mm^2 concrete joint planes.

Figure 9: An assemble FG dowel with load cells for double shear testing in 50 t Instron testing machine

Table 3: Single and double shear test results with different grouts

a) **Encapsulation Grout: BU100**

Test	Initial ave axial load (kN)	Final ave axial load (kN)	Peak shear load (kN)	Peak double joint plane shear strength (MPa)	Peak shear per joint plane (MPa)	Contribution from concrete joint surface (%)	shear strength less joint surface shear (MPa)	Direct single shear test (guillotine) ave value from Table 2 (MPa)	Increase (%)
1	2.5	28.7	163.9	431.2	215.6	10	194	133.5	49
2	4.5	43.4	182.9	481.6	240.6	15	205	133.5	58
3	5	62.0	204.7	538.5	269.2	15	229	133.5	76
4	15	31.2	219.7	578.0	289.0	20	231	133.5	78
5	20	40.0	258.1	679.0	339.5	25	255	133.5	96
6*	25	66.2	191.8	504.6	252.3	30	177	133.5	36

* Sample 6 - twisted dowel

b)   Encapsulation Grout: TD80

Test	Initial ave axial load (kN)	Final ave axial load (kN)	Peak shear load (kN)	Peak double joint plane shear strength (MPa)	Peak shear per joint plane (MPa)	Contribution from concrete joint surface (%)	shear strength less joint surface shear (MPa)	Direct single shear test (guillotine) ave value from Table 2 (MPa)	Increase (%)
7	2.5	26.9	206.3	542.6	271.3	10	244	133.5	88
8	7.5	49.2	178.5	469.6	234.8	15	200	133.5	54
9	10	20.6	266.6	701.2	350.6	15	298	133.5	229
10	22.5	50.2	296.1	779.0	389.5	15	331	133.5	255
11	25	53.7	172.4	453.5	226.8	25	170	133.5	31
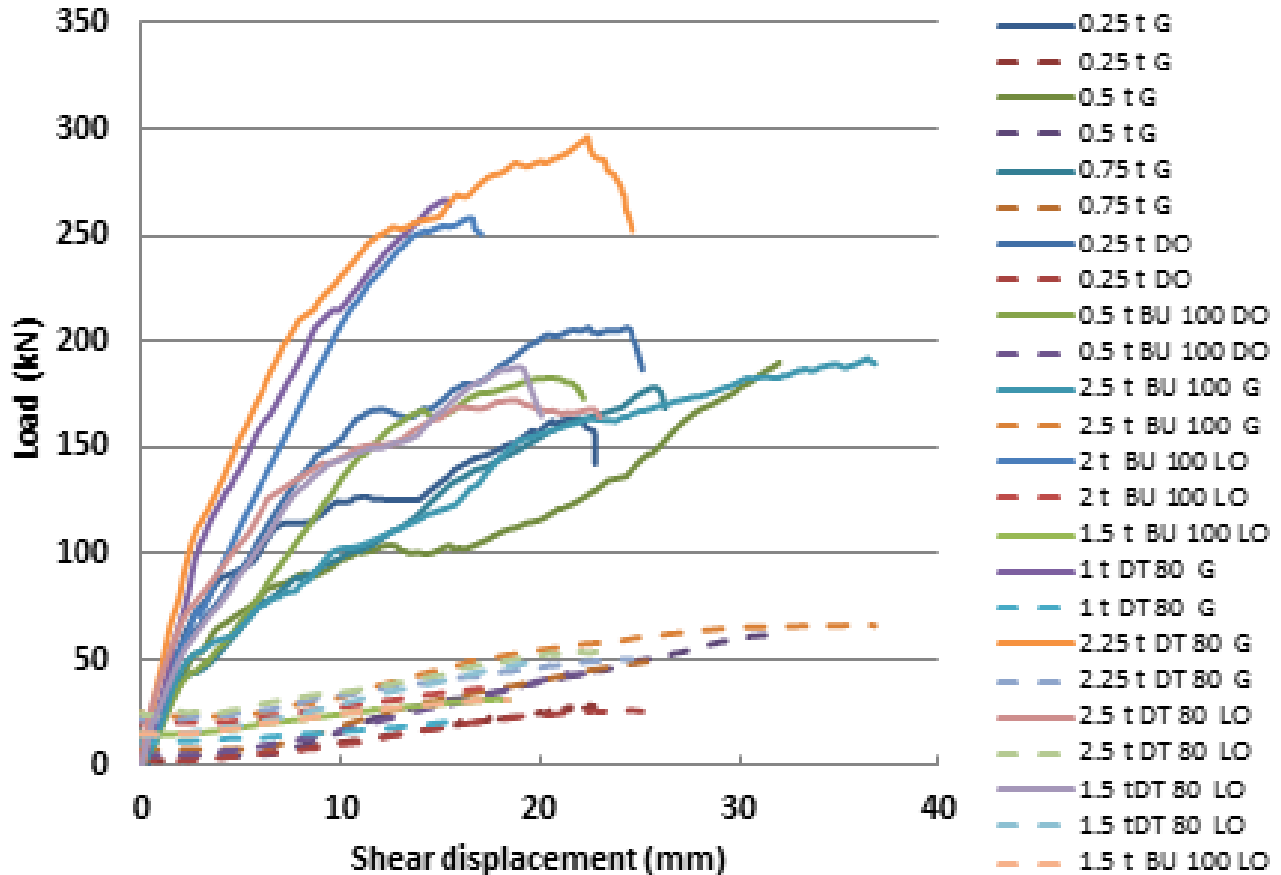
Figure 10- Shear pretention loads versus vertical displacement of double shear testing of 11 dowels

Impact of concrete strength

Further studies on the impact of the concrete strength on the double shear strength value of the dowel, a series of tests were undertaken in 40 MPa and 60 MPa concrete strength respectively. Four double shear tests were carried in 60 MPa strength concrete assemblies. Each double shear test was made in different pretension load of 2.5, 5, 10 and 15 kN respectively. Tests were made using 40 mm hexagonal nut with spherical ends. Another set if three tests were also made in 40 MPa concrete.

Table 4 shows initial axial loads, the peak axial loads, the peak shear loads and the equivalent single shear strength of four 22 mm dowels double shear tested in 60 MPa concrete blocks.
Figure 1 shows graphically the combined results from all four tests. The figure shows both the shear load and axial pretension loads for all samples. The shear strength values of the dowel appears to be influenced by the level of pretension loads, which is an expected variation and in agreement with various tests undertaken in both solid rebar and cable bolts. In general, the shear strength of the dowel was increased with increasing pretension loads.

Table 4: Double shear axial and shear loads of dowels tested in 60 MPa concrete

Sample	Initial Axial Load (kN)	Peak Axial Load 1 (kN)	Peak Axial Load 2 (kN)	Peak Shear Load (kN)	Shear Strength (MPa)
1B	2.5	15.91	13.64	220.74	290.34
2B	5	25.73	22.39	213.03	280.20
3B	10	22.60	27.79	242.70	319.23
4B	15	29.83	44.14	262.48	345.25
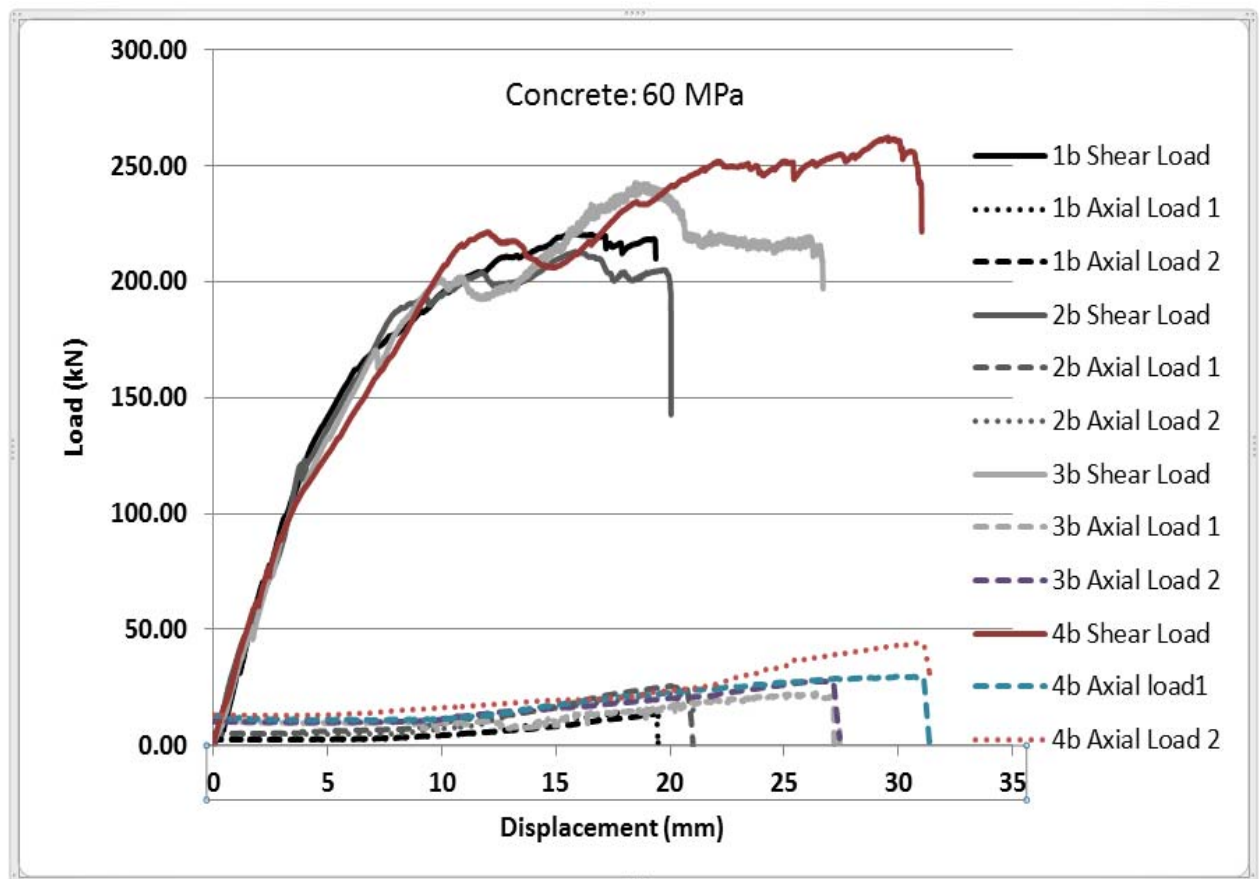
Figure 11: Double shear load–displacement profile of dowels axial and shear loads in 60 MPa concrete blocks

Punch shear test

Using the punch shear box, shown in Figure 12a, a series of punch shear tests were carried out on FG dowel samples to determine the shear strength of FG dowels. 3 mm thick discs were sliced perpendicular to the dowel axis to examine the shear strength properties of dowels parallel to the strands or FG elements lay, while 3 mm strips were cut parallel to the dowel axis to evaluate the shear strength of the FG elements bonding. Figure 12 b shows typical samples prepared for testing in punch shear apparatus. Tables 5 and 6 show results of punch shear tests. Values of the shear strength were determined by using the following equation;

$$\tau = \frac{F}{3.142 \ x \ T \ x \ D} \tag{2}$$

where;

F = applied load, τ = shear strength, T = Sample thickness and D = Punch diameter
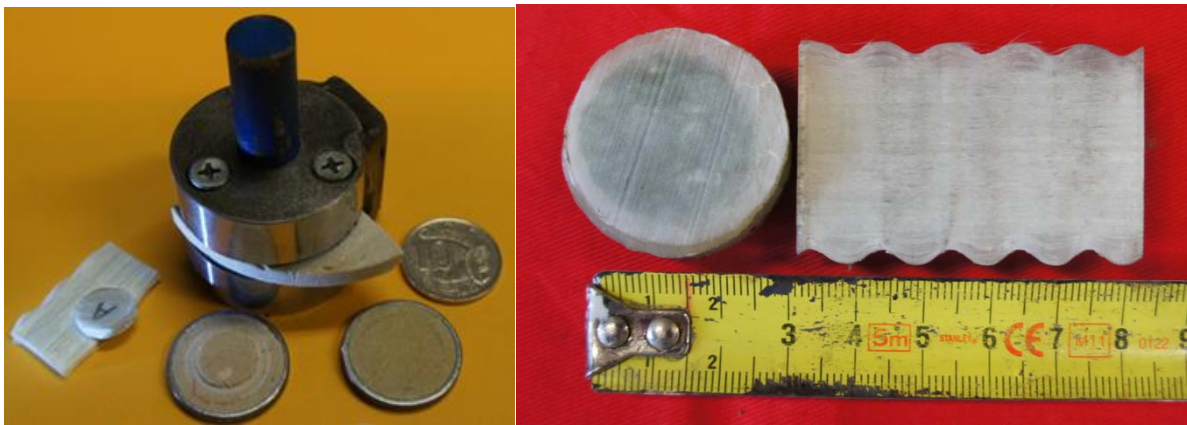
(a) Punch shear apparatus   (b) FG dowel samples perpendicular and parallel dowel axis

Figure 12: (a) Punch shear apparatus and (b) 33 samples FG strip cut out   (i) perpendicular and (ii) parallel to dowel axis, for shear testing

From Table 5, the average shear strength value of six samples punch tested parallel to the direction of the dowel is shown to be 22.35 MPa, and the average shear strength value of testing three samples perpendicular to the direction of the dowel axis as shown in Table 6 is 104.01 MPa. It is clear that there is an obvious difference in shear strength in the ration of 4.7:1 in favour of perpendicular to dowel axis or dowel strands compared with parallel to dowel axis. The low shear strength values parallel to the dowel axis may be due to the resin strength holding the fibres together, which is resisting the shear force. The average shear strength value shown in Table 5 strikingly similar to the average shear strength value of 21 days old standard oil based bolting as reported by Gilbert (2014)

Table 5: Punch test results of samples cut parallel to dowel axis

Sample	MN	T (m)	D (m)	τ (MPa)
A	0.0021	0.00249	0.0127	21.12
B	0.0022	0.00253	0.0128	21.70
C	0.0023	0.00279	0.0126	20.64
D	0.0028	0.00336	0.0126	20.98
E	0.0040	0.00363	0.0127	27.97
F	0.0011	0.00178	0.0127	15.38
G	0.0039	0.00342	0.0127	28.67
			Average	22.35

Table 6: Punch test results of samples cut perpendicular to dowel axis

Sample	Punch load (MN)	T (m)	D (m)	τ (MPa)
A	0.012	0.00297	0.0128	102.22
B	0.012	0.00302	0.0127	102.30
C	0.013	0.00302	0.0129	107.50
			Average	104.01

CONCLUSIONS

This study demonstrated that the guillotine method of testing dowels yields lower shear values than results obtained from testing dowels by double shear testing in concrete. Double shear testing in concrete represent a realistic way of simulating the strength property of the composite material in rock and *in situ*. The study also found that:

a)   Shear strength values of the FG dowels were higher with higher pretension loads.

b)   Increased pretension loads greater than 22.5 kN caused dowel ends to twist, affecting double shear strength values.

c)   Shear load values of dowels are affected by the grout type, with average shear values obtained from testing FG dowels tested with grout TD80 was higher than test results with BU100 grout, despite the fact that BU100 grout has relatively superior strength in comparison with TD80 grout.

d)   Low shear strength results of testing dowel parallel to the dowel axis in comparison to the shear values perpendicular to FG strands lay may be indicative of the resin strength holding the fibres together and resisting the shear force. Shear strength values shown in Table 3 are comparable to the shear strength of a typical oil based standard chemical resin used for bolting installation.

REFERENCES

Lowenstein, K.L. 1973, *The Manufacturing Technology of Continuous Glass Fibers*. New York: Elsevier Scientific. pp. 2–94. ISBN 0-444-41109-7.

American Standard for Testing Materials (ASTM. C-759). 1991, Standard test method for compressive strength of chemical –resistant mortar, grouts, monolithic surfacings and polymer concretes.

British Standard BS 7861- Parts 1 and 2. 2009, Strata Reinforcement support system components used in Coal Mines-Part 1. Specification for rock bolting and Part 2: Specification for Flexible systems for roof reinforcement.

International Standard ISO 10406-1. 2008, Fibre-reinforced polymer (FRP) reinforcement if concrete – test methods, part 1: FRP bars and grits, First edition, 40 p.

South African Standard SANS1534. 2004, Resin capsules for use with tendon based support systems, published by *Standards South Africa*.

Gibert, D. 2014, Study of fibre glass strength properties, undergraduate thesis, *University of Wollongong*.

INDEX TO AUTHORS